12-31-2010

Design and Synthesis of Beta-Hairpin Peptidomimetics for Modulating Integrin Mediated Cell Adhesion, Abeta Fibrillogenesis and p53-MDM2 Protein-Protein Interactions

Priyesh Jain
University of South Florida

Design & Synthesis of β-hairpin Peptidomimetics for Modulating Integrin Mediated Cell Adhesion, Abeta Fibrillogenesis and p53-MDM2 Protein-Protein Interactions

by

Priyesh Jain

A dissertation submitted in partial fulfillment
of the requirements for the degree of
Doctor of Philosophy
Department of Chemistry
College of Arts and Sciences
University of South Florida

Major Professor: Mark McLaughlin, Ph.D.
Jon Antilla, Ph.D.
Roman Manetsch, Ph.D.
Jianfeng Cai, Ph.D.

Date of Approval:
July 6, 2010

Keywords: β-sheet conformation, Cyclic Peptides, Cyclic III peptide, Multiple Myeloma, Peptide Nucleic Acids

DEDICATION

To my father late Shri Jayantiprasad Jain and

mother Smt. Jinendraprabha Jain

To my brothers and sisters

To my wife Parul

To my mentors Mark and Malshe

To my friends

ACKNOWLEDGEMENTS

I would like to thank my eldest brother, Pradeep Jain, my mother Jinendraprabha and family members who had inspired me to pursue the Doctorate degree. I would also thank my beloved wife, Parul, who has always supported me and helped me to accomplish this deed. I also thank my mentor, Dr. McLaughlin for his support, motivation, invaluable ideas and advise during my graduate career. He has helped me a lot in molding my career from polymer chemist to medicinal chemist. I also thank Dr. Lori Hazlehurst and her group members for performing biological activity studies for cyclic III peptide project. I am very thankful to Dr. Vasudha Sharma for agreeing to chair my Defense Committee. I would also like to acknowledge Dr. Sergiy Borysov at USF Health Byrd Alzheimer's Institute for carrying out biological assays for abeta fibrillogenesis inhibitors project. I thank all my committee members, Dr. Antilla, Dr. Roman and Dr. Cai for their invaluable suggestions. I would also like to thank Daniel Santiago who helped me with molecular modeling studies. I would like to acknowledge Dr. Ted Gauthier and Phil Murray for teaching me solid phase peptide synthesis and characterization. I also thank David Badger for performing all ^{2}D NMR experiments for the cyclic peptidomimetics. I also thank my previous and current group members: Dr. Woogie, Sridhar, Dr. Laura, Missy, Mingzhou, Mehul, Dr. Kiran, Dr. Stephanie, Dr. Tanaji, Dr. Mohan, Hyun Joo, Yi and Fenger for their constant support and encouragement. Finally I would like to thank the Department of Chemistry and Moffitt Cancer Research Center for providing me support and facilities to carry out my research work.

TABLE OF CONTENTS

LIST OF TABLES

LIST OF FIGURES

LIST OF SCHEMES

LIST OF ABBREVIATIONS

AA = Amino acid

AD = Alzheimer's Disease

Aib = α-aminoisobutyric acid

AOP = 7-Azabenzotriazol-1-yloxytris(dimethylamino)phosphonium hexafluorophosphate

APP = Amyloid Precursor Protein

ATP = Adenosine Triphosphate

Aβ = Amyloid Beta

Boc = tert-Butyloxy carbonyl

BOP = Benzotriazole-1-yl-oxy-tris-(dimethylamino)-phosphonium hexafluorophosphate

BOP-Cl = Bis(2-oxo-3-oxazolidinyl)phosphonic chloride

BroP = Bromotris(dimethylamino)phosphonium hexafluorophosphate

Bts-Cl = benzothiazole-2-sulfonylchloride

CD = Circular Dichroism

CHCA = α-Cyano-4-hydroxycinnamic acid

CHDA = 1,4-cyclohexanedicarboxylic acid

CPNA = Cysteine Based Peptide Nucleic acid

DBU = 1,8-Diazabicyclo[5.4.0]undec-7-ene

DCC = N,N'-dicyclohexylcarbodiimide

DCM = Dichloromethane

DIC = N,N'-diisopropylcarbodiimide

DIEA = N,N-Diisopropylethylamine

DMF = N,N-Dimethyl Formamide

DMSO = Dimethylsulfoxide

DPPA = Azidodiphenoxyoxophosphorane

DNA = Deoxyribonucleic acid

ECM = Extracellular matrix

EDC = 1-ethyl-3-[3-(dimethylamino)propyl]carbodiimide

ELISA = Enzyme-linked immunosorbent assay

Et_3SiH = Triethylsilane

Fmoc = 9-Fluorenylmethoxycarbonyl

Fmoc-Cl = 9-Fluorenylmethoxycarbonyl chloride

Fmoc-OSu = 9-Fluorenylmethyl *N*-succinimidyl carbonate

FN = Fibronectin

FTIR = Fourier Transform InfraRed

GPNA = Guanidine based Peptide Nucleic acid

HATU = *N,N,N′,N′*-Tetramethyl-*O*-(7-azabenzotriazol-1-yl)uronium hexafluorophosphate

HBTU = 2-(1H-Benzotriazole-1-yl)-1,1,3,3-tetramethyluronium hexafluorophosphate

HCTU = *N*,*N*,*N′*,*N′*-Tetramethyl-*O*-(6-chloro-1*H*-benzotriazol-1-yl)uronium hexafluorophosphate

HOBT = 1-hydroxybenzotriazole

HOPfp = pentafluorophenol

HPLC = High-performance liquid chromatography

III = Integerin Interaction Inhibitors

KDa = kilodalton

MBHA = 4 - Methylbenzhydrylamine resin

MDM2 = murine double minute 2

MDR = Multi-drug resistant

Meu = α-N-methylated Leucine

MM = Multiple myeloma

MRD = Minimal Residual Disease

m-RNA = Messenger RNA

NMM = N-Methylmorpholine

NMP = N-Methylpyrrolidone

NOE = Nuclear Overhauser effect

ONBSCl = ortho-nitrobenezenesulfonyl chloride

PDB = Protein Data Bank

PNA = Peptide Nucleic acid

PTSCl = p-Toluenesulfonyl chloride

PyAOP = 7-Azabenzotriazol-1-yloxy)tripyrrolidinophosphonium hexafluorophosphate

PyBOP = (1-Hydroxy-1H-benzotriazolato-O)tri-1-yrrolidinylphosphorus(1+) hexafluorophosphate(1-)

ROS = Reactive Oxygen Species

S_N2 = Nucleophilic Substitution bimolecular

SPPS = Solid Phase Peptide Synthesis

TBAI = Tetrabutylammonium iodide

TATU = 2-(7-Azabenzotriazole-1-yl)-1,1,3,3-tetramethyluronium tetrafluoroborate

TBTU = 2-(1H-Benzotriazole-1-yl)-1,1,3,3-tetramethyluronium tetrafluoroborate

TEA = Triethylamine

TEMPO = 2,2,6,6-tetramethylpiperidinoxyl

TFA = Trifluoroacetic acid

TFMSA = Trifluoromethanesulfonic acid

THF = Tetrahydrofuran

ThT = Thioflavin T

TLC = Thin Layer Chromatography

TMS = Tetramethylsilane

TMSCl = Chlorotrimethylsilane

Design & Synthesis of β-hairpin Peptidomimetics for Modulating Integrin Mediated Cell Adhesion, Abeta Fibrillogenesis and p53-MDM2 Protein-Protein Interactions

Priyesh Jain

ABSTRACT

Inhibiting therapeutically important protein-protein interactions has been a tremendous challenge for medicinal chemists. The folded 3D structures of peptides and proteins, mainly comprise secondary structural elements i.e α-helices and β-sheet have created an opportunity to design small molecules and peptidomimetic inhibitors of protein-protein interaction (PPI). Hence, information about the formation and stabilization of these secondary structures is vital for designing future drugs. In this dissertation, several cyclic beta-hairpin peptidomimetics that mimic the recognition surface have been designed and synthesized as inhibitors for different targets such as integrin mediated extracellular matrix -cell adhesion in multiple myeloma, p53-MDM2 PPI, amyloid beta fibrillogenesis inhibitor. Cyclization of linear peptides to restrict the number of conformations available to the linear peptide can increase its affinity for the target as well as increase its proteolytic resistance. In this study, different beta turn promoters that increase the propensity of cyclic peptides to adopt beta-sheet structures have been designed and synthesized. Chapter two discusses the design and synthesis of several cyclic III (Integrin Interaction Inhibitor) peptides that block adhesion of integrins to extracellular matrix components in Multiple Myeloma tumor cells. These cyclic peptides, as assayed by

TOPRO 3 assay were more potent than the parent linear peptide with a bio-activity of 1.08 µM. We have also studied structure activity relationships (SAR) of these cyclic III peptide analogs to increase the potency and bioavailability of these peptides.

Chapter three describes the application of cyclic beta-hairpin peptidomimetics to inhibit abeta fibrillogenesis that is responsible for Alzheimer's disease. We have successfully designed and synthesized cyclic peptides that target the hydrophobic region (17-21) of abeta fibril which is believed to cause self aggregation and plaque formation. We have also successfully explored these cyclic beta-hairpin peptides to disrupt p53-MDM2 interactions. Chapter five discusses the design and synthesis of novel cysteine based Peptide Nucleic Acid (PNA) monomers that are aimed to increase cellular uptake by introducing positively charged species attached to the cysteine side chain. We have successfully synthesized CPNA monomers and made efforts to make PNA oligomers.

CHAPTER ONE:

INTRODUCTION

1.1 General overview of peptides and proteins

Proteins are macromolecules consisting of 20 different natural amino acids linked together by amide bonds to form linear chains. Linear chains consisting of 2 to 100 amino acids with molecular weight up to 10 KDa are usually termed as peptides whereas longer polypeptides with defined structures are classified as proteins. The total number of different proteins that can be made from 20 different amino acids is huge. A 10 amino acids chain can have up to 20^{10} possible sequences or 10 trillion structurally different molecules. The biological activity of a protein depends on its three dimensional conformation. Peptides often have many different conformations and can randomly change whereas proteins are relatively rigid with one or a handful of preferred conformations. The primary structure of a polypeptide or protein is the sequence of amino acids linked together by peptide bond. As shown in fig. 1.1a, the peptide C-N bond has partial double bond character due to resonance, which restricts free rotation around the peptide bond (1). Proteins fold themselves into well defined secondary and tertiary structures. The secondary structure of proteins usually stems from the geometry of bond angle between amino acids and hydrogen bonds betweens adjacent amino acids residues. The main secondary structures of protein are: the α-helix, the β-pleated sheet and the β-turn. The tertiary structure of a protein describes the overall three-dimensional

arrangement of the atoms or shape of a protein. As shown in Fig. 1.1b, the peptide structure is always interpreted in terms of dihedral angles between adjacent planar peptide groups. The dihedral angle for free rotation around C^{α}–N bond is represented by angle Φ whereas rotation about C^{α}–C is denoted by Ψ.

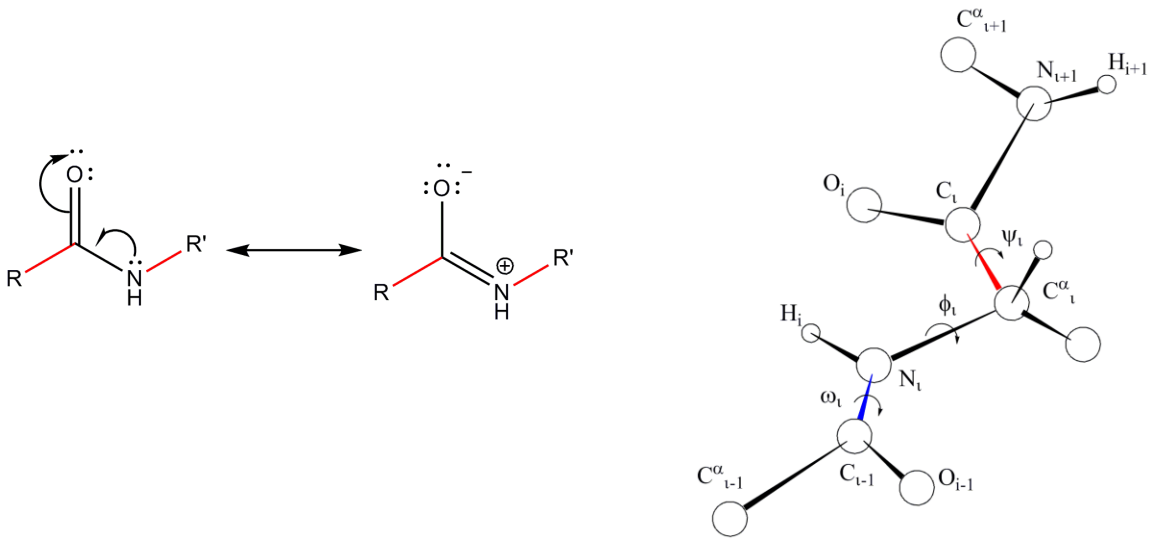

Fig. 1.1 (a) Resonance in planar peptide bonds (b) Various dihedral angles observed in linear peptide chains.

Table 1.1 Dihedral angles for secondary structural elements in peptides

Conformation	**Dihedral angle (degree)**		**Residues per turn**
	Φ	**Ψ**	
Right-handed α-helix	-57	-47	3.6
Anti-parallel β-sheet	-139	+135	2.0
Parallel β-sheet	-119	+113	2.0
Type I β-turn*	-60(-90)	-30(0)	3.0
Type II β-turn*	-60(+90)	+120(0)	3.0

For the β-turn, angle outside parenthesis is for ith+1 residue and within parenthesis is for ith+2 residue of the turn (2).

The right handed α-helix accounts for approximately 31% of all protein structures whereas β-sheets and β-turns accounts for 28% and 25% respectively (3). These secondary and tertiary structures are stabilized by noncovalent interactions such as hydrogen bonds, Van der Waals interactions, hydrophobic effects and steric interactions. The folded 3D structures of peptides and proteins have created an opportunity to design small molecules and peptidomimetics to mimic the recognition surface involved in various protein-protein interactions responsible for causing several diseases.

1.2 β-Sheet and β-hairpins

β-Sheet and β-hairpins are key recognition motifs that bind to many protein-protein and protein-DNA interactions that are important for many biological functions and also in causing some diseases. So far, the α-helix secondary structure has been widely studied. The study of β-sheets was not widely adopted due to the fact that these peptides quickly undergo self-association to form large, insoluble, quaternary β-sheet structures, which makes detailed thermodynamic and structural characterization of these secondary structures very difficult (4,5). β-sheets consist of two or more paired β-strands arranged in parallel or antiparallel fashion. In parallel β-sheets, the individual β-strands run in the same direction and are usually characterized by 12 atom hydrogen bonded rings (Fig.1.2a). In antiparallel β-sheets, the individual β-strands run in the opposite directions and are usually characterized by alternating 10 and 14 atom hydrogen bonded rings (Fig.1.2b). Table 1.1 clearly depicts the dihedral angles found in parallel and anti-parallel beta sheets. Antiparallel β-sheets have shorter (linear) H bonds whereas parallel β-sheet have slightly longer H bonds. Both parallel and antiparallel β-sheets have adjacent side chain residues running in opposite directions, thereby exhibiting an

extended conformation. Thus β-sheets offer three different recognition sites: interaction either via top or bottom faces of the sheet or via hydrogen bonding with amide hydrogen on each side of the sheet. Parallel β-sheets are usually seen in the hydrophobic interior of proteins whereas antiparallel β-sheets with amphipathic character are usually found at the surface of proteins.

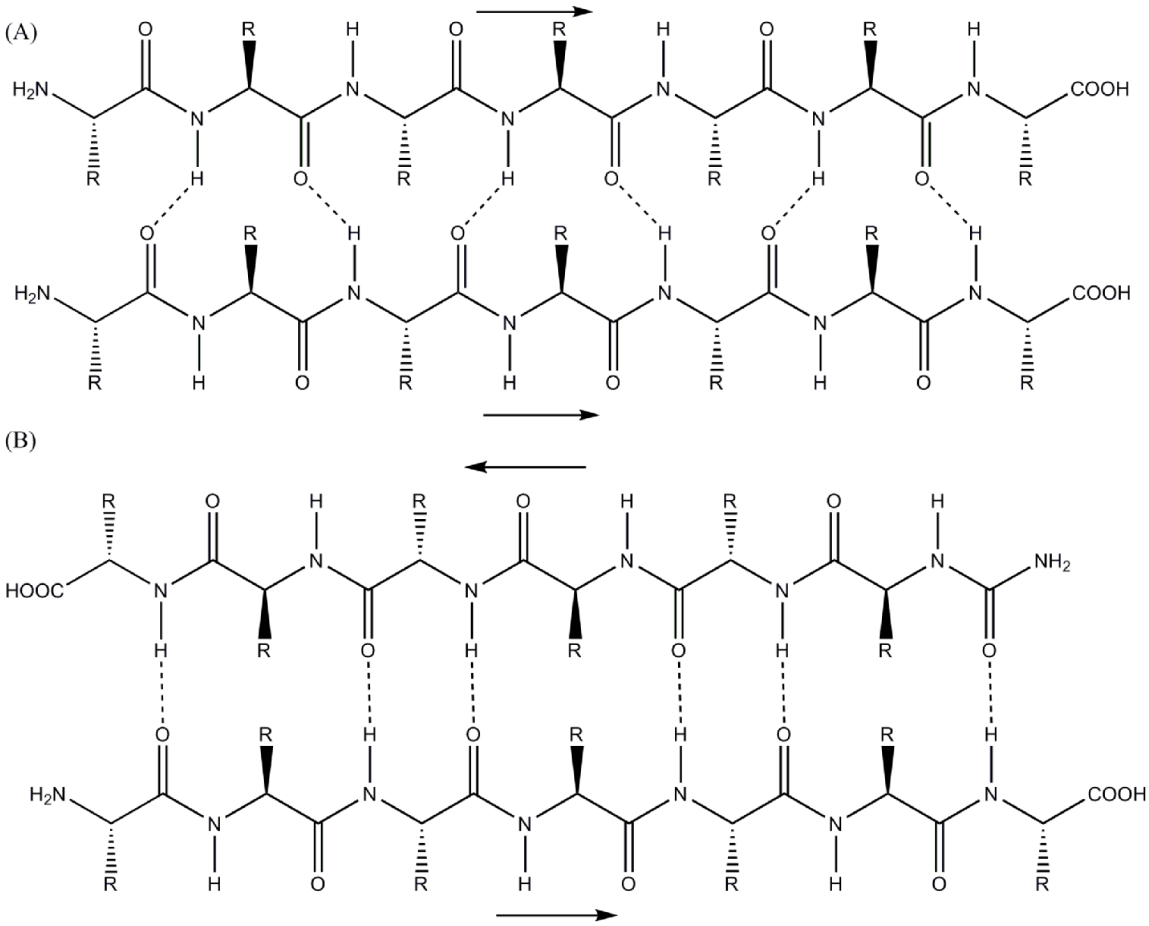

Fig. 1.2 Schematic representation of (A) parallel and (B) antiparallel β-sheets. H bonds are indicated by dashed lines whereas side chains of amino acids are represented by R. The arrow head indicates direction from N to C terminus of the β-sheet.

The β-turn is another important protein structure which allows the polypeptide chain to change the direction abruptly by 180^{o} and allows the protein to adopt a more globular compact shape (6-8). β-turns usually consists of loops formed from four amino

acid residues where the hydrogen bonding from ith and ith +3 residue is important in stabilizing the turn (Fig. 1.3).

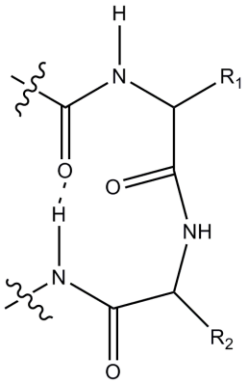

Fig. 1.3 The β-turn

Another very interesting secondary structure found at protein-protein interfaces is the β-hairpin motif (9-11). A β-hairpin is a simple motif that contains two antiparallel strands connected by a short connecting loop sequence of two to five amino residues that stabilizes the hairpin structure (Fig. 1.4). The β-hairpin scaffold is very interesting since it is used by many proteins for bimolecular recognition. 3D structure analysis of β-hairpins revealed that β-hairpins vary widely in hydrogen-bonding pattern between strands and most of hairpin loops have less than 5 residues (12).

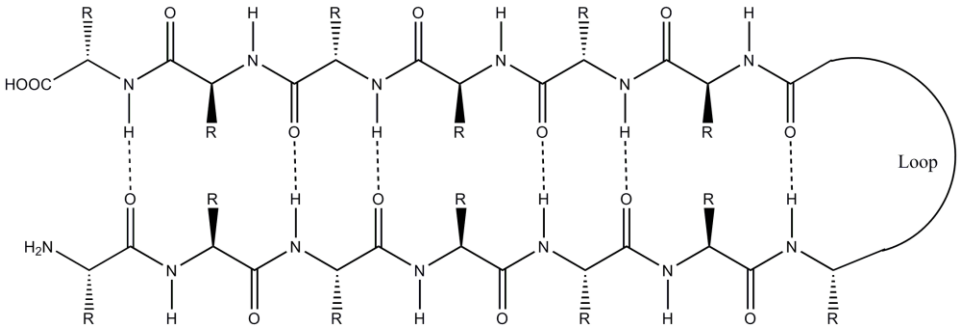

Fig. 1.4 β-hairpin

The simplest approach to design a β-hairpin mimetic is to transplant a hairpin loop of protein with a known structure onto a template that stabilizes the β-hairpin to form a conformationally defined macrocyclic structure. The template serves as a β-turn promoter and nucleates the cyclic β-sheet formation. The template structure plays an important role on macrocylic β-hairpin stability. Various research groups have incorporated natural or unnatural amino acids in the β-turn position of a β-hairpin and have studied β-hairpin folding and the stability of linear peptides in aqueous solution (13-18). As shown in Fig. 1.5, Blanco and co-workers have used the L-Asn-Gly dipeptide template as a β-turn promoter which folds and forms β-hairpin structure in water.

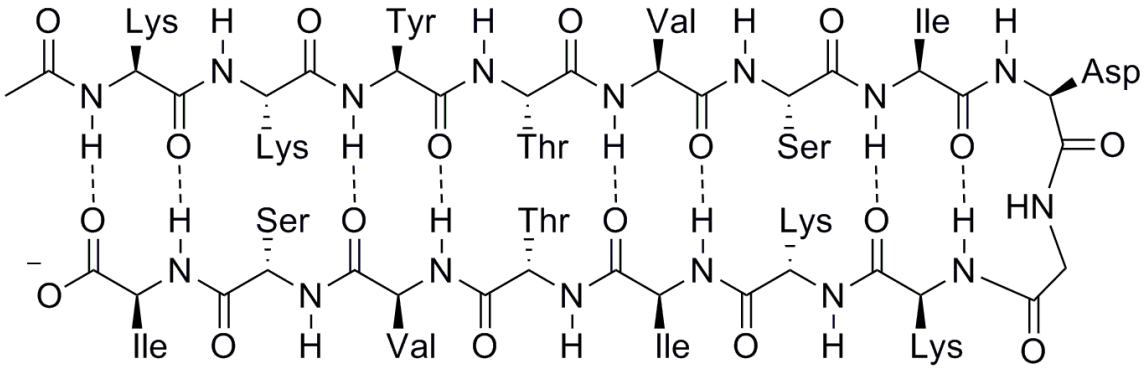

Fig. 1.5 16 amino acid residue peptide with Asn-Gly dipeptide template as turn promoter

Gellman and co-workers have utilized D-Pro-Gly template to form stable β-hairpins in aqueous solution (Fig. 1.6) (14). They found that the D-Pro-Gly template was better than Asn-Gly and use of D-amino acid increases the propensity of linear peptides to adopt the β-hairpin conformation.

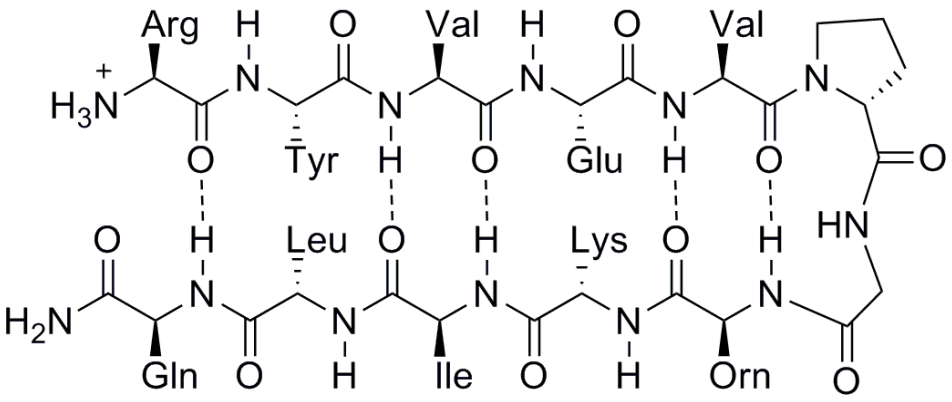

Fig. 1.6 12 amino acid residue Gellman peptide with D-Pro-Gly dipeptide template

It has been reported that achiral α-aminoisobutyric acid (Aib) forms a β-turn when used with D-α-amino acid or achiral α-amino acids. Balaram and co-workers have shown that peptides with the Aib-Xaa (Xaa= D-Ala, D-Val, D-Pro, D-Gly) dipeptide template adopts β-turn conformations in organic solvents (19). Hammer, Barany, Veglia and co-workers have shown that Aib-D-Ala and Aib-Gly adopts a β-turn conformation in water (20). They have compared the conformation of Gellman's peptide (Fig. 1.6) by replacing the D-Pro-Gly dipeptide β-turn inducer by Aib-D-Ala (Balram's dipeptide template), Aib-Gly and demonstrated by NMR studies that these peptides (Fig. 1.7) adopt type I' β-turn conformations in water.

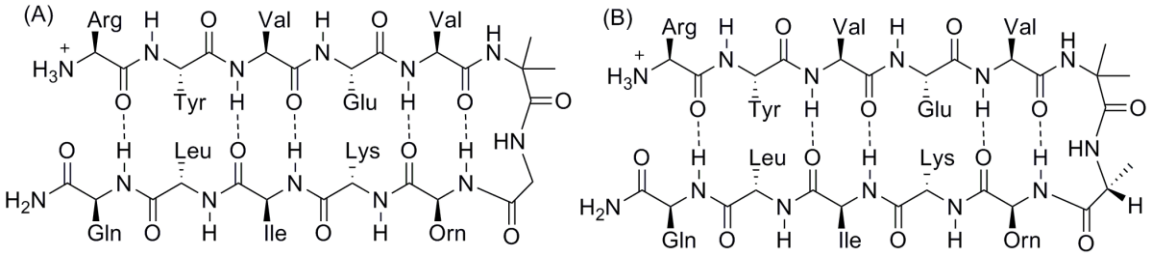

Fig. 1.7 Hammer's design of β-hairpin structures with (a) Aib-Gly and (B)Aib-D-Ala dipeptide units introduced as a β-turn inducer in Gellman's peptide sequence.

Balaram and co-workers have also reported several expanded β-turn mimics with D-Pro-Xaa (Xaa= β-,γ-, and δ- amino acid) dipeptide template (21). They have shown that peptides with α,β and α,γ residues at the turn adopt β-hairpin structures in methanol.

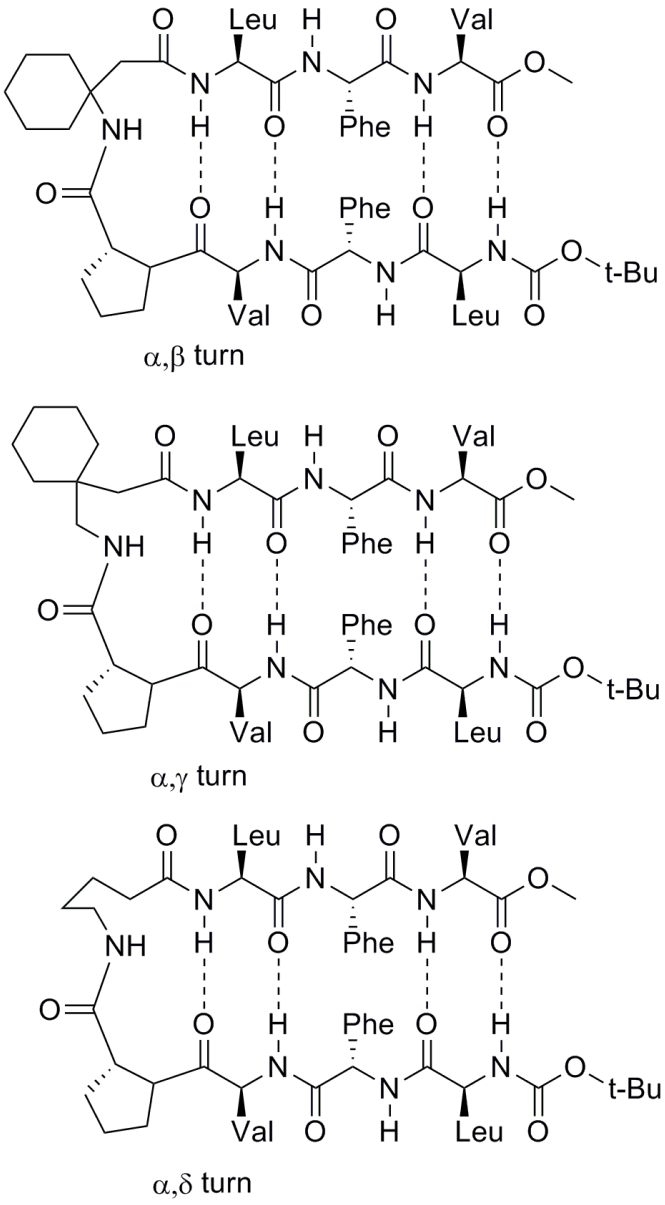

Fig. 1.8 Balaram's design of β-hairpins with extended α,β, α,γ and α,δ turn promoter.

Guan have reported a 1,4-disubstituted 1,2,3-triazole based β-turn promoter that induces β-hairpin structures for peptides in chloroform (22). Silvani have reported

tetrahydroisoquinoline based turn promoter to induce β-hairpin structures for smaller peptides in chloroform (23). Several research groups have reported new β-turn promoter that induce β-hairpin formation for linear peptides (24). Fig.1.10 lists some of the β-turn promoters reported for inducing β-sheet structure formation.

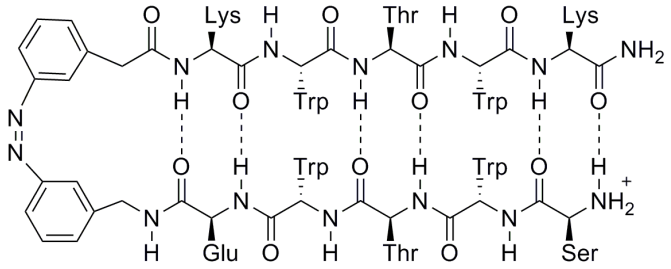

cis-azobenzene turn

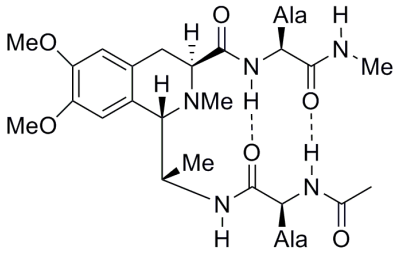

tetrahydroisoquinoline-based turn promoter

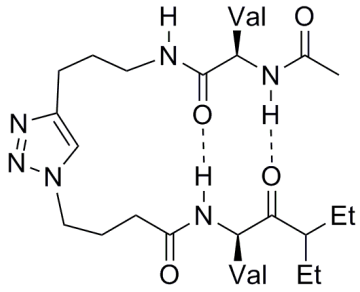

1,2,3-triazole based β- turn promoter

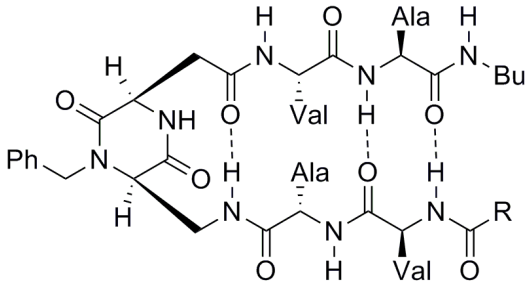

diketopiperazine based β- turn promoter

Fig. 1.9 Different β-turn promoters for inducing β-hairpin structures for linear peptides

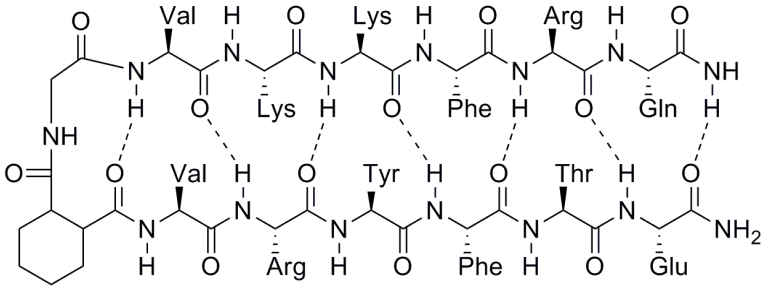

Fig. 1.10 Parallel β-sheet formation using CHDA-Gly diacid linker

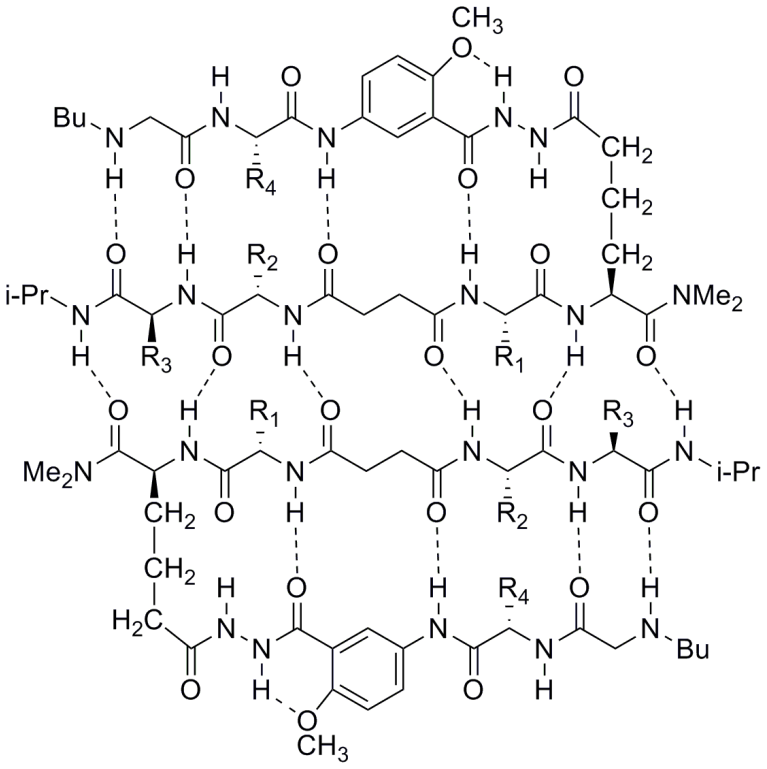

Fig. 1.11 Artificial β-sheets consisting of parallel β-sheet dimer with succinic diacid linkers and β-strand and β-turn mimic.

Recently Gellman and co-workers have reported the first diacid linker, CHDA-Gly turn promoter that promotes β-sheet formation in water (25). The CHDA-Gly turn promoter aligns two β-strands in parallel orientation as shown in Fig.1.10. Nowick and Levine have recently reported the synthesis of artificial β-sheets that dimerize through parallel interstrand β-sheet interations in chloroform (26). Parallel β-sheet interactions are important in the aggregation of peptides such as Aβ peptide aggregation observed in Alzheimer's disease.

1.3 Cyclic β-hairpin peptidomimetics

Generally the bioactivity of proteins arises from a small local segment of protein surface formed by these secondary structures, so molecules based on these structures would in principle serve as antagonists. Hence a simple approach for medicinal chemists

is to design drugs would mimic the β-sheet/strand regions of proteins recognized by other proteins or DNA. However the linear peptides have the disadvantages of being conformationally flexible, existing as random structures in aqueous solution. Linear peptides have low bioavailability, are easily susceptible to degradation by proteases and poor pharmacological properties. There are two strategies for solving these issues. The first approach involves restricting the degrees of freedom available to the linear peptide through cyclization to form macrocycles. Molecules which are conformationally preorganized or have fixed shape that can be recognized by a receptor will have higher affinity for that receptor due to a diminished loss of entropy for adopting that shape. Nature frequently uses cyclization technique to force peptides to adopt bioactive conformations. Naturally occurring peptide antibiotics such as gramicidin S and θ-defensin have been used and studied extensively for creating β-sheet structures. Cyclic peptides also cannot as readily be recognized by proteolytic enzymes.

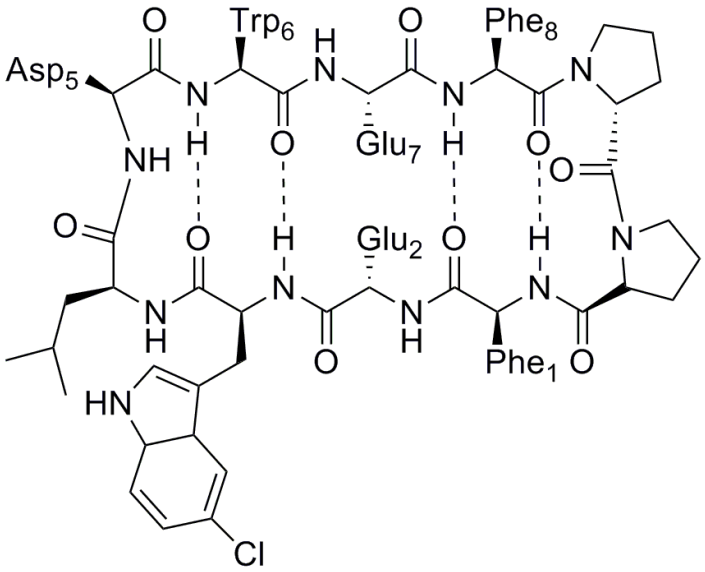

Fig. 1.12 Robinson's cyclic β-hairpin design as inhibitors of p53/MDM2 interaction.

As shown in Fig.1.12, Robinson and co-workers have utilized this approach in mimicking the α-helix of p53 with a cyclic β-hairpin to inhibit p53/MDM2 interaction. They have designed a cyclic beta-hairpin scaffold mounted on a D-Pro-L-Pro beta-turn promoter template that holds the side chains of phenylalanine and tryptophan residues in the correct relative positions, so that they could interact with their respective binding sites on MDM2 protein (27). This dipeptide template adopts a stable type II' β-turn that is ideal for inducing β-hairpin conformations. Kopple and co-workers have also used this template to design cyclic hexapeptides that exhibit β-sheet structures with type II' β-turn (28). This cyclic β-hairpin peptide design developed by Robinson has been explored to design inhibitors for several bimolecular targets. Shankaramma have synthesized a cyclic macrocylic β-hairpin mimetic of the cationic antimicrobial peptide Protegrin I by using the DPro-LPro dipeptide template (Fig.1.13) (29). Robinson & co-workers have also reported β-hairpin mimetics with a mixed peptide-peptoid backbone that have shown excellent antimicrobial activity (Fig.1.14) (30). They have also synthesized a series of cyclic β-hairpin mimetics based on a trypsin inhibitor from sunflower seeds (31).

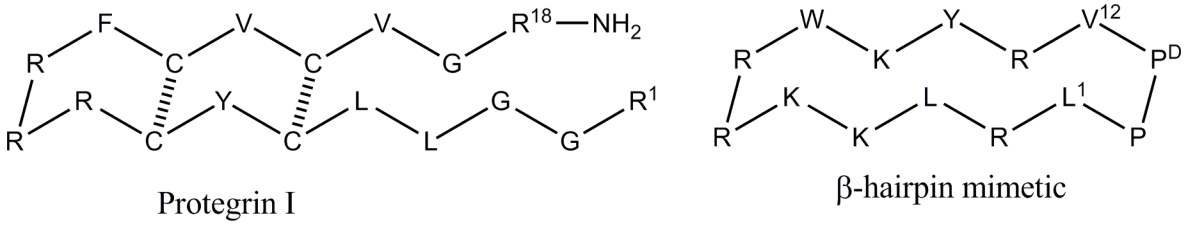

Fig. 1.13 β-hairpin mimetic of cationic antimicrobial peptide Protegrin I.

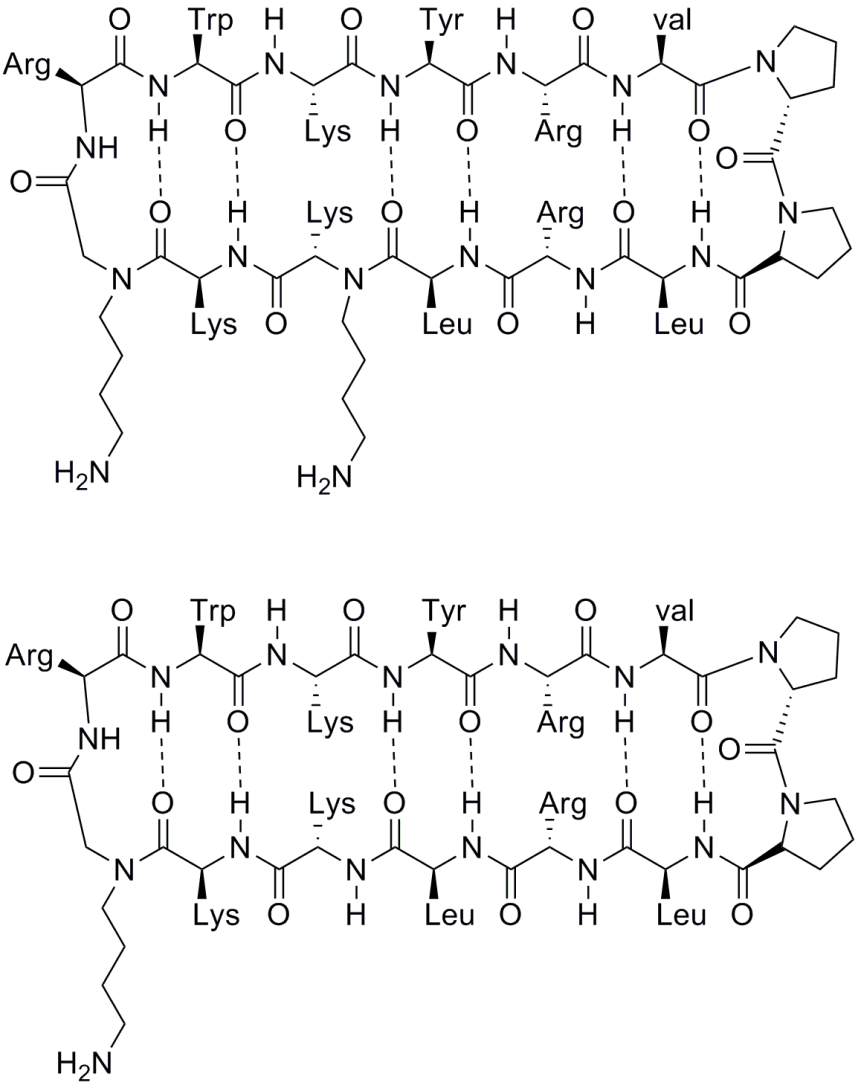

Fig. 1.14 β-hairpin mimetic of antimicrobial peptides with mixed peptide-peptoid backbone.

Nowick and co-workers have reported the synthesis of a triple-stranded artificial β-sheet that adopts β-sheet like conformation in organic solvents (Fig.1.15a)(32). Recently, they have developed several macrocyclic peptides containing a pentapeptide strand, β-strand mimic and two ornithine based β-turn promoters (33-34). These 42-membered cyclic peptides adopt β-sheet conformations in water (Fig.1.15b). Ornithine α-

amino groups provide a site that allows synthesis of bivalent peptides connected by a linker of suitable length (Fig.1.15c).

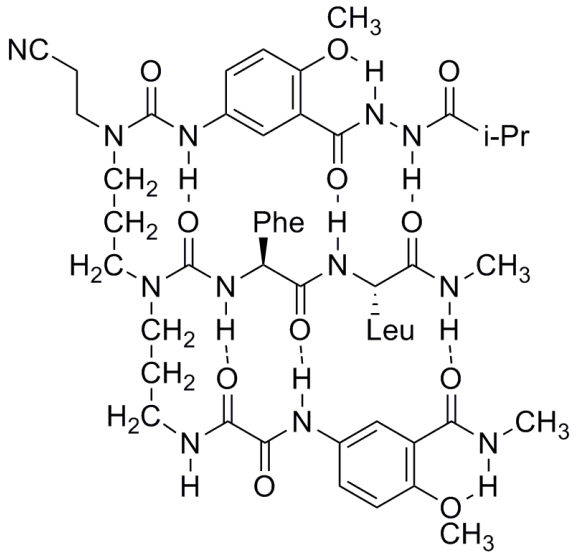

Fig. 1.15a Nowick's design for triple stranded artificial β-sheet.

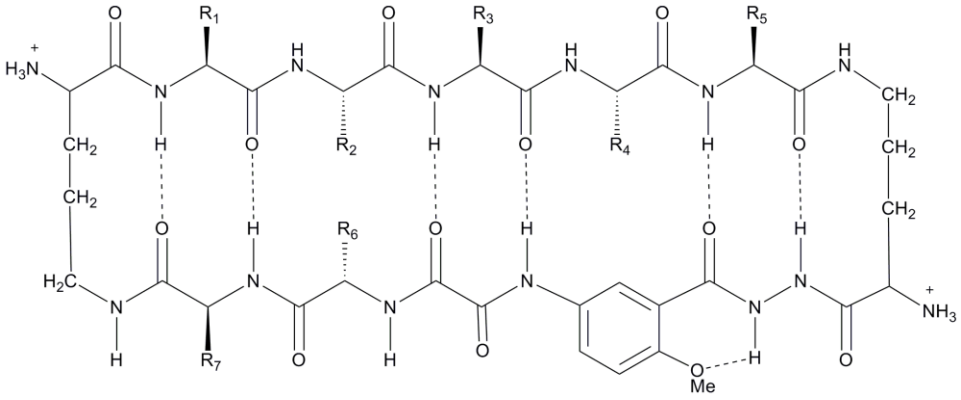

Fig. 1.15b 42-membered macrocyclic β-sheet peptide mimic containing β-strand & β-turn mimic.

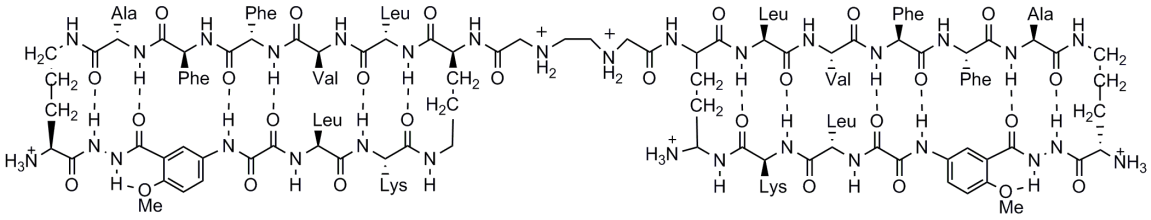

Fig. 1.15c Macrocyclic β-sheet peptide mimic containing β-strand & β-turn mimic.

As shown in Fig.1.16, the methylsulfonamido aminoethyl glycine and proline based ether-peptidomimetic amino acid have been designed and synthesized to induce β-sheet conformations for synthesizing cyclic β-haipin peptidomimetics to inhibit protein-protein interactions. The core residues mimicking the recognition surface are placed in the recognition strand whereas non-recognition strand residues can be modified to optimize the bioavailability and bioactivity of the designed peptide. N- to C- terminus cyclization of linear peptides to restrict the number of conformations available to the linear peptide increases the affinity of the cyclized peptide for its target. Peptidomimetics obtained after incorportation of methylsulfonamido aminoethyl glycine turn promoters are believed to adopt β-sheet extended structures. Replacement of the aminoethyl glycine turn promoter with the D-Proline derived ether-peptidomimetic turn promoter should further constrain the β-hairpin and increase its binding affinity for the target.

It is known through cited literature that adhesion of leukemia tumor cell to extracellular matrix components via integrin influences cell survival and inhibits drug induced apoptosis. Various research groups have made efforts to design drugs that mimic integrin recognition surfaces, inhibiting protein-protein interaction and thereby inducing cell death through apoptotic pathways. A linear 10 amino acid residue peptide referred as D-HYD1 has been reported to block adhesion of tumor cells to extracellular matrix. Our proposed strategy of cyclic β-hairpin peptidomimetics design that carries the core region of D-HYD1 in the recognition strand are expected to block adhesion of integrins (glycoprotein) to extracellular matrix components in prostate, multiple myeloma, and lung tumor cells.

(a)

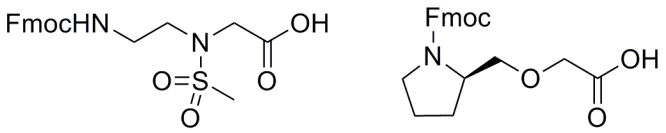

(b)

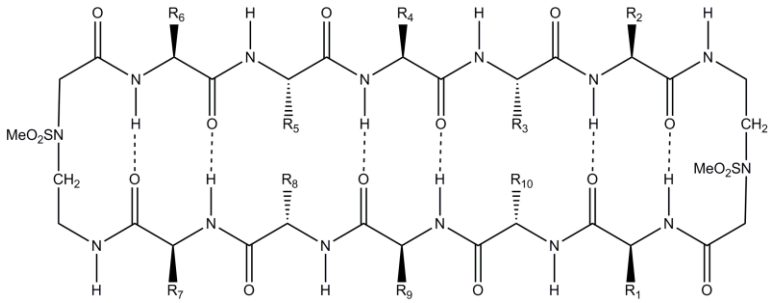

(c)

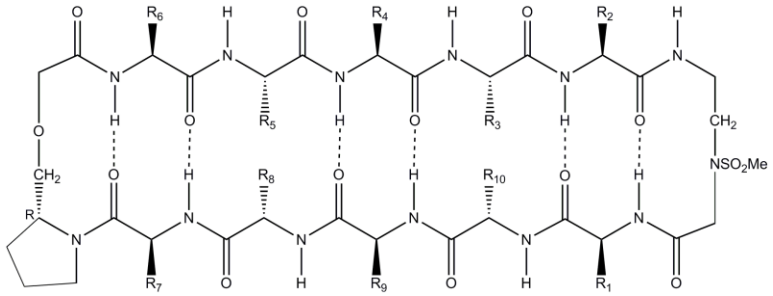

Fig. 1.16 (a) Designed methylsulfonamide aminoethyl glycine and proline based ether-peptidomimetic amino acid turn promoters (b) Proposed cyclic β-hairpin peptidomimetic with aminoethyl glycine turn promoter to inhibit adhesion of leukemia cells to extracellular matrix (c) Cyclic β-hairpin peptidomimetic with proline based ether-peptidomimetic amino acid turn promoter.

Another well known example is the p53/MDM2 protein-protein interactions observed in many cancers. Various research groups have developed drugs that mimic the p53 recognition surface that binds to MDM2 and inhibits the protein-protein interactions. Fig.1.17 shows the 9-membered cyclic peptide that has been designed to mimic the α-helix of p53 with cyclic β-hairpin to inhibit p53/MDM2 interaction.

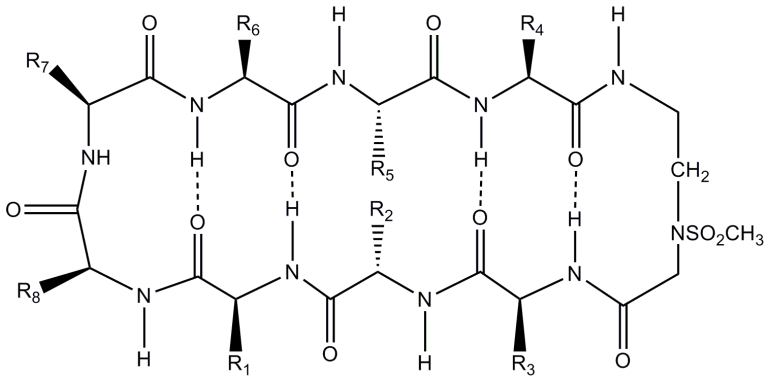

Fig. 1.17 Proposed cyclic β-hairpin mimetic of α-helix of p53.

In the last two decades many neurological disorders such as Alzheimer's disease (AD), Parkinson's disease, mad-cow disease, Huntington's disease and many other prion diseases have been to be caused by protein misfolding without any alteration of the protein 'primary structure'. It was found that aggregation or self-association of amyloid fibrils, consisting of 40-42 amino acid Aβ peptides formed insoluble β-sheet plaques that were responsible for causing AD. Many researchers have shown that the hydrophobic core region (residues 17-21) of Aβ peptide is critical for fibril formation. Based on these reports we propose the design and synthesis of cyclic β-hairpin peptides that bind specifically to this hydrophobic region and prevent abeta β-sheet aggregation (Fig.1.18). The recognition strand of the designed cyclic peptide would interact with the growing Aβ fibril whereas the non-recognition strand would have residues that would inhibit aggregation from the other face of the assembly.

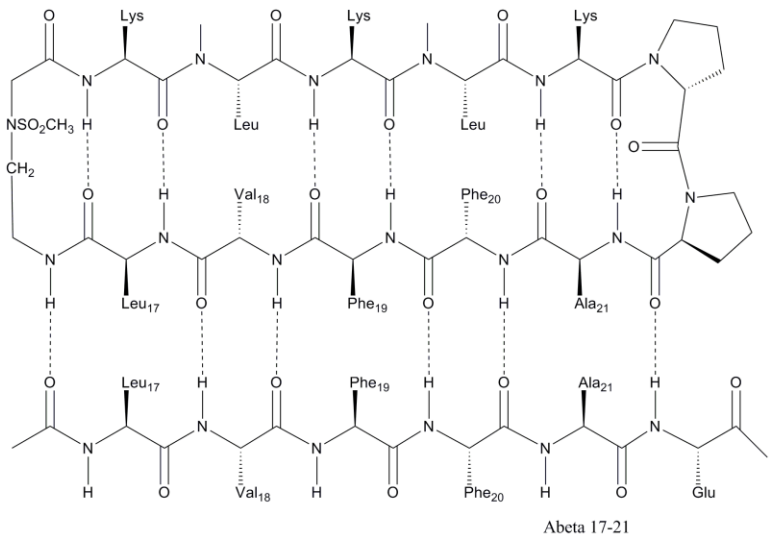

Fig. 1.18 Cyclic β-hairpin peptidomimetic targeting hydrophobic core region (17-21) of Aβ peptide.

1.4 Solid Phase Peptide Synthesis

In 1959, Merrifield conceived the idea that if peptide is bound to an insoluble support then any unreacted reagents left at the end of each reaction step can be simply removed by general solvent wash, thereby reducing the time required for purification and synthesis of the desired compound. This idea led him to pioneer a new field in chemistry called solid-phase synthesis for which he was awarded Nobel Prize in 1984. Solid-phase synthesis is widely used by chemist to carry out chemical reactions on a solid support to prepare libraries of organic compounds, oligomers and complex molecules that are difficult to synthesize using solution-phase synthesis. During the last six decades, Solid-Phase Peptide Synthesis (SPPS) has evolved as the primary route for synthesizing a great diversity of peptides and proteins. The basic concept of synthesizing peptides using SPPS is described in Fig.1.19. The peptide chain is assembled on polymeric resin solid support by stepwise addition of α-amino acid residues in the C to N direction. Fmoc and Boc protecting group strategies are widely used for synthesizing peptides on resin. Fmoc

chemistry has been widely adopted for most solid-phase peptide synthesis since this strategy has been shown to be more reliable. The greatest advantage of employing Fmoc SPPS strategy is that it is chemically compatible with most of the commercially available peptide synthesizers. The use of extremely hazardous and corrosive chemicals for deprotection step in Boc SPPS limits its application on an automated synthesizer.

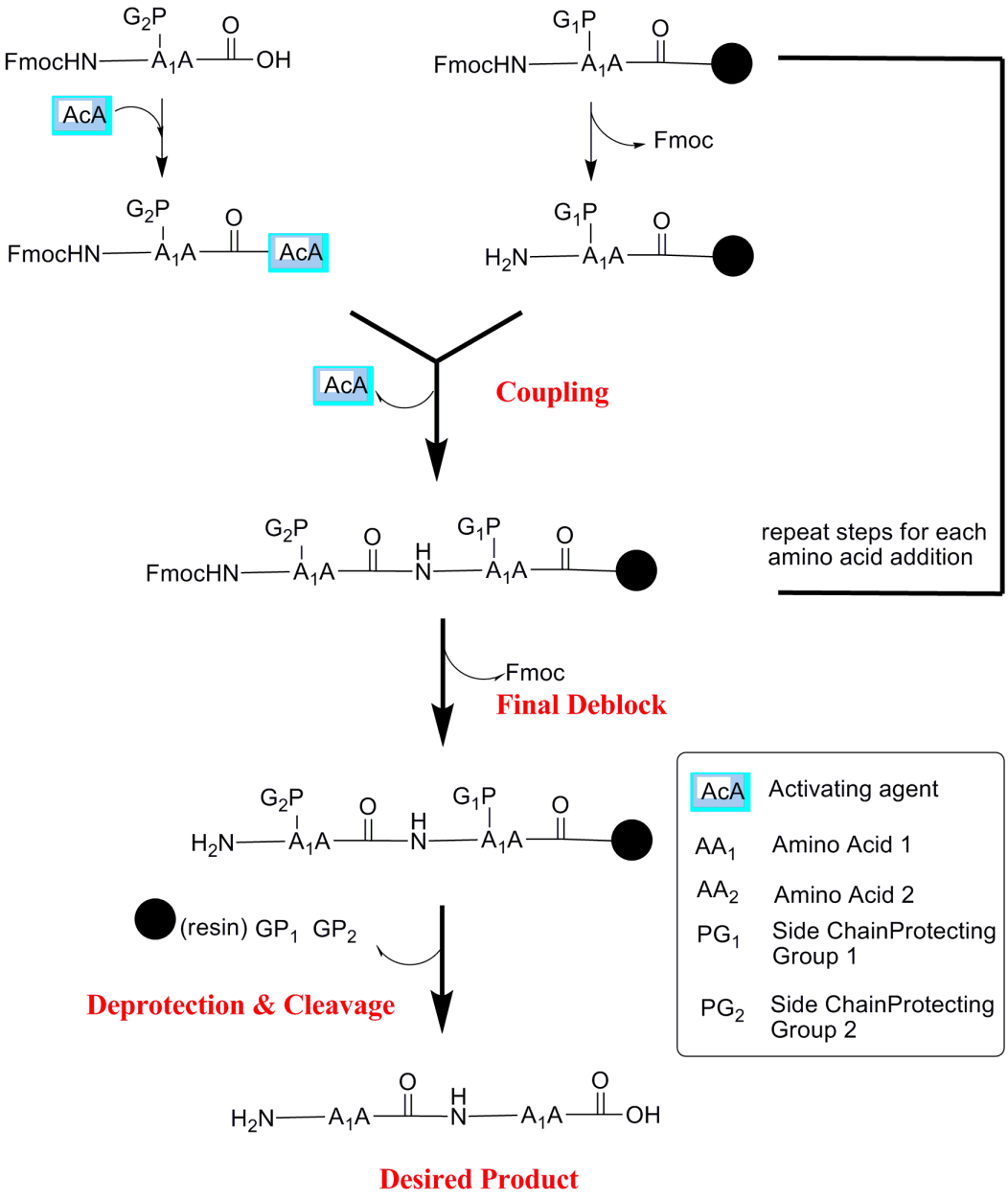

Fig. 1.19 General protocol for solid-phase peptide synthesis.

After base treatment, the peptide is washed several times with a mixture of solvents and then a mixture consisting of an activated amino acid and base is added to the peptide in the reactor to couple the next amino acid. There are four different kinds of coupling agents used for carboxyl activation in SPPS:

1. Carbodiimides
2. Symmetrical anhydrides
3. Activated Esters
4. Uronium based coupling reagents

Carbodiimides are widely preferred activation reagents (35). These reagents produce insoluble ureas in some of the solvents that are used in SPPS and thus interfere in peptide purification. Symmetrical anhydrides can be generated in situ from two equivalents of amino acid and one equivalent of carbodiimide reagent. The generated urea can be filtered off and the synthesized coupling agents can then be used for coupling. The most commonly used activated esters for peptide coupling are those derived from pentafluorophenol (HOPfp) and HODhbt (36). During last three decades, coupling reagents based on phosphonium and uronium salts have been widely used for synthesizing peptides. These in situ activation reagents are highly efficient in peptide couplings and reduces racemization or side-product formation. Fig.1.20 lists some of the common activating agents used. Other coupling reagents used for peptide coupling include amino acid halides and azides (37, 38). The activated acids can be prepared and purified prior to coupling or can be generated in situ be addition of reagents such as cyanuric chloride or fluoride to give acid chlorides or fluorides. Diphenyl phosphorylazide directly converts carboxyl groups to an acylazide intermediate.

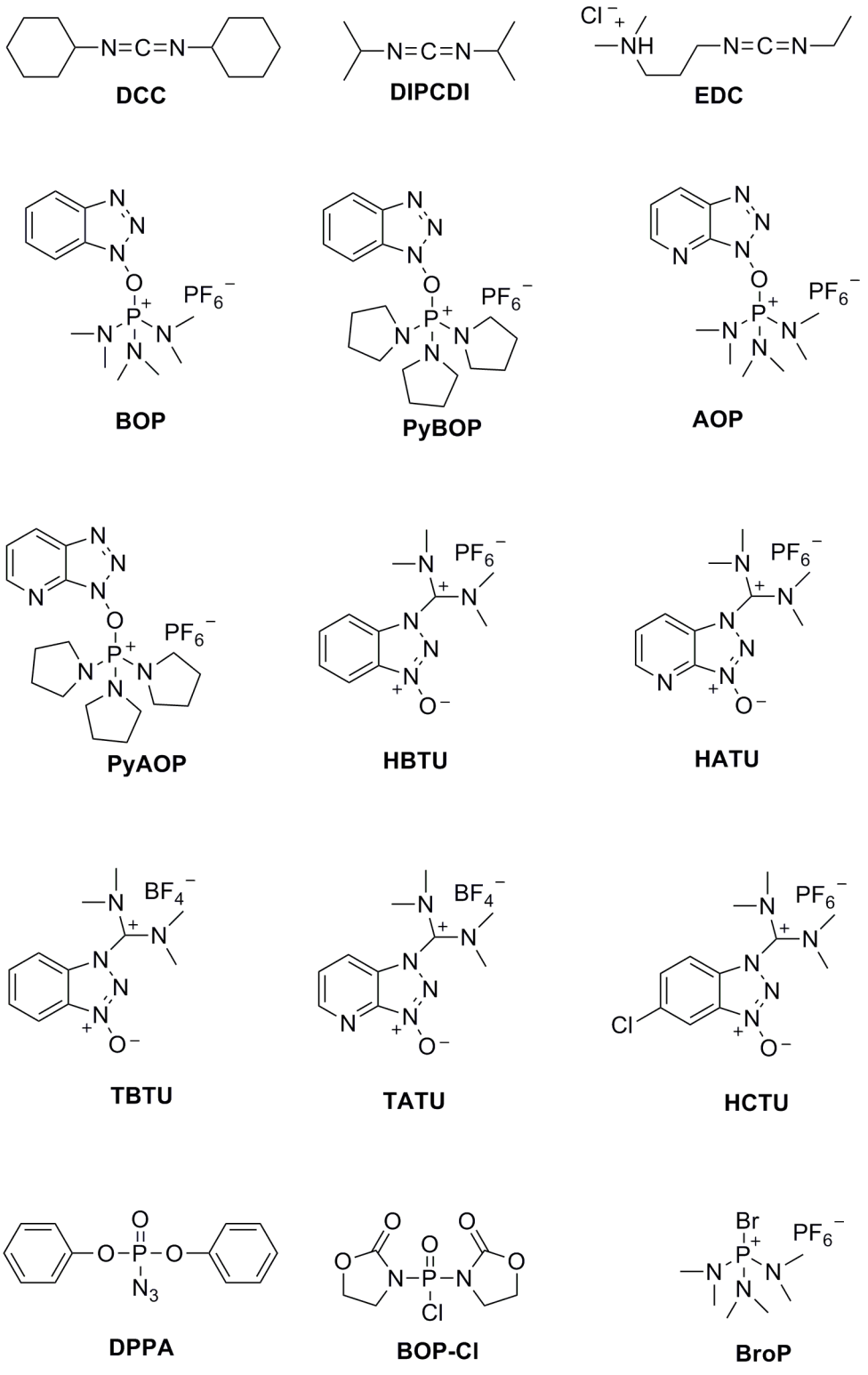

Fig. 1.20 Common coupling reagents used in SPPS.

All cyclic β-hairpin peptidomimetics designed for the different targets (chapter 2, 3 &4) will be synthesized on the Symphony peptide synthesizer, Protein Technologies Instrument, using Fmoc SPPS strategy. Typically, a linear precursor will be assembled on solid support, 2-Chlorotrityl chloride resin, and then macrocyclized and deprotected in solution phase. SPPS strategy has also been adopted to synthesize PNA oligomers which is described in detail in chapter five.

1.5 Cysteine based Peptide Nucleic Acid (CPNA)

PNA (Peptide Nucleic Acids) are DNA mimics in which the deoxyribose phosphate diester backbone is replaced by a pseudo-peptide backbone while the four natural nucleobases are retained. PNA consists of repeating N-(2-aminoethyl)-glycine units in which the nucleobase is attached to the glycine nitrogen via a methylene carbonyl linker. The acyclic, achiral and neutral backbone makes PNA set apart from DNA. The neutral backbone of PNA allows stronger binding between complementary PNA/DNA strands than between complementary DNA/DNA strands. PNAs have been demonstrated as potential candidates for gene-targeting drugs but some disadvantages have limited its applications. These include low cellular uptake caused by poor cell membrane permeability and poor aqueous solubility. To increase cellular uptake we propose the design of novel CPNA (cysteine based PNA) scaffolds by introducing positive charge species attached to the cysteine side chains. An attempt to synthesize cysteine based Peptide nucleic acid (CPNA) monomers and oligomers containing all four nucleobases is described in chapter five.

1.6 Structural Analysis of Peptides

The 3D structural analysis of peptides and proteins can be carried out by several experimental techniques such as X-ray crystallography, solution nuclear magnetic resonance (NMR) spectroscopy, circular dichroism (CD) spectroscopy and Fourier transform infrared spectroscopy (FTIR). X-ray analysis is a widely preferred technique for structural elucidation of peptides. Solution NMR spectroscopy is another powerful tool used since the last three decades. The NMR input for conformational studies of peptides depends on NOE (nuclear Overhauser effects) and coupling constants. NOE studies detect the interactions involved by measuring interproton distances of 5 Å or less while the coupling constants give information about torsion angles. The whole set of NOE constraints is then plugged in computational software and an energy minimization experiment is carried out to search for optimized solution structures of peptides and proteins.

Circular Dichroism (CD) is another important technique for determining the conformations of peptides and proteins in solution. CD spectroscopy measures the difference in absorbance of right- and left-circularly polarized light by a substance. Bands in the far UV region of CD spectra (260-190 nm) are analyzed for the different secondary structural of peptides and proteins i.e. alpha helix, parallel and antiparallel beta sheet, beta turn, etc. Fig.1.21. shows various secondary structural elements in CD spectra of polypeptides in solution (39). All cyclic β-hairpin peptides synthesized will be characterized for their secondary structures using CD and NMR experiments.

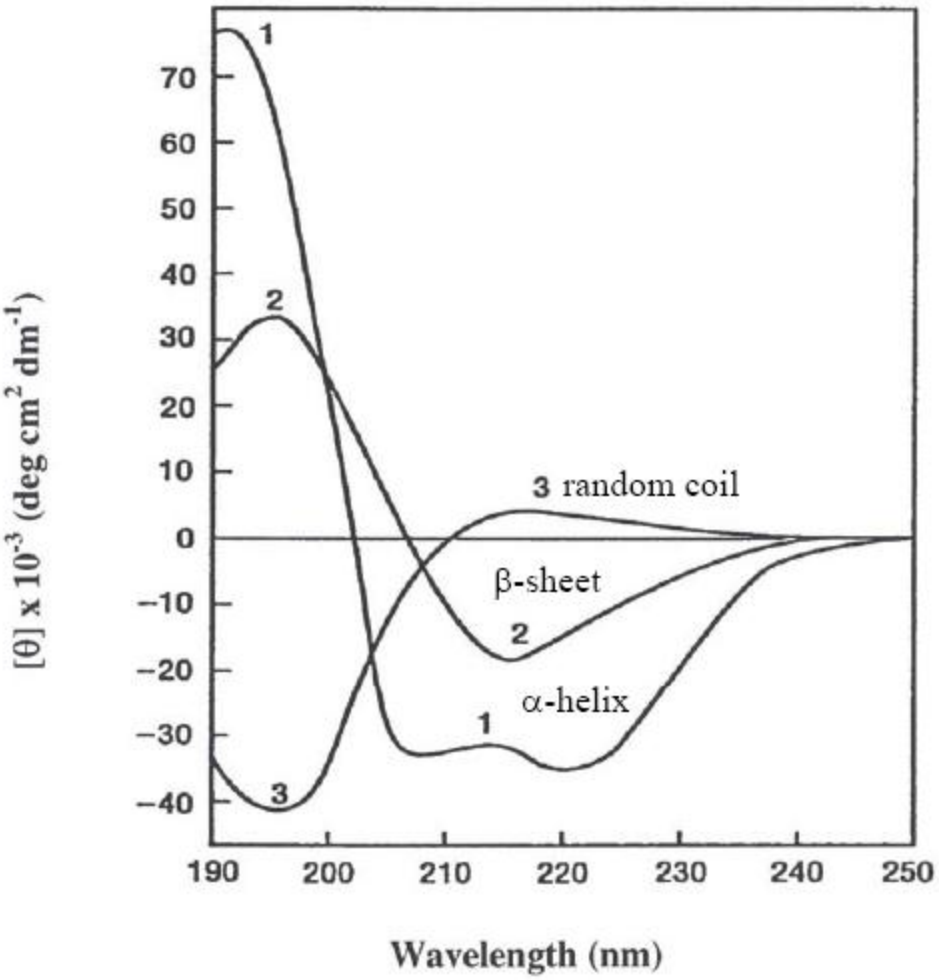

Fig. 1.21 CD spectra of secondary structural elements in peptides and proteins.

FTIR technique is used for examining peptides that shows self-association or aggregation behavior. In IR spectra each compounds has its own set of absorption bands. In FTIR, characterstic bands for peptides and proteins include Amide I and Amide II arising from the amide bond (40). The stretching vibrations of C=O leads to Amide I bands where bending vibrations of the N-H bonds leads to amide II bands. The location of both amide I and amide II bands are very sensitive to the secondary structure of peptides and proteins.

1.7 References

1. Patrick, G. L., *An Introduction to Medicinal Chemistry, 2nd Edition*. Oxford University Press, New York, 2005; pp.24.

2. Creighton, T. E. *Proteins: Structure and Molecular Properties*; 2nd ed; W. H.Freeman and Co.: New York, 1993; pp. 65-68.

3. Walton, A. G. *Polypeptides and Protein Structure*; Elsevier: New York, 1981; pp. 49-55.

4. Pauling, L.; Corey, R. B., Configurations of polypeptide chains with favored orientations around single bonds: two new pleated sheets. *Proc. Natl. Acad. Sci. U. S. A.* **1951,** *37*, 729-40.

5. Pauling, L.; Corey, R. B.; Branson, H. R., The structure of proteins: two hydrogen-bonded helical configurations of the polypeptide chain. *Proc. Natl. Acad. Sci. U. S. A.* **1951,** *37*, 205-11.

6. Dyson, H. J.; Rance, M.; Houghten, R. A.; Lerner, R. A.; Wright, P. E., Folding of immunogenic peptide fragments of proteins in water solution. I. Sequence requirements for the formation of a reverse turn. *J. Mol. Biol.* **1988,** *201* (1), 161-200.

7. Hutchinson, E. G.; Thornton, J. M., A revised set of potentials for Î²-turn formation in proteins. *Protein Sci.* **1994,** *3* (12), 2207-16.

8. Sibanda, B. L.; Blundell, T. L.; Thornton, J. M., Conformation of beta-hairpins in protein structures. A systematic classification with applications to modelling by homology, electron density fitting and protein engineering. *J. Mol. Biol.* **1989,** *206* (4), 759-77.

9. Blanco, F. J.; Jimenez, M. A.; Herranz, J.; Rico, M.; Santoro, J.; Nieto, J. L., NMR evidence of a short linear peptide that folds into a beta -hairpin in aqueous solution. *J. Am. Chem. Soc.* **1993,** *115* (13), 5887-8.

10. Blanco, F. J.; Rivas, G.; Serrano, L., A short linear peptide that folds into a native stable beta-hairpin in aqueous solution. *Nat Struct Biol* **1994,** *1* (9), 584-90.

11. Searle, M. S.; Williams, D. H.; Packman, L. C., A short linear peptide derived from the N-terminal sequence of ubiquitin folds into a water-stable non-native beta-hairpin. *Nat Struct Biol* **1995,** *2* (11), 999-1006.

12. Sibanda, B. L.; Thornton, J. M., Beta-hairpin families in globular proteins. *Nature* **1985,** *316* (6024), 170-4.

13. Ramirez-Alvarado, M.; Blanco Francisco, J.; Serrano, L., De novo design and structural analysis of a model beta -hairpin peptide system. *Nat Struct Biol* **1996,** *3* (7), 604-612.

14. Gellman, S. H., Minimal model systems for beta sheet secondary structure in proteins. *Curr. Opin. Chem. Biol.* **1998,** *2* (6), 717-725.

15. Searle, M. S., Peptide models of protein beta -sheets: design, folding and insights into stabilising weak interactions. *J. Chem. Soc., Perkin Trans. 2* **2001,** (7), 1011-1020.

16. Venkatraman, J.; Shankaramma, S. C.; Balaram, P., Design of Folded Peptides. *Chem. Rev. (Washington, D. C.)* **2001,** *101* (10), 3131-3152.

17. Searle, M. S.; Ciani, B., Design of beta -sheet systems for understanding the thermodynamics and kinetics of protein folding. *Curr. Opin. Struct. Biol.* **2004,** *14* (4), 458-464.

18. Hughes, R. M.; Waters, M. L., Model systems for beta -hairpins and beta -sheets. *Curr. Opin. Struct. Biol.* **2006,** *16* (4), 514-524.

19. Aravinda, S.; Shamala, N.; Rajkishore, R.; Gopi, H. N.; Balaram, P., A crystalline beta -hairpin peptide nucleated by a type I' Aib-D-Ala beta -turn: evidence for cross-strand aromatic interactions. *Angew. Chem., Int. Ed.* **2002,** *41* (20), 3863-3865.

20. Masterson, L. R.; Etienne, M. A.; Porcelli, F.; Barany, G.; Hammer, R. P.; Veglia, G., Nonstereogenic alpha -aminoisobutyryl-glycyl dipeptidyl unit nucleates type I' beta -turn in linear peptides in aqueous solution. *Biopolymers* **2007,** *88* (5), 746-753.

21. Rai, R.; Vasudev, P. G.; Ananda, K.; Raghothama, S.; Shamala, N.; Karle, I. L.; Balaram, P., Hybrid peptides: expanding the beta turn in peptide hairpins by the insertion of beta -, gamma -, and delta -residues. *Chem.--Eur. J.* **2007,** *13* (20), 5917-5926.

22. Oh, K.; Guan, Z., A convergent synthesis of new beta -turn mimics by click chemistry. *Chem. Commun. (Cambridge, U. K.)* **2006,** (29), 3069-3071.

23. Lesma, G.; Meschini, E.; Recca, T.; Sacchetti, A.; Silvani, A., Synthesis of tetrahydroisoquinoline-based pseudopeptides and their characterization as suitable reverse turn mimetics. *Tetrahedron* **2007,** *63* (25), 5567-5578.

24. Ressurreicao, A. S. M.; Bordessa, A.; Civera, M.; Belvisi, L.; Gennari, C.; Piarulli, U., Synthesis and Conformational Studies of Peptidomimetics Containing a New Bifunctional Diketopiperazine Scaffold Acting as a beta -Hairpin Inducer. *J. Org. Chem.* **2008,** *73* (2), 652-660.

25. Freire, F.; Fisk, J. D.; Peoples, A. J.; Ivancic, M.; Guzei, I. A.; Gellman, S. H., Diacid Linkers That Promote Parallel beta -Sheet Secondary Structure in Water. *J. Am. Chem. Soc.* **2008,** *130* (25), 7839-7841.

26. Levin, S.; Nowick, J. S., An Artificial beta -Sheet That Dimerizes through Parallel beta -Sheet Interactions. *J. Am. Chem. Soc.* **2007,** *129* (43), 13043-13048.

27. Fasan, R.; Dias, R. L. A.; Moehle, K.; Zerbe, O.; Vrijbloed, J. W.; Obrecht, D.; Robinson, J. A., Using a beta -hairpin to mimic an alpha -helix: Cyclic peptidomimetic inhibitors of the p53-HDM2 protein-protein interaction. *Angew. Chem., Int. Ed.* **2004,** *43* (16), 2109-2112.

28. Bean, J. W.; Kopple, K. D.; Peishoff, C. E., Conformational analysis of cyclic hexapeptides containing the D-Pro-L-Pro sequence to fix beta -turn positions. *J. Am. Chem. Soc.* **1992,** *114* (13), 5328-34.

29. Shankaramma, S. C.; Athanassiou, Z.; Zerbe, O.; Moehle, K.; Mouton, C.; Bernardini, F.; Vrijbloed, J. W.; Obrecht, D.; Robinson, J. A., Macrocyclic hairpin mimetics of the cationic antimicrobial peptide protegrin I: a new family of broad-spectrum antibiotics. *ChemBioChem* **2002,** *3* (11), 1126-1133.

30. Shankaramma, S. C.; Moehle, K.; James, S.; Vrijbloed, J. W.; Obrecht, D.; Robinson, J. A., A family of macrocyclic antibiotics with a mixed peptide-peptoid beta -hairpin backbone conformation. *Chem. Commun. (Cambridge, U. K.)* **2003,** (15), 1842-1843.

31. Descours, A.; Moehle, K.; Renard, A.; Robinson, J. A., A new family of beta -hairpin mimetics based on a trypsin inhibitor from sunflower seeds. *ChemBioChem* **2002,** *3* (4), 318-323.

32. Nowick, J. S.; Cary, J. M.; Tsai, J. H., A Triply Templated Artificial beta -Sheet. *J. Am. Chem. Soc.* **2001,** *123* (22), 5176-5180.

33. Woods, R. J.; Brower, J. O.; Castellanos, E.; Hashemzadeh, M.; Khakshoor, O.; Russu, W. A.; Nowick, J. S., Cyclic Modular beta -Sheets. *J. Am. Chem. Soc.* **2007,** *129* (9), 2548-2558.

34. Khakshoor, O.; Demeler, B.; Nowick, J. S., Macrocyclic beta -Sheet Peptides That Mimic Protein Quaternary Structure through Intermolecular beta -Sheet Interactions. *J. Am. Chem. Soc.* **2007,** *129* (17), 5558-5569.

35. Barany, G.; Merrifield, R.B. *The Peptides: Analysis, Synthesis, Biology*; Gross, E., Meienhofer, J. Eds.; Academic Press: New York, NY, 1979; Vol. 2.

36. Kovacs, J.; Kisfaludy, L.; Ceprini, M. Q., Optical purity of peptide active esters prepared by N,N'-dicyclohexylcarbodiimide and complexes of N,N'-

dicyclohexylcarbodiimide-pentachlorophenol and N,N'-dicyclohexylcarbodiimide-pentafluorophenol. *J. Am. Chem. Soc.* **1967,** *89* (1), 183-4.

37. Carpino, L. A.; Beyermann, M.; Wenschuh, H.; Bienert; Michael, Peptide Synthesis via Amino Acid Halides. *Acc. Chem. Res.* **1996,** *29* (6), 268-274.

38. Ninomiya, K.; Shioiri, T.; Yamada, S., Amino acids and peptides. XII. Phosphorus in organic synthesis. VIII. Reaction of malonic acid half esters with diphenyl phosphorazidate. *Chem. Pharm. Bull.* **1974,** *22* (6), 1398-1404.

39. Greenfield, N. J.; Fasman, G. D., Computed circular dichroism spectra for the evaluation of protein conformation. *Biochemistry* **1969,** *8* (10), 4108-16.

40. Haris, P. I.; Chapman, D., The conformational analysis of peptides using Fourier transform IR spectroscopy. *Biopolymers* **1995,** *37* (4), 251-63.

CHAPTER TWO:

NOVEL CYCLIC III PEPTIDES TARGETING INTEGRIN MEDIATED CELL ADHESION IN MULTIPLE MYELOMA

2.1 Introduction

Multiple Myeloma (MM) is an incurable malignancy which frequently exhibits relapse due to unsuccessful elimination of minimal residual disease (MRD). Current standard chemotherapeutic treatments that target apoptotic cell death pathways have proven to be unsuccessful in treating this disease, due to the strong multi-drug resistance (MDR) emergence by tumor cells (1). MRD is found in the bone marrow indicating that the bone marrow microenvironment is essential for tumor cell survival (2). The bone marrow is rich in extracellular matrices. Hazlehurst and co-workers have shown that adhesion of leukemia and multiple myeloma cells to the extracellular matrix component fibronectin (FN) influences cell survival and inhibits drug induced apoptotic cell death (3-9). Various research groups have targeted integrin mediated cell adhesion to increase the efficacy of standard cytotoxic drugs that predominantly use the apoptotic cell death pathways. Cell deaths in mammals have been reported to occur mainly via three different pathways. Type I cell death or apoptosis usually occurs with alteration of mitochondrial membrane potential, followed by subsequent release of cytochrome C and activation of caspases, ultimately leading to shut down of cell machinery. Type II cell death or autophagy is independent of activation of caspases and is usually observed with the

formation of double membrane vesicles (autophagosomes) (10, 11). It is usually the default cell death pathway and may occur when apoptotic mechanisms fails. Type III cell death pathway or necrosis is seen with rupture of plasma membrane, swelling of cytoplasmic organelles, decrease in ATP levels and an increase in reactive oxygen species (ROS) (12). The majority of cancer cells follow the apoptotic pathway to induce cell death. Hence, the majority of current standard chemotherapeutic agents are developed to induce apoptosis in tumor cells. With the emergence of multi-drug resistance of tumor cells for currently used standard cytotoxic drugs that follow the apoptotic pathway, development of cytotoxic drugs that follow an alternative cell death pathway would be an effective strategy in tumor cell killing.

Using combinatorial peptide libraries and a functional binding assay, Kit Lam and Anne Cress and co-workers were able to identify several peptides that inhibited β1 integrin mediated adhesion of prostate cancer cells to fibronectin, laminin and collagen IV (13). They identified a synthetic all D-amino acid peptide referred as HYD1(kikmviswkg) that blocks binding of epithelial prostate carcinoma cells to extracellular matrix components (14,15). Hazlehurst and co-workers have shown that use of HYD1 peptide in blocking β1 integrin mediated adhesion increased the efficacy of standard cytotoxic drugs used to treat Multiple myeloma (16). HYD1 induces cell death in multiple myeloma as a single agent in vitro and in vivo. HYD1 treatment did not trigger the activation of caspases nor did it induce DNA fragmentation. HYD1 treatment seemed to cause necrotic cell death as shown by loss of mitochondrial membrane potential, loss of cellular ATP and an increase in ROS production.

Hazlehurst and co-workers performed truncation studies on the C and N terminus and identified MVISW as a likely core region of linear D-HYD1 responsible for biological activity. They have demonstrated that HYD1 has an IC_{50} value 33 μM when assayed for H929 multiple myeloma tumor cells using FACS analysis for cell death. It is well known that any molecule which is conformationally preorganized or fixed into a shape which can be recognized by a target will have higher affinity for that target, at the expense of entropy loss for adopting that conformation (17). Cyclization of linear peptides to form cyclic peptidomimetics, imposes constraints in the number of conformations available to the linear peptide. The constraint further stabilizes the bound conformation of the peptide. Also, cyclization of the linear peptide to form cyclic peptides makes the amide bonds less recognizable by various proteases.

Based on the structural information of D-HYD1 peptide, we proposed the design and synthesis of novel cyclic III (Integrin Interaction Inhibitors) peptide analogs for optimizing the efficacy of the parent peptide (Fig.2.1). The introduction of a novel beta turn promoter in the cyclic peptide design will further constrain the recognition portion of cyclic peptide specifically into an extended or beta-sheet like conformation. All cyclic peptides were more potent as compared to linear D-HYD1 when assayed using TOPRO3 protocol. The alanine scan of the recognition strand carrying core residues has also been investigated to determine critical residues responsible for bioactivity of cyclic peptides. Furthermore we have also proved that all cyclic peptidomimetics adopt beta sheet conformation as confirmed by circular dichroism and NMR studies.

(A) Cyclic D-HYD1 2.18

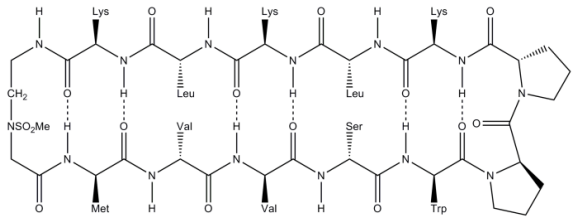

(B) Cyclic III Peptide 2.17

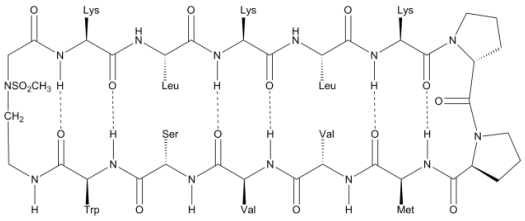

(C) Cyclic III Peptide 2.1

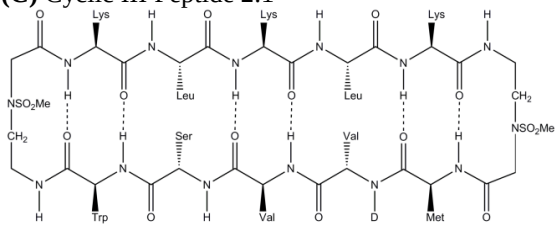

(D) Cyclic III Peptide 2.7

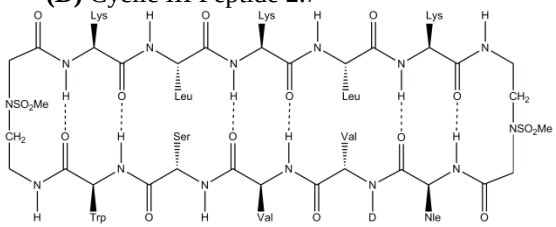

(E) Retro-inverso Cyclic III Peptide 2.10

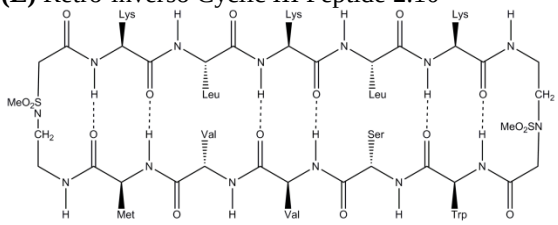

Fig. 2.1 Proposed cyclic III peptide analogs of linear HYD1 peptide with L-WSVVM and D-MVVSW as key residues on recognition strand.

2.2 Results & Discussion

2.2.1 Peptide design

Hazlehurst and co-workers have systematically carried out truncated N and C terminus studies and identified MVISW as the likely core region of linear D-HYD1 required for biological activity. Using this information and the finding that valine for isoleucine replacement gave a more active D-HYD1 analog, we developed a cyclized version of D-HYD1 that is designed to display the core sequence (MVVSW) in the recognition strand and (KLKLK) as the non-recognition strand. The designed cyclic peptidomimetic exhibited an extended or beta-sheet-like conformation (Fig. 2.1). N- to C-terminus cyclization of linear peptides to restrict the number of conformations available to the linear peptide increases the affinity of the cyclized peptide for its target when the constraint stabilizes the bound conformation of the peptide. As a starting point for the rational design, we did energy minimization studies on similar designed beta-hairpin cyclic peptides for inhibiting abeta fibrillogenesis (Fig. 2.2 & Fig. 2.3). Energy minimizations were carried out by keeping all backbone atoms fixed to refine the spatial position of side chain residues. Energy minimization studies suggested that introduction of the novel turn promoter and the Robinson template (D-Pro-L-Pro) at the turns gave stable hairpin peptide with all of the internal H-bonds intact. Table 2.1. depicts the energy minization values for different turn promoters used in designing these stable cyclic peptides. Based on energy minimization studies data, we synthesized cyclic D-HYD1 with the methylsulfonamide aminoethyl glycine as turn promoters. As per the cell inhibition assay TOPRO 3, the cyclic D-HYD1 peptide was found to be twice as active as linear D-HYD1.

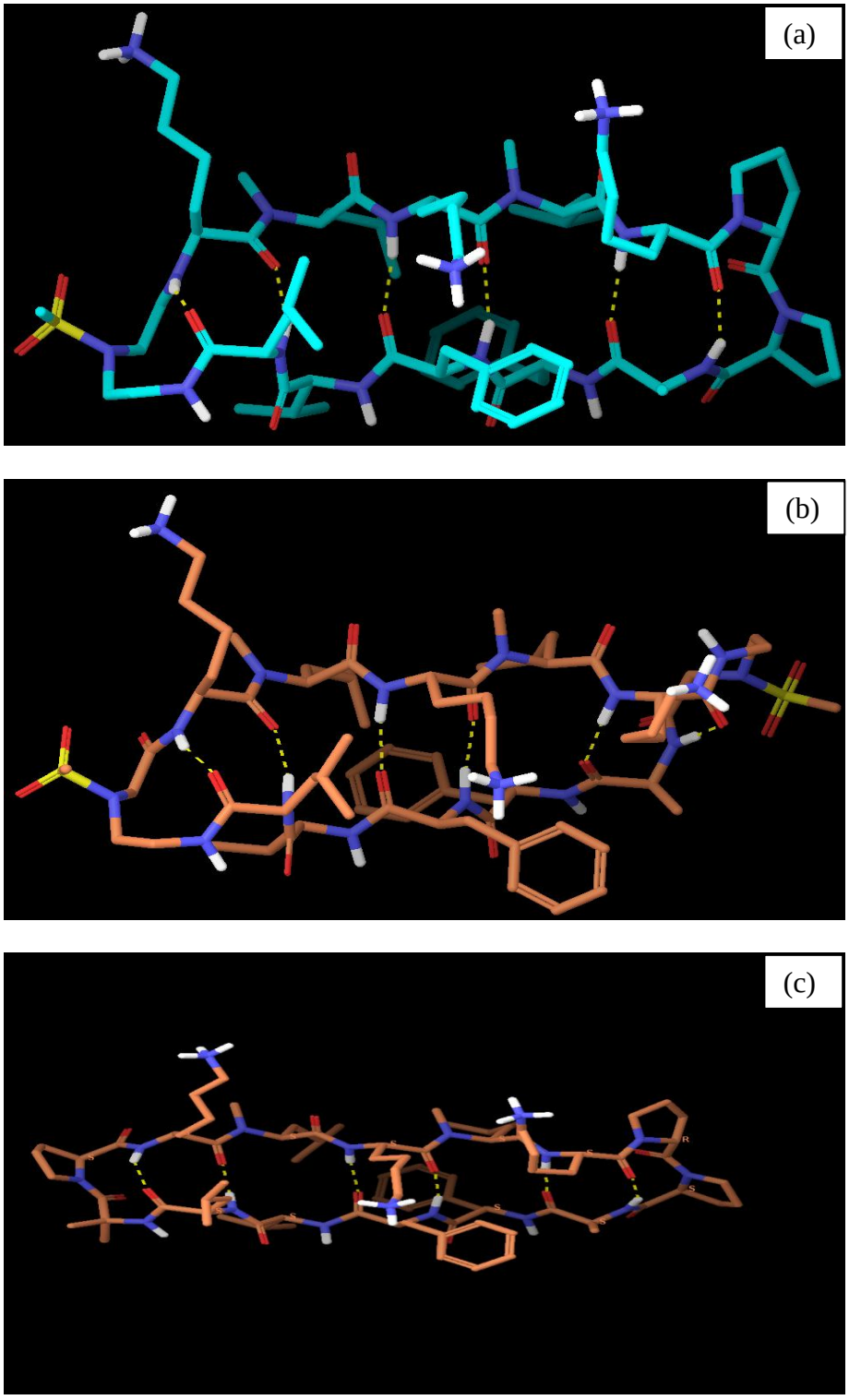

Fig. 2.2 Stereo drawing of cyclic abeta peptides obtained after energy minimization procedure. Cyclic Aβ peptides designed using (a) L-Pro-D-Pro and methylsulfonamido aminoethyl glycine (b) two methylsulfonamido aminoethyl glycine units and (c) L-Pro-D-Pro and L-Pro-Aib turn promoters.

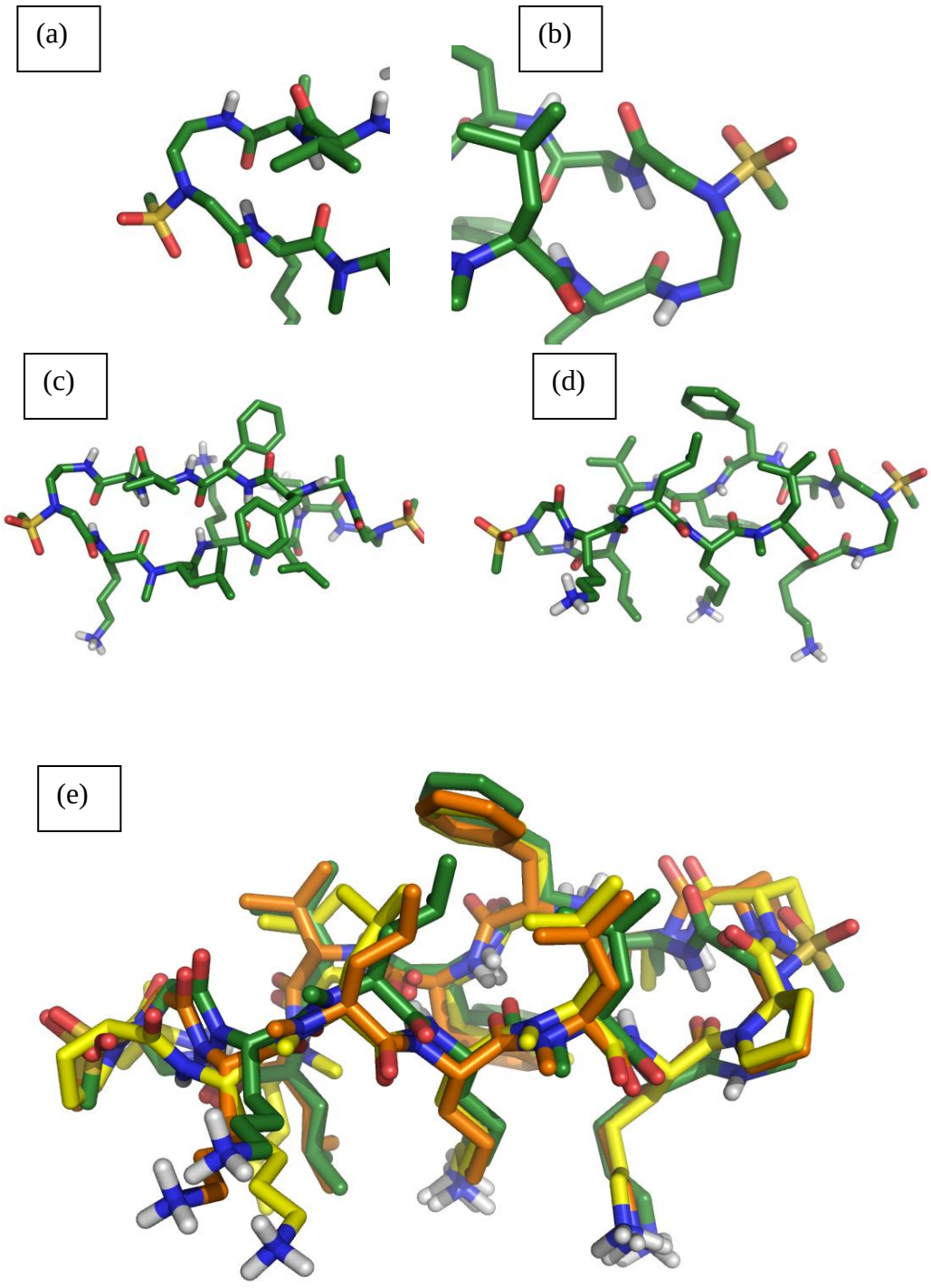

Fig. 2.3 Cyclic Abeta peptide designed with different β-turn promoters. (a) Turn 1 (b) Turn 2 (c) top view (d) side view of cyclic abeta peptide with the methylsulfonamido aminoethyl glycine turns and (e) super-imposed pose for cyclic abeta peptides with different turn promoters.

Table 2.1 Turn Promoters used in synthesis of cyclic peptidomimetics.

	Turn1	**Turn 2**	**Energy Minimization**
1	Methylsulfonamido aminoethyl glycine	D-Pro-L-Pro	-2100 Kcal
2	Methylsulfonamido aminoethyl glycine	Methylsulfonamido aminoethyl glycine	-2400 Kcal
3	L-Pro-Aib	D-Pro-L-Pro	-1400 Kcal

We also further investigated the inverso- and retro-inverso- cyclic III peptide analogs for their potential to block beta integrin mediated cell adhesion. Retro-inverso design of biologically active peptides is a well known strategy to design all D-amino acid peptides from potentially bioactive all L-peptide sequences with increased stability (18-21). Retro-inverso peptide analogs have a similar placement of side chain residues as observed for cyclic D-HYD1 and hence similar or better effect in bioactivity was anticipated for retro-inverso analogs. It was surprisingly found that retro-inverso analogs had better bioactivity than cyclic D-HYD1 analogs whereas cyclic III was twice more active as cyclic D-HYD1 (Table 2.2). In an effort to optimize the bioactivity of cyclic III, it was essential to determine the key residues most critical to the bioactivity of cyclic III peptide.

2.2.2 Structure Activity Relationship of cyclic III peptide

The key residues of cyclic III peptide responsible for biological activity have been identified by performing sequential alanine substitution analysis on the recognition strand of the peptide analog. We expected two or more of the recognition strand residues to be responsible for bio-activity of resulting cyclic III analogs. As anticipated, bioactivity data

revealed tryptophan, valine and methionine in peptides **2.2**, **2.4** and **2.6** respectively as key residues critical for binding of cyclic III to integrins (Table 2.2). Replacement of alanine for the serine in peptide **2.2** drastically improved the bioactivity of cyclic III analog. Oxidation of methionine side chain has been observed during peptide isolation for some cyclic III analogs through HPLC. This problem was overcome by replacing the methionine side chain with a structurally similar and chemically stable side chain such as norleucine. To our surprise, introduction of the norleucine into the recognition strand of peptide **2.7** increased bioactivity drastically. We therefore anticipated that the recognition strand WAVVN (N= Norleucine) would further improve the bioactivity of the cyclic III analogs. After the determination of critical residues responsible for bioactivity of cyclic III peptide, efforts have been made to further enhance the bioactivity by making slight changes such as increased hydrophobicity or slightly decreased hydrophobicity in the recognition strand. As shown in Table 2.2, replacement of norleucine in peptide **2.9** with more hydrophobic tryptophan did not alter the bioactivity appreciably. Cress and co-workers have previously reported that another peptide RZ-3 (KMVIYWKAG) similar to HYD1 inhibited adhesion of prostate tumor cells to ECM proteins or human dermal fibroblasts (22). To further optimize our scaffold for enhancement of bioactivity of cyclic III peptide design, we synthesized cyclic peptide **2.8** with the RZ-3 (WYVVN) core sequence in the recognition strand. Peptide **2.8** had similar bioactivity as our optimized cyclic III analog.

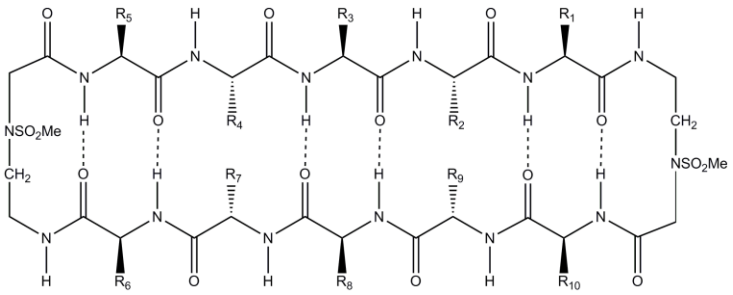

Table 2.2 Structure-Activity Relationship studies of cyclic III peptide analogs.

Peptide	R_1	R_2	R_3	R_4	R_5	R_6	R_7	R_8	R_9	R_{10}	IC_{50}
2.1	**K**	**L**	**K**	**L**	**K**	**W**	**S**	**V**	**V**	**M**	**15.5±7.7**
2.2	**K**	**L**	**K**	**L**	**K**	**A**	**S**	**V**	**V**	**M**	**57.1±22**
2.3	**K**	**L**	**K**	**L**	**K**	**W**	**A**	**V**	**V**	**M**	**4.1±1.9**
2.4	**K**	**L**	**K**	**L**	**K**	**W**	**S**	**A**	**V**	**M**	**19.0±6.9**
2.5	**K**	**L**	**K**	**L**	**K**	**W**	**S**	**V**	**A**	**M**	**6.2±2.7**
2.6	**K**	**L**	**K**	**L**	**K**	**W**	**S**	**V**	**V**	**A**	**31.1±7.6**
2.7	**K**	**L**	**K**	**L**	**K**	**W**	**S**	**V**	**V**	**N***	**2.6±1.3**
2.8	**K**	**L**	**K**	**L**	**K**	**W**	**Y**	**V**	**V**	**N***	**2.9±1.3**
2.9	**K**	**L**	**K**	**L**	**K**	**W**	**A**	**V**	**V**	**W**	**5.9**
2.10	**K**	**L**	**K**	**L**	**K**	**M**	**V**	**V**	**S**	**W**	**5.9±3.4**
2.11	**K**	**L**	**K**	**L**	**K**	**N***	**V**	**V**	**A**	**W**	**12.3**
2.12	**K**	**L**	**K**	**L**	**K**	**A**	**V**	**V**	**A**	**W**	**21.9**
2.13	**K**	**L**	**K**	**L**	**K**	**N***	**A**	**V**	**A**	**W**	**25.9**
2.14	**K**	**L**	**K**	**L**	**K**	**N***	**V**	**A**	**A**	**W**	**41.3**
2.15	**K**	**L**	**K**	**L**	**K**	**N***	**V**	**V**	**A**	**A**	**2.8**
2.16	**K**	**L**	**K**	**L**	**K**	**F**	**V**	**V**	**A**	**W**	**9.7**

N* = Nor-Leucine

2.2.3 Structure Activity Relationship of Retro-inverso cyclic III analog

After determining that serine and methionine replacement with alanine and tryptophan residues yielded cyclic III peptides with improved bioactivity, we attempted to study structure activity relationship for the retro-inverso cyclic III analog. A sequential alanine scan was carried out with NVVAW as the core sequence in the recognition strand. It was found that replacement of norleucine (peptide **2.12**) and valine in peptide **2.13** & **2.14** are critical for the bioactivity of the retro-inverso peptides. There was an unexpected improvement in bioactivity for peptide **2.15** where tryptophan was substituted for alanine.

2.2.4 Design of cyclic HYD1 analogs with constrained ether-peptidomimetic β-turn promoter

After optimizing the recognition strand for obtaining increased bioactivity for cyclic III analogs, efforts were made to further constrain the cyclic peptide by introduction of a constrained oxygenated turn promoter (Fig.2.4a) at one turn and the methylsulfonamido aminoethyl glycine as the other turn. The introduction of an ether-peptidomimetic amino acid (proline or 2-piperidine carboxylic acid derivative) as a constrained turn promoter will probably further reduce the degrees of freedom available to the cyclic peptide and possibly increase its affinity for binding to the target. Conformational search and energy minimization studies were carried out using GLIDE software to ensure that all intramolecular hydrogen bonds are sustained within the cyclic beta-hairpin like scaffold (Fig. 2.4 b-d). Conformational search and energy minimization studies suggested that introduction of the five membered ring D-Proline derivatized ether-peptidomimetic was favorable in stabilizing and sustaining the intramolecular hydrogen-bonding within the cyclic III analog. Based on this information, we synthesized

cyclic III analog with the proline derived ether-peptidomimetic at one turn and methylsulfonamide amino ethyl glycine as other turn gave an impressive bioactivity of 1.08 µM when assayed using TOPRO3 protocol.

(a)

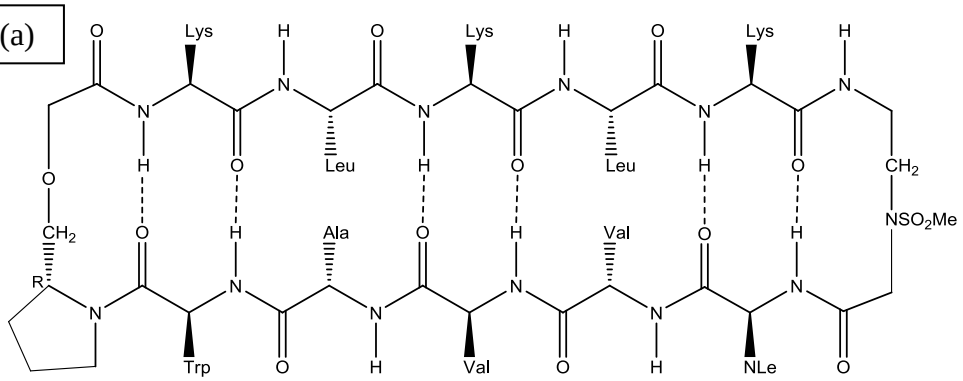

(b)

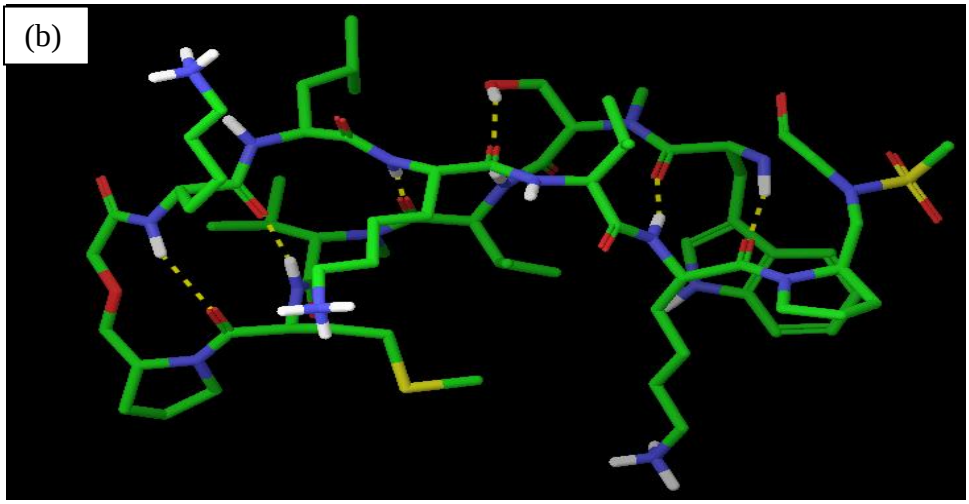

(c)

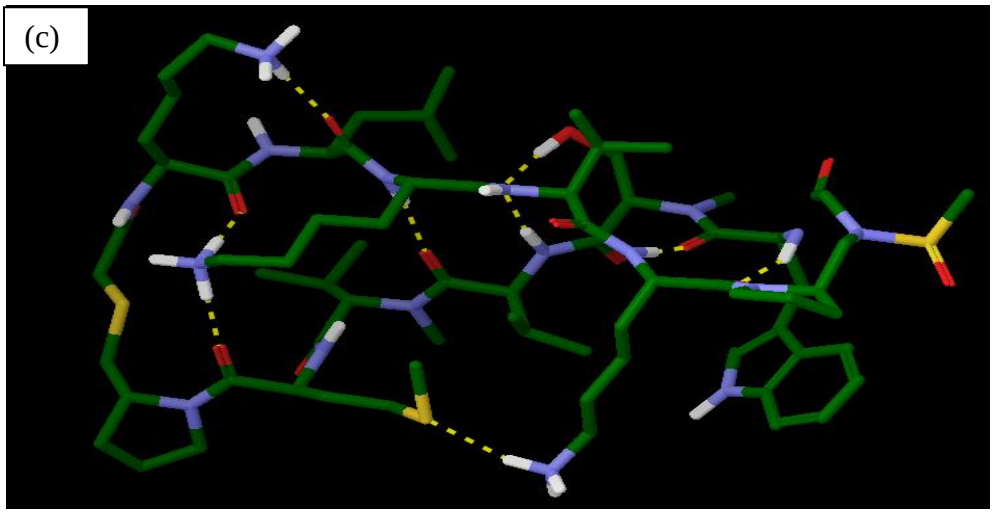

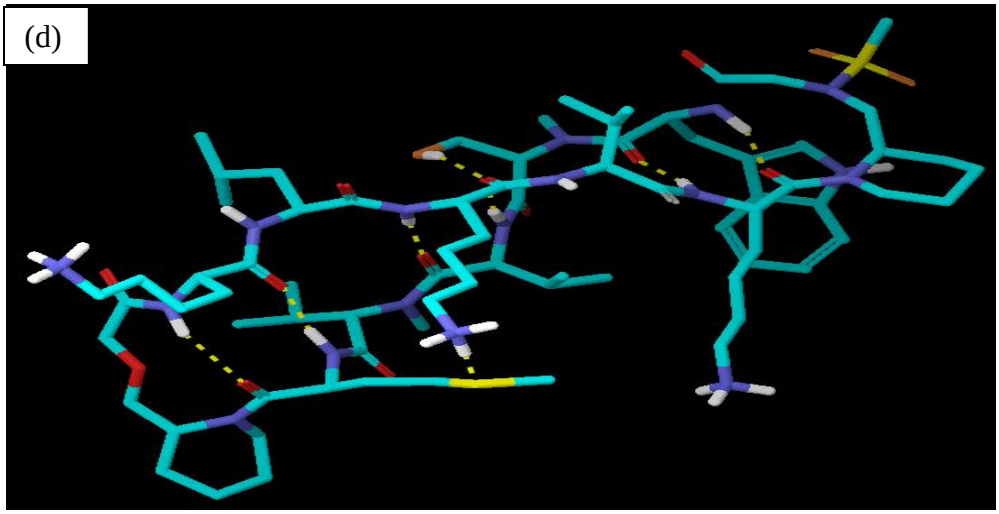

Fig. 2.4 Cyclic III analogs with constrained β-turn promoter. (a) proline derived ether-peptidomimetic turn promoter, (b), (c) and (d) represents conformational search for the ether-peptidomimetic turn promoter, thioether peptidomimetic turn promoter and piperidine derived ether-peptidomimetic turn promoter.

As shown in figure 2.4d, computational studies suggested that when ether peptidomimetic was replaced with the thioether derivative it disrupts internal hydrogen bonding within the cyclic III peptide.

2.2.5 Optimization of Non-recognition strand

The non-recognition strand of cyclic III peptide was optimized to determine if it has any effect on bioactivity. A similar bioactivity observed for cyclic D-HYD1 and the cyclic III peptides suggest extensive peptide backbone interactions are absent or minimal since these two analogs have opposite backbone sequences. This hypothesis was tested by replacing the amino acid residues that have exo amide hydrogens with N-methylated amino acid residues. We first replaced all leucine residues in the non-recognition strand with N-methyl glycine (sarcosine) (Fig.2.5a). We anticipated that N-methylation of the exo amides will not significantly change III conformation but it should stabilize cyclic beta-hairpin and eliminate possible peptide aggregation due to beta-sheet like

dimerization or oligomerization of one or more cyclic III analogs. Surprisingly, we found that this cyclic III analog with sarcosine residues in the non-recognition strand and the ether-peptidomimetic amino acid as the turn promoter did not show any bioactivity. We believe that the introduction of too many constraints in the molecule might have caused disruption of the internal hydrogen bonding which stabilizes the cyclic peptide.

(a)

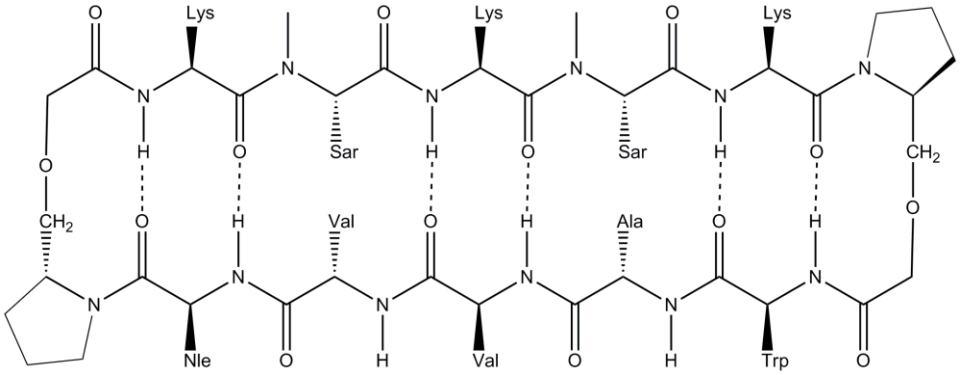

(b)

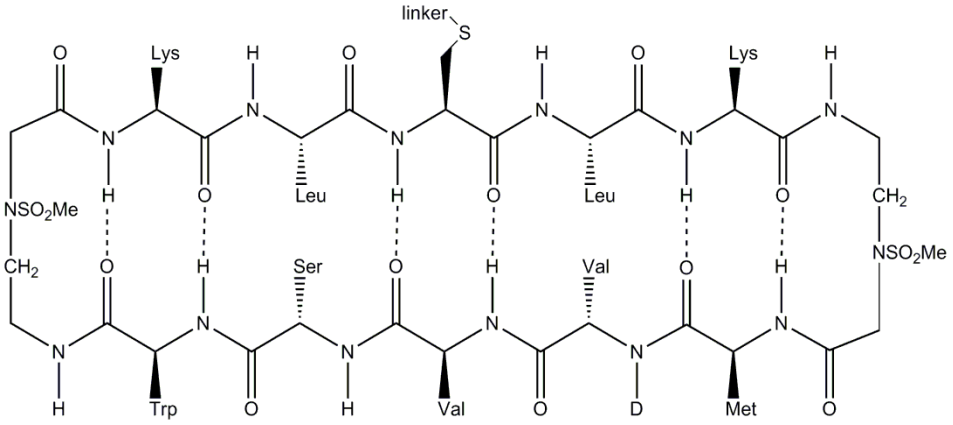

Fig. 2.5 (a) Retro-inverso cyclic III analog with ether-peptidomimetic amino acid turn promoter and N-methylated glycine residue in non-recognition strand. (b) cyclic III analog with membrane seeking linker attached to the cysteine residue in the non-recognition strand.

Cyclic HYD1 analogs with membrane seeking linker in the non-recognition strand

It is presumed that the target of the cyclic III monomer is extracellular. We hypothesize that integrin clustering could enable an avidity effect on the cyclic III analog binding. Hence attachment of a long membrane-seeking fatty acid tail connected via oligoethyleneoxide linker to the cysteine side chain in the non-recognition strand should enhance the bioactivity of these III analogs (Fig. 2.5b). We have attempted to attach laurate, $H_3C(CH_2)_{11}$-$(OCH_2CH_2)_5$-$OCH_2CH_2NHCOCH_2Br$ to the cysteine side chain in the non-recognition strand as per reported procedure (23). MALDI-TOF data clearly suggested that the membrane seeking linker was attached to the cysteine side chain but we could not get appreciable yield to carry out bioassay experiments. A lysine monomer with a laurate side chain attached to the ε-nitrogen has also been synthesized with an aim to incorporate these monomers directly during solid phase peptide synthesis. This strategy should improve the bioavailability of these cyclic III analogs. Recently, several reports have appeared in the literature describing the use of bivalent linkers to target G-protein coupled receptors (24-29). The use of bivalent linkers exhibited increased potency as compared to monovalent counterparts. Based on these cited reports, we propose the design of dimeric cyclic III analogs separated by the bivalent hexaethylene glycol derived linker $BrCH_2CONHCH_2CH_2(OCH_2CH_2)_4CH_2CH_2NHCOCH_2Br$. These membrane-seeking dimeric cyclic III analogs should probably be more bioactive than underivatized cyclic III analogs. We have been successful in synthesizing bivalent electrophilic linkers for making dimeric cyclic III analogs but have failed in attaching these linkers to the thiol side chain of the cysteine in the non-recognition strand.

2.2.6 Synthesis of β- turn promoters and cyclic III peptides

All cyclic peptidomimetics were synthesized on 2-chlorotrityl chloride resin as solid support and Fmoc solid phase peptide synthesis strategy as shown in scheme 2.1. The linear peptides were synthesized and selectively cleaved from the resin without cleaving side chain Boc-groups using trifluoroethanol as the cleaving agent. The linear peptide is then cyclized in solution under dilute conditions to afford crude cyclized peptide in modest yields. We have made a few attempts to do on-resin cylization of linear peptides but failed in our endeavor to synthesize cyclic peptides.

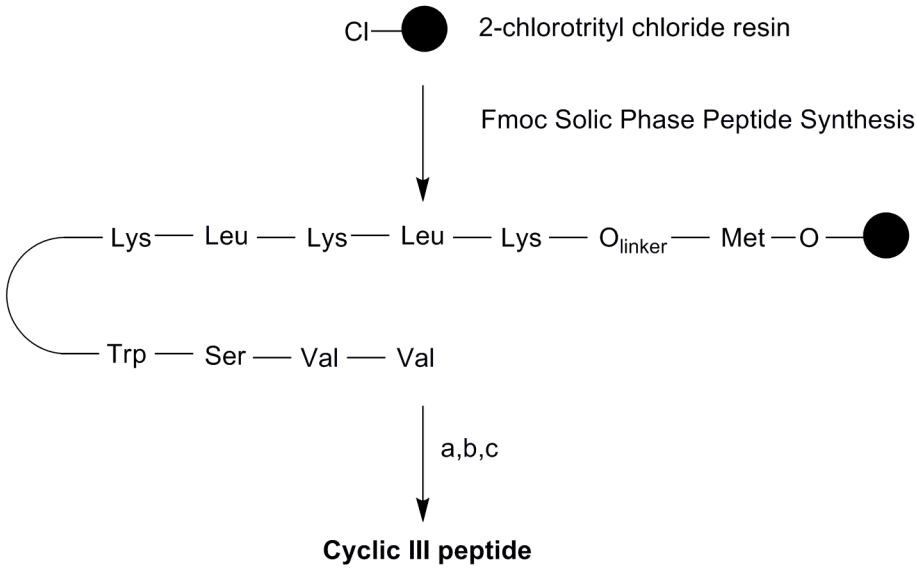

(a) 20% Trifluoroethanol in DCM, rt (b) HATU, DIEA, DMF (c) 95%TFA, Et_3SiH, H_2O

Scheme 2.1 Solid-Phase synthesis of cylic III analogs.

Scheme 2.2 describes the synthesis of the methylsulfonamide aminoethyl glycine turn promoter. Selective mono-alkylation of excess ethylene diamine with tert-butyl bromoacetate was carried out under dilute conditions to give compound **2.2** in 85% yield (30). Compound **2.2** is taken up in the next step without further purification and selective Fmoc protection of the primary amine is achieved to give crude fmoc-protected

aminoethyl glycinate **2.3**. The crude reaction mixture is then washed with dilute hydrochloric acid, stored overnight in the deep freezer, resulting in precipitation of pure compound **2.3** as the hydrochloride salt that can be stored for several months in the refrigerator (Scheme 2.2). Mesylation of the secondary amine with methanesulfonyl chloride afforded compound **2.4** that precipitates from ethyl acetate solution under cold conditions. Deprotection of the t-butyl group was achieved by employing 4M HCl in dioxane to give the desired compound **2.5** in excellent yield.

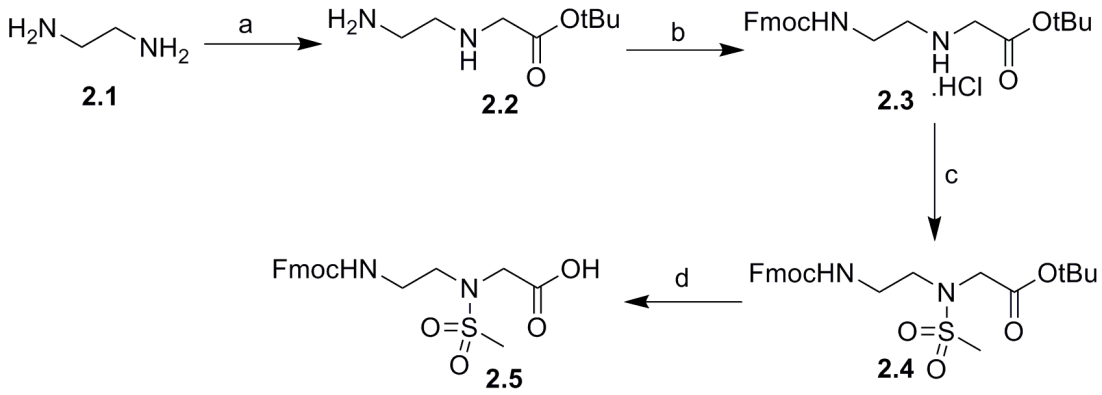

(a) $BrCH_2CO_2tBu$, THF, 85% (b) FmocNOSu, DIEA, DCM, 90% (c) $MeSO_2Cl$, DIEA, THF, 88% (d) 1,4-Dioxane,4M HCl, quant.

Scheme 2.2 Synthesis of the methylsulfonamido aminoethyl glycine beta turn promoter.

As shown in scheme 2.3, the ether peptidomimetic amino acid was prepared from commercially available Boc-D-Prolinol. First, O-alkylation of **2.6** with tert-butyl bromoacetate afforded compound **2.7** in 77% yield (31, 32). Selective removal of the Boc protecting group of compound **2.7** using trifluoroacetic acid in DCM (1:4) gave compound **2.8**. Fmoc-group protection of the secondary amine **2.8** with FmocOSu followed by acidic cleavage of the tert-butyl ester group gave the proline derived ether-peptidomimetic **2.10** in 79% yield. The N-ethylated beta turn promoter **2.15** was synthesized to determine if the additional constraint further stabilizes the secondary

structure of the cyclic peptide and increase its affinity for the target. Compound **2.15** was prepared from 2-ethyl ethanolamine as shown in scheme 2.4. Boc protection of the secondary amine **2.11** followed by O-alkylation with tert-butyl bromoacetate gave the fully protected compound **2.12** in 89% yield. Selective deprotection of the Boc group of compound **2.12** followed by Fmoc protection of the resulting amine gave compound **2.14**. Final cleavage of the tert-butyl ester in compound **2.14** afforded desired N-ethylated turn promoter **2.15** in 85% yield.

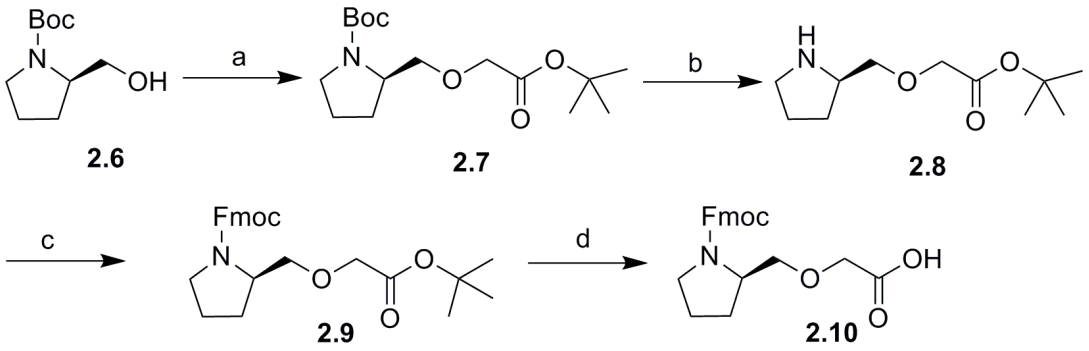

(a) NaOH, toluene, $BrCH_2CO_2t$-bu, TBAI, 77% (b) TFA/DCM (4:1) quant. (c) FmocOSu, DIEA, DCM, 79% (d) TFA/DCM,Triethylsilane, quant.

Scheme 2.3 Synthesis of ether-peptidomimetic amino acid.

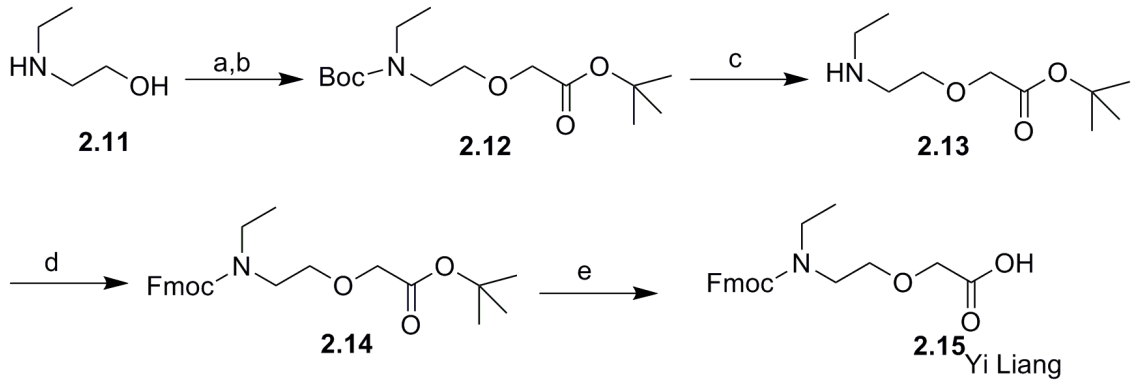

(a) $(Boc)_2O$, DCM, (b) NaOH, toluene, $BrCH_2CO_2t$-bu, TBAI, 89% (c) TFA/DCM (3:1), 90% (d) FmocOSu, DIEA,DCM, 85% (e) TFA/DCM,Triethylsilane, quant.

Scheme 2.4 Synthesis of the N-Ethylated beta turn promoter.

The membrane-seeking linkers and bivalent linkers proposed for making membrane-seeking and dimeric/oligomeric cyclic III analogs were synthesized to target avidity effect arising due to integrin clustering near the cell membrane surface (scheme 2.5). Synthesis of azides derived from the ethylene glycol derivatives have been previously reported by Bonger et. al.(33). Azide **2.18** was prepared from the corresponding ethylene glycol derivative **2.16** by transformation to the p-toluenesulfonate ester **2.17** followed by displacement of the esters with sodium azide. Hydrogenation of compound **2.18** with 10% Pd/C in methanol afforded primary amine **2.19** in quantitative yield. Acetylation of primary amine **2.19** with bromoacetyl bromide afforded the desired linker **2.20** in 93% yield. Bis-azide **2.23** required for making bivalent linkers was prepared from the corresoponding hexaethylene glycol using the above mentioned strategy in 85% yield. The diamine **2.24** was finally acetylated to give bis-bromoacetylated hexaethylene glycol **2.25** in 81% yield. Compound **2.20** and **2.25** can be stored in refrigerator at -20^0C for several weeks.

Another attractive strategy proposed for making membrane-seeking linkers involved synthesis of lysine monomers with the side chain acetylated with lauroyl chloride. These modified amino acids would be incorporated into the sequence like other residues for the synthesis of the linear peptide on the resin. Based on these proposed ideas, lauryl and biotin groups have been attached to the ε-nitrogen of Fmoc-lysine to give compounds **2.28** and **2.29,** respectively (scheme 2.6).

(A)

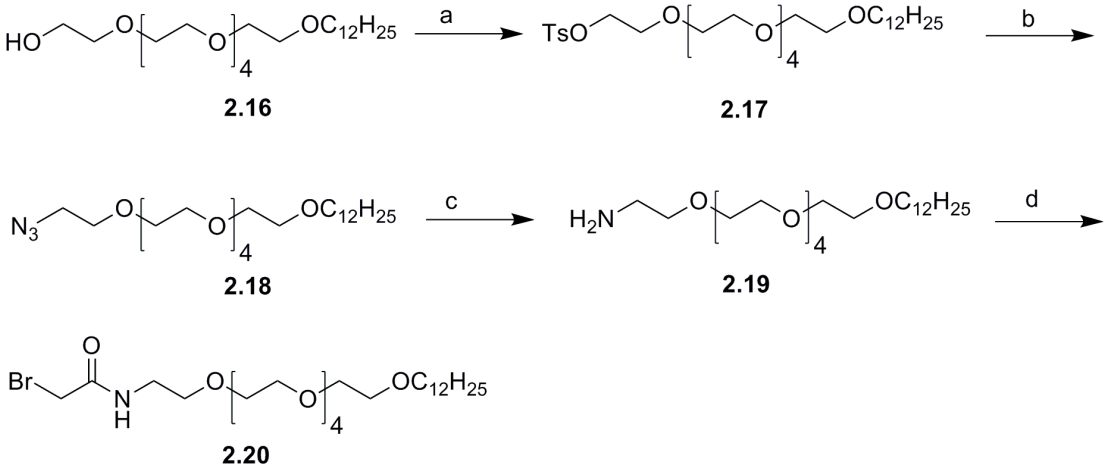

(a) PTSCl, KOH, DCM,85% (b) NaN_3, DMF, 96% (c) Pd/C, MeOH, quant. (d) $BrCH_2COBr$, Na_2CO_3, DCM,93%

(B)

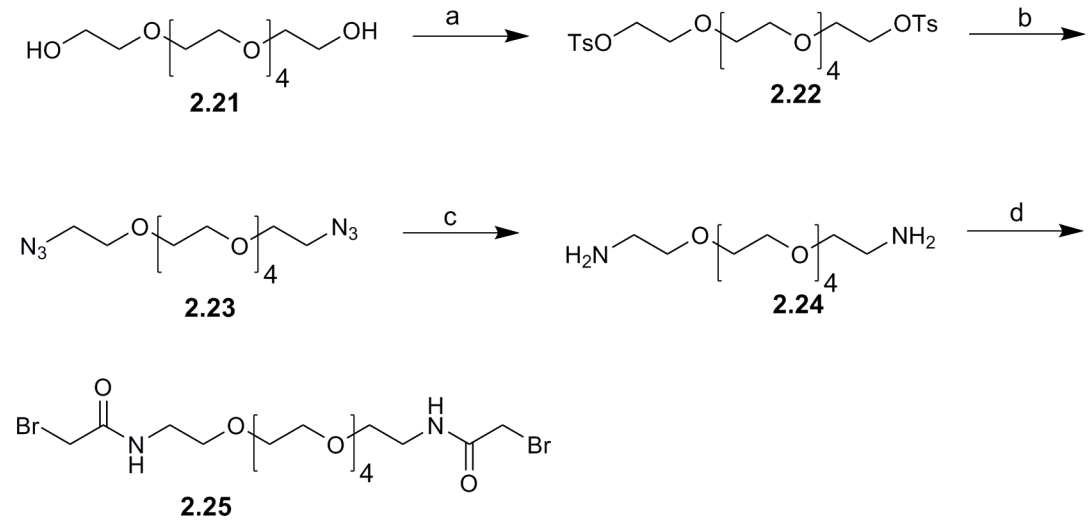

(a) PTSCl, KOH, DCM, 74% (b) NaN_3, DMF, 85% (c) Pd/C, MeOH, quant. (d) $BrCH_2COBr$, Na_2CO_3, DCM, 81%

Scheme 2.5 Synthetic routes for preparing (a) membrane-seeking linkers and (b) bivalent linkers for making dimeric or oligomeric cyclic III analogs.

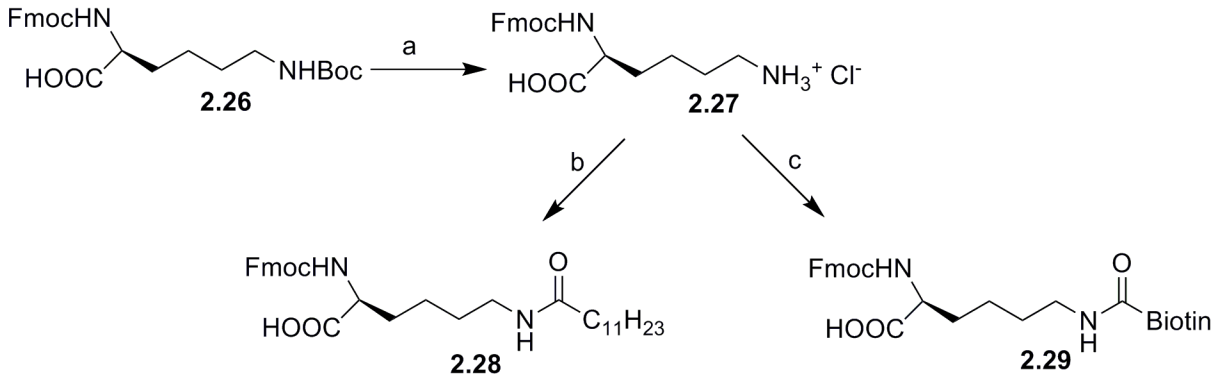

(a) 1,4 Dioxane, HCl (b) $C_{11}H_{23}COCl$, Na_2CO_3, dioxane (c) 4M NaOH, Biotin-NHS pH 8-8.5

Scheme 2.6 Synthesis of Fmoc-Lys(lauroyl)-OH and Fmoc-Lys(biotin)-OH.

2.2.7 Conformational studies of cyclic Peptides using Circular Dicroism

Circular dichroism (CD) is a sensitive measure of the secondary structure of peptides and proteins. CD spectroscopy measures the difference in absorbance of right- and left-circularly polarized light by a substance. Peptides usually show absorption in the ultraviolet region of the spectrum from the peptide bonds and side chains of the amino acids in the sequence. Various reports cited in the literature have shown that CD spectra from 260-190 nm is analyzed for the different secondary structural of peptides and proteins i.e. alpha helix, parallel and antiparallel beta sheet, beta turn, etc (34, 35). The lowest energy transition in the peptide chromophore is an n - Π* transition observed at 210-220 nm with weak intensity. The peptide with a β-sheet structure usually exhibits an absorption minima around 210 nm and a relatively strong absorption maxima around 190 nm. Peptide conformational studies using CD are mainly characterized by comparing analysis of the overall shape of the CD spectra with standard peptide spectra.

The conformational study of all cyclic III peptides were carried out in buffered aqueous solutions. The CD spectra of the cyclic peptide with Robinson's template and the novel methylsulfonamide glycine turn promoter and peptide **2.1** are shown in Fig.2.6a.

Fig. 2.6b shows the CD spectra for cyclic peptides **2.4**, **2.6**, **2.7** and **2.10** in 7 mM sodium acetate buffer at a concentration of 200 µM at pH 7 and 25^{0}C. All these cyclic peptides displayed similar, but different characteristic CD bands: negative absorption minima around 200 nm and strong positive absorption maxima around 185-190 nm. These characteristic CD bands are strongly indicative of a beta-sheet or beta-turn secondary structures. These peptides shows strong absorption at higher concentration indicating a possible dimeric or oligomeric species in aqueous buffered solutions.

(A)

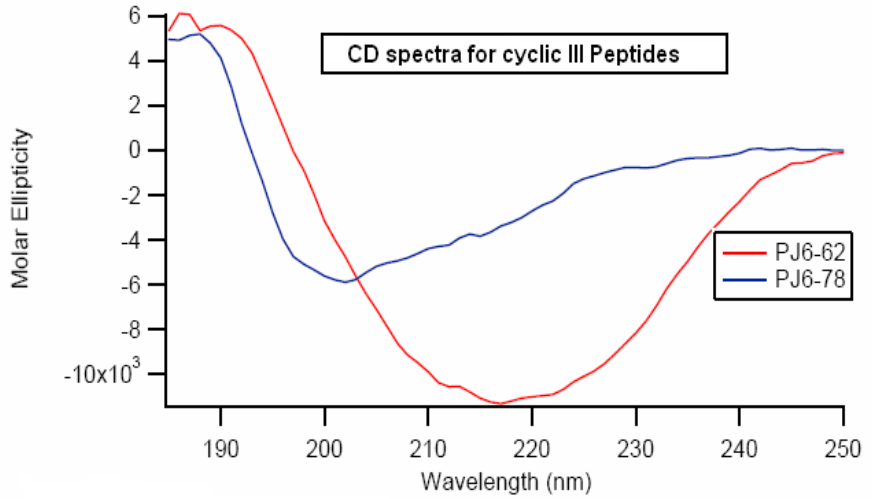

(B)

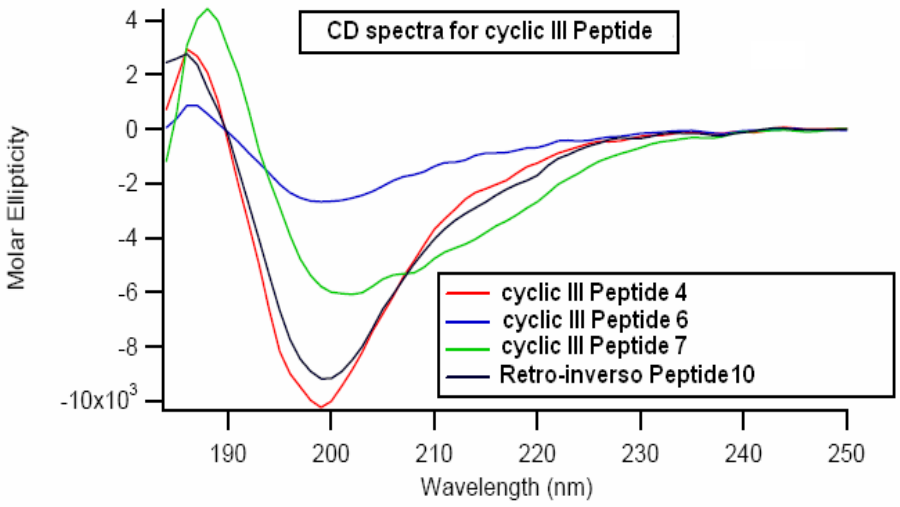

Fig. 2.6 Circular dichroism studies for cyclic III (A) peptides 2.1, 2.17 and (B) peptides 2.4, 2.6, 2.7, 2.10 in 7 mM sodium acetate buffer at a concentration of 200 µM at pH 7.

To check the validity of turn promoters to induce β-hairpin structure, turn promoters 2.5 and 2.10 were replaced by D-Pro-Gly in linear Gellman's peptide (fig. 2.7). CD spectra of these peptides indicated that oxygenated turn promoter produced well defined β-hairpin secondary structures in linear peptide as compared to methylsulfonamido aminoethyl glycine turn promoter.

(A) (B)

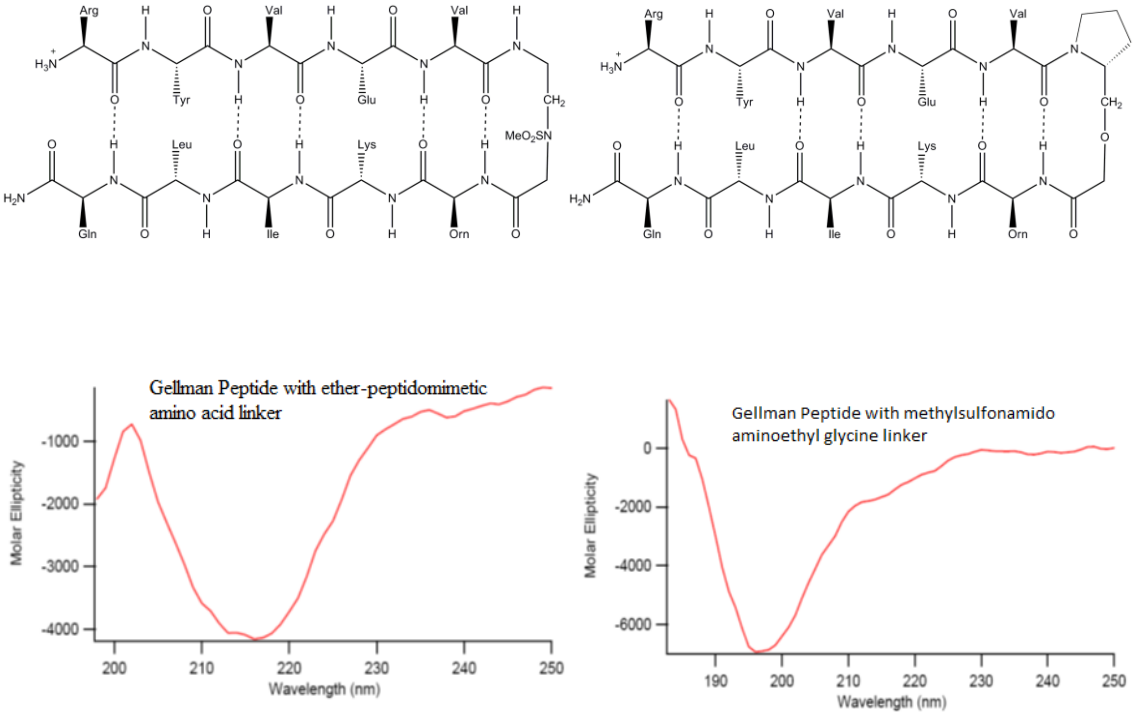

Fig. 2.7. Circular dichroism studies for validating the linkers (A) methylsulfonamido aminoethyl glycine and (B) ether-peptidomimetic amino acid in inducing secondary structures in Gellman peptide.

2.2.8 NMR studies for determination of structure of cyclic peptides in solution†

Complete peak assignments were only done for cyclic peptides **2.4** and **2.17** and are shown in Table 2.3 and Table 2.4. Assignments for both the recognition sequence and the non-recognition sequence, omitting the turns, were done for the remainder of the peptides. In an effort to de-clutter the 2D spectra sets, the NMR experiments were run in 100% D_2O to remove the exchangeable amide and Lysine ε-NH protons from the spectrum. Even without information from the amide and lysine ε-NH protons, the results from our NMR experiments clearly show that the peptides have all adopted a *β*-hairpin structure.

Table 2.3 NMR assignments for peptide **2.4.**

	α	β	γ	δ	ε
PNA Turn	3.465^S, 4.047^R		3.490^S, 3.529^R	3.334	SO_2Me = 3.050
Lys-1	4.423	1.657, 1.770	1.305	1.589	2.879
Leu-2	4.042	1.994	1.955	0.904, 0.929	
Lys-3	4.072	1.613, 1.740	1.149, 1.281	1.506	2.776
Leu-4	4.160	1.418, 1.525	1.359	0.645, 0.768	
Lys-5	4.311	1.823	1.452	1.691	2.996
PNA Turn	3.891^S, 4.062^R		3.500^S, 3.612^R	3.236	SO_2Me = 3.045
Trp-6	4.609	3.123, 3.206	7.151, 7.160, 7.239, 7.473, 7.654		(5H, 2H, 6H, 7H, 4H)
Ser-7	4.599	3.720, 3.822			
Ala-8	4.531	1.183			
Val-9	4.575	1.618	0.797, 0.924		
Met-10	4.599	1.999, 2.234	2.532, 2.664		2.077

R = Pro-R, S = Pro-S

† All NMR run and analyzed by David B. Badger

Table 2.4 NMR assignments for peptide **2.17.**

	α	β	γ	δ	ε
L-Pro-1	4.531	2.111, 2.219	1.940, 2.077	3.705, 3.949	
D-Pro-2	4.741	2.155, 2.287	1.896, 2.004	3.539, 3.793	
Lys-3	4.541	1.662, 1.789	1.242, 1.349	1.564	2.864
Leu-4	4.985	1.730	1.530	0.777, 0.851	
Lys-5	4.291	1.667, 1.794	1.261, 1.403	1.564	2.947
Leu-6	4.536	1.569	1.505	0.811, 0.812	
Lys-7	4.379	1.745, 1.784	1.403	1.667	2.977
PNA Turn	3.563^{S}, 3.866^{R}		3.348	3.162	SO_2Me = 3.030
Trp-10	4.692	3.128, 3.226	7.121, 7.146, 7.229, 7.473, 7.561		(5H, 2H, 6H, 7H, 4H)
Ser-11	4.599	3.837			
Val-12	4.267	1.989	0.802, 0.880		
Val-13	4.130	1.940	0.665, 0.875		
Met-14	4.482	2.107	2.434, 2.551		2.121

R = Pro-R, S = Pro-S

Supporting our CD results, both the chemical shifts of the amino acid α-hydrogen protons (H_α) and the NOE data indicate that the peptides are in a *β*-hairpin conformation. Our NMR results agree with previous empirical analysis which has shown that when *β*-sheets are formed, there is a downfield shift in the H_α resonances (36, 37). The majority of the amino acid H_α's in our peptides are shifted significantly downfield such that their values indicate a β-hairpin conformation.

2.2.9 Analysis and Characterization of Our Novel Turn Promoter

H_α and NOE NMR analysis of peptide **2.17**, which contains both the Robinson *β*-hairpin turn promoter template (38) (D-Pro-L-Pro) and the methylsulfonamido aminoethyl glycine turn, confirms the structure of this peptide as a *β*-sheet. This peptide

was then remade using the methylsulfonamido aminoethyl glycine in place of the Robinson template as the β-hairpin turn promoter to give peptide **2.1**. The resulting H_α chemical shifts for this peptide show it is also a β-sheet.

A comparison between the H_α shifts of these two peptides reveals a many similarities. Most of the H_α's on the non-recognition side of peptide **2.1** have shifted upfield relative to **2.17**, suggesting that the structure is less like a β-sheet. While 3 of these residues have only shifted about 0.2 ppm or less upfield, Leu2's shift of about 0.7 ppm suggests a fair amount of structural change. Interestingly, the only H_α on the non-recognition strand that has an upfield shift is Lys1. More importantly however, all but one of the H_α's on the recognition side of the peptide have shifted downfield indicating a β-sheet conformation. The H_α of Ser7 is the only one that has shifted upfield. Looking at the fact that the H_α's on residues Met10 and Lys1 have shifted downfield after the β-hairpin turn promoter was changed from the Robinson template to our methylsulfonamido aminoethyl glycine turn, it suggests that our turn promoter allows for more β-hairpin-like character at this end of the peptide. Thus, our turn may be a better β-hairpin promoter for certain peptide sequences.

Although most of the H_α shifts were small, about 0.2 ppm or less, there was a large shift in two of the H_α's which appears to be highly structurally significant. While the Leu2's H_α shifted upfield 0.704 ppm, Val9's H_α shifted downfield 0.532 ppm. This suggests that the leucine α proton is not predominatly adopting a β-sheet conformation. This is most likely due to steric interactions from the γ-protons of Val9 which is directly across from Leu2. Presumably as a direct result of Leu2's structural conformational

change, Lys3's H_α is shifted 0.215ppm (the second largest shift) upfield which removes a small amount of its β-sheet character and thus is further evidence supporting this claim.

An examination of the other peptides reveals a similar phenomenon. The Leu2 H_α is always shifted upfield and the residue in position 9 is always shifted downfield, with the exception of peptide **2.10**, in comparison with peptide **2.17**. This can be explained by the fact that the D-Pro-L-Pro turn in the Robinson template is very structurally rigid, forcing those residues close to it into a β-hairpin conformation. However, our turn is much more flexible, thus allowing the residues close to the turn to be less rigid in their orientations. It is probably this flexibility that allows the Leu2 H_α to deviate from the β-sheet configuration. NOE analysis supports this view. In peptide **2.17**, strong NOEs were observed between the H_α's of Leu4 and Val13 as well as a small NOE between the H_α's of Leu4 and Val12. However, in peptide **2.1** the NOE between the H_α's of Leu2 and Val9 was only of low intensity. In its place, there was a strong NOE between the H_α's of Leu2 and Leu4. Additionally, a semi-strong NOE was observed between the H_α of Leu2 and only 1 γ-CH_3 group of Val9. This significant reduction in NOE cross-peak intensity between the Leu and Val H_α's combined with the appearance of a new strong cross-peak between the two Leu H_α's is strong evidence in support of this structural picture.

The replacement of the Robinson template by our turn slightly increases the distance between the two sides of the β-sheet. This is due to the fact that this turn isn't rigidly fixed into a certain conformation thereby allowing the chain to expand and contract, much like an accordion. It is this accordion-like action that allows the distance between the two sides of the β-sheet to change. This change in distance can be seen by

the decrease in NOE intensity between the Leu and Val residues mentioned previously. NOEs also show the disappearance of the following; a strong NOE between the ε protons of Met14 and the H_α of Lys3, a strong NOE between the γ_1 protons of Val12 and the β and β′ protons of Lys5. Also, the intensity of the NOE interaction between the γ_2 protons of Val12 and the β proton of Lys5 dropped from being semi-strong to being quite low upon replacement of the Robinson turn.

The methylsulfonamido aminoethyl glycine turn itself can be broken down into two parts for discussions sake. The first part is the CH_2 side between the carbonyl and the N-Mesyl group, which we will refer to as the α-protons. The second part is the CH_2-CH_2 side between the N-Mesyl group and the amide NH, which will be referred to as the γ and δ-protons as shown in Figure 2.7.

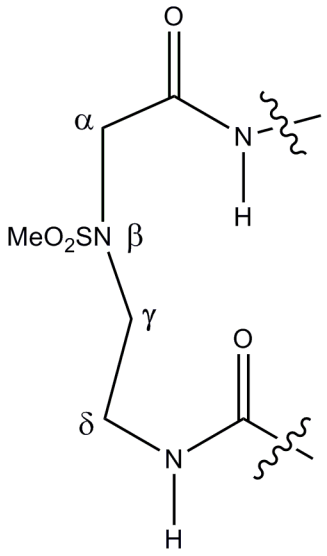

Fig. 2.8 Labeled positions on the methylsulfonamido aminoethyl glycine turn.

The flexibility of the turn is not just limited to adjusting the distance between the two sides. Rather, NOE analysis shows the existence of 2 distinct conformations. Newman projections of the two different conformations viewed down the δ-γ bond

showing specific steric interactions can be seen in Figure 2.8. The first conformation (a) exists as an eclipsed conformer which puts it in the higher energy state of the two. However, the bulky N-Ms group points down and away from the *β*-sheet, eliminating all steric interactions and placing it in the lowest energy state. The second conformation (b) exists as the staggered conformer, thus being the lower energy of the two. This time however, the bulky N-Ms group points directly into the center of the *β*-sheet causing large amounts of steric interactions with the backbone forcing the N-Ms group into a very high energy state. Therefore, it can be assumed that the bulky N-Ms group drives the turn's preference for the (a) conformation, picking the lower total energy conformer with the least amount of steric interactions.

Interestingly, conformer (a) may also be slightly favored because the Pro-R γ-proton (labeled as H') is eclipsed with the amide NH and the Pro-R δ-proton is eclipsed with the nitrogen from the N-Ms group. The proton attached to the amide NH is pointed out away from the backbone of the peptide while the lone pair on this nitrogen is pointed upwards towards the inside of the β-sheet. Additionally, the lone pair on the nitrogen from the N-Ms group points out towards the middle of the two δ-protons. There is the potential for a favorable attractive interaction (39,40) between the lone pairs on these nitrogens and their respective protons. This would forgive some of the strain caused from being in the eclipsed conformation further reducing the total energy of the (a) conformation making it more favorable.

Indeed, this favorable attractive interaction is supported by the chemical shifts of the respective protons. In peptide **2.4** for both turns, the Pro-R γ-protons are shifted

downfield relative to the Pro-S γ-protons meaning a decrease in shielding as is expected with the interaction of the lone pair of electrons on the amide nitrogen.

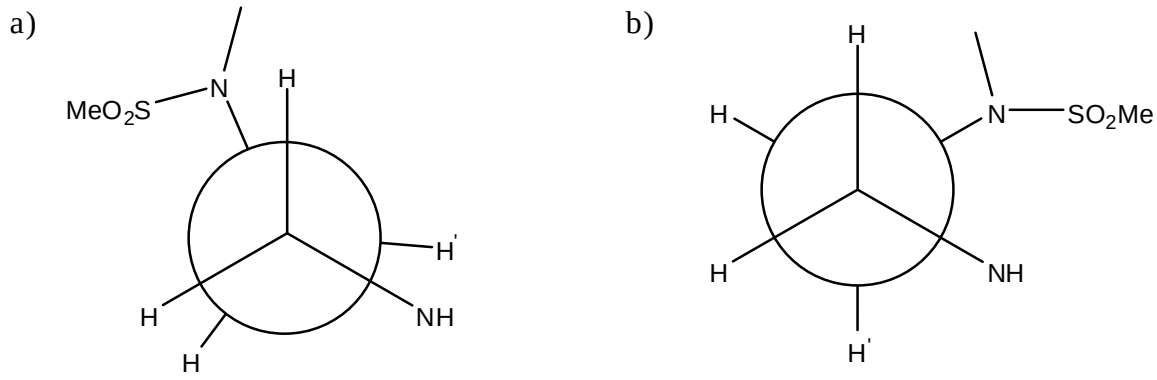

Fig. 2.9 Newman Projections of the *β*-turn viewed down the δ-γ bond: (a) N-Ms pointing down and away from the *β*-sheet; (b) N-Ms pointing into the center of the *β*-sheet.

For all but one of the peptides, the turn's geminal γ-protons are non-identical giving rise to a Pro-R proton and a Pro-S proton. Peptide **2.17** is the only one where these protons are identical. This is most likely caused by the Robinson turn locking the methylsulfonamido aminoethyl glycine turn into a more rigid conformation. Observations that support this analysis can be seen by the significant (0.08ppm and greater) upfield shift of both the γ and δ resonances from **2.4** to **2.17**. The α protons, with the exception of the equatorial one in **2.17**, experience a much larger (0.18ppm and greater) upfield shift than either of these two. Thus, this side of the peptide looks less like a *β*-sheet when the Robinson turn is used to induce the *β*-hairpin.

Because only 1 peak is seen for these protons, the turn's γ-protons must exist in somewhat similar environments and the turn's conformation must be different enough from the two mentioned above. Fig.2.9 is a Newman projection viewed down the δ-γ bond of what this altered conformation might look like which is supported by NOEs.

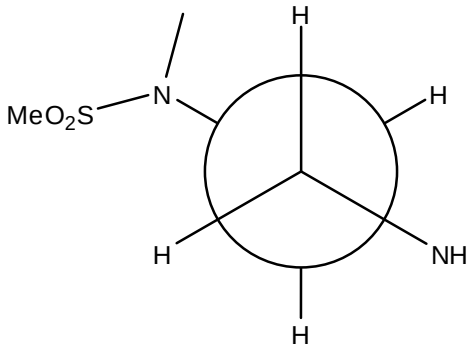

Fig. 2.10. Newman Projection of the structurally locked *β*-turn viewed down the δ-γ bond.

2.2.10 Peptide Structural Characterization via NOE

In conjunction with the chemical shifts of the α-protons, the NOE data was used to help determine the 3D structure of peptides. Peptide **2.4** was used as a general model for all the peptides. Cross-strand analysis reveals many NOEs between the Tryp6 and Lys5 residues, specifically between Tryp4H-LysεH, Tryp5H-LysβH, Tryp5H-LysεH, Tryp6H-LysγH and TrypβH-LysεH to name a few. These suggest that the tryptophan ring sits between the two strands at an angle with the indole ring facing the rest of the peptide. Additionally, peptide **2.1** also shows a NOE between TrypβH-LysβH, evidence that the ring spends part of its time in an alternate position between the two strands.

Chemical shift analysis supports these two pictures, showing that the tryptophan ring occupies one of two positions depending on the adjacent residues. With the exception of the H_α's, all of the protons in Lys5 are downfield of their respective ones in either Lys3 or Lys1 even though Lys5 is cross-strand from Tryp6 which would suggest an upfield shift due to interaction with the aromatic rings. The first picture deals with those peptides that contain a valine at residue 8. Here, the aromatic ring of Tryp6 and the hydrophobic γ-methyl groups Val8 are oriented with each other such that one face of the

tryptophan ring is interacting with the valine via intra-pair van der Waal's contacts (41) while the other face is interacting slightly with the Lys5 protons via cation-π interaction (42) causing them to slightly shift upfield. This is supported by the chemical shifts of the valine in position 8 because the protons interacting with the tryptophan ring shift upfield as is expected due to the increased shielding from the ring. The chemical shifts of Lys5 also show a small amount of upfield shift which indicates packing against the tryptophan ring. However, peptide **2.6** does not follow this model. While the Val8 H_α does shift upfield, the β and γ-protons shift downfield which means the face of the Tryptophan ring is not interacting with that valine. Instead, all of Lys3's protons shift upfield with the exception of H_α and new prominent NOEs can be seen between Lys3 and Tryp6. This combined with the fact that there was very little shift, up or downfield, of Lys5's protons means one face of the Tryptophan ring is now interacting with Lys3 rather than with Val8. This is probably due to the replacement of the methionine with an alanine thus reducing the van der Waal's interactions with Lys3.

The second picture is for peptide **2.4**, which lacks a valine at residue 8. In this picture, the tryptophan ring sits between the two strands partially over the turn and is at an angle with the indole ring facing the rest of the peptide. Here, there is less interaction between the face of the tryptophan ring and the protons of Lys5. Therefore, the Lys5 resonances are shifted slightly downfield. In either picture however, the Lys1 and Lys3 are more upfield due to interactions with each other and the methionine.

Interestingly, peptide **2.4** shows only a small NOE between the H_α's of Leu4 and Ser7, much like the Leu2-Val9 interaction mentioned above. There are however a few notable NOEs between serine and leucine4 which include SerβH-LeuδH, SerβH-LeuβH

and SerβH-Leuβ′H. These imply that the leucine is oriented such that the β-protons point into the *β*-sheet while the δ-methyl's are pointing down and away from the *β*-sheet. It is also important to note the chemical shift of the serine H_α. There is no difference in the serine H_α chemical shift between peptides **2.17** and **2.4**, this is due to the fact that in **2.17**, the Robinson turn helps to keep everything in a tight β-sheet and in **2.4**, the tryptophan ring is over the turn. However, in peptides **2.1** and **2.7**, the tryptophan ring is above the serine H_α shielding it and causing an upfield shift. In peptide **2.6**, the serine H_α is significantly downfield suggesting that the tryptophan ring isn't above it; this is supported by the NOE data.

The NOEs between the Ala8 and Lys3 residues are of significant intensity, The alanine β-proton shows an NOE with the β, β′, δ and γ-protons of Lys3. Although the other peptides possess a valine at position 8, they show the same NOEs with Lys3 and some even show NOEs to Lys1 and Lys5. These cross-strand and diagonal cross-strand NOEs imply that all of the Lysine's are oriented over the *β*-sheet itself and that when there is a valine in position 8, it's γ-methyl groups are aligned with the *β*-sheet and point in opposite directions.

The valine in position 9 has several NOEs, while most are with Leu2 there is one with Leu4 which is quite intense. A few of those with Leu2 include Valγ_2H-LeuγH, Valγ_2H-LeuδH, Valγ_2H-LeuβH, ValβH-LeuαH and ValαH-LeuδH. The NOE with Leu4 is between Valγ_1H and LeuδH. Although the intensity of the NOE between the H_α's of Val9 and Leu2 is quite low, the strengths of the NOEs just mentioned provide compelling evidence that this part of the peptide is indeed a *β*-sheet.

NOEs from Met10 describe an interesting side-chain structure and a particular orientation with Lys1. Some of these include MetεH-LysαH, Metβ′H-Lysβ′H, Metβ′H-LysεH and MetαH-LysεH. Since these residues are attached to either side of the turn, their cross-strand NOEs are proof that the turn does in fact make a *β*-sheet rather than a random coil. Additionally, NOEs are also observed between Met10 and Lys3. Some of the most significant ones are MetεH-LysεH, MetγH-LysεH and MetβH-LysεH. These diagonal cross-strand NOEs help to reinforce the fact that these peptides exist as *β*-sheets despite the lack of a strong NOE between the H_α's of Leu2 and Val9. These NOEs suggest that the methionine side chain is specifically interacting with the two lysine side chains. In addition to the standard Van der Waals interactions, weak hydrogen bonding (43) may exist between the methionine sulfur and the lysine ε-NH protons holding the chains closer in space thus giving rise to more and stronger NOEs between the chains. This idea is supported by the fact that when methionine is replaced by nor-leucine in **2.7**, both the amount and the intensity of the cross-strand NOEs decrease significantly. Furthermore, both the ε and γ-methylenes of the Lys1 experience a significant downfield shift upon the replacement with norleucine. Replacing the methionine residue with a more hydrophobic one removes the hydrogen bonding and causes a change in the side chain conformation, which is evident in **2.7**.

2.3 Experimental Procedures

2.3.1 Materials and Methods

Organic and inorganic reagents (ACS grade) were obtained from commercial sources and used without further purification, unless otherwise noted. Fmoc-protected amino acids and the coupling agent HCTU were obtained from Protein Technologies,

Calbiochem-Novabiochem, or Chem-impex International. 2-Chlorotrityl chloride resin was purchased from Anaspec Inc. All linear peptides were synthesized on the Symphony peptide synthesizer, Protein Technologies Instruments. Solvents for peptide synthesis and reverse-phase HPLC were obtained from Applied Biosystems. Other chemicals used were obtained from Aldrich and were of the highest purity commercially available. Thin layer chromatography (TLC) was performed on glass plates (Whatman) coated with 0.25 mm thickness of silica gel 60Å (# 70-230 mesh). All ^{1}H and ^{13}C NMR spectra were recorded on Bruker 250 MHz, Varian INOVA 400 MHz spectrometer in $CDCl_3$ or unless otherwise specified and chemical shifts are reported in ppm (δ) relative to internal standard tetramethylsilane (TMS). High resolution mass spectra were obtained on an Agilent LC-MSD-TOF.

2.3.2 Peptide Synthesis & Purification

Cyclic III peptide with D-Pro-L-Pro and N-(2-aminoethyl)-N-methylsulfonamido glycine beta-turn promoters.

2-Chlorotrityl chloride resin was treated with Fmoc-Pro-OH and then immediately Fmoc-deprotected using 20% piperidine/2% DBU in DMF. Fmoc quantification of resin indicated a loading of 0.19 mmol/g of resin. For a 25 μmol synthesis, 132 mg of resin was charged to the peptide reaction vessel on a Protein Technologies Symphony Peptide Synthesizer. For each coupling step, 5 equivalents of Fmoc-amino acid and 7.5 equivalents of HCTU are dissolved in 0.4 M NMM in DMF to equal 20 equivalents of NMM, which is added to the reactor. Each coupling reaction was carried out for 10 mins followed by NMP washes. Fmoc deprotection was done using 20% piperidine/2% DBU in DMF for (2 x 2.5 mins). The amino acids used for peptide synthesis were coupled in the following order: Fmoc-D-Pro-OH, Fmoc-Lys(Boc)-OH,

Fmoc-Leu-OH, Fmoc-Lys(Boc)-OH, Fmoc-Leu-OH, Fmoc-Lys(Boc)-OH, Fmoc-$NHCH_2CH_2N(O_2SCH_3)CH_2COOH$, Fmoc-Trp(Boc)-OH, Fmoc-Ser(t-Bu)-OH, Fmoc-Val-OH, Fmoc-Val-OH, and Fmoc-Met-OH. After synthesis of the protected linear HYD1, the resin was transferred to a manual peptide synthesis vessel and treated with 5 mL of a cleavage solution of 20% trifluoroethanol in DCM for 2 hours. The resin was filtered and washed with 5 mL of cleavage solution. This cleavage cycle was repeated twice. The combined organic filtrates were concentrated to give crude protected linear III peptide. The crude III peptide was dissolved in 15 mL of 1% v/v DIEA in DMF and treated with 4 equivalents of HCTU for one hour. After one hour, the reaction mixture was concentrated to give crude protected cyclized III peptidomimetic. The crude peptidomimetic was then treated with a 10 mL solution of 87.5% TFA/5% H_2O/5% phenol/2.5% triethylsilane for 30 mins. The reaction mixture was concentrated and the thick viscous liquid was triturated twice with 10 mL of cold diethyl ether. The reaction contents were centrifuged to give crude cyclic III peptidomimetic. The crude peptidomimetic was dissolved in a solution of 0.1% TFA in H_2O and freeze-dried to give a white fluffy powder. All cyclic III peptides and peptidomimetics were purified using semi-preparative reverse phase HPLC (5 µM particle size C_{18} AAPPTEC spirit column, 25 x 2.12 cm) with eluents: A = 0.1% HCO_2H in H_2O, B = 0.1% HCO_2H in H_3CCN. The purification was carried out using a gradient of 5-50% B Buffer over 40 min with a flow rate 20 mL/minute using 222 nm UV detection. All peaks with retention times expected for peptides were collected and lyophilized. The purified peptides were analyzed using similar analytical HPLC conditions and found to have >95% purity and were structurally characterized using a Bruker Autoflex MALDI-TOF instrument with α-cyano hydroxyl

cinnamic acid (CHCA) as matrix. We have also characterized the secondary structure of selected cyclic III peptidomimetics and they show concentration independent CD spectra in pH 7.0 sodium acetate buffer at concentrations of 200 μM indicative of beta-sheet-like conformations with a minima around 200 nm for cyclic III and a maxima around 190 nm as expected. This supports the assertion of cyclic beta-hairpin-like structure.

Cyclic III peptides with two N-(2-aminoethyl)-N-methylsulfonamidoglycine beta-turn promoters.

2-Chlorotrityl chloride resin was treated with Fmoc-Met-OH and then immediately Fmoc-deprotected using 20% piperidine/2% DBU in DMF. Fmoc quantification of resin indicated a loading of 0.24 mmol/g of resin. For a 25 μmol synthesis, 104 mg of resin was charged to the peptide reaction vessel on a Protein Technologies Symphony Peptide Synthesizer. Everything else was the same as above except the amino acids were coupled in the following order: Fmoc-$NHCH_2CH_2N(O_2SCH_3)CH_2COOH$, Fmoc-Lys(Boc)-OH, Fmoc-Leu-OH, Fmoc-Lys(Boc)-OH, Fmoc-Leu-OH, Fmoc-Lys(Boc)-OH, Fmoc-$NHCH_2CH_2N(O_2SCH_3)CH_2COOH$, Fmoc-Trp(Boc)-OH, Fmoc-Ser(t-Bu)-OH, Fmoc-Val-OH, and Fmoc-Val-OH. We saw no evidence of Met C-terminal racemization from the C-terminal peptide cyclization step, which can be detected by the appearance of diastereomeric peptide side products in the HPLC analysis.

Synthesis of cyclic HYD1 analogs with membrane seeking linker 20 attached to the cysteine side chain on the non-recognition strand.

A stock solution of linker **2.20** (2.3 mg, 4 μmol) in 600 μL DMF was prepared and 42 μL (0.28 μmol) of this stock solution was added to cyclic peptide (1.8 mg, 1.1 μmol). 20% (v/v) DMF in 0.1M Tris-HCl buffer (pH = 8) was then added and the

mixture was stirred for 3-4 hours under inert atmosphere. 200 µL DMF/ mg peptide was used. After completion of the reaction, the reaction contents were quenched by addition of 1M HCl to pH 2. MALDI-TOF analysis of the crude mixture showed the product peak along with the unreacted peptide peak .

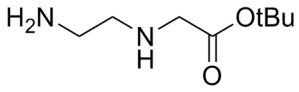

tert-Butyl N-(2-aminoethyl) glycine 2.2

A solution of tert-butyl bromoacetate (27.6 mL, 0.18 mol) in 150 mL DCM was added dropwise to a solution of ethylenediamine (100 mL, 1.5 mol) in 700 mL DCM at 0^{o}C for a period of 30 mins. The reaction mixture was allowed to warm to room temperature and stirred for 15 hours. The reaction mixture was then washed with (2 x 150 mL) water. The aqueous layer was re-extracted with DCM (3 x 100 mL). The combined organic washes were dried using sodium sulfate and then filtered. The solution was concentrated in vacuo to dryness and was used in next step without further purification (27.4 gm, 85%). ^{1}H NMR (250 MHz, $CDCl_3$) δ 3.30 (s, 2H), 2.83 – 2.76 (m, 2H), 2.72 – 2.64 (m, 2H), 1.60 (b, 3H), 1.47 (s, 9H). ^{13}C NMR (63 MHz, $CDCl_3$) ppm 171.54, 80.59, 51.70, 51.21, 41.34, 27.78.

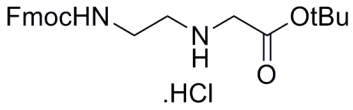

tert-Butyl N-[2-(N-9-fluorenylmethoxycarbonyl)aminoethyl]glycinate hydrochloride 2.3

Compound **2.2** (22 gm, 0.13 mol) was dissolved along with DIEA (22 mL, 0.13 mol) in DCM (1000 mL) and N-(9-fluorenylmethoxycarbonyloxy) succinimide (41 gm, 0.12 mol) in 300 mL DCM was added dropwise over one hour. The reaction contents were stirred overnight and washed with (3 x 100 mL) 1M HCl solution and brine solution (100 mL). The organic contents were dried using Na_2SO_4 and filtered. The solution was partially concentrated to 50 mL and cooled in deep freezer (-20^oC) for overnight. The white precipitate formed was filtered and washed with DCM. The precipitates were vacuum dried to give compound **2.3** as the hydrochloride salt (43.1 gm, 90%). ^1H NMR (400 MHz, DMSO d_6) δ 9.51 (s, 2H), 7.88 (d, *J* = 7.5 Hz, 2H), 7.70 (d, *J* = 7.4 Hz, 2H), 7.65 (d, *J* = 5.5 Hz, 1H), 7.41 (t, *J* = 7.4 Hz, 2H), 7.33 (t, *J* = 7.3 Hz, 2H), 4.31 (d, *J* = 6.7 Hz, 2H), 4.23 (d, *J* = 6.6 Hz, 1H), 3.86 (s, 2H), 3.49 – 3.26 (m, 2H), 3.02 (t, *J* = 5.9 Hz, 2H), 1.45 (s, 9H). ^{13}C NMR (101 MHz, DMSO d_6) ppm 165.52, 156.21, 143.77, 140.70, 127.60, 127.04, 125.17, 120.09, 82.91, 65.64, 54.91, 47.19, 46.63, 46.37, 36.59, 27.59.

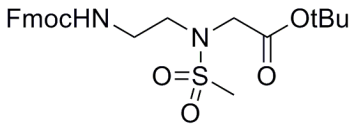

tert-Butyl N-[2-(N-9-fluorenylmethoxycarbonyl)aminoethyl N-methylsulfonamido glycinate 2.4

Compound **2.3** (5.0 gm, 11.5 mmol) was suspended in 50 mL of THF and DIEA (4.0 mL, 23.1 mmol) was added to it at 0^oC. Methanesulfonyl chloride (0.9 mL, 11.5 mmol) was added dropwise for period of 10 mins. The reaction mixture was stirred for two hours and allowed to warm to room temperature. The mixture was evaporated to dryness in vacuum and the residue was partitioned between DCM and water. The organic layer was partially concentrated and kept in the refrigerator overnight. The white precipitate that formed was

filtered and dried in vacuuo. (4.8 gm, 88%) ^{1}H NMR (250 MHz, $CDCl_3$) δ 7.76 (d, *J* = 7.1 Hz, 2H), 7.61 (d, *J* = 7.3 Hz, 2H), 7.44 – 7.27 (m, 5H), 5.48 (s, 1H), 4.38 (d, *J* = 7.1 Hz, 2H), 4.28 – 4.18 (m, 1H), 4.02 (s, 2H), 3.38 (d, *J* = 12.6 Hz, 4H), 3.01 (s, 3H), 1.48 (s, 9H).^{13}C NMR (63 MHz, $CDCl_3$) ppm 169.04, 156.58, 143.93, 141.30, 127.69, 127.09, 125.18, 119.96, 82.97, 66.95, 49.45, 47.94, 47.19, 39.71, 39.20, 28.04.

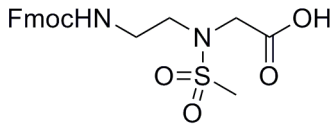

2-(N-(2-(((9H-fluoren-9-yl)methoxy)carbonylamino)ethyl)methylsulfonamido)acetic acid 2.5

Compound **2.4** (4.8 gm, 10 mmol) was dissolved in 1,4-dioxane and 4M HCl was added to it. After completion of the reaction, reaction contents were filtered to give compound **2.5** as white solid in quantitative yield (4.1 gm). ^{1}H NMR (400 MHz, DMSO d_6) δ 12.93 (s, 1H), 7.90 (d, *J* = 7.5 Hz, 2H), 7.69 (d, *J* = 7.4 Hz, 2H), 7.43 (t, *J* = 7.4 Hz, 2H), 7.34 (t, *J* = 7.3 Hz, 2H), 4.32 (d, *J* = 6.9 Hz, 2H), 4.23 (t, *J* = 6.8 Hz, 1H), 4.01 (s, 2H), 3.36 (s, 1H), 3.29 (t, *J* = 6.3 Hz, 2H), 3.20 (dd, *J* = 12.0, 6.0 Hz, 2H), 2.98 (s, 3H). ^{13}C NMR (101 MHz, DMSO) ppm 170.99, 156.13, 143.88, 140.73, 127.60, 127.06, 125.13, 120.10, 65.45, 48.25, 46.98, 46.74, 39.02, 38.87.

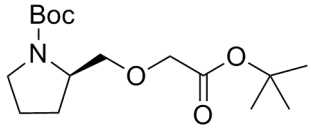

I-tert-butyl 2-((2-tert-butoxy-2-oxoethoxy)methyl)pyrrolidine-1-carboxylate 2.7

To a solution of **2.6** (0.5 gm, 2.5 mmol) in toluene (10 mL) were added 30% NaOH solution (6 mL), tert-butyl bromoacetate (0.73 mL, 5.0 mmol) and TBAI (0.46 gm, 1.2 mmol) at 0^{o}C. The reaction was carried out for 3 hrs until the TLC showed complete

consumption of starting material. The reaction mixture was diluted with water (5 mL) before extracting with ethyl acetate (3 x 20 mL). The combined organic layer was washed with 1M HCl (10 mL), brine (10 mL) and dried over Na_2SO_4. The organic layer was concentrated to leave a residue which was further purified by column chromatography to give compound **2.7** (0.6 gm) in 77% yield. ^{1}H NMR (250 MHz, $CDCl_3$) δ 3.89 (s, 2H), 3.88 – 3.81 (m, 1H), 3.55 (d, *J* = 6.1 Hz, 1H), 3.26 (s, 2H), 1.88 (tdt, *J* = 28.0, 23.0, 9.0 Hz, 4H), 1.40 (s, 9H), 1.39 (s, 9H). ^{13}C NMR (63 MHz, $CDCl_3$) ppm 169.69, 154.47, 81.45, 79.21, 72.04, 68.96, 56.30, 46.40, 28.49, 28.08, 23.78, 22.88.

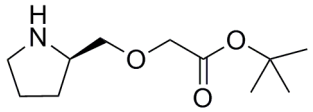

1-tert-butyl 2-(pyrrolidin-2-ylmethoxy)acetate 2.8

Compound **2.7** (0.6 gm, 1.8 mmol) was dissolved in 15 mL DCM and 5 mL trifluoroacetic acid was added to it. The reaction contents were stirred until the starting material was completely consumed. The reaction mixture was concentrated to dryness in vacuo and was used in the next step without further purification.

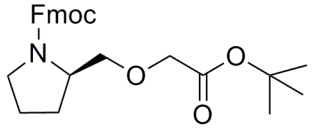

I-(9H-fluoren-9-yl)methyl 2-((2-tert-butoxy-2-oxoethoxy)methyl)pyrrolidine-1-carboxylate 2.9

Compound **2.8** (0.5 gm, 1.8 mmol) was dissolved in 20 mL DCM and DIEA (1.0 mL, 5.4 mmol) was added to it. The reaction mixture was cooled to 0^{o}C and FmocOSu (0.6 gm, 1.8 mmol) was added to it. The reaction contents were allowed to warm to room

temperature and stirred for two hours. The reaction mixture was concentrated in vacuo and residue was partitioned between DCM (20 mL) and H_2O (15 mL). The organic layer was dried, filtered, concentrated and chromatographed using EtOAc/Hexane (4:1) as eluent to give compound **2.9** (0.55 gm) in 79%yield. ^{1}H NMR (250 MHz, $CDCl_3$) δ 7.61 (d, *J* = 7.4 Hz, 2H), 7.45 (d, *J* = 7.1 Hz, 2H), 7.28 – 7.13 (m, 4H), 4.39 (d, *J* = 5.6 Hz, 1H), 4.22 (d, *J* = 5.8 Hz, 1H), 4.08 (t, *J* = 6.9 Hz, 1H), 3.91 – 3.78 (m, 2H), 3.59 (d, *J* = 3.6 Hz, 1H), 3.55 – 3.48 (m, 1H), 3.47 – 3.38 (m, 1H), 3.33 – 3.17 (m, 2H), 1.87 – 1.43 (m, 4H), 1.32 (s, 9H).

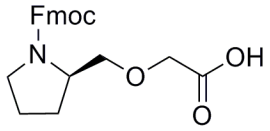

I-2-((1-(((9H-fluoren-9-yl)methoxy)carbonyl)pyrrolidin-2-yl)methoxy)acetic acid 2.10

Compound **2.9** (0.6 gm, 1.3 mmol) was dissolved in 10 mL DCM and 10 mL trifluoroacetic acid was added to it. The reaction contents were stirred until the starting material was completely consumed to give compound **2.10** in quantitative yield. ^{1}H NMR (400 MHz, $CDCl_3$) δ 7.76 (d, *J* = 7.5 Hz, 2H), 7.58 (d, *J* = 7.3 Hz, 2H), 7.40 (t, *J* = 7.4 Hz, 2H), 7.32 (t, *J* = 7.4 Hz, 2H), 4.64 (t, *J* = 23.4 Hz, 1H), 4.43 (s, 1H), 4.21 (t, *J* = 26.2 Hz, 3H), 3.77 (d, *J* = 20.2 Hz, 1H), 3.61 (d, *J* = 23.2 Hz, 1H), 3.41 (t, *J* = 34.1 Hz, 3H), 3.00 (d, *J* = 36.5 Hz, 1H), 1.88 (d, *J* = 42.5 Hz, 4H). ^{13}C NMR (101 MHz, $CDCl_3$) ppm 174.54, 159.10, 144.01, 127.99, 127.38, 125.22, 120.20, 72.71, 71.81, 68.49, 67.94, 47.45, 47.11, 29.93, 23.97.

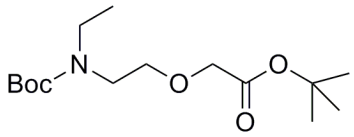

tert-butyl 2-(2-(tert-butoxycarbonyl(ethyl)amino)ethoxy)acetate 2.12

2-ethylaminoethanol (2.2 mL, 23.7 mmol) was dissolved in DCM (10 mL) and cooled to 0^{o}C. $(Boc)_2O$ (5.2 gm, 23.7 mmol) dissolved in DCM (20 mL) was added to it and the reaction was monitored by TLC until the starting material was completely consumed. The reaction mixture was partitioned between DCM (50 mL) and H_2O (20 mL). The organic layer was further washed with 1M HCl (15 mL) and brine (15 mL). The organic layer was dried, filtered, and concentrated to give tert-butyl ethyl(2-hydroxyethyl) carbamate (3.8 gm) in 90 % yield. To a solution of the Boc protected compound (1.0 gm, 5.3 mmol) in toluene (15 mL) were added 30% NaOH solution (12 mL), tert-butyl bromoacetate (1.6 mL, 10.6 mmol) and TBAI (1.0 gm, 2.65 mmol) at 0^{o}C. The reaction was carried out for 3 hrs until the TLC showed complete consumption of starting material. The reaction mixture was diluted with water (10 mL) before extracting with ethyl acetate (3 x 20 mL). The combined organic layer was washed with 1M HCl (20 mL), brine (20 mL) and dried over Na_2SO_4. The organic layer was concentrated to leave a residue which was further purified by column chromatography to give compound **2.12** in (1.45 gm) in 90 % yield. ^{1}H NMR (400 MHz, $CDCl_3$) δ 3.86 (d, *J* = 8.6 Hz, 2H), 3.52 (s, 2H), 3.25 (d, *J* = 37.1 Hz, 4H), 1.36 (t, *J* = 8.7 Hz, 18H), 0.99 (dd, *J* = 14.7, 7.1 Hz, 3H). ^{13}C NMR (101 MHz, $CDCl_3$) ppm 169.62, 155.68, 81.63, 79.45, 70.32, 69.05, 46.63, 43.41, 42.88, 28.56, 28.19, 13.76.

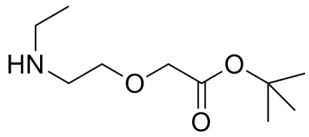

tert-butyl 2-(2-(ethylamino)ethoxy)acetate 2.13

Compound **2.12** (1.5 gm, 5.1 mmol) was dissolved in 15 mL DCM and 5 mL trifluoroacetic acid was added to it. The reaction contents were stirred until the starting material was completely consumed. The reaction mixture was concentrated to dryness in vacuo and was used directly in the next step without further purification.

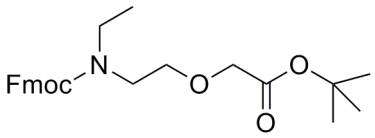

tert-butyl 2-(2-((((9H-fluoren-9-yl)methoxy)carbonyl)(ethyl)amino)ethoxy)acetate 2.14

Compound **2.13** (1.6 gm, 5.1 mmol) was dissolved in 20 mL DCM and DIEA (2.7 mL, 15.4 mmol) was added to it. The reaction mixture was cooled to 0^{o}C and FmocOSu (1.7 gm, 5.1 mmol) was added to it. The reaction contents were allowed to warm to room temperature and stirred for two hours. The reaction mixture was concentrated in vacuo and the residue was partitioned between DCM (40 mL) and H_2O (15 mL). The organic layer was dried, filtered, concentrated, and chromatographed to give compound **2.14** in (1.78 gm) 85% yield. ^{1}H NMR (250 MHz, $CDCl_3$) δ 7.78 (d, *J* = 7.2 Hz, 2H), 7.62 (d, *J* = 6.4 Hz, 2H), 7.46 – 7.28 (m, 4H), 4.58 – 4.39 (m, 2H), 4.32 – 4.20 (m, 1H), 3.91 (d, *J* = 38.7 Hz, 2H), 3.68 (d, *J* = 4.3 Hz, 1H), 3.49 (b, 1H), 3.40 – 3.17 (m, 4H), 1.51 (s, 9H), 1.16 – 0.96 (m, 3H). ^{13}C NMR (63 MHz, $CDCl_3$) ppm 169.50, 156.15, 144.18, 141.40, 127.64, 127.06, 124.94, 119.95, 81.61, 69.99, 68.94, 67.11, 47.42, 47.05, 43.45, 28.13, 13.62.

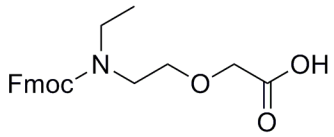

2-(2-((((9H-fluoren-9-yl)methoxy)carbonyl)(ethyl)amino)ethoxy)acetic acid 2.15

Compound **2.14** (1.8 gm, 4.2 mmol) was dissolved in 10 mL DCM and 10 mL of trifluoroacetic acid was added to it. The reaction contents were stirred until the starting material was completely consumed to give compound **2.15** in quantitative yield. ^{1}H NMR (400 MHz, DMSO d_6) δ 7.87 (d, *J* = 7.4 Hz, 2H), 7.64 (d, *J* = 7.3 Hz, 2H), 7.40 (t, *J* = 7.4 Hz, 2H), 7.33 (t, *J* = 7.1 Hz, 2H), 4.41 (d, *J* = 5.8 Hz, 2H), 4.29 – 4.25 (m, 1H), 3.99 – 3.86 (m, 2H), 3.49 (s, 1H), 3.29 (s, 1H), 3.26 – 3.12 (m, 4H), 3.11 – 3.02 (m, 1H), 0.89 (d, *J* = 67.3 Hz, 3H). ^{13}C NMR (101 MHz, DMSO d_6) ppm 171.49, 155.15, 154.81, 144.03, 140.85, 127.53, 127.06, 124.82, 120.02, 68.84, 68.55, 67.47, 66.19, 51.35, 46.82, 46.09, 45.70, 42.38, 41.94, 13.32, 12.95.

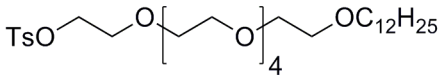

3,6,9,12,15,18-hexaoxatriacontyl 4-methylbenzenesulfonate 2.17

Hexaethylene glycol monododecyl ether **2.16** (1.0 gm, 2.2 mmol) and p-toluenesulfonyl chloride (0.6 gm, 2.2 mmol) were dissolved in DCM (15 mL). Powdered KOH (0.5 gm, 8.8 mmol) was added to it in small lots so that temperature remains below 5^{o}C. The reaction was carried out for 3 hrs. The reaction mixture was partitioned between DCM (15 mL) and 10% $NaHCO_3$ (10 mL). The organic layer was dried using Na_2SO_4, filtered and concentrated to give a clear oil. This oil was chromatographed using flash silica to give compound **2.17** (1.1 gm) in 85% yield. ^{1}H NMR (250 MHz, $CDCl_3$) δ 7.87 – 7.73 (m, 2H), 7.35 (d, *J* = 8.0 Hz, 2H), 4.23 – 4.08 (m, 2H), 3.76 – 3.53 (m, 22H), 3.45 (t, *J* =

6.8 Hz, 2H), 1.56 (dd, *J* = 13.5, 6.7 Hz, 2H), 1.26 (s, 18H), 0.88 (t, *J* = 6.6 Hz, 3H). ^{13}C NMR (63 MHz, $CDCl_3$) ppm 144.80, 132.96, 129.83, 127.99, 71.54, 70.74, 70.57, 70.04, 69.26, 68.66, 31.92, 29.64, 29.50, 29.36, 26.09, 22.69, 21.66, 14.15.

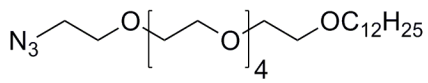

1-azido-3,6,9,12,15,18-hexaoxatriacontane 2.18

Compound **2.17** (1.3 gm, 2.1 mmol) was dissolved in DMF (15 mL) and NaN_3 (0.3 gm, 4.3 mmol) was added to it. The reaction mixture was heated at 80^{o}C for 18 hrs. The reaction mixture was concentrated in vacuo and chromatographed using EtOAc/Hexane (4:1) as eluent to give compound **2.18** (1.1 gm) in 96% yield. ^{1}H NMR (250 MHz, $CDCl_3$) δ 3.76 – 3.66 (m, 20H), 3.65 – 3.59 (m, 2H), 3.45 (dt, *J* = 8.1, 5.0 Hz, 4H), 1.61 (dd, *J* = 13.3, 6.6 Hz, 2H), 1.30 (s, 18H), 0.92 (t, *J* = 6.6 Hz, 3H). ^{13}C NMR (63 MHz, $CDCl_3$) ppm 71.54, 70.69, 70.66, 70.62, 70.58, 70.04, 50.66, 31.91, 29.66, 29.63, 29.61, 29.49, 29.35, 26.08, 22.68, 14.13.

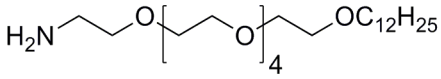

3,6,9,12,15,18-hexaoxatriacontan-1-amine 2.19

Compound **2.18** (0.7 gm, 2.1 mmol) was taken up in MeOH and 10% Pd/C was added to it. Hydrogenation was carried overnight at 50 psi. The reaction contents were filtered over diatomaceous earth and concentrated to give compound **2.19** (0.83 gm) in 84% yield.

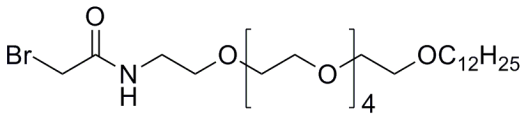

2-bromo-N-3,6,9,12,15,18-hexaoxatriacontylacetamide 2.20

Compound **2.19** (0.7 gm, 1.6 mmol) was suspended in 8 mL DCM and 8 mL saturated aqueous Na_2CO_3 solution was added to it. The reaction mixture was cooled to 0^oC and bromoacetyl bromide (0.4 gm, 1.8 mmol) was added to it. The reaction contents were allowed to warm to room temperature and stirred for two hours. The reaction mixture was concentrated in vacuo and residue was partitioned between EtOAc (20 mL) and H_2O (15 mL). The organic layer was dried, filtered, concentrated and chromatographed using EtOAc/Hexane (4:1) as eluent to give compound **2.20** (0.66 gm) in 93% yield. ^1H NMR (250 MHz, $CDCl_3$) δ 7.09 (s, 1H), 3.86 (s, 2H), 3.65 – 3.52 (m, 22H), 3.51 – 3.35 (m, 4H), 1.63 – 1.43 (m, 2H), 1.24 (s, 20H), 0.86 (t, *J* = 6.4 Hz, 3H). ^{13}C NMR (63 MHz, $CDCl_3$) ppm 165.79, 71.52, 70.56, 70.33, 70.02, 69.34, 39.92, 31.90, 29.60, 29.48, 29.33, 29.12, 26.07, 22.67, 14.13.

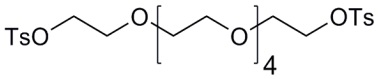

3,6,9,12,15-pentaoxaheptadecane-1,17-diyl bis(4-methylbenzenesulfonate) 2.22

Hexaethylene glycol **2.21** (1.0 gm, 3.5 mmol) and p-toluenesulfonyl chloride (1.4 gm, 7.1 mmol) were dissolved in DCM (10 mL). Powdered KOH (1.6 gm, 28.3 mmol) was added to it in small lots so that temperature remains below 5^oC. The reaction was carried out for 3 hrs. The reaction mixture was partitioned between DCM (15 mL) and 10% $NaHCO_3$ (10 ml). The organic layer was dried using Na_2SO_4, filtered, and concentrated to give a clear oil. The crude oil was chromatographed using flash silica to give compound **2.22**

(1.54 gm) in 74% yield. ^{1}H NMR (250 MHz, $CDCl_3$) δ 7.80 (d, *J* = 8.3 Hz, 4H), 7.35 (d, *J* = 8.0 Hz, 4H), 4.20 – 4.12 (m, 4H), 3.72 – 3.65 (m, 4H), 3.62 (s, 7H), 3.58 (s, 8H), 2.45 (s, 6H). ^{13}C NMR (63 MHz, $CDCl_3$) ppm 144.86, 132.91, 129.86, 127.97, **70.71**, 70.59, 70.53, 70.48, 69.30, 68.65, 21.66.

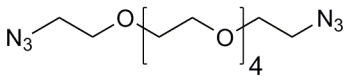

1,17-diazido-3,6,9,12,15-pentaoxaheptadecane 2.23

Compound **2.22** (1.5 gm, 2.6 mmol) was dissolved in DMF (15 mL) and NaN_3 (0.7 gm, 10.4 mmol) was added to it. The reaction mixture was heated at 80^{0}C for 18 hrs. The reaction mixture was concentrated in vacuo and chromatographed using EtOAc/Hexane (4:1) as eluent to give compound **2.23** (0.74 gm) in 85% yield. ^{1}H NMR (250 MHz, $CDCl_3$) δ 3.71 – 3.63 (m, *J* = 5.8, 2.8 Hz, 5H), 3.39 (t, *J* = 5.0 Hz, 1H).

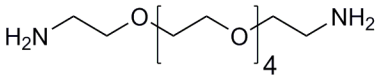

3,6,9,12,15-pentaoxaheptadecane-1,17-diamine 2.24

Compound **2.23** (0.75 gm, 2.1 mmol) was taken up in MeOH and 10% Pd/C was added to it. Hydrogenation was carried overnight at 50 psi. The reaction contents were filtered over diatomaceous earth and concentrated to give compound **2.24**.

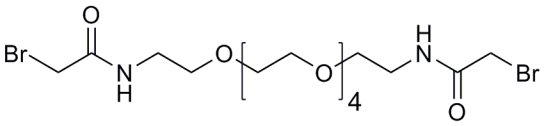

N,N'-(3,6,9,12,15-pentaoxaheptadecane-1,17-diyl)bis(2-bromoacetamide) 2.25

Compound **2.24** (0.6 gm, 2.1 mmol) was suspended in 10 mL DCM and 10 mL saturated aqueous Na_2CO_3 solution was added to it. The reaction mixture was cooled to 0^{o}C and

bromoacetyl bromide (1.0 gm, 4.7 mmol) was added to it. The reaction contents were allowed to warm to room temperature and stirred for two hours. The reaction mixture was concentrated in vacuo and the residue was partitioned between EtOAc (20 mL) and H_2O (15 mL). The organic layer was dried, filtered, concentrated and chromatographed using EtOAc/Hexane (4:1) as eluent to give compound **2.25** (0.93 gm) in 81% yield. ^{1}H NMR (250 MHz, $CDCl_3$) δ 3.90 (s, 4H), 3.67 (d, *J* = 6.2 Hz, 16H), 3.63 – 3.57 (m, 5H), 3.49 (dd, *J* = 10.1, 5.1 Hz, 4H). ^{13}C NMR (63 MHz, $CDCl_3$) ppm 166.02, 70.56, 70.28, 69.44, 39.95, 29.17.

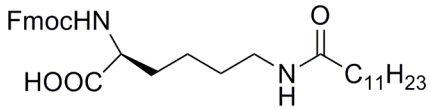

(S)-2-(((9H-fluoren-9-yl)methoxy)carbonylamino)-6-dodecanamidohexanoic acid 2.28

Fmoc-Lys(Boc)-OH (2.5 gm, 5.3 mmol) **2.26** was dissolved in 15 mL 1,4-dioxane and 15 mL 4M HCl was added to it. After completion of the reaction, the reaction mixture was concentrated in vacuo. The white solid was filtered and dried to give compound **2.27** as the hydrochloride salt in quantitative yield. Compound **2.26** (1.0 gm, 2.5 mmol) was dissolved in 15 mL dioxane and sodium carbonate (0.8 gm, 7.4 mmol) in 15 mL H_2O was added dropwise at 0^{o}C. After 5 min, lauroyl chloride (0.6 mL, 2.6 mmol) in 10 mL dioxane was added to the reaction mixture. The reaction mixture was allowed to warm to room temperature and stirred overnight. After completion of reaction, the reaction contents were taken up in 125 mL DCM and washed with saturated $NaHCO_3$ (1 x 20 mL), 1M HCl (1 x 10 mL) and brine (1 x 20 mL). The organic layer was dried, filtered, concentrated, and chromatographed to give compound **2.28** as white solid in 72 %

yield. ^{1}H NMR (400 MHz, cdcl$_3$) δ 7.74 (d, *J* = 7.5 Hz, 2H), 7.59 (t, *J* = 8.0 Hz, 2H), 7.37 (t, *J* = 7.4 Hz, 2H), 7.30 – 7.25 (m, 2H), 5.82 (s, 2H), 4.49 – 4.30 (m, 3H), 4.19 (t, *J* = 7.2 Hz, 1H), 3.31 – 3.13 (m, 2H), 2.18 – 2.11 (m, 2H), 1.92 – 1.76 (m, 1H), 1.65 – 1.35 (m, 6H), 1.28 – 1.19 (m, 17H), 0.87 (dd, *J* = 8.5, 5.3 Hz, 3H). ^{13}C NMR (101 MHz, CDCl$_3$) ppm 175.29, 174.63, 156.53, 143.93, 141.48, 127.92, 127.30, 125.40, 120.17, 67.30, 53.83, 47.36, 39.30, 36.99, 32.13, 29.84, 29.73, 29.57, 29.52, 26.02, 22.91, 22.36, 14.35.

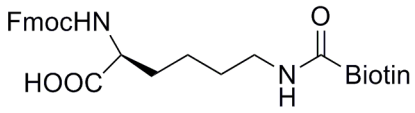

(S)-2-(((9H-fluoren-9-yl)methoxy)carbonylamino)-6-(5-((3aS,4S,6aR)-2-oxohexahydro-1H-thieno[3,4-d]imidazol-4-yl)pentanamido)hexanoic acid 2.29

Compound **2.27** (0.4 gm, 1.0 mmol) was dissolved in 10 mL DCM and DIEA (0.5 mL, 2.9 mmol) was added to it. Chlorotrimethyl silane (0.25 mL, 2.0 mmol) was added and reaction contents were heated until a homogenous solution was obtained. After 30 mins, the reaction contents were cooled to 0^{o}C and Biotin-Onp (0.4 gm, 1.0 mmol) were added. The reaction was stirred for 3 hrs and washed with 5% NaHCO$_3$ (10 mL), 1M HCl (1 x 10 mL). The organic layers were filtered, dried and concentrated. To the resulting crude reaction mass was added 15 mL cold MeOH. The resulting gelatinous white solid was filtered, washed with MeOH to afford pure Fmoc-Lys(Biotin)-OH **2.29** as white solid in 65% yield. ^{1}H NMR (250 MHz, DMSO) δ 12.64 (s, 1H), 7.91 (d, *J* = 7.4 Hz, 2H), 7.74 (d, *J* = 7.4 Hz, 2H), 7.43 (t, *J* = 7.1 Hz, 2H), 7.34 (t, *J* = 7.0 Hz, 2H), 6.45 (s, 1H), 6.39 (s, 1H), 4.27 (m, 4H), 4.16 – 4.08 (m, 1H), 3.91 (m, 1H), 3.06 (m, 3H), 2.82 (dd, *J* = 12.4, 5.0 Hz, 1H), 2.57 (d, *J* = 12.4 Hz, 1H), 2.05 (t, *J* = 7.1 Hz, 2H), 1.74 – 1.23 (m, 12H). ^{13}C NMR (63 MHz, DMSO) ppm 174.01, 171.79, 162.68, 156.12, 143.77, 140.68, 127.62,

127.05, 125.28, 120.10, 65.56, 60.99, 59.13, 55.40, 53.78, 46.61, 38.14, 35.19, 30.43, 28.74, 28.20, 28.00, 25.29, 23.08.

Circular Dichroism Measurement

Circular dichroism experiments were carried out at room temperature on the Aviv (Model # 210) spectropolarimeter flushed with nitrogen. The samples were prepared as stock solutions in sodium acetate buffer and diluted to the desired concentration for measurements. Each spectra was collected from 250 to 184 nm using a 0.1 cm path length cylindrical quartz cell. Each spectrum was recorded as an average of three scans taken at a spectral bandwidth of 1 nm. All spectra were corrected for buffer contributions and presented in units of molar ellipticity.

NMR Spectroscopy

All deuterated reagents and solvents were purchased from Cambridge Isotopes. NMR samples were made by dissolving 1-2 mg peptide in 100 μL D_2O and then adjusting the pD to 4.0 (uncorrected) with either 50 mM NaOAc-d_3 or 50 mM AcOH-d_4 to yield a final concentration between 3-7 mM. Chemical shifts are reported in parts per million (ppm) relative to 0.5 mM DSS. NMR experiments were run and processed on a three-channel Varian Inova 500MHz instrument at 298.1 K using a 3-mm I.D. RT probe equipped with Z-axis PFGs running VnmrJ 2.2D. Spectra were then analyzed using ACD labs NMR Manager version 11.0. 1D NMR spectra were collected using 32K data points, between 16 and 64 scans were collected using a 0.5 s delay and 1 s presaturation. 2D TOCSY and NOESY experiments were run with a 5000 Hz window in both dimensions. TOCSY experiments were run with a mixing time of 60 ms, a 0.5 s relaxation delay followed by 1 s of presaturation and 512 increments in the f_1 dimension

with 32 transients per increment (collecting 4096 data points per transient in the f_2 dimension). Zero-filling was then applied using 4096 points for each dimension. NOESY experiments were performed using a 500 ms mixing time, 1 s of presaturation and 512 increments of 32 transients each (collecting 4096 data points per transient in the f_2). Zero-filling was then applied using 4096 points for each dimension. Presaturation was used to suppress the water resonance both during the relaxation delay and during the mixing time. All spectra were analyzed using standard window functions (Gaussian without shifting). Assignments were made by using standard methods as described by Wüthrich (44).

2D NMR Data

Table 2.5 NMR assignments for peptide **2.1.**

	α	β	γ	δ	ε
Lys-1	4.574	1.657, 1.765	1.286	1.589	2.879
Leu-2	4.281	1.945	1.622	0.923, 0.845	
Lys-3	4.076	1.642, 1.759	1.285, 1.373	1.588	2.874
Leu-4	4.349	1.554	1.427	0.782, 0.767	
Lys-5	4.262	1.774, 1.823	1.402, 1.432	1.642	2.976
Trp-6	4.701	3.172	7.140, 7.121, 7.238, 7.473, 7.590		(5H, 2H, 6H, 7H, 4H)
Ser-7	4.462	3.778			
Val-8	4.320	1.911	0.772, 0.816		
Val-9	4.662	1.637	0.801, 0.874		
Met-10	4.643	1.989, 2.155	2.522, 2.575		2.072

Table 2.6a NMR assignments for peptide **2.6.**

	α	B	γ	δ	ε
Lys-1	4.516	1.745, 1.647	1.291	1.564	2.869
Leu-2	4.282	1.540	1.427	0.787, 0.768	
Lys-3	4.081	1.750, 1.638	1.339, 1.261	1.555	2.845
Leu-4	4.311	1.946	1.892	0.836, 0.763	
Lys-5	4.438	1.823, 1.779	1.423	1.662	2.977
Trp-6	4.668	3.153, 3.172	7.146, 7.141, 7.244, 7.478, 7.615		(5H, 2H, 6H, 7H, 4H)
Ser-7	4.697	3.754, 3.803			
Val-8	4.184	1.950	0.860, 0.934		
Val-9	4.629	1.623	0.792, 0.865		
Ala-10	4.419	1.383			

Table 2.6b NMR assignments for peptide **2.7.**

	α	β	γ	δ	ε
Lys-1	4.590	1.638, 1.731	1.310, 1.388	1.589	2.943
Leu-2	4.375	1.985	1.618	0.836, 0.914	
Lys-3	4.086	1.682, 1.750	1.266, 1.369	1.584	2.869
Leu-4	4.292	1.579	1.467	0.807, 0.821	
Lys-5	4.287	1.691, 1.799	1.379, 1.437	1.623	2.943
Trp-6	4.595	3.246, 3.207	7.112, 7.141, 7.239, 7.483, 7.581		(2H, 5H, 6H, 7H, 4H)
Ser-7	4.453	3.802			
Val-8	4.639	1.589	0.811, 0.861		
Val-9	4.673	2.038	0.880, 0.895		
Nor-10	4.453	1.794	1.711	1.276	0.851

Table 2.6c NMR assignments for peptide **2.10.**

	α	β	γ	δ	ε
Lys-1	4.345	1.770, 1.819	1.393, 1.437	1.687	2.977
Leu-2	4.365	1.633	1.525	0.875, 0.905	
Lys-3	4.052	1.608, 1.731	1.354	1.535	2.943
Leu-4	4.531	1.657	1.535	0.851, 0.895	
Lys-5	4.174	1.652, 1.770	1.345	1.379	2.967
Met-6	4.453	1.941, 2.048	2.498, 2.562		2.083
Val-7	4.096	2.009	0.924, 0.939		
Val-8	4.517	1.496	0.782, 0.816		
Ser-9	4.512	3.774, 3.754			
Trp-10	4.834	3.212, 3.436	7.141, 7.234, 7.268, 7.493, 7.630		(5H, 6H, 2H, 7H, 4H)

For the NOE figures below, arrows drawn in red indicate a weak NOE enhancement. Arrows drawn in green indicate a medium NOE enhancement while those drawn in black indicate a strong NOE enhancement.

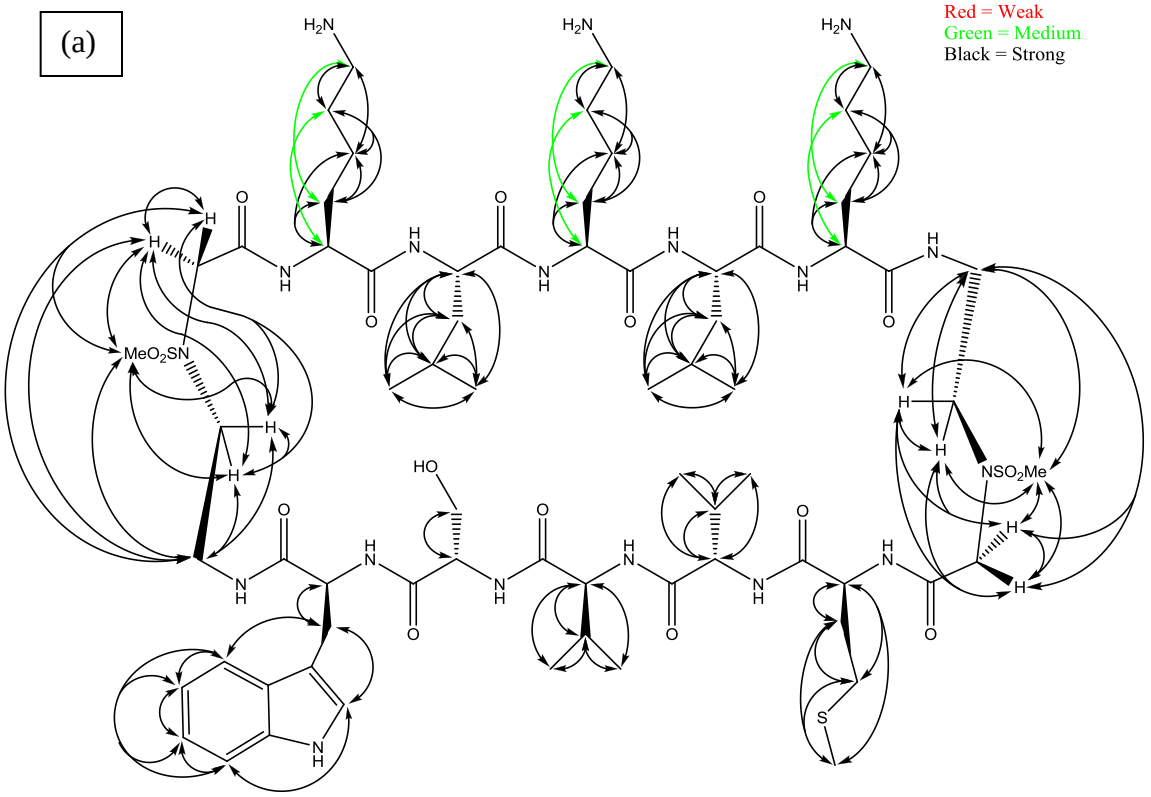
(a)
Red = Weak
Green = Medium
Black = Strong
H_2N
MeO_2SN
HO
NSO_2Me
S

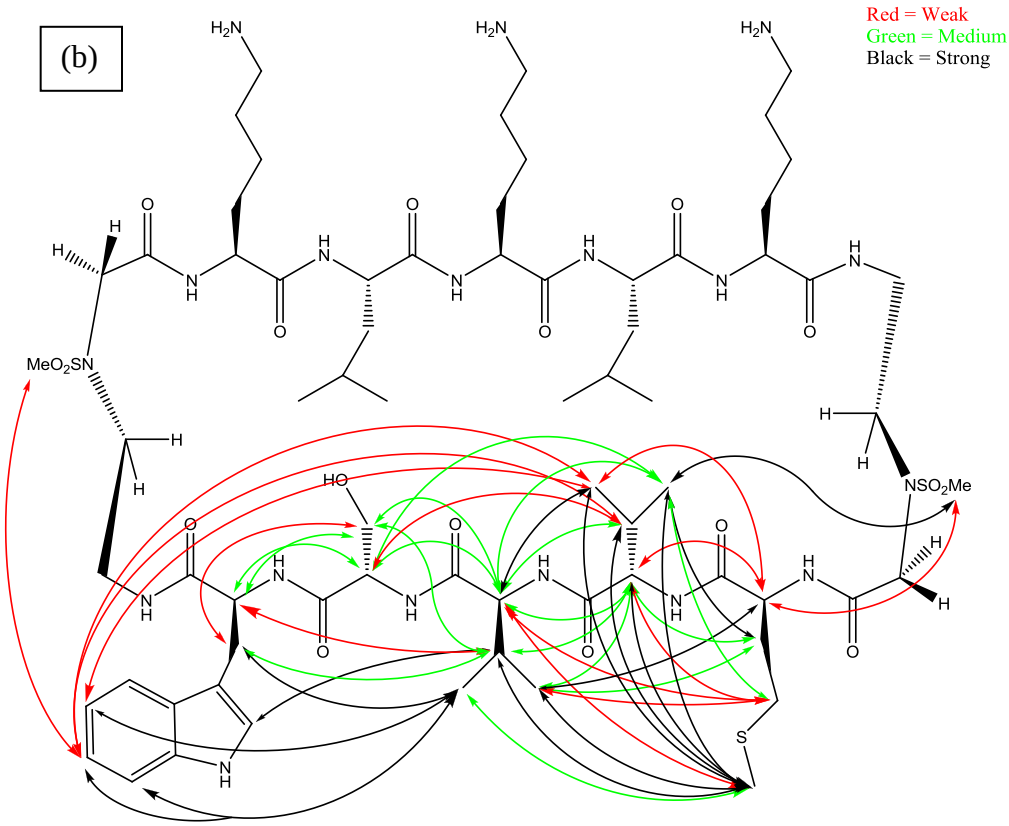
(b)
Red = Weak
Green = Medium
Black = Strong
H_2N
MeO_2SN
HO
NSO_2Me
S

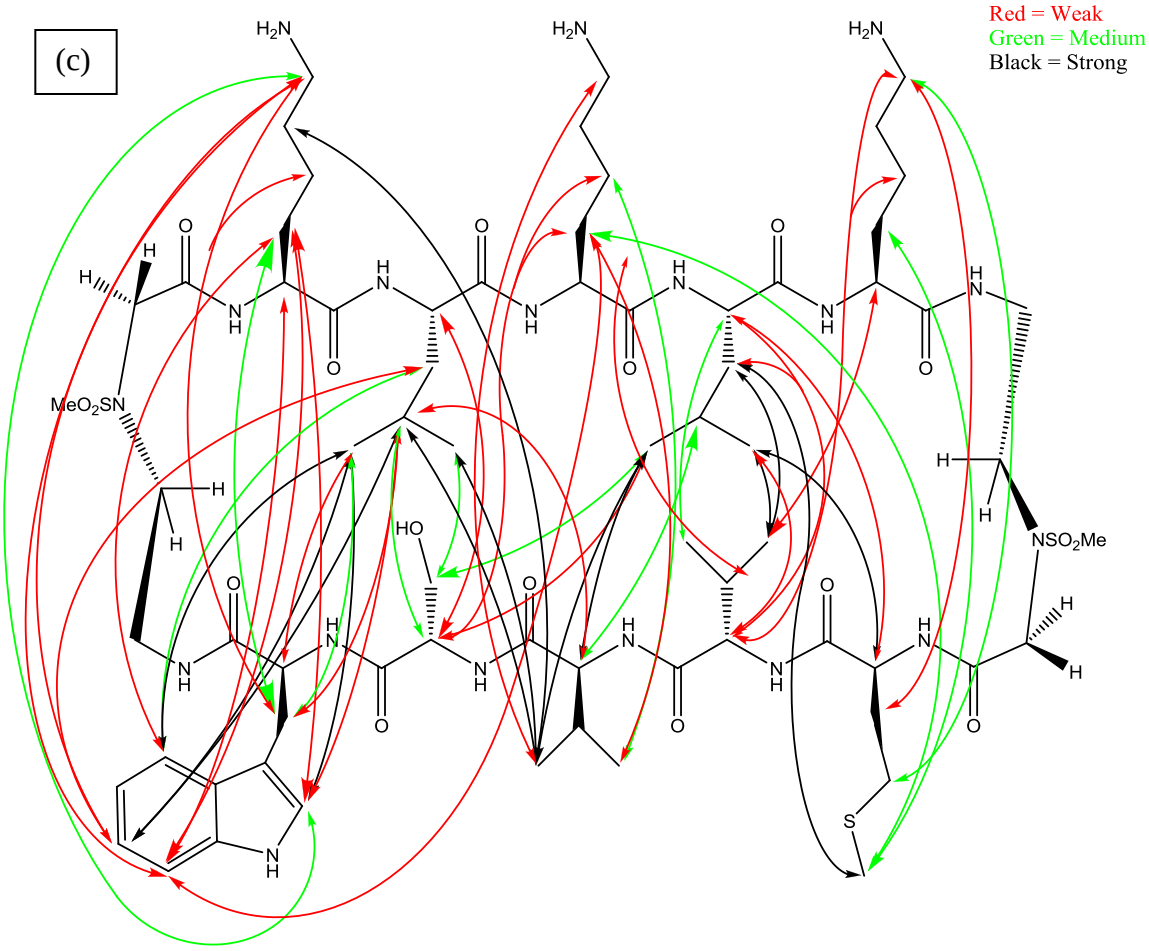

Fig. 2.10 Peptide **2.1** NOEs: (a) Intra-residue NOEs; (b) Same-strand NOEs; (c) Cross-strand NOEs.

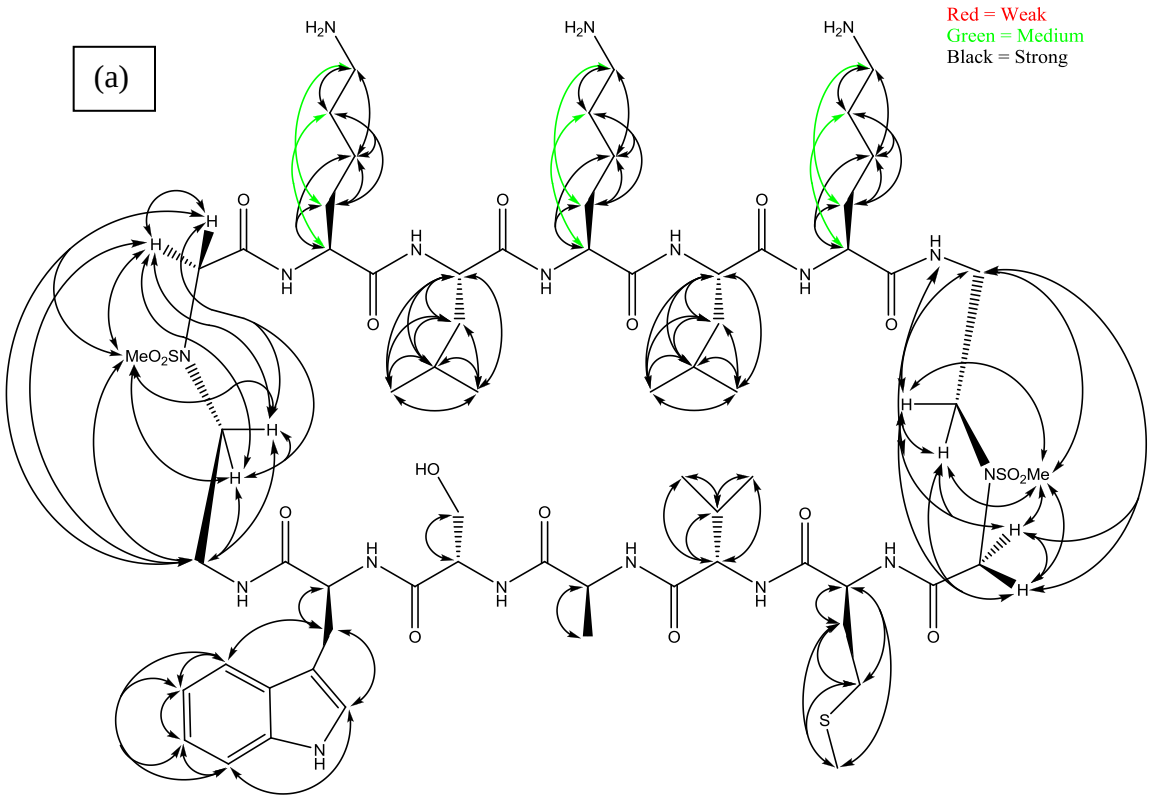
(a)
Red = Weak
Green = Medium
Black = Strong
H_2N
MeO_2SN
HO
NSO_2Me
S

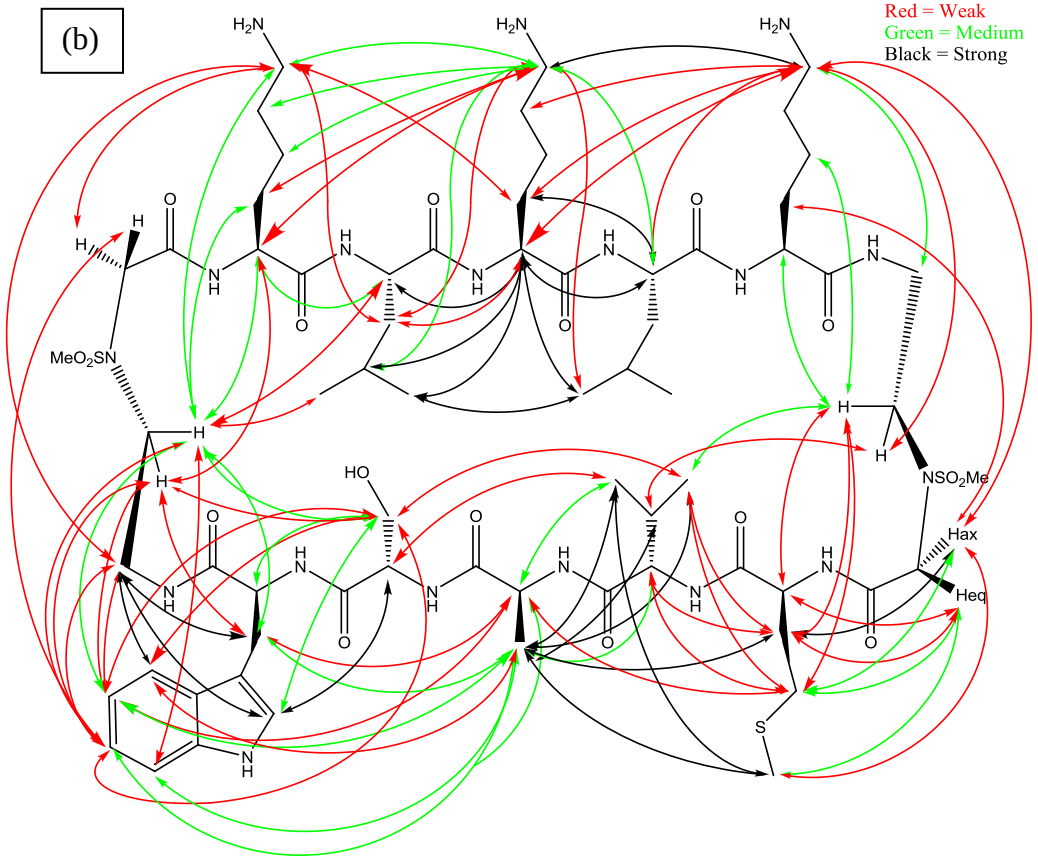
(b)
Red = Weak
Green = Medium
Black = Strong
H_2N
MeO_2SN
HO
NSO_2Me
Hax
Heq
S

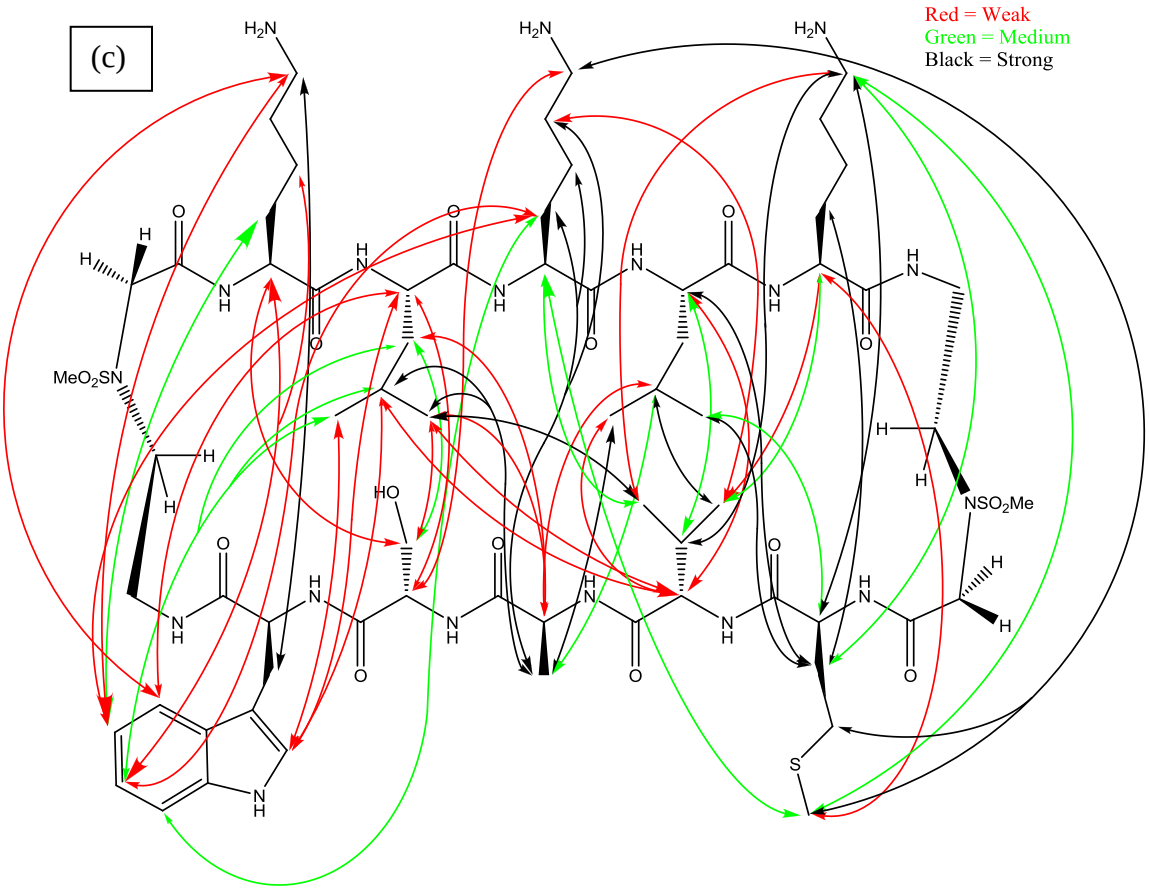

Fig. 2.11 Peptide **2.4** NOEs: (a) Intra-residue NOEs; (b) Same-strand NOEs; (c) Cross-strand NOEs.

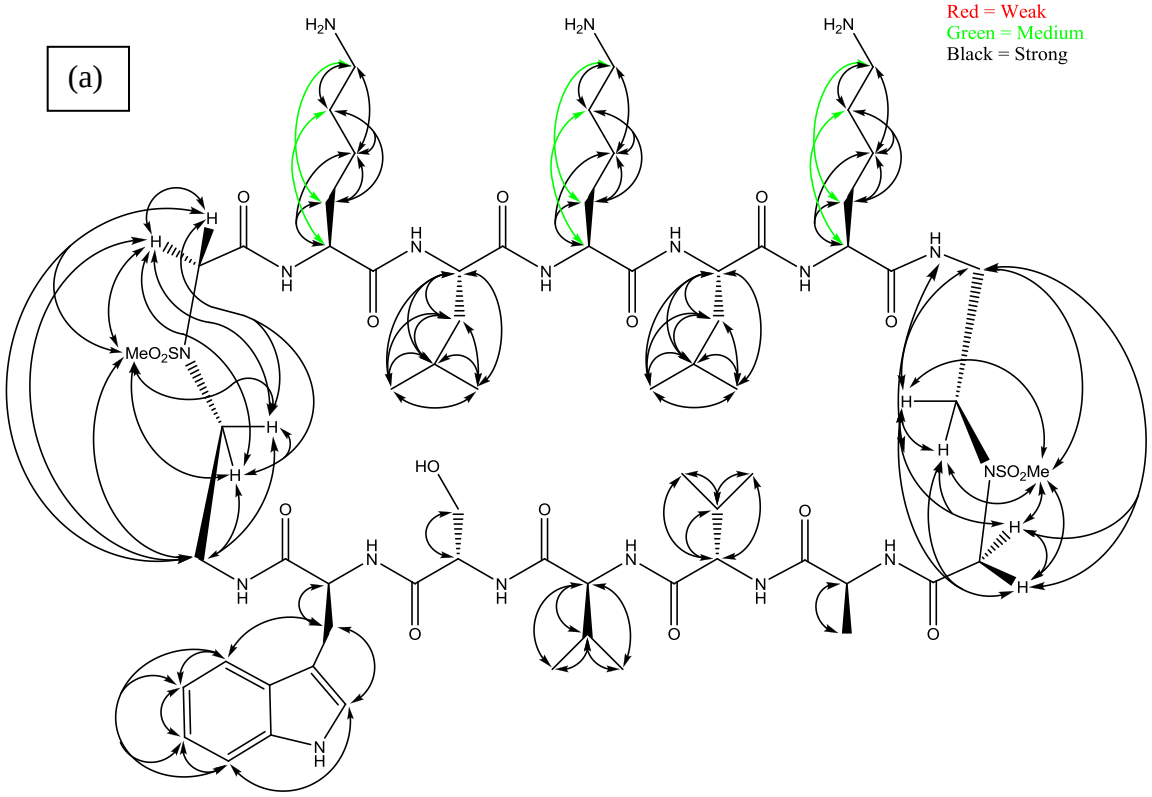
(a)
Red = Weak
Green = Medium
Black = Strong
H_2N
MeO_2SN
HO
NSO_2Me

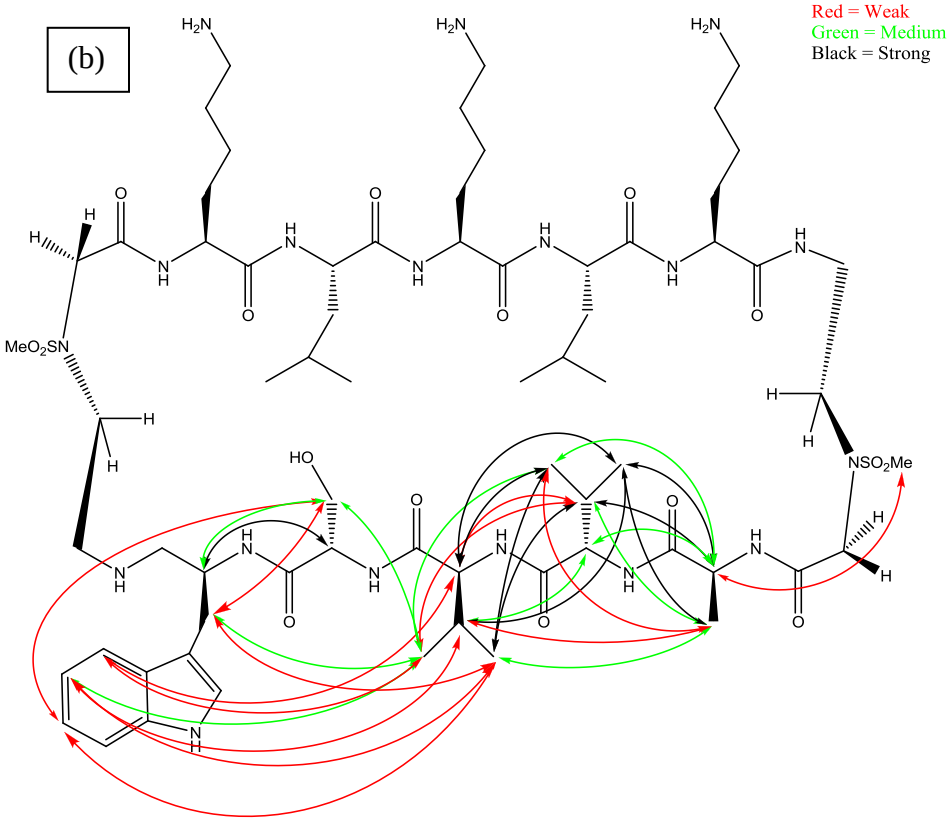
(b)
Red = Weak
Green = Medium
Black = Strong
H_2N
MeO_2SN
HO
NSO_2Me

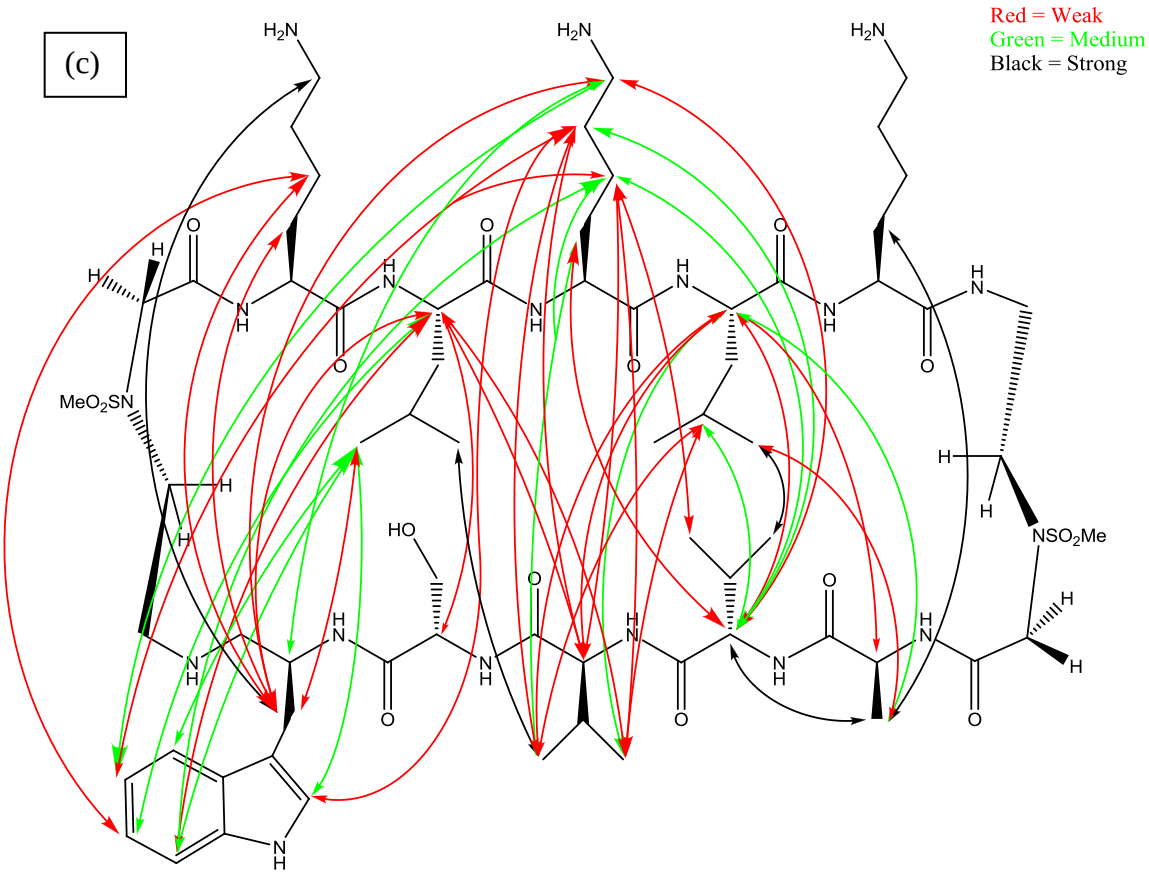

Fig. 2.12 Peptide **2.6** NOEs: (a) Intra-residue NOEs; (b) Same-strand NOEs; (c) Cross-strand NOEs.

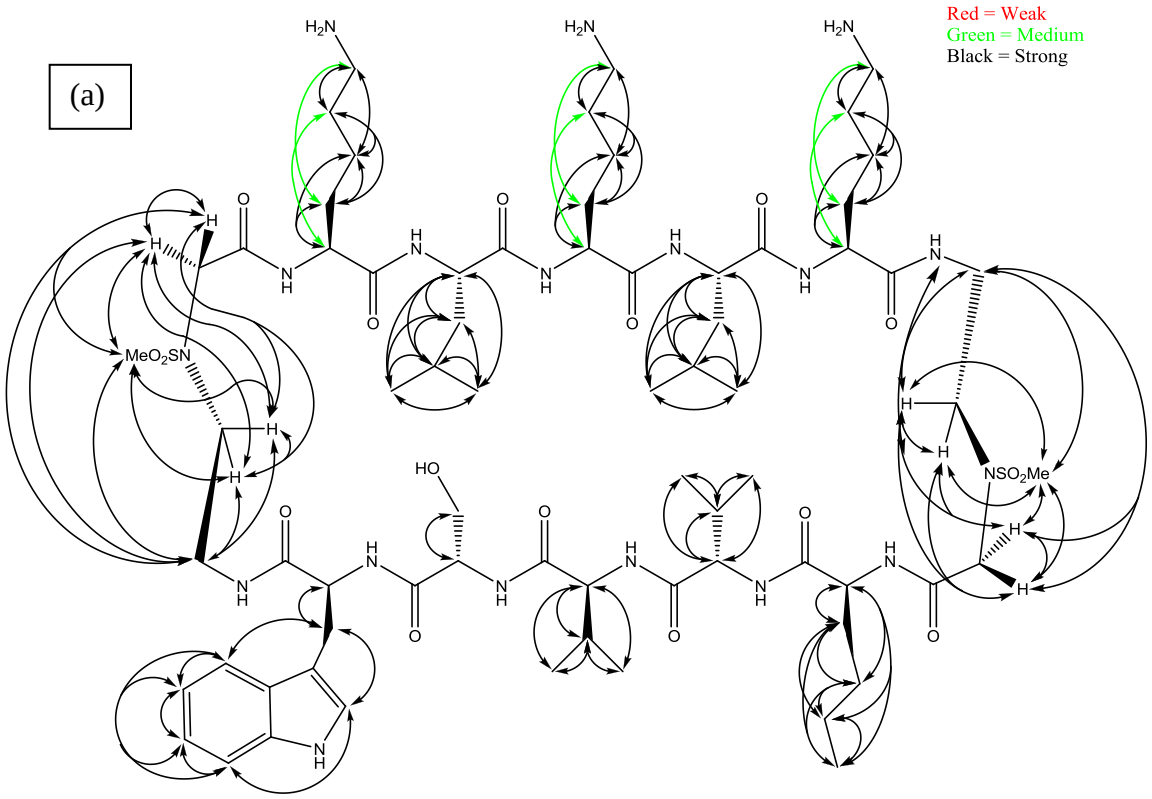
(a)
Red = Weak
Green = Medium
Black = Strong
H_2N
MeO_2SN
NSO_2Me
HO

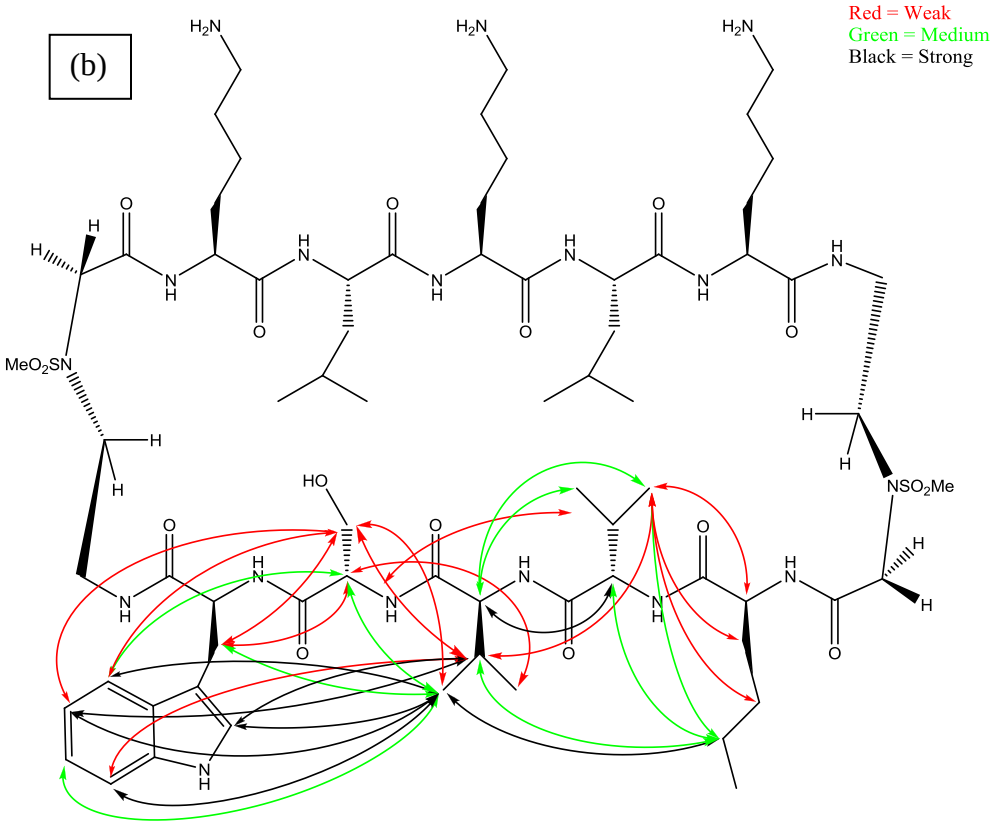
(b)
Red = Weak
Green = Medium
Black = Strong
H_2N
MeO_2SN
NSO_2Me
HO

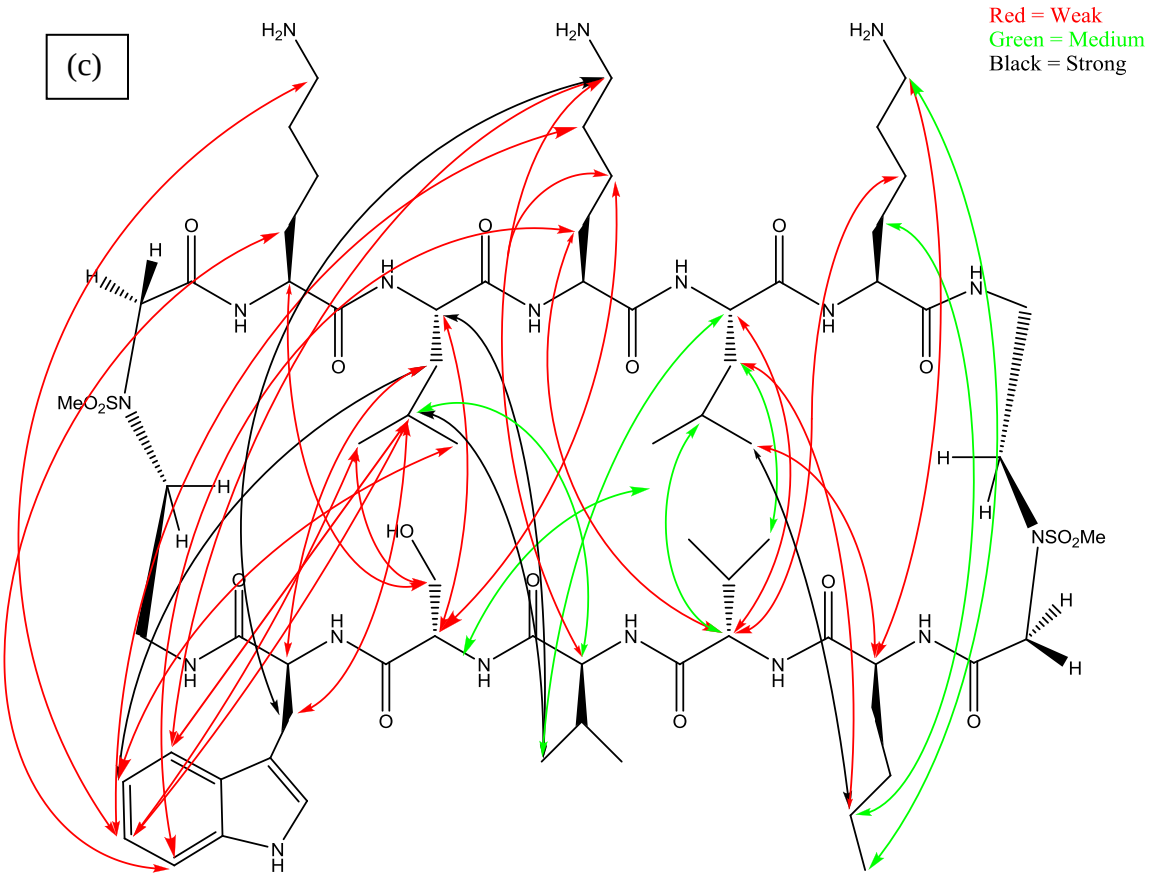

Fig. 2.13 Peptide **2.7** NOEs: (a) Intra-residue NOEs; (b) Same-strand NOEs; (c) Cross-strand NOEs.

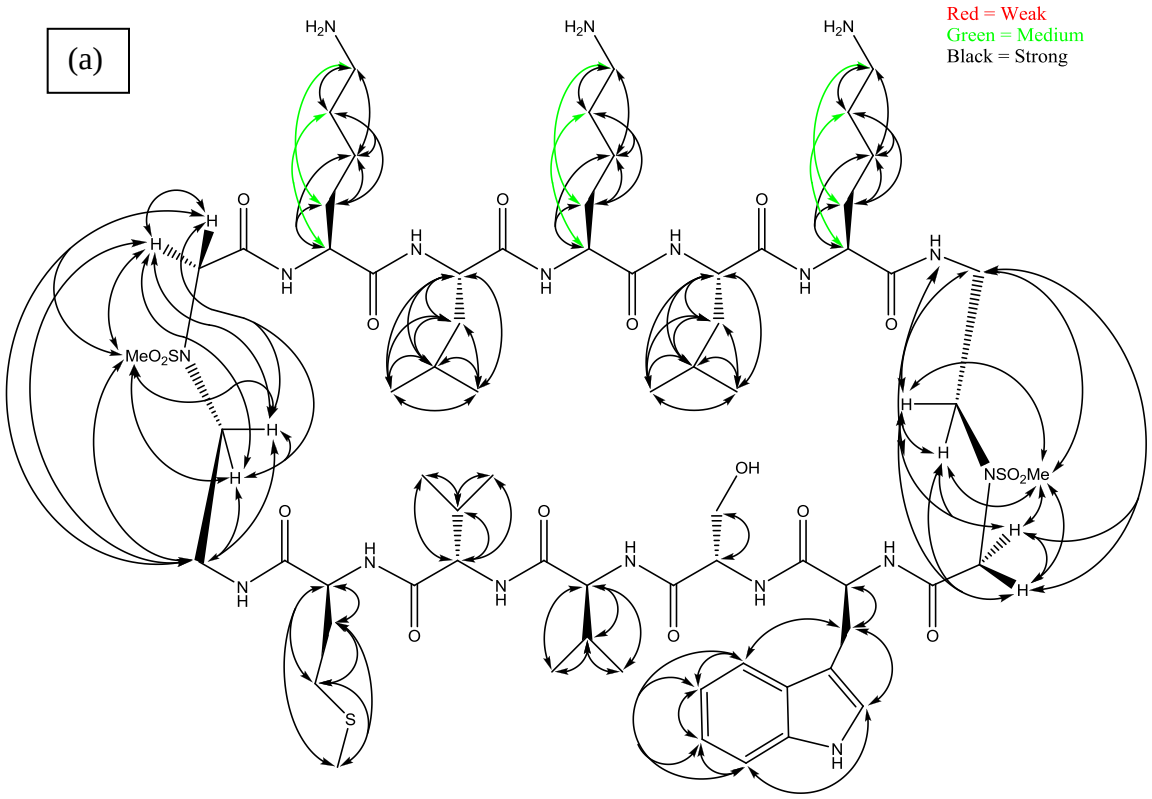
(a)
Red = Weak
Green = Medium
Black = Strong

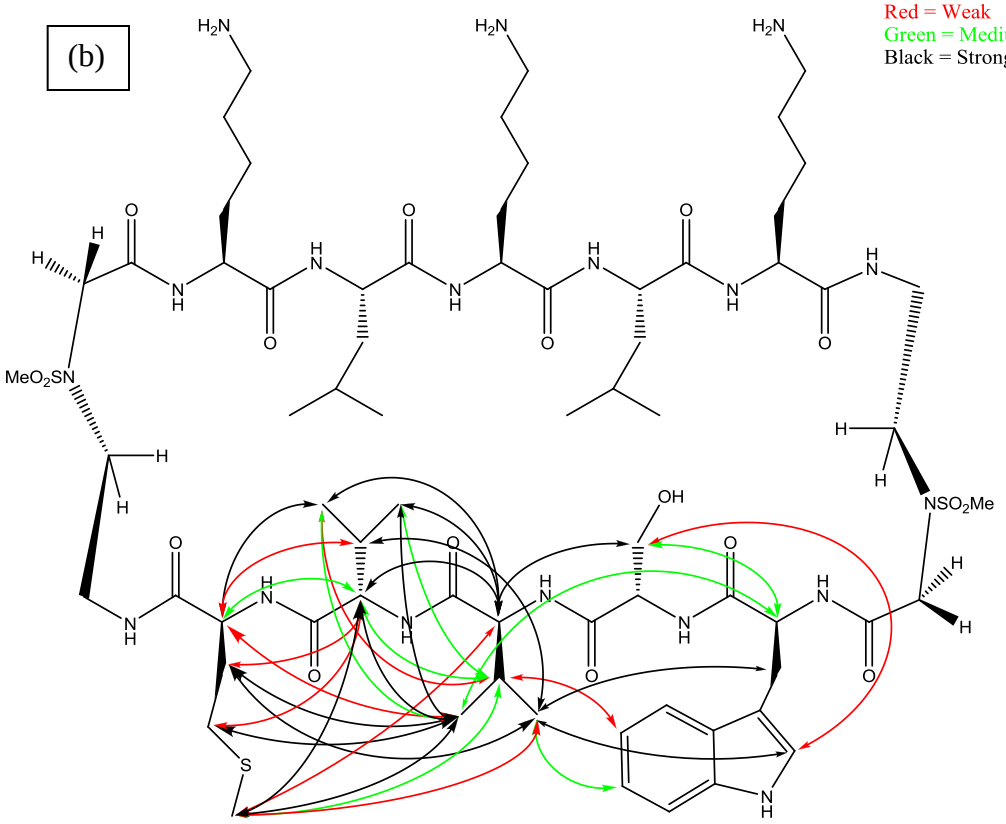
(b)
Red = Weak
Green = Medium
Black = Strong

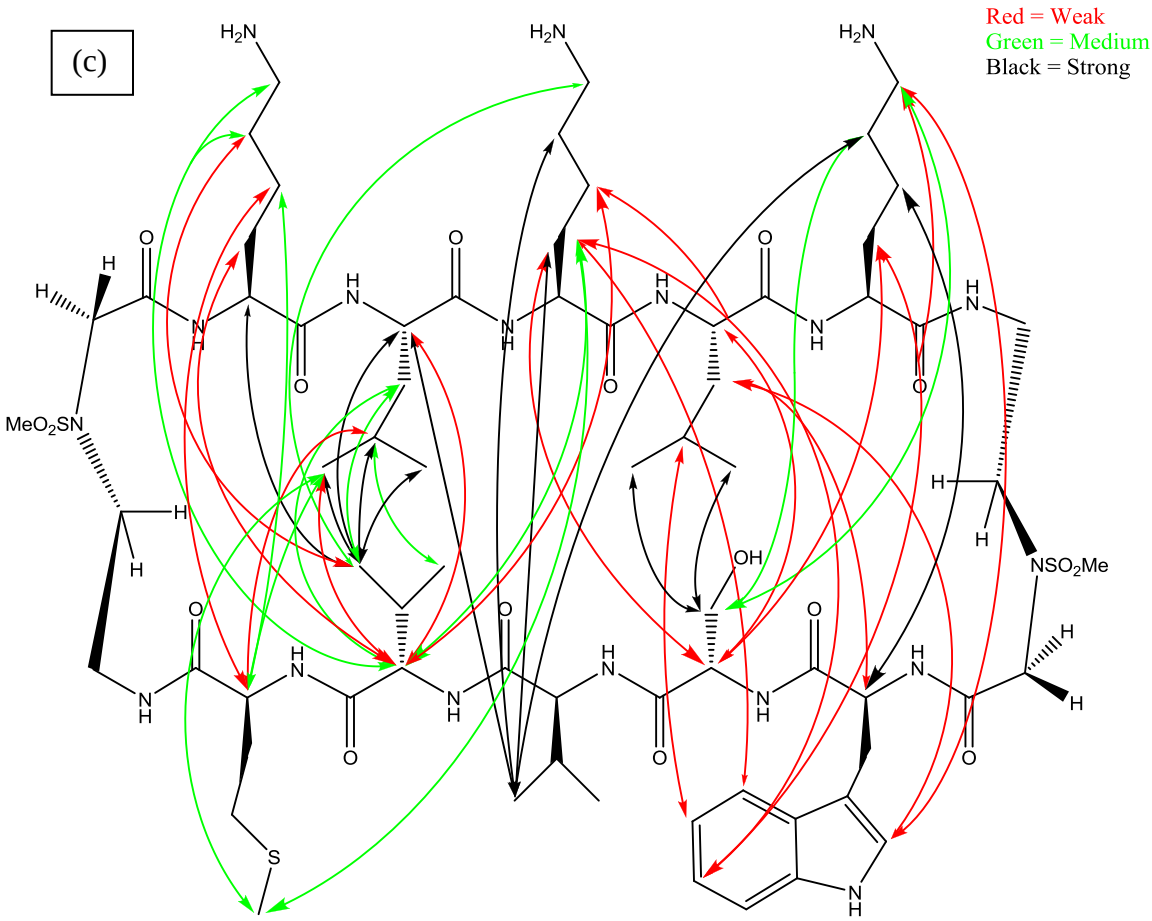

Fig. 2.14 Peptide **2.10** NOEs: (a) Intra-residue NOEs; (b) Same-strand NOEs; (c) Cross-strand NOEs.

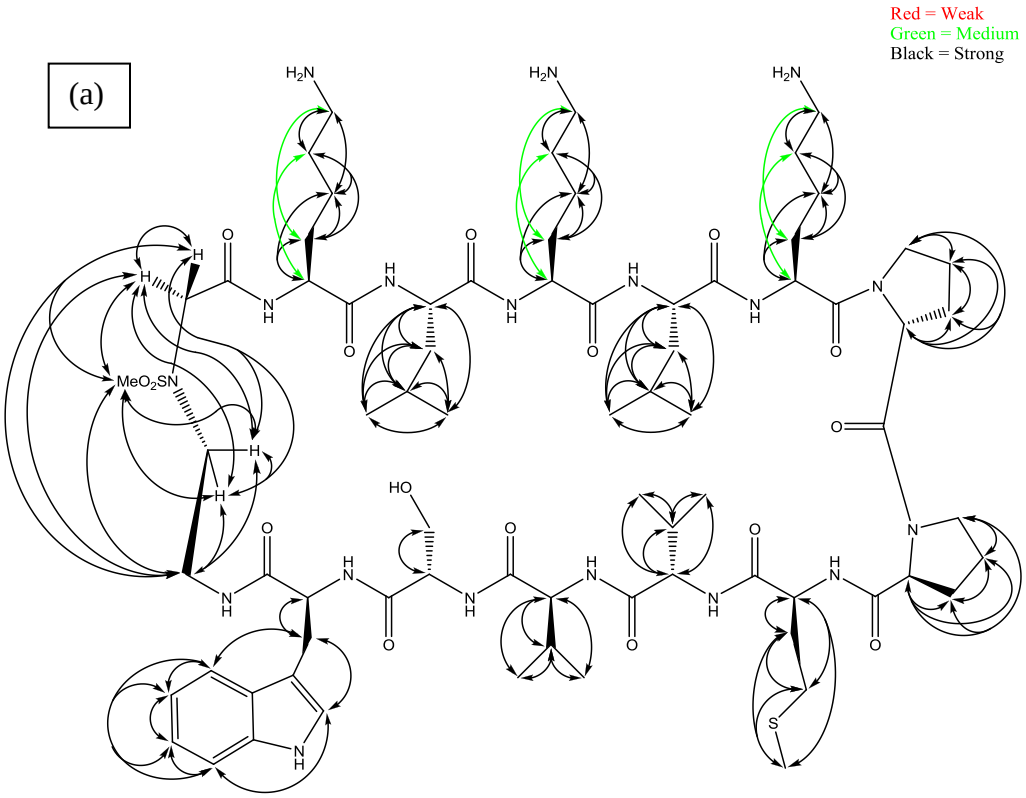
(a)
Red = Weak
Green = Medium
Black = Strong
H_2N
MeO_2SN
HO
S

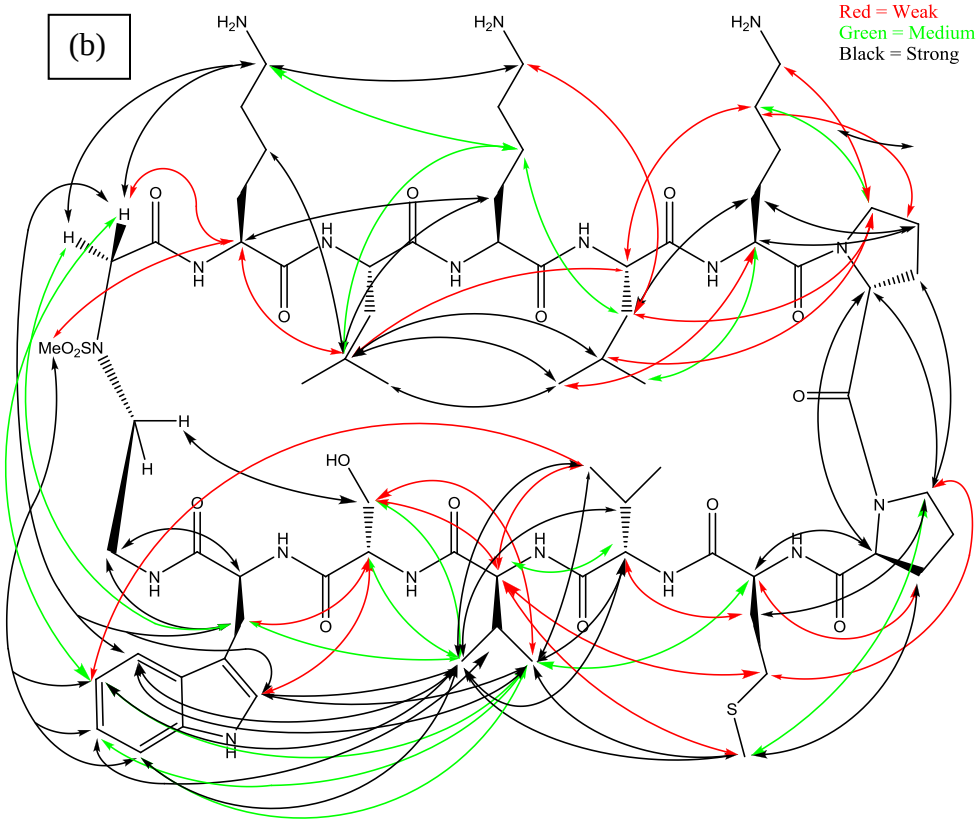
(b)
Red = Weak
Green = Medium
Black = Strong
H_2N
MeO_2SN
HO
S

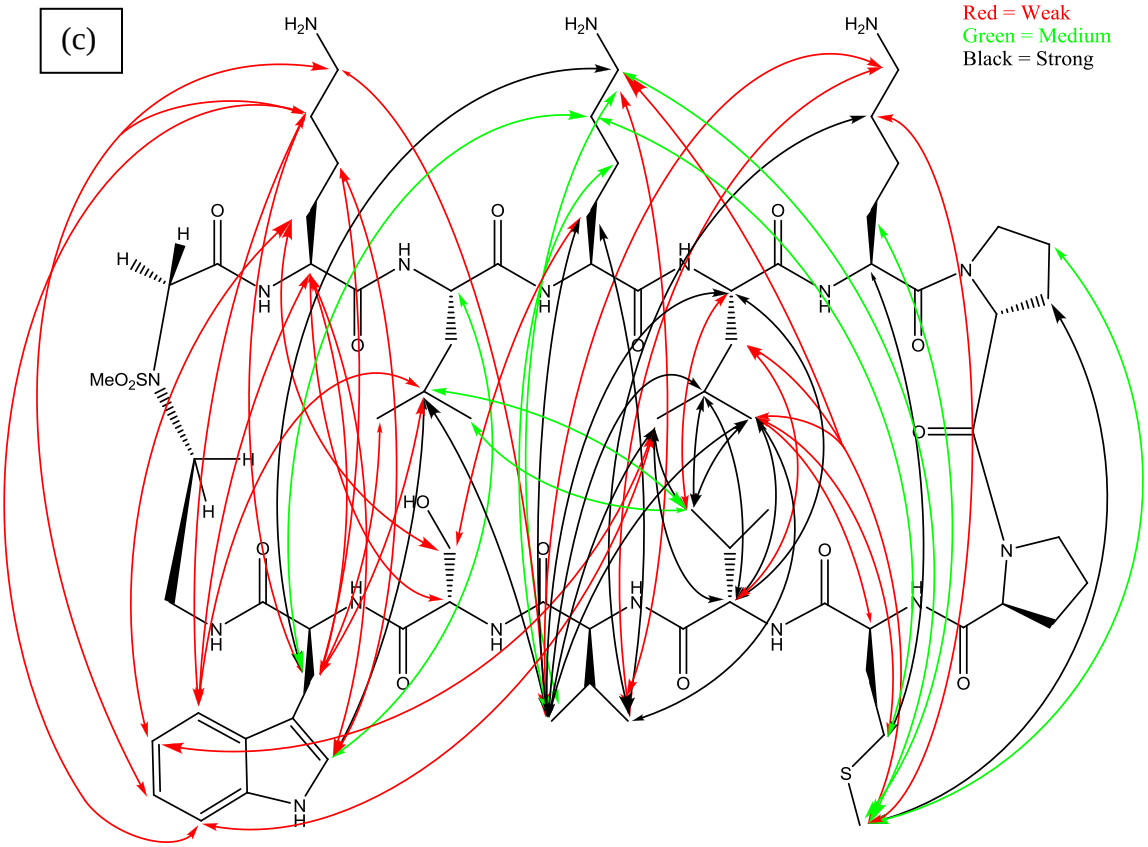

Fig. 2.15 Peptide **2.17** NOEs: (a) Intra-residue NOEs; (b) Same-strand NOEs; (c) Cross-strand NOEs.

2.4 Refereneces

1. Hazlehurst, L. A.; Enkemann, S. A.; Beam, C. A.; Argilagos, R. F.; Painter, J.; Shain, K. H.; Saporta, S.; Boulware, D.; Moscinski, L.; Alsina, M.; Dalton, W. S., Genotypic and Phenotypic Comparisons of de Novo and Acquired Melphalan Resistance in an Isogenic Multiple Myeloma Cell Line Model. *Cancer Res.* **2003,** *63* (22), 7900-7906.

2. Meads, M. B.; Hazlehurst, L. A.; Dalton, W. S., The Bone Marrow Microenvironment as a Tumor Sanctuary and Contributor to Drug Resistance. *Clin. Cancer Res.* **2008,** *14* (9), 2519-2526.

3. Hazlehurst, L. A.; Damiano, J. S.; Buyuksal, I.; Pledger, W. J.; Dalton, W. S., Adhesion to fibronectin via beta 1 integrins regulates p27kip1 levels and contributes to cell adhesion mediated drug resistance (CAM-DR). *Oncogene* **2000,** *19* (38), 4319-4327.

4. Hazlehurst, L. A.; Valkov, N.; Wisner, L.; Storey, J. A.; Boulware, D.; Sullivan, D. M.; Dalton, W. S., Reduction in drug-induced DNA double-strand breaks associated with beta 1 integrin-mediated adhesion correlates with drug resistance in U937 cells. *Blood* **2001,** *98* (6), 1897-1903.

5. Hazlehurst, L. A.; Foley, N. E.; Gleason-Guzman, M. C.; Hacker, M. P.; Cress, A. E.; Greenberger, L. W.; De Jong, M. C.; Dalton, W. S., Multiple mechanisms confer drug resistance to mitoxantrone in the human 8226 myeloma cell line. *Cancer Res.* **1999,** *59* (5), 1021-1028.

6. Hazlehurst, L. A.; Argilagos, R. F.; Emmons, M.; Boulware, D.; Beam, C. A.; Sullivan, D. M.; Dalton, W. S., Cell Adhesion to Fibronectin (CAM-DR) Influences Acquired Mitoxantrone Resistance in U937 Cells. *Cancer Res.* **2006,** *66* (4), 2338-2345.

7. Hazlehurst, L. A.; Argilagos, R. F.; Dalton, W. S., beta 1 integrin mediated adhesion increases Bim protein degradation and contributes to drug resistance in leukaemia cells. *Br. J. Haematol.* **2007,** *136* (2), 269-275.

8. Hazlehurst, L. A.; Landowski, T. H.; Dalton, W. S., Role of the tumor microenvironment in mediating de novo resistance to drugs and physiological mediators of cell death. *Oncogene* **2003,** *22* (47), 7396-7402.

9. Matsunaga, T.; Takemoto, N.; Sato, T.; Takimoto, R.; Tanaka, I.; Fujimi, A.; Akiyama, T.; Kuroda, H.; Kawano, Y.; Kobune, M.; Kato, J.; Hirayama, Y.; Sakamaki, S.; Kohda, K.; Miyake, K.; Niitsu, Y., Interaction between leukemic-cell VLA-4 and stromal fibronectin is a decisive factor for minimal residual disease of acute myelogenous leukemia. *Nat. Med. (N. Y., NY, U. S.)* **2003,** *9* (9), 1158-1165.

10. Gozuacik, D.; Kimchi, A., Autophagy as a cell death and tumor suppressor mechanism. *Oncogene* **2004,** *23* (16), 2891-2906.

11. Bursch, W.; Hochegger, K.; Torok, L.; Marian, B.; Ellinger, A.; Hermann, R. S., Autophagic and apoptotic types of programmed cell death exhibit different fates of cytoskeletal filaments. *J. Cell Sci.* **2000,** *113* (7), 1189-1198.

12. Golstein, P.; Kroemer, G., Cell death by necrosis: towards a molecular definition. *Trends Biochem. Sci.* **2007,** *32* (1), 37-43.

13. Pennington, M. E.; Lam, K. S.; Cress, A. E., The use of a combinatorial library method to isolate human tumor cell adhesion peptides. *Mol. Diversity* **1996,** *2* (1/2), 19-28.

14. Sroka Thomas, C.; Marik, J.; Pennington Michael, E.; Lam Kit, S.; Cress Anne, E., The minimum element of a synthetic peptide required to block prostate tumor cell migration. *Cancer Biol Ther* **2006,** *5* (11), 1556-62.

15. Sroka Thomas, C.; Pennington Michael, E.; Cress Anne, E., Synthetic D-amino acid peptide inhibits tumor cell motility on laminin-5. *Carcinogenesis* **2006,** *27* (9), 1748-57.

16. Nair, R. R.; Emmons, M. F.; Cress, A. E.; Argilagos, R. F.; Lam, K.; Kerr, W. T.; Wang, H.-G.; Dalton, W. S.; Hazlehurst, L. A., HYD1-induced increase in reactive oxygen species leads to autophagy and necrotic cell death in multiple myeloma cells. *Mol. Cancer Ther.* **2009,** *8* (8), 2441-2451.

17. Loughlin, W. A.; Tyndall, J. D. A.; Glenn, M. P.; Fairlie, D. P., Beta-Strand Mimetics. *Chem. Rev. (Washington, DC, U. S.)* **2004,** *104* (12), 6085-6117.

18. Chorev, M.; Goodman, M., A dozen years of retro-inverso peptidomimetics. *Acc. Chem. Res.* **1993,** *26* (5), 266-73.

19. Fletcher, M. D.; Campbell, M. M., Partially Modified Retro-Inverso Peptides: Development, Synthesis and Conformational Behavior. *Chem. Rev. (Washington, D. C.)* **1998,** *98* (2), 763-795.

20. Nair, D. T.; Kaur, K. J.; Singh, K.; Mukherjee, P.; Rajagopal, D.; George, A.; Bal, V.; Rath, S.; Rao, K. V. S.; Salunke, D. M., Mimicry of native peptide antigens by the corresponding retro-inverso analogs is dependent on their intrinsic structure and interaction propensities. *J. Immunol.* **2003,** *170* (3), 1362-1373.

21. Taylor, E. M.; Otero, D. A.; Banks, W. A.; O'Brien, J. S., Retro-inverso prosaptide peptides retain bioactivity, are stable in vivo, and are blood-brain barrier permeable. *J. Pharmacol. Exp. Ther.* **2000,** *295* (1), 190-194.

22. DeRoock, I. B.; Pennington, M. E.; Sroka, T. C.; Lam, K. S.; Bowden, G. T.; Bair, E. L.; Cress, A. E., Synthetic peptides inhibit adhesion of human tumor cells to extracellular matrix proteins. *Cancer Res.* **2001,** *61* (8), 3308-3313.

23. Xu, W.; Taylor, J. W., A template-assembled model of the N-peptide helix bundle from HIV-1 Gp-41 with high affinity for C-peptide. *Chem. Biol. Drug Des.* **2007,** *70* (4), 319-328.

24. Soulier, J.-L.; Russo, O.; Giner, M.; Rivail, L.; Berthouze, M.; Ongeri, S.; Maigret, B.; Fischmeister, R.; Lezoualc'h, F.; Sicsic, S.; Berque-Bestel, I., Design and Synthesis of Specific Probes for Human 5-HT4 Receptor Dimerization Studies. *J. Med. Chem.* **2005,** *48* (20), 6220-6228.

25. Carrithers, M. D.; Lerner, M. R., Synthesis and characterization of bivalent peptide ligands targeted to G-protein-coupled receptors. *Chem. Biol.* **1996,** *3* (7), 537-542.

26. Tejada, F. R.; Nagy, P. I.; Xu, M.; Wu, C.; Katz, T.; Dorsey, J.; Rieman, M.; Lawlor, E.; Warrier, M.; Messer, W. S., Jr., Design and Synthesis of Novel Derivatives of the Muscarinic Agonist Tetra(ethylene glycol) (3-methoxy-1,2,5-thiadiazol-4-yl) [3-(1-Methyl-1,2,5,6-tetrahydropyrid-3-yl)-1,2,5-thiadiazol-4-yl] Ether (CDD-0304): Effects of Structural Modifications on the Binding and Activity at Muscarinic Receptor Subtypes and Chimeras. *J. Med. Chem.* **2006,** *49* (25), 7518-7531.

27. Rajeswaran, W. G.; Cao, Y.; Huang, X.-P.; Wroblewski, M. E.; Colclough, T.; Lee, S.; Liu, F.; Nagy, P. I.; Ellis, J.; Levine, B. A.; Nocka, K. H.; Messer, W. S., Jr., Design, Synthesis, and Biological Characterization of Bivalent 1-Methyl-1,2,5,6-tetrahydropyridyl-1,2,5-thiadiazole Derivatives as Selective Muscarinic Agonists. *J. Med. Chem.* **2001,** *44* (26), 4563-4576.

28. Peng, X.; Knapp, B. I.; Bidlack, J. M.; Neumeyer, J. L., Synthesis and Preliminary In vitro Investigation of Bivalent Ligands Containing Homo- and Heterodimeric Pharmacophores at micro , delta , and k Opioid Receptors. *J. Med. Chem.* **2006,** *49* (1), 256-262.

29. Daniels, D. J.; Lenard, N. R.; Etienne, C. L.; Law, P.-Y.; Roerig, S. C.; Portoghese, P. S., Opioid-induced tolerance and dependence in mice is modulated by the distance between pharmacophores in a bivalent ligand series. *Proc. Natl. Acad. Sci. U. S. A.* **2005,** *102* (52), 19208-19213.

30. Thomson, S. A.; Josey, J. A.; Cadilla, R.; Gaul, M. D.; Hassman, C. F.; Luzzio, M. J.; Pipe, A. J.; Reed, K. L.; Ricca, D. J.; et al., Fmoc mediated synthesis of peptide nucleic acids. *Tetrahedron* **1995,** *51* (22), 6179-94.

31. Kuwahara, M.; Arimitsu, M.; Shigeyasu, M.; Saeki, N.; Sisido, M., Hybridization between Oxy-Peptide Nucleic Acids and DNAs: Dependence of Hybrid Stabilities on the Chain-Lengths, Types of Base Pairs, and the Chain Directions. *J. Am. Chem. Soc.* **2001,** *123* (20), 4653-4658.

32. Kuwahara, M.; Arimitsu, M.; Sisido, M., Synthesis of delta -amino acids with an ether linkage in the main chain and nucleobases on the side chain as monomer units for oxy-peptide nucleic acids. *Tetrahedron* **1999,** *55* (33), 10067-10078.

33. Bonger, K. M.; van den Berg, R. J. B. H. N.; Heitman, L. H.; Ijzerman, A. P.; Oosterom, J.; Timmers, C. M.; Overkleeft, H. S.; van der Marel, G. A., Synthesis and evaluation of homo-bivalent GnRHR ligands. *Bioorg. Med. Chem.* **2007,** *15* (14), 4841-4856.

34. Creighton, T. E. *Protein: Structures and Molecular Properties*, 2nd ed.; W. H.Freeman and Co.: New York, 1993.

35. Tilstra, L.; Mattice, W. L. In *Circular Dichroism and the Conformational Analysis of Biomolecule*. Fasman, G. D. ed; Plenum Press: New York, 1996.

36. Wishart, D.S.; Sykes, B.D.; Richards, F.M. *Biochemistry* **1992**, *31*, 1647-1651

37. Wishart, D. S.; Sykes, B. D.; Richards, F. M. *J. Mol. Biol.* **1991**, *222*, 311-333

38. Favre, M.; Moehle, K.; Jiang, L.; Pfeiffer, B.; Robinson, J.A. *J. Am. Chem. Soc.* **1999**, *121*, 2679-2685

39. Bertrand, R. D.; Compton, R. D.; Verkade J.G. *J. Am. Chem. Soc.* **1970**, *92*, 2702-2709

40. Yamamoto, Y.; Iwafune, K.; Nanai, N.; Ōsawa, A.; Chûjô, R.; Suzuki, T. *Eur. J. Biochem.* **1991**, *198*, 299-306

41. Hutchinson, E.G; Sessions, R.B; Thornton J.M.; Woolfson D.N. *Protein Sci*. **1998**, *7*, 2287-2300

42. Hughes, R.M.; Waters M.L. *J. Am. Chem. Soc*. **2005**, *127*, 6518-6519

43. Zhou, P.; Tian, F.; Lv, F.; Shang, Z. *Proteins Struct. Funct. Bioinf.* **2009**, *76*, 151-163

44. Wüthrich, K. *NMR of Proteins and Nucleic Acids*; Wiley-Interscience Publication: New York, 1986.

CHAPTER THREE:

CYCLIC β- HAIRPIN PEPTIDOMIMETICS AS POTENTIAL Aβ FIBRILLOGENESIS INHIBITOR

3.1 Introduction

Substantial information amassed from genetic, animal modeling, and biochemical data, reveals that self aggregation of fibrillar amyloid beta (Aβ) peptides is responsible for insoluble, neuritic plaque formation in the brains of patients with Alzheimer's disease (AD). These Aβ peptides are byproducts of cleavage of transmembrane protein, Amyloid Precursor Protein (APP) by successive action of two aspartyl proteases, β- and γ-secretases (1-3). β-secretase cleaves APP to produce a membrane bound 99 amino acid long C-terminal stub which is successively cleaved by γ-secretase releasing Aβ peptides. Depending on the exact cleavage point by γ-secretase, Aβ exists in three isoforms: Aβ38, Aβ40 and Aβ42. Aβ40 is more abundantly produced in nature but Aβ42 is more fibrillogenic and associated with diseased states (4-7). The mere presence of Aβ peptides in brains and cerebrospinal fluids does not cause neurodegenerative diseases (8). These Aβ peptides are disordered in monomeric state, but adopt ordered beta sheet conformations to form amyloid plaques upon aggregation (9,10). Hence disruption of Aβ aggregation has been a major area of research in treating Alzheimer's disease. Efforts have been made by various research groups to design small molecule inhibitors or peptidomimetics that could potentially inhibit Aβ aggregation, fibrillization, and plaque

formation. Fig. 3.1 shows some promising small molecule and peptidomimetic inhibitors developed for inhibiting Aβ aggregation (11).

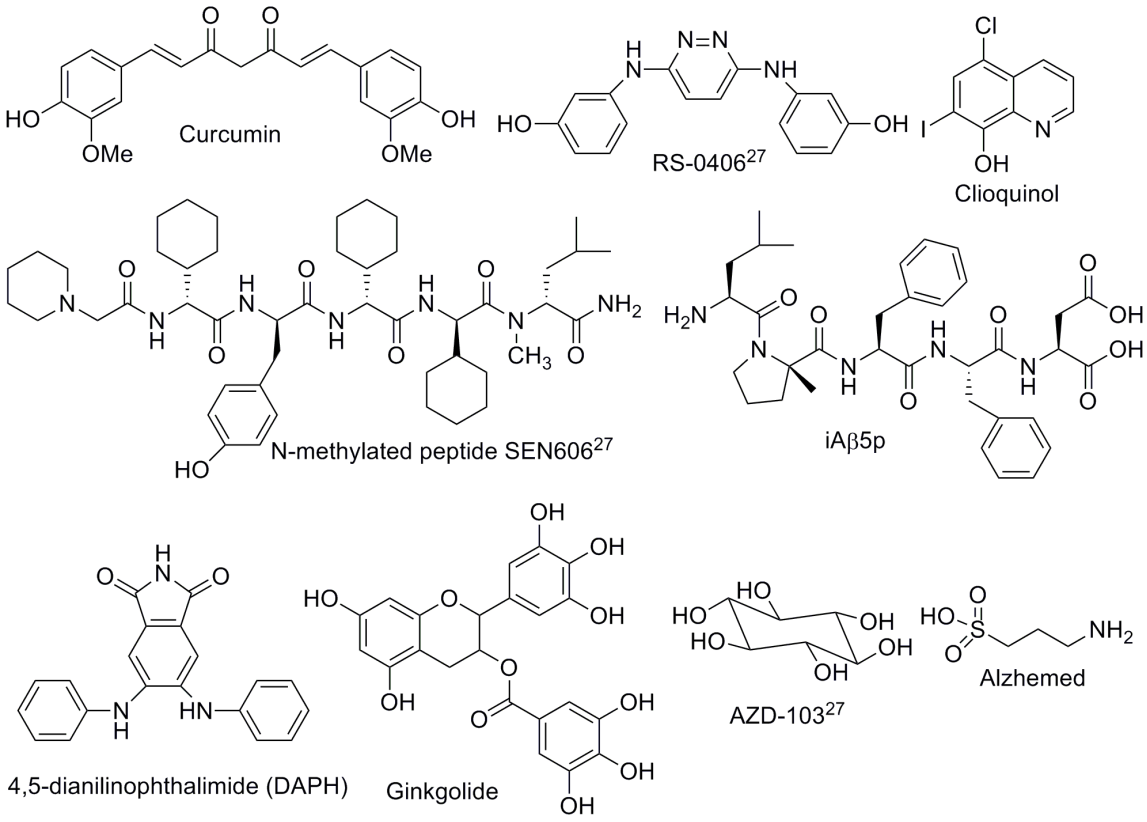

Fig. 3.1 Examples of some potential Aβ aggregation inhibitors

Peptide based inhibitors for inhibiting Aβ aggregation

Since Aβ peptides self-oligomerize, the first strategy for developing Aβ aggregation inhibitors was to start with short peptide fragment homologous to the full length wild-type peptide. Tjernberg and co-workers first developed synthetic peptides homologous to the core section (16-20) (KLVFF) of full-length Aβ and showed that this peptide was able to bind full-length Aβ, thereby preventing self-assembly into fibrils (12). Soto also developed peptidomimetics targeting the core region of Aβ especially residues 17-21 (LVFFA) (13,14). They developed peptides with partial homology of core

region 17-21 of Aβ, having key positions replaced with proline. Proline residues were introduced to reduce the β-sheet-forming propensity of the peptide (LPFFD, RDLPFFDVPID) without losing its hydrophobicity. The β-sheet breaker peptides designed from all D-amino acids (LPFFD) were equally effective as the L-peptide versions but it was more stable, smaller and hydrophobic enough to penetrate blood brain barrier (15).

Murphy and co-workers targeted the core region (15-25) of Aβ and designed peptide with a disrupting element attached to the C-terminus, linked to the recognition element. The recognition element would interact specifically with Aβ whereas the disrupting element would interfere with normal fibril self-association mechanism and alter Aβ aggregation pathways (16-18). Residues 16-20 of the core of Aβ were more potent as recognition elements as compared to residues 15-25. Murphy showed that the disrupting element containing at least three lysine residues (KLVFFKKKKKK) was most potent at preventing Aβ toxicity and caused largest change in Aβ aggregation kinetics and aggregate morphology.

The use of N-methylated amino acids in peptides for inhibition of Aβ and improving peptide stability in vivo have been explored by various research groups (19-23). Momany have shown that N-methylation promotes β-sheet formation by locking the residue into β-sheet conformation (24). Doig and co-workers have shown that N-methylation generates soluble monomeric β-sheet peptides. One side of the N-methylated peptide forms hydrogen bonding with the Aβ fibril whereas the outer edge having N-methyl groups in place of backbone NH groups blocks hydrogen bonding. Meredith reported N-methylated peptides corresponding to the core region 16-22 and 16-20 of Aβ

and have shown that these peptides prevented Aβ fibril formation and even dissolved pre-formed fibrils (25, 26). N-methylated peptides have been shown to have high proteolytic resistance, solubility, blood brain barrier permeability and a high β-sheet forming propensity.

Based on these finding by various research groups, we aim to target the hydrophobic core region 17-21 (LVFFA) of full length Aβ peptide. We propose the design and synthesis of cyclic β-hairpin peptide that binds specifically to this hydrophobic region and prevents β-sheet aggregation. Figure 3.2 clearly explains the inhibition mechanism of Aβ fibrils using cyclic peptides. The recognition strand of the cyclic peptide would interact with the Aβ fibril whereas the non-recognition strand would have residues that would inhibit aggregation from the other face of the assembly. The introduction of novel beta turn promoter in the cyclic structure stabilizes the extended conformation and provides stability to the cyclic structure. All of our cyclic peptides exhibit β-sheet character as characterized by circular dichroism and ^{1}H NMR studies. We have also designed and synthesized cyclic N-methylated peptides to prevent abeta fibrillogenesis. The designed N-methylated β-hairpin is believed to cap the growing fibril, prevent further oligomerization and even solubilize preformed Aβ fibrils. The Aβ fibril inhibition of all cyclic β-hairpin peptides synthesized has been studied using Thioflavin T fluorometry assay.

(a)

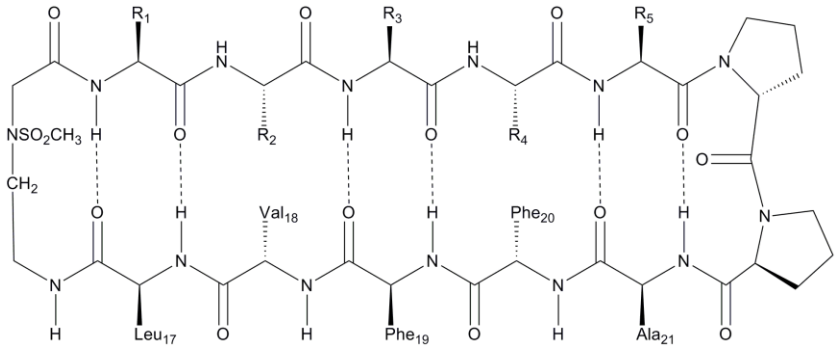

(b)

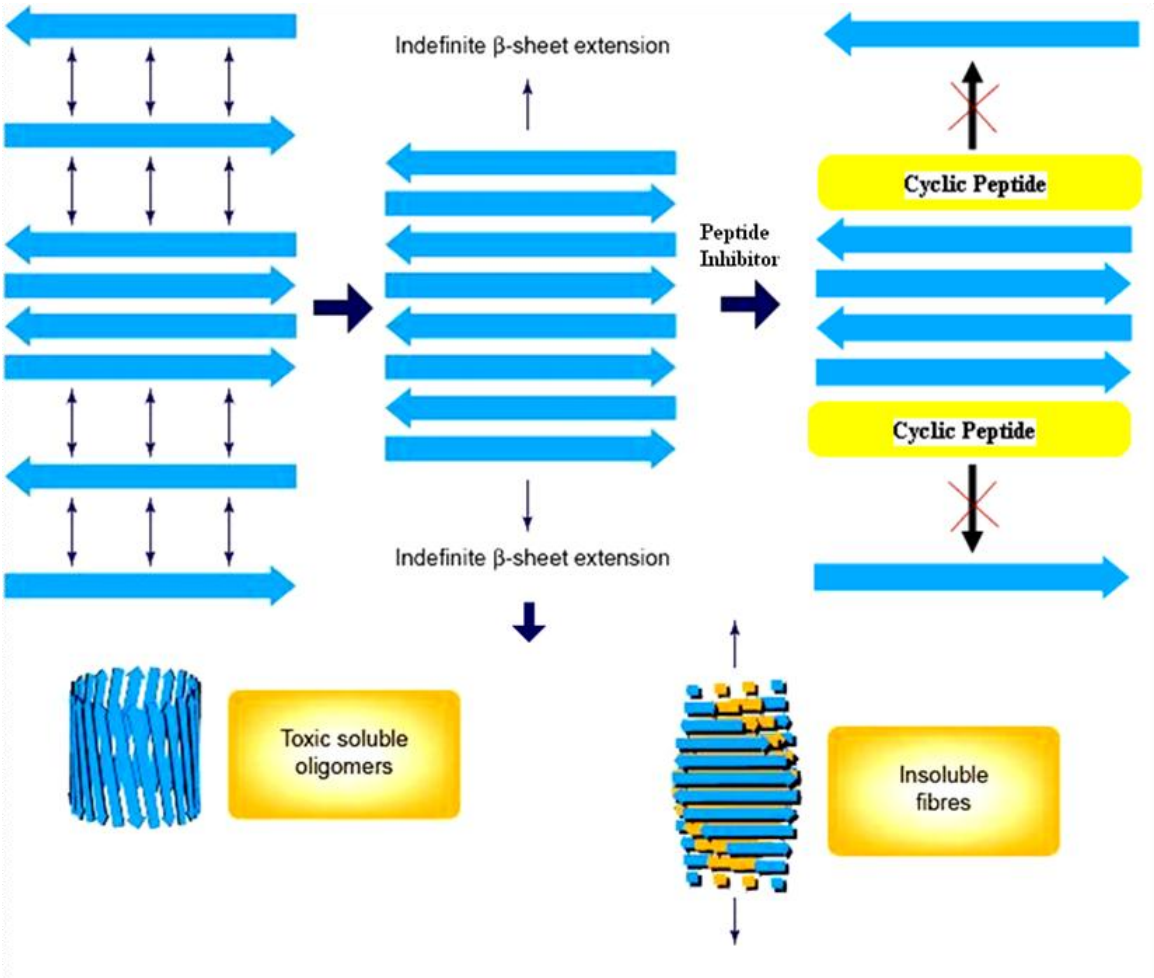

Fig. 3.2 (a) Proposed cyclic peptidomimetic fibrillogenesis inhibitor (b) Aβ peptide aggregation mechanism and fibril inhibition using proposed cyclic peptide.

3.2 Results & Discussion

3.2.1 Peptide design

Our design of cyclic peptide inhibitors for Aβ fibril is based on the hypothesis that peptides, which contain the hydrophobic core of Aβ (LVFFA) in the recognition strand, can interact with the corresponding residues of Aβ growing fibril via inter-strand hydrogen bonding and side chain-side chain interactions, whereas the non-recognition strand could have residues that would prevent further aggregation on other face of the assembly. Cyclization greatly restricts the number of conformations available to the linear peptide and thus induces distinct secondary structures. The proposed cyclic Aβ peptide is believed to exhibit secondary beta-sheet structure which we confirmed by circular dichroism and NMR studies. Also, cyclic peptides become resistant to proteolysis. It has been reported that short linear Aβ peptides containing the hydrophobic core (LVFFA) with N-methylated derivatives have been effective in inhibiting fibril formation and inducing secondary structure in short peptides (27,28). Our strategy involves incorporation of N-methylated leucine or sarcosine in the non-recognition strand that would eliminate any possible hydrogen bonding arising due to dangling amide hydrogens on the opposite face. Thus we hypothesized that cyclic peptides with this design could have strong affinity for the surfaces of β-sheet assemblies of Aβ and prevent further aggregation by blocking a face of the assembly. Fig. 3.3 shows the proposed design of cyclic Aβ peptidomimetic with novel designed methylsulfonamido aminoethyl glycine turn promoter and Robinson's template (D-Pro-L-Pro). The incorporation of a beta turn promoter in the cyclic structure stabilizes the extended conformation and provides proteolytic stability to the cyclic hairpin. The designed cyclic peptide could

interact with the growing fibril in either the parallel or anti-parallel fashion (Fig. 3.3). To support our rational design, we did energy minimization studies on designed cyclic Aβ peptides designed to inhibit abeta fibrillogenesis as described in the previous chapter 2. Energy minimization studies suggested that introduction of the novel turn promoter and the Robinson template (D-Pro-L-Pro) at the turns gave stable hairpin peptides with all internal H-bonds intact. As per computational studies, the stability of cyclic hairpin further improved when both turns were replaced by methylsulfonamido aminoethyl glycine linker. Based on energy minimization studies data, we have synthesized a series of cyclic Aβ peptides as shown in Table 3.1.

It has been previously reported that amino acid residues that are restrained to a limited range of backbone torsion angles may be used as turn promoters in the design of α-helix and β-hairpins (29). Conformationally constrained amino acids such as α-amino isobutyric acid (Aib) and related $C^{\alpha,\alpha}$ dialkylated are strong α-helix and beta turn promoters. D-Pro-Aib sequences strongly favor type II' turn conformations, which have been used to design and synthesize β-hairpin structures (30). We have also synthesized cyclic abeta peptides with D-Pro-Aib and Robinson's template as turn promoters.

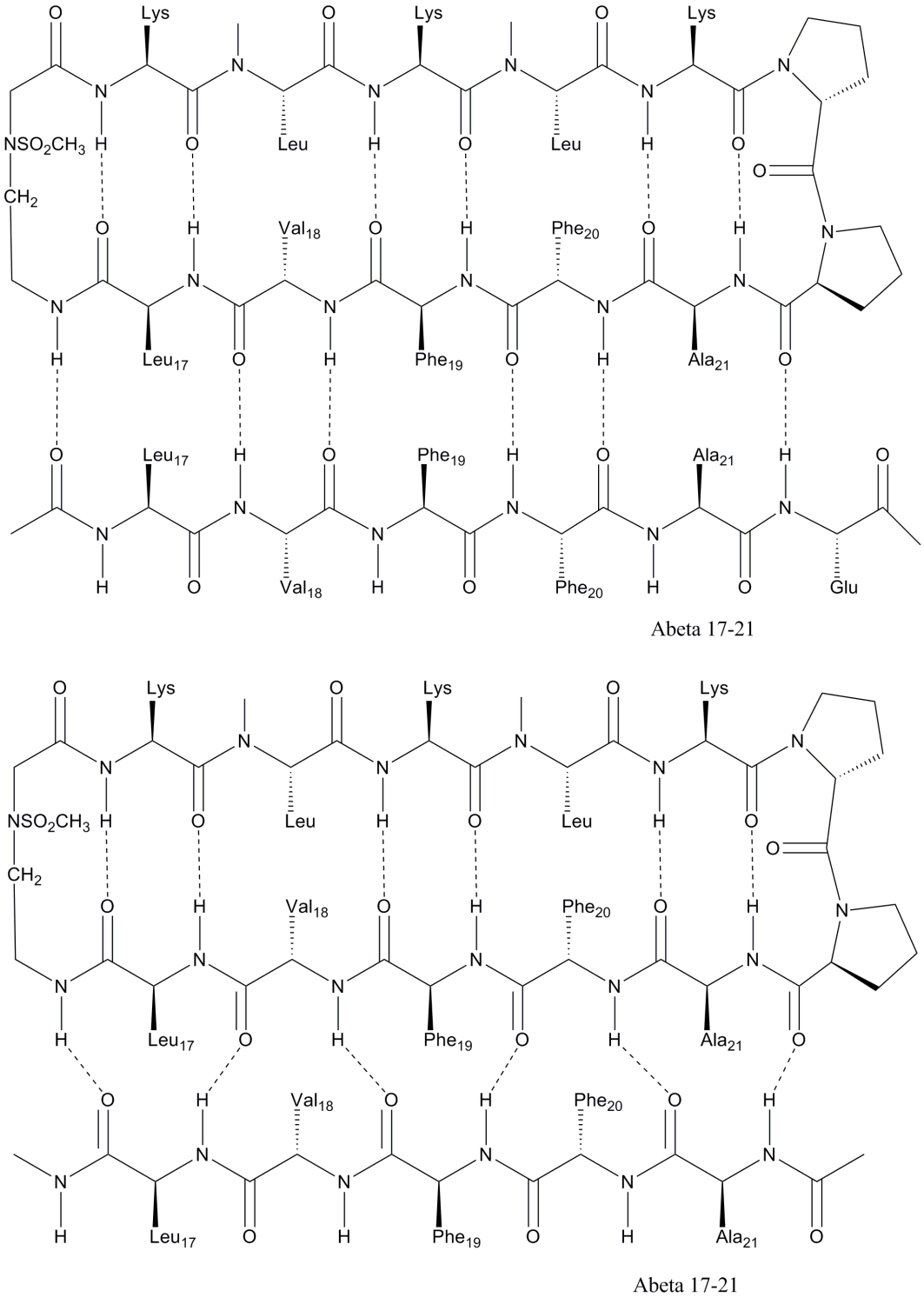

Fig. 3.3 (a) Anti-parallel & (b) parallel interactions of proposed cyclic Aβ peptide with growing Aβ fibril.

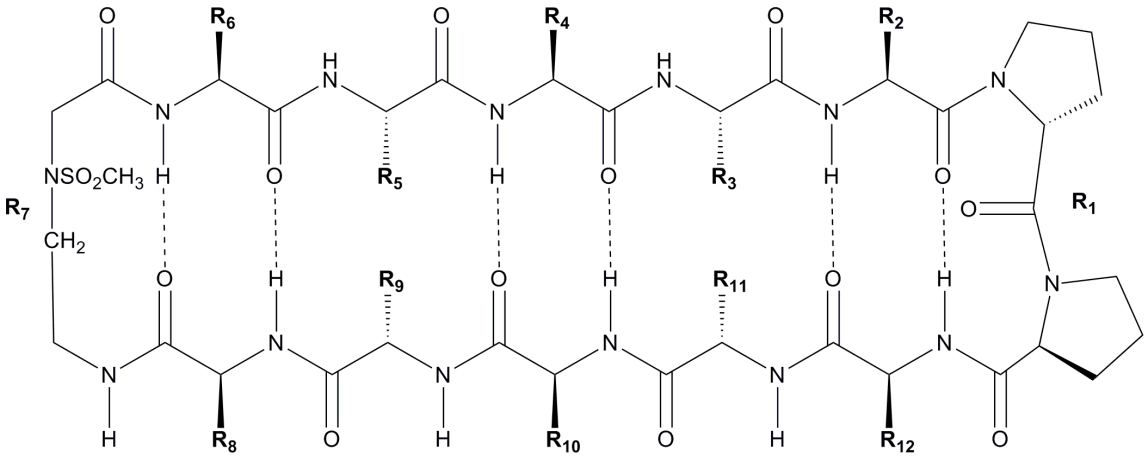

Table 3.1 Primary sequences of cyclic Aβ-hairpin peptidomimetics.

Peptide	R_1	R_2	R_3	R_4	R_5	R_6	R_7	R_8	R_9	R_{10}	R_{11}	R_{12}
3.1	**X**	**K**	**L**	**K**	**L**	**K**	**O**	**L**	**V**	**F**	**F**	**A**
3.2	**X**	**K**	**Meu**	**K**	**Meu**	**K**	**O**	**L**	**V**	**F**	**F**	**A**
3.3	**O**	**K**	**L**	**K**	**L**	**K**	**O**	**L**	**V**	**F**	**F**	**A**
3.4	**O**	**K**	**Meu**	**K**	**Meu**	**K**	**O**	**L**	**V**	**F**	**F**	**A**
3.5	**X**	**K**	**Sar**	**K**	**Sar**	**K**	**O**	**L**	**V**	**F**	**F**	**A**
3.6	**X**	**K**	**G**	**K**	**G**	**K**	**O**	**L**	**V**	**F**	**F**	**A**
3.7	**O**	**K**	**L**	**K**	**L**	**K**	**O**	**K**	**L**	**V**	**F**	**F**

X = ^{D}Pro-^{L}Pro Meu = N-methylated Leucine Sar = Sarcosine O = methylsulfonamido aminoethyl glycine ($NH_2CH_2CH_2N(O_2SCH_3)CH_2COOH$).

All synthesized cyclic peptides were tested for their potential to inhibit Aβ aggregation using Thioflavin T (ThT) binding assays. Thioflavin T is known to fluoresce upon binding to Aβ fibrils and the intensity of fluorescence is a measure of fibril content. The extent of fibril formation of each sample was determined by addition of varying concentrations of cyclic Aβ peptide and 5 μL of Aβ 1-42 solution to a 50 μL of a

thioflavin T solution. The fluorescence of the thioflavin T was measured by monitoring emission at 528 ± 20 nm with an excitation of 485 ± 20. Multiple experiments were conducted to determine the effect of cyclic peptides on beta-amyloid fibril formation. It can be seen from ThT binding assay data that peptide **3.6** prevented fibril formation of Aβ 1-42 *in vitro*. As can be seen in Fig. 3.4, a molar ratio of 1:2 (inhibitor: Aβ1-42) is capable of inhibiting abeta fibrillogenesis. Designed cyclic Peptides **3.1**, **3.2** & **3.4** were less potent in inhibiting fibril formation.

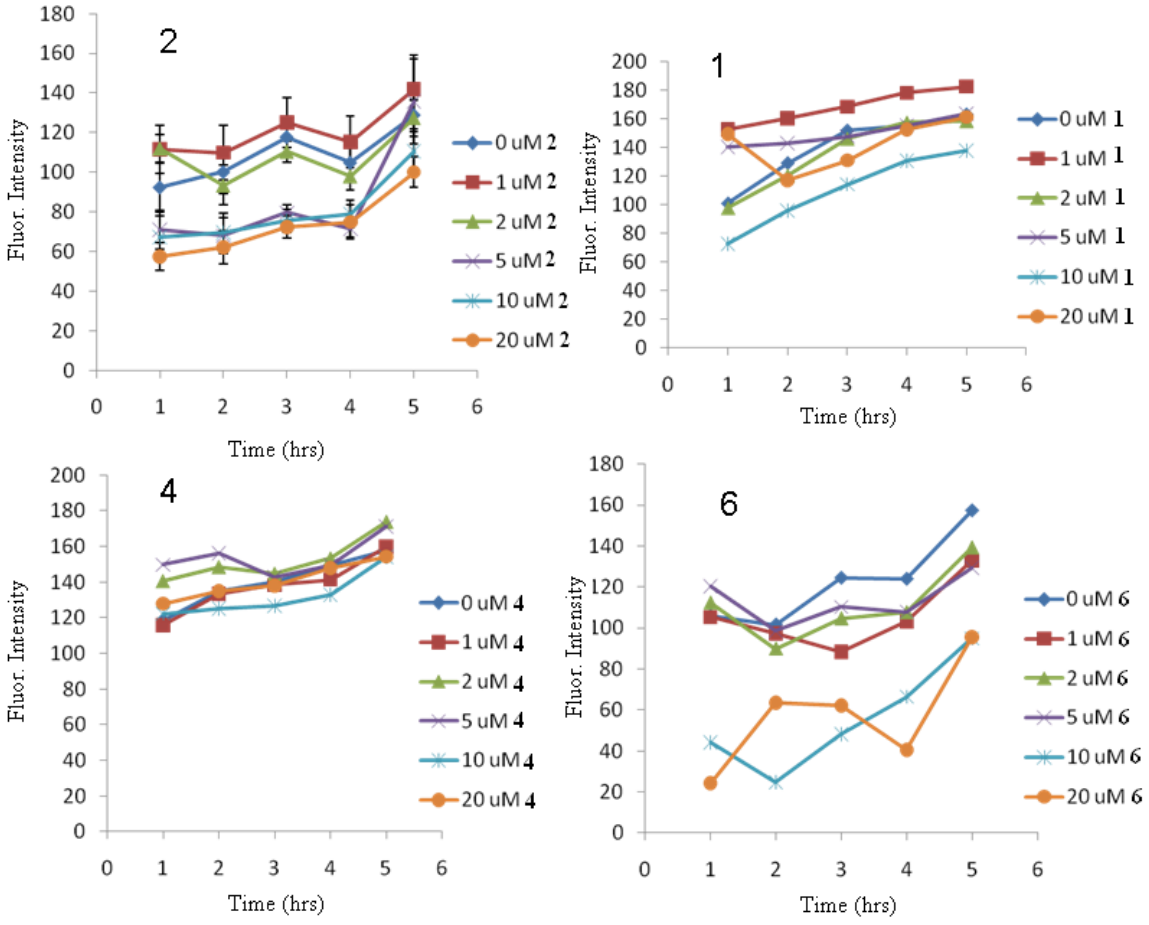

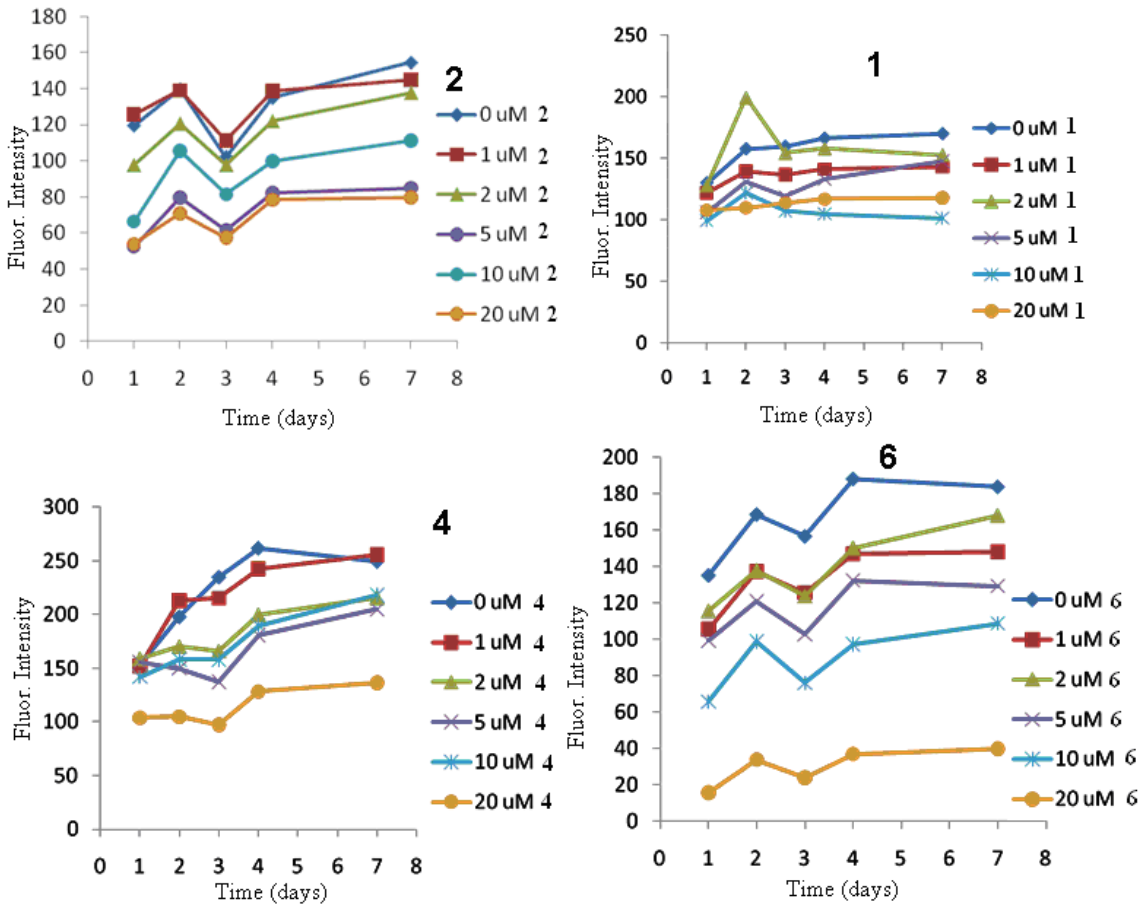

Fig. 3.4 Effects of cyclic Aβ peptides **3.1, 3.2, 3.4** and **3.6** on oligomerization of Aβ 1-42 *in vitro.* Beta-amyloid (Aβ 1-42) at 5 μM monomer concentration was mixed with cyclic peptides at 1 μM, 2 μM, 5 μM, 10 μM, and 20 μM. 50 μM Thioflavin T was then added to Aβ peptide solution. The fibril formation was measured at various time as the change in fluorescent emission at 528 nm with excitation at 450 nm.

In our search of more potent Aβ fibrillogenesis inhibitors we designed another cyclic peptide that had a hydrophobic core (KLVFF) of Aβ 16-20 in the recognition strand. We were able to synthesize this peptide but were unsuccessful in isolation.

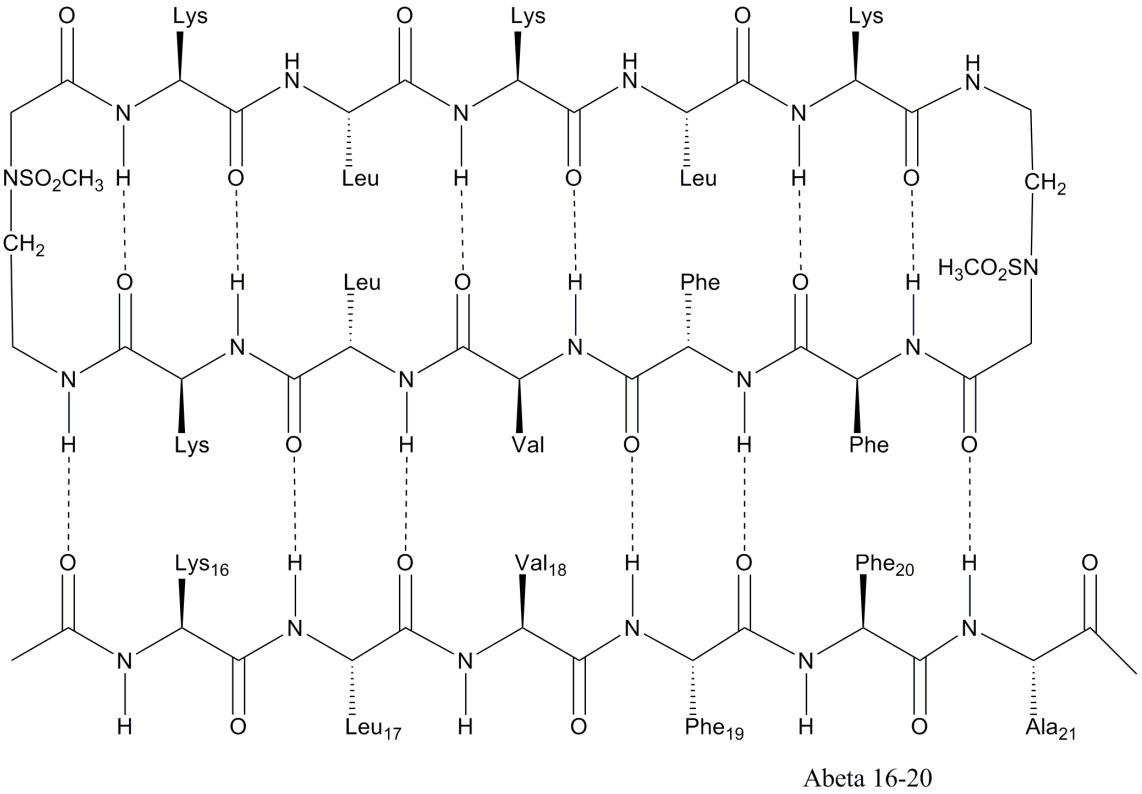

Fig. 3.5 Proposed cyclic Aβ peptide with KLVFF as core residues in recognition strand interacting with fragment 16-20 of growing Aβ fibril.

All cyclic peptidomimetics were synthesized on 2-chlorotrityl chloride resin as solid support and standard solid phase Fmoc amino acid chemistry as described in chapter 2 (31). Coupling was carried out in most cases using standard chemistry of HCTU in N-methyl pyrrolidone (NMP) with double coupling for each residue. The exceptions were cyclic peptides **3.2** & **3.4**, which required extended coupling times because of the difficulty of coupling amino acids following a N-methyl residue. These peptides were manually synthesized first to optimize coupling conditions for attaching the amino acid residue following the N-methyl residue. Coupling efficiency for each amino acid was monitored using UV quantification for dibenzofulvene-derived chromophore released on deprotection of the Fmoc-protecting group using 20% piperidine/2% DBU in DMF. It was seen that double coupling of unmethylated amino

acids following N-methyl residue coupling for 3 hours gave quantitative conversion. Only two coupling reactions had to be double coupled for 3 hrs, whereas the remaining were coupled for 10 mins each cycle. After optimizing and successfully synthesizing peptides **3.2** & **3.4** manually, we tried to synthesize these peptides on Protein Technologies Symphony synthesizer using optimized conditions for manual synthesis. To our surprise none of the peptides were synthesized. When N-methyl-Leu was replaced with commercially available and less hindered N-methyl-Gly (Sarcosine), peptide **3.5** was synthesized on synthesizer using the same optimized conditions for manual synthesis. All linear peptides were cleaved from the resin and cyclized under dilute conditions as described in chapter 2. The crude cyclic peptides were then purified by HPLC and characterized by MALDI-TOF and NMR analysis.

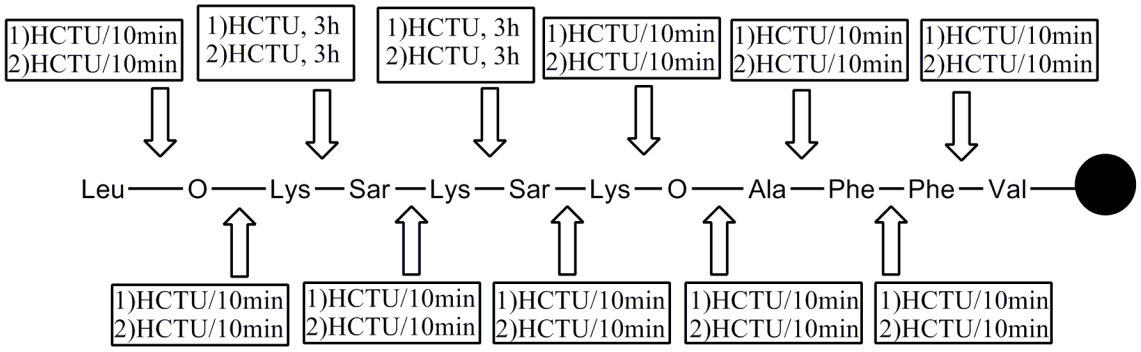

Fig. 3.6 Synthesis protocol for coupling step for peptide **3.5** on PTI symphony synthesizer.

Various methods have been reported for the synthesis of α-N-methylated amino acids (32-36). All α-N-methylated amino acids were synthesized using a two step protocol. The first step involves 5-oxazolidinone formation by condensation of commercially available Fmoc-amino acids with paraformaldehyde in the minimum amount of toluene using microwave irradiation. All the reactions were carried out in an

unmodified domestic microwave oven operated at 2450 MHz frequency at 80% power. 5-Oxazolidinone formation was monitored by TLC and the reaction was completed in 2 mins. Treatment of oxazolidinones with excess triethylsilane in TFA:DCM (1:1) resulted in ring opening with reduction to give α-N-methylated amino acids **3.3a-c** in good yields.

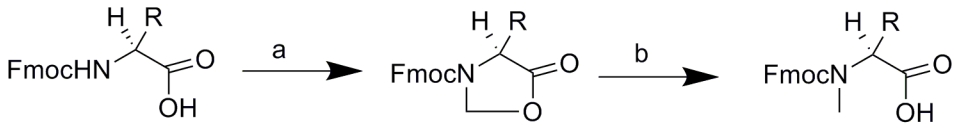

1 **2** **3**

		Yield(%)	
	R	2	3
a	$CH_2CH(CH_3)_2$	95	96
b	$(CH_2)_2NHCO_2Allyl$	98	92
c	$CH(CH_3)_2$	92	95

(a) $(CH_2)_nO$, PTSA (Cat.), Toluene microwave 45 sec (b) Et_3SiH, TFA, DCM

Scheme 3.1 Synthesis of N-methylated amino acids via reduction of 5-oxazolidines.

Most of the reported methodologies have limited or no applications to N-methylated amino acids with functionalized side chains and are not suitable for Fmoc-solid phase chemistry. We have synthesized N-methylated lysine by a second protocol employing o-nitrobenzenesulfonyl chloride (ONBSCl) as protecting group as shown in scheme 3.2 (37,38). Our strategy was to use the o-NBS group to protect and activate the amino group. The acidic proton of the sulfonamide is then easily removed by a relatively weak base such as DBU allowing softer conditions for N-methylation specifically on α-amino group. The removal of the o-NBS protecting group is achieved with mercaptoethanol and DBU in DMF. The resulting secondary amine is acylated with Fmoc-Cl to give the N-methylated protected ester **3.9**. The deprotection of the allyl

protecting group with $Pd(PPh_3)_4$ in the presence of NMM gives Fmoc-protected α-N-methylated lysine in good yield.

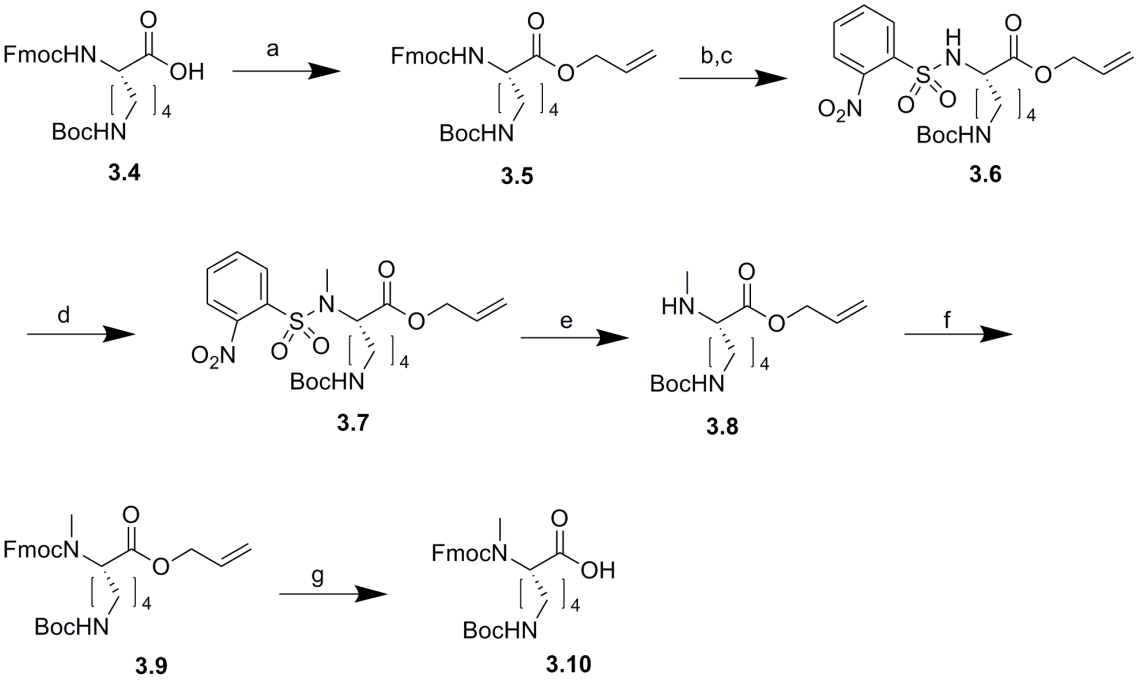

(a) Cs_2CO_3, Allyl Bromide, DMF (b) 2% DBU, 20% Piperidine in DMF (c) oNBSCl, Et_3N, DCM, rt
(d) DBU, $(CH_3)_2SO_4$, DMF, 0^0C (e) $SHCH_2CH_2OH$, DBU, DMF (f) Fmoc-Cl, DIPEA, DCM rt
(g) $Pd(PPh_3)_4$, NMM, DCM rt

Scheme 3.2 Synthesis of Fmoc α-N-methyl Lys(Boc)-OH.

We have also synthesized a N-methylated lysine derivative in good yields using a solid phase strategy. This methodology involves the use of 2-chlorotrityl chloride resin to temporarily protect the carboxylic group of the α-amino acid as shown in scheme 3.3.

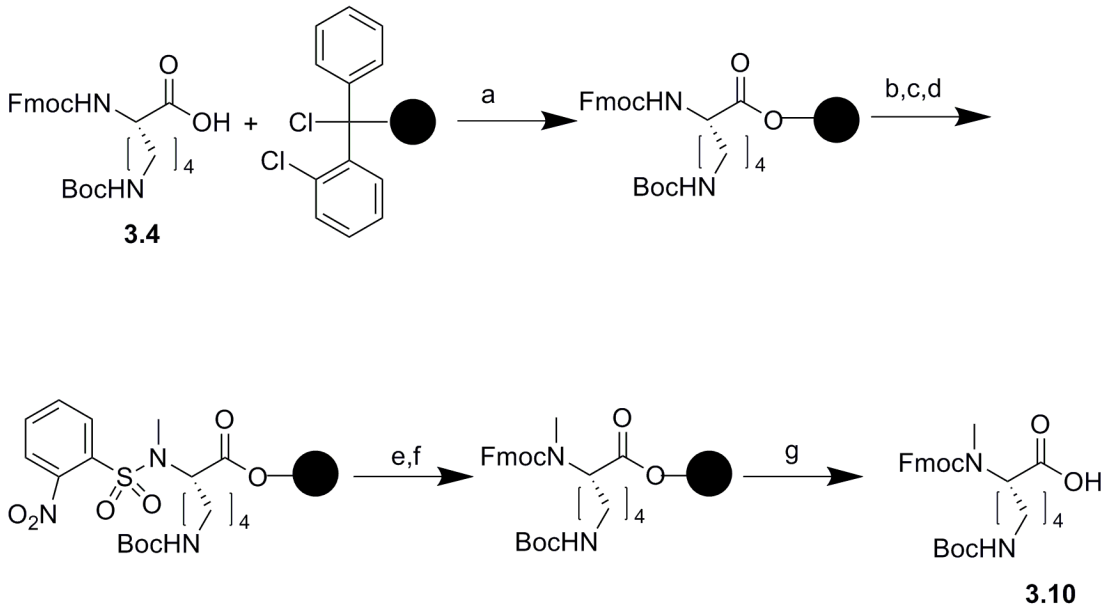

(a) DIEA, DCM (b) 2% DBU, 20% Piperidine in DMF (c) oNBSCl, Et_3N, DCM, rt (d) DBU, $(CH_3)_2SO_4$, DMF, 0^0C (e) $SHCH_2CH_2OH$, DBU, DMF (f) Fmoc-Cl, DIPEA, DCM rt (g)20%Trifluoroethanol in DCM, rt

Scheme 3.3 Solid Phase Synthesis of Fmoc α-N-Methyl-Lys(Boc)-OH.

3.2.2 Conformational studies of cyclic Peptides using Circular Dichroism

The conformational study of all cyclic III peptides were carried out in buffered aqueous solutions. The CD spectra of cyclic Aβ-hairpin peptide with Robinson's template and novel sulfonamide glycine turn promoter (peptide **3.1)** are shown in Fig. 3.7. CD spectra for cyclic peptide **3.1** was take in 7 mM phosphate buffer at a concentration of 200 µM at pH 7 and 25^0C. As expected the CD spectra showed a negative absorption minima around 200 nm and strong positive absorption maxima around 185-190 nm. These characterstic CD bands are strongly indicative of a beta sheet or beta turn secondary structures.

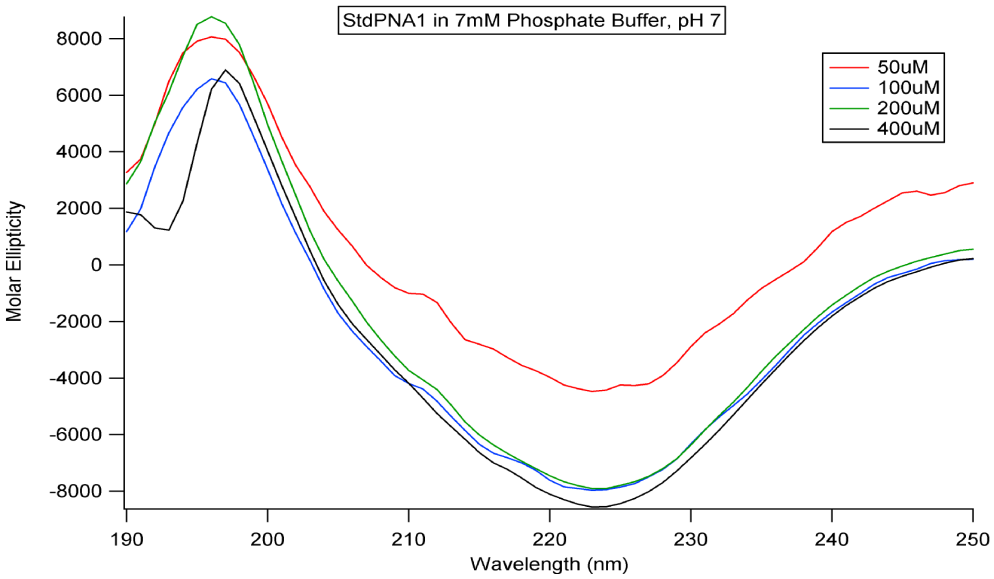

Fig. 3.7 CD spectra for determining β-sheet conformation, for different concentration of cyclic Aβ hairpin **3.2** prepared in 7 mM phosphate buffer.

3.3 Experimental Procedures

3.3.1 Materials and Methods

Organic and inorganic reagents (ACS grade) were obtained from commercial sources and used without further purification, unless otherwise noted. Fmoc-protected amino acids and the coupling agent HCTU were obtained from Protein Technologies, Calbiochem-Novabiochem, or Chem-impex International. 2-Chlorotrityl chloride resin was purchased from Anaspec Inc. All linear peptides were synthesized on the Symphony peptide synthesizer, Protein Technologies Instruments. Solvents for peptide synthesis and reverse-phase HPLC were obtained from Applied Biosystems. Other chemicals used were obtained from Aldrich and were of the highest purity commercially available. Thin layer chromatography (TLC) was performed on glass plates (Whatman) coated with 0.25 mm thickness of silica gel 60Å (# 70-230 mesh). All ^{1}H,^{13}C and ^{2}D NMR spectra were recorded on Bruker 250 MHz, Varian INOVA 400 MHz spectrometer in $CDCl_3$ or unless

otherwise specified and chemical shifts are reported in ppm (δ) relative to internal standard tetramethylsilane (TMS). High resolution mass spectra were obtained on an Agilent LC-MSD-TOF.

3.3.2 Peptide Synthesis & Purification

Cyclic Aβ-hairpin peptide with ^{D}Pro-^{L}Pro and N-(2-aminoethyl)-N-methylsulfonamido glycine beta-turn promoters.

2-Chlorotrityl chloride resin was treated with Fmoc-Pro-OH and then immediately Fmoc-deprotected using 20% piperidine/2% DBU in DMF. Fmoc quantification of resin indicated a loading of 0.19 mmol/g of resin. For a 25 μmol synthesis, 132 mg of resin was charged to the peptide reaction vessel on a Protein Technologies Symphony Peptide Synthesizer. For each coupling step, 5 equivalents of Fmoc-amino acid and 7.5 equivalents of HCTU are dissolved in 0.4 M NMM in DMF to equal 20 equivalents of NMM, which is added to the reactor. Each coupling reaction was carried out for 10 mins followed by NMP washes. Fmoc deprotection was done using 20% piperidine/2% DBU in DMF for (2 x 2.5 mins). The amino acids used for peptide synthesis were coupled in the following order: Fmoc-^{D}Pro-OH, Fmoc-Lys(Boc)-OH, Fmoc-Leu-OH, Fmoc-Lys(Boc)-OH, Fmoc-Leu-OH, Fmoc-Lys(Boc)-OH, Fmoc-$NHCH_2CH_2N(O_2SCH_3)CH_2COOH$, Fmoc-Leu-OH, Fmoc-Val-OH, Fmoc-Phe-OH, Fmoc-Phe-OH, and Fmoc-Ala-OH. After synthesis of the protected linear Aβ peptide, the resin was transferred to a manual peptide synthesis vessel and treated with 5 mL of a cleavage solution of 20% trifluoroethanol in DCM for 2 hrs. The resin was filtered and washed with 5 mL of cleavage solution. This cleavage cycle was repeated twice. The combined organic filtrates were concentrated to give crude protected linear Aβ peptide. The crude Aβ peptide was dissolved in 15 mL of 1% v/v DIEA in DMF and treated with

4 equivalents of HCTU for one hour. After one hour, the reaction mixture was concentrated to give crude protected cyclized Aβ-hairpin peptidomimetic. The crude peptidomimetic was then treated with a 10 mL solution of 87.5% TFA/5% H_2O/5% phenol/2.5% triethylsilane for 30 minutes. The reaction mixture was concentrated and the thick viscous liquid was triturated twice with 10 mL of cold diethyl ether. The reaction contents were centrifuged to give crude cyclic Aβ peptidomimetic. The crude peptidomimetic was dissolved in a solution of 0.1% TFA in H_2O and freeze-dried to give a white fluffy powder. All Aβ-hairpin peptides were purified using preparative reverse phase HPLC (5 μM particle size C_{18} AAPPTEC spirit column, 25 x 2.12 cm) with eluents: A = 0.1% HCO_2H in H_2O, B = 0.1% HCO_2H in H_3CCN. The purification was carried out using a gradient of 5-50% B Buffer over 40 min with a flow rate 20 mL/minute using 222 nm UV detection. All peaks with retention times expected for peptides were collected and lyophilized. The purified peptides were analyzed using similar analytical HPLC conditions and found to have >95% purity and were structurally characterized using a Bruker Autoflex MALDI-TOF instrument with α-cyano hydroxy cinnamic acid (CHCA) as matrix. We have also characterized the secondary structure of selected cyclic peptidomimetics and they show concentration independent CD spectra in pH 7.2 phosphate buffer indicative of beta-sheet-like conformations with a minima at 218 nm and a maxima at 190 nm for cyclic Aβ-hairpin peptide as expected. This supports the assertion of cyclic beta-hairpin-like structures.

General Procedure for the synthesis of N-Fmoc-5-oxazoldinone

A mixture of Fmoc-amino acid (10 mmol), paraformaldehyde (60 mmol) and p-toluenesulfonic acid (1 mmol) was suspended in toluene (10 mL) in a pyrex microwave

vial. The vial was placed in a beaker filled with sand and exposed to microwave irradiation in a domestic microwave operating at 2450 MHz frequency and 80% power for 45 sec. After completion of the reaction, an additional 25 mL of ethyl acetate was added and the reaction mixture was washed with water (1 x 20 mL). The organic layer was dried, filtered, concentrated and chromatographed using EtOAc/Hexane (1:4) as eluent to give the 5-oxazolidinone in good yields.

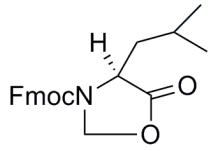

(9H-fluoren-9-yl)methyl 4-isobutyl-5-oxooxazolidine-3-carboxylate 3.2a

Compound **3.2a** was obtained as oil and purified by column chromatography using EtOAc/Hexane (1:4). Yield: (3.5 gm, 95 %). ^{1}H NMR (400 MHz, $CDCl_3$) δ 7.72 (d, *J* = 7.5 Hz, 2H), 7.51 (d, *J* = 7.3 Hz, 2H), 7.39 – 7.34 (m, 2H), 7.32 – 7.26 (m, 2H), 5.39 – 5.15 (m, 1H), 4.97 (d, *J* = 4.5 Hz, 1H), 4.58 (b, 2H), 4.17 – 4.04 (m, 2H), 2.33 (s, 2H), 1.77 – 1.30 (m, 3H), 0.94 – 0.69 (m, 6H). ^{13}C NMR (101 MHz, $CDCl_3$) ppm 172.55, 170.98, 143.77, 143.70, 141.61, 129.26, 128.45, 128.10, 127.37, 125.55, 124.85, 120.32, 63.87, 60.45, 53.49, 53.41, 47.45, 39.42, 39.36, 22.86, 21.09.

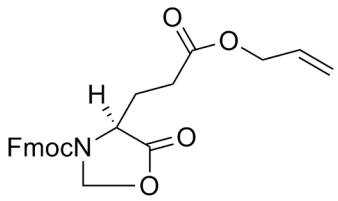

(9H-fluoren-9-yl)methyl4-(3-(allyloxy)-3-oxopropyl)-5-oxooxazolidine-3-carboxylate

Compound **3.2b** was obtained as white foam and purified by column chromatography using EtOAc/Hexane (1:1). Yield: (4.1 gm, 98 %). ^{1}H NMR (400 MHz, $CDCl_3$) δ 7.74 (d, *J* = 7.5 Hz, 2H), 7.51 (d, *J* = 7.4 Hz, 2H), 7.38 (td, *J* = 7.4, 4.0 Hz, 2H), 7.30 (t, *J* = 7.4 Hz, 2H), 5.94 – 5.82 (m, 1H), 5.33 – 5.19 (m, 3H), 5.02 (d, *J* = 4.4 Hz, 1H), 4.71 – 4.57 (m, 2H), 4.52 (d, *J* = 5.0 Hz, 1H), 4.19 (t, *J* = 5.3 Hz, 1H), 2.52 – 2.04 (m, 3H), 1.95 – 1.70 (m, 1H). ^{13}C NMR (101 MHz, $CDCl_3$) ppm 171.82, 153.06, 143.51, 141.59, 132.19, 128.18, 127.47, 124.80, 120.33, 118.75, 77.72, 67.59, 65.59, 54.04, 47.34, 29.33, 25.85.

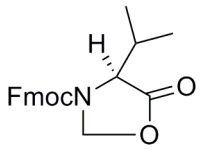

(9H-fluoren-9-yl)methyl 4-isopropyl-5-oxooxazolidine-3-carboxylate 3.2c

Compound **3.2c** was obtained as pale yellow oil and purified by column chromatography using EtOAc/Hexane (1:1). Yield: (3.2 gm, 92 %). ^{1}H NMR (400 MHz, $CDCl_3$) δ 7.73 (d, *J* = 7.5 Hz, 2H), 7.51 (d, *J* = 7.4 Hz, 2H), 7.38 (t, *J* = 7.4 Hz, 2H), 7.30 (t, *J* = 7.4 Hz, 2H), 5.45 – 5.17 (m, 1H), 4.97 (d, *J* = 4.6 Hz, 1H), 4.68 – 4.53 (m, 2H), 4.21 – 4.14 (m, 1H), 3.66 – 3.52 (m, 1H), 1.80 – 1.58 (m, 1H), 1.09 – 0.76 (m, 6H). ^{13}C NMR (101 MHz, $CDCl_3$) ppm 171.41, 153.42, 143.62, 141.65, 128.15, 127.42, 124.75, 120.30, 78.43, 67.22, 60.06, 47.41, 31.12, 17.98.

General Procedure for the synthesis of N-Fmoc-N-Methyl Amino Acid

5-Oxazolidinone (1 equiv.) was dissolved in 20 mL DCM and 20 mL TFA, triethylsilane (3 equiv.) were added. The reaction mixture was stirred overnight at room temperature. The reaction contents were then concentrated in vacuo and reconcentrated three times to

remove residual TFA. The resultant crude oil was crystallized with 5% ether in hexane to give a white solid in good yields.

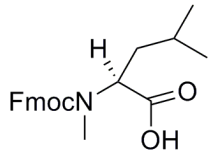

2-((((9H-fluoren-9-yl)methoxy)carbonyl)(methyl)amino)-4-methylpentanoic acid 3.3a

Compound **3.3a** was obtained as a white powder. Yield: (3.3 gm, 96 %) ^{1}H NMR (250 MHz, $CDCl_3$) δ 7.75 (t, *J* = 7.9 Hz, 2H), 7.57 (dd, *J* = 12.8, 6.6 Hz, 2H), 7.45 – 7.26 (m, 4H), 4.65 – 4.51 (m, 1H), 4.51 – 4.18 (m, 3H), 2.86 (d, *J* = 4.7 Hz, 3H), 1.81 – 1.40 (m, 3H), 1.04 – 0.71 (m, 6H). ^{13}C NMR (101 MHz, $CDCl_3$) ppm 178.42, 161.50, 149.28, 146.21, 133.07, 133.00, 132.52, 132.43, 130.44, 130.24, 125.52, 72.12, 61.56, 52.18, 42.48, 42.17, 35.61, 35.34, 29.84, 28.54, 28.33, 26.43.

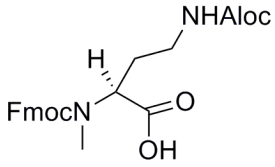

2-((((9H-fluoren-9-yl)methoxy)carbonyl)(methyl)amino)-5-(allyloxy)-5-oxopentanoic acid 3.3b

Compound **3.3b** was obtained as a white powder. Yield: (4.1 gm, 92%) ^{1}H NMR (400 MHz, DMSO-d_6) δ 12.93 (s, 1H), 7.88 (d, *J* = 6.8 Hz, 2H), 7.64 (t, *J* = 6.5 Hz, 2H), 7.41 (t, *J* = 7.0 Hz, 2H), 7.33 (d, *J* = 2.9 Hz, 2H), 5.97 – 5.84 (m, 1H), 5.28 (d, *J* = 17.3 Hz, 1H), 5.18 (d, *J* = 10.2 Hz, 1H), 4.53 (s, 2H), 4.42 – 4.32 (m, 2H), 4.32 – 4.26 (m, 1H), 2.74 (s, 3H), 2.29 (d, *J* = 7.0 Hz, 1H), 2.19 (d, *J* = 17.5 Hz, 2H), 2.07 – 1.80 (m, 1H). ^{13}C NMR (101 MHz, DMSO-d_6) ppm 172.04, 171.84, 156.02, 143.75, 140.78, 132.65,

127.65, 127.10, 125.00, 120.09, 117.70, 117.65, 66.84, 64.45, 58.07, 46.74, 30.96, 30.19, 23.44.

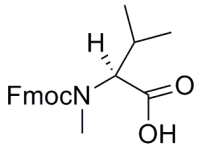

2-((((9H-fluoren-9-yl)methoxy)carbonyl)(methyl)amino)-3-methylbutanoic acid 3.3c

Compound **3.3c** was obtained as a white powder. Yield: (3.2 gm, 95%) ^{1}H NMR (400 MHz, DMSO-d_6) δ 11.29 (s, 1H), 7.85 (s, 2H), 7.63 (s, 2H), 7.35 (d, *J* = 29.8 Hz, 4H), 4.40 (d, *J* = 26.4 Hz, 2H), 4.27 (s, 2H), 2.76 (s, 3H), 2.05 (d, *J* = 31.9 Hz, 1H), 1.14 – 0.70 (m, 6H). ^{13}C NMR (101 MHz, DMSO-d_6) ppm 171.76, 171.58, 155.86, 155.25, 143.65, 143.51, 140.62, 127.39, 126.84, 124.70, 119.82, 66.61, 63.58, 46.59, 46.53, 29.92, 26.75, 26.63, 19.48, 19.42, 18.58, 18.28.

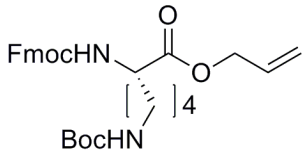

allyl 1-(9H-fluoren-9-yl)-13,13-dimethyl-3,11-dioxo-2,12-dioxa-4,10-diazatetra-decane-5-carboxylate 3.5

Fmoc-Lys(Boc)-OH (2.0 gm, 4.2 mmol) was suspended in dry methanol (12 mL) and cesium carbonate (0.7 gm, 2.1 mmol) was added to it. After forming homogenous solution, the reactions contents were stirred at room temperature for 2 hrs under inert atmosphere. The mixture was then concentrated to give white foam, which was redissolved in DMF (15 mL). Allyl bromide (3.7 mL, 42.4 mmol) was then added and reaction was stirred overnight. After completion of reactions, the contents were taken up in 200 mL ethyl acetate and washed with water (1 x 30 mL) and brine (1 x 30 mL). The

organic layer was dried over Na_2SO_4, filtered, concentrated and flash chromatographed to give compound **3.5** (1.8 gm, 82%) as colorless foam. R_f = 0.25 (1:3 ethyl acetate: hexane). ^{1}H NMR (400 MHz, $CDCl_3$) δ 7.71 (d, *J* = 7.5 Hz, 2H), 7.61 – 7.54 (m, 2H), 7.35 (t, *J* = 7.4 Hz, 2H), 7.26 (t, *J* = 7.3 Hz, 2H), 5.85 (ddd, *J* = 16.3, 10.7, 5.4 Hz, 1H), 5.77 (d, *J* = 7.0 Hz, 1H), 5.29 (d, *J* = 17.2 Hz, 1H), 5.20 (d, *J* = 10.4 Hz, 1H), 4.80 (s, 1H), 4.60 (s, 2H), 4.40 – 4.32 (m, 2H), 4.18 (t, *J* = 6.8 Hz, 1H), 3.06 (s, 2H), 1.91 – 1.52 (m, 4H), 1.41 (s, 9H), 1.37 (b, 2H). ^{13}C NMR (101 MHz, $CDCl_3$) ppm 172.10, 155.99, 143.79, 143.63, 141.12, 131.46, 127.55, 126.92, 124.98, 119.81, 118.69, 78.83, 66.84, 65.72, 53.75, 47.02, 39.89, 31.80, 29.42, 28.31, 22.35.

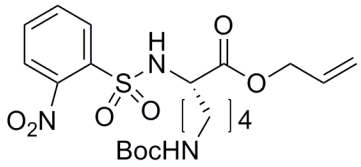

allyl 6-(tert-butoxycarbonylamino)-2-(2-nitrophenylsulfonamido)hexanoate 3.6

Compound **3.5** (1.8 gm, 3.5 mmol) was dissolved in 20 mL DCM and 5 mL 20% piperidine / 2% DBU was added to it. After complete deprotection of the Fmoc group, the resulting primary amine was quickly purified by passing over a pad of silica gel and used in the next step without further purification. The amine (0.94 gm, 3.3 mmol) was taken up in 20 mL DCM and DIEA (0.84 mL, 4.8 mmol) was added. o-Nitrobenzenesulfonyl chloride (1.1 gm, 5.0 mmol) in 10 mL DCM was added slowly at 0 ^{o}C. The reaction was stirred for 2 hrs by monitoring the conversion of starting material by TLC. After completion of the reaction, the crude mixture was further diluted with 50 mL DCM and washed with (1 x 15 mL) 5% Na_2CO_3 solution, water (1 x 20 mL) and brine (1 x 20 mL). The combined organic layers were dried, filtered, concentrated and chromatographed to

give compound **3.6** (1.12 gm, 73%). ^{1}H NMR (250 MHz, $CDCl_3$) δ 8.10 – 8.04 (m, 1H), 7.95 – 7.90 (m, 1H), 7.77 – 7.70 (m, 2H), 6.12 (d, *J* = 9.2 Hz, 1H), 5.67 (ddt, *J* = 17.3, 10.2, 5.9 Hz, 1H), 5.23 – 5.19 (m, 1H), 5.15 (dd, *J* = 1.7, 1.2 Hz, 1H), 4.54 (s, 1H), 4.38 – 4.31 (m, 2H), 4.24 – 4.15 (m, 1H), 3.14 – 3.05 (m, 2H), 1.98 – 1.53 (m, 6H), 1.45 (s, 9H). ^{13}C NMR (101 MHz, $CDCl_3$) ppm 170.37, 155.72, 147.19, 133.58, 133.35, 132.61, 130.74, 130.04, 125.01, 118.61, 78.34, 65.64, 56.24, 39.65, 32.12, 28.85, 28.01, 21.96.

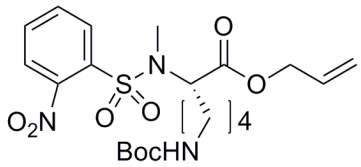

allyl 6-(tert-butoxycarbonylamino)-2-(N-methyl-2-nitrophenylsulfonamido) hexanoate 3.7

Compound **3.6** (1.12 gm, 2.4 mmol) was dissolved in 15 mL DMF and $(CH_3)_2SO_4$ (0.3 mL, 3.5 mmol), CH_3I (0.2 mL, 3.5 mmol) was added along with DBU (0.8 mL, 4.7 mmol) as base. The reaction was completed in 15 mins, as monitored by TLC. The solvent was removed in vacuo and crude reaction contents were purified by flash chromatography to give compound **3.7** (1.2 gm, 93%) as a pale yellow oil. ^{1}H NMR (250 MHz, $CDCl_3$) ppm 8.07 – 8.02 (m, 1H), 7.71 – 7.66 (m, 2H), 7.65 – 7.58 (m, 1H), 5.84 – 5.65 (m, 1H), 5.20 (ddd, *J* = 9.6, 7.4, 1.3 Hz, 2H), 4.66 (dd, *J* = 10.6, 4.9 Hz, 1H), 4.54 (s, 1H), 4.50 – 4.44 (m, 2H), 3.17 – 3.06 (m, 2H), 2.97 (d, *J* = 3.3 Hz, 3H), 1.85 – 1.55 (m, 6H), 1.44 (s, 9H).

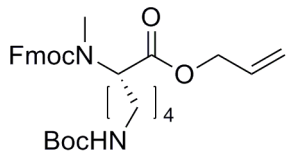

allyl 1-(9H-fluoren-9-yl)-4,13,13-trimethyl-3,11-dioxo-2,12-dioxa-4,10-diaza tetradecane-5-carboxylate 3.9

Compound **3.7** (1.15 gm, 2.4 mmol) was dissolved in 10 mL DMF and mercaptoethanol (1.7 mL, 23.6 mmol) along with DBU (1.8 mL, 11.8 mmol) was added at 0^{o}C. After completion of reaction in 10 mins, the solvent was removed from reaction mixture and the crude mixture was quickly purified over pad of silica gel to give secondary amine **3.8** (0.6 gm, 85%). This secondary amine was used without further purification. The secondary amine (0.14 gm, 0.5 mmol) was dissolved in 6 mL DCM and Fmoc-Cl (0.26 gm, 0.9 mmol), DIEA (0.3 mL, 1.4 mmol) were added. The reaction was stirred overnight at room temperature. The reaction mixture was concentrated in vacuo and subjected to flash chromatography to give compound **3.9** (0.18 gm, 77%) as a white foam. ^{1}H NMR (400 MHz, $CDCl_3$) δ 7.65 (d, *J* = 7.1 Hz, 2H), 7.57 – 7.43 (m, 2H), 7.31 – 7.19 (m, 4H), 5.86 – 5.71 (m, 1H), 5.26 – 5.09 (m, 2H), 4.96 – 4.71 (m, 1H), 4.55 – 4.42 (m, 2H), 4.40 – 4.28 (m, 2H), 4.19 – 4.08 (m, 1H), 3.07 – 2.93 (m, 2H), 2.76 (d, *J* = 7.1 Hz, 3H), 1.95 – 1.60 (m, 2H), 1.37 (d, *J* = 8.6 Hz, 9H), 1.31 – 0.99 (m, 4H). ^{13}C NMR (101 MHz, $CDCl_3$) ppm 170.67, 170.34, 156.55, 155.83, 155.70, 144.57, 143.60, 143.47, 140.89, 131.42, 131.35, 127.30, 126.93, 126.67, 126.49, 124.66, 124.61, 124.34, 119.58, 119.44, 118.04, 78.36, 67.27, 66.96, 65.17, 64.69, 58.02, 50.07, 46.82, 39.79, 30.18, 29.89, 29.02, 28.06, 27.81, 22.83.

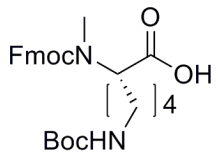

1-(9H-fluoren-9-yl)-4,13,13-trimethyl-3,11-dioxo-2,12-dioxa-4,10-diazatetradecane-5-carboxylic acid 3.10

Compound **3.9** (0.18 gm, 0.34 mmol) was dissolved in anhydrous 10 mL DCM and $Pd(PPh_3)_4$ (39 mg, 0.03 mmol), NMM (0.17 gm, 1.7 mmol) were added to it. After 2 hrs, another fresh lot of catalyst (39 mg, 0.03 mmol) was added and reaction was stirred for another 2 hrs. The reaction contents were concentrated and purified by flash chromatography to give compound **3.10** (0.13 gm, 80%) as a white solid. ^{1}H NMR (400 MHz, $CDCl_3$) δ 10.30 (b, 1H), 7.75 (t, *J* = 8.8 Hz, 2H), 7.62 – 7.53 (m, 2H), 7.42 – 7.27 (m, 4H), 4.81 (dd, *J* = 10.5, 4.4 Hz, 1H), 4.69 – 4.53 (m, 1H), 4.50 – 4.38 (m, 2H), 4.30 – 4.19 (m, 1H), 3.09 (d, *J* = 13.2 Hz, 2H), 2.86 (d, *J* = 10.6 Hz, 3H), 2.03 – 1.69 (m, 2H), 1.44 (d, *J* = 8.8 Hz, 9H), 1.40 – 1.11 (m, 4H). ^{13}C NMR (101 MHz, $CDCl_3$) ppm 175.71, 157.28, 156.53, 144.04, 143.88, 141.39, 127.76, 127.13, 125.10, 124.90, 120.02, 67.90, 67.62, 58.39, 47.31, 41.42, 40.28, 30.69, 30.48, 29.41, 28.48, 28.14, 23.37.

3.4 References

1. Haass, C.; Schlossmacher, M. G.; Hung, A. Y.; Vigo-Pelfrey, C.; Mellon, A.; Ostaszewski, B. L.; Lieberburg, I.; Koo, E. H.; Schenk, D.; Teplow, D. B.; et al., Amyloid beta-peptide is produced by cultured cells during normal metabolism. *Nature* **1992,** *359* (6393), 322-5.

2. Seubert, P.; Vigo-Pelfrey, C.; Esch, F.; Lee, M.; Dovey, H.; Davis, D.; Sinha, S.; Schlossmacher, M.; Whaley, J.; Swindlehurst, C.; et al., Isolation and quantification of soluble Alzheimer's beta-peptide from biological fluids. *Nature* **1992,** *359* (6393), 325-7.

3. Shoji, M.; Golde, T. E.; Ghiso, J.; Cheung, T. T.; Estus, S.; Shaffer, L. M.; Cai, X. D.; McKay, D. M.; Tintner, R.; Frangione, B.; et al., Production of the Alzheimer amyloid beta protein by normal proteolytic processing. *Science* **1992,** *258* (5079), 126-9.

4. Burdick, D.; Soreghan, B.; Kwon, M.; Kosmoski, J.; Knauer, M.; Henschen, A.; Yates, J.; Cotman, C.; Glabe, C., Assembly and aggregation properties of synthetic Alzheimer's A4/beta amyloid peptide analogs. *J Biol Chem* **1992,** *267* (1), 546-54.

5. Jarrett, J. T.; Berger, E. P.; Lansbury, P. T., Jr., The carboxy terminus of the beta amyloid protein is critical for the seeding of amyloid formation: implications for the pathogenesis of Alzheimer's disease. *Biochemistry* **1993,** *32* (18), 4693-7.

6. Vigo-Pelfrey, C.; Lee, D.; Keim, P.; Lieberburg, I.; Schenk, D. B., Characterization of beta-amyloid peptide from human cerebrospinal fluid. *J Neurochem* **1993,** *61* (5), 1965-8.

7. Walsh, D. M.; Tseng, B. P.; Rydel, R. E.; Podlisny, M. B.; Selkoe, D. J., The oligomerization of amyloid beta-protein begins intracellularly in cells derived from human brain. *Biochemistry* **2000,** *39* (35), 10831-9.

8. Pike, C. J.; Walencewicz, A. J.; Glabe, C. G.; Cotman, C. W., In vitro aging of beta-amyloid protein causes peptide aggregation and neurotoxicity. *Brain Res* **1991,** *563* (1-2), 311-4.

9. Kirschner, D. A.; Abraham, C.; Selkoe, D. J., X-ray diffraction from intraneuronal paired helical filaments and extraneuronal amyloid fibers in Alzheimer disease indicates cross-beta conformation. *Proc. Natl. Acad. Sci. U. S. A.* **1986,** *83* (2), 503-7.

10. Benzinger, T. L. S.; Gregory, D. M.; Burkoth, T. S.; Miller-Auer, H.; Lynn, D. G.; Botto, R. E.; Meredith, S. C., Two-Dimensional Structure of beta -Amyloid(10-35) Fibrils. *Biochemistry* **2000,** *39* (12), 3491-3499.

11. Amijee, H.; Madine, J.; Middleton, D. A.; Doig, A. J., Inhibitors of protein aggregation and toxicity. *Biochem. Soc. Trans.* **2009,** *37* (4), 692-696.

12. Tjernberg, L. O.; Naeslund, J.; Lindqvist, F.; Johansson, J.; Karlstroem, A. R.; Thyberg, J.; Terenius, L.; Nordstedt, C., Arrest of beta -amyloid fibril formation by a pentapeptide ligand. *J. Biol. Chem.* **1996,** *271* (15), 8545-8.

13. Soto, C.; Kindy, M. S.; Baumann, M.; Frangione, B., Inhibition of Alzheimer's amyloidosis by peptides that prevent beta -sheet conformation. *Biochem. Biophys. Res. Commun.* **1996,** *226* (3), 672-680.

14. Poduslo, J. F.; Curran, G. L.; Kumar, A.; Frangione, B.; Soto, C., beta -sheet breaker peptide inhibitor of Alzheimer's amyloidogenesis with increased blood-brain

barrier permeability and resistance to proteolytic degradation in plasma. *J. Neurobiol.* **1999,** *39* (3), 371-382.

15. Soto, C.; Sigurdsson, E. M.; Morelli, L.; Kumar, R. A.; Castano, E. M.; Frangione, B., beta -Sheet breaker peptides inhibit fibrillogenesis in a rat brain model of amyloidosis: implications for Alzheimer's therapy. *Nat. Med. (N. Y.)* **1998,** *4* (7), 822-826.

16. Ghanta, J.; Shen, C. L.; Kiessling, L. L.; Murphy, R. M., A strategy for designing inhibitors of beta-amyloid toxicity. *J Biol Chem* **1996,** *271* (47), 29525-8.

17. Pallitto, M. M.; Ghanta, J.; Heinzelman, P.; Kiessling, L. L.; Murphy, R. M., Recognition sequence design for peptidyl modulators of beta -amyloid aggregation and toxicity. *Biochemistry* **1999,** *38* (12), 3570-3578.

18. Lowe, T. L.; Strzelec, A.; Kiessling, L. L.; Murphy, R. M., Structure-Function Relationships for Inhibitors of beta -Amyloid Toxicity Containing the Recognition Sequence KLVFF. *Biochemistry* **2001,** *40* (26), 7882-7889.
19. Bodles Angela, M.; El-Agnaf Omar, M. A.; Greer, B.; Guthrie David, J. S.; Irvine, G. B., Inhibition of fibril formation and toxicity of a fragment of alpha-synuclein by an N-methylated peptide analogue. *Neurosci Lett* **2004,** *359* (1-2), 89-93.

20. Gordon, D. J.; Meredith, S. C., Probing the Role of Backbone Hydrogen Bonding in beta -Amyloid Fibrils with Inhibitor Peptides Containing Ester Bonds at Alternate Positions. *Biochemistry* **2003,** *42* (2), 475-485.

21. Kapurniotu, A.; Schmauder, A.; Tenidis, K., Structure-based design and study of non-amyloidogenic, double N-methylated IAPP amyloid core sequences as inhibitors of IAPP amyloid formation and cytotoxicity. *J. Mol. Biol.* **2002,** *315* (3), 339-350.

22. Kokkoni, N.; Stott, K.; Amijee, H.; Mason Jody, M.; Doig Andrew, J., N-Methylated peptide inhibitors of beta-amyloid aggregation and toxicity. Optimization of the inhibitor structure. *Biochemistry* **2006,** *45* (32), 9906-18.

23. Yan, L.-M.; Tatarek-Nossol, M.; Velkova, A.; Kazantzis, A.; Kapurniotu, A., Design of a mimic of nonamyloidogenic and bioactive human islet amyloid polypeptide (IAPP) as nanomolar affinity inhibitor of IAPP cytotoxic fibrillogenesis. *Proc. Natl. Acad. Sci. U. S. A.* **2006,** *103* (7), 2046-2051.

24. Manavalan, P.; Momany, F. A., Conformational energy studies on N-methylated analogs of thyrotropin releasing hormone, enkephalin, and luteinizing hormone-releasing hormone. *Biopolymers* **1980,** *19* (11), 1943-73.

25. Gordon, D. J.; Sciarretta, K. L.; Meredith, S. C., Inhibition of beta -Amyloid(40) Fibrillogenesis and Disassembly of beta -Amyloid(40) Fibrils by Short beta -

Amyloid Congeners Containing N-Methyl Amino Acids at Alternate Residues. *Biochemistry* **2001,** *40* (28), 8237-8245.

26. Gordon, D. J.; Tappe, R.; Meredith, S. C., Design and characterization of a membrane permeable N-methyl amino acid-containing peptide that inhibits Abeta 1-40 fibrillogenesis. *J. Pept. Res.* **2002,** *60* (1), 37-55.

27. Hughes, E.; Burke, R. M.; Doig, A. J., Inhibition of toxicity in the beta -amyloid peptide fragment beta -(25-35) using N-methylated derivatives: a general strategy to prevent amyloid formation. *J. Biol. Chem.* **2000,** *275* (33), 25109-25115.

28. Doig, A. J., A three stranded beta -sheet peptide in aqueous solution containing N-methyl amino acids to prevent aggregation. *Chem. Commun. (Cambridge)* **1997,** (22), 2153-2154.

29. Mahalaxmi, R.; Balaram, P. Methods in Molecular Biology, vol. 340: Protein Design: Methods and Applications, R.Guerois and M.L. de la Paz , Eds., Humana Press Inc., Totowa, NJ.

30. Cammish, L. E.; Kates, S. A. Instrumentation for automated solid phase peptide synthesis. In *Fmoc Solid Phase Peptide Synthesis*, Chan, W. C. and White, P. D. Eds., Oxford, 2000, pp 277-302.

31. Tantry, S. J.; Kantharaju; Suresh Babu, V. V., Microwave accelerated efficient synthesis of N-fluorenylmethoxycarbonyl/t-butoxycarbonyl/benzyloxycarbonyl-5-oxazolidinones. *Tetrahedron Lett.* **2002,** *43* (51), 9461-9462.

32. .Freidinger, R. M.; Hinkle, J. S.; Perlow, D. S., Synthesis of 9-fluorenylmethyloxycarbonyl-protected N-alkyl amino acids by reduction of oxazolidinones. *J. Org. Chem.* **1983,** *48* (1), 77-81.

33. Ben-Ishai, D., Reaction of acylamino acids with paraformaldehyde. *J. Am. Chem. Soc.* **1957,** *79*, 5736-8.

34. Zhang, S.; Govender, T.; Norstroem, T.; Arvidsson, P.I., An improved synthesis of Fmoc-N-methyl-α-amino acids. *J. Org. Chem.* **2005,** 70(17), 6918-6920.

35. Biron, E.; Chatterjee, J.; Kessler, H., Optimized selective N-methylation of peptides on solid support. *J. Pept. Sci.* **2006,** *12* (3), 213-219.

36. Bowman, W. R.; Coghlan, D. R., A facile method for the N-alkylation of alpha -amino esters. *Tetrahedron* **1997,** *53* (46), 15787-15798.

37. Reichwein, J. F.; Liskamp, R. M. J., Site-specific N-alkylation of peptides on the solid phase. *Tetrahedron Lett.* **1998,** *39* (10), 1243-1246.

38. Fukuyama, T.; Jow, C.-K.; Cheung, M., 2- and 4-nitrobenzenesulfonamides: exceptionally versatile means for preparation of secondary amines and protection of amines. *Tetrahedron Lett.* **1995,** *36* (36), 6373-4.

CHAPTER FOUR:

CYCLIC β- HAIRPIN PEPTIDOMIMETICS: TARGETING p53-MDM2 PROTEIN-PROTEIN INTERACTIONS

4.1 Introduction

The tumor suppressor protein p53 plays a pivotal part in protection from tumor development that arises due to various forms of cellular stress pathways such as DNA damage, hypoxia, telomere shortening etc (1,2). p53 is a potent transcription factor that regulates multiple downstream genes implicated in cell cycle control, apoptosis, antiangiogenesis and senescence. It is estimated that half of all human tumors express p53 is disabled by mutations in its DNA-binding domain and becomes inactive as a transcription factor (3). Growth suppressive and proapoptotic activity of p53 could harm proliferating cells that are not under stress (4). The levels of p53 in cells are controlled by its negative regulator MDM2 (an oncoprotein) through an autoregulatory feedback loop mechanism (5,6). Under cellular stress, nuclear p53 level gets elevated that transcriptionally transactivates the MDM2 gene, resulting in MDM2 binding to p53 (fig.4.1). This results in an increase in MDM2 expression. In turn, MDM2 binds to p53, blocks its transactivation domain and transports p53 to the cytoplasm where MDM2, acts as an E3 ubiquitin protein ligase and promotes p53 ubiquitination and degradation by the proteaosome (7-14). On response to cellular stress, p53 gets phosphorylated on specific serine residue near the MDM2 binding domain, thereby decreasing the affinity of p53 for

MDM2 (15). Over expression of MDM2 inhibits p53 function, leading to uncontrolled proliferation of tumor cells. These tumor cells become resistant to standard chemotherapeutic treatment and do not undergo programmed cell death or apoptosis.

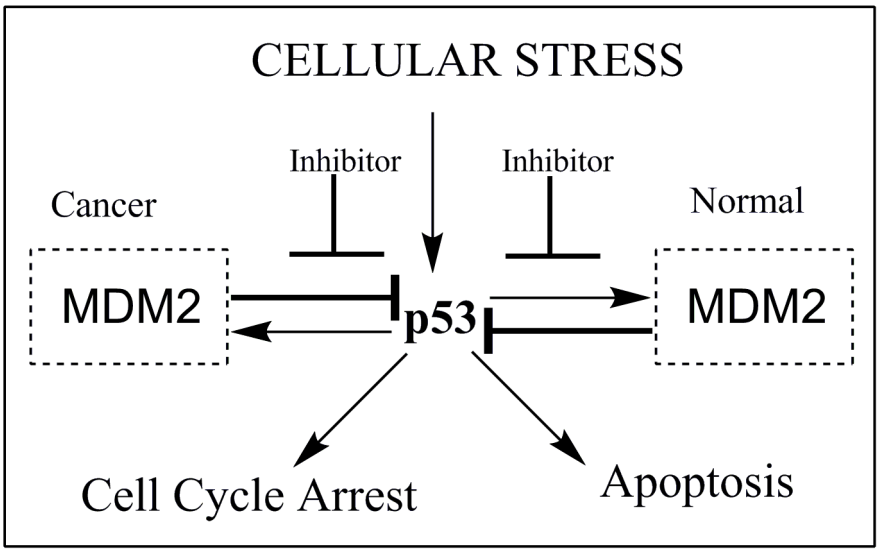

Fig. 4.1 Modulation of p53-MDM2 interactions. Cellular stress triggers the p53 response pathway. The p53-MDM2 autoregulatory feedback loop modulates the amount of p53. Over expression of MDM2 in human cancer leads to p53 ubiquitination to disable the p53 network. Designed inhibitors should complex with MDM2 and block its interaction with p53.

MDM2 interacts through its NH_2 terminal domain with an α-helix present in the NH_2 terminal transactivation domain of p53 and blocks its transcriptional activity directly. The hydrophobic side of the p53 α-helix formed by the amino acids phenylalanine, tryptophan and leucine fit deeply into the hydrophobic cleft of MDM2. Since MDM2 is seen to be over expressed in certain cancers, it may reduce the functional activity of p53-dependent cancer therapies. Hence disruption of p53/MDM2 interaction is a viable therapeutic target for the treatment of cancer. Various small molecule inhibitors, retroinverso peptides, peptoids, terphenyls, β-hairpins, p-oligobenzamides, β-peptides have been developed to mimic the recognition surface of the α-helix of p53. These

inhibitors occupy the p53-binding pocket in MDM2, thereby preventing protein-protein interaction, and thus, facilitate the p53 tumor suppressor function to inhibit cancer cells. Among small molecule inhibitors, Nutlin (cis-imidazolines) emerged as a potent and selective small molecule antagonist of p53/MDM2 interaction with both in vitro and in vivo activity (16). Figure 4.2. shows some promising small molecule and proteomimetic scaffold based inhibitors for p53/MDM2 interaction.

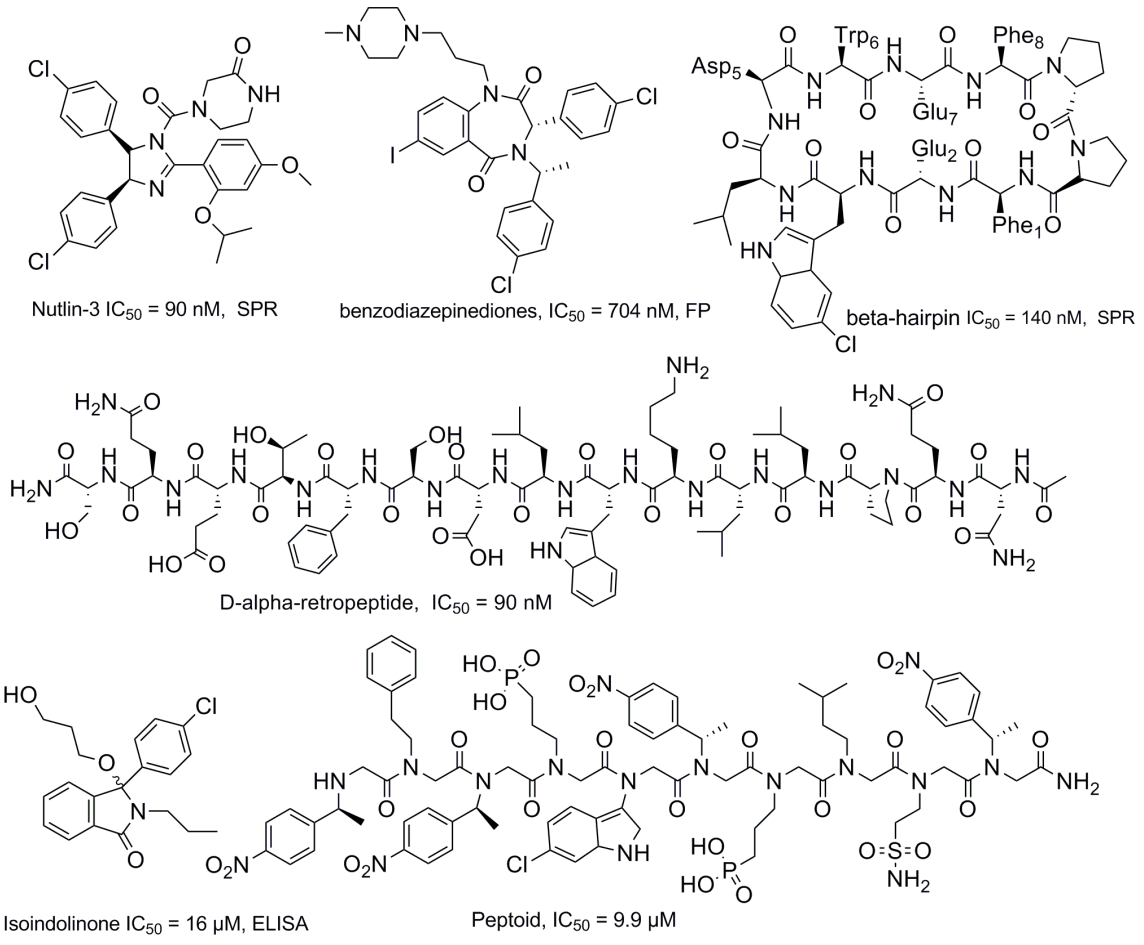

Fig. 4.2 Small molecule and peptidomimetic inhibitors of p53/MDM2 interactions.

Robinson mimicked the α-helix of p53 with a cyclic β-hairpin to inhibit p53/MDM2 interaction. The cyclic beta-hairpin scaffold mounted on ^{D}Pro-^{L}Pro template holds the side chains of phenylalanine and tryptophan residues in the correct relative

positions, so that they could interact with their respective binding sites on MDM2 (17). This scaffold exhibited poor cellular uptake. In this present work, we have made an attempt to synthesize cyclic β-hairpin peptidomimetics mimicking the α-helix of p53 using our novel β- turn promoter, to disrupt p53/MDM2 protein-protein interactions. The incorporation of novel β- turn promoter will further facilitate in stabilizing the cyclic β-hairpin. We have also made an attempt to synthesize morpholino derivatives of serine and lysine and incorporate them into the non-recognition strand of the proposed cyclic β-hairpin with an aim to improve the bioavailability and cellular permeability of the cyclic peptides. The synthesis of the chiral β-turn promoters have also been attempted to improve the binding affinity of these molecules to MDM2.

4.2 Results & Discussions

4.2.1 Peptide Design

The crystal structure of a p53-derived peptide (residues 15-29) in complex with the inhibitory domain of MDM2 (residue 17-125) as revealed by Pavletich and workers suggested that the peptide adopts an α-helical backbone conformation (18). The side chains of Phe19, Trp23 and Leu26 align along one face of the helix and inserts deep into hydrophobic clefts on the surface of MDM2 (fig.4.3a). The binding energy for this protein-protein interaction arises due to van der Waals interactions of these three p53 side chains with the surface of MDM2. The C-terminal end of the helix is less tightly bound leading to a type I β-turn for the segment between Trp23 and Leu26. Robinson and coworkers found that the distance between C_α atoms of Phe19 and Trp23 residues on one face of the MDM2-bound p53 α-helix is same as the distance between C_α atoms of ith and ith+2 residues along one strand (recognition strand) of a β-hairpin. They proposed a

cyclic β-hairpin scaffold that would hold Trp and Phe residues in the correct relative positions so that they could interact with p53 binding site on MDM2. Our design for making cyclic β-hairpin peptides as p53-MDM2 inhibitors involves, Phe19, Trp23 and Leu26 residues aligned along one face of the recognition strand. We hypothesized that incorporation of a novel sulfonamido aminoethyl glycine β-turn promoter at the turns would further facilitate in stabilizing the β-hairpin conformation. As shown in Fig.4.3 (b), β-hairpin mimetic designed as scaffold for p53-MDM2 inhibitors was found to be a weak lead with an IC_{50} greater than 150 μM in an ELISA assay.

(A)

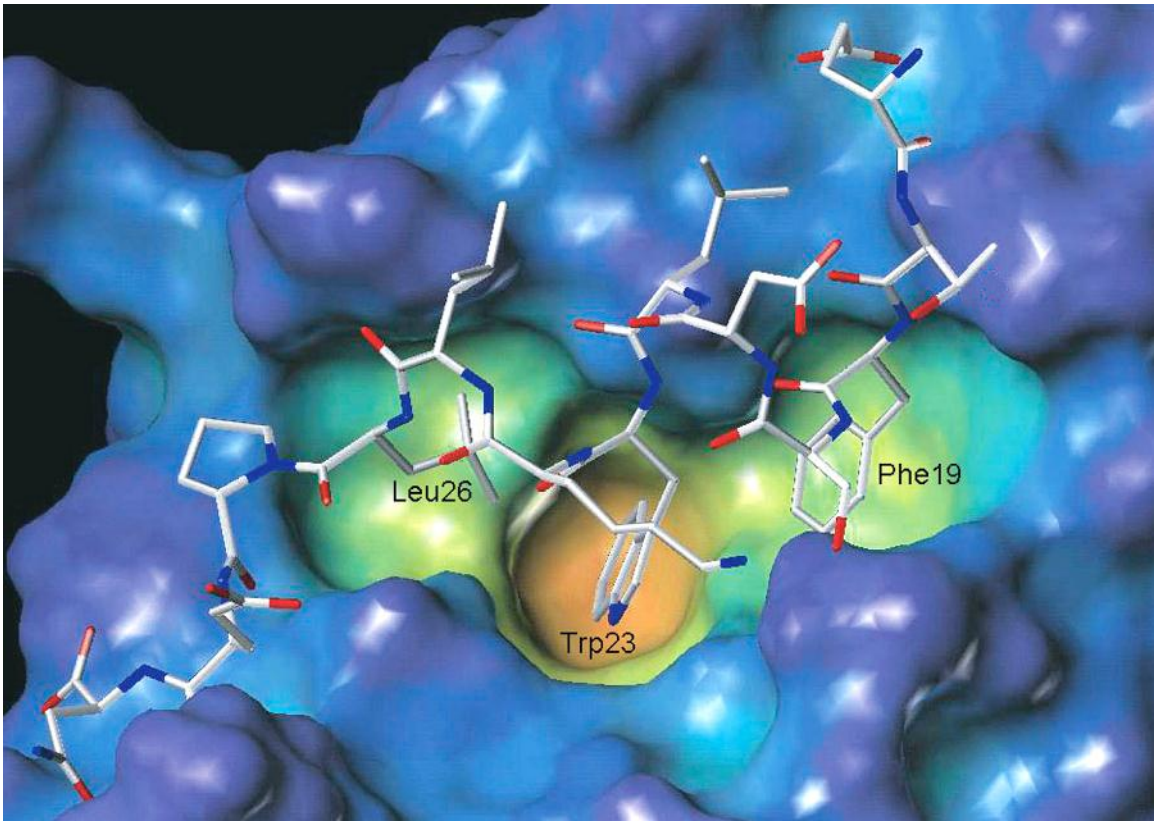

(B)

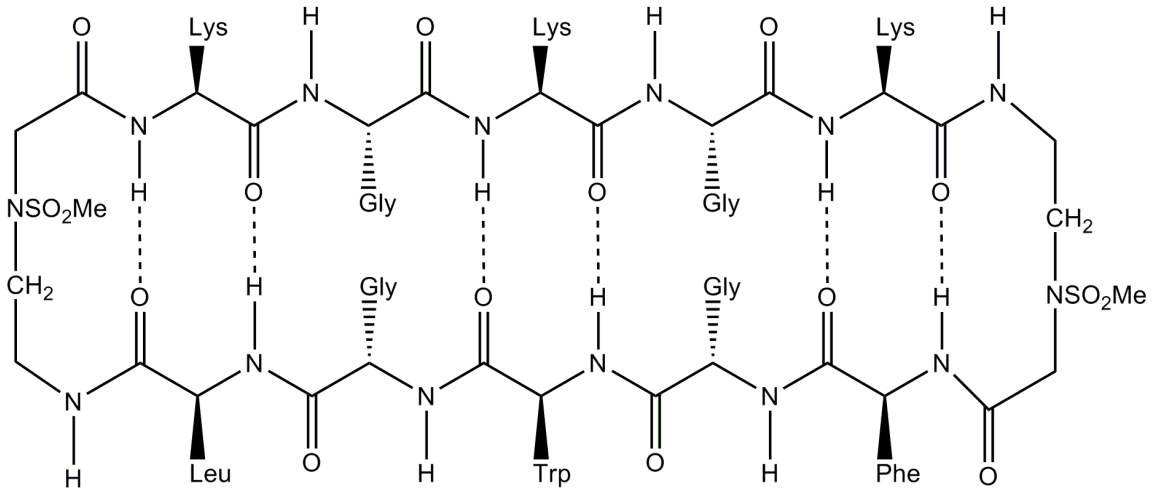

Fig. 4.3 (A) Crystal structure of complex consisting of a p53-derived peptide and MDM2. (B) Proposed β-hairpin mimetic scaffold with novel sulfonamido aminoethyl glycine turn promoters.

In an attempt to design bioactive peptides for inhibiting p53-MDM2 interaction we tried to shorten the β-hairpin loop to eight residue loop as shown in (Table.4.1). The eight residue loop with Leu and glutamic acid residues populated along the β turn was preorganized into a regular β-hairpin. We found that this scaffold is bioactive with an IC_{50} of 35 μM. With this design as our lead scaffold, we tried to study structure activity relationship with an aim to obtain β-hairpin mimetics with enhanced bioactivity. Table 4.1 depicts the structure activity relationship of designed β-hairpin mimetics as p53-MDM2 inhibitors. After obtaining peptide **4.1** as lead molecule we tried to replace aspartic acid with leucine at the β-turn. We found that this mimetic had IC_{50} of 2 μM. In another attempt, we tried to populate the β-turn with Leu and Trp residues. Here we tried to populate the three residues around the β-turn so that we could achieve maximum binding.

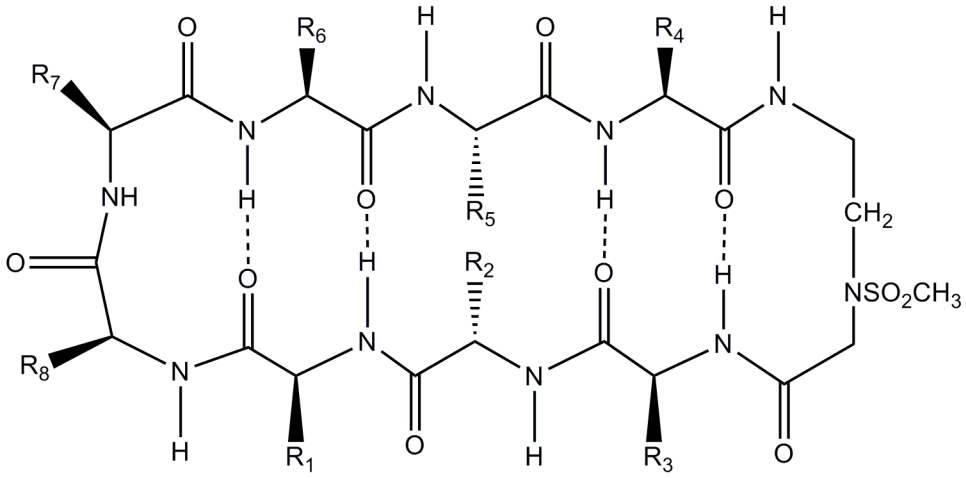

Table 4.1 Structure activity relationship of cyclic β-hairpin peptidomimetics.

Peptide	**R_1**	**R_2**	**R_3**	**R_4**	**R_5**	**R_6**	**R_7**	**R_8**	**IC50 (μM)**
4.1	W	K	F	F	K	W	D	L	35
4.2	W	K	F	F	K	W	L	L	2
4.3	W	S_M	F	F	S_M	W	L	L	>125
4.4	F	K	F	L	K	W	L	W	ND

S_M = Morpholine derivatized serine ND= Not determined yet

To check the bioavailability of the designed cyclic peptidomimetics, we carried out quikPro calculation for log P data for previously designed cyclic abeta and cyclic III peptides. We found that designed cyclic peptidomimetics are too hydrophilic with log P outside the range of acceptable limits. We proposed to decrease the hydrophilicity by incorporating morpholine derivatized lysine and serine derivatives into the non-recognition strand of the peptidomimetics. This more hydrophobic lysine analog reduces the basic character of the epsilon nitrogen and removes two of the three hydrogen bond donors in the physiologically relevant protonated form of this side chain. As seen from Table 4.2, incorporation of the morpholine derivative brings the log P values for cyclic

abeta and cyclic III peptides within the range of acceptable limits. To test this idea, we synthesized cyclic peptide **4.3** with the lysine replaced with the morpholine derivative. The peptide was synthesized successfully as characterized initially by MALDI-TOF but isolation and purification problems were encountered. We tested the crude peptide for p53-MDM2 inhibition, which did not give us expected results.

Table 4.2 QuikPro calculations for LogP data for cyclic abeta and cyclic III peptides.

Peptide	Log P (Octanol/Water)
Cyclo (7,8) $^{L}P^{1}\ ^{D}P^{2}\ K^{3}\ L^{4}\ K^{5}\ L^{6}\ K^{7}\ O^{8}\ M^{9}\ V^{10}\ I^{11}\ S^{12}\ W^{13}$	**-3.078**
Cyclo (7,8) $^{L}P^{1}\ ^{D}P^{2}\ K_{M}{}^{3}\ L^{4}\ K_{M}{}^{5}\ L^{6}\ K_{M}{}^{7}\ O^{8}\ M^{9}\ V^{10}\ I^{11}\ S^{12}\ W^{13}$	**-1.369**
Cyclo (1,12) $M^{1}\ V^{2}\ I^{3}\ S^{4}\ W^{5}\ O^{6}\ K^{7}\ L^{8}\ K^{9}\ L^{10}\ K^{11}\ O^{12}$	**-4.224**
Cyclo (1,12) $M^{1}\ V^{2}\ I^{3}\ S^{4}\ W^{5}\ O^{6}\ K_{M}{}^{7}\ L^{8}\ K_{M}{}^{9}\ L^{10}\ K_{M}{}^{11}\ O^{12}$	**-2.445**
Cyclo (7,8) $^{L}P^{1}\ ^{D}P^{2}\ K^{3}\ L^{4}\ K^{5}\ L^{6}\ K^{7}\ O^{8}\ W^{9}\ S^{10}\ V^{11}\ V^{12}\ M^{13}$	**-3.077**
Cyclo (7,8) $^{L}P^{1}\ ^{D}P^{2}\ K_{M}{}^{3}\ L^{4}\ K_{M}{}^{5}\ L^{6}\ K_{M}{}^{7}\ O^{8}\ W^{9}\ S^{10}\ V^{11}\ V^{12}\ M^{13}$	**-0.818**

O= Methylsulfonamido aminoethyl glycine turn promoter

In a quest for obtaining improved bioactive peptides we further constrained the cyclic peptide by introduction of a constrained oxygenated turn promoter (fig. 4.4) at one turn. The introduction of an ether-peptidomimetic amino acid (proline or 2-piperidine carboxylic acid derivative) as a constrained turn promoter will further reduce the degrees of freedom available to the cyclic peptide and possibly increase its affinity for binding to the target. As shown in figure 4.4, this cyclic peptidomimetic had an IC_{50} of 2 µM, similar to that of peptide 4.2.

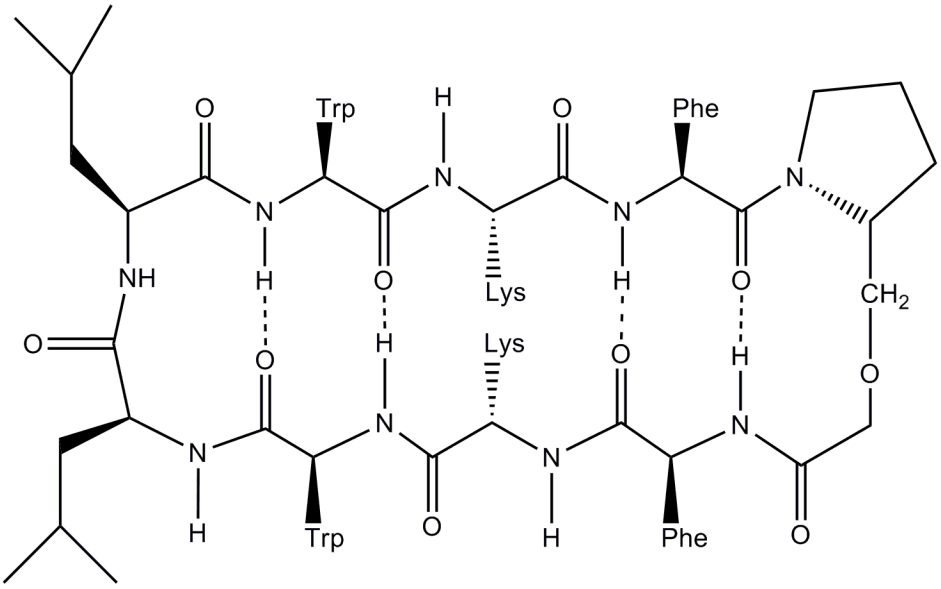

Fig. 4.4 Cyclic betahairpin peptide with proline derived ether-peptidomimetic turn promoter.

To further improve our lead scaffold, we designed a chiral reduced amide dipeptide β-turn promoter decorated with different alkyl groups at the turn as shown in fig. 4.5a. To support our design, we did computational studies by incorporating these reduced amide dipeptide β-turn promoters into the eight residue β-hairpin scaffold. It was seen that chiral turn promoter populated with tryptophan residues at the turn inserts deep into the hydrophobic pocket of MDM2 (fig. 4.5c). When superimposed, this mimetic had side chain residues perfectly aligned with the corresponding ligand residues as shown in Fig.4.5b. Fig.4.5c shows the docking and interactions of this peptide in the active site of MDM2. The key to this mimetic lies in the synthesis of the reduced amide dipeptide β-turn promoter. An attempt to make the reduced amide dipeptide β-turn promoter with Leu side chains is described.

(A)

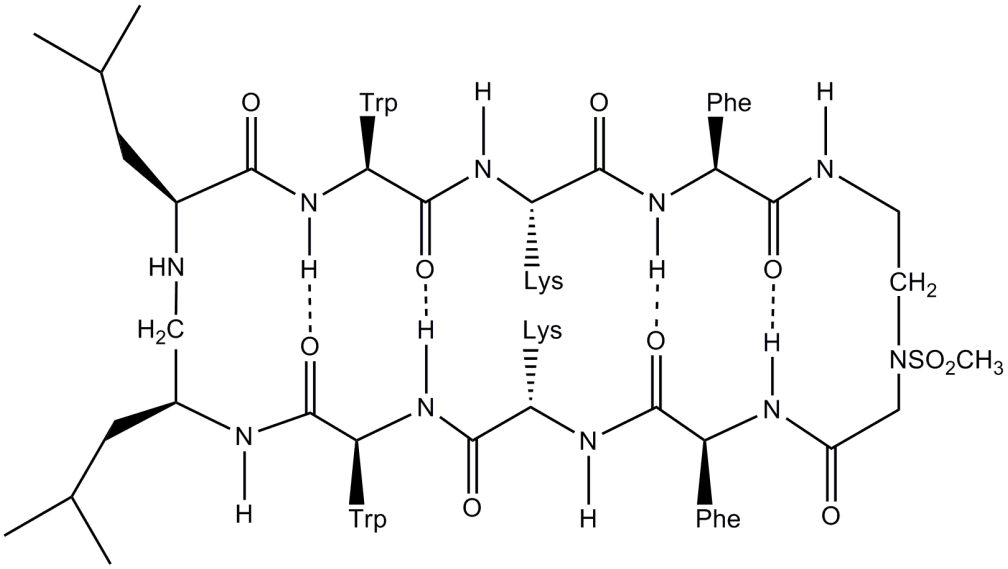
O
Trp
H
N
O
Phe
H
N
N
N
HN
H
O
Lys
H
O
CH2
H2C
O
H
Lys
O
H
NSO2CH3
N
N
N
N
N
H
Trp
O
H
Phe
O

(B)

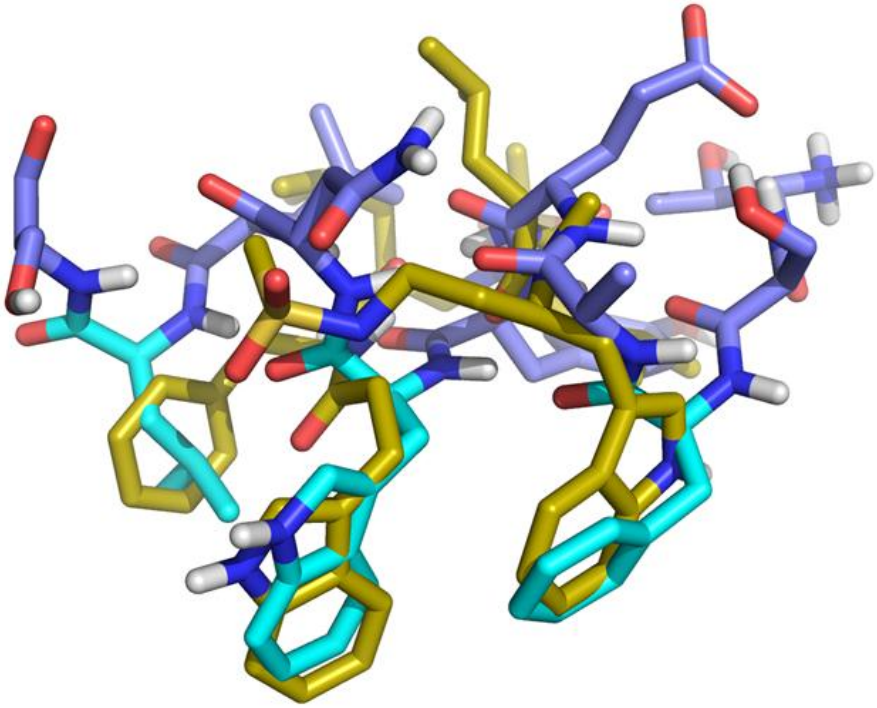

(C)

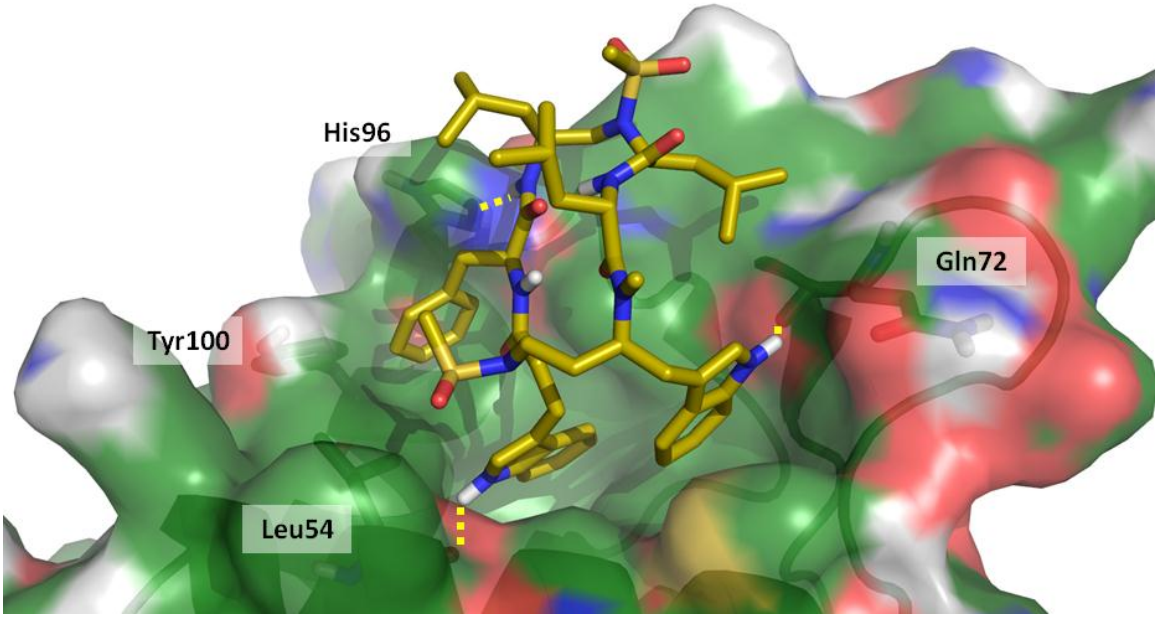

Fig. 4.5 (a) Proposed cyclic p53-MDM2 peptidomimetics with chiral reduced amide dipeptide β-turn promoter with leucine residues (b) reduced amide dipeptides β-turn promoter superimposed with ligand (PDB 2axi). (c) proposed cyclic p53-MDM2 hairpin peptide docked into the active site of MDM2 (PDB 2axi).

All cyclic peptidomimetics were synthesized on 2-chlorotrityl chloride resin as solid support and standard solid phase Fmoc amino acid chemistry as described in chapter 2. Coupling was carried out in most cases using standard chemistry of HCTU in N-methyl pyrrolidone (NMP) with double coupling for each residue. The synthesized linear peptides were selectively cleaved from the resin without cleaving Boc groups on certain residues using dilute trifluoroethanol as the cleaving agent. The linear peptide is then cyclized in solution under dilute conditions to afford crude cyclized peptide in modest yields.

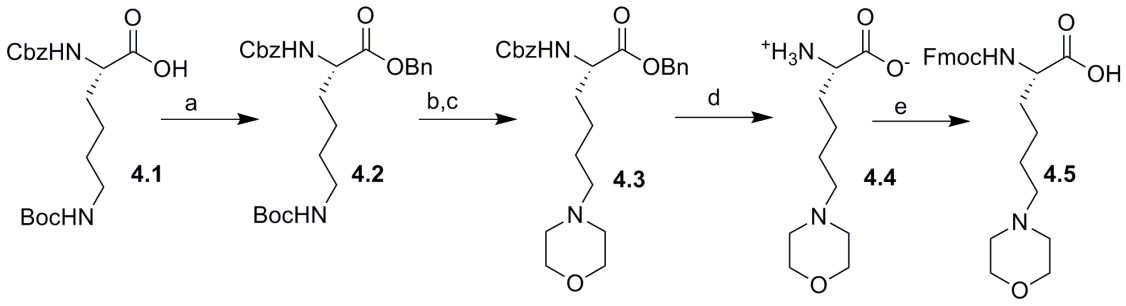

(a) $PhCH_2Br$, DIEA, CH_3CN, 92% (b) TFA/DCM 0^oC (c) 2-Bromo ethyl ether, $NaHCO_3$, toluene, reflux, 78%

(d) Pd/C, MeOH, quant. (e)TMSCl, DCM, DIEA, Fmoc-Cl

Scheme 4.1 Synthesis of Morpholino derivative of lysine.

The morpholino derivative of lysine was synthesized from commercially available CbzLys(Boc)-OH as shown in scheme 4.1. The key step in this scheme was the formation of morpholine ring. Compound **4.2** was subjected to Boc-deprotection using TFA/DCM followed by reflux of resulting amine with 2-bromo ethyl ether to give key compound **4.3** in 78% yield. Compound **4.3** was hydrogenated using 10% Pd/C in methanol to give completely deprotected amino acid **4.4**. The primary amine was then protected with a Fmoc protecting group using Bolin's procedure to give desired morpholine derivative **4.5** in low yields. Hence an alternative route of preparing morpholine derivatives of serine was investigated using two different protecting group strategies.

(A)

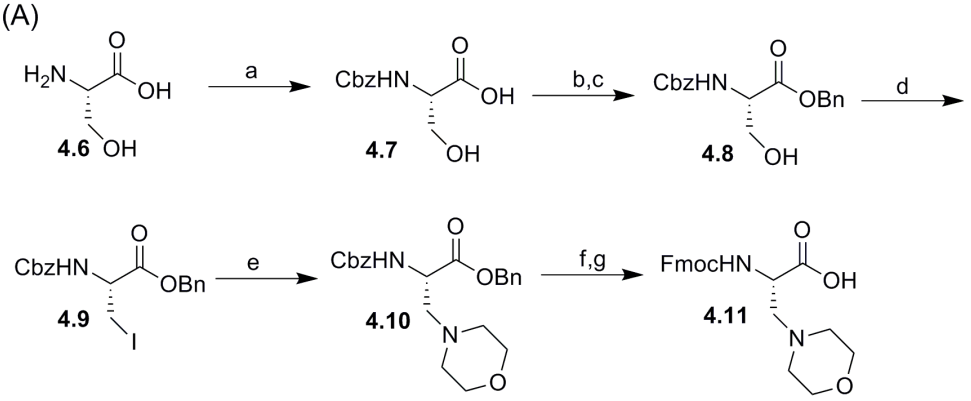

(a) $NaHCO_3$, Cbz-Cl, THF:H_2O, 87% (b) Cs_2CO_3, MeOH, (c) DMF, $PhCH_2Br$, 79% (d) PPh_3, Imidazole, I_2, DCM, 70% (e) K_2CO_3, DMF, Morpholine, 84% (f) H_2 (Pd/C), MeOH (g) DCM, TMS-Cl, Fmoc-OSu, DIEA, 49%

(B)

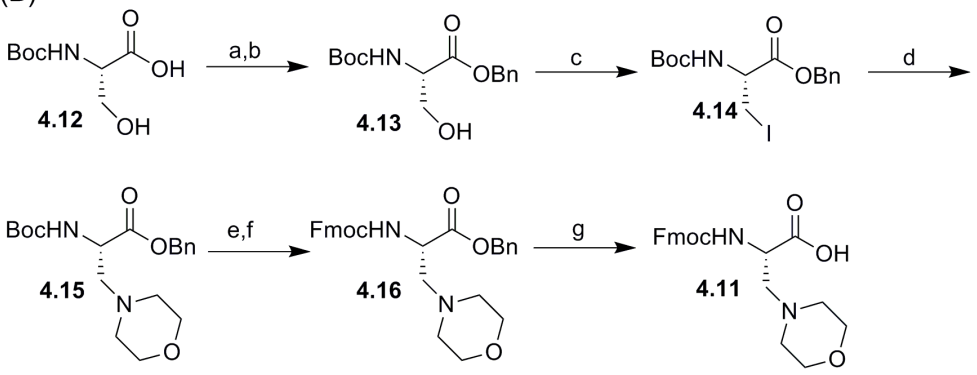

(a) Cs_2CO_3, MeOH, (b) DMF, $PhCH_2Br$ (c) PPh_3, Imidazole, I_2, DCM, (d) K_2CO_3, DMF, Morpholine, (e) TFA,DCM (f) DCM, Fmoc-OSu, DIEA (g)H_2 (Pd/C), MeOH

Scheme 4.2 Synthetic routes for morpholino derivative of serine (a) using Cbz protecting groups (b) using Boc/Cbz protecting group strategy.

In scheme 4.2(a), the morpholino compound **4.10** was synthesized by transformation of hydroxyl group to iodide followed by S_N2 displacement of iodide with morpholine. Compound **4.10** is subjected to hydrogenation followed by Fmoc protection of resulting amine to give desired compound **4.11** in moderate yield 49%. An alternative strategy was formulated to maximize yield for compound **4.11**. Scheme 4.2b describes the synthesis of the morpholino derivative of serine using commercially available Boc Ser-OH **4.12**. Compound **4.15** was synthesized using the same procedure as described for

the preparation of compound **4.10**. Compound **4.14** was then subjected to Boc deprotection using TFA/DCM followed by protection of the resulting amine with Fmoc group to give fully protected morpholino derivative **4.16**. Hydrogenation of **4.16** with 10% Pd/C gave desired compound **4.11** in good yields.

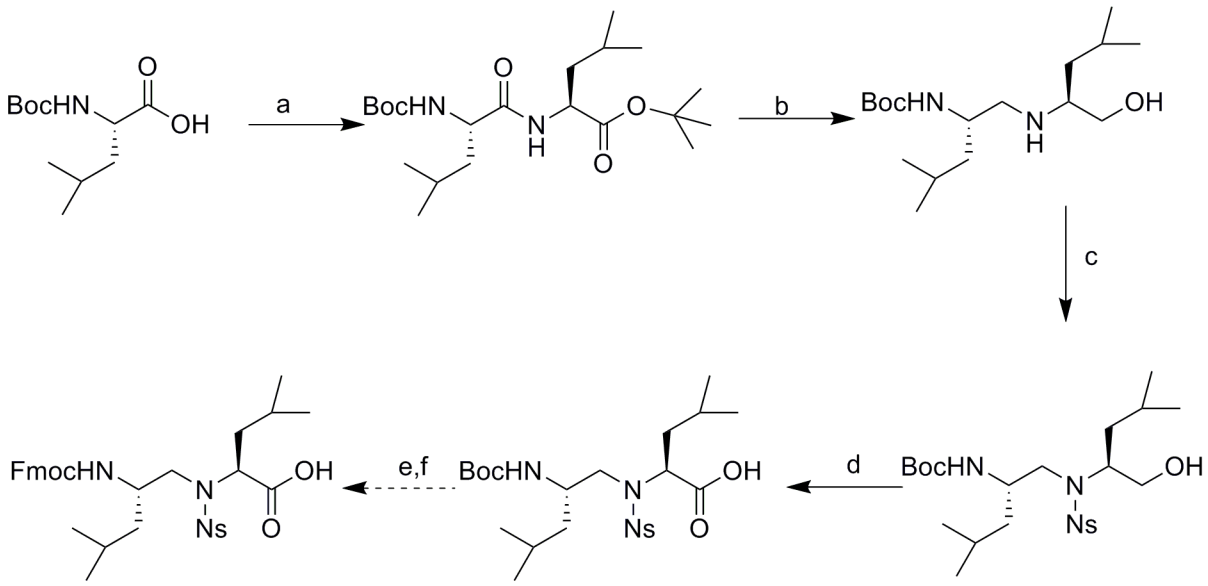

(a) IBC,NMM,THF, H-Leu-O^{t}bu.HCl, 86% (b) 65% Vitride in toluene, toluene, 80% (c) ONBS-Cl, $NaHCO_3$, H_2O/Dioxane, 85% (d) TEMPO, Trichloroisocyanuric acid, 10% $NaHCO_3$, 42% (e) TFA/DCM (f) TMS-Cl, DIEA,Fmoc-OSu, DCM

Scheme 4.3 Synthesis of proposed reduced amide dipeptides β-turn promoter populated with Leu side chains.

The synthesis of reduced amide dipeptides β-turn promoter **4.22** was carried out by making a dipeptide unit **4.18**. Compound **4.18** was then reduced using 65% Vitride in toluene to give compound **4.19**. The secondary amine was selectively protected with ortho-nitrobenezenesulfonyl chloride (ONBSCl) to give compound **4.20** in good yield. Oxidation of the resulting alcohol **4.20** using TEMPO and trichloroisocyanuric acid as oxidizing agent gave the corresponding acid **4.21** in low yield (19). We did not achieve

success in synthesizing Fmoc-protected amino acid **4.22** using standard Bolin's procedure.

4.3. Experimental Procedures

4.3.1 Materials and Methods

Organic and inorganic reagents (ACS grade) were obtained from commercial sources and used without further purification, unless otherwise noted. Fmoc-protected amino acids and the coupling agent HCTU were obtained from Protein Technologies, Calbiochem-Novabiochem, or Chem-impex International. 2-Chlorotrityl chloride resin was purchased from Anaspec Inc. All linear peptides were synthesized on the Symphony peptide synthesizer, Protein Technologies Instruments. Solvents for peptide synthesis and reverse-phase HPLC were obtained from Applied Biosystems. Other chemicals used were obtained from Aldrich and were of highest purity commercially available. Thin layer chromatography (TLC) was performed on glass plates (Whatman) coated with 0.25 mm thickness of silica gel 60Å (# 70-230 mesh). All ^{1}H and ^{13}C NMR spectra were recorded on Bruker 250 MHz, Varian INOVA 400 MHz spectrometer in $CDCl_3$ or unless otherwise specified and chemical shifts are reported in ppm (δ) relative to internal standard tetramethylsilane (TMS). High Resolution mass spectra were obtained on an Agilent LC-MSD-TOF.

4.3.2 Peptide Synthesis & Purification

Cyclic β-hairpin peptidomimetic with (2-aminoethyl)-N-methylsulfonamido glycine beta-turn promoter.

2-Chlorotrityl chloride resin was treated with Fmoc-Phe-OH and then immediately Fmoc-deprotected using 20% piperidine/2% DBU in DMF. Fmoc

quantification of resin indicated a loading of 0.18 mmol/g of resin. For a 25 μmol synthesis, 139 mg of resin was charged to the peptide reaction vessel on a Protein Technologies Symphony Peptide Synthesizer. For each coupling step, 5 equivalents of Fmoc amino acid and 7.5 equivalents of HCTU are dissolved in 0.4 M NMM in DMF to equal 20 equivalents of NMM, which is added to the reactor. Each coupling reaction was carried out for 10 minutes followed by NMP washes. Fmoc deprotection was done using 20% piperidine/2% DBU in DMF for (2 x 2.5 minutes). The amino acids used for peptide synthesis were coupled in the following order: Fmoc-Lys(Boc)-OH, Fmoc-Trp(Boc)-OH, Fmoc-Leu-OH, Fmoc-Leu-OH, Fmoc-Trp(Boc)-OH Fmoc-Lys(Boc)-OH, Fmoc-Phe-OH and Fmoc-$NHCH_2CH_2N(O_2SCH_3)CH_2COOH$. After synthesis of the protected linear peptide, the resin was transferred to a manual peptide synthesis vessel and treated with 5 mL of a cleavage solution of 20% trifluoroethanol in DCM for 2 hours. The resin was filtered and washed with 5 mL of cleavage solution. This cleavage cycle was repeated twice. The combined organic filtrates were concentrated to give crude protected linear peptide. The crude peptide was dissolved in 15 mL of 1% v/v DIEA in DMF and treated with 4 equivalents of HCTU for one hour. After one hour, the reaction mixture was concentrated to give crude protected cyclized β-hairpin peptidomimetic. The crude peptidomimetic was then treated with a 10 mL solution of 87.5% TFA/5% H_2O/5% phenol/2.5% triethylsilane for 30 minutes. The reaction mixture was concentrated and the thick viscous liquid was triturated twice with 10 mL of cold diethyl ether. The reaction contents were centrifuged to give crude cyclic β-hairpin peptidomimetic. The crude peptidomimetic was dissolved in a solution of 0.1% TFA in H_2O and freeze-dried to give a white fluffy powder. All cyclic peptides were purified using preparative reverse phase

HPLC (5 µM particle size C_{18} AAPPTEC spirit column, 25 x 2.12 cm) with eluents: A = 0.1% HCO_2H in H_2O, B = 0.1% HCO_2H in H_3CCN. The purification was carried out using a gradient of 5-50% B Buffer over 40 min with a flow rate 20 mL/minute using 222 nm UV detection. All peaks with retention times expected for peptides were collected and lyophilized. The purified peptides were analyzed using similar analytical HPLC conditions and found to have >95% purity and were structurally characterized using a Bruker Autoflex MALDI-TOF instrument with α-cyano hydroxy cinnamic acid (CHCA) as matrix.

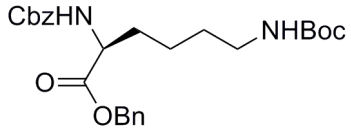

N-α-benzyloxycarbonyl-N-ε-(tert-butoxycarbonyl)lysine benzyl ester (4.2)

N-ε-(tert-butoxycarbonyl)-N-α-carbobenzyloxylysine **4.1**(1 gm, 2.6 mmol) was dissolved in 25 mL dry acetonitrile and diisopropylethylamine (0.47 mL, 2.8 mmol) was added. Benzyl bromide (0.33 mL, 2.8 mmol) was subsequently added and the reaction mixture was stirred under argon at room temperature for two days. The reaction mixture was concentrated in vacuo and the residue was partitioned between DCM (25 mL) and water (15 mL). The organic layer was dried using Na_2SO_4, filtered and concentrated to give a clear oil. The crude oil was chromatographed over flash silica with EtOAc/Hexane (1:1) to give compound **4.2** (0.95 gm, 78%). ^{1}H NMR (400 MHz, $CDCl_3$) ppm 7.43 – 7.24 (m, 10H), 5.42 (s, 1H), 5.23 – 5.06 (m, 4H), 4.53 (b, 1H), 4.40 (d, *J* = 4.9 Hz, 1H), 3.12 – 2.94 (m, 2H), 1.88 – 1.63 (m, 2H), 1.46 – 1.25 (m, 13H). ^{13}C NMR (101 MHz, $CDCl_3$) δ 172.35, 156.13, 136.33, 135.40, 128.73, 128.61, 128.44, 128.27, 79.24, 67.23, 67.10, 53.89, 40.11, 32.25, 29.65, 28.52, 22.36.

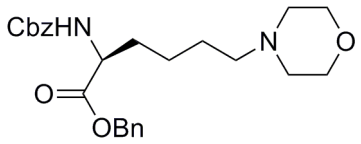

(R)-benzyl 2-(benzyloxycarbonylamino)-6-morpholinohexanoate (4.3)

Compound **4.2** (0.95 gm, 2 mmol) was dissolved in 20 mL DCM and 10 mL trifluoroacetic acid was added to it. The reaction contents were stirred until the starting material was completely consumed. The reaction mixture was concentrated to dryness in vacuo and used directly in the next step without further purification. The deprotected amine was suspended in 20 mL toluene and sodium bicarbonate (0.55 gm, 6 mmol), 2-bromoethyl ether (0.56 gm, 2.4 mmol) was added to it. The system was flushed with argon and reaction contents were refluxed for 24 hrs. The reaction mixture was concentrated in vacuo and the residue was partitioned between EtOAc (25 mL) and dilute $NaHCO_3$ (15 mL). The organic layer was dried using Na_2SO_4, filtered and concentrated to give crude oil. The crude oil was chromatographed over flash silica with EtOAc:Hexane (2:1) to give compound **4.3** (0.7 gm, 79%). ^{1}H NMR (250 MHz, DMSO) ppm 7.80 (d, *J* = 7.7 Hz, 1H), 7.48 – 7.19 (m, 10H), 5.13 (t, *J* = 5.1 Hz, 2H), 5.09 – 4.97 (m, 2H), 4.16 – 3.98 (m, 1H), 3.62 – 3.46 (m, 4H), 2.51 (dt, *J* = 3.5, 1.7 Hz, 1H), 2.34 – 2.24 (m, 4H), 2.19 (t, *J* = 6.8 Hz, 2H), 1.69 (dt, *J* = 15.2, 6.3 Hz, 2H), 1.48 – 1.20 (m, 4H). ^{13}C NMR (63 MHz, DMSO) ppm 172.33, 156.16, 136.89, 135.94, 128.39, 128.33, 128.03, 127.79, 127.73, 127.23, 66.14, 65.84, 65.47, 57.99, 53.89, 53.29, 30.52, 25.30, 23.29. m/z 441.2377 $(M+H)^+$

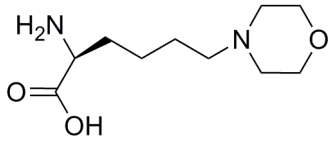

(S)-2-amino-6-morpholinohexanoic acid (4.4)

Compound **4.3** (0.7 gm, 1.6 mmol) was dissolved in MeOH and 10% Pd/C was added to it. Hydrogenation was carried overnight at 50 psi. The reaction contents were filtered over diatomaceous earth and concentrated to give compound **4.4**. This compound was used in the next step without further purification.

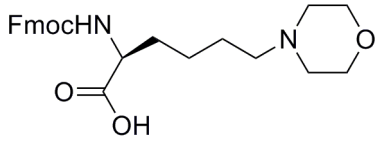

(S)-2-(((9H-fluoren-9-yl)methoxy)carbonylamino)-6-morpholinohexanoic acid (4.5)

Compound **4.4** (0.32 gm, 1.5 mmol) was suspended in 15 mL anhydrous DCM and DIEA (0.73 mL, 4.19 mmol), TMSCl (0.53 mL, 4.2 mmol) were added to it. The reaction mixture became homogenous on gentle reflux for one hour. After one hour, the reaction mixture was cooled to 0 ^{0}C, and Fmoc-OSu (0.71 gm, 2.1 mmol) was added. The progress of the reaction was monitored by TLC. The reaction content was concentrated and flash chromatographed to give compound **4.5** in low yields**.** m/z 439.2227 $(M+H)^{+}$

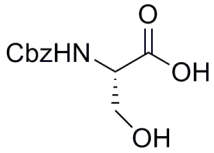

(R)-2-(benzyloxycarbonylamino)-3-hydroxypropanoic acid (4.7)

To a stirred suspension of $NaHCO_3$ (10 gm, 12 mmol) in THF:H_2O (50 mL) was added L-serine (5 gm, 47.5 mmol) in small lots. After 15 mins, benzyl chloroformate (7.5 mL, 52.5 mmol) was added dropwise over a period of 30 mins. The reaction was carried out

for 2 hrs and then diethyl ether (50 mL) was added to it. The aqueous layer was acidified to pH 2~3 with 1N HCl solution and extracted with ethyl acetate (2 x 50 mL). The combined organic layer was further washed with 1N HCl (25 mL) and brine (50 mL), dried over Na_2SO_4. The reaction mixture was concentrated to dryness in vacuo and further crystallized with ethyl acetate/hexane to give **4.7** (9.9 gm) in 87 % yield. ^{1}H NMR (250 MHz, MeOD) ppm 7.46 – 7.28 (m, 5H), 5.14 (s, 2H), 4.30 (t, *J* = 4.4 Hz, 1H), 3.97 – 3.77 (m, 2H). ^{13}C NMR (101 MHz, CD_3OD) ppm 173.72, 158.41, 137.93, 129.37, 128.93, 128.77, 68.01, 67.68, 63.03, 57.58. m/z 240.0866 $(M+H)^+$

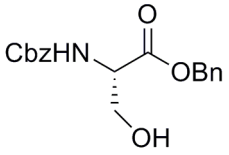

(R)-benzyl 2-(benzyloxycarbonylamino)-3-hydroxypropanoate (4.8)

Compound **4.7** (5 gm, 20.8 mmol) was dissolved in dry methanol (25 mL) and Cs_2CO_3 (3.4 gm, 10.4 mmol) was added to it at 0 ^{0}C. After 10 mins, methanol was removed at reduced pressure and the reaction contents were taken in DMF (30 mL). Benzyl bromide (20 mL, 167 mmol) was added in excess and the reaction was stirred overnight at room temperature. After completion of reaction, the reaction mixture was concentrated and partitioned between DCM (200 mL) and water (50 mL). The organic layer was dried, filtered, concentrated and chromatographed to give compound **4.8** (5.4 gm) in 79% yield. ^{1}H NMR (400 MHz, $CDCl_3$) ppm 7.46 – 7.30 (m, 10H), 5.71 (s, 1H), 5.22 (s, 2H), 5.12 (s, 2H), 4.55 – 4.43 (m, 1H), 4.09 – 3.88 (m, 3H), 2.11 (s, 1H). ^{13}C NMR (101 MHz, $CDCl_3$) ppm 170.49, 156.25, 136.25, 135.30, 128.89, 128.78, 128.49, 128.42, 128.36, 67.76, 67.46, 63.65, 56.40. m/z 330.1324 $(M+H)^+$

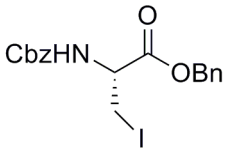

(S)-benzyl 2-(benzyloxycarbonylamino)-3-iodopropanoate (4.9)

To a stirred solution of **4.8** (2 gm, 6 mmol) in dry DCM (10 mL) was added a pre-mixed solution of PPh_3 (2.38 gm, 9 mmol), iodine (2.31 gm, 9 mmol) and imidazole (0.75 gm, 10.9 mmol) in 30 mL dry DCM. The reaction mixture was stirred at room temperature for 2 hrs. After completion of reaction, the reaction mixture was concentrated in vacuo and chromatographed using EtOAc:Hexane (1:9) as eluent to give compound **4.9** (1.7 gm) 70% as white solid. ^{1}H NMR (250 MHz, $CDCl_3$) ppm 7.67 – 7.49 (m, 10H), 5.84 (d, *J* = 7.2 Hz, 1H), 5.42 (s, 2H), 5.33 (d, *J* = 0.6 Hz, 2H), 4.82 (dt, *J* = 7.5, 3.7 Hz, 1H), 3.88 – 3.71 (m, 2H). ^{13}C NMR (63 MHz, $CDCl_3$) ppm 169.15, 155.43, 135.94, 134.72, 128.77, 128.71, 128.66, 128.62, 128.34, 128.16, 68.17, 67.33, 54.04, 7.44. m/z 440.0345 $(M+H)^+$

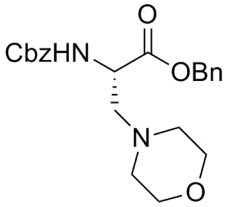

(R)-benzyl 2-(benzyloxycarbonylamino)-3-morpholinopropanoate (4.10)

To a solution of **4.9** (1.0 gm, 2.3 mmol) in dry DMF (15 mL) were added K_2CO_3 (0.81 gm, 5.9 mmol) and morpholine (0.45 mL, 5.3 mmol) at room temperature. The reaction mixture was stirred overnight until TLC showed disappearance of starting material. After completion of reaction, the reaction mixture was concentrated in vacuo and chromatographed to give compound **4.10** (0.76 gm) 84% as pale yellow liquid. ^{1}H NMR (250 MHz, DMSO d_6) ppm 7.80 (d, *J* = 7.7 Hz, 1H), 7.48 – 7.19 (m, 10H), 5.13 (t, *J* =

5.1 Hz, 2H), 5.09 – 4.97 (m, 2H), 4.16 – 3.98 (m, 1H), 3.62 – 3.46 (m, 4H), 2.51 (dt, *J* = 3.5, 1.7 Hz, 1H), 2.34 – 2.24 (m, 4H), 2.19 (t, *J* = 6.8 Hz, 2H), 1.69 (dt, *J* = 15.2, 6.3 Hz, 2H), 1.48 – 1.20 (m, 4H). ^{13}C NMR (63 MHz, DMSO d_6) ppm 171.48, 155.92, 136.84, 135.90, 128.36, 128.33, 128.00, 127.82, 127.77, 66.03, 65.87, 65.56, 58.54, 53.11, 52.11. m/z 399.1917 $(M+H)^+$

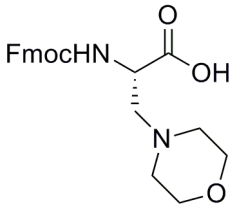

(S)-2-(((9H-fluoren-9-yl) methoxy) carbonylamino)-3-morpholinopropanoic acid (4.11)

Compound **4.10** (0.9 gm, 2.3 mmol) was taken in MeOH and 10% Pd/C was added to it. Hydrogenation was carried overnight at 50 psi. The reaction contents were filtered over diatomaceous earth and concentrated to give the intermediate zwitterion (0.36 gm, 2.1 mmol). This compound was used in the next step without further purification. This compound was suspended in 15 mL anhydrous DCM and DIEA (0.73 mL, 4.2 mmol), TMSCl (0.53 mL, 4.2 mmol) was added to it. The reaction mixture became homogenous on gentle reflux for one hour. After one hour, the reaction mixture was cooled to 0^{o}C, and Fmoc-OSu (0.71 gm, 2.1 mmol) was added. The progress of the reaction was monitored by TLC. The reaction contents were concentrated and flash chromatographed to give compound **4.11** (0.41 gm, 49%). ^{1}H NMR (400 MHz, $CDCl_3$) ppm 7.74 (d, *J* = 7.3 Hz, 2H), 7.57 (d, *J* = 6.6 Hz, 2H), 7.33 (dt, *J* = 36.2, 6.9 Hz, 4H), 6.01 (s, 1H), 4.43 – 4.31 (m, 2H), 4.27 (s, 1H), 4.17 (t, *J* = 6.2 Hz, 1H), 3.92 – 3.69 (m, 4H), 3.28 – 2.91 (m, 5H), 2.63 – 2.30 (m, 1H). ^{13}C NMR (101 MHz, $CDCl_3$) ppm 172.57, 156.14, 144.02, 141.53,

127.97, 127.26, 125.27, 120.21, 67.16, 64.86, 58.07, 52.99, 50.44, 47.35. m/z 397.1755 $(M+H)^+$.

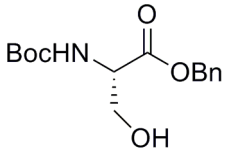

(S)-benzyl 2-(tert-butoxycarbonylamino)-3-hydroxypropanoate (4.13)

Compound **4.12** (4.0 gm, 19 mmol) was dissolved in dry methanol (25 mL) and Cs_2CO_3 (3.2 gm, 9.7 mmol) was added to it at 0^oC. After 10 mins, methanol was removed at reduced pressure and the reaction contents were taken up in DMF (30 mL). Benzyl bromide (18.6 mL, 156 mmol) was added in excess and the reaction was stirred overnight at room temperature. After completion of reaction, the reaction mixture was concentrated and partitioned between DCM (200 mL) and water (50 mL).The organic layer was dried, filtered, concentrated and chromatographed to give compound **4.13** (5.1 gm) in 87% yield.. ^{1}H NMR (400 MHz, $CDCl_3$) ppm 7.42 – 7.20 (m, 5H), 5.64 (d, *J* = 7.4 Hz, 1H), 5.18 (d, *J* = 20.2 Hz, 2H), 4.37 (s, 1H), 3.89 (dd, *J* = 41.7, 10.1 Hz, 2H), 3.17 (s, 1H), 1.40 (s, 9H). ^{13}C NMR (101 MHz, $CDCl_3$) ppm 171.09, 156.05, 135.51, 128.76, 128.56, 128.32, 80.39, 67.46, 63.37, 56.08, 28.48.

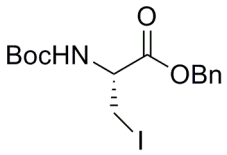

(R)-benzyl 2-(tert-butoxycarbonylamino)-3-iodopropanoate (4.14)

To a stirred solution of **4.13** (5.0 gm, 17 mmol) in dry DCM (10 mL) was added a pre-mixed solution of PPh_3 (6.7 gm, 25.5 mmol), iodine (6.4 gm, 25.5 mmol) and imidazole (0.75 gm, 30.6 mmol) in 100 mL dry DCM. The reaction mixture was stirred at room

temperature for 2 hrs. After completion of reaction, the reaction mixture was concentrated in vacuo and chromatographed using EtOAc:Hexane (1:9) as eluent to give compound **4.14** (4.8 gm) 70% as a white solid. ^{1}H NMR (400 MHz, $CDCl_3$) ppm 7.46 – 7.25 (m, 5H), 5.36 (d, *J* = 4.8 Hz, 1H), 5.20 (t, *J* = 5.1 Hz, 2H), 4.54 (d, *J* = 3.0 Hz, 1H), 3.56 (dd, *J* = 11.2, 6.6 Hz, 2H), 1.44 (s, 9H). ^{13}C NMR (101 MHz, $CDCl_3$) ppm 169.68, 155.04, 135.06, 129.11, 128.85, 128.77, 80.68, 68.16, 53.91, 28.48, 7.99. m/z 428.0383 $(M+Na)^{+}$.

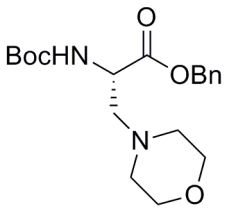

(S)-benzyl 2-(tert-butoxycarbonylamino)-3-morpholinopropanoate (4.15)

To a solution of **4.13** (3.5 gm, 8.6 mmol) in dry DMF (30 mL) were added K_2CO_3 (3.1 gm, 22.4 mmol) and morpholine (1.71 mL, 19.8 mmol) at room temperature. The reaction mixture was stirred overnight until TLC showed disappearance of starting material. After completion of reaction, the reaction mixture was concentrated in vacuo and chromatographed to give compound **4.14** (2.65 gm) 84% as a pale yellow liquid.^{1}H NMR (400 MHz, $CDCl_3$) ppm 7.98 – 7.79 (m, 1H), 7.38 – 7.22 (m, 6H), 5.25 (d, *J* = 17.4 Hz, 1H), 5.22 – 4.93 (m, 2H), 4.56 (d, *J* = 18.3 Hz, 1H), 4.27 (d, *J* = 5.4 Hz, 1H), 3.48 (t, *J* = 4.3 Hz, 3H), 2.83 (d, *J* = 7.5 Hz, 1H), 2.77 (s, 1H), 2.59 (t, *J* = 9.5 Hz, 2H), 2.35 – 2.20 (m, 4H), 1.40 – 1.25 (m, 9H). m/z 365.2109 $(M+H)^{+}$.

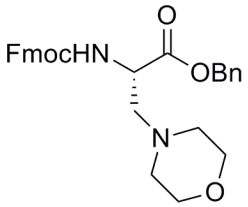

(S)-benzyl 2-(((9H-fluoren-9-yl)methoxy)carbonylamino)-3-morpholinopropanoate (4.16)

Compound **4.15** (0.79 gm, 2.2 mmol) was dissolved in 10 mL DCM and 10 mL TFA was added to it. After completion of the reaction, the residue was reconcentrated three times with DCM to remove residual TFA. The crude residue (1.06 gm, 2.2 mmol) was dissolved in 20 mL DCM and DIEA (1.32 mL, 7.6 mmol), FmocOSu (0.69 gm, 2.1 mmol) was added. After completion of the reaction, the reaction contents were diluted with 50 mL DCM and washed with water (1 x 15 mL) and brine (1 x 15 mL). The organic layer was then dried, filtered, concentrated and subjected to flash chromatography to give compound **4.16** (0.95 gm, 91%).^{1}H NMR (250 MHz, $CDCl_3$) ppm 7.68 (d, *J* = 7.2 Hz, 2H), 7.52 (d, *J* = 6.4 Hz, 2H), 7.39 – 7.14 (m, 9H), 5.60 (d, *J* = 6.2 Hz, 1H), 5.11 (dd, *J* = 29.2, 11.8 Hz, 2H), 4.33 (d, *J* = 6.6 Hz, 3H), 4.16 (s, 1H), 3.49 (s, 4H), 2.64 (d, *J* = 4.7 Hz, 2H), 2.29 (s, 4H).^{13}C NMR (63 MHz, $CDCl_3$) ppm 171.59, 155.97, 143.95, 143.77, 141.34, 135.22, 129.26, 128.63, 127.76, 127.10, 125.11, 120.04, 67.27, 67.08, 66.85, 59.09, 53.74, 52.36, 47.18 m/z 487.2095 $(M+H)^+$.

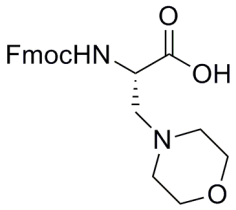

(S)-2-(((9H-fluoren-9-yl)methoxy)carbonylamino)-3-morpholinopropanoic acid (4.11)

Compound **4.16** (0.5 gm, 1.6 mmol) was taken up in MeOH and 10% Pd/C was added to it. Hydrogenation was carried overnight at 50 psi. The reaction contents were filtered through diatomaceous earth and concentrated to give compound **4.11** (0.35 gm, 87%). m/z 397.1755 $(M+H)^+$.

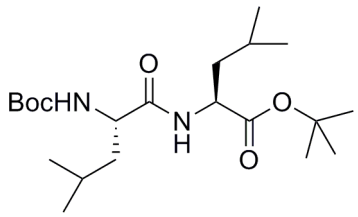

(S)-tert-butyl 2-((R)-2-(tert-butoxycarbonylamino)-4-methylpentanamido)-4-methylpentanoate (4.18)

Dipeptide **4.18** was synthesized from Boc-Leu-OH monohydrate (3.0 gm, 13 mmol) and leucine tert-butyl ester hydrochloride (2.9 gm, 13 mmol) as per the procedure for mixed anhydride coupling using N-methylmorpholine (4.3 mL, 39 mmol) and isobutyl chloroformate (1.7 mL, 13 mmol) using THF (60 mL) as solvent. After completion of the reaction, reaction contents were washed with water (1 x 25 mL), brine (1 x 25 mL) and filtered, dried and concentrated. The dipeptide **4.18** was obtained as white needles (4.48 gm, 86.4%) after crystallization using EtOAc/Hexane as solvent. ^{1}H NMR (250 MHz, $CDCl_3$) ppm 6.38 (d, 1H), 4.89 (d, *J* = 8.3 Hz, 1H), 4.41 (td, *J* = 8.5, 5.4 Hz, 1H), 4.10 – 3.95 (m, 1H), 1.65 – 1.45 (m, 6H), 1.39 (d, *J* = 2.1 Hz, 9H), 1.38 – 1.36 (m, 9H), 0.92 (s, 1H), 0.90 – 0.84 (m, 13H). m/z 387.3225 $(M+H)^+$.

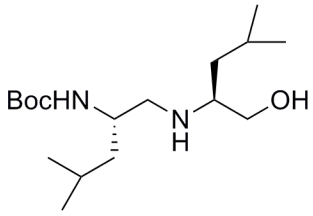

tert-butyl (R)-1-((S)-1-hydroxy-4-methylpentan-2-ylamino)-4-methylpentan-2-ylcarbamate (4.19)

Compound 4.18 (3.4 gm, 9.5 mmol) was taken up in 60 mL toluene and a solution of 65% Vitride in toluene (22 mL, 71 mmol) was added to it at 0 ^{o}C. The reaction contents were refluxed for one hour, cooled to room temperature and poured into cold 0.5 M citric acid solution at pH 2~3. The compound was then extracted with (2 x 100 mL) ethyl acetate and dried over Na_2SO_4. The combined organic layers were concentrated in vacuo to give compound 4.20 (2.4 gm) in 80% yield. ^{1}H NMR (250 MHz, $CDCl_3$) ppm 4.47 (b, 1H), 3.85 – 3.69 (m, 1H), 3.62 (dd, *J* = 10.7, 3.8 Hz, 1H), 3.28 – 3.18 (m, 1H), 2.73 – 2.67 (m, 1H), 2.63 (d, *J* = 5.6 Hz, 2H), 1.74 – 1.56 (m, 2H), 1.46 (s, 9H), 1.41 – 1.13 (m, 5H), 0.93 (dd, *J* = 6.5, 4.8 Hz, 12H). ^{13}C NMR (63 MHz, $CDCl_3$) ppm 156.13, 63.54, 56.88, 51.68, 49.00, 42.57, 41.38, 28.40, 24.94, 23.16, 23.08, 22.71, 22.21. m/z 317.2725 $(M+H)^{+}$.

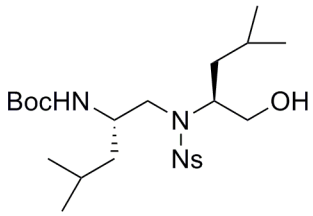

tert-butyl (R)-1-(N-((S)-1-hydroxy-4-methylpentan-2-yl)-2-itrophenylsulfonamido)-4-methylpentan-2-ylcarbamate (4.20)

To a stirred solution of $NaHCO_3$ (2.9 gm, 34 mmol) in 10 mL water was added **4.18** (1.8 gm, 5.7 mmol) in 15 mL dioxane. The reaction contents were cooled to 0^{o}C in ice-bath

and ONBSCl (2.5 gm, 11 mmol) in 10 mL dioxane was added slowly with vigorous stirring. The reaction was stirred overnight at room temperature. The reaction contents were then poured onto ether (50 mL), washed with 2N NH_4OH (1 x 20 mL), water (1 x 20 mL) and cold 0.5M citric acid (1 x 20 mL). The organic contents were then dried, filtered, and concentrated in vacuo to give **4.20** (2.43 gm, 85.3%) yield. ^{1}H NMR (250 MHz, $CDCl_3$) ppm 8.13 – 8.04 (m, 1H), 7.65 – 7.60 (m, 2H), 7.57 – 7.52 (m, 1H), 4.77 (d, *J* = 7.9 Hz, 1H), 3.87 – 3.66 (m, 2H), 3.64 – 3.58 (m, 2H), 3.29 (t, *J* = 8.4 Hz, 2H), 2.66 (b, 1H), 1.70 – 1.50 (m, 2H), 1.35 (s, 9H), 0.86 (dd, *J* = 6.5, 3.9 Hz, 6H), 0.70 (dd, *J* = 16.6, 5.4 Hz, 6H). ^{13}C NMR (63 MHz, $CDCl_3$) ppm 155.86, 147.96, 133.66, 131.82, 124.14, 79.32, 67.08, 63.33, 58.99, 48.90, 42.57, 39.09, 28.38, 24.81, 24.75, 23.28, 22.61, 22.24, 22.05. m/z 524.2397 $(M+Na)^+$.

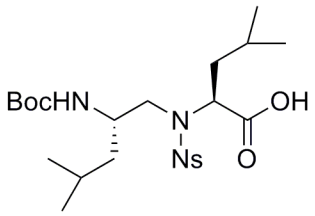

(S)-2-(N-((R)-2-(tert-butoxycarbonylamino)-4-methylpentyl)-2-nitrophenyl-sulfonamido)- 4-methylpentanoic acid (4.21)

Compound **4.20** (1.9 gm, 3.7 mmol) was dissolved in 50 mL acetone and 15 mL 15% $NaHCO_3$ was added to it. Then sodium bromide (76 mg, 0.7 mmol), TEMPO (11.6 mg, 0.07 mmol) and trichloroisocyanuric chloride (1.73 gm, 7.4 mmol) were sequentially added. After completion of reaction, the reaction contents were extracted with ethyl acetate (1 x 50 mL). The organic contents were dried, filtered, concentrated, and purified by column chromatography to give **4.21** (0.8 gm) in 40 % yield. ^{1}H NMR (250 MHz, $CDCl_3$) ppm 9.05 (b, 1H), 8.06 – 7.96 (m, 1H), 7.68 – 7.59 (m, 2H), 7.54 (dd, *J* = 7.3, 1.8

Hz, 1H), 4.77 (b, 1H), 4.55 – 4.42 (m, 1H), 3.98 – 3.65 (m, 1H), 3.58 – 3.04 (m, 2H), 1.46 – 1.32 (m, 11H), 0.90 – 0.79 (m, 12H). ^{13}C NMR (63 MHz, $CDCl_3$) ppm 175.65, 155.84, 148.06, 134.02, 133.95, 131.70, 131.57, 131.43, 131.36, 124.31, 124.17, 81.63, 79.31, 59.42, 58.75, 50.08, 48.52, 42.79, 38.58, 28.38, 28.08, 24.65, 24.31, 23.64, 23.15, 22.55, 22.24, 21.35, 20.91. m/z 538.2193 $(M+Na)^+$.

4.4 References

1.Vogelstein, B.; Lane, D.; Levine, A. J., Surfing the p53 network. *Nature* **2000,** *408* (6810), 307-10.

2.Vousden, K. H.; Lu, X., Live or let die: the cell's response to p53. *Nat. Rev. Cancer* **2002,** *2* (8), 594-604.

3.Hainaut, P.; Hollstein, M., p53 and human cancer. The first ten thousand mutations. *Adv. Cancer Res.* **2000,** *77*, 81-137, 1 color plate.

4.Moll, U. M.; Petrenko, O., The MDM2-p53 Interaction. *Mol. Cancer Res.* **2003,** *1* (14), 1001-1008.

5.Bond, G. L.; Hu, W.; Levine, A. J., MDM2 is a central node in the p53 pathway: 12 years and counting. *Curr. Cancer Drug Targets* **2005,** *5* (1), 3-8.

6.Fischer Peter, M.; Lane David, P., Small-molecule inhibitors of the p53 suppressor HDM2: have protein-protein interactions come of age as drug targets? *Trends Pharmacol Sci* **2004,** *25* (7), 343-6

7.Momand, J.; Zambetti, G. P.; Olson, D. C.; George, D.; Levine, A. J., The mdm-2 oncogene product forms a complex with the p53 protein and inhibits p53-mediated transactivation. *Cell (Cambridge, Mass.)* **1992,** *69* (7), 1237-45.

8.Roth, J.; Dobbelstein, M.; Freedman, D. A.; Shenk, T.; Levine, A. J., Nucleo-cytoplasmic shuttling of the hdm2 oncoprotein regulates the levels of the p53 protein via a pathway used by the human immunodeficiency virus rev protein. *Embo J.* **1998,** *17* (2), 554-564.

9.Tao, W.; Levine, A. J., Nucleocytoplasmic shuttling of oncoprotein Hdm2 is required for Hdm2-mediated degradation of p53. *Proc Natl Acad Sci U S A* **1999,** *96* (6), 3077-80.

10.Pickart, C. M., Mechanisms underlying ubiquitination. *Annu. Rev. Biochem.* **2001,** *70*, 503-533.

11.Haupt, Y.; Maya, R.; Kazaz, A.; Oren, M., Mdm2 promotes the rapid degradation of p53. *Nature (London)* **1997,** *387* (6630), 296-299.

12.Honda, R.; Tanaka, H.; Yasuda, H., Oncoprotein MDM2 is a ubiquitin ligase E3 for tumor suppressor p53. *FEBS Lett.* **1997,** *420* (1), 25-27.

13.Kubbutat, M. H. G.; Jones, S. N.; Vousden, K. H., Regulation of p53 stability by Mdm2. *Nature (London)* **1997,** *387* (6630), 299-303.

14.Harris, C. C., Protein-protein interactions for cancer therapy. *Proc Natl Acad Sci USA* **2006,** *103* (6), 1659-1660.

15.Jimenez, G. S.; Khan, S. H.; Stommel, J. M.; Wahl, G. M., p53 regulation by post-translational modification and nuclear retention in response to diverse stresses. *Oncogene* **1999,** *18* (53), 7656-7665.

16.Vassilev, L. T.; Vu, B. T.; Graves, B.; Carvajal, D.; Podlaski, F.; Filipovic, Z.; Kong, N.; Kammlott, U.; Lukacs, C.; Klein, C.; Fotouhi, N.; Liu, E. A., In Vivo Activation of the p53 Pathway by Small-Molecule Antagonists of MDM2. *Science (Washington, DC, U. S.)* **2004,** *303* (5659), 844-848.

17.Fasan, R.; Dias, R. L. A.; Moehle, K.; Zerbe, O.; Vrijbloed, J. W.; Obrecht, D.; Robinson, J. A., Using a beta-hairpin to mimic an alpha -helix: Cyclic peptidomimetic inhibitors of the p53-HDM2 protein-protein interaction. *Angew. Chem., Int. Ed.* **2004,** *43* (16), 2109-2112.

18.Kussie, P. H.; Gorina, S.; Marechal, V.; Elenbaas, B.; Moreau, J.; Levine, A. J.; Pavletich, N. P., Structure of the MDM2 oncoprotein bound to the p53 tumor suppressor transactivation domain. *Science (Washington, D. C.)* **1996,** *274* (5289), 948-953.

19.Luca Leonora, D.; Luca Joao Bosco Assis, D., Marie Rennotte, educator and medical doctor: elements for a historical and biographical, social and medical study. *Hist Cienc Saude Manguinhos* **2003,** *10* (2), 703-25.

CHAPTER FIVE:

DESIGN AND SYNTHESIS OF PEPTIDE NUCLEIC ACID OLIGOMERS

5.1 Introduction

Many human diseases are caused by over-, under-, or misproduction of specific proteins. Defects in the gene cause production of m-RNAs which codes for a non-functional protein. Many diseases can be controlled by curbing production of these non functional proteins (1). Thus, if single strands of DNA can be synthesized, the base sequence could be studied and manipulated to treat various diseases. Gene expression can be regulated by binding of an oligonucleotide or oligonucleotide analogue to double stranded DNA or single stranded RNA. PNA (Peptide Nucleic Acids) is an extremely good DNA mimic in which the deoxyribose phosphate diester backbone is replaced by a pseudo-peptide backbone while the four natural nucleobases are retained. This new backbone designed using computer models is structurally similar to the deoxyribose phosphate backbone, synthetically accessible and amenable to automated assembly synthesis (2, 3) (Fig. 5.1).

PNA consists of repeating N-(2-aminoethyl)-glycine units in which the nucleobase is attached to the glycine nitrogen via a methylene carbonyl linker. The acyclic, achiral and neutral backbone makes PNA set apart from DNA (4). The neutral backbone of PNA allows stronger binding between complementary PNA/DNA strands than between complementary DNA/DNA strands as determined by Tm's (Melting

Temperature). This is attributed to lack of charge repulsion between the PNA strand and the DNA strand. PNA also binds to DNA with greater specificity. A mismatch in a PNA/DNA duplex is more destabilizing than a mismatch in a DNA/DNA duplex (5, 6).

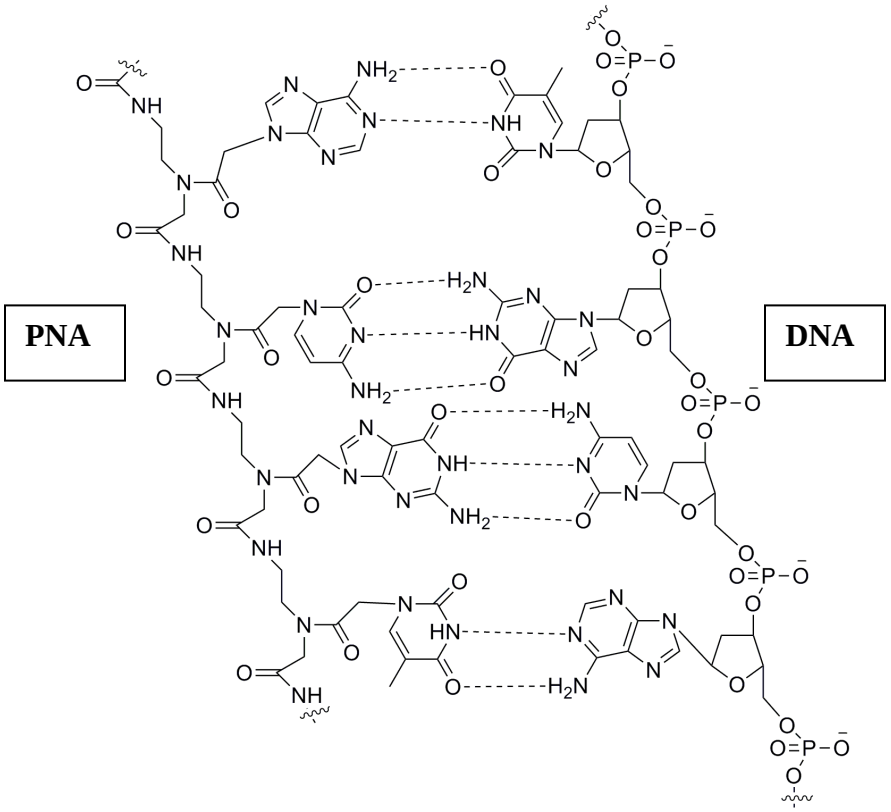

Fig. 5.1 Structures of PNA and DNA.

PNA can bind to DNA or RNA strands in antiparallel or parallel orientations. In antiparallel orientations, a DNA or RNA strand in 5' to 3' orientation binds to a complementary PNA strand such that the carboxyl end of PNA is directed towards the 5' end of DNA or RNA and the amino end is directed towards the 3' end of DNA/RNA. The neutral polyamide backbone of PNA offers enzymatic stability, making PNA resistant to both proteases and nucleases (7). PNAs form stable triplexes PNA-DNA-PNA in which one PNA strand hybridizes to DNA by Watson-crick base pairing while other binds the same strand via the Hoogsten mode.

All of the above properties makes PNA an important tool for designing gene therapeutic drugs (antisense and antigene) and in genetic diagnostics (8). Although PNAs have been demonstrated as potential candidates for gene-targeting drugs, some disadvantages have limited applications. These include low cellular uptake caused by poor cell membrane permeability and poor aqueous solubility (9, 10). This is due to uncharged property of PNAs whereas nucleic acid oligonucleotides bearing negative charges can penetratate the cell membrane by endocytosis (11). In order to increase the cellular uptake of PNAs various strategies have been explored during the last decade. These includes microinjection, electroporation, and attachment to cell penetrating peptides (12). Since a positive charge will enhance attraction of molecules to cell membrane, some researchers have tried to introduce positively charged residues such as lysine and arginine into PNA molecules to increase cellular uptake of PNAs. Ly's group synthesized GPNA with arginine side chain attached to PNA backbone (7, 13). Inspired by this idea to increase cellular uptake by introducing positive charge species into PNA, an attempt to synthesize cysteine based Peptide nucleic acid (CPNA) monomers and oligomers containing all four nucleobases was made. The proposed target molecule is shown in figure 5.2.

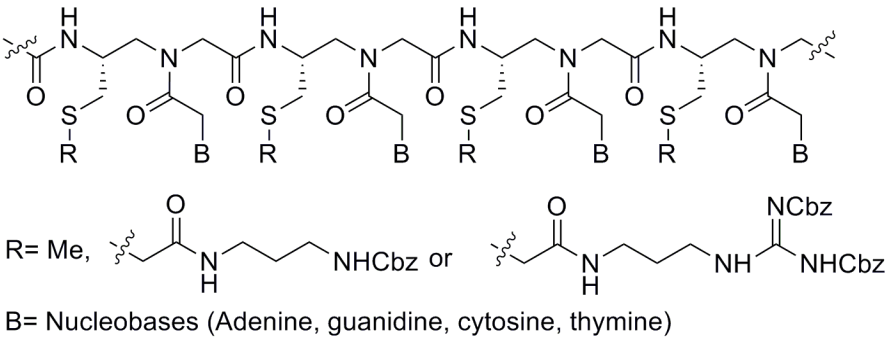

Fig. 5.2 Proposed CPNA design for antisense applications.

CPNA monomers are derived from cysteine with positively charged guanidine units in the side chain. The thiol group in cysteine allows us to attach various alkyl groups designed to improve the properties of PNA. The presence of the thiol group usually interferes in solid phase synthesis too. This might be the reason for no report of PNAs based on cysteine. The introduction of positively charge residues on PNA is expected to increase aqueous solubility and cellular uptake of PNAs. We have also made efforts to synthesize standard Peptide Nucleic Acids monomers with an aim to make hybrid PNAs. In this chapter, the synthesis of standard and CPNA monomers, modified nucleobases and an effort to synthesize PNA oligomers is described.

5.2 Results and Discussion

5.2.1 Synthesis of CPNA monomers

Synthesis of PNA oligomers is based on solid phase peptide synthesis protocols. The scheme for protecting amino groups of PNA monomers is based on either Boc or Fmoc chemistry. Scheme 5.1 shows the synthesis of four CPNA monomers using Fmoc protecting groups on primary amine of backbone and Cbz protecting groups on the exocyclic amino groups of nucleobases. The backbone protecting groups must be orthogonal in their requirement from removal from PNA during oligomer synthesis i.e Cbz protecting groups on nucleobases must be stable to conditions used for removal of Fmoc protecting group from terminal amine. The use of Fmoc protection groups offers advantages of milder synthesis conditions and improved monomer solubility.

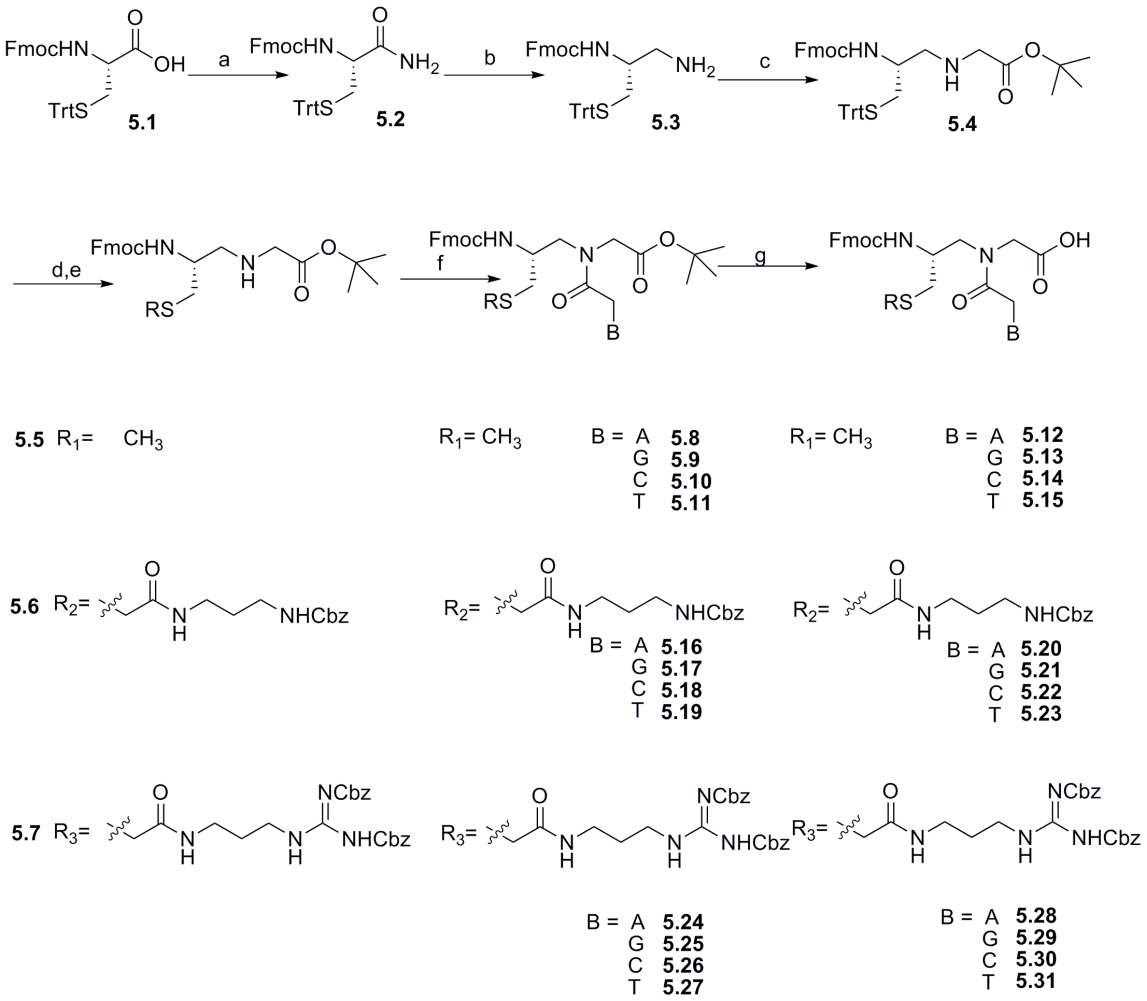

(a) DCC, HOBT, NH_4OH, THF 92% (b) BH_3,THF, THF 72% (c) $BrCH_2CO_2tbu$, DIEA, THF 82% (d) TFA, Et_3SiH, DCM (e) RBr, NaOH, EtOH 92% (f) BCH_2COOH, HATU, DIEA, DMF 70% (g) $HCl_{(g)}$, dioxane quant.

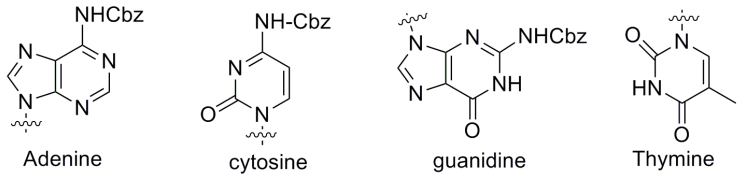

Scheme 5.1 Synthetic strategy for making CPNA monomers.

Various research groups have used the reductive amination route (14) to synthesize PNA backbone but our PNA is synthesized by a novel S_N2 route. Synthesis of CPNA monomers involves activation of commercially available Fmoc(Cys)Trt-COOH

using DCC followed by attack of nucleophile to enable formation of Amide **5.2**. Selective reduction of **5.2** with BH_3 in THF yields primary amine **5.3** in 65% yield. Alkylation of terminal amine **5.3** with tert-butyl bromoacetate via S_N2 reaction followed by aqueous workup gives **5.4** in 82% yield. Deprotection of acid labile trityl protecting group in **5.4** using triflouro acetic Acid followed by alkylation of resulting thiol with various alkylating agents (methyl iodide, guanidium) enabled us to introduce positive charge residue on the side chain of PNAs. The next step involves coupling of nucleobase acetic acids to unreactive secondary amine in **5.5, 5.6, 5.7** to give fully protected CPNA monomers in 80% yield. Finally, the t-butyl ester was deprotected with HCl in dioxane to give CPNA monomers in quantitative yield.

During synthesis of amide, the by-product N,N'-DCC urea is mostly removed by filtration, but trace amounts still remain and is often difficult to remove. Other activating agents such as EDC, DIC were also used as an alternative. These activating agents were equally efficient to DCC with similar yields. Excess amount of ammonium hydroxide should be avoided as it often leads to cleavage of base labile Fmoc group, thereby decreasing the yields of amide. This reaction should be carried out at low temperature ~10-15^{0}C. Larger reaction time and elevated temperatures often resulted in low yields of amide. Borane reduction of amide to give primary amine was tricky reaction. Concentration of pure amine after column chromatography usually cleaved Fmoc protecting group which causes a reduction in yield. This problem was eliminated by making use of trityulation technique for purifying crude amine. During synthesis of compound **5.4**, excess amount of alkylating agent caused formation of some dialkylated compound along with desired monoalkylated compound. Also cleavage of Fmoc

protecting group was seen when base slight excess of DIEA was used. This problem was solved by using 1equivalent of alkylating agent and 1.05 equivalent of base. The reaction temperature also determined the amount of dialkylated compound formed. A significant amount of dialkylated compound was formed when the reaction was carried at room temperature for longer time as well as some Fmoc cleavage was also observed. The reaction was done at 10-15^{0}C for 10 hours and then at room temperature for two hours. The reaction rate was slow but no dialkylated compound and Fmoc cleavage was observed. Deprotection of trityl group in compound **5.4** and then alkylation of resulting thiol was done in a single pot. Extreme dilute conditions were employed while using TFA deprotection of trityl group. Dilute conditions enabled t-butyl to remain intact. Alkylation of thiol was done using slight excess of base followed by addition of slight excess of alkylating agent. Coupling of nucleobase acetic acids to CPNA submonomers gave monomers in good yield. Purification of these polar based coupled CPNA monomers was tedious, particularly Guanidine coupled CPNA monomer purification gave low yields.

Deprotection of t-butyl ester from fully protected CPNA monomer using HCl/Dioxane gave final monomers in quantitative yields but removal of residual dioxane from monomers was difficult.

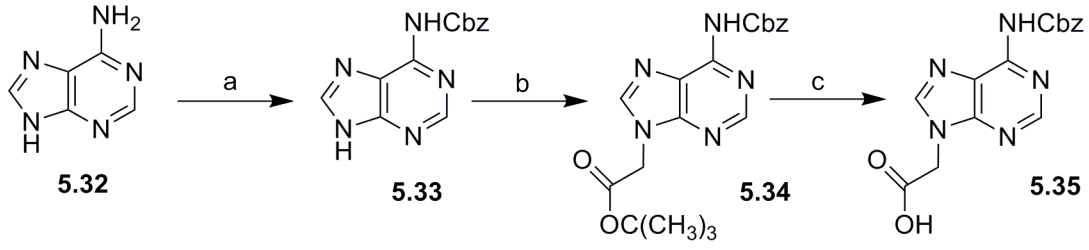

(a) NaH, Cbz-Cl, DMF (b) $BrCH_2CO_2t$-Bu, K_2CO_3, Cs_2CO_3, DMF (c) TFA, Et_3SiH, CH_2Cl_2

Scheme 5.2 Synthesis of Cbz protected Adenine acetic acid nucleobase for CPNA.

Synthesis of Adenine Acetic Acid used for coupling to PNA backbone is shown in scheme 5.2. Several procedures for synthesizing nucleobase acetic acids have been reported till now (15, 16, 17). The exocyclic amine of adenine was first protected with acid labile Cbz protecting group using benzyl chloroformate to give **5.33**. Compound **5.33** was then alkylated with t-butyl bromoacetate in DMF using potassium carbonate and cesium carbonate to give a mixture of N-7 and N-9 alkylated products. The desired N-9 alkylated produced was separated using column chromatography in 49% yield. Removal of the t-butyl ester with TFA in DCM gave compound **5.35** in 92% yields along with a loss of Cbz group. The loss of Cbz group in this reaction was suppressed by using slight excess of cation scavenger triethylsilane in the reaction mixture.

The solid phase synthesis of CPNA monomers posed a great challenge to us. We have been able to synthesize dimers of nucleobase coupled CPNA monomers using solution phase coupling. Synthesis of purine based CPNA monomers and their coupling during solid phase synthesis was difficult. Solid phase coupling for obtaining CPNA oligomers (18-mer) was attempted but it did not yield promising results. The synthesis of standard peptide nucleic acid monomers was attempted with an aim to make hybrid PNAs consisting of standard PNA and CPNA monomers. This strategy will help us to modulate the positive charge on PNA, required for achieving cellular permeability.

5.2.2 Synthesis of standard PNA monomers

Scheme 5.3 depicts the synthesis of standard PNA monomers using orthogonal Fmoc/t-butyl strategy as cited in reported literature procedures. Selective monoalkylation of excess ethylene diamine with t-butyl bromoacetate gave compound **5.37**. This material was utilized in next step without further purification. Fmoc protection of the primary

amine in **5.37** followed by acidic workup gave compound **5.38** as Hydrochloride salt. This compound can be stored indefinitely in deep freezer. Coupling of nucleobase acetic acids to PNA backbone was achieved using HATU and DIEA in DMF to give nucleobase coupled PNA esters. Finally deprotection of t-butyl group using HCl gas in dioxane gave peptide nucleic acid monomers in good yields.

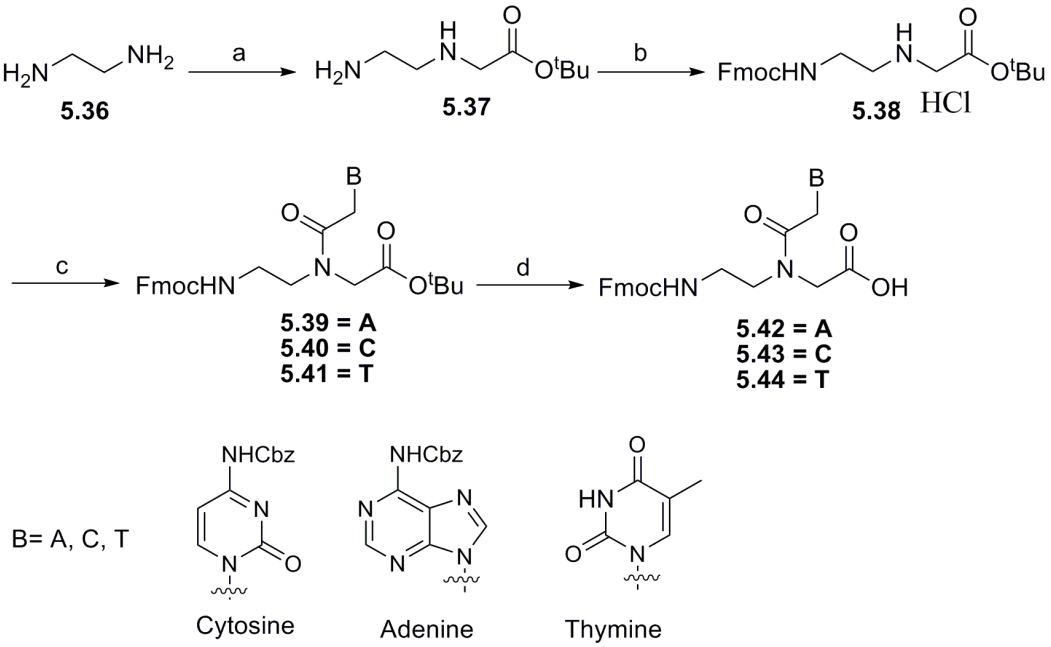

(a) $BrCH_2CO_2{}^tBu$, THF, 0°C-rt, 85% (b) FmocOSu, DIEA, DCM, rt, 12h, 90% (c) BCH_2COOH, HATU, DIEA, DMF, 75-80% (d) 1,4-Dioxane, $HCl_{(g)}$, quant.

Scheme 5.3 Synthesis of standard PNA monomers using Fmoc/t-butyl strategy.

The solid phase synthesis of standard PNA monomers was carried out on MBHA resin solid support using standard Fmoc protecting group strategy. We were able to synthesize 12mer PNA oligomer with sequence NH_2LysTTACATCTTTTC-COOH along with truncated byproducts. The purification of PNA using RPLC became difficult and we were not successful in obtaining purified PNA out of the column. We sought for alternative strategies for making standard peptide nucleic acid. Lee and coworkers have synthesized self-activated cyclic PNA monomers and an efficient method for

synthesizing PNA oligomer using benzothiazole-2-sulfonyl (Bts) protecting group. Scheme 5.4 shows the synthesis of cyclic Bts protected PNA monomers carried out as per cited literature procedure (18).

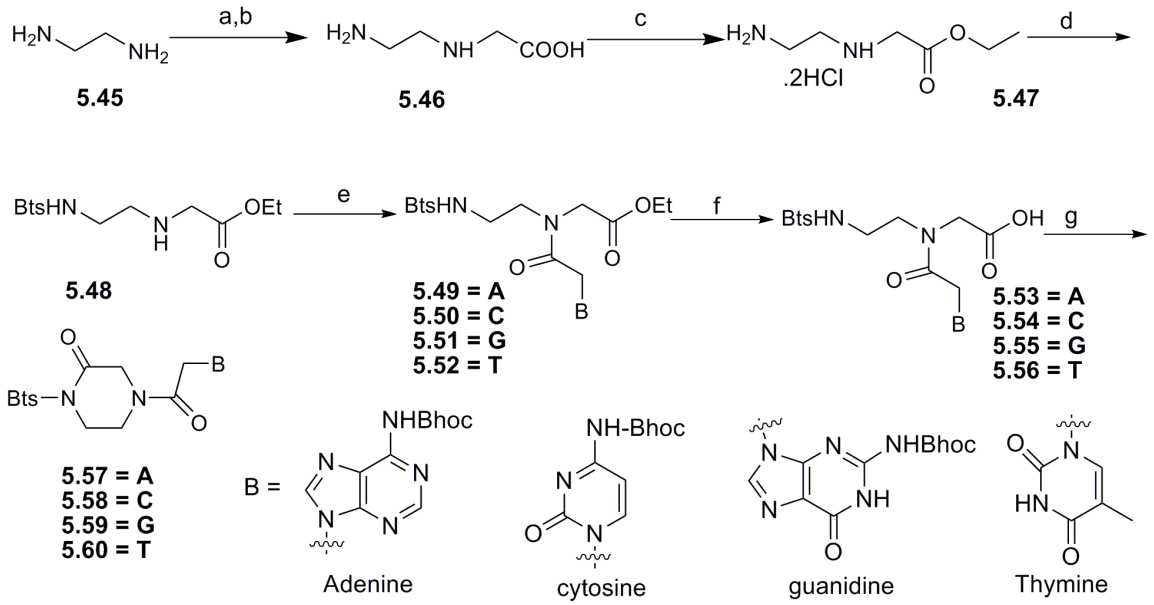

(a)CHOCOOH, MeOH (b) Pd/C, MeOH, 62% (c) EtOH,HCl, reflux (d) BtsCl, DCM, TEA 72%

(e) B-CH_2COOH, HATU, DIEA, DMF, 65% (f)LiOH, THF:H_2O(1:1), 80-90% (g)EDC, DMF 85-90%

Scheme 5.4 Synthesis of Cyclic Bts PNA monomers.

Compound **5.48** was prepared by treating **5.47** with Bts-Cl synthesized from 2-meracaptobenzothioazole in 72% yield (19, 20). Nucleobases used for coupling were protected with Bhoc group due to its stability towards nucleophiles and ease of deprotection. Nucleobase acetic acids were prepared as per reported literature and coupled to **5.48** using HATU and DIEA in DMF (21). The corresponding esters (**5.49-5.52**) were hydrolysed using LiOH to give corresponding acids (**5.53-5.56**) in 80-90% yield. The acids (5.53-5.56) were then readily cyclized using EDC to give cyclic Bts protected PNA monomers in 85-90% yield. Scheme 5.5 describes the solid phase synthesis of PNA oligomer using cyclic Bts monomers.

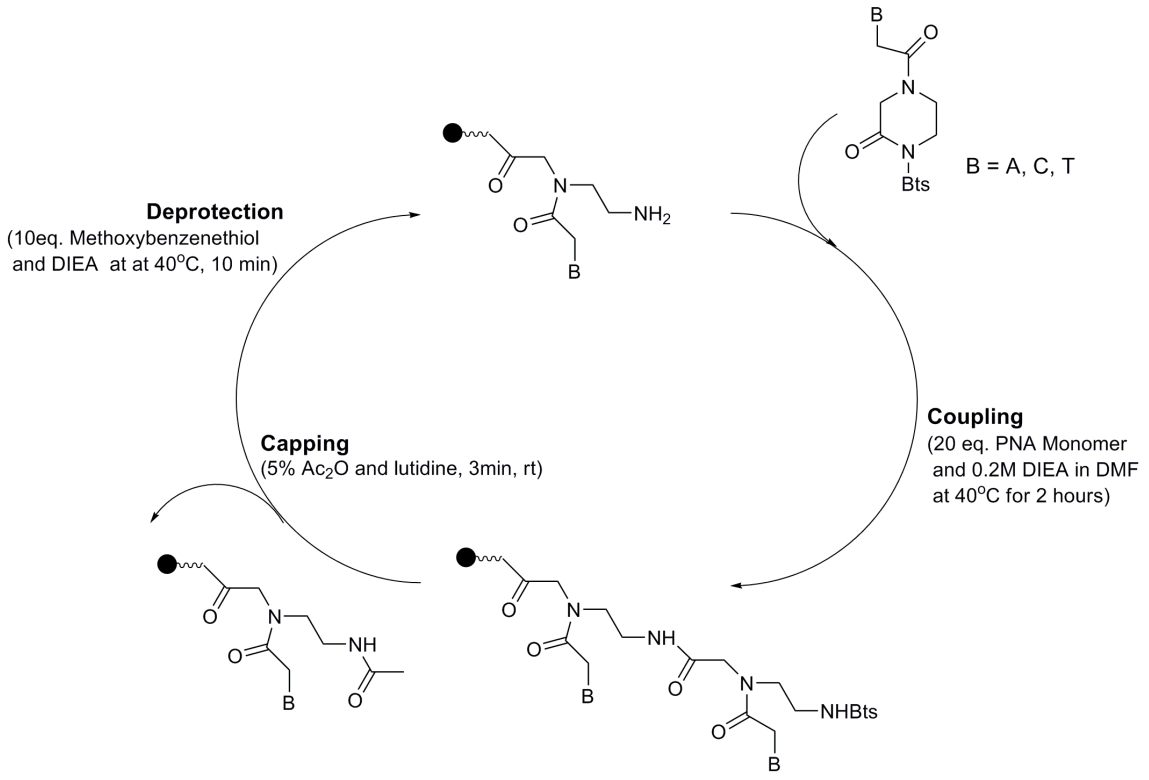

Scheme 5.5 Solid phase synthesis of standard PNA using cyclic Bts protecting group.

Bts group activates carbonyl of piperazinone to be readily attacked by primary amine of PNA and is easily removed by thiols in presence of base after the coupling reaction. PNA synthesis was carried out on CLEAR amino resin loaded with PAL linker that allows cleavage of PNA under acidic conditions. Coupling was carried out at 40^{o}C for two hours and unreacted amine of PNA was capped by Ac_2O/Lutidine. The Bts group was removed by 1M 4-Methoxybenzethiol and 1M DIEA in DMF. The greatest advantage of using cyclic Bts protected monomers is that they do not require preactivation or extremely anhydrous conditions. Also we can recover unused monomers since no coupling agents are involved. MALDI-TOF analysis of the crude PNA synthesis suggested we were able to synthesize desired PNA alongwith truncated byproducts using this strategy but we could not quantify it into appreciable yields.

5.3 Experimental Procedures

5.3.1 Materials and Methods

Organic and inorganic reagents (ACS grade) were obtained from commercial sources and used without further purification, unless otherwise noted. Fmoc-protected amino acids and the coupling agent HCTU were obtained from Protein Technologies, Calbiochem-Novabiochem, or Chem-impex International. 2-Chlorotrityl chloride resin was purchased from Anaspec Inc. All linear peptides were synthesized on the Symphony peptide synthesizer, Protein Technologies Instruments. Solvents for peptide synthesis and reverse-phase HPLC were obtained from Applied Biosystems. Other chemicals used were obtained from Aldrich and were of highest purity commercially available. Thin layer chromatography (TLC) was performed on glass plates (Whatman) coated with 0.25 mm thickness of silica gel 60Å (# 70-230 mesh). All ^{1}H and ^{13}C NMR spectra were recorded on Bruker 250 MHz, Varian INOVA 400 MHz spectrometer in $CDCl_3$ or unless otherwise specified and chemical shifts are reported in ppm (δ) relative to internal standard tetramethylsilane (TMS). High Resolution mass spectra were obtained on an Agilent LC-MSD-TOF.

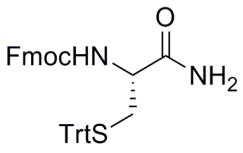

(R)-(9H-fluoren-9-yl)methyl1-amino-1-oxo-3-(tritylthio)propan-2-ylcarbamate (5.2)

To a solution of **5.1**(10.00 g, 17.05 mmol), HOBT (2.76 gm, 20.0 mmol) and DCC (4.23 gm, 20.0 mmol) in THF (100 mL) was added 28% NH_4OH (2.45 mL, 20.0 mmol) at 0°C. After 2hr of stirring at 0°C, the reaction mixture was filtered through diatomaceous earth

and the filtrate was concentrated, diluted with ethyl acetate, and washed with water and brine. The organic layer was then dried over sodium sulfate, concentrated and subjected to flash column chromatography to give **5.2**(9.25 g, 92 %) as white solid. R_f = 0.45 (50:50 ethyl acetate: hexane)) ^{1}H NMR (400MHz, $CDCl_3$) δ 2.65(m, 2H), 4.12 (q, J = 7.14, 1H), 4.17 (t, J = 6.52, 1H), 4.41 (d, J = 4.92, 2H), 5.02 (d, J = 7.54, 1H), 5.48 (s, 1H), 5.74 (s, 1H), 7.23 (m, 11H), 7.38 (dd, J = 7.6 & 11.0, 8H), 7.36 (d, J = 7.36, 2H), 7.74 (m, 2H). ^{13}C NMR (400MHz, $CDCl_3$) δ 25.94, 33.94, 53.5, 60.10, 67.4, 120.01, 124.99, 126.94, 127.07, 127.10, 127.75, 127.77, 128.08, 129.55, 141.35, 143.66, 144.28, 156.76, 172.72. m/z 585.2 $(M+H)^+$

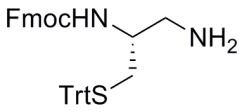

(R)- (9H-fluoren-9-yl) methyl 1-amino-3-(tritylthio) propan-2-ylcarbamate (5.3).

To a solution of **5.2**(9.25 gm, 15.8 mmol) in THF(30 mL was added 1 M Borane·THF complex (34.76 mL, 34.76 mmol) at 0°C and After stirring at 0°C for 3 hrs, reaction mixture was then heated to 70°C and stirred for 12 hrs. Reaction mixture was cooled to 0°C and quenched by MeOH. The reaction mixture was concentrated and diluted with MeOH and concentrated again in vacuo. The concentrated oil was subjected to flash column chromatograph to afford **5.3**(6.5 gm) in a 72 % yield. R_f = 0.50 (90:10 ethyl acetate: methanol)) ^{1}H NMR (400 MHz, $CDCl_3$) δ 0.78 (m, 2H), 2.37 (d, J = 20.25, 2H), 2.63 (s, 2H), 4.20 (t, J = 6.74, 1H), 4.40 (d, J = 6.62, 2H), 4.81 (s, 1H), 7.25 (m, 11H), 7.41 (m, 8H), 7.59 (d, J = 7.39, 2H), 7.75 (m, 2H).). ^{13}C NMR (400 MHz, $CDCl_3$) δ

24.94, 25.62, 33.96, 44.56, 47.30, 52.42, 66.90, 119.96 125.03, 126.81, 127.03, 127.68, 127.97, 129.58, 141.34, 143.91, 144.54, 155.92. m/z 571.2 $(M+H)^+$

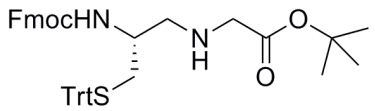

[2-(9H-Fluoren-9-ylmethoxycarbonylamino)-3-tritylsulfanyl-propylamino]-acetic acid tert-butyl ester (5.4)

To a solution of **5.3** (1.8 gm, 3.2 mmol) in THF(20 mL) was added tert-butyl bromoacetate (0.47 mL, 3.2 mmol) and DIEA (0.576 ml, 3.31 mmol) at 0°C. The reaction mixture was slowly allowed to warm to room temperature. The reaction mixture was concentrated in vacuo, diluted with EtOAc and washed with brine. The organic layer was dried over sodium sulfate, concentrated in vacuo and subjected to a flash column chromatography to give **5.4**(2.2 gm, 82%). R_f = 0.73 (50:50 ethyl acetate: hexane)) ^{1}H NMR (400 MHz, $CDCl_3$) δ 0.868 (d, J = 7.09, 2H), 0.97 (d, J = 6.55, 1H), 1.25 (s, 2H), 1.45 (s, 9H), 2.46 (m, 4H), 3.17 (s, 2H), 4.20 (s, 1H), 4.35 (d, J = 6.71, 2H), 5.10 (m, 1H), 7.25 (m, 11H), 7.4 (m, 8H), 7.59 (d, J = 7.31, 2H), 7.75 (d, J = 7.49, 2H). ^{13}C NMR (400 MHz, $CDCl_3$) δ 29.51, 35.3, 47.6, 49.5, 50.2, 67.6, 67.52, 81.9, 120.1, 125.8, 127.43, 127.9, 128.05, 129.88, 140.7, 144.2, 145.5, 156.2, 172.1. m/z 685.2 $(M+H)^+$

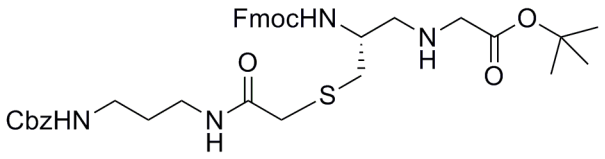

(R)-tert-butyl 13-(((9H-fluoren-9-yl)methoxy)carbonylamino)-3,9-dioxo-1-phenyl-2-oxa-11-thia-4,8,15-triazaheptadecan-17-oate (5.6)

To a stirred solution of **5.4** (1.5 gm, 2.1 mmol) in DCM (50 mL) at 0°C was added TFA (4 mL). The reaction mixture was treated with triethylsilane (0.35 mL, 2.1 mmol). The reaction mixture was stirred for 30 min at 0°C and concentrated in vacuo. The crude product was dissolved in EtOH (20 mL) and the solution was cooled to 0^0C. Aqueous NaOH (2N, 3.3 mL, 6.6 mmol) was added slowly to the solution followed by addition of the alkyl bromide, (0.86 gm, 2.6 mmol). The reaction was stirred for 4 hrs at 0°C. After the removal of organic solvents in vacuo, the residue was diluted with EtOAc and washed with water and brine. The organic layer was dried over sodium sulfate, concentrated in vacuo and subjected to a flash column chromatography to give **5.6**(1.4 gm, 92 %). R_f = 0.4 (100% ethyl acetate) ^{1}H NMR (400 MHz, $CDCl_3$) δ 1.44 (d, J = 7.17, 9H), 1.63 (s, 2H), 2.75 (m, 2H), 3.24 (m, 8H), 3.52 (s, 2H), 4.06 (s, 1H), 4.17 (q, 1H), 4.33 (d, 2H), 5.03 (s, 2H), 5.4 (s, 1H), 6.58 (b, 1H), 7.28 (m, 7H), 7.37 (t, J = 7.47, 2H), 7.45 (m, 1H), 7.58 (d, 2H) 7.73 (d, J = 7.52, 2H). m/z 691.2 $(M+H)^+$

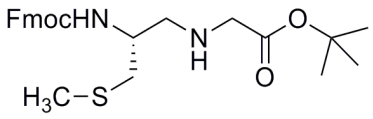

[2-(9H-Fluoren-9-ylmethoxycarbonylamino)-3-methylsulfanyl-propylamino]-acetic acid tert-butyl ester (5.5)

R_f = 0.52 (50:50 ethyl acetate: hexane)) ^{1}H NMR (250 MHz, $CDCl_3$) δ 1.43 (d, J = 19.9, 9H), 2.116 (s, 2H), 2.78 (m, 4H), 3.28 (s, 2H), 3.85 (s, 1H), 4.21 (t, J = 6.78, 1H), 4.39 (s, 2H), 5.55 (s, 1H), 7.33 (ddd, J = 5.57, 12.76 & 17.63, 4H), 7.61 (d, J = 7.28, 2H), 7.74 (d, J = 7.27, 2H). ^{13}C NMR (400 MHz, $CDCl_3$) δ 16.19, 28.12, 36.81, 47.28, 50.29, 51.01, 51.65, 66.58, 81.42, 119.94, 125.11, 127.03, 127.64, 141.3, 143.95, 156.13, 171.64. m/z 457.2$(M+H)^+$

General procedure for Base coupling

(R)-tert-butyl13-(((9H-fluoren-9-yl)methoxy)carbonylamino)-15-(2-(5-methyl-2,4-dioxo-3,4-dihydropyrimidin-1(2H)-yl)acetyl)-3,9-dioxo-1-phenyl-2-oxa-11-thia-4,8,15-triazaheptadecan-17-oate (5.19)

To a stirring solution of **5.6**(1.18 gm, 1.7 mmol), HATU (0.78 gm, 2.04mmol) and thymine acetic acid (0.47 gm, 2.6 mmol) in DMF was added TEA (0.71 mL) at room temperature for 4 hrs. The reaction mixture was diluted with EtOAc, washed with cold water and brine, dried over sodium sulfate, concentrated in vacuo and subjected to a flash column chromatography to give **5.19**(1.38 gm, 95%).

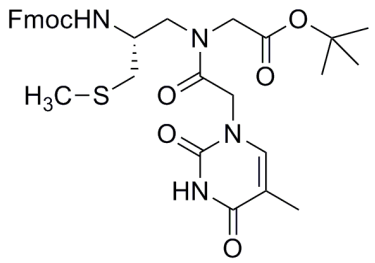

{[2-(9H-Fluoren-9-ylmethoxycarbonylamino)-3-methylsulfanyl-propyl]-[2-(5-methyl-2,4-dioxo-3,4-dihydro-2H-pyrimidin-1-yl)-acetyl]-amino}-acetic acid tert-butyl ester (5.8).

R_f = 0.51 (100% ethyl acetate)) ^{1}H NMR (400 MHz, $CDCl_3$) δ 1.47 (d, J = 27.2, 9H), 2.93 (s, 3H), 2.01 (s, 1H), 2.1 (d, J = 22.8, 3H), 2.6-2.72 (m, 2H), 2.8 (d, J = 0.58, 2H), 4.09 (m, 2H), 4.21 (m, 1H), 4.41 (d, J = 10.32, 2H), 4.74 (b, 1H), 7.23 (d, J = 6.09, 1H), 7.3 (d, J = 6.28, 2H), 7.51 (dd, J = 4.46 & 8.43, 1H), 7.66 (m, 2H), 7.78 (d, J = 7.27, 2H), 8.42 (dd, J = 1.36 & 8.43, 1H), 8.72 (d, J = 4.46, 1H). m/z 645.1 $(M+Na)^+$

General procedure for deprotecting carboxylic acid

Synthesis of (R)-13-(((9H-fluoren-9-yl)methoxy)carbonylamino)-15-(2-(5-methyl-2,4-dioxo-3,4-dihydropyrimidin-1(2H)-yl)acetyl)-3,9-dioxo-1-phenyl-2-oxa-11-thia-4,8,15-triazaheptadecan-17-oic acid (**5.23)**.

HCl gas was passed through a solution of **5.19**(1.38 gm, 1.6 mmol) in dioxane for 20 minutes. The reaction mixture was then stirred at r.t for 2 hrs followed by concentration in vacuo to give **5.23** (1.2 gm, quantitative yield).

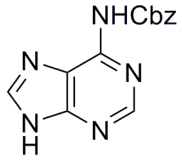

6-N-(Benzyloxycarbonyl) adenine (5.33)

Sodium Hydride (6.07 gm, 252 mmol), washed with hexane (3 times), was taken up in DMF (100 mL) in an ice-bath. Adenine (5 gm, 7 mmol), **5.32**, was then added in small lots. The suspension was stirred for 5 minutes and then benzyl chloroformate (11.6 gm, 81.5 mmol) was added dropwise. The reaction mixture was stirred for 4 hours, poured into ice-cooled water (250 mL) and pH was adjusted to 7 with 1 N HCl. The yellow precipitate was washed with water and ether to give crude product. Recrystallization with

DCM gave 5.12 gm of **5.33** in a 51 % yield. ^{1}H NMR (400MHz, DMSO) δ 5.3 (s, 2H), 7.3-7.5 (m, 5H), 8.4 (s, 1H), 8.6 (s, 1H) m/z 270.0 $(M+H)^+$

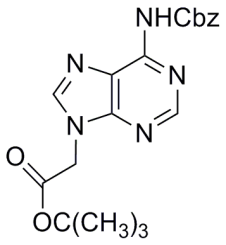

6-N-(Benzyloxycarbonyl)-9-(tert-butoxycarbonylmethyl) adenine (5.34)

5.33 (4 gm, 14.8 mmol) was taken up in DMF (25 mL). Anhydrous Cs_2CO_3 (0.48 gm, 1.48 mmol) and anhydrous K_2CO_3 (2.04 gm, 14.8 mmol) was added to it. After stirring for 5 minutes, tert-butyl bromoacetate (2.64 mL, 17.8 mmol) was added dropwise. After stirring for 24 hours, the mixture was concentrated, diluted in EtOAc, washed with water (10 mL) and ethyl acetate (35 mL). The organic layer was dried over sodium sulfate, concentrated, and subjected to column chromatography to give 2.85 gm of **5.34** in a 49 % yield. Rf = 0.33, (50:50 EtOAc:Hexane) ^{1}H NMR (400 MHz, $CDCl_3$) δ 8.78 (s, 1H), 8.09 (s, 1H), 7.25-7.35 (m, 5H), 5.3 (s, 2H), 4.89 (s, 2H), 1.47 (s, 9H). m/z 384.1$(M+H)^+$

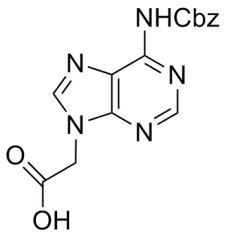

6-N-(Benzyloxycarbonyl)-9-(carboxymethyl) adenine 5.35

Triethylsilane (11.4 ml) was added to a solution of **5.34** (2.85 gm, 7.43 mmol) in anhydrous DCM (10 mL) and then TFA (15 mL) was added dropwise at 0^0C. After 5 min, the reaction mixture was allowed to warm to room temperature and stirred for 10 hrs. The mixture was concentrated and any volatile impurities were removed by

azeotroping with $CHCl_3$ (3 times) to give a crude product as white foam. Recrystallization with acetone gave 2.23 g of **5.35** in a 92 % yield. ^{1}H NMR (400 MHz, DMSO) δ 5.05 (s, 2H), 5.2 (s, 2H), 7.2-7.3 (m, 5H), 8.4 (s, 1H), 8.6 (s, 1H), 10.7 (s, 1H). m/z 326.0 $(M-H)^+$

Synthesis for compound **5.38** has been reported in chapter two.

General procedure for coupling of Cbz protected nucleobases to PNA backbone

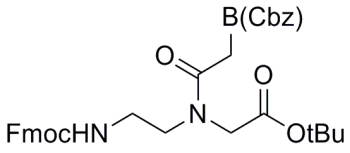

To a stirring solution of **5.38** (1.0 eq.), HATU (1.2 eq) and thymine acetic acid (1.2 eq.) in DMF was added TEA (3 eq.) at room temperature for 4 hrs. The reaction mixture was diluted with EtOAc, washed with cold water and brine, dried over sodium sulfate, concentrated in vacuo and subjected to a flash column chromatography to give corresponding esters **5.39-5.41** in 75-80% yield.

General procedure for deprotection of esters 5.39-5.41

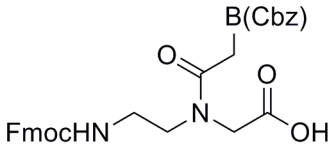

Corresponding esters **5.39-5.41** were dissolved in 1, 4-dioxane and $HCl_{(g)}$ was passed into solution for 10 min. The reaction mixture was stirred for another one hour and concentrated in vacuo and dried to give the corresponding acids.

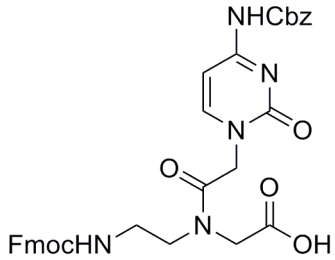

N-[2-(N-9-fluorenylmethoxycarbonyl)aminoethyl]-N-[[4-N-(benzloxycarbonyl)-cytosine-1-yl]acetyl]glycine 5.43

Yield: 86%, White solid. ^{1}H NMR (400 MHz, DMSO) δ 7.89 – 7.81 (m, 3H), 7.65 (d, *J* = 6.9 Hz, 2H), 7.42 – 7.26 (m, 10H), 7.00 – 6.93 (m, 1H), 5.16 (s, 2H), 4.79 (s, 1H), 4.60 (s, 1H), 4.34 – 4.23 (m, 2H), 4.20 (s, 2H), 3.96 (s, 1H), 3.45 – 3.01 (m, 5H).

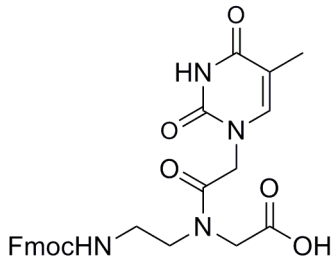

N-[2-N-(N-9-Fluorenylmethoxycarbonyl)aminoethyl]-N-[(thymin-1-yl)acetyl]-glycine (5.44)

Yield: 89%, White solid. ^{1}H NMR (400 MHz, DMSO) δ 11.24 (d, *J* = 7.0 Hz, 1H), 7.85 (d, *J* = 7.5 Hz, 2H), 7.65 (d, *J* = 7.3 Hz, 2H), 7.38 (t, *J* = 7.4 Hz, 3H), 7.29 (dd, *J* = 7.3, 6.6 Hz, 3H), 4.62 (s, 1H), 4.44 (s, 1H), 4.28 (dd, *J* = 16.0, 6.9 Hz, 2H), 4.22 – 4.14 (m, 2H), 4.05 – 3.77 (m, 2H), 3.38 (t, *J* = 6.3 Hz, 1H), 3.30 (t, *J* = 6.6 Hz, 1H), 3.22 (d, *J* = 5.9 Hz, 1H), 3.07 (dd, *J* = 12.3, 6.1 Hz, 1H), 1.69 (s, 3H).

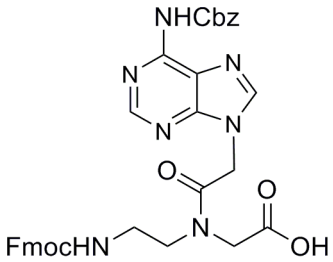

N-[2-(N-9-fluorenylmethoxycarbonyl)aminoethyl]-N-[[6-N-(benzyloxycarbonyl) adenin-9-yl]glycine (5.42)

Yield: 82% White solid. ^{1}H NMR (400 MHz, DMSO) δ 8.56 (d, *J* = 19.3 Hz, 1H), 8.49 – 8.45 (m, 1H), 7.84 (d, *J* = 7.5 Hz, 2H), 7.67 – 7.61 (m, 2H), 7.50 – 7.46 (m, 1H), 7.45 – 7.42 (m, 2H), 7.39 – 7.34 (m, 4H), 7.34 – 7.30 (m, 1H), 7.29 – 7.25 (m, 2H), 5.35 (s, 1H), 5.19 (d, *J* = 18.2 Hz, 3H), 4.33 (d, *J* = 7.1 Hz, 2H), 4.28 – 4.14 (m, 3H), 3.97 (s, 1H), 3.55 – 3.50 (m, 1H), 3.33 (d, *J* = 15.4 Hz, 2H).

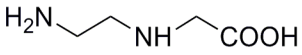

N-(2-Aminoethyl) glycine (5.46)

Ethylene diamine (18 mL, 27 mmol) was dissolved in methanol (26 mL) and glyoxylic acid monohydrate (8.4 gm, 91 mmol) in 2 6mL of H_2O was added slowly at 0^{o}C. After stirring for 20 mins, 5% Pd/C is added to the mixture and hydrogenation was carried out at 50 psi at room temperature. After filtering the mixture, the filtrate was concentrated and residue was reconcentrated twice with toluene (2 x 25 mL). Methanol (15 mL) was added to the crude residue stirring vigorously at 0^{o}C. After 15 mins, the white precipitates that formed were filtered off and washed with cold methanol. A second crop of precipitate was obtained from concentration of the mother liquor. The white precipitates were combined and dried to give compound **5.46** in 62% yield. ^{1}H NMR (250 MHz, D_2O)

δ 3.22 (s, 2H), 2.99 (dd, *J* = 9.5, 3.4 Hz, 2H), 2.85 (t, *J* = 6.0 Hz, 2H). m/z 118.13 $(M+H)^+$

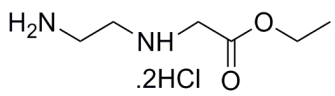

Ethyl N-(2-aminoethyl) glycinate dihydrochloride (5.47)

Compound **5.46** (10 gm, 84.7 mmol) was suspended in ethanol and HCl gas was passed into the suspension. The mixture was refluxed overnight and cooled to 0^oC. The product was filtered off and dried in vacuo to give compound **5.47** in quantitative yield. ^1H NMR (250 MHz, D_2O) δ 4.25 (q, *J* = 7.2 Hz, 2H), 4.04 (s, 2H), 3.82 (s, 1H), 3.54 – 3.27 (m, 5H), 1.23 (t, *J* = 7.2 Hz, 3H). m/z 147.10 $(M+H)^+$

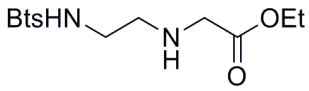

N-[2-(Benzothiazole-2-sulfonylamino)-ethyl]-glycine ethyl ester (5.48)

Compound **5.47** (3.2 gm, 15 mmol) was suspended in 100 mL DCM and TEA (7.5 mL, 58.4 mmol) was added slowly at room temperature. Then Bts-Cl (3.5 gm, 15 mmol) dissolved in 50 mL DCM was added over a period of 10 minutes. The reaction was stirred for 3 hours at room temperature and washed with water (50 mL). The organic layer was dried, filtered, concentrated and purified by column chromatography to give compound **5.48** in 72% yield. ^1H NMR (250 MHz, $CDCl_3$) δ 8.20 – 8.13 (m, 1H), 8.01 – 7.94 (m, 1H), 7.64 – 7.51 (m, 2H), 4.13 (q, *J* = 7.1 Hz, 2H), 3.38 (s, 2H), 3.34 (d, *J* = 5.9 Hz, 2H), 2.88 – 2.81 (m, 2H), 1.23 (t, *J* = 7.1 Hz, 3H).

General Procedure for synthesizing compounds (5.53-5.56)

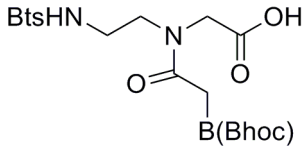

To a stirred solution of 5.48 (1.0 eq.), nucleobase acetic acid (1.0 eq.), HOBT (1.2 eq.) and DCC (1.2 eq.) in DMF was added DIEA (1.5 eq.) at room temperature. The reaction mixture was stirred overnight and concentrated to leave crude residue. The residue was dissolved in DCM and the precipitates were filtered. The filtrate was washed with 1M cold HCl solution, sat. $NaHCO_3$ solution and brine. The residue was then triturated with ethyl alcohol to give protected ester (**5.49-5.52**). The protected esters were suspended in THF:H_2O (1:1) mixture, solution of lithium hydroxide (2 eq.) in water was then added and the reaction mixture was stirred at room temperature for one hour. After completion of the reaction, the reaction contents were acidified to pH ~ 2-3 by dropwise addition of 1M HCl at 0^oC. The resulting solution was extracted with ethyl acetate, dried, filtered, and concentrated to dryness in vacuo to afford compounds **5.53-5.56** in 80-90% yield.

General procedure for synthesizing cyclic Bts protected PNA monomers

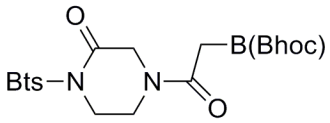

To a mixture of Bts protected PNA monomers (**5.53-5.56**) (1.0 eq.) in DMF was added EDCI (1.2 eq.) and stirred for 6 hours at room temperature. After completion of the reaction, solvent was removed by evaporation and residue was dissolved in DCM. The solution was washed with cold 1M HCl and water. The organic contents were dried,

filtered, concentrated and purified by flash chromatography to give cyclized Bts protected PNA monomers in 85-90% yield.

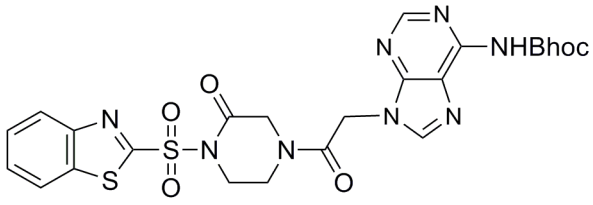

1-(Benzothiazole-2-sulfonyl)-4-{[6-N-(benzhydryloxycarbonyl)-adenine-9-yl]-acetyl}-piperazin-2-one) (5.57)

Yield: 87%, white solid. ^{1}H NMR (250 MHz, DMSO) δ 10.91 (s, 1H), 8.60 (d, *J* = 4.3 Hz, 1H), 8.33 (ddd, *J* = 13.4, 7.5, 2.2 Hz, 3H), 7.74 (dd, *J* = 6.4, 2.5 Hz, 2H), 7.54 (d, *J* = 7.1 Hz, 4H), 7.39 (t, *J* = 9.9, 4.6 Hz, 4H), 7.33 – 7.26 (m, 2H), 6.83 (s, 1H), 5.41 (s, 1H), 5.30 (s, 1H), 4.59 (s, 1H), 4.30 (s, 2H), 4.11 (s, 2H), 3.89 (s, 1H). m/z 683.147 $(M+H)^{+}$

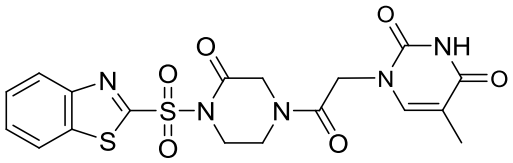

1-(Benzothiazole-2-sulfonyl)-4-[(thymin-1-yl)-acetyl]-piperazin-2-one (5.60)

Yield: 92%, white solid. ^{1}H NMR (400 MHz, DMSO) δ 11.27 (d, *J* = 7.2 Hz, 1H), 8.32 (d, *J* = 4.8 Hz, 1H), 8.24 (s, 1H), 7.72 – 7.67 (m, 2H), 7.31 (s, 1H), 7.24 (s, 1H), 4.65 (s, 1H), 4.55 (s, 1H), 4.39 (s, 1H), 4.25 (s, 1H), 4.18 (s, 1H), 4.04 (s, 1H), 3.96 – 3.90 (m, 1H), 3.86 – 3.80 (m, 1H), 1.71 (s, 3H). ^{13}C NMR (101 MHz, DMSO) δ 167.03, 166.45, 166.31, 165.03, 164.44, 151.87, 151.73, 142.66, 142.58, 137.24, 129.10, 128.68, 125.64, 124.07, 108.89, 60.42, 49.47, 48.80, 48.62, 47.70, 46.84, 46.68, 42.40, 12.58. LCMS (ESI) m/z 464.07 (MH^{+})

5.4 General Procedure for PNA synthesis using Fmoc/Cbz protecting group strategy

PNA oligomer synthesis was carried out on Protein Technologies Instrument PTI Symphony synthesizer. MBHA resin was first swollen manually in NMP for 45 minutes and downloaded with Fmoc-Lys(Boc)-OH to a substitution level of ~0.15mmol/g. Fmoc deprotection was then carried out using 20% piperidine/2%DBU in NMP and the resin is washed with NMP (5x), DCM (5x). Coupling was carried out using 5 equivalents of Fmoc protected PNA monomers, 5 equivalents HCTU and 10 eq. NMM in NMP. After coupling the resin was washed again with NMP (5x), DCM (5x). This cycle was repeated for each base coupled. After the last coupling the Fmoc group was deprotected and PNA oligomer was cleaved off from the resin using following procedure: The resin was swelled in TFA once. Two solutions were prepared:

Solution 1	**Solution 2**
TFA/dimethylsulphide/m-cresol (1:3:1)	TFA/TFMSA (9:1)

1 mL of each solution was added to resin first and swirled for one hour. Here the protecting groups on the immobilized oligomer are removed first. Then 1 mL of a third solution TFMSA/TFA/m-cresol (2:8:1) was added to the reaction vessel and swirled for another 1.5 hrs. The black solution was poured out in ether (6-7 mL). The white solid was precipitated out by centrifugation and the precipitate was washed with ether. The ether was decanted and precipitates were freeze-dried. Different PNA oligomers synthesized using various orthogonal protecting group strategies are listed in Table 5.1.

Table 5.1 PNA sequences synthesized on PTI synthesizer using different protecting group strategies.

Sequence	Protecting Group	Expected	Observed
LysTTCCC	Fmoc/Cbz	1181.177	1180.736
Lys-TTCTTCCTTCTTC-NH_2	Fmoc/Cbz	3532.132	3532.902
Lys-TTCTTCCTTCTTC-NH_2	Preactivated OPf esters	3532.132	3532.071
CO_2HCTTTTCTACATTLysNH_2	Bts/Bhoc	3312.3477	3312.0891
GlyTTCC	Fmoc/Cbz (CPNA)	1364.5131	1364.5138

5.5 References

1. Ge, R.; Heinonen, J.E.; Svahn, M.J.; Smith, C.I. *The Faseb Journal*, **2007**, 21, 1902.

2. Nielsen, P.E.: *Peptide Nucleic Acids: Protocols and Applications* Horizon Scientific Press. Norfolk, **2004**.

3. Nielsen, P.E.; Egholm, M.; Buchardt, O. *Bioconjugate Chem.*, **1994**, 5, 3-7.

4. Nielsen, P.E. *Letters in Peptide Science*, **2003**, 10, 135-147

5. Ganesh, K.N.; Nielsen, P.E. *Current Organic Chemistry*, **2000**, 4, 931-943.

6. Shakeel, S.; Karim, S.; Arif, A. *J. Chem technol biotechnol.*, **2006**, 81, 892-899.

7. Andrasi, A.D.; Rapireddy, S.; Bhattacharya, B.; Nielsen, J.H.; Zon, G.; Ly, D.H. *J. Am. Chem. Soc.*, **2006**, 128, 16104-16112.

8. Nielsen, P.E. *Acc. Chem. Res.*, **1999**, 32, 624-630.

9. Koning, M.C.; Marel, G.A.; Overhand, M. *Current Opinion in Chemical Biology*, **2003**, 7, 734-740.

10. Li, X.; Zhang, L.; Lu, J.; Chen, Y.; Zhang, Li. *Bioconjugate Chemistry*, **2003**, 14, 153-157.

11. Wang, G.; Xu, X.S. *Cell Research*, **2004**, 14, 111-116.

12. Zhou, P.; Andrasi, A.D.; Bhattacharya, B.; Nielsen, J.H.; Ly, D.H. *Bioorganic & Medicinal Chemistry Letters*, **2006**, 16, 4931-4935.

13. Andrasi, A.D.; Rapireddy, S.; Bhattacharya, B.; Nielsen, J.H.; Zon, G.; Ly, D.H. *J. Am. Chem. Soc.*, **2003**, 125, 6878-6879.

14. Dose, C.; Seitz, O. *Organic Letters*, **2005**, 7, 4365-4368.

15. Kofoed, T.; Hansen, H.F.; Orum, H.; Koch, T. *J. Peptide Sci.*, **2001**, 7, 402-412.

16. Thomson, S.A.; Josey, J.A.; Cadilla, R.; Gaul, M.D.; Hassman, C.F.; Luzzio, M.J.; Pipe, A.J.; Reed, K.L.; Ricca, D.J.; Wiethe, R.W.; Noble, S.A. *Tetrahedron*, **1995**, 51, 6179-6194.

17. Hyrup, B.; Nielsen, P.E. *Bioorganic & Medicinal Chemistry*, **1996**, 4, 5-23.

18. Lee, H.; Jeon, J.H.; Lim, J.C.; Choi, H.; Yoon, Y.; Kim, S.K. *Organic Letters*, **2007**, 9(17), 3291-3293.

19. Vedejs, E.; Lin, S.; Klapars, A.; Wang, J. *J. Am. Chem. Soc.*, 1996, 118, 9796.

20. Will, D.W.; Breipohl, G.; Langner, D.; Knolle, J.; Uhlmann, E. *Tetrahedron*, **1995**, 51, 12069.

21. Debaene, F.; Winssinger, N. *Organic Letters*, **2003**, 5(23), 4445.

APPENDICES

APPENDIX A: Selected ^{1}H and ^{13}C NMR Spectra

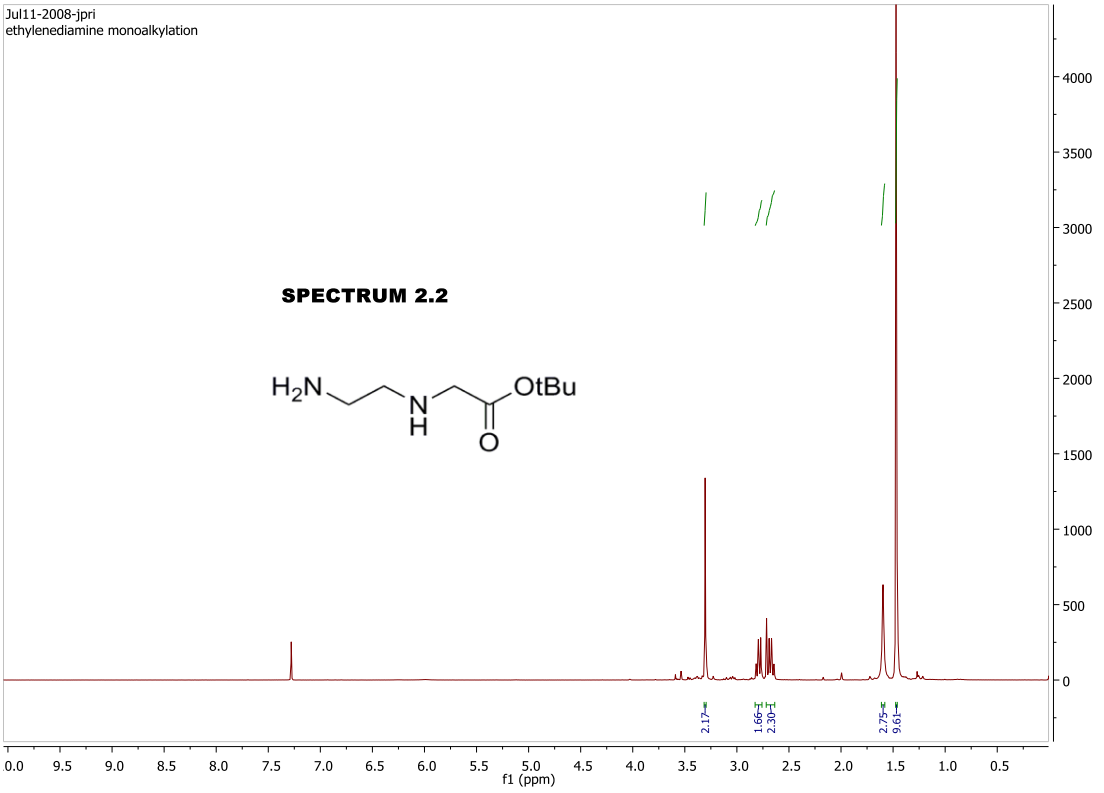

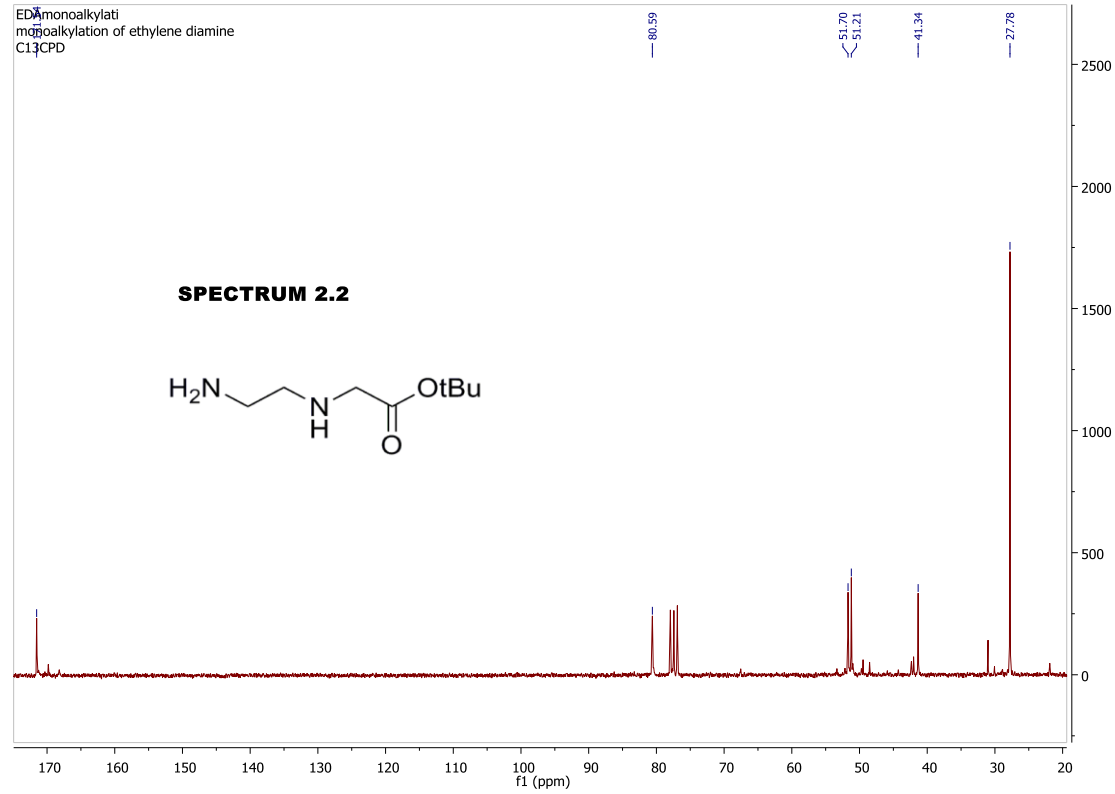

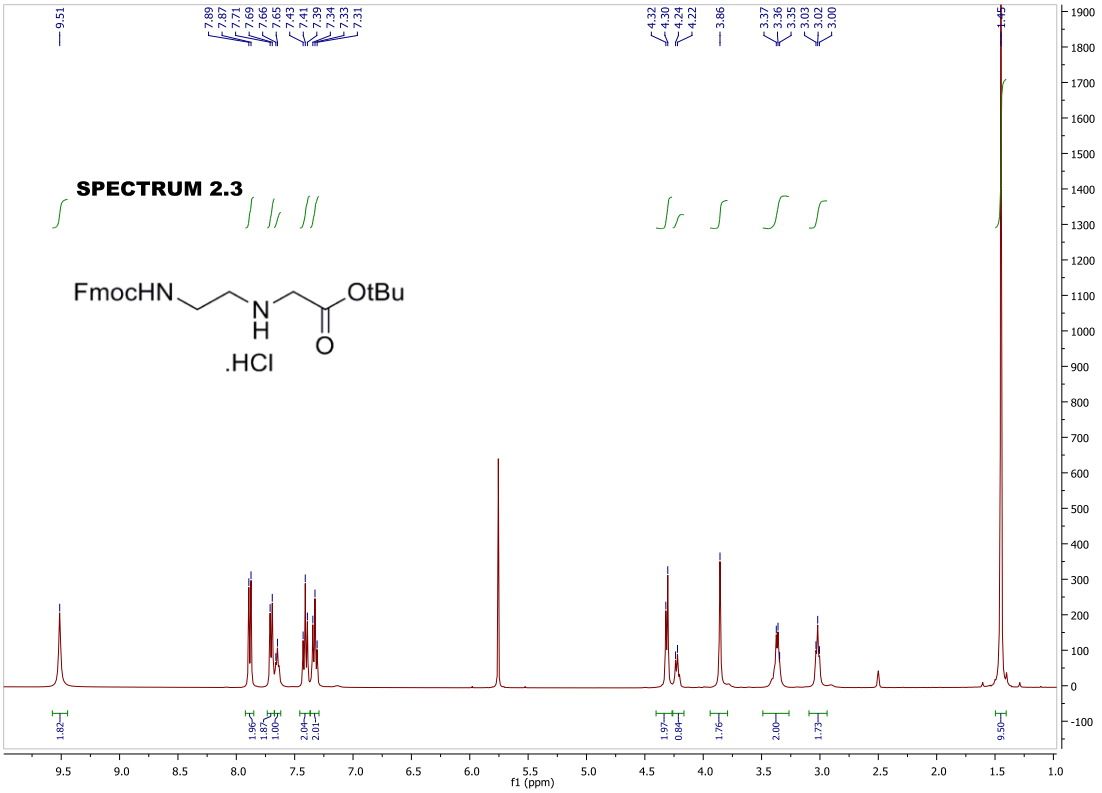
SPECTRUM 2.3
FmocHN
N
H
OtBu
O
.HCl
f1 (ppm)

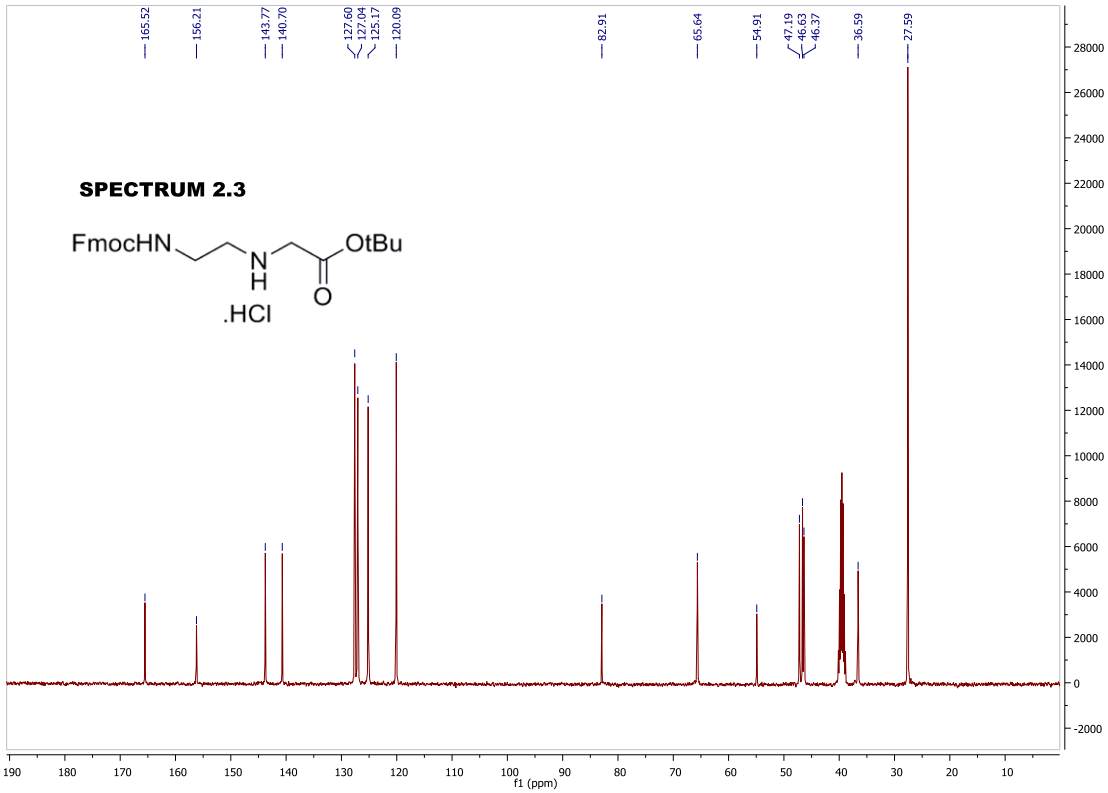
SPECTRUM 2.3
FmocHN
N
H
OtBu
O
.HCl
f1 (ppm)

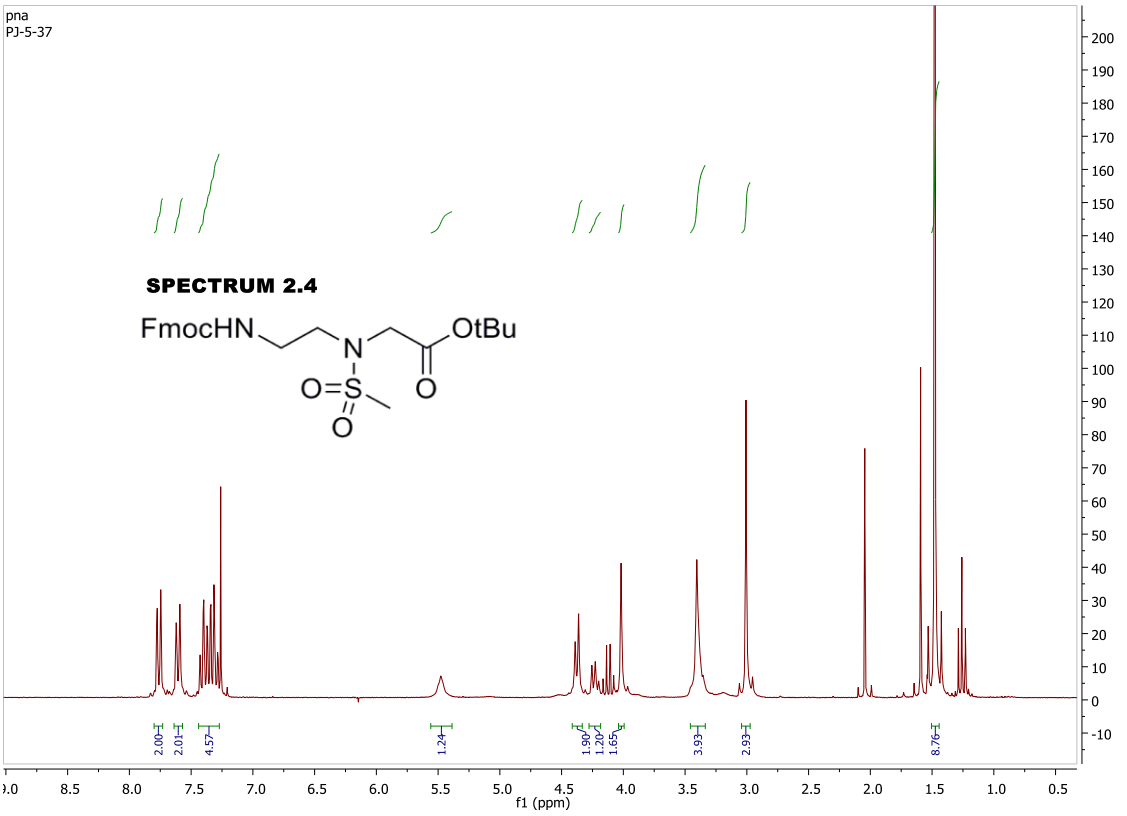
pna
PJ-5-37
SPECTRUM 2.4
FmocHN
OtBu
f1 (ppm)

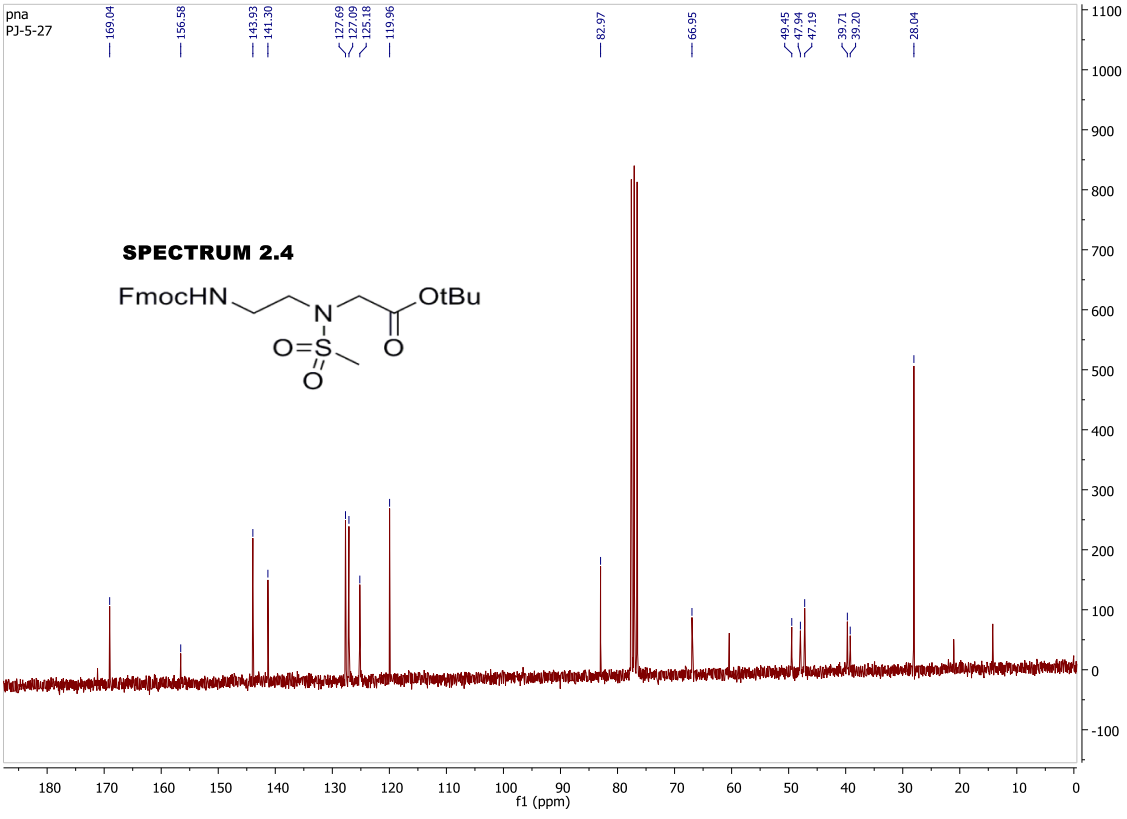
pna
PJ-5-27
SPECTRUM 2.4
FmocHN
OtBu
f1 (ppm)

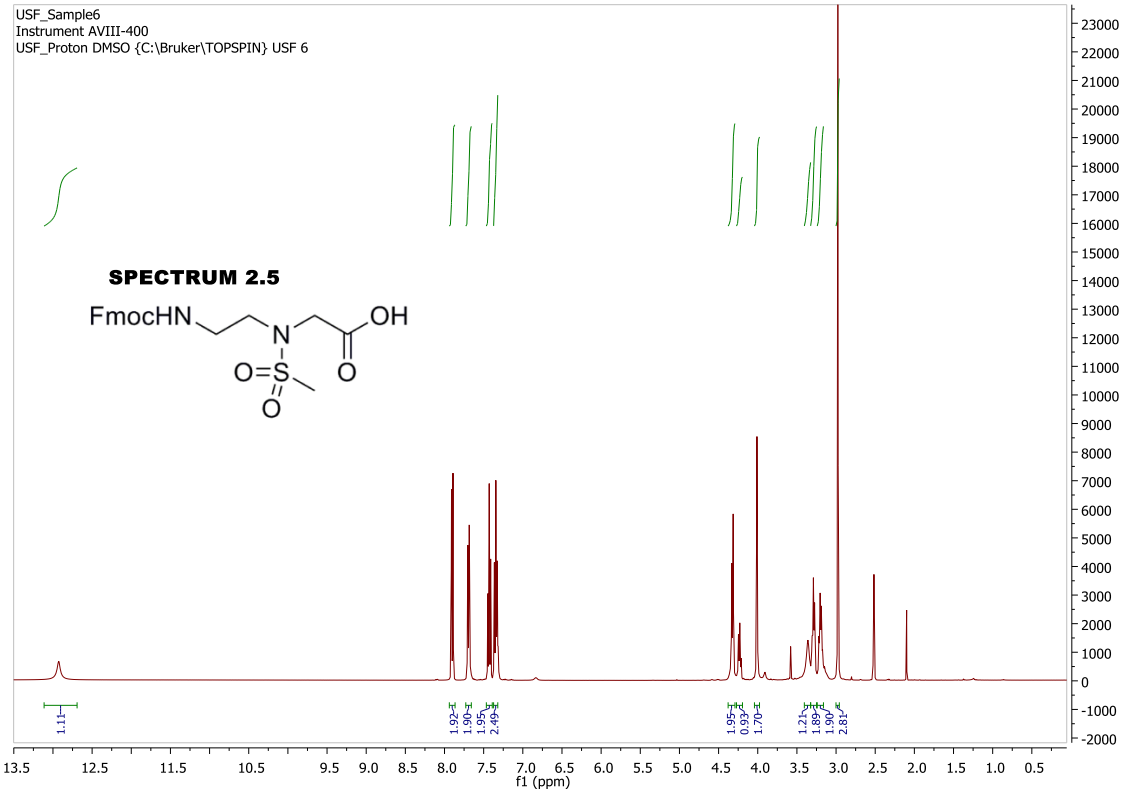
USF_Sample6
Instrument AVIII-400
USF_Proton DMSO {C:\Bruker\TOPSPIN} USF 6
SPECTRUM 2.5
FmocHN
N
OH
O=S
O
O
f1 (ppm)

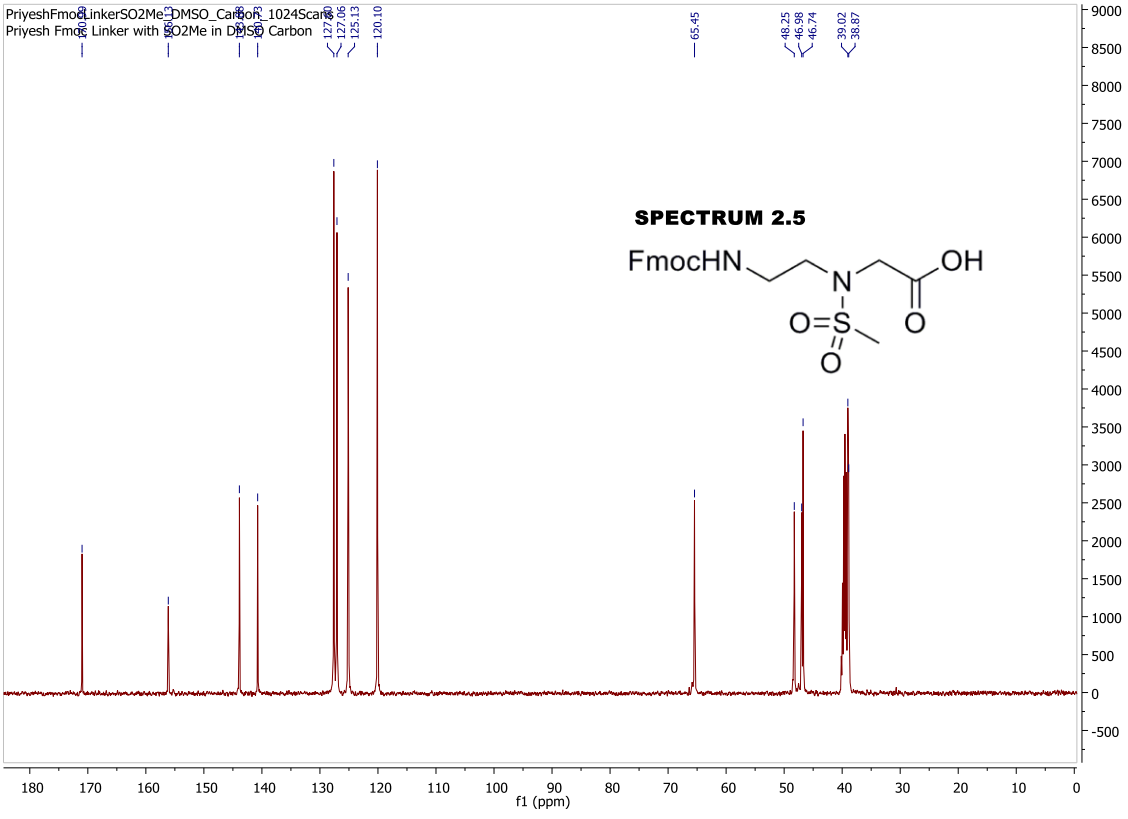
PriyeshFmocLinkerSO2Me_DMSO_Carbon_1024Scans
Priyesh Fmoc Linker with SO2Me in DMSO Carbon
SPECTRUM 2.5
FmocHN
N
OH
O=S
O
O
f1 (ppm)

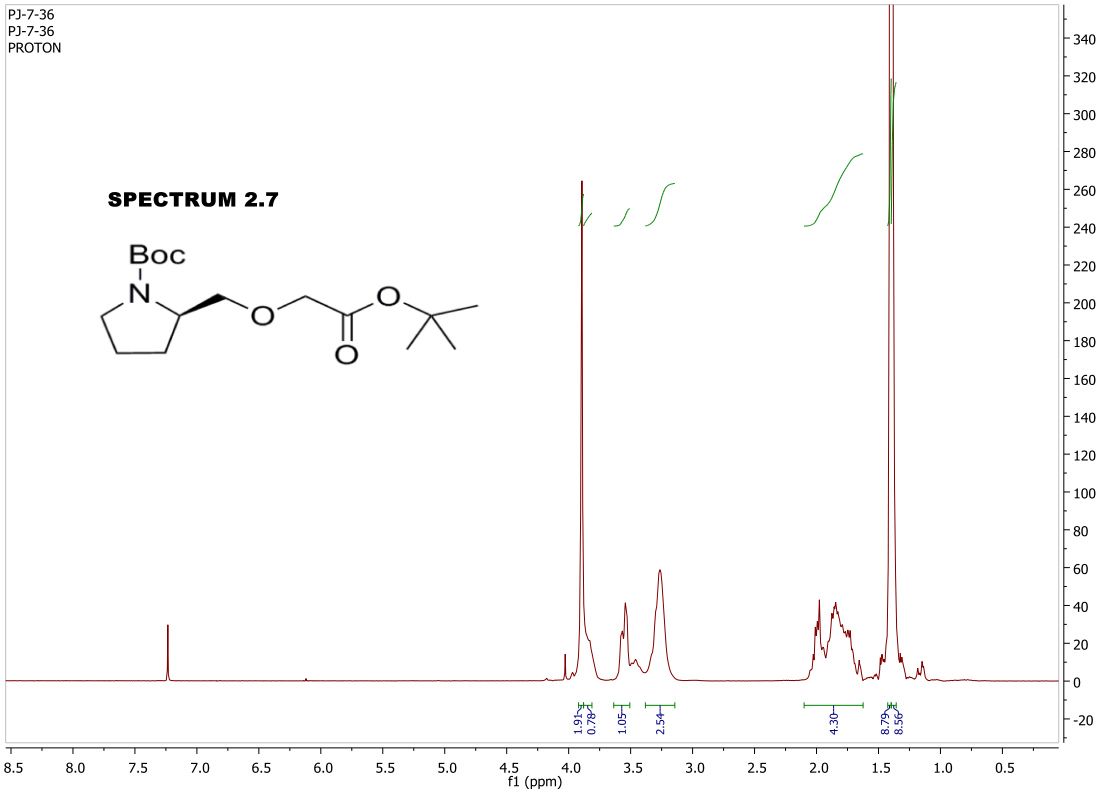
PJ-7-36
PJ-7-36
PROTON
SPECTRUM 2.7
Boc
N
O
O
O
1.91
0.78
1.05
2.54
4.30
8.79
8.56
f1 (ppm)

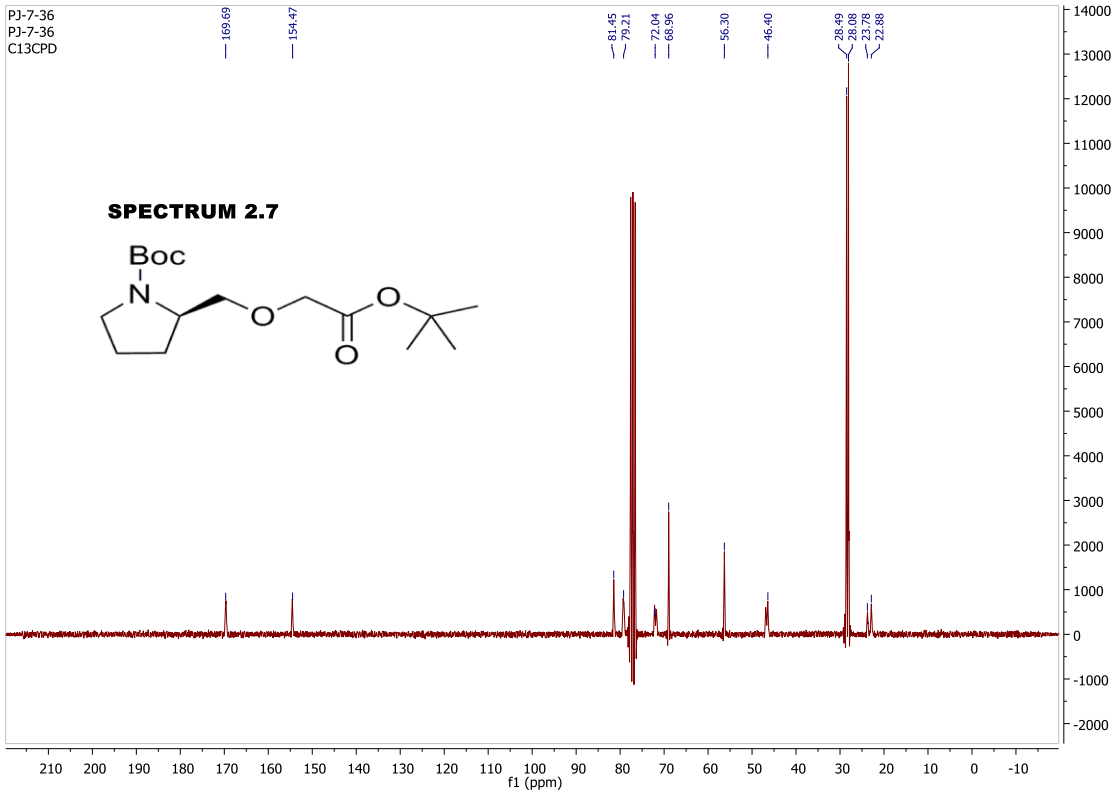
PJ-7-36
PJ-7-36
C13CPD
169.69
154.47
81.45
79.21
72.04
68.96
56.30
46.40
28.49
28.08
23.78
22.88
SPECTRUM 2.7
Boc
N
O
O
O
f1 (ppm)

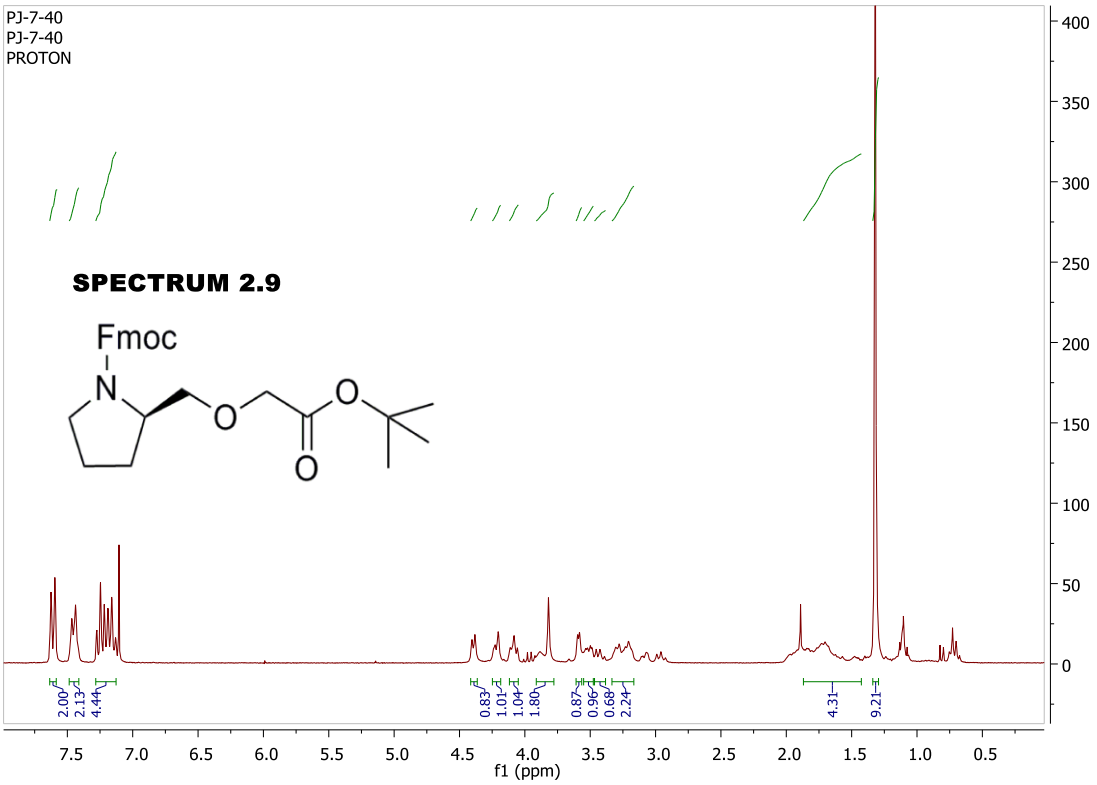
PJ-7-40
PJ-7-40
PROTON
SPECTRUM 2.9
Fmoc
N
O
O
O
2.00
2.13
4.44
0.83
1.01
1.04
1.80
0.87
0.96
0.68
2.24
4.31
9.21
7.5
7.0
6.5
6.0
5.5
5.0
4.5
4.0
3.5
3.0
2.5
2.0
1.5
1.0
0.5
f1 (ppm)
400
350
300
250
200
150
100
50
0

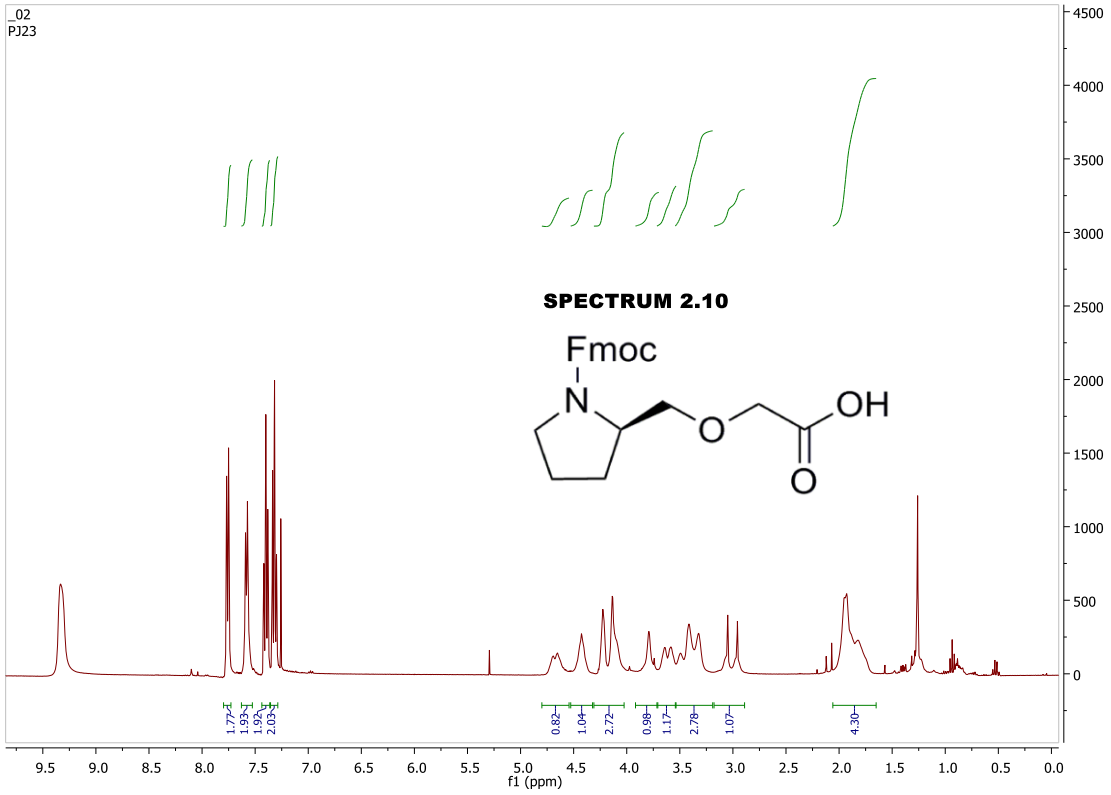
_02
PJ23
SPECTRUM 2.10
Fmoc
N
O
OH
O
1.77
1.93
1.92
2.03
0.82
1.04
2.72
0.98
1.17
2.78
1.07
4.30
f1 (ppm)

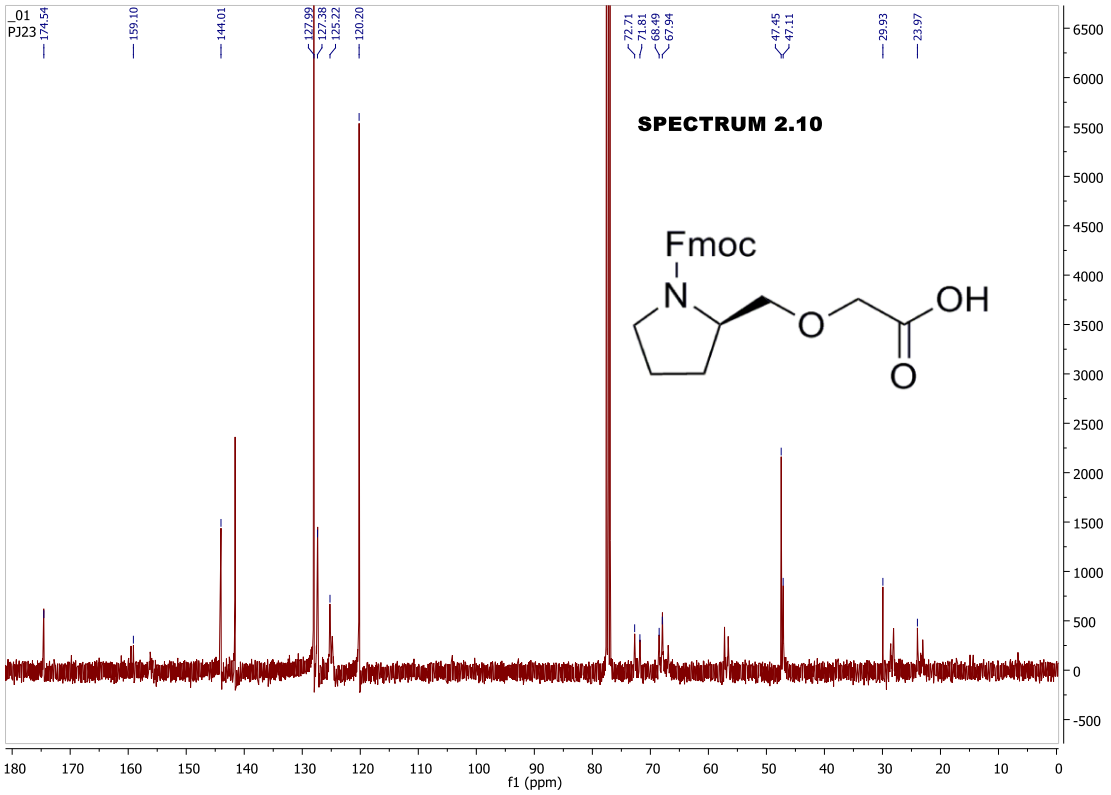
_01
PJ23
174.54
159.10
144.01
127.99
127.38
125.22
120.20
72.71
71.81
68.49
67.94
47.45
47.11
29.93
23.97
SPECTRUM 2.10
Fmoc
N
O
OH
O
f1 (ppm)

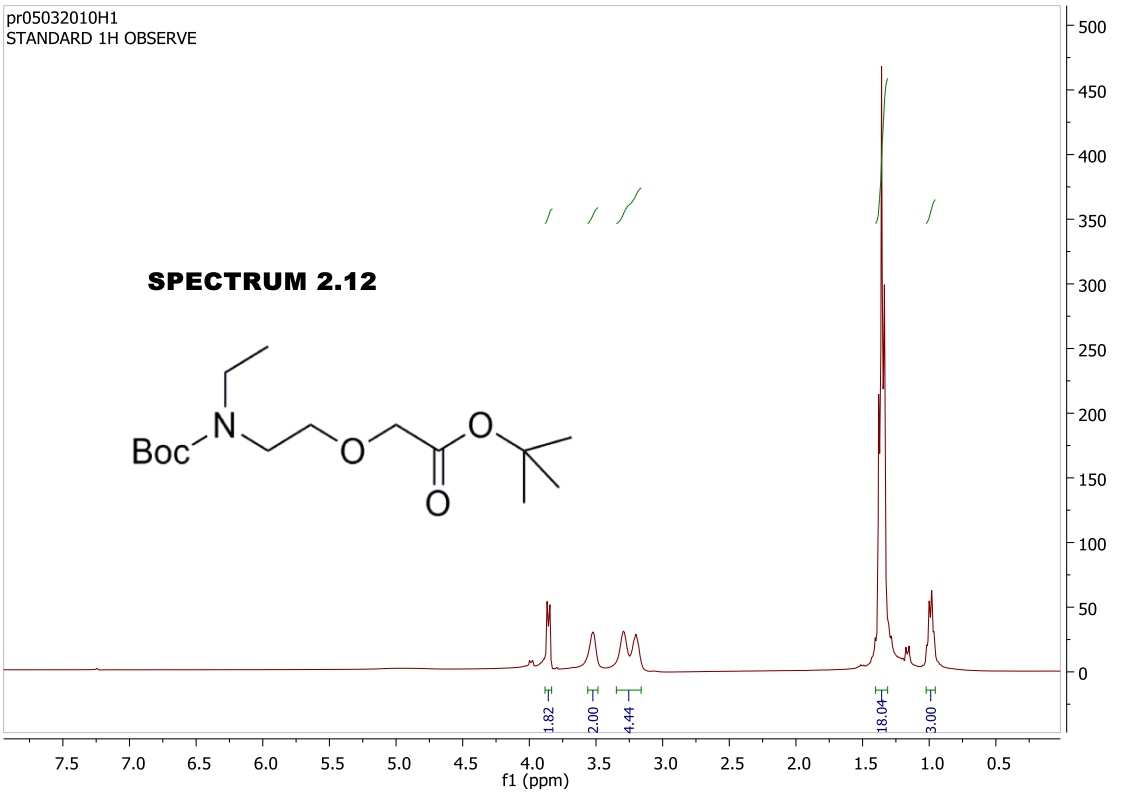
pr05032010H1
STANDARD 1H OBSERVE
SPECTRUM 2.12
Boc
N
O
O
O
1.82
2.00
4.44
18.04
3.00
f1 (ppm)

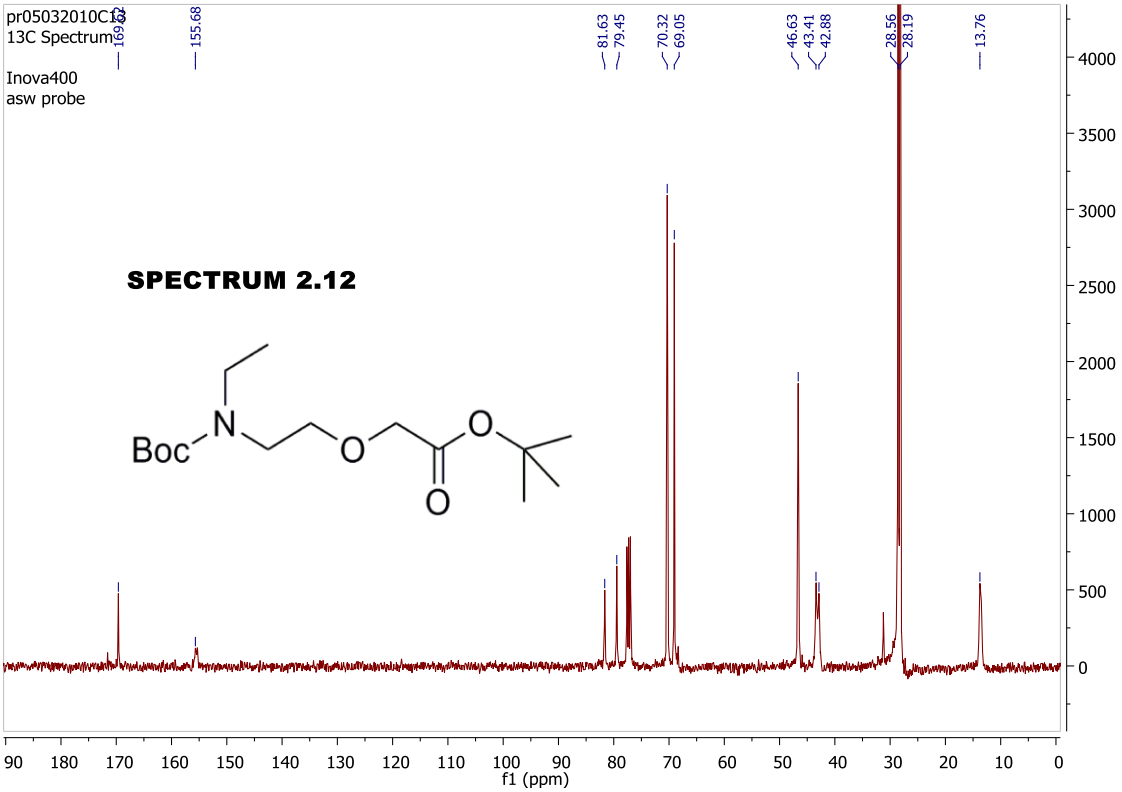
pr05032010C13
13C Spectrum
Inova400
asw probe
169.42
155.68
81.63
79.45
70.32
69.05
46.63
43.41
42.88
28.56
28.19
13.76
SPECTRUM 2.12
Boc
N
O
O
O
f1 (ppm)

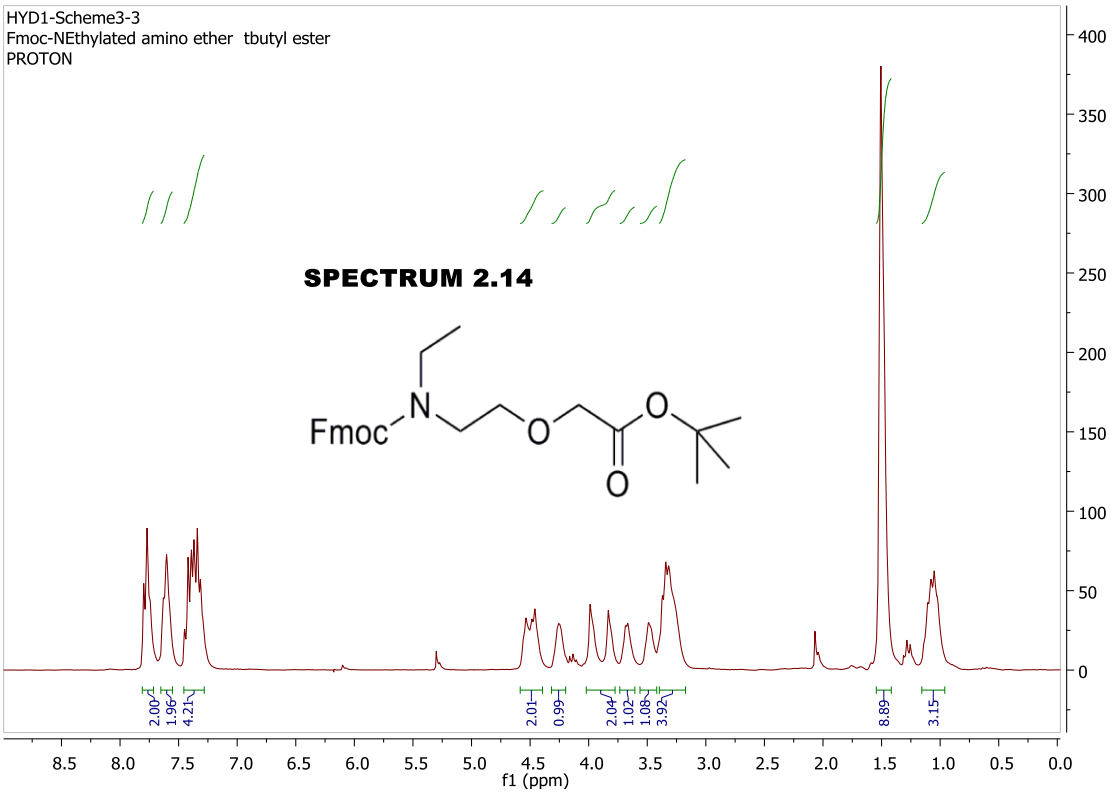
HYD1-Scheme3-3
Fmoc-NEthylated amino ether tbutyl ester
PROTON
SPECTRUM 2.14
Fmoc
N
O
O
O
2.00
1.96
4.21
2.01
0.99
2.04
1.02
1.08
3.92
8.89
3.15
f1 (ppm)

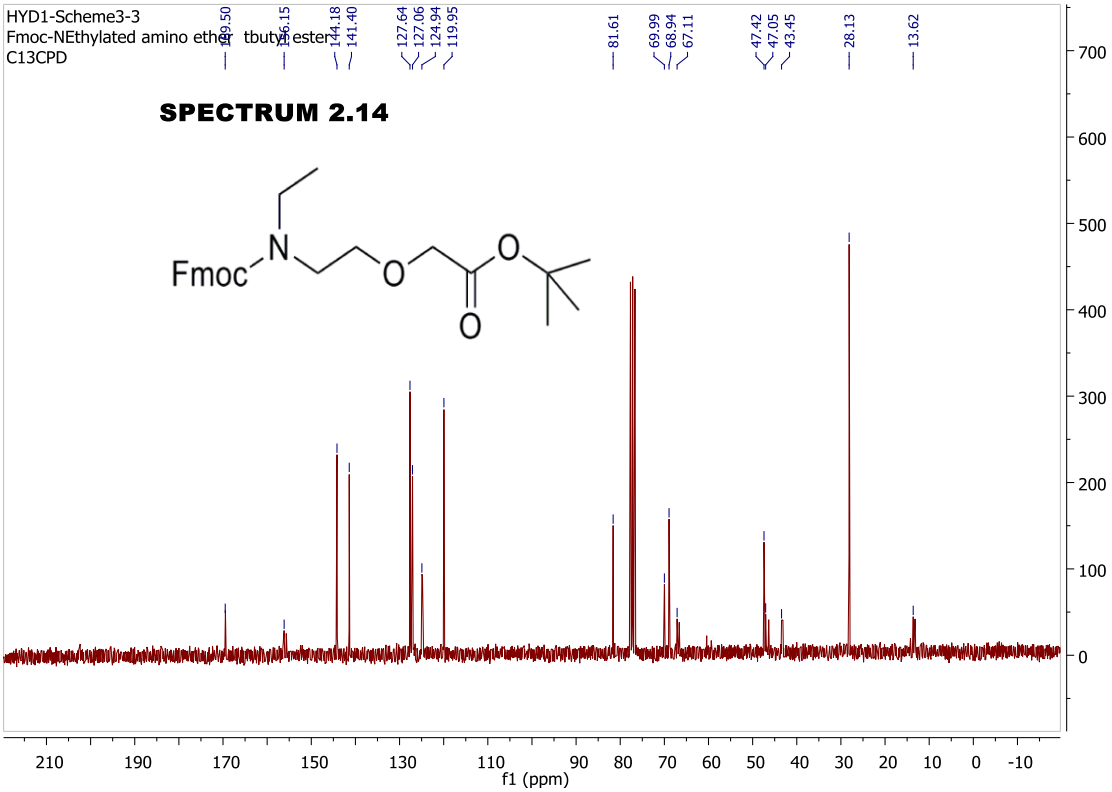
HYD1-Scheme3-3
Fmoc-NEthylated amino ether tbutyl ester
C13CPD
SPECTRUM 2.14
Fmoc
N
O
O
O
f1 (ppm)

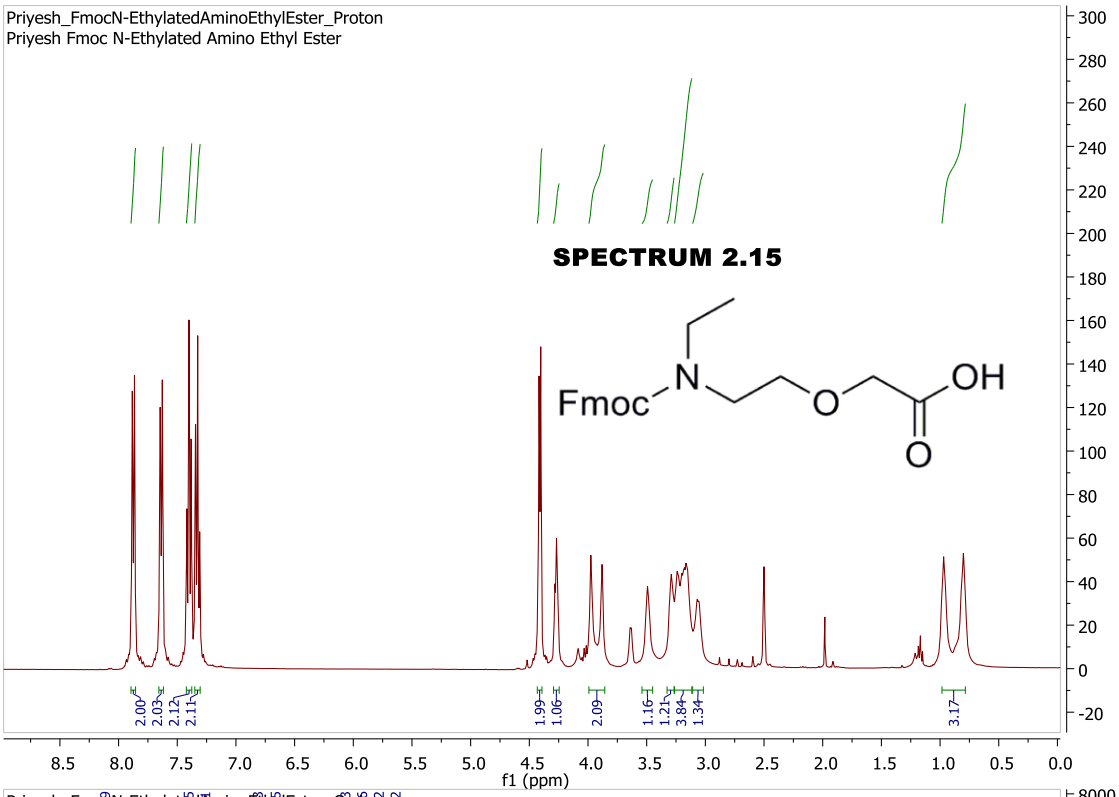
Priyesh_FmocN-EthylatedAminoEthylEster_Proton
Priyesh Fmoc N-Ethylated Amino Ethyl Ester
SPECTRUM 2.15
Fmoc
N
O
OH
O
f1 (ppm)

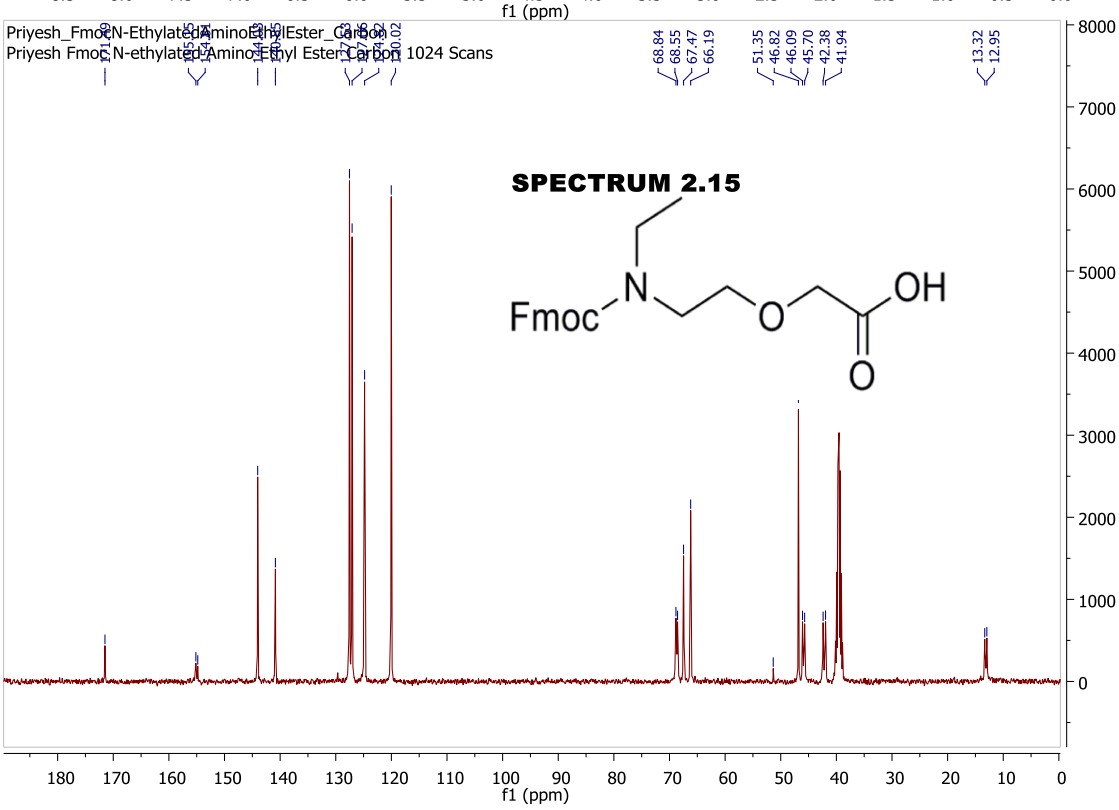
Priyesh_FmocN-EthylatedAminoEthylEster_Carbon
Priyesh Fmoc N-ethylated Amino Ethyl Ester Carbon 1024 Scans
68.84
68.55
67.47
66.19
51.35
46.82
46.09
45.70
42.38
41.94
13.32
12.95
SPECTRUM 2.15
Fmoc
N
O
OH
O
f1 (ppm)

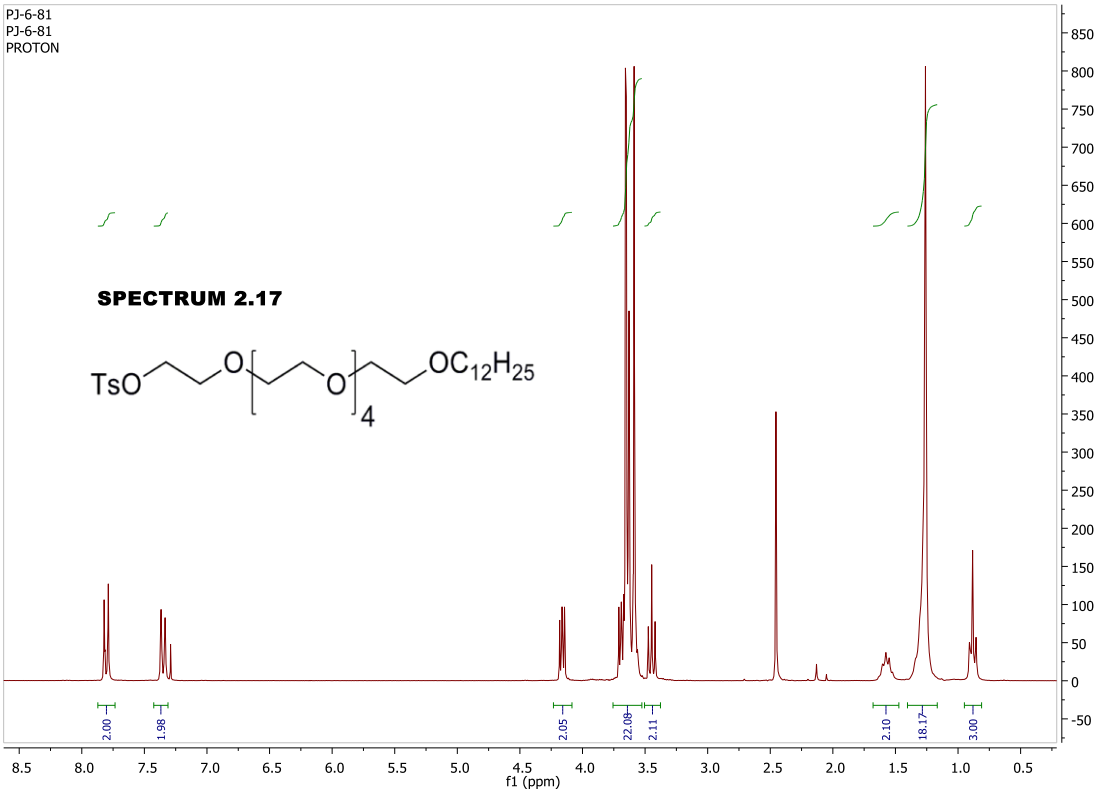
PJ-6-81
PJ-6-81
PROTON
SPECTRUM 2.17
TsO
O
O
4
OC12H25
2.00
1.98
2.05
22.09
2.11
2.10
18.17
3.00
f1 (ppm)

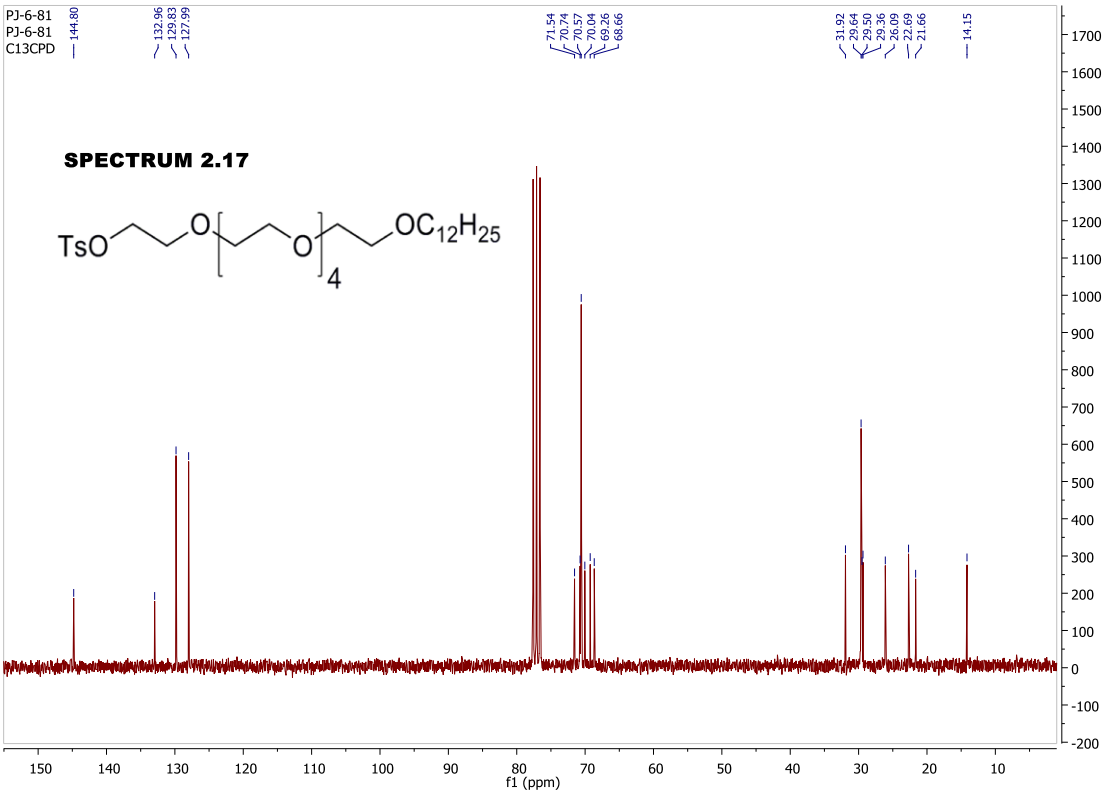
PJ-6-81
PJ-6-81
C13CPD
144.80
132.96
129.83
127.99
71.54
70.74
70.57
70.04
69.26
68.66
31.92
29.64
29.50
29.36
26.09
22.69
21.66
14.15
SPECTRUM 2.17
TsO
O
O
4
OC12H25
f1 (ppm)

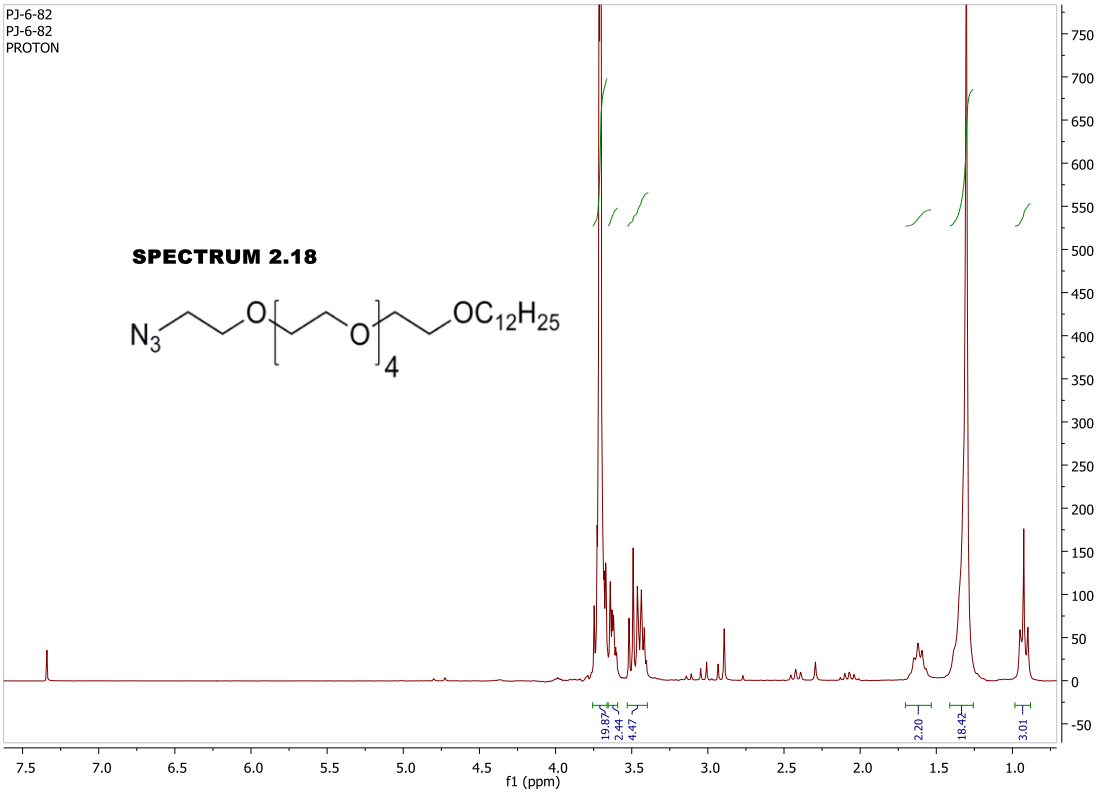
PJ-6-82
PJ-6-82
PROTON
SPECTRUM 2.18
N3
O
O
4
OC12H25
19.87
2.44
4.47
2.20
18.42
3.01
f1 (ppm)

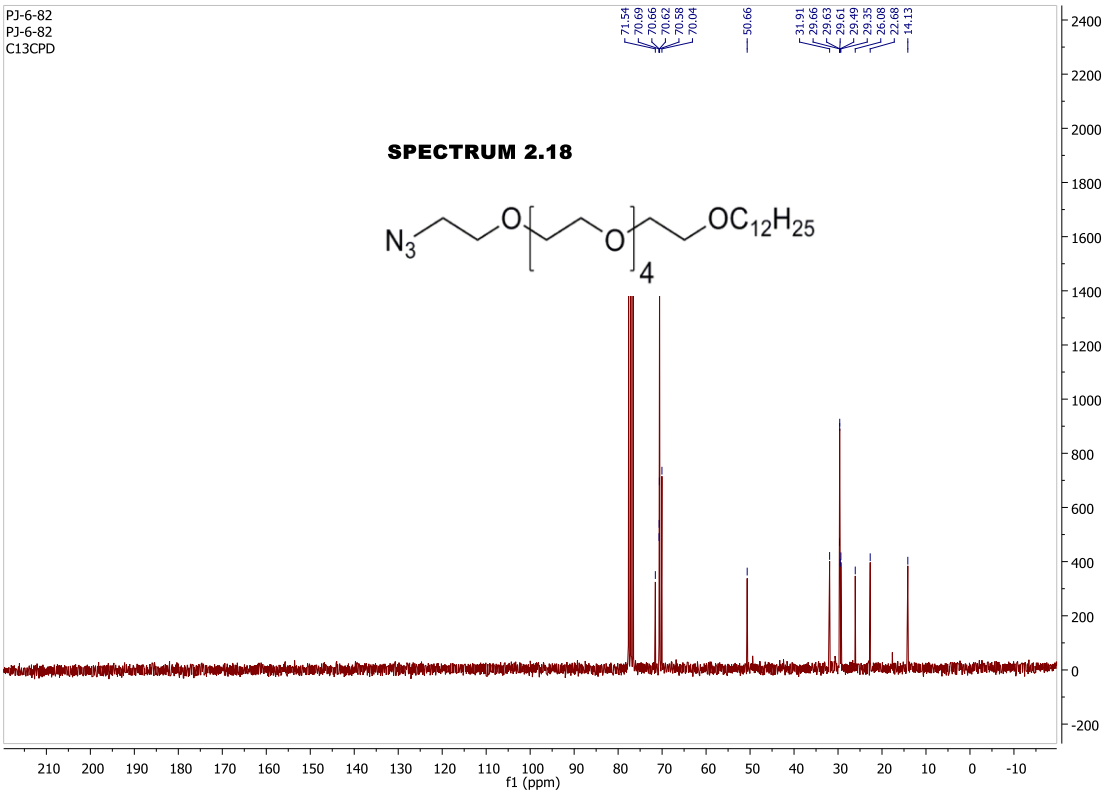
PJ-6-82
PJ-6-82
C13CPD
71.54
70.69
70.66
70.62
70.58
70.04
50.66
31.91
29.66
29.63
29.61
29.49
29.35
25.68
22.68
14.13
SPECTRUM 2.18
N3
O
O
4
OC12H25
f1 (ppm)

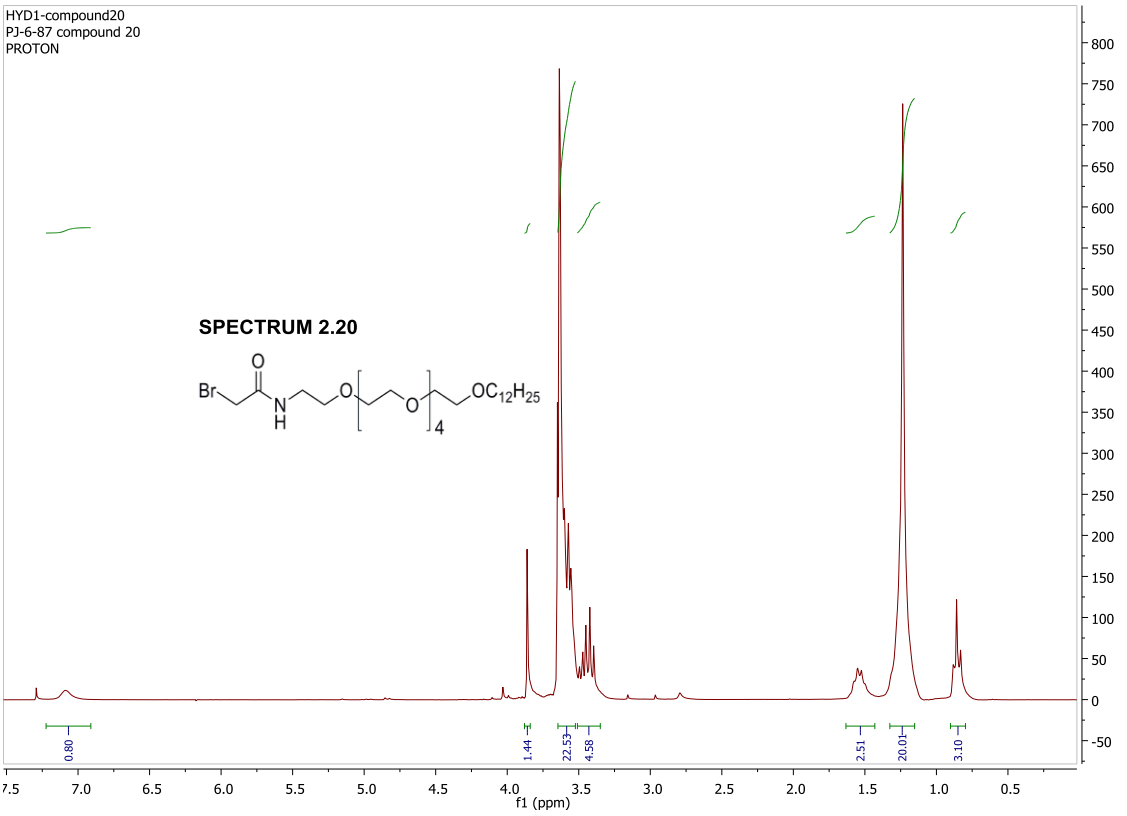
HYD1-compound20
PJ-6-87 compound 20
PROTON
SPECTRUM 2.20
Br
O
N
H
O
O
4
OC12H25
0.80
1.44
22.53
4.58
2.51
20.01
3.10
f1 (ppm)

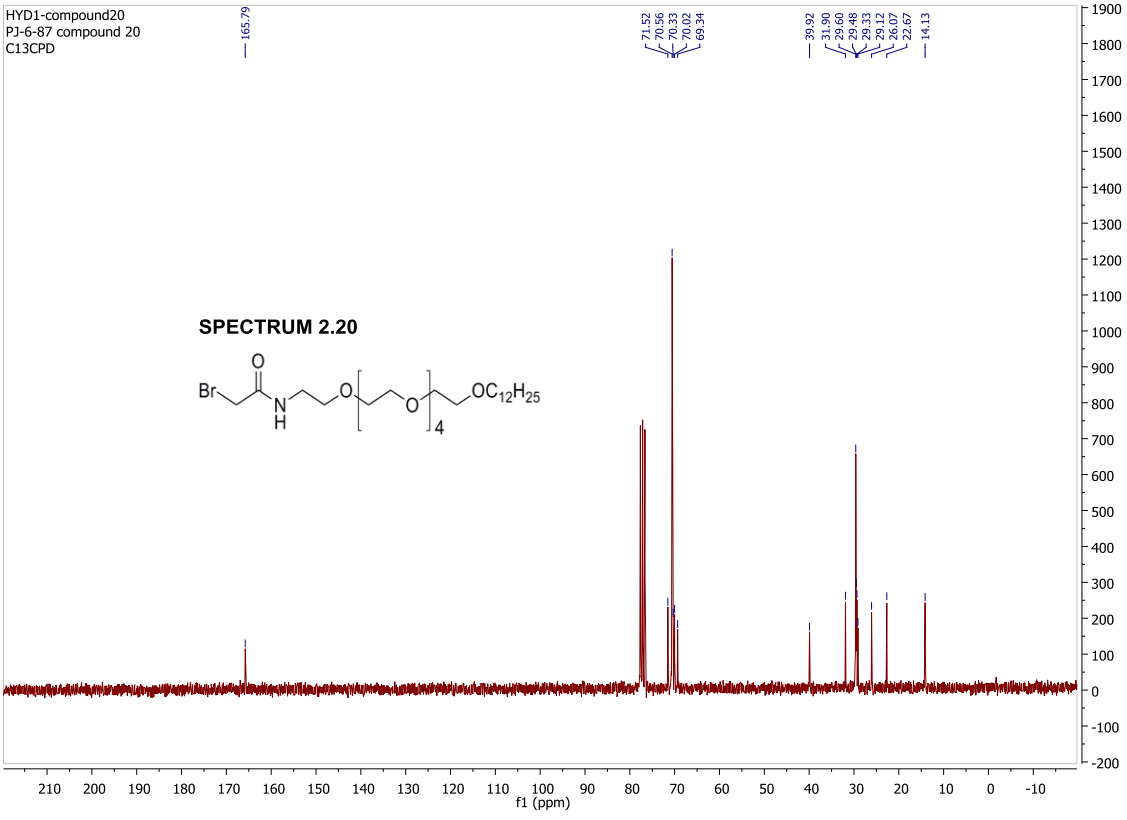
HYD1-compound20
PJ-6-87 compound 20
C13CPD
165.79
71.52
70.56
70.33
70.02
69.34
39.92
31.90
29.60
29.48
29.33
29.12
26.07
22.67
14.13
SPECTRUM 2.20
Br
O
N
H
O
O
4
OC12H25
f1 (ppm)

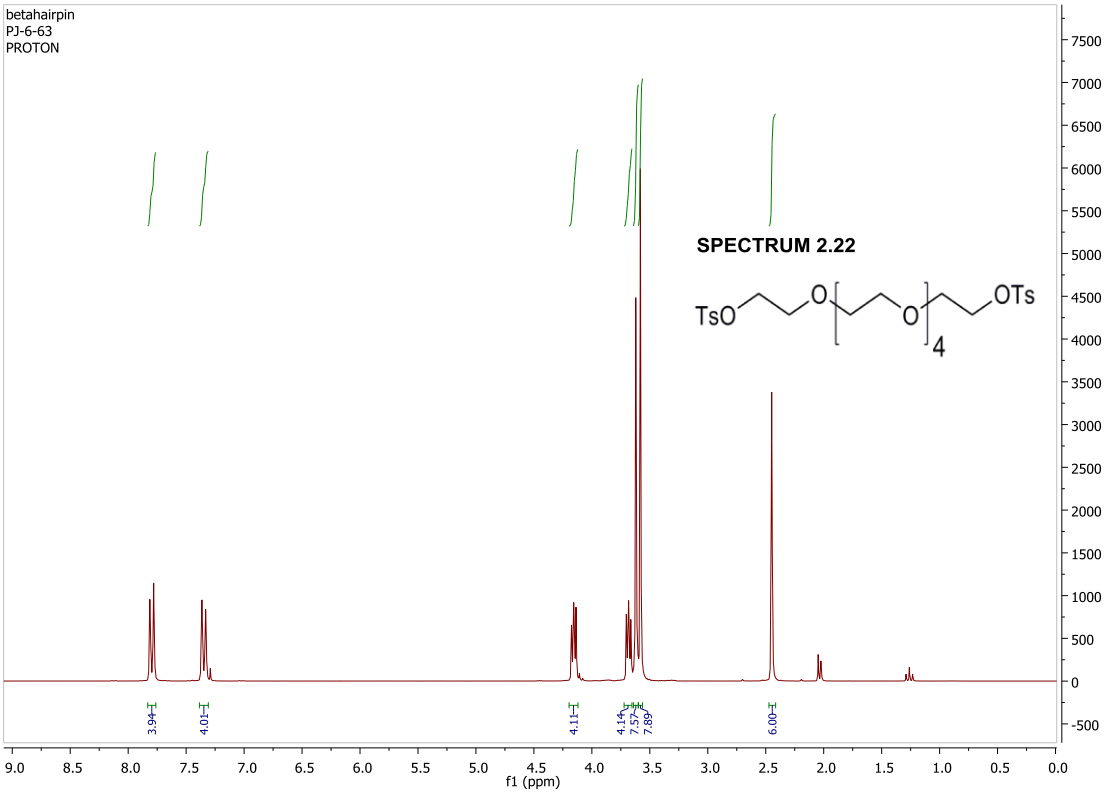
betahairpin
PJ-6-63
PROTON
SPECTRUM 2.22
TsO
O
O
4
OTs
3.94
4.01
4.11
4.14
7.57
7.89
6.00
f1 (ppm)

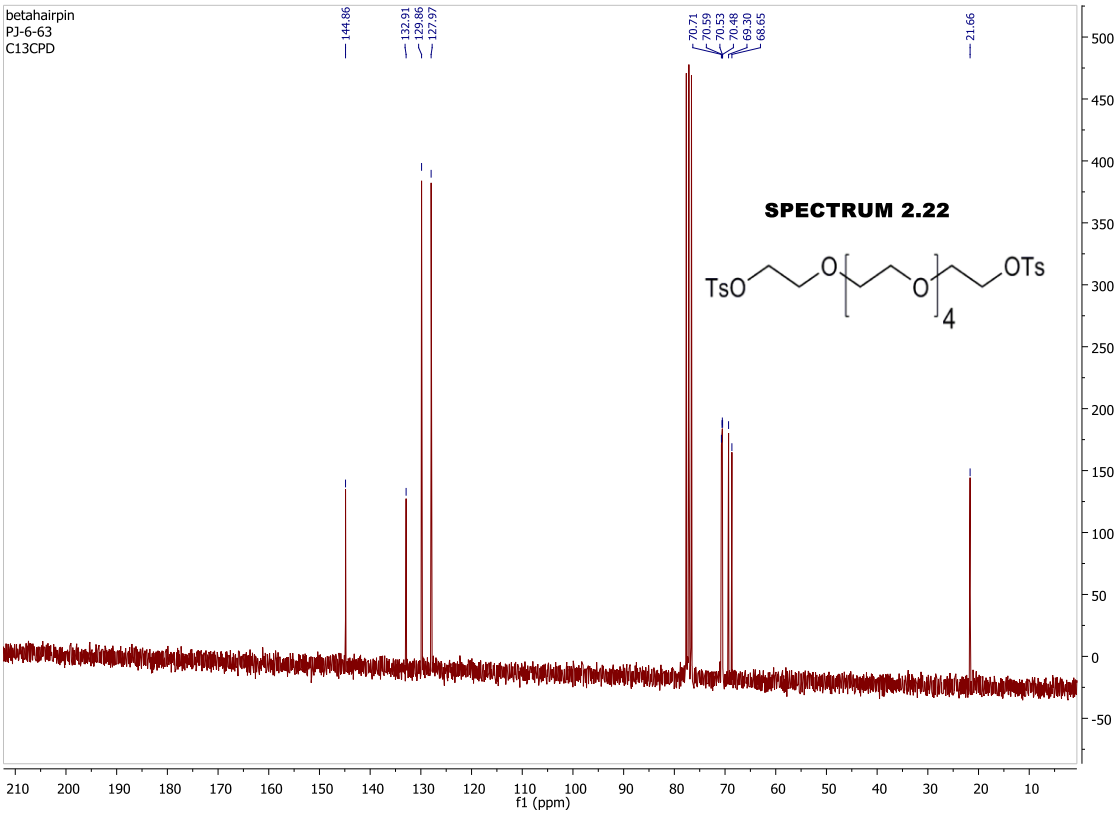
betahairpin
PJ-6-63
C13CPD
144.86
132.91
129.86
127.97
70.71
70.59
70.53
70.48
69.30
68.65
21.66
SPECTRUM 2.22
TsO
O
O
4
OTs
f1 (ppm)

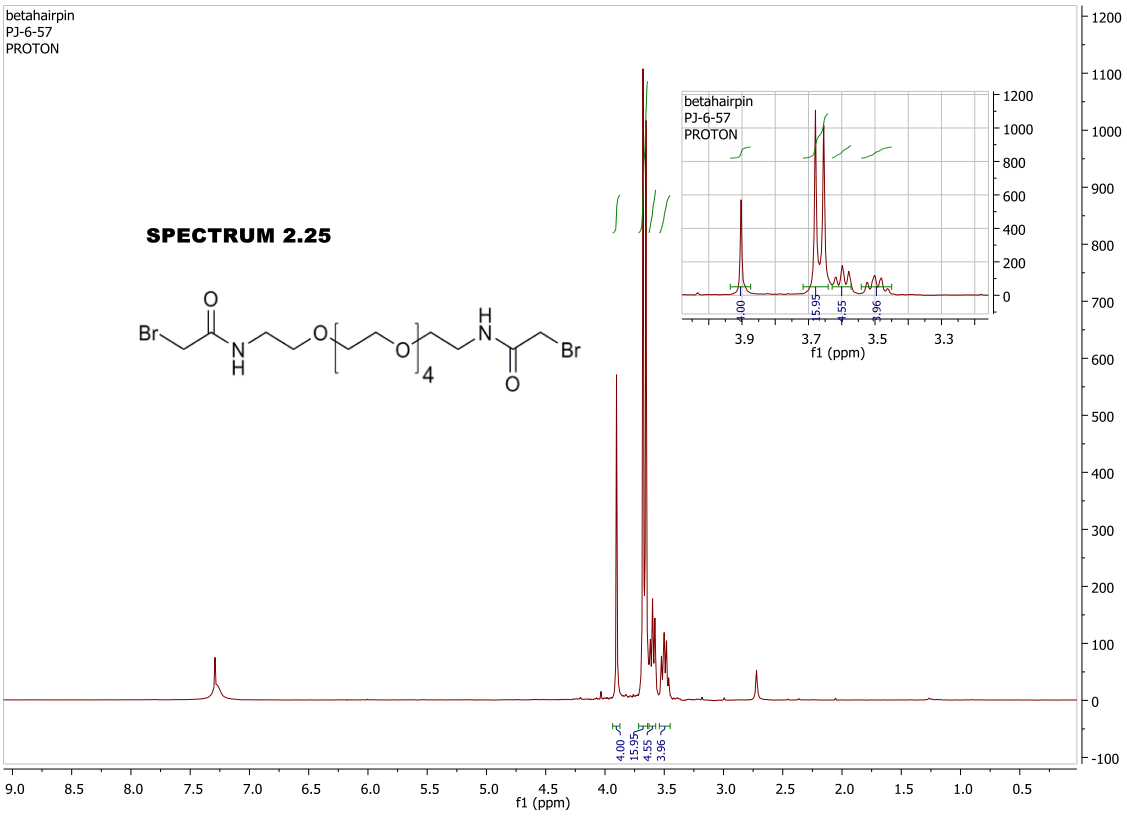
betahairpin
PJ-6-57
PROTON
SPECTRUM 2.25
Br
O
N
H
O
O
4
H
N
O
Br
4.00
15.95
4.55
3.96
f1 (ppm)

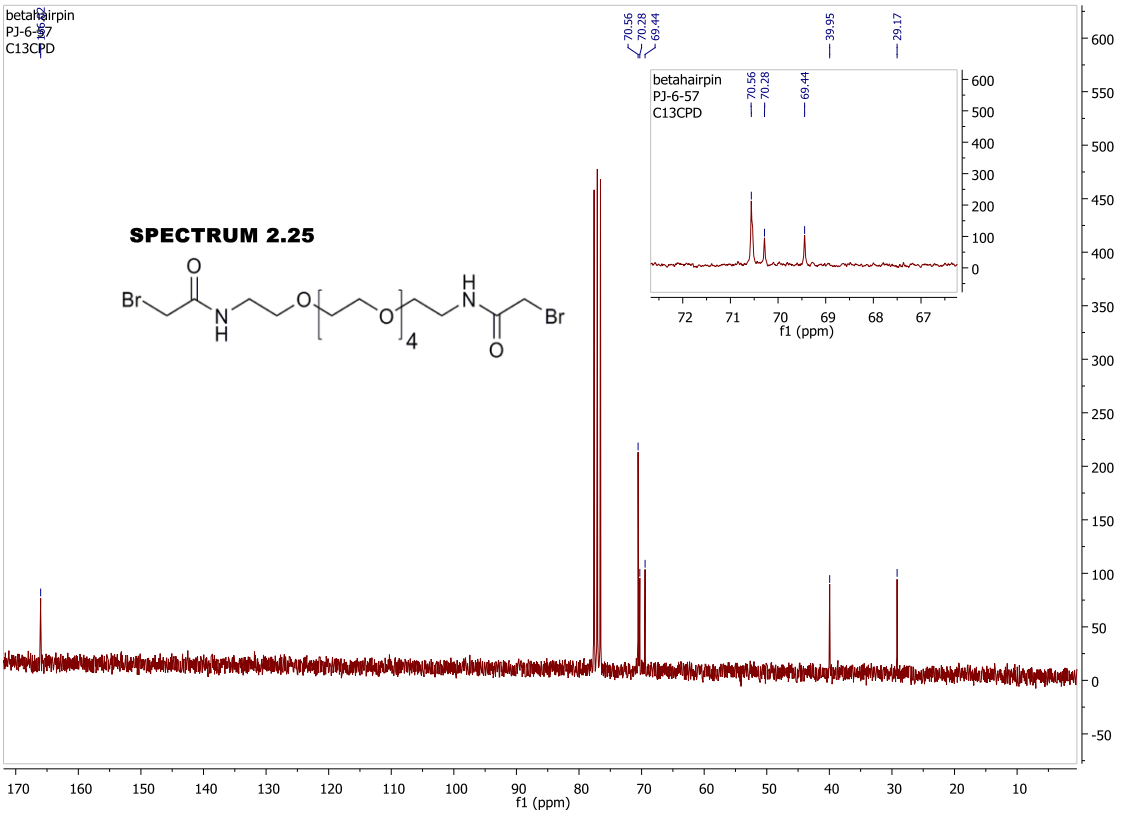
betahairpin
PJ-6-57
C13CPD
70.56
70.28
69.44
39.95
29.17
SPECTRUM 2.25
Br
O
N
H
O
O
4
H
N
O
Br
f1 (ppm)

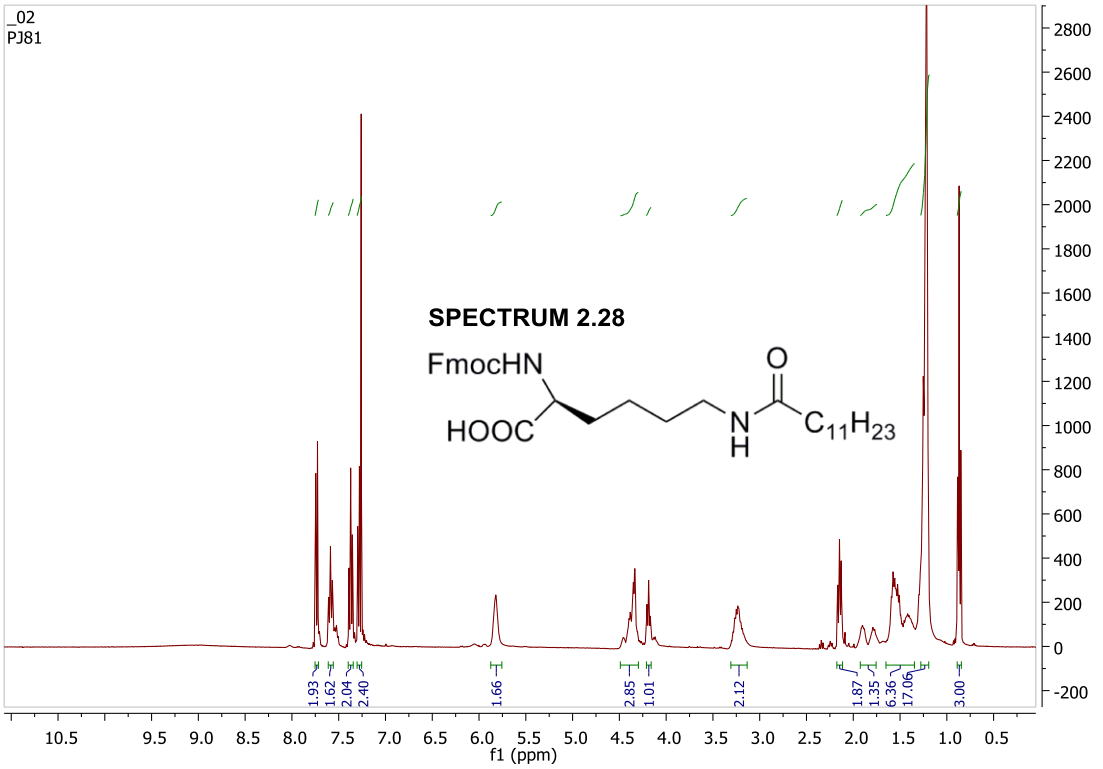
_02
PJ81
SPECTRUM 2.28
FmocHN
HOOC
O
N
H
C11H23
1.93
1.62
2.04
2.40
1.66
2.85
1.01
2.12
1.87
1.35
6.36
17.06
3.00
f1 (ppm)

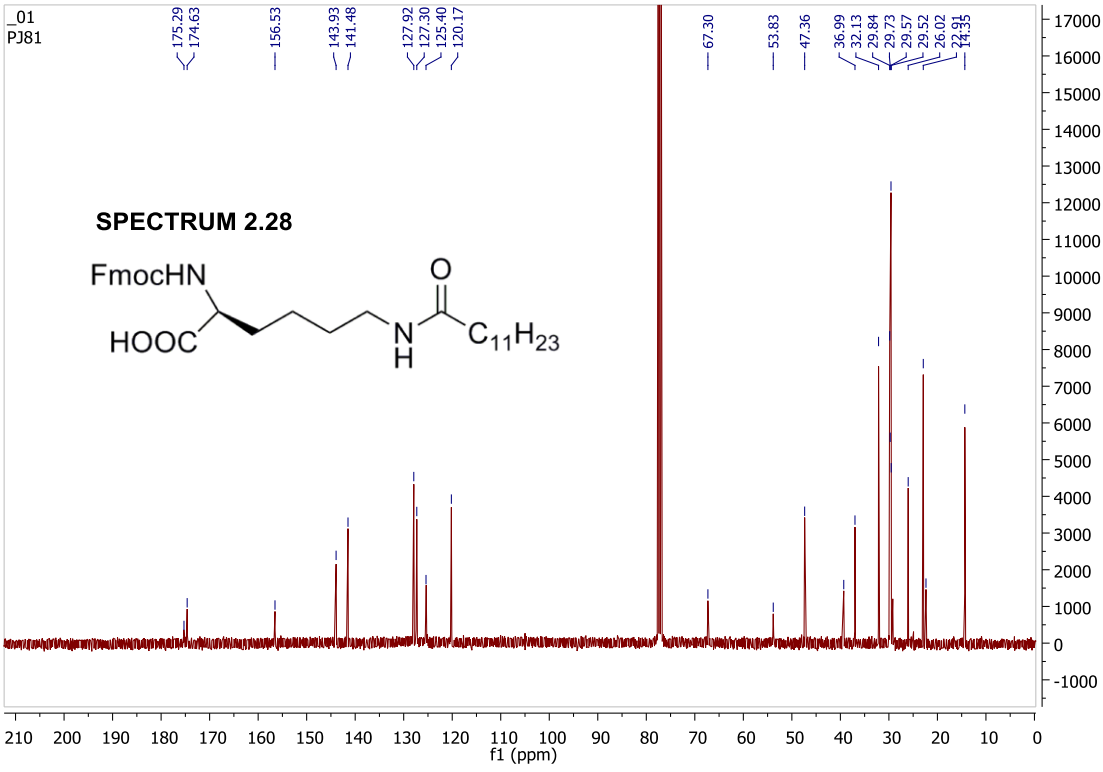
_01
PJ81
175.29
174.63
156.53
143.93
141.48
127.92
127.30
125.40
120.17
67.30
53.83
47.36
36.99
32.13
29.84
29.73
29.57
29.52
26.02
22.91
14.35
SPECTRUM 2.28
FmocHN
HOOC
O
N
H
C11H23
f1 (ppm)

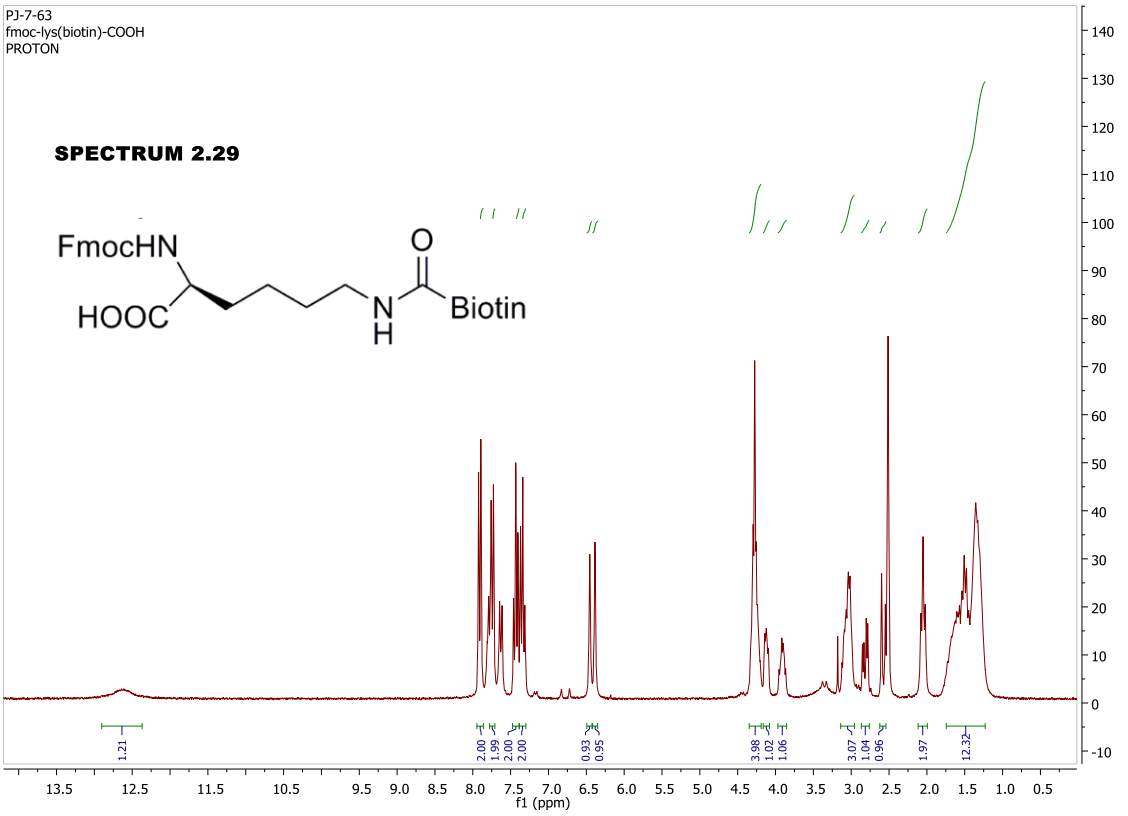
PJ-7-63
fmoc-lys(biotin)-COOH
PROTON
SPECTRUM 2.29
FmocHN
HOOC
O
N
H
Biotin
1.21
2.00
1.99
2.00
2.00
0.93
0.95
3.98
1.02
1.06
3.07
1.04
0.96
1.97
12.32
f1 (ppm)

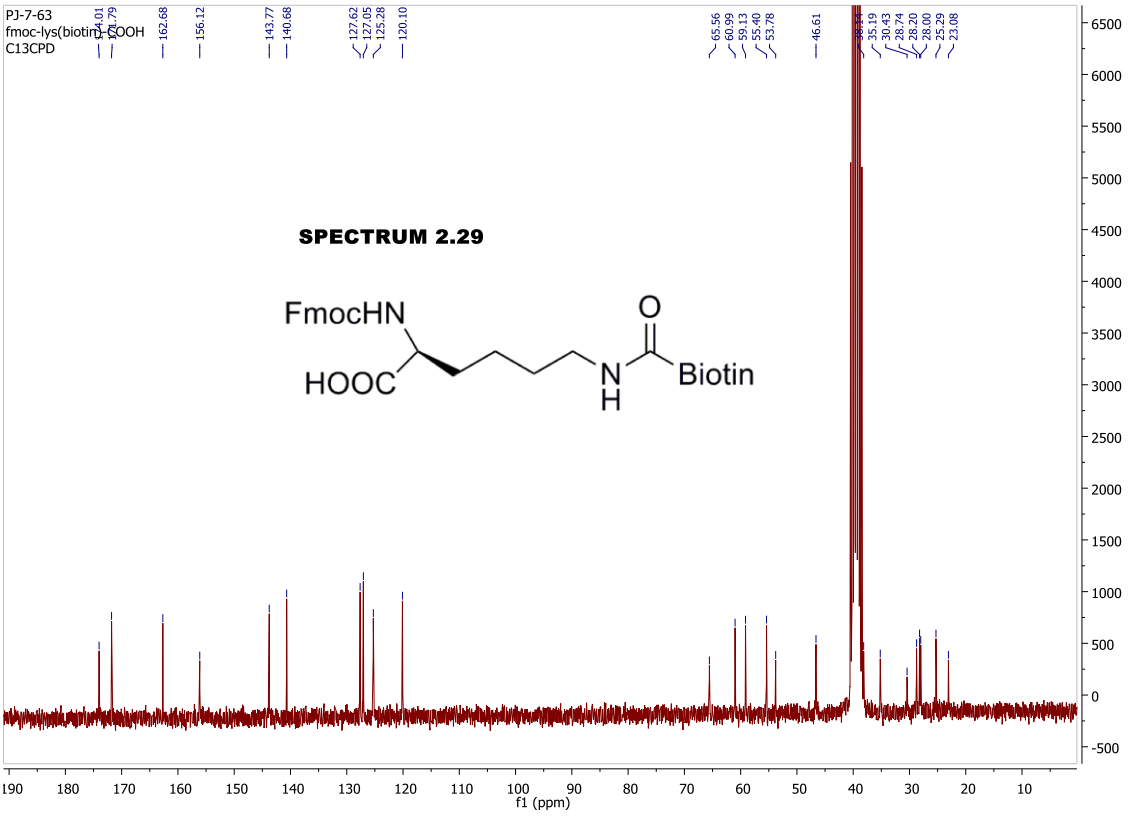
PJ-7-63
fmoc-lys(biotin)-COOH
C13CPD
174.01
171.79
162.68
156.12
143.77
140.68
127.62
127.05
125.28
120.10
65.56
60.99
59.13
55.40
53.78
46.61
35.19
30.43
28.74
28.20
28.00
25.29
23.08
SPECTRUM 2.29
FmocHN
HOOC
O
N
H
Biotin
f1 (ppm)

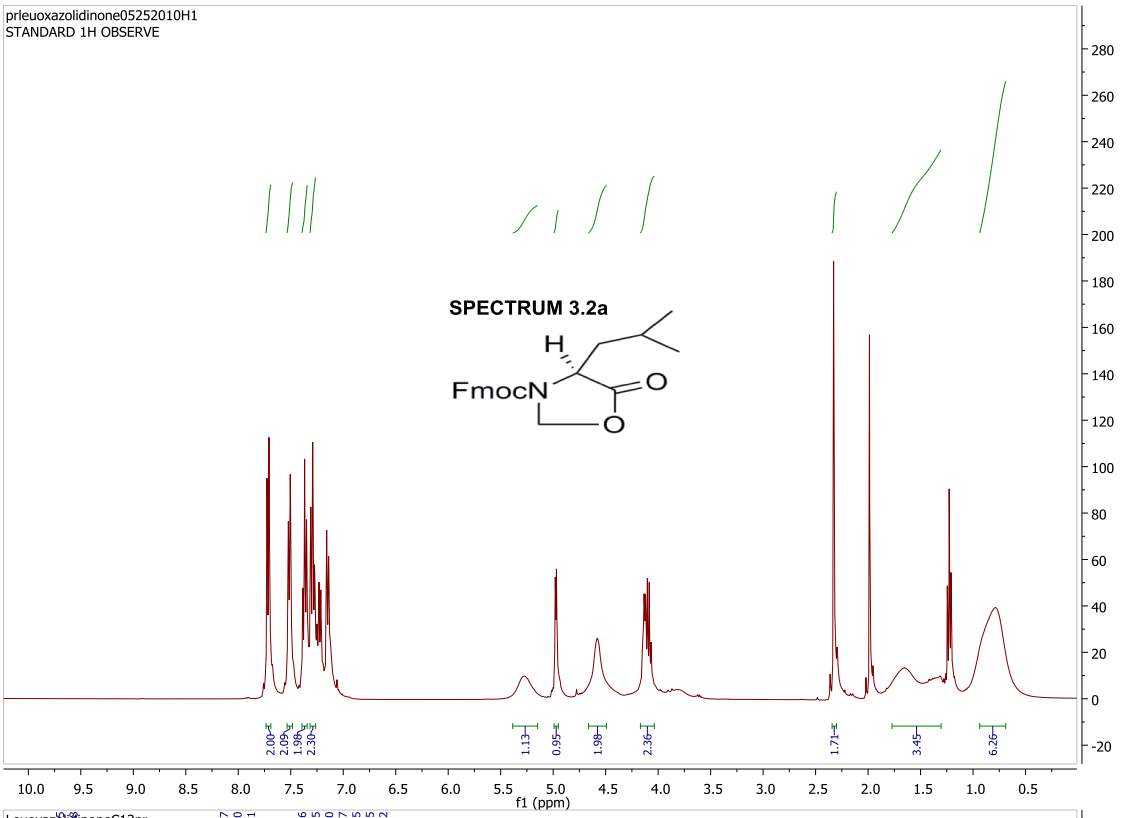
prleuoxazolidinone05252010H1
STANDARD 1H OBSERVE
SPECTRUM 3.2a
H
FmocN
O
O
2.00
2.05
1.98
2.30
1.13
0.95
1.98
2.36
1.71
3.45
6.26
f1 (ppm)

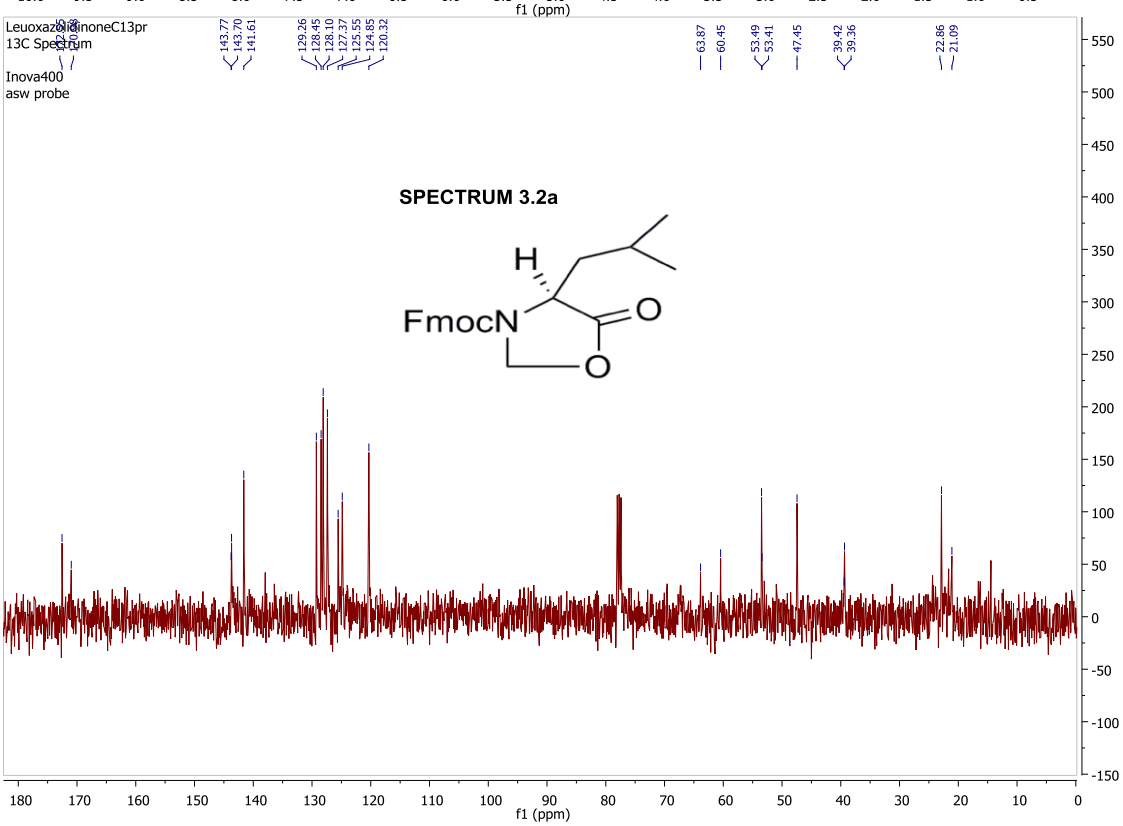
LeuoxazolidinoneC13pr
13C Spectrum
Inova400
asw probe
143.77
143.70
141.61
129.26
128.45
128.10
127.37
125.55
124.85
120.32
63.87
60.45
53.49
53.41
47.45
39.42
39.36
22.86
21.09
SPECTRUM 3.2a
H
FmocN
O
O
f1 (ppm)

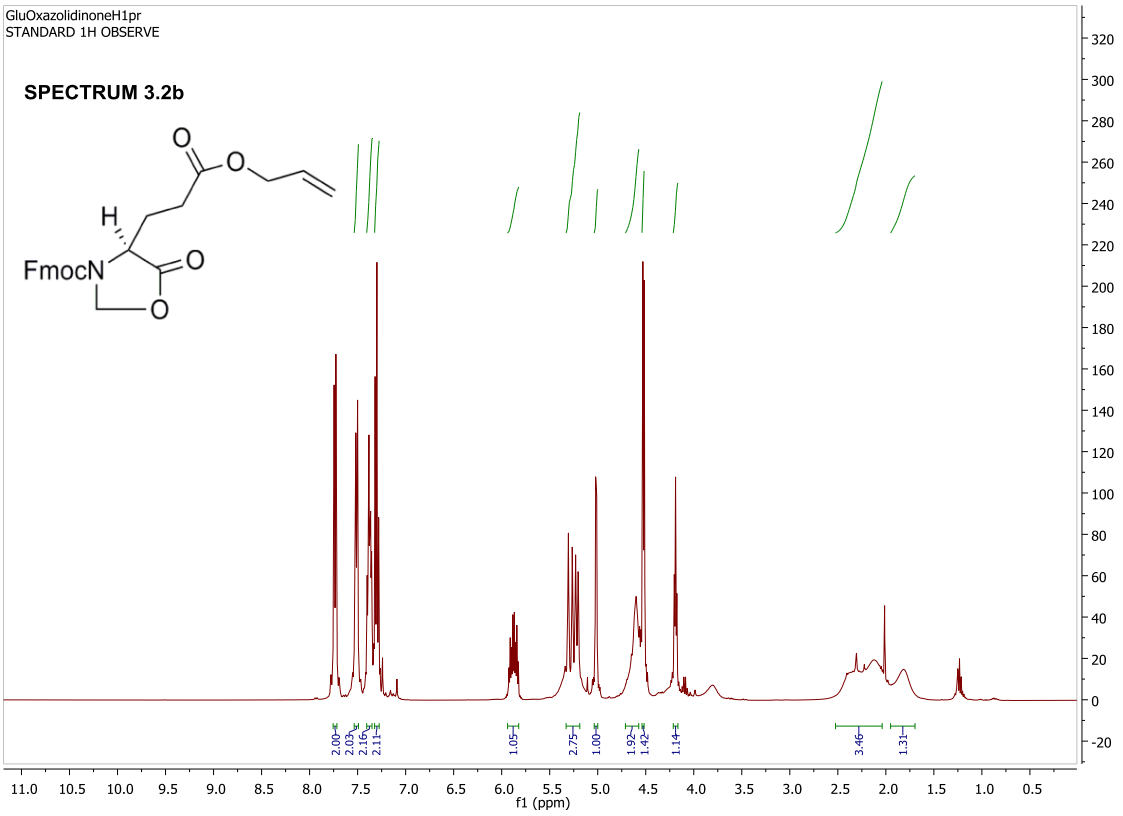
GluOxazolidinoneH1pr
STANDARD 1H OBSERVE
SPECTRUM 3.2b
FmocN
f1 (ppm)

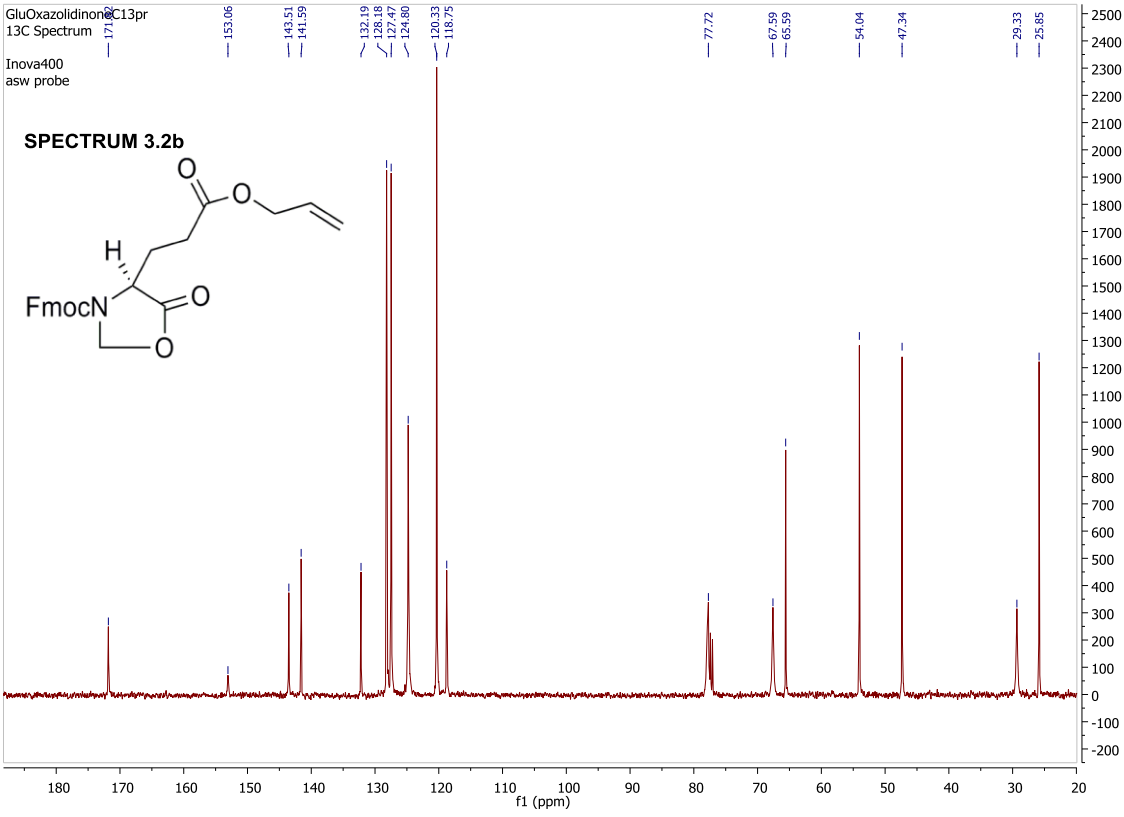
GluOxazolidinoneC13pr
13C Spectrum
Inova400
asw probe
SPECTRUM 3.2b
FmocN
f1 (ppm)

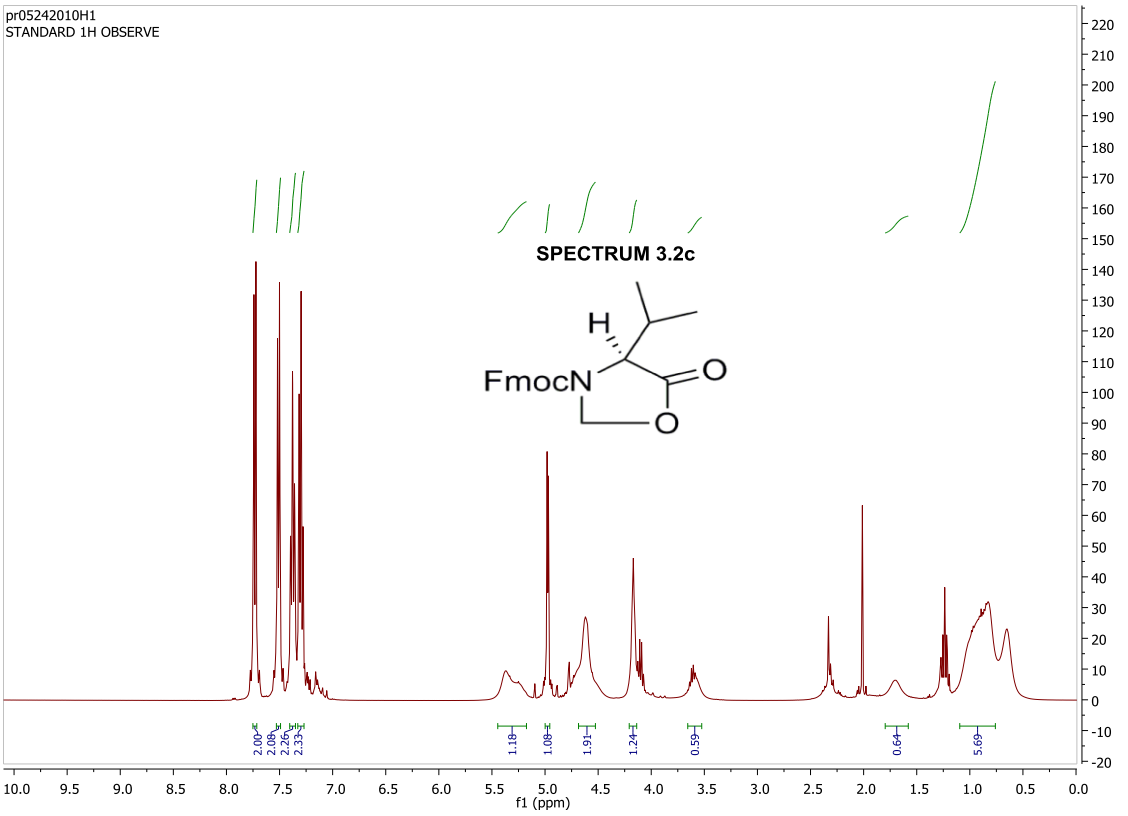
pr05242010H1
STANDARD 1H OBSERVE
SPECTRUM 3.2c
H
FmocN
O
O
2.00
2.08
2.26
2.33
1.18
1.08
1.91
1.24
0.59
0.64
5.69
f1 (ppm)

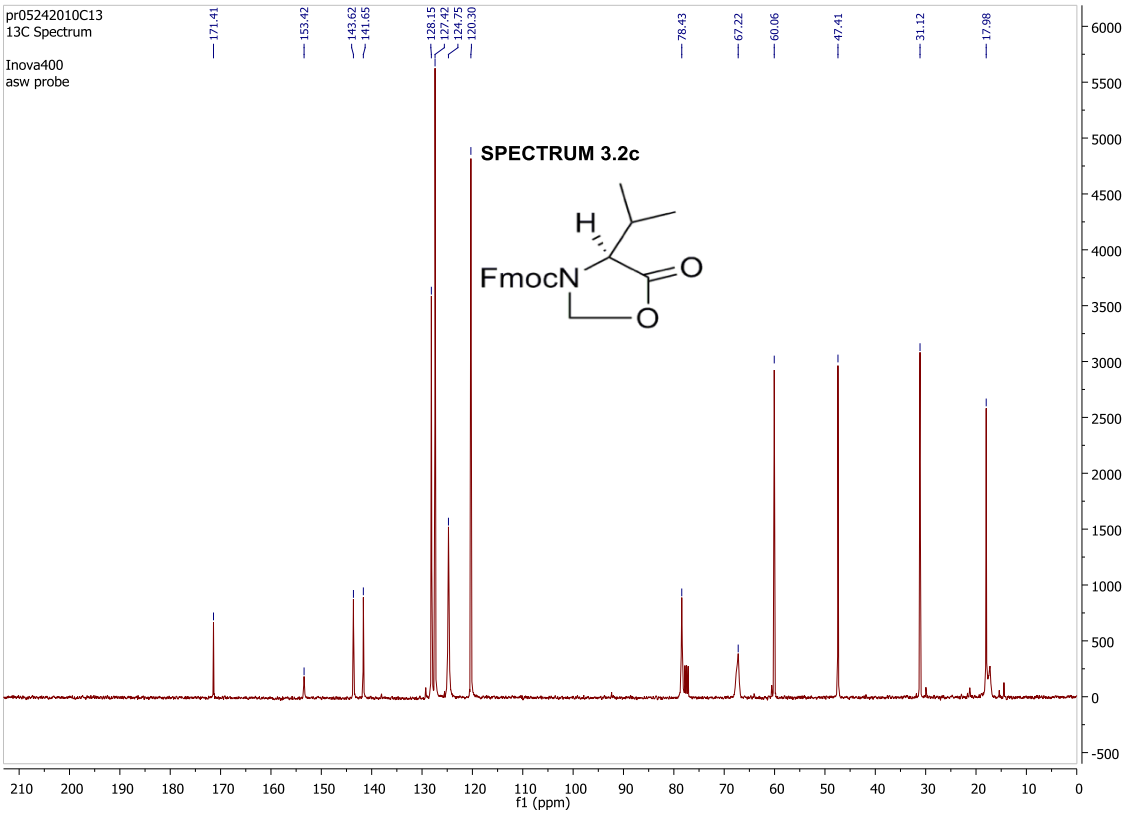
pr05242010C13
13C Spectrum
Inova400
asw probe
171.41
153.42
143.62
141.65
128.15
127.42
124.75
120.30
78.43
67.22
60.06
47.41
31.12
17.98
SPECTRUM 3.2c
H
FmocN
O
O
f1 (ppm)

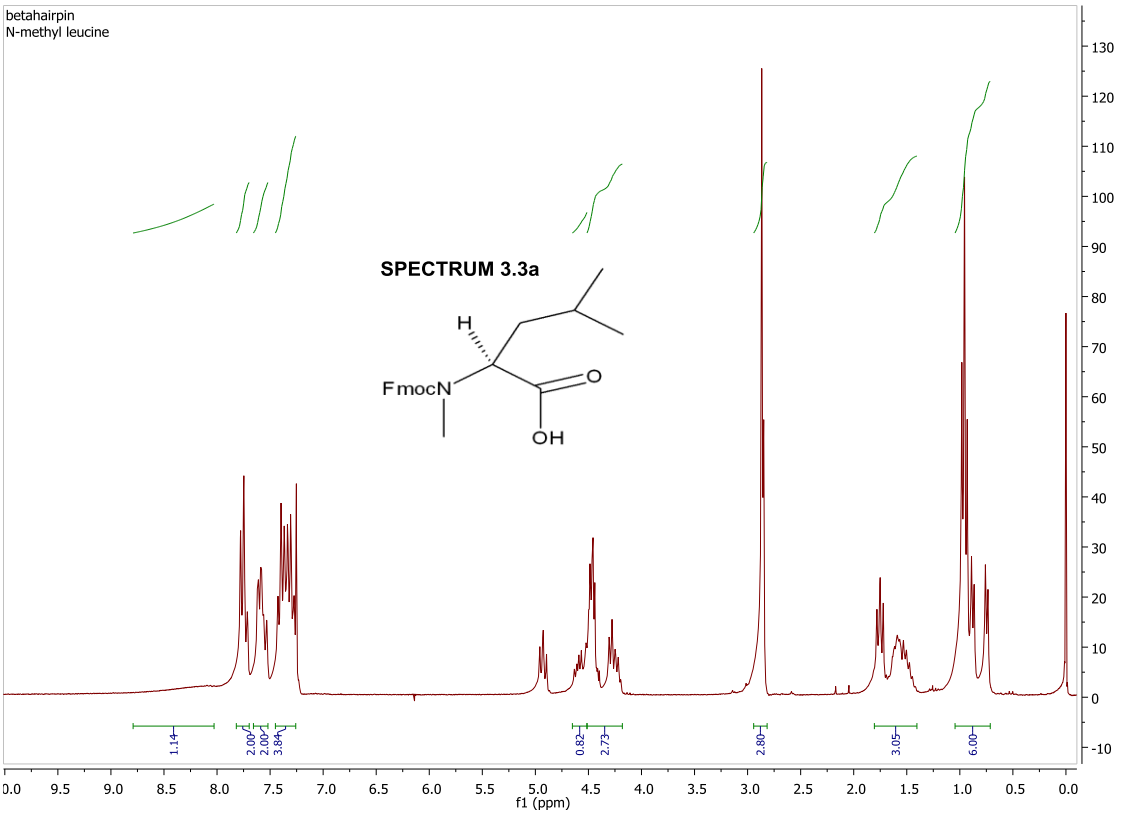
betahairpin
N-methyl leucine
SPECTRUM 3.3a
H
FmocN
O
OH
1.14
2.00
2.00
3.84
0.82
2.73
2.80
3.05
6.00
f1 (ppm)

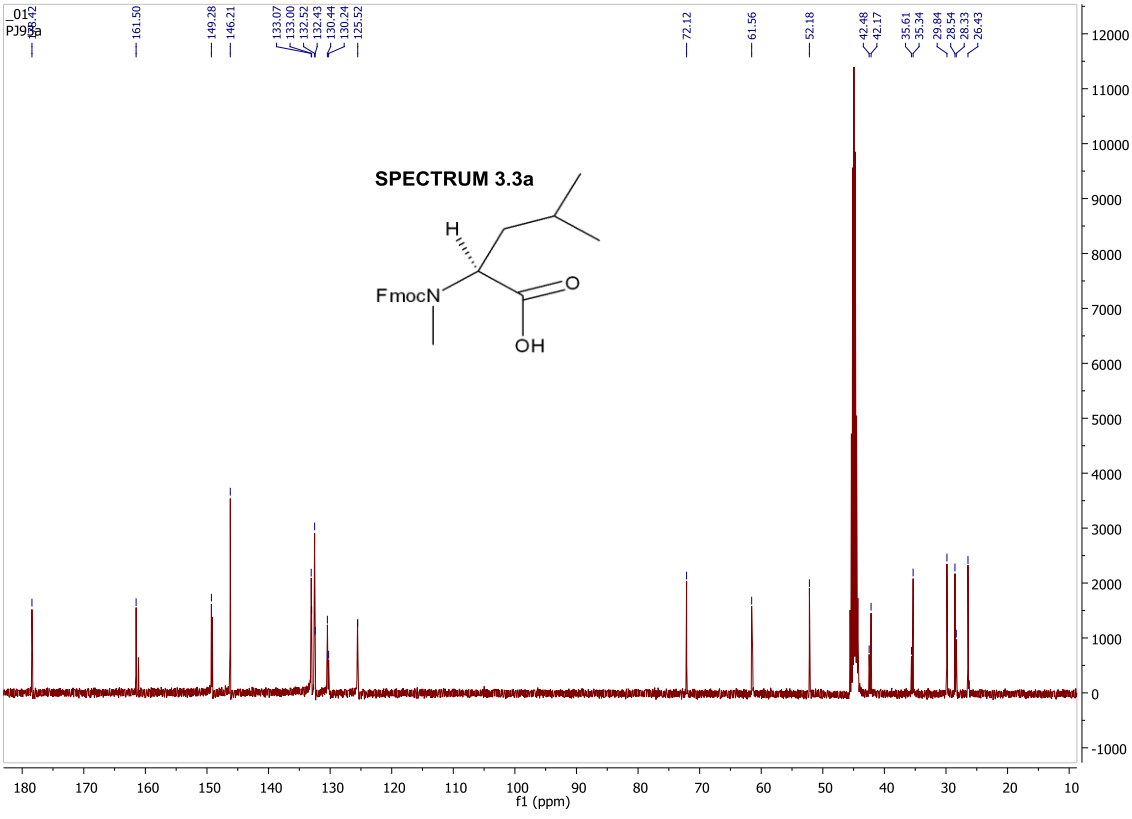
_01
PJ958a
161.50
149.28
146.21
133.07
133.00
132.52
132.43
130.44
130.24
125.52
72.12
61.56
52.18
42.48
42.17
35.61
35.34
29.84
28.54
28.33
26.43
SPECTRUM 3.3a
H
FmocN
O
OH
f1 (ppm)

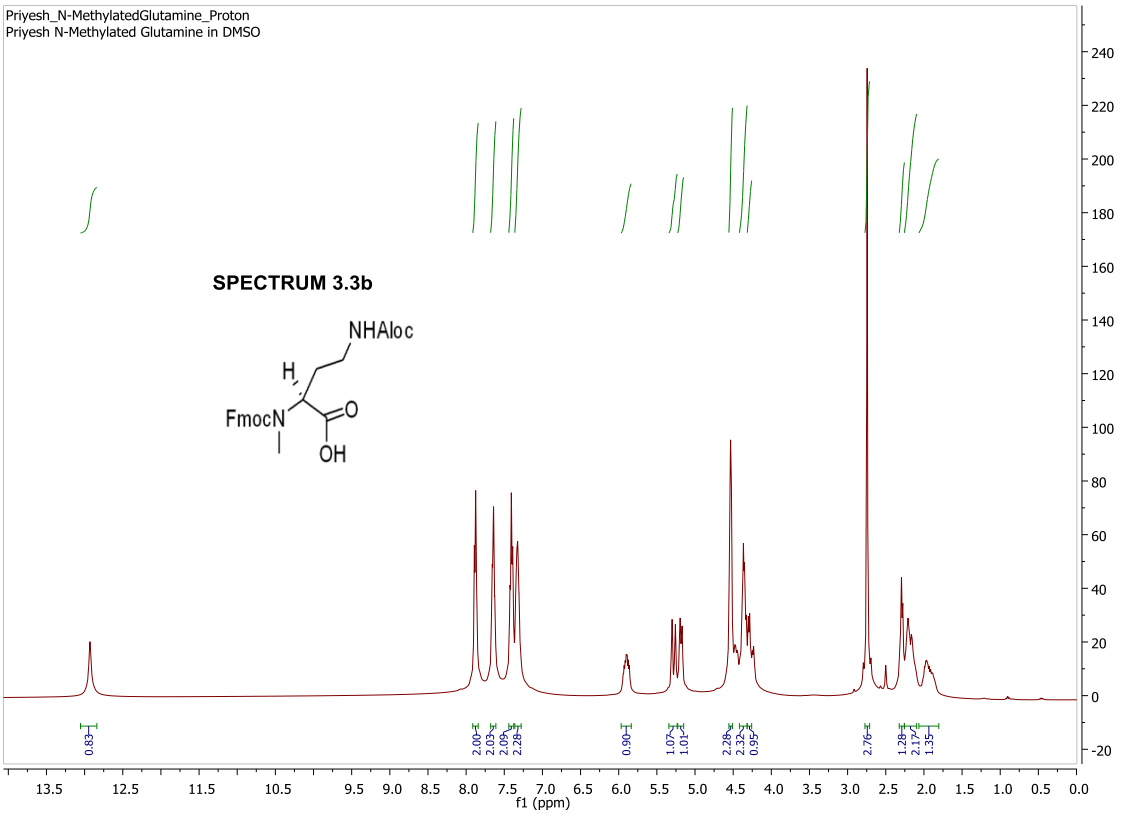
Priyesh_N-MethylatedGlutamine_Proton
Priyesh N-Methylated Glutamine in DMSO
SPECTRUM 3.3b
NHAloc
H
FmocN
O
OH
f1 (ppm)

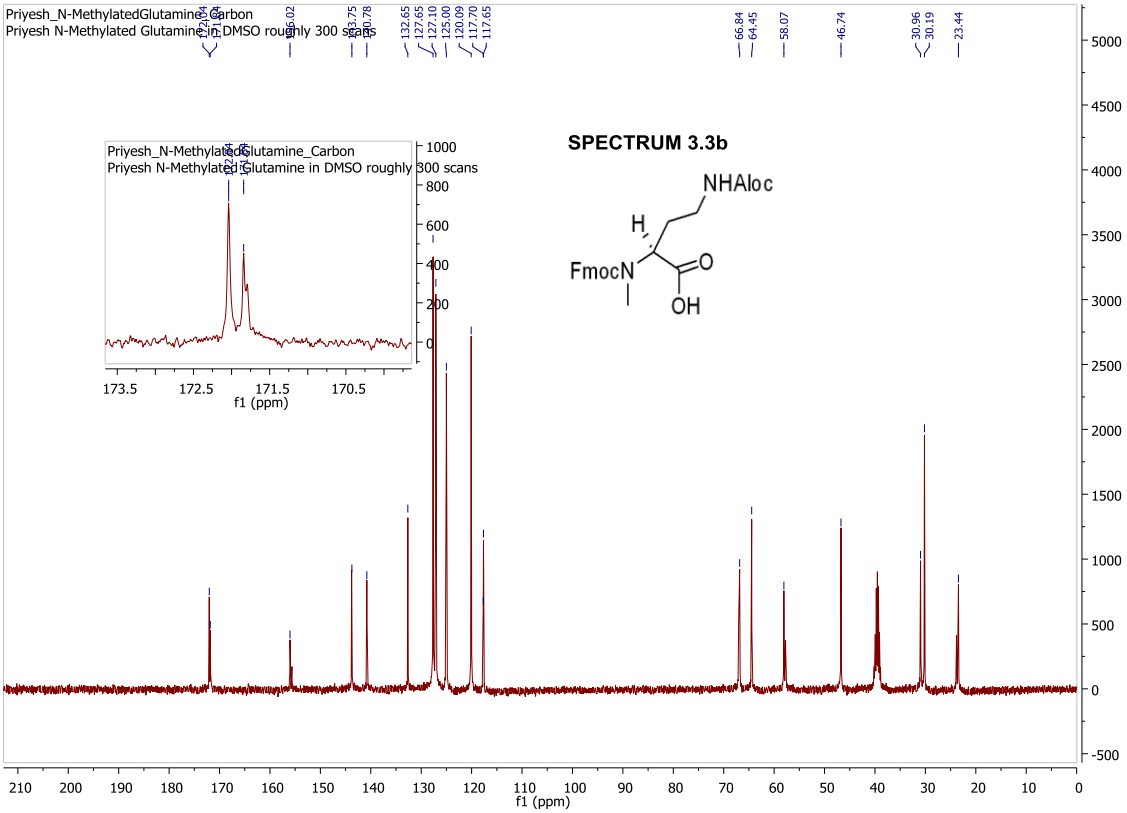
Priyesh_N-MethylatedGlutamine_Carbon
Priyesh N-Methylated Glutamine in DMSO roughly 300 scans
SPECTRUM 3.3b
NHAloc
H
FmocN
O
OH
f1 (ppm)

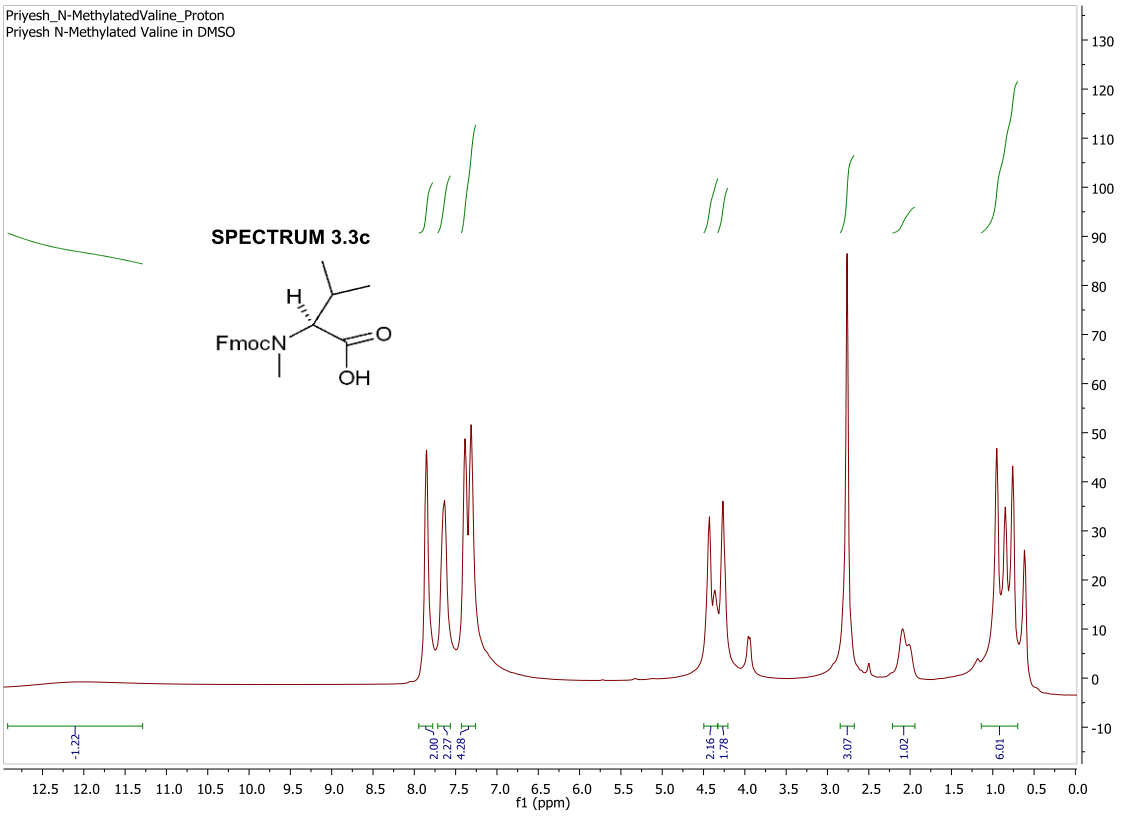
Priyesh_N-MethylatedValine_Proton
Priyesh N-Methylated Valine in DMSO
SPECTRUM 3.3c
FmocN
H
O
OH
-1.22
2.00
2.27
4.28
2.16
1.78
3.07
1.02
6.01
f1 (ppm)

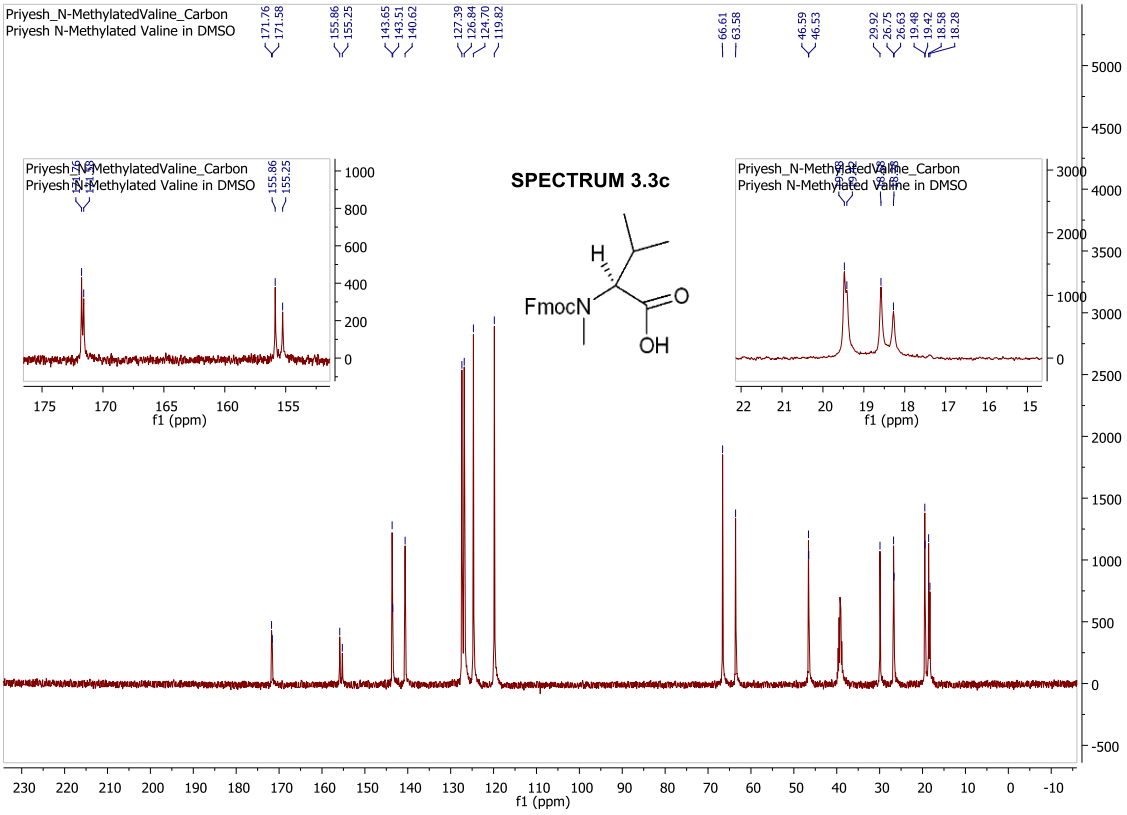
Priyesh_N-MethylatedValine_Carbon
Priyesh N-Methylated Valine in DMSO
171.76
171.58
155.86
155.25
143.65
143.51
140.62
127.39
126.84
124.70
119.82
66.61
63.58
46.59
46.53
29.92
26.75
26.63
19.48
19.42
18.58
18.28
SPECTRUM 3.3c
FmocN
H
O
OH
f1 (ppm)

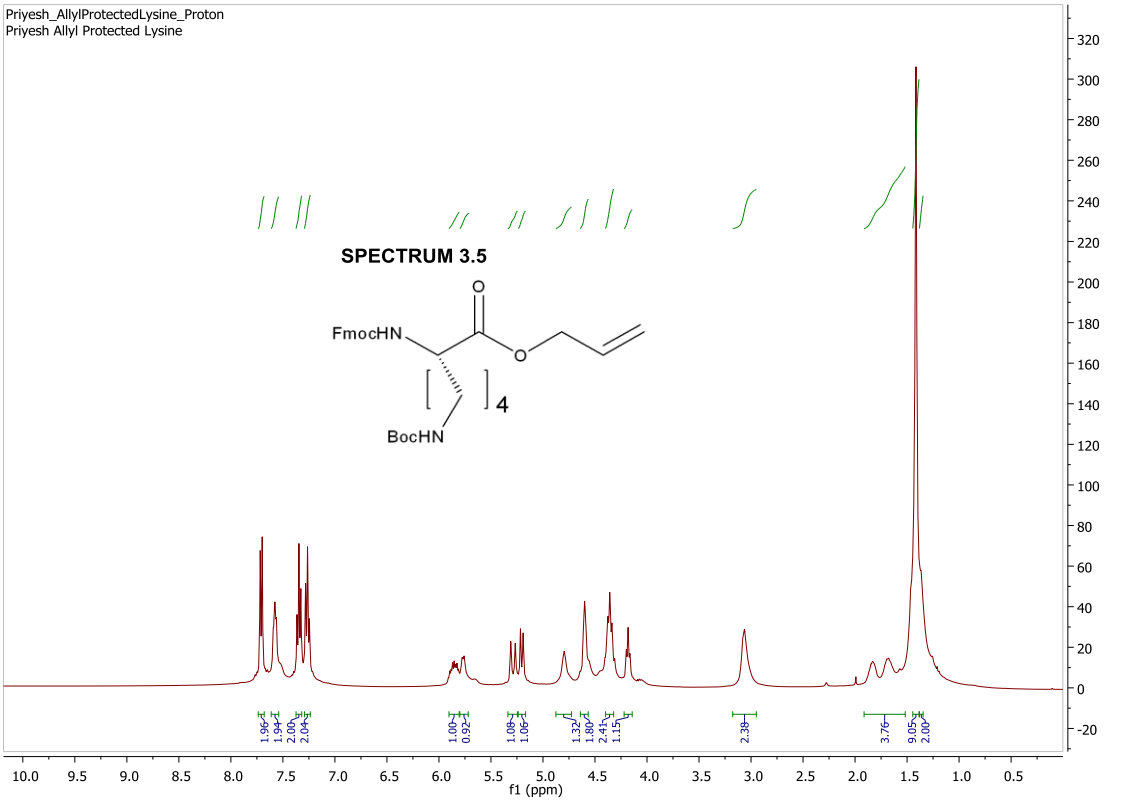
Priyesh_AllylProtectedLysine_Proton
Priyesh Allyl Protected Lysine
SPECTRUM 3.5
FmocHN
BocHN
4
f1 (ppm)

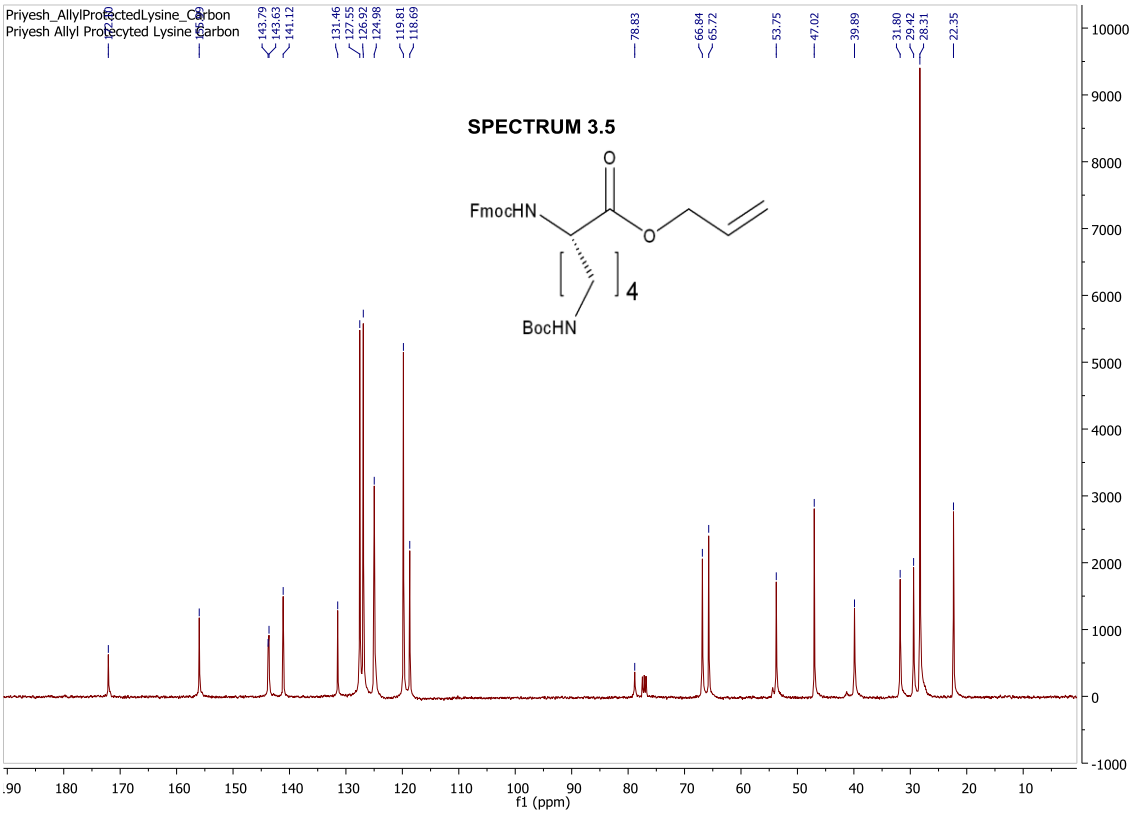
Priyesh_AllylProtectedLysine_Carbon
Priyesh Allyl Protecyted Lysine Carbon
143.79
143.63
141.12
131.46
127.55
126.92
124.98
119.81
118.69
78.83
66.84
65.72
53.75
47.02
39.89
31.80
29.42
28.31
22.35
SPECTRUM 3.5
FmocHN
BocHN
4
f1 (ppm)

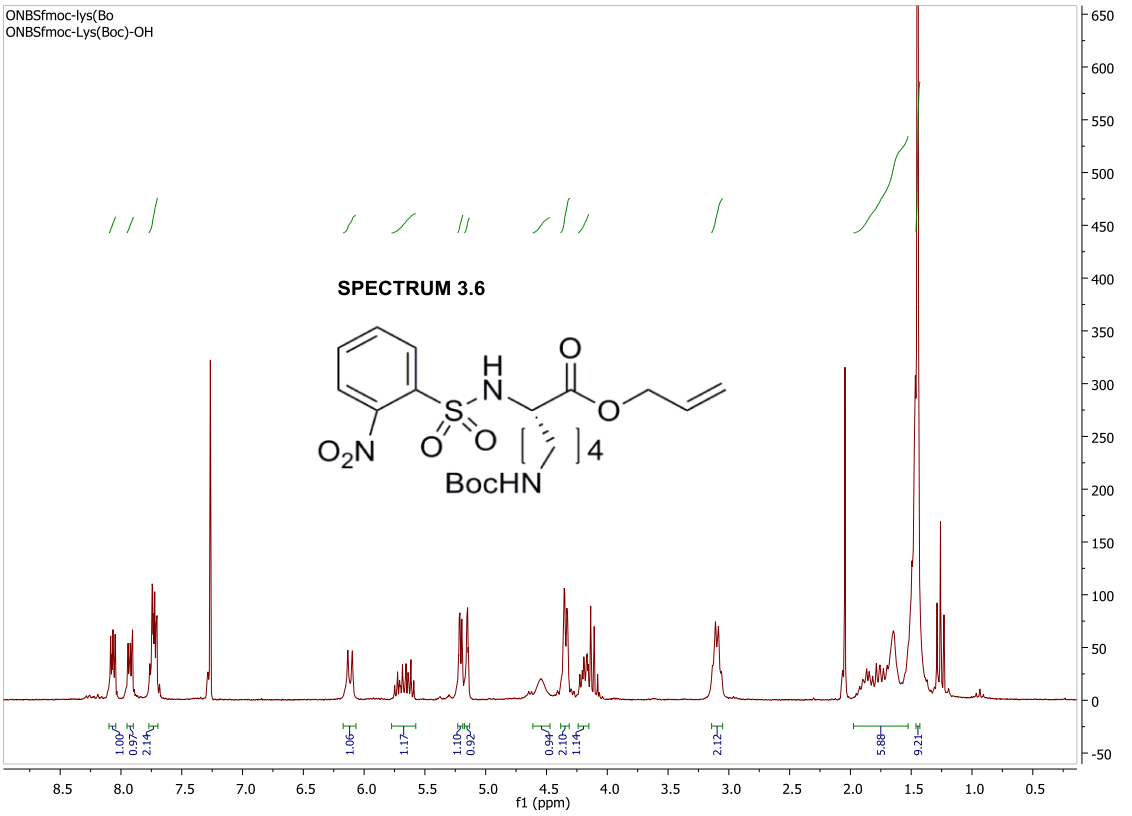
ONBSfmoc-lys(Bo
ONBSfmoc-Lys(Boc)-OH
SPECTRUM 3.6
f1 (ppm)

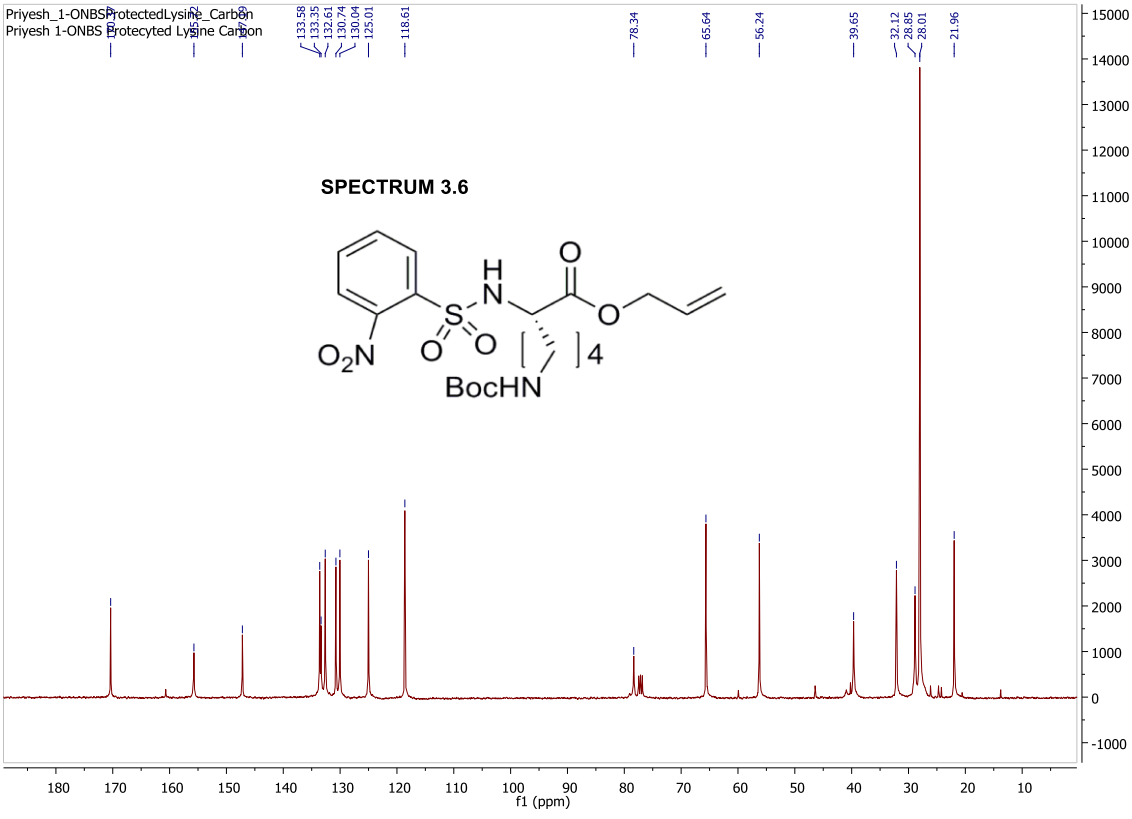
Priyesh_1-ONBSProtectedLysine_Carbon
Priyesh 1-ONBS Protecyted Lysine Carbon
SPECTRUM 3.6
f1 (ppm)

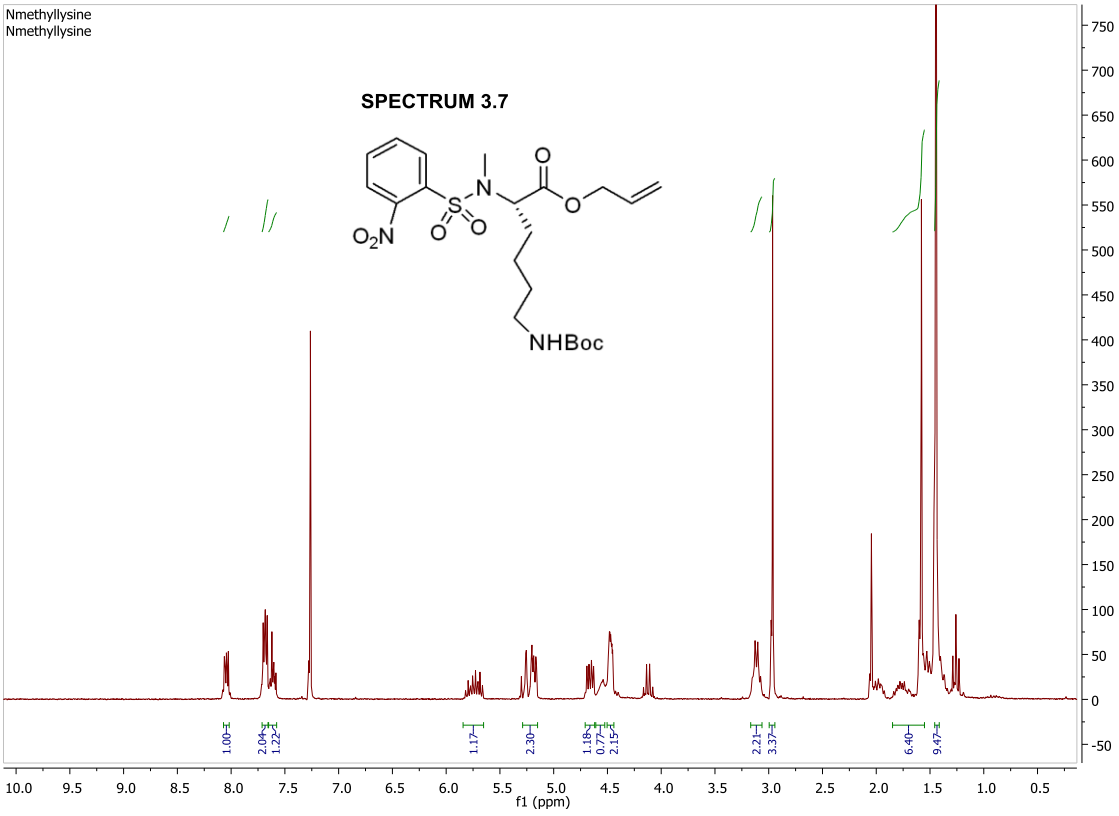
Nmethyllysine
Nmethyllysine
SPECTRUM 3.7
NHBoc
f1 (ppm)

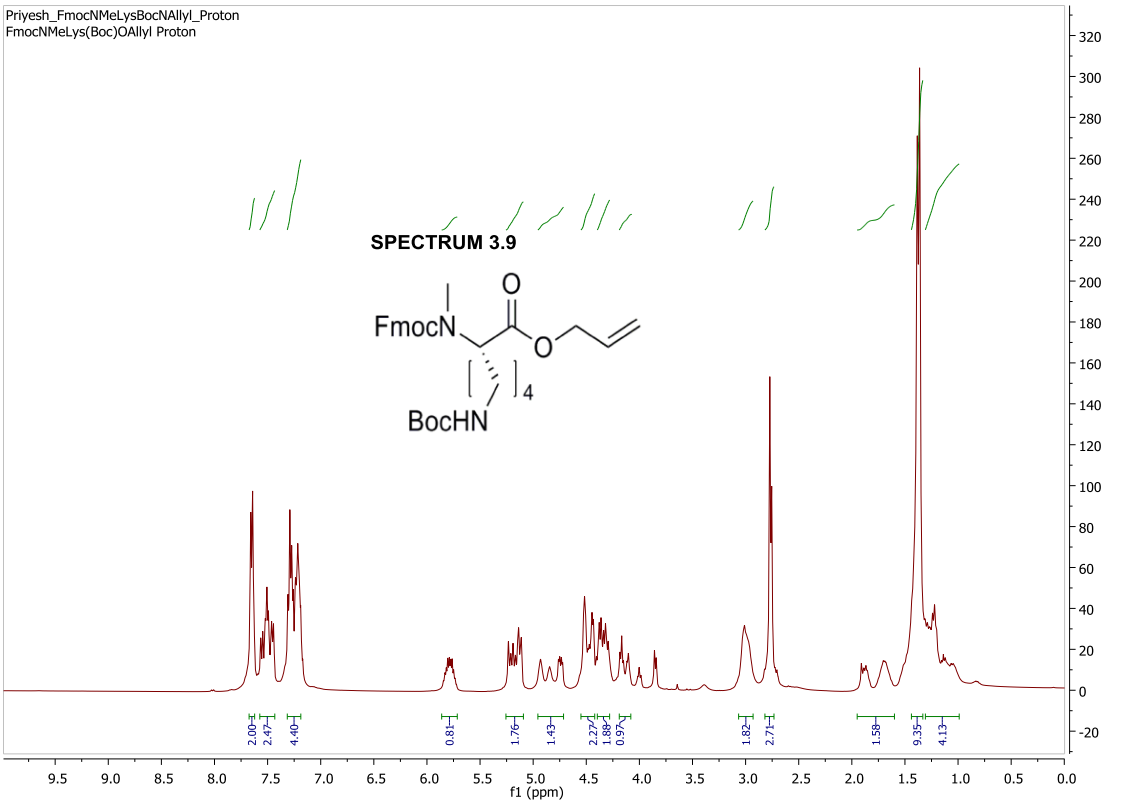
Priyesh_FmocNMeLysBocNAllyl_Proton
FmocNMeLys(Boc)OAllyl Proton
SPECTRUM 3.9
FmocN
O
O
4
BocHN
2.00
2.47
4.40
0.81
1.76
1.43
2.27
1.88
0.97
1.82
2.71
1.58
9.35
4.13
f1 (ppm)

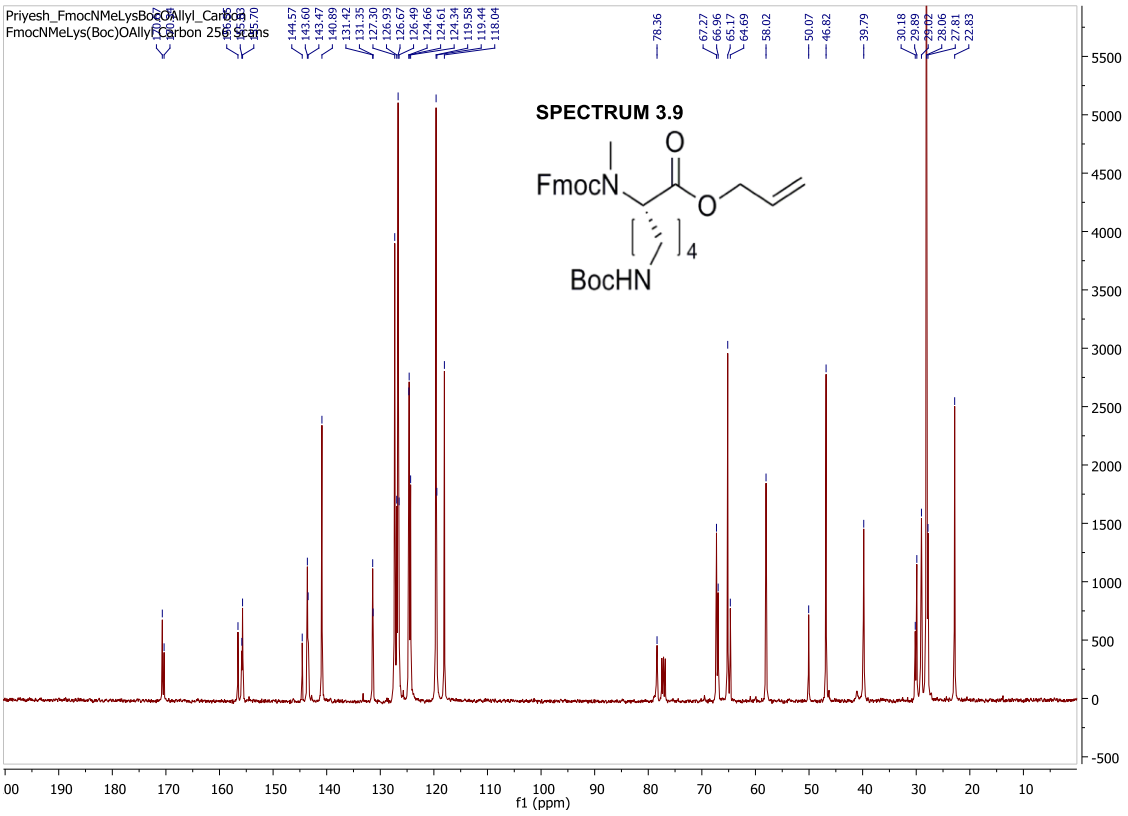
Priyesh_FmocNMeLysBocOAllyl_Carbon
FmocNMeLys(Boc)OAllyl Carbon 256 Scans
144.57
143.60
143.47
140.89
131.42
131.35
127.30
126.93
126.67
126.49
124.66
124.61
124.34
119.58
119.44
118.04
78.36
67.27
66.96
65.17
64.69
58.02
50.07
46.82
39.79
30.18
29.89
29.02
28.06
27.81
22.83
SPECTRUM 3.9
FmocN
O
O
4
BocHN
f1 (ppm)

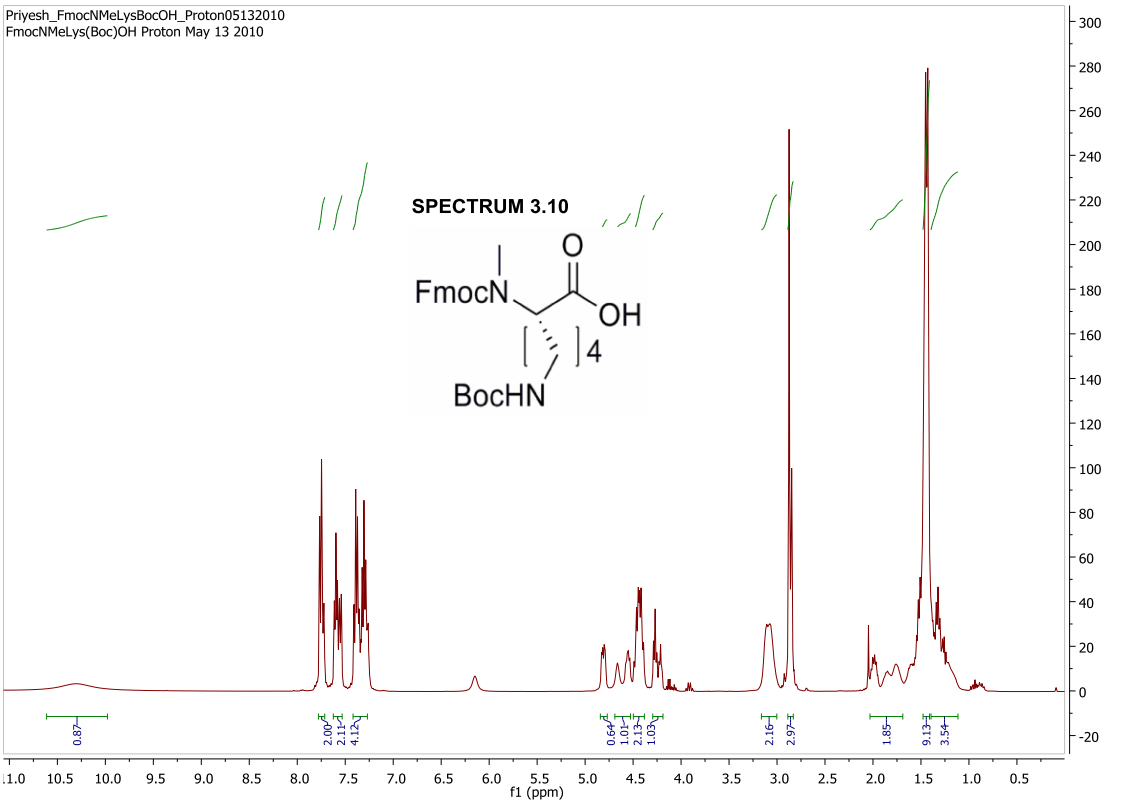
Priyesh_FmocNMeLysBocOH_Proton05132010
FmocNMeLys(Boc)OH Proton May 13 2010
SPECTRUM 3.10
FmocN
O
OH
4
BocHN
f1 (ppm)

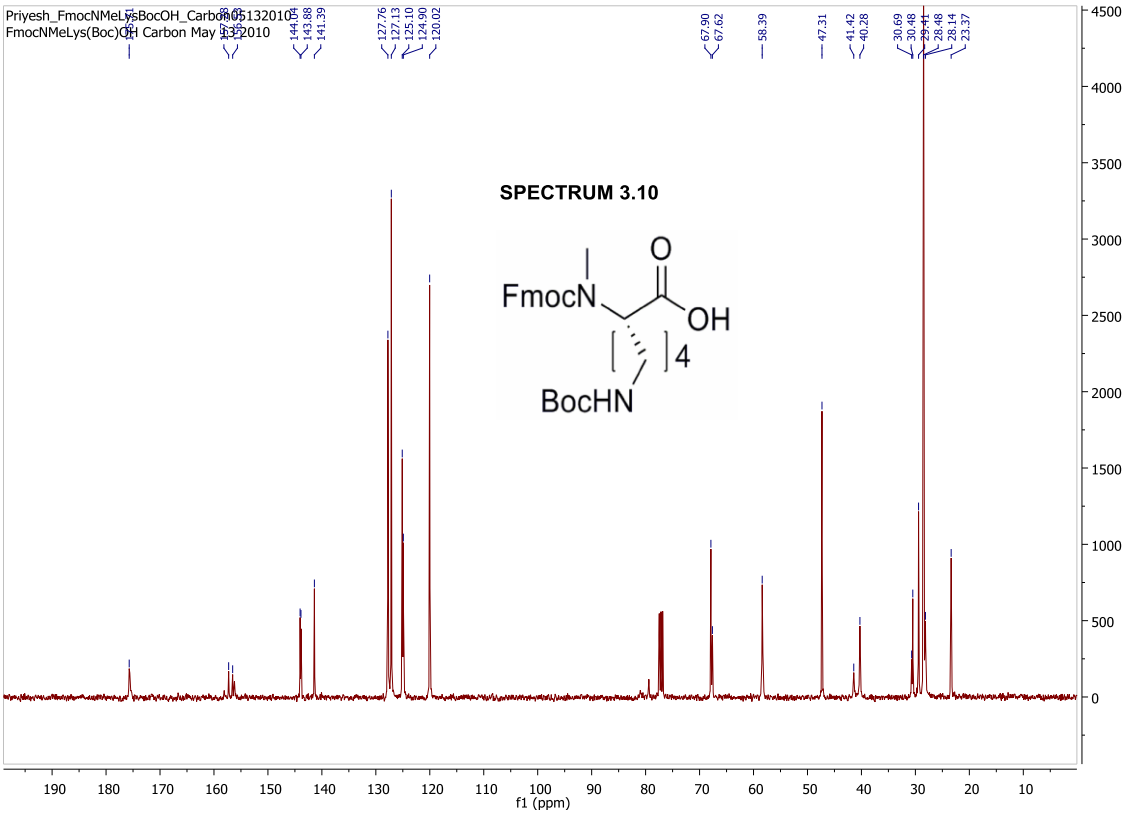
Priyesh_FmocNMeLysBocOH_Carbon05132010
FmocNMeLys(Boc)OH Carbon May 13 2010
SPECTRUM 3.10
FmocN
O
OH
4
BocHN
f1 (ppm)

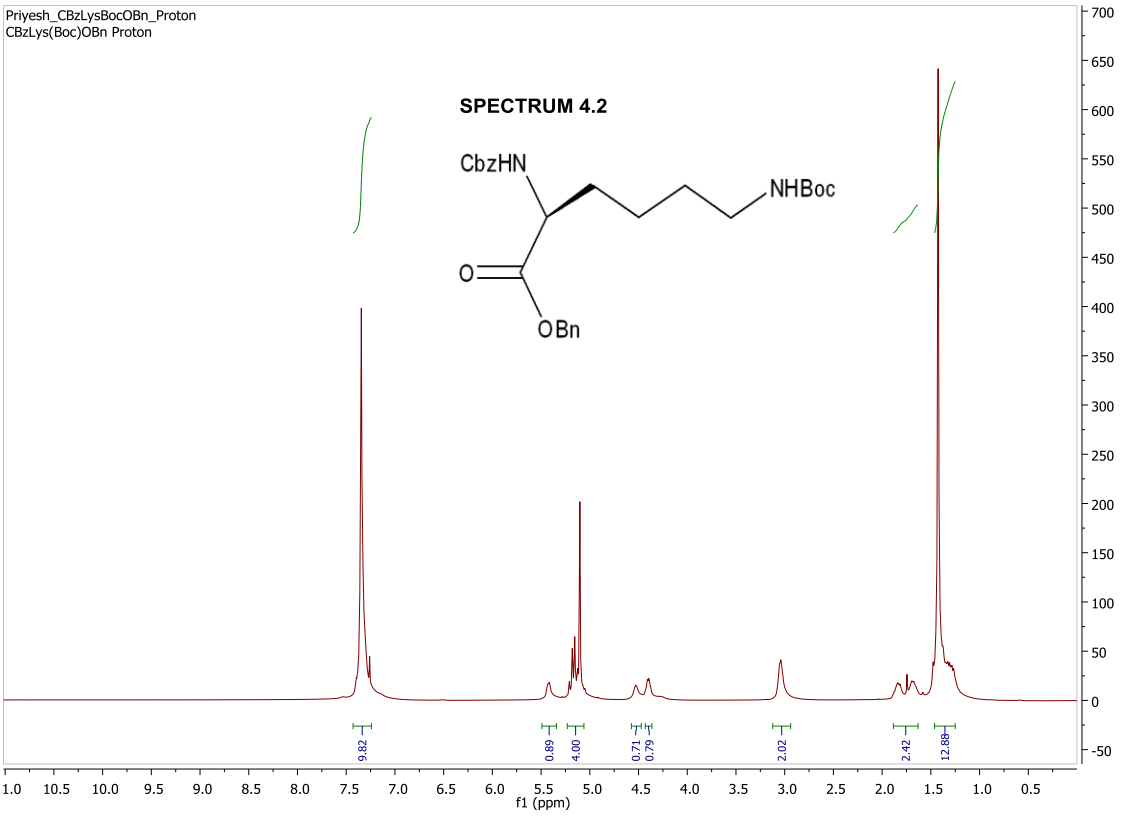
Priyesh_CBzLysBocOBn_Proton
CBzLys(Boc)OBn Proton
SPECTRUM 4.2
CbzHN
NHBoc
O
OBn
9.82
0.89
4.00
0.71
0.79
2.02
2.42
12.88
f1 (ppm)

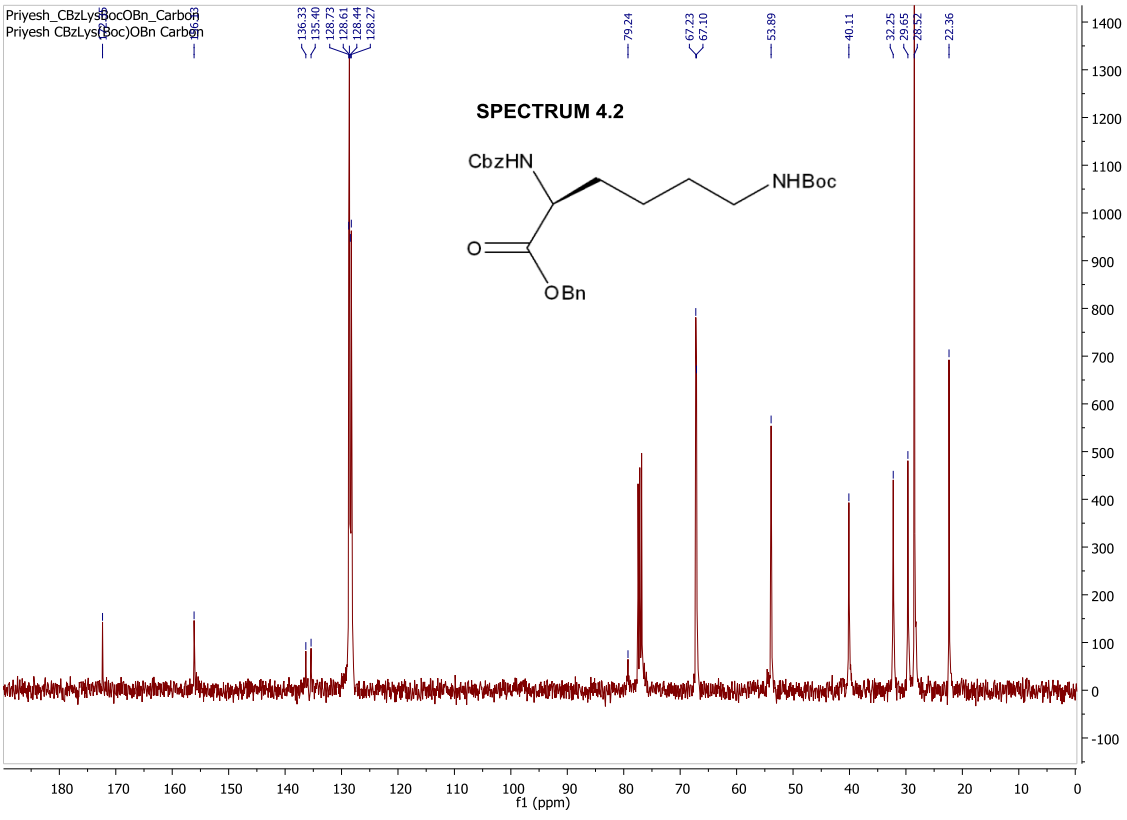
Priyesh_CBzLysBocOBn_Carbon
Priyesh CBzLys(Boc)OBn Carbon
136.33
135.40
128.73
128.61
128.44
128.27
79.24
67.23
67.10
53.89
40.11
32.25
29.65
28.52
22.36
SPECTRUM 4.2
CbzHN
NHBoc
O
OBn
f1 (ppm)

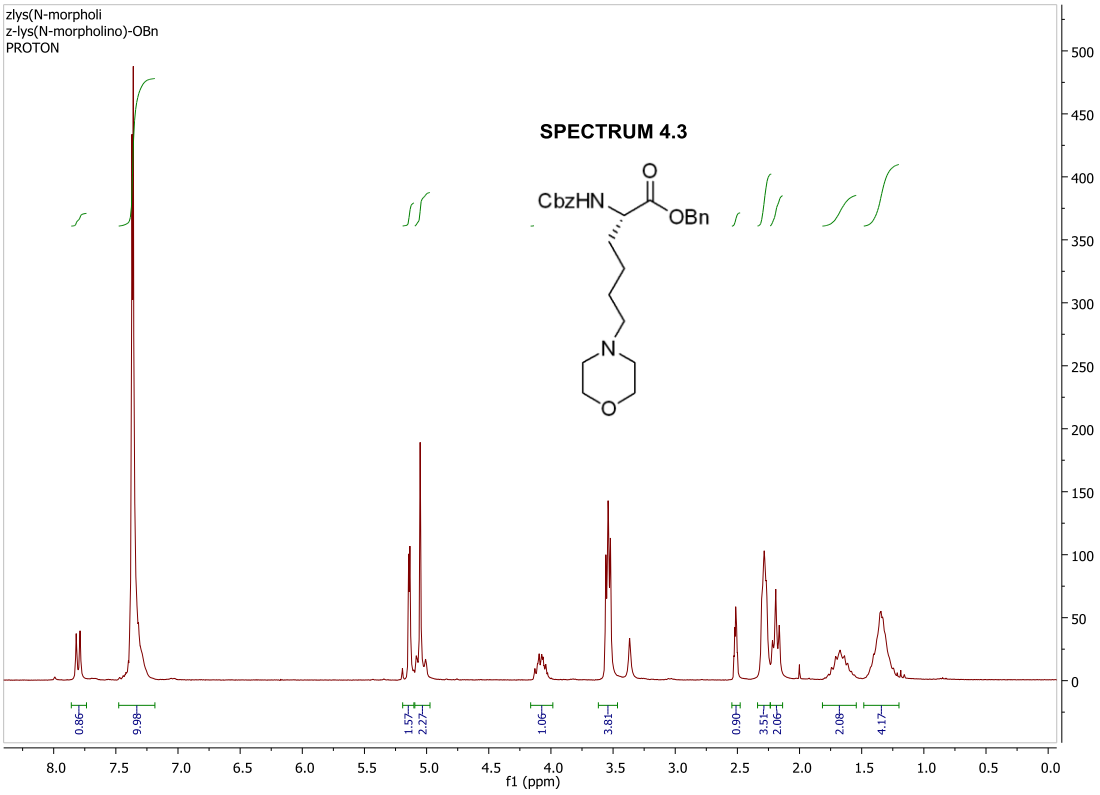
zlys(N-morpholi
z-lys(N-morpholino)-OBn
PROTON
SPECTRUM 4.3
CbzHN
OBn
N
O
0.86
9.98
1.57
2.27
1.06
3.81
0.90
3.51
2.06
2.08
4.17
f1 (ppm)

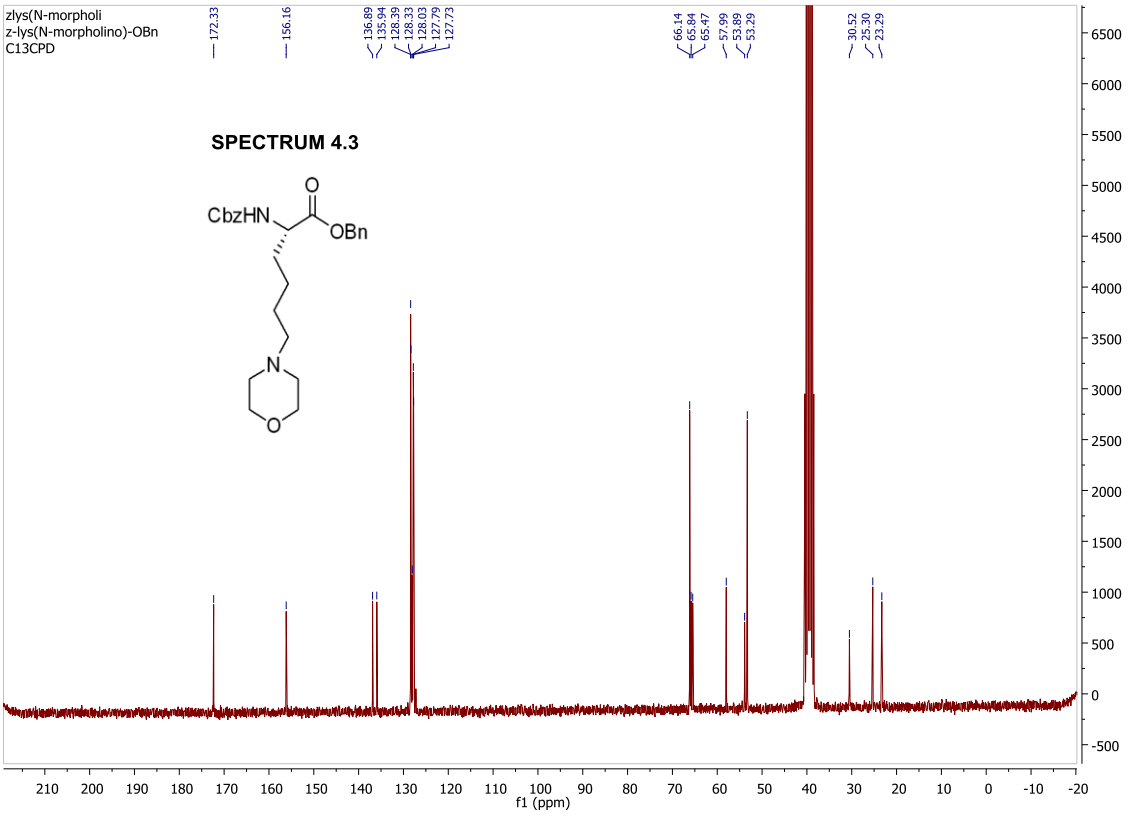
zlys(N-morpholi
z-lys(N-morpholino)-OBn
C13CPD
172.33
156.16
136.89
135.94
128.39
128.33
128.03
127.79
127.73
66.14
65.84
65.47
57.99
53.89
53.29
30.52
25.30
23.29
SPECTRUM 4.3
CbzHN
OBn
N
O
f1 (ppm)

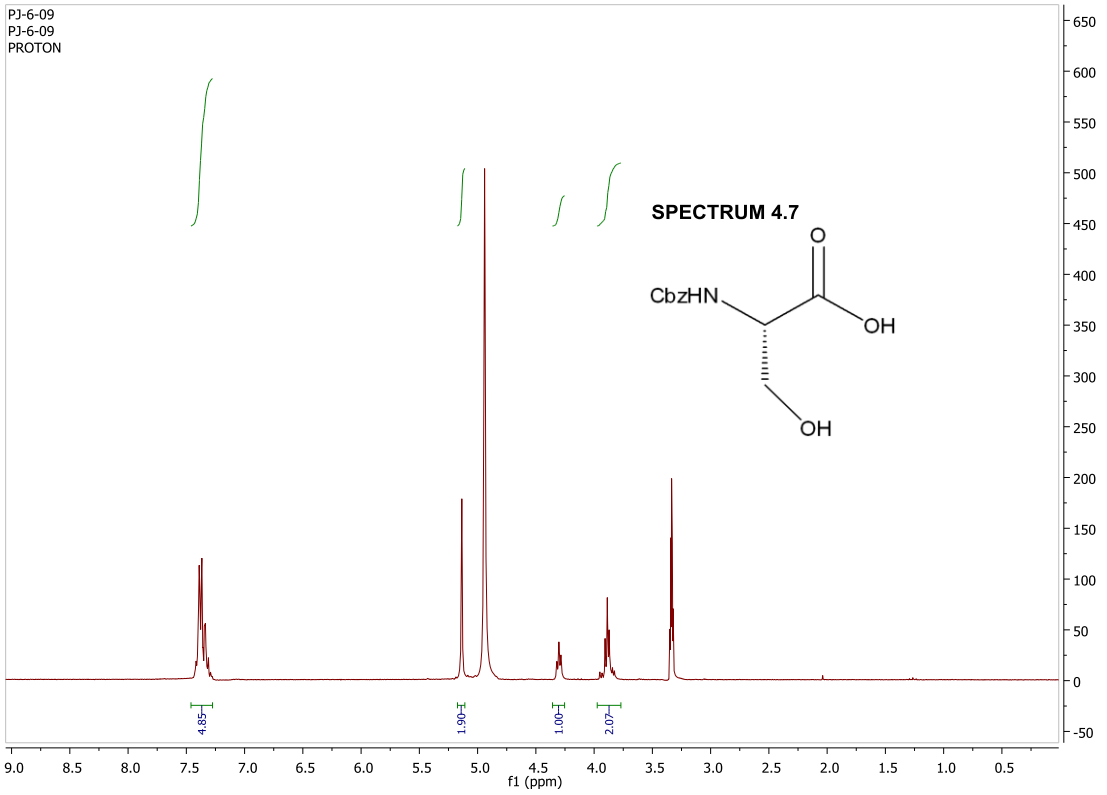
PJ-6-09
PJ-6-09
PROTON
SPECTRUM 4.7
CbzHN
OH
OH
O
4.85
1.90
1.00
2.07
f1 (ppm)

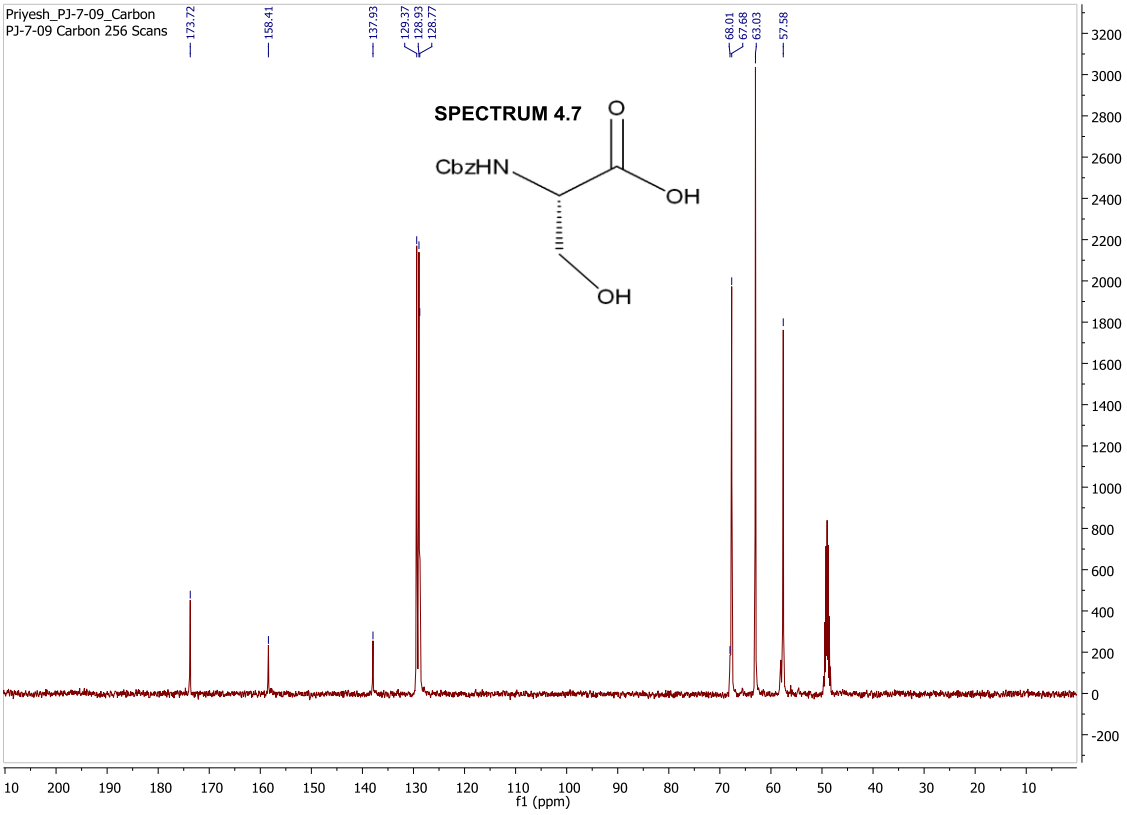
Priyesh_PJ-7-09_Carbon
PJ-7-09 Carbon 256 Scans
173.72
158.41
137.93
129.37
128.93
128.77
68.01
67.68
63.03
57.58
SPECTRUM 4.7
CbzHN
OH
OH
O
f1 (ppm)

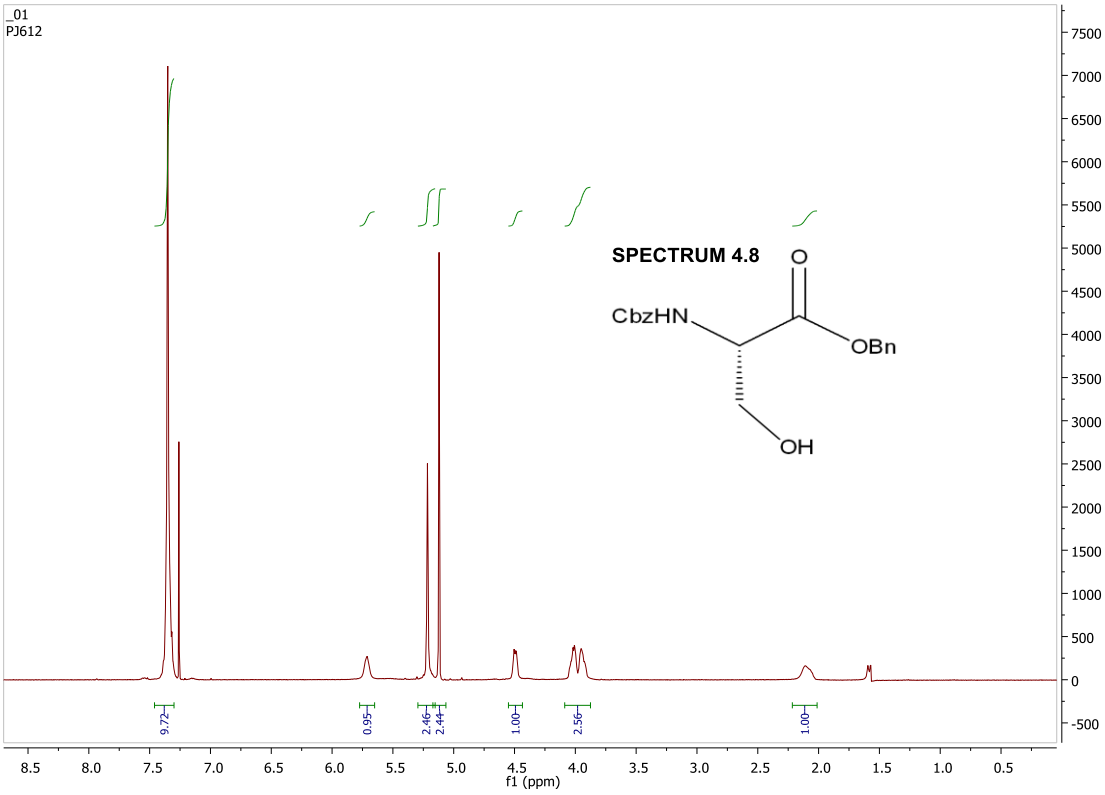
_01
PJ612
SPECTRUM 4.8
CbzHN
OBn
OH
f1 (ppm)

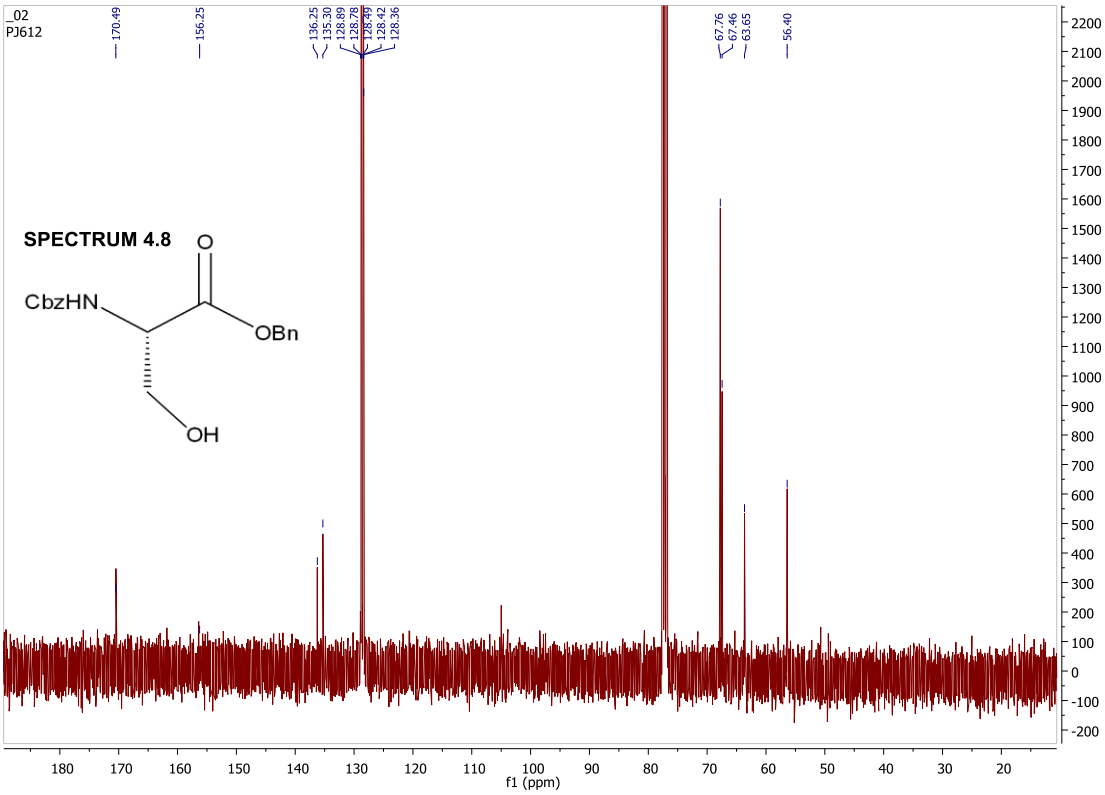
_02
PJ612
170.49
156.25
136.25
135.30
128.89
128.78
128.49
128.42
128.36
67.76
67.46
63.65
56.40
SPECTRUM 4.8
CbzHN
OBn
OH
f1 (ppm)

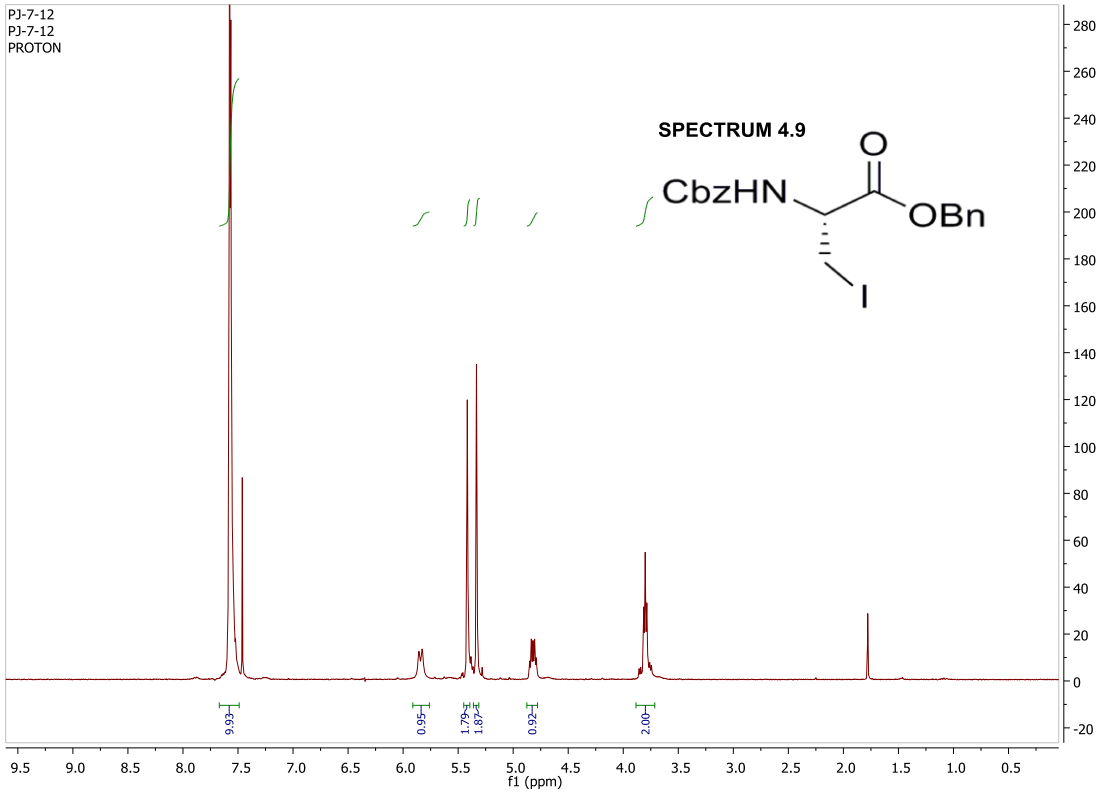
PJ-7-12
PJ-7-12
PROTON
SPECTRUM 4.9
CbzHN
O
OBn
I
9.93
0.95
1.79
1.87
0.92
2.00
f1 (ppm)

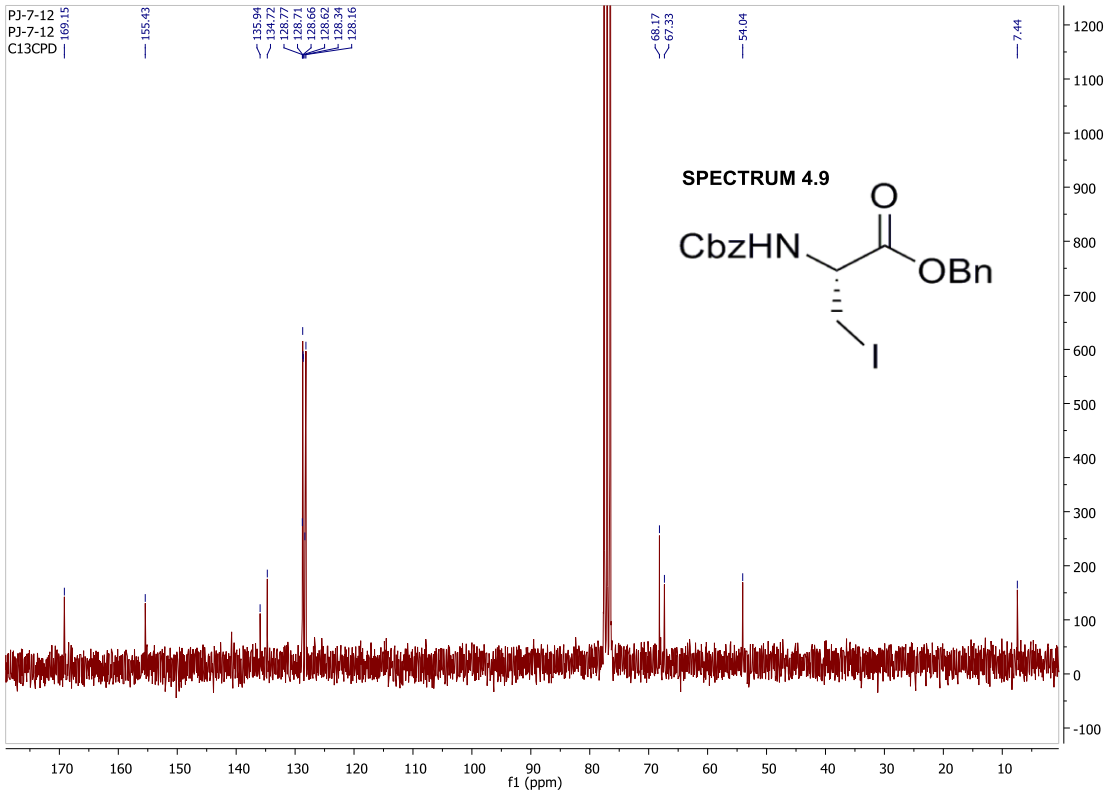
PJ-7-12
PJ-7-12
C13CPD
169.15
155.43
135.94
134.72
128.77
128.71
128.66
128.62
128.34
128.16
68.17
67.33
54.04
7.44
SPECTRUM 4.9
CbzHN
O
OBn
I
f1 (ppm)

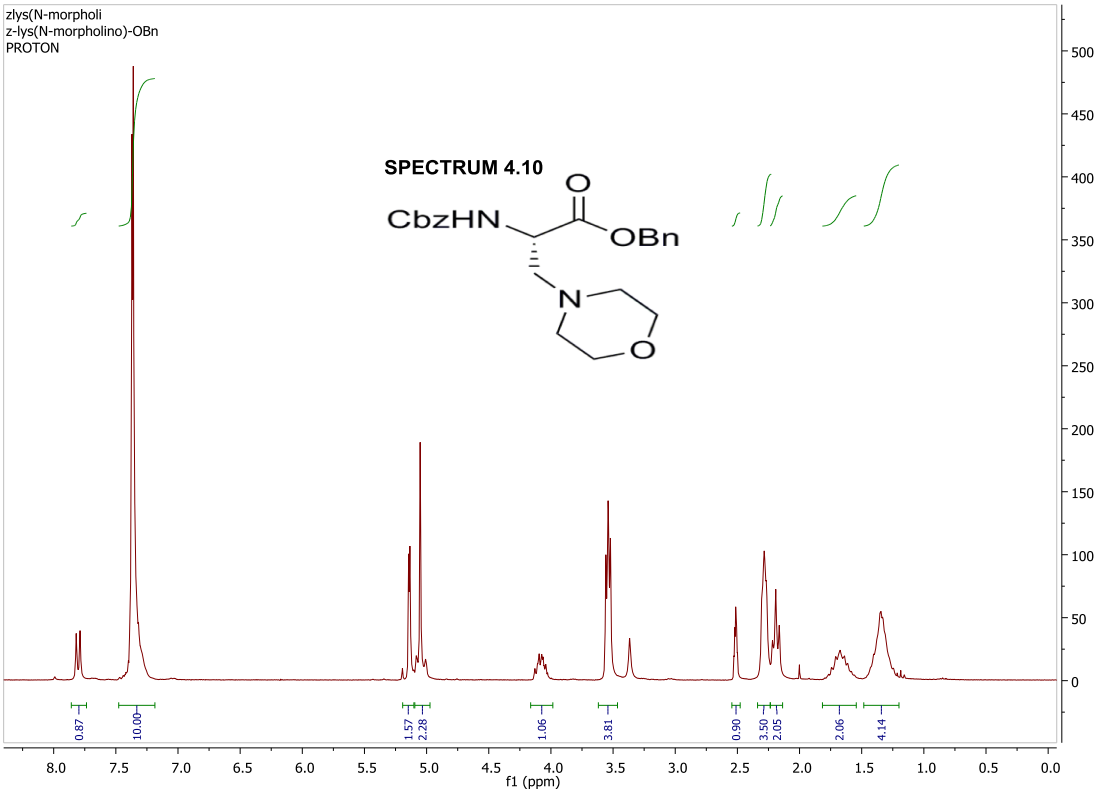
zlys(N-morpholi
z-lys(N-morpholino)-OBn
PROTON
SPECTRUM 4.10
CbzHN
OBn
N
O
f1 (ppm)

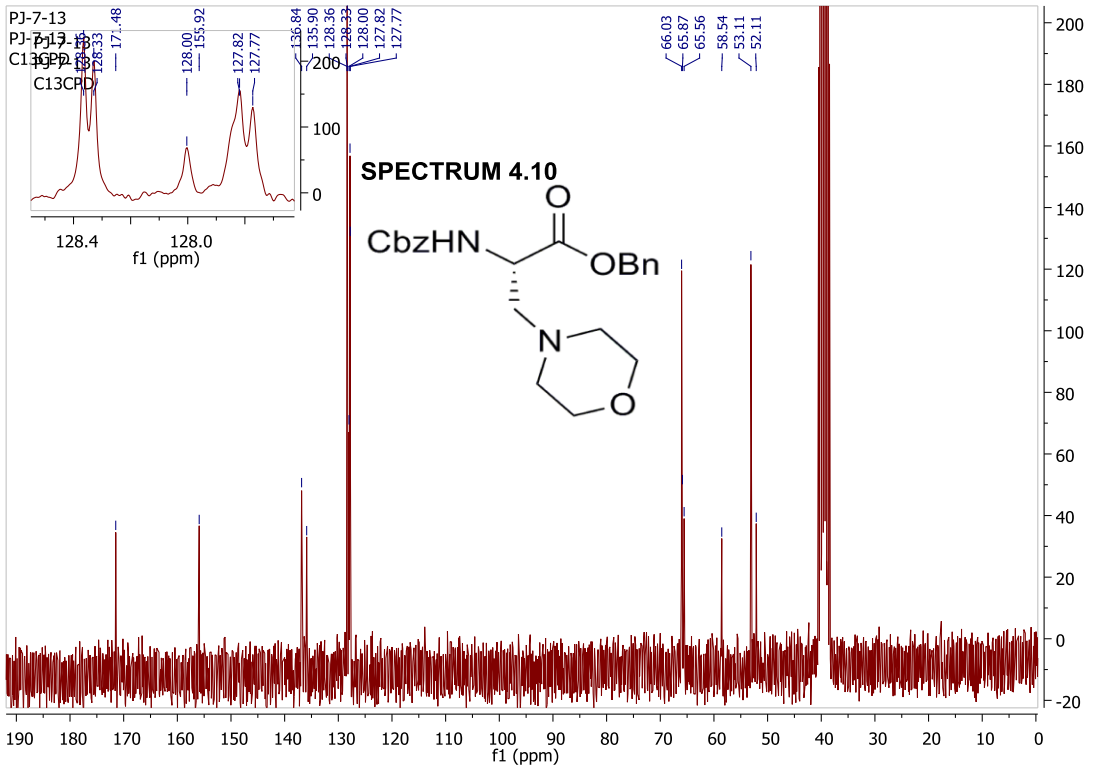
PJ-7-13
C13CPD
SPECTRUM 4.10
CbzHN
OBn
N
O
f1 (ppm)

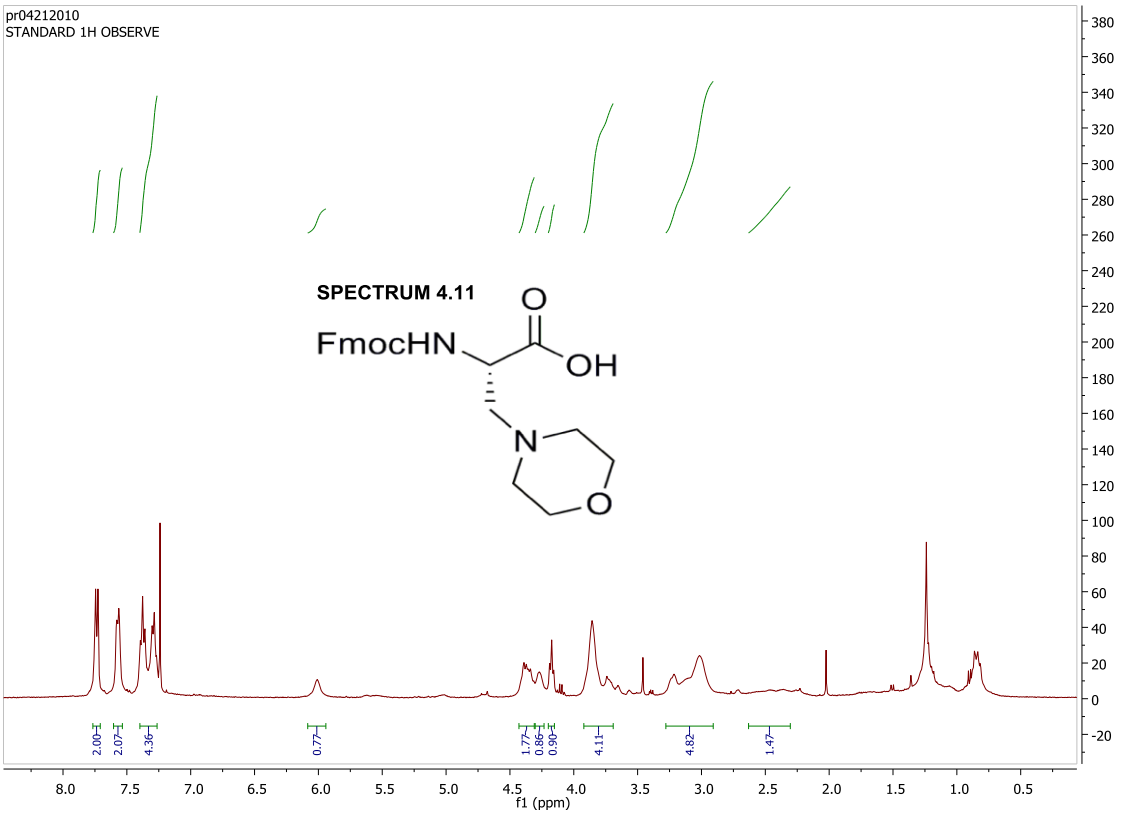
pr04212010
STANDARD 1H OBSERVE
SPECTRUM 4.11
FmocHN
OH
O
N
O
2.00
2.07
4.36
0.77
1.77
0.86
0.90
4.11
4.82
1.47
f1 (ppm)

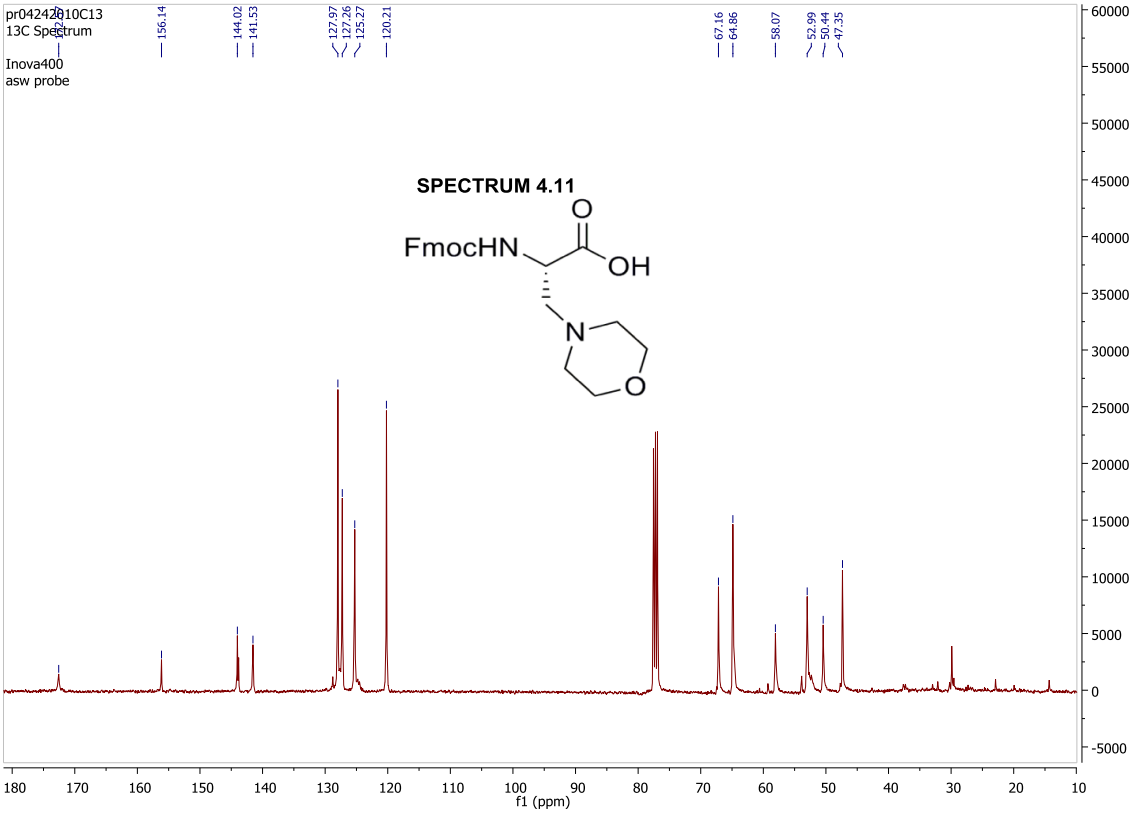
pr04242010C13
13C Spectrum
Inova400
asw probe
156.14
144.02
141.53
127.97
127.26
125.27
120.21
67.16
64.86
58.07
52.99
50.44
47.35
SPECTRUM 4.11
FmocHN
OH
O
N
O
f1 (ppm)

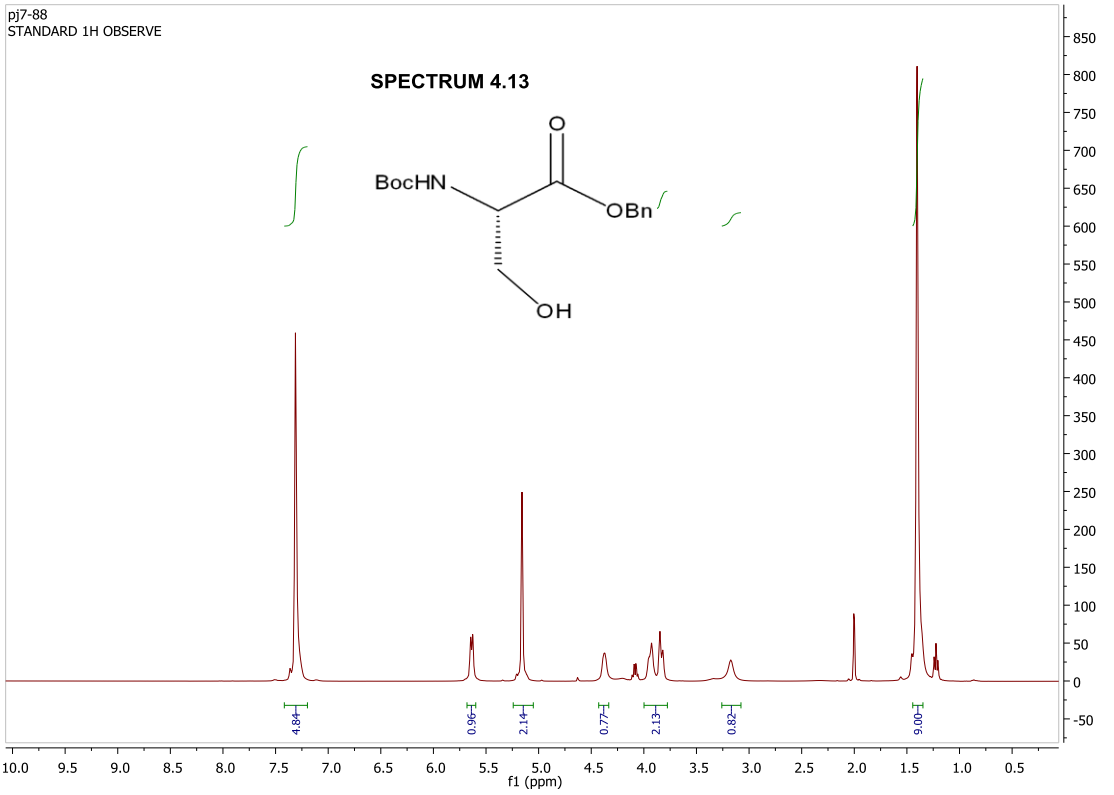
pj7-88
STANDARD 1H OBSERVE
SPECTRUM 4.13
BocHN
OBn
OH
4.84
0.96
2.14
0.77
2.13
0.82
9.00
f1 (ppm)

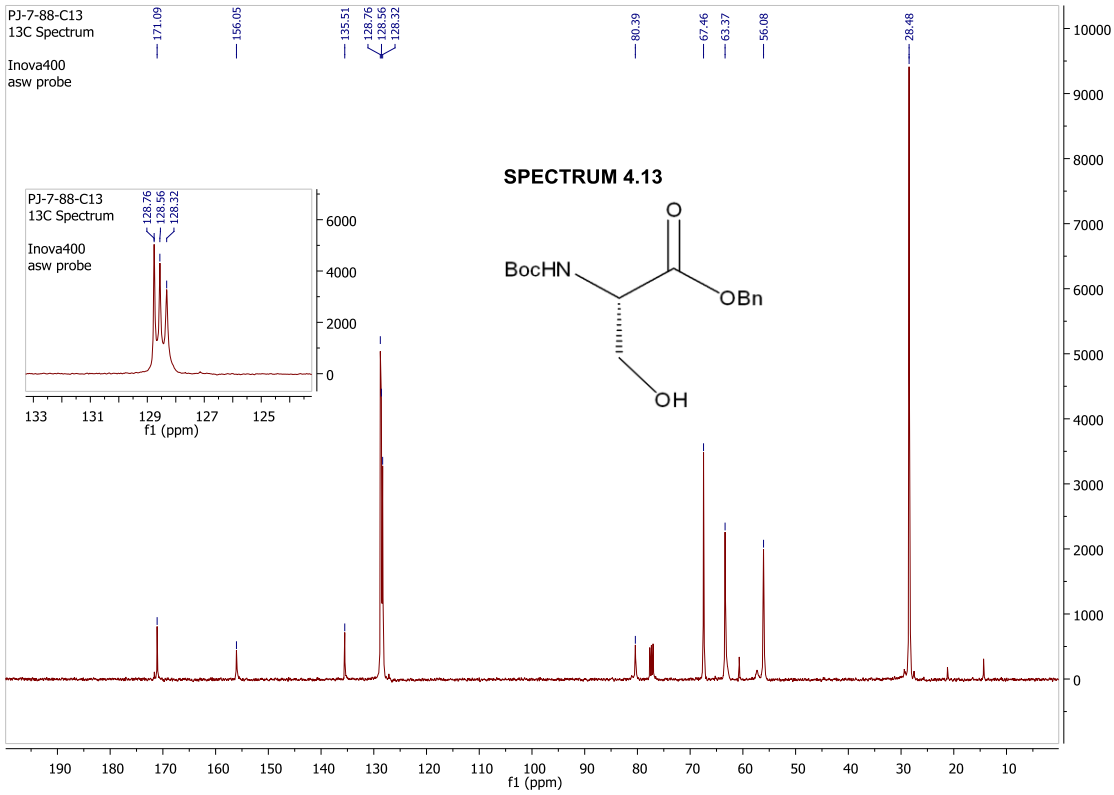
PJ-7-88-C13
13C Spectrum
Inova400
asw probe
171.09
156.05
135.51
128.76
128.56
128.32
80.39
67.46
63.37
56.08
28.48
SPECTRUM 4.13
BocHN
OBn
OH
f1 (ppm)

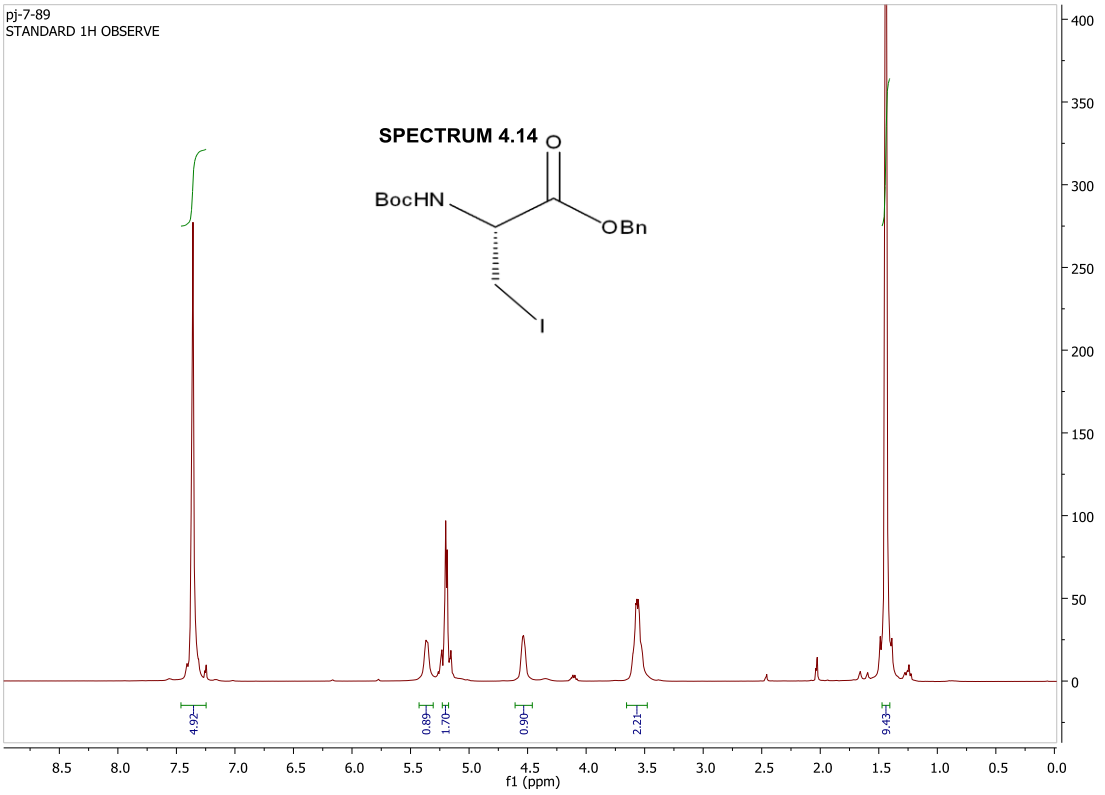
pj-7-89
STANDARD 1H OBSERVE
SPECTRUM 4.14
BocHN
OBn
I
4.92
0.89
1.70
0.90
2.21
9.43
f1 (ppm)

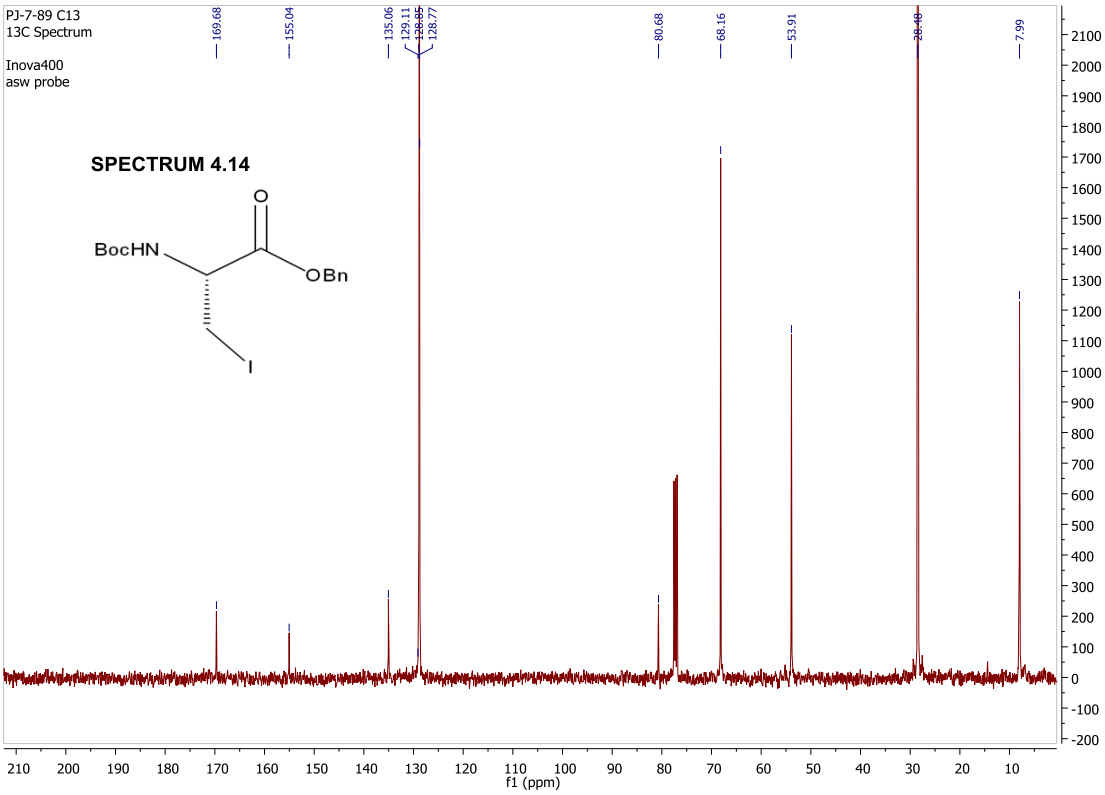
PJ-7-89 C13
13C Spectrum
Inova400
asw probe
169.68
155.04
135.06
129.11
128.77
80.68
68.16
53.91
28.48
7.99
SPECTRUM 4.14
BocHN
OBn
I
f1 (ppm)

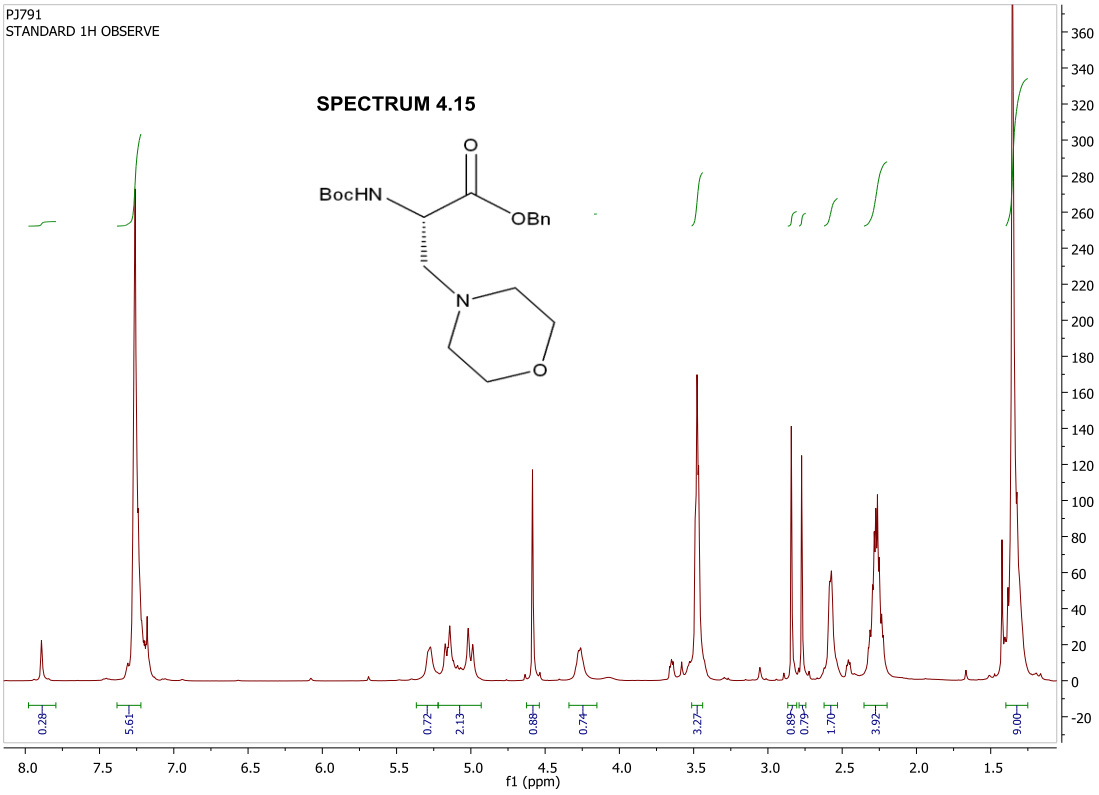
PJ791
STANDARD 1H OBSERVE
SPECTRUM 4.15
BocHN
OBn
N
O
O
0.28
5.61
0.72
2.13
0.88
0.74
3.27
0.89
0.79
1.70
3.92
9.00
f1 (ppm)

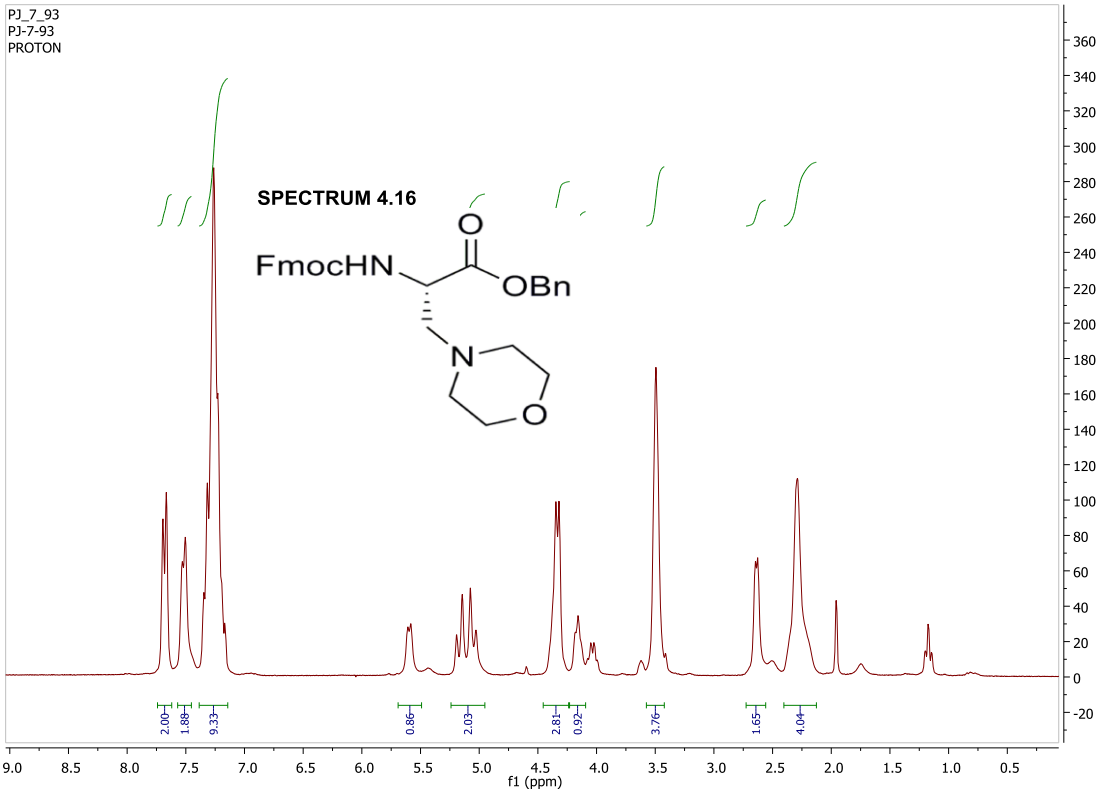
PJ_7_93
PJ-7-93
PROTON
SPECTRUM 4.16
FmocHN
OBn
O
N
O
2.00
1.88
9.33
0.86
2.03
2.81
0.92
3.76
1.65
4.04
f1 (ppm)

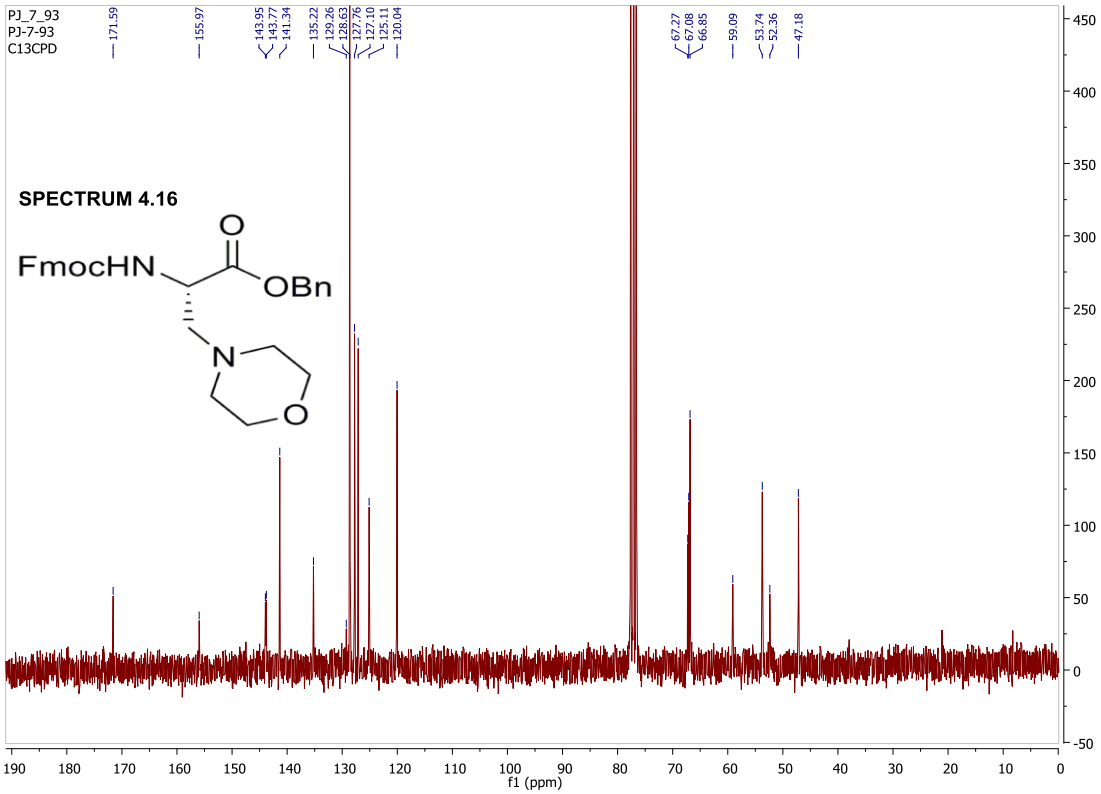
PJ_7_93
PJ-7-93
C13CPD
171.59
155.97
143.95
143.77
141.34
135.22
129.26
128.63
127.76
127.10
125.11
120.04
67.27
67.08
66.85
59.09
53.74
52.36
47.18
SPECTRUM 4.16
FmocHN
OBn
O
N
O
f1 (ppm)

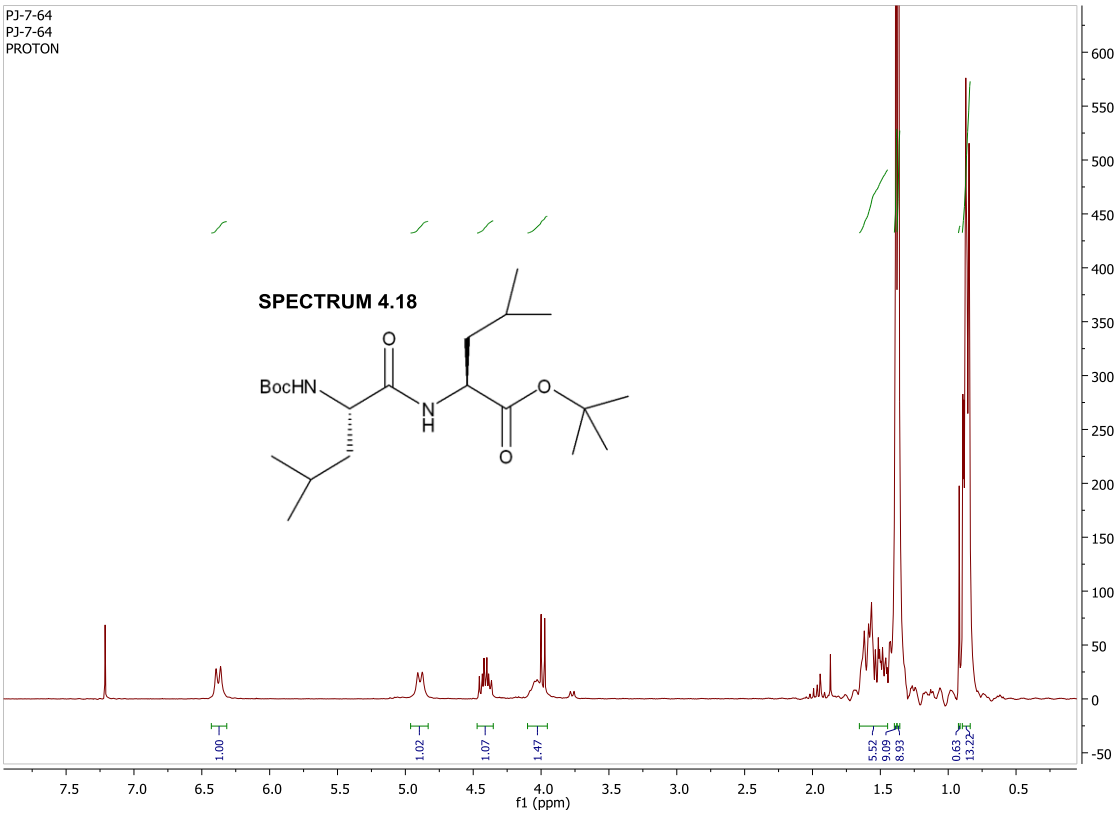
PJ-7-64
PJ-7-64
PROTON
SPECTRUM 4.18
BocHN
O
N
H
O
O
1.00
1.02
1.07
1.47
5.52
9.09
8.93
0.63
13.22
f1 (ppm)

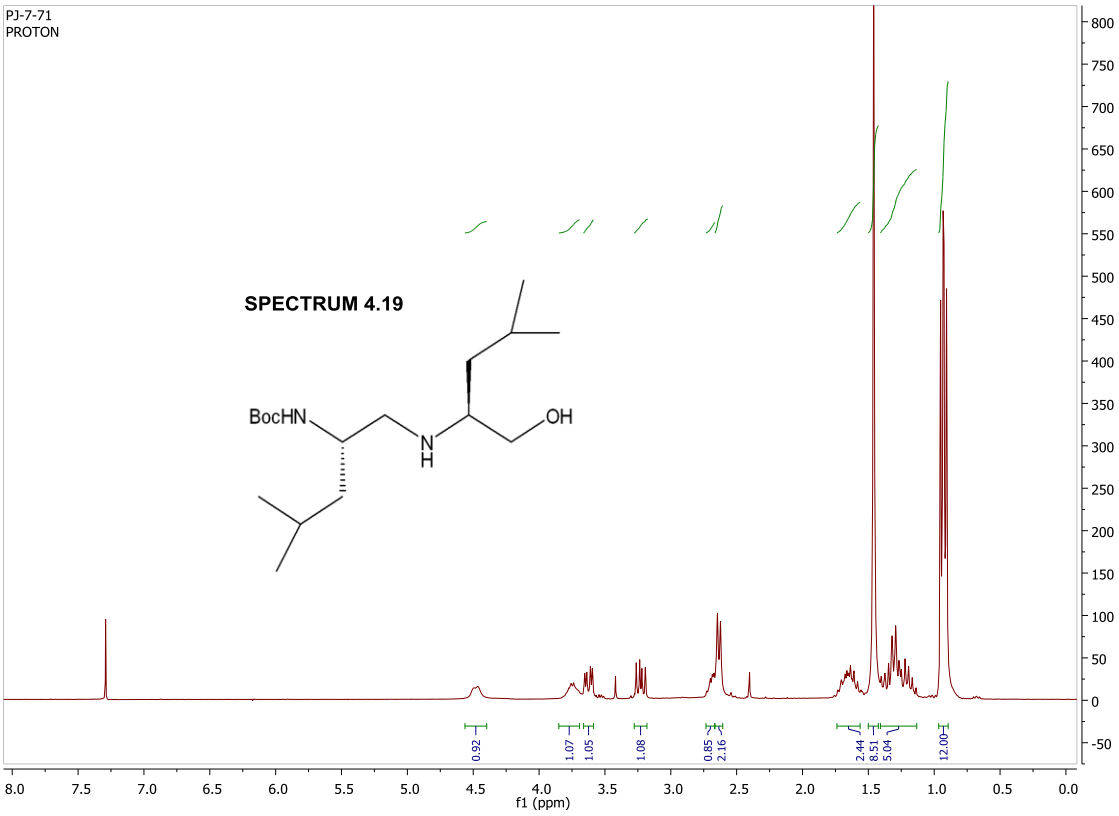
PJ-7-71
PROTON
SPECTRUM 4.19
BocHN
OH
N
H
0.92
1.07
1.05
1.08
0.85
2.16
2.44
8.51
5.04
12.00
f1 (ppm)

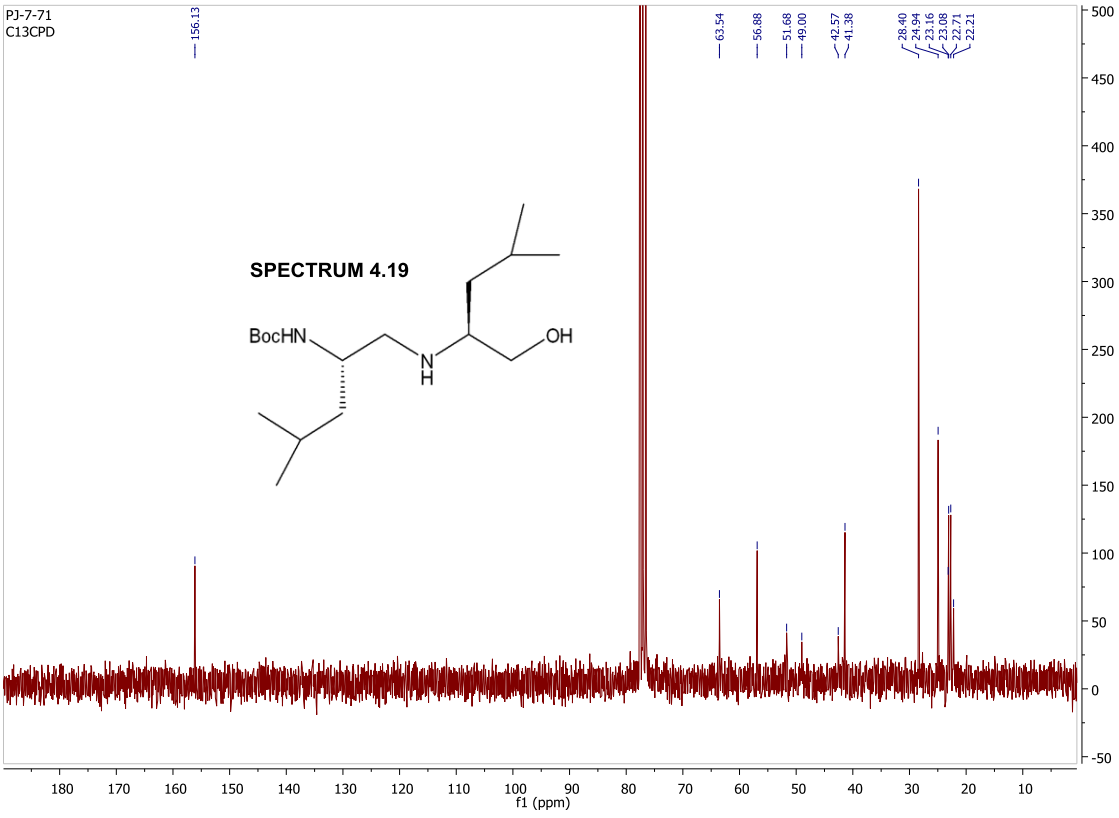
PJ-7-71
C13CPD
156.13
63.54
56.88
51.68
49.00
42.57
41.38
28.40
24.94
23.16
23.08
22.71
22.21
SPECTRUM 4.19
BocHN
OH
N
H
f1 (ppm)

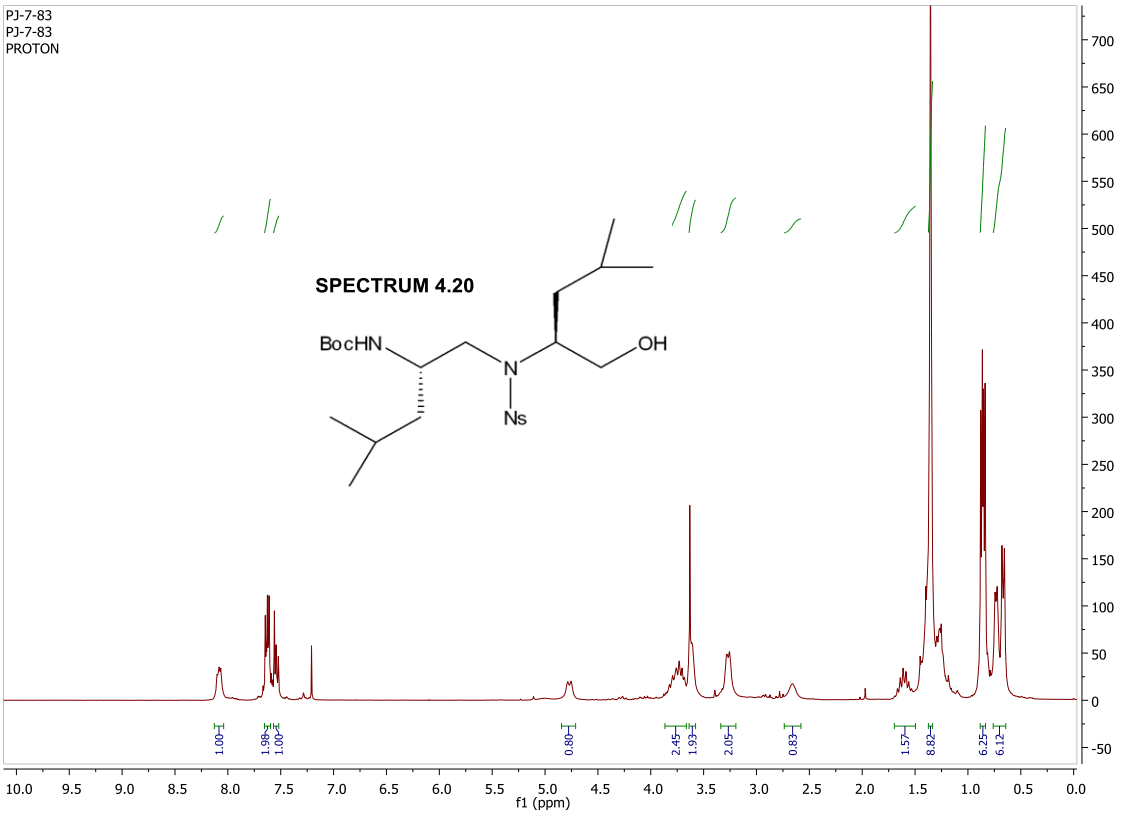
PJ-7-83
PJ-7-83
PROTON
SPECTRUM 4.20
BocHN
N
OH
Ns
1.00
1.98
1.00
0.80
2.45
1.93
2.05
0.83
1.57
8.82
6.25
6.12
f1 (ppm)

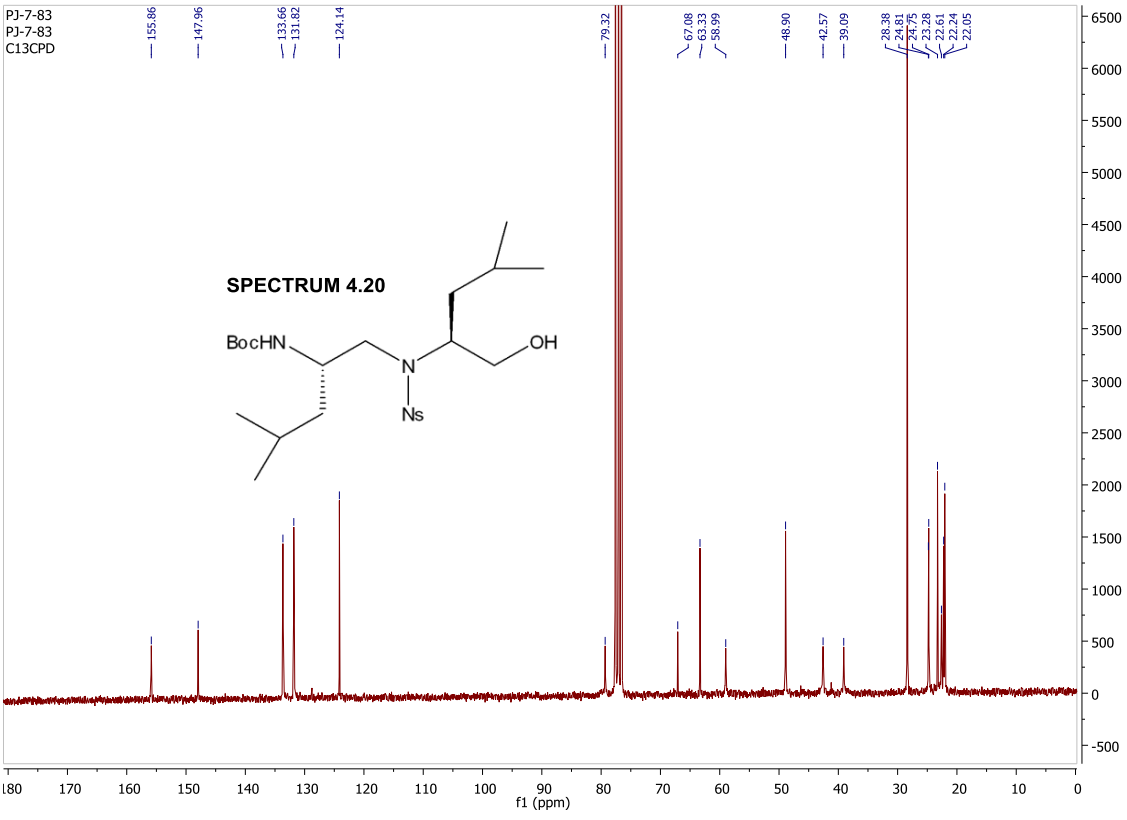
PJ-7-83
PJ-7-83
C13CPD
155.86
147.96
133.66
131.82
124.14
79.32
67.08
63.33
58.99
48.90
42.57
39.09
28.38
24.81
24.75
23.28
22.61
22.24
22.05
SPECTRUM 4.20
BocHN
N
OH
Ns
f1 (ppm)

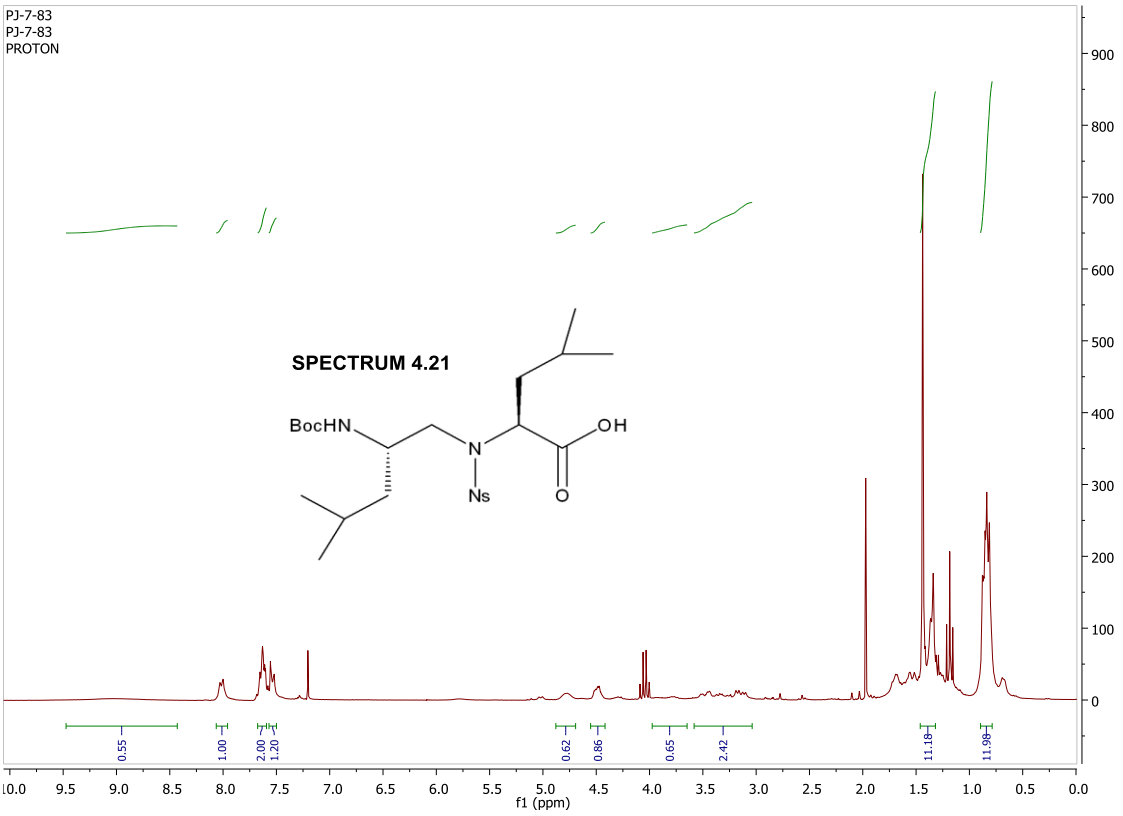
PJ-7-83
PJ-7-83
PROTON
SPECTRUM 4.21
BocHN
N
Ns
OH
O
0.55
1.00
2.00
1.20
0.62
0.86
0.65
2.42
11.18
11.90
f1 (ppm)

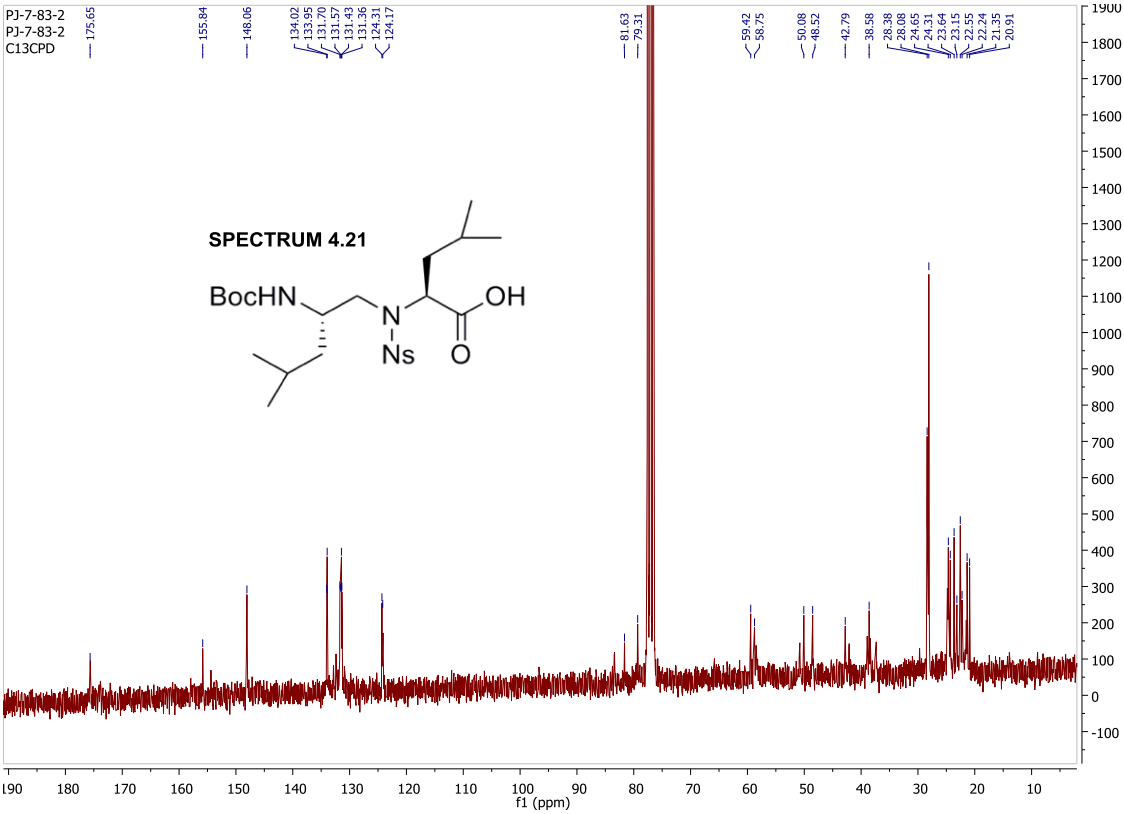
PJ-7-83-2
PJ-7-83-2
C13CPD
175.65
155.84
148.06
134.02
133.95
131.70
131.57
131.43
131.36
124.31
124.17
81.63
79.31
59.42
58.75
50.08
48.52
42.79
38.58
28.38
28.08
24.65
24.31
23.64
23.15
22.55
22.24
21.35
20.91
SPECTRUM 4.21
BocHN
N
Ns
OH
O
f1 (ppm)

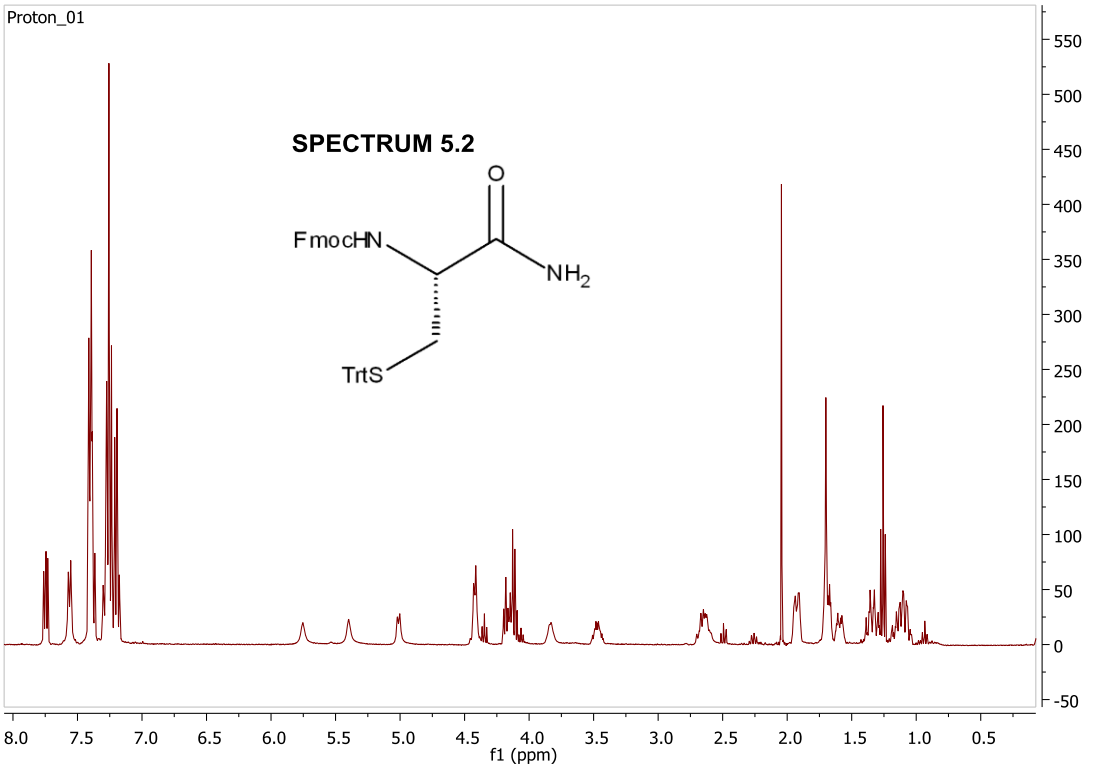
Proton_01
SPECTRUM 5.2
FmocHN
O
NH2
TrtS
550
500
450
400
350
300
250
200
150
100
50
0
-50
8.0
7.5
7.0
6.5
6.0
5.5
5.0
4.5
4.0
3.5
3.0
2.5
2.0
1.5
1.0
0.5
f1 (ppm)

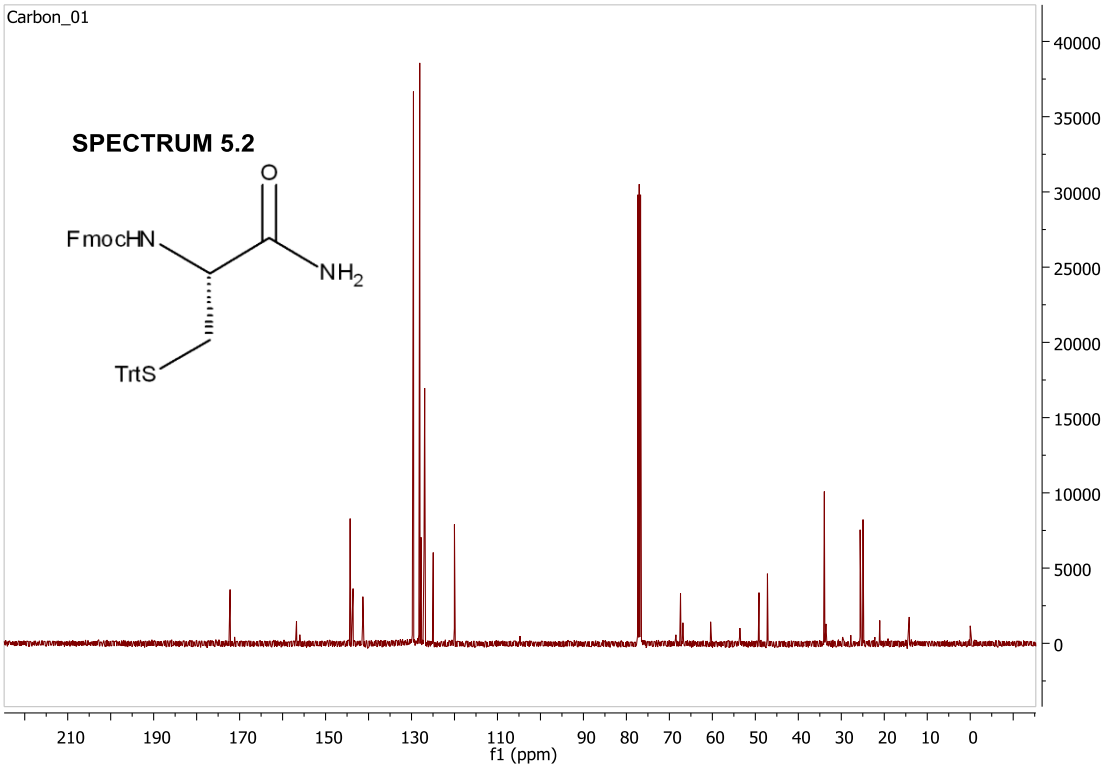
Carbon_01
SPECTRUM 5.2
FmocHN
O
NH2
TrtS
40000
35000
30000
25000
20000
15000
10000
5000
0
210
190
170
150
130
110
90
80
70
60
50
40
30
20
10
0
f1 (ppm)

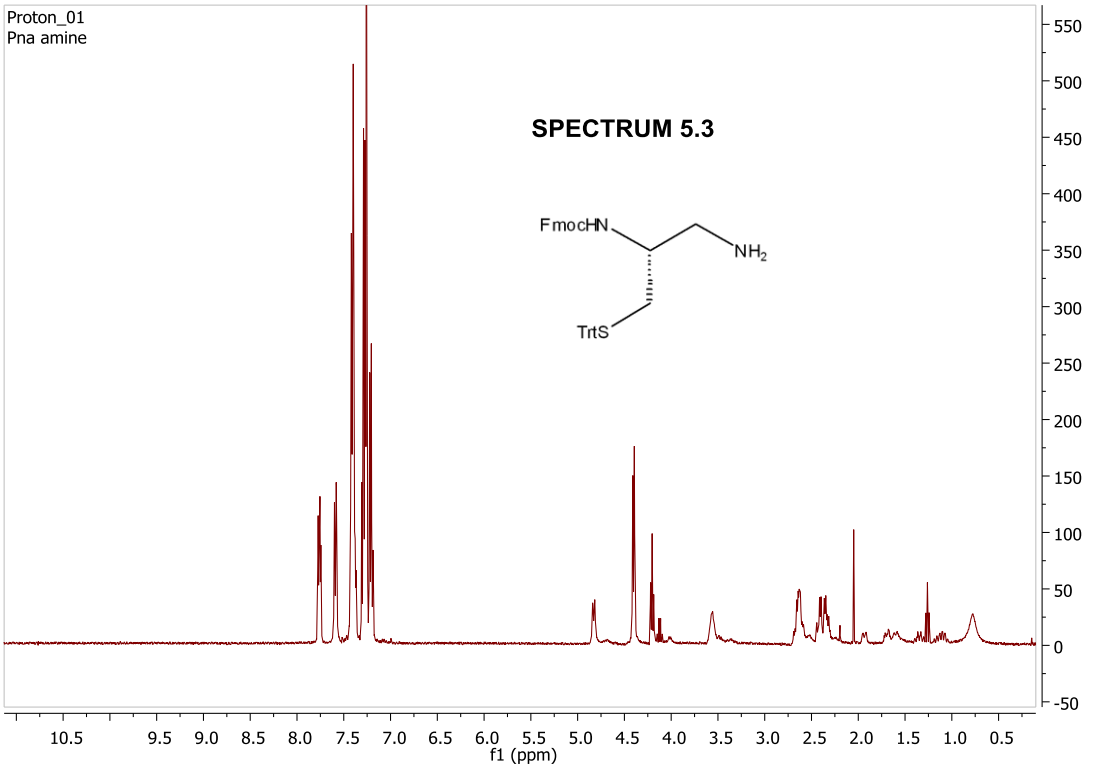
Proton_01
Pna amine
SPECTRUM 5.3
FmocHN
NH2
TrtS
f1 (ppm)

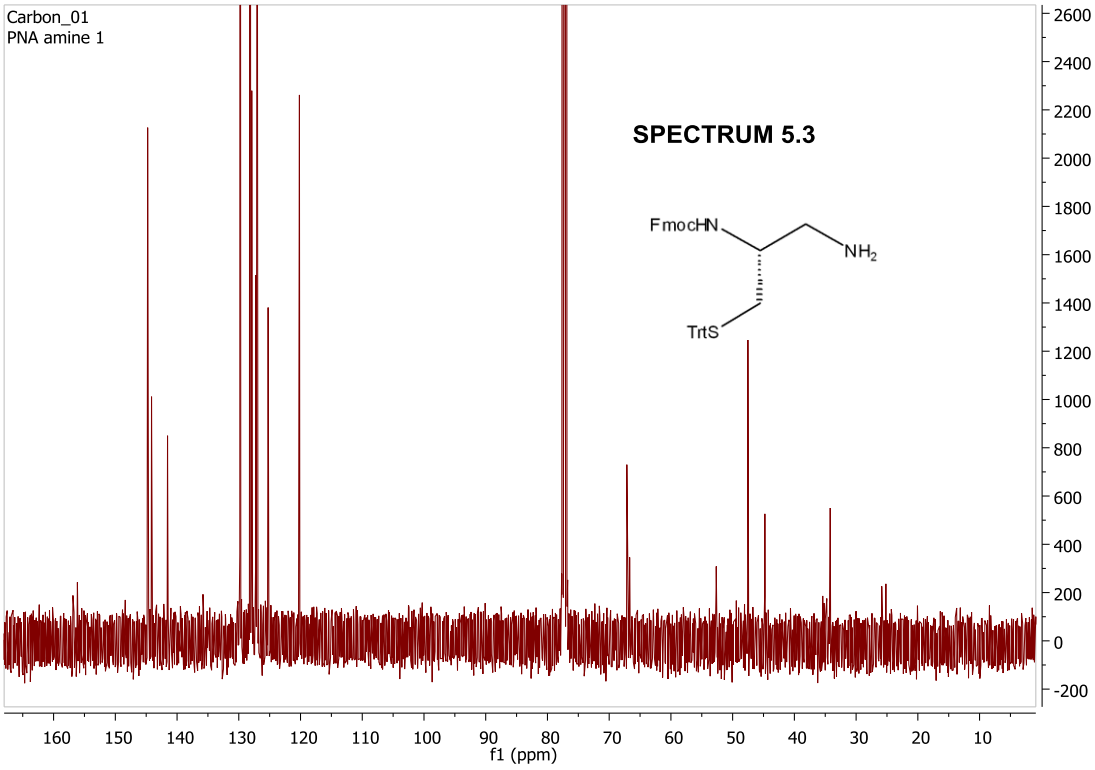
Carbon_01
PNA amine 1
SPECTRUM 5.3
FmocHN
NH2
TrtS
f1 (ppm)

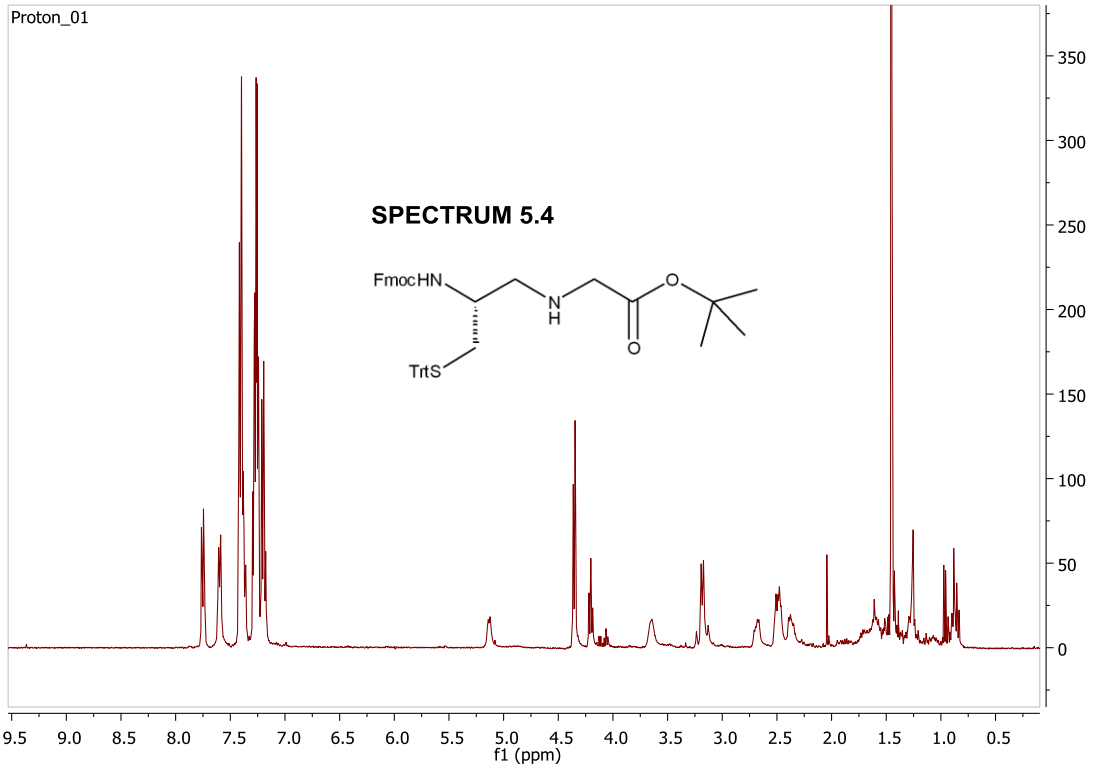
Proton_01
SPECTRUM 5.4
FmocHN
N
H
O
O
TrtS
350
300
250
200
150
100
50
0
9.5 9.0 8.5 8.0 7.5 7.0 6.5 6.0 5.5 5.0 4.5 4.0 3.5 3.0 2.5 2.0 1.5 1.0 0.5
f1 (ppm)

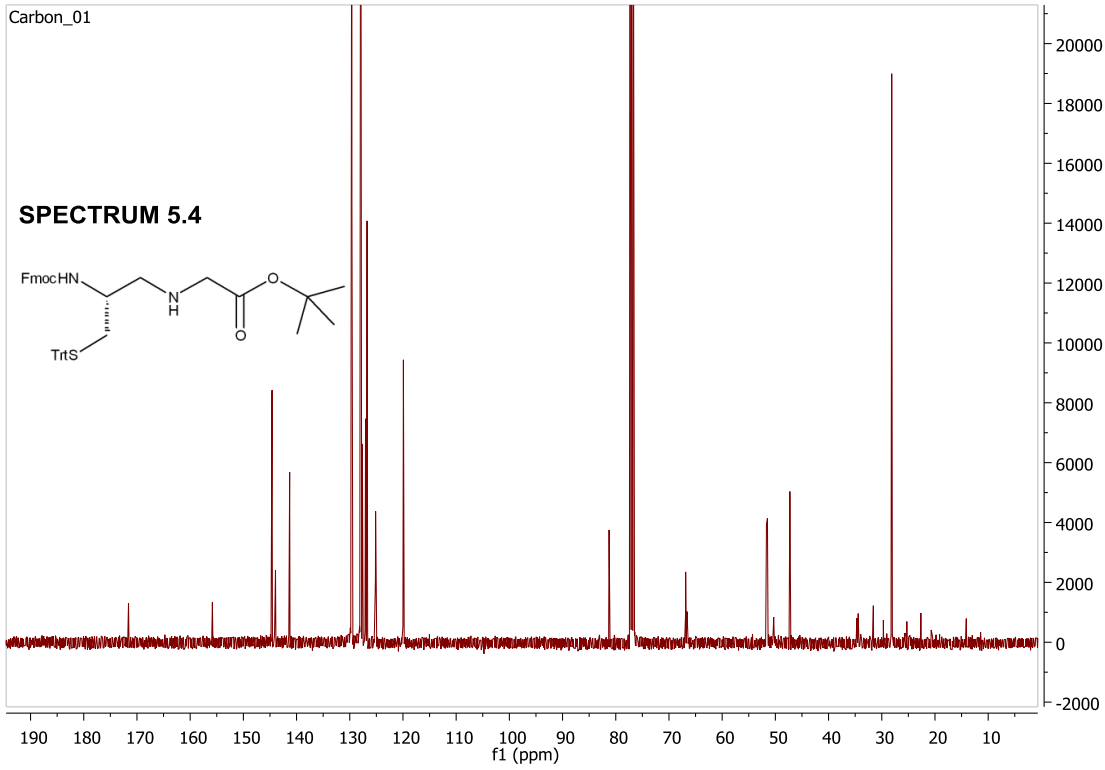
Carbon_01
SPECTRUM 5.4
FmocHN
N
H
O
O
TrtS
20000
18000
16000
14000
12000
10000
8000
6000
4000
2000
0
-2000
190 180 170 160 150 140 130 120 110 100 90 80 70 60 50 40 30 20 10
f1 (ppm)

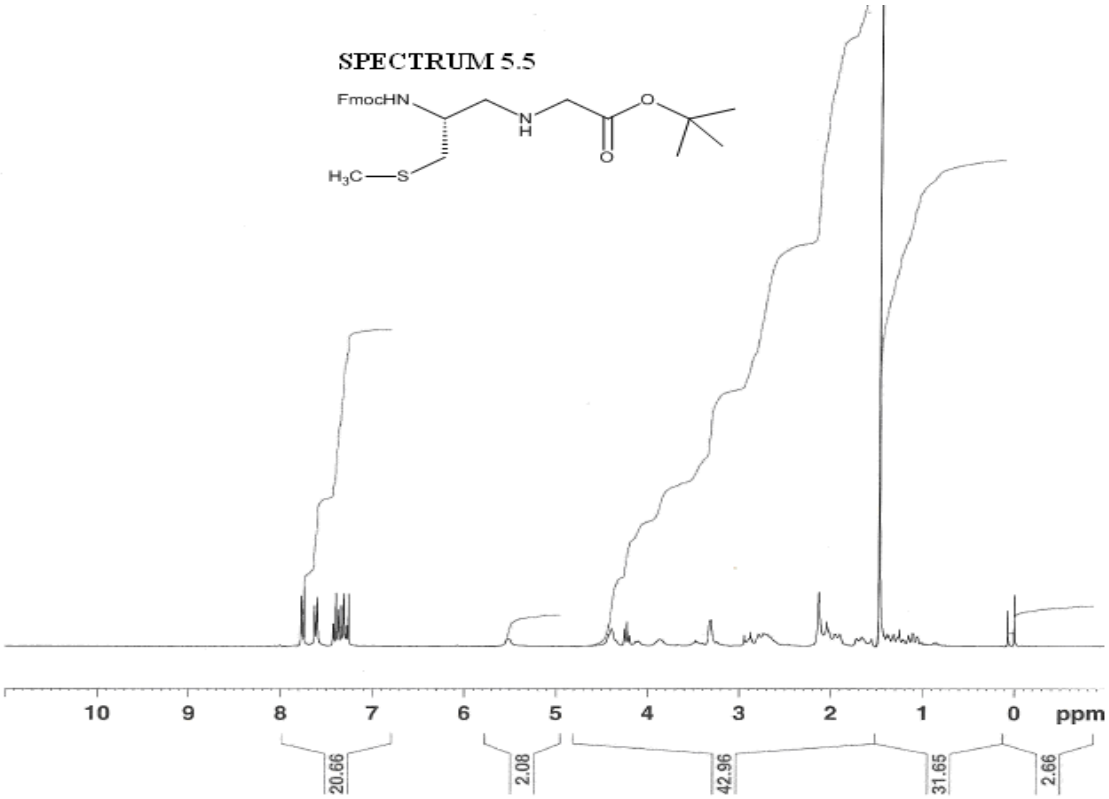

fmoc-smethylation-pj-3-10
C13CPD

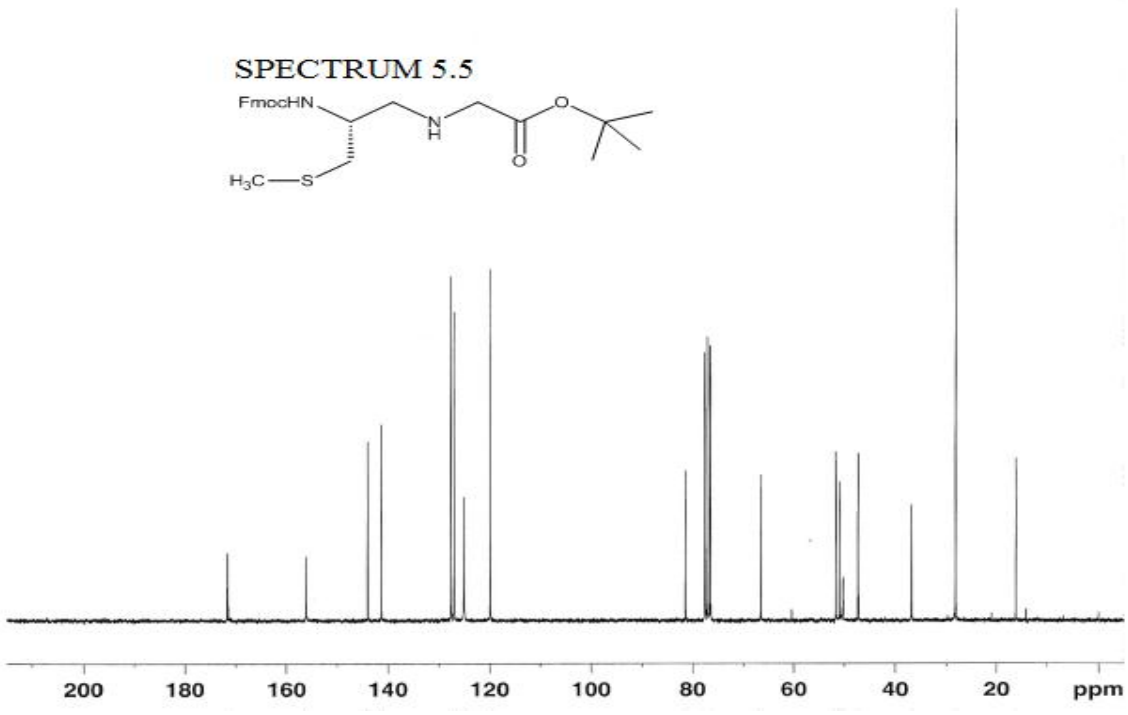

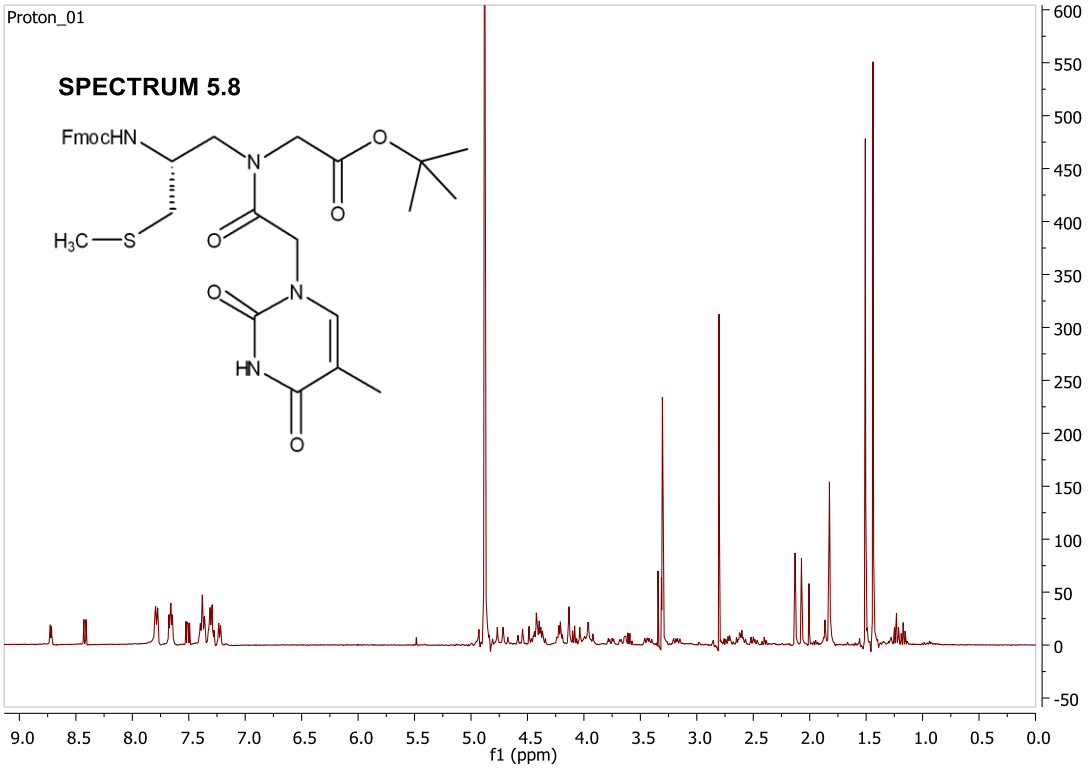
Proton_01
SPECTRUM 5.8
FmocHN
N
O
O
H3C
S
O
O
N
HN
O
600
550
500
450
400
350
300
250
200
150
100
50
0
-50
9.0
8.5
8.0
7.5
7.0
6.5
6.0
5.5
5.0
4.5
4.0
3.5
3.0
2.5
2.0
1.5
1.0
0.5
0.0
f1 (ppm)

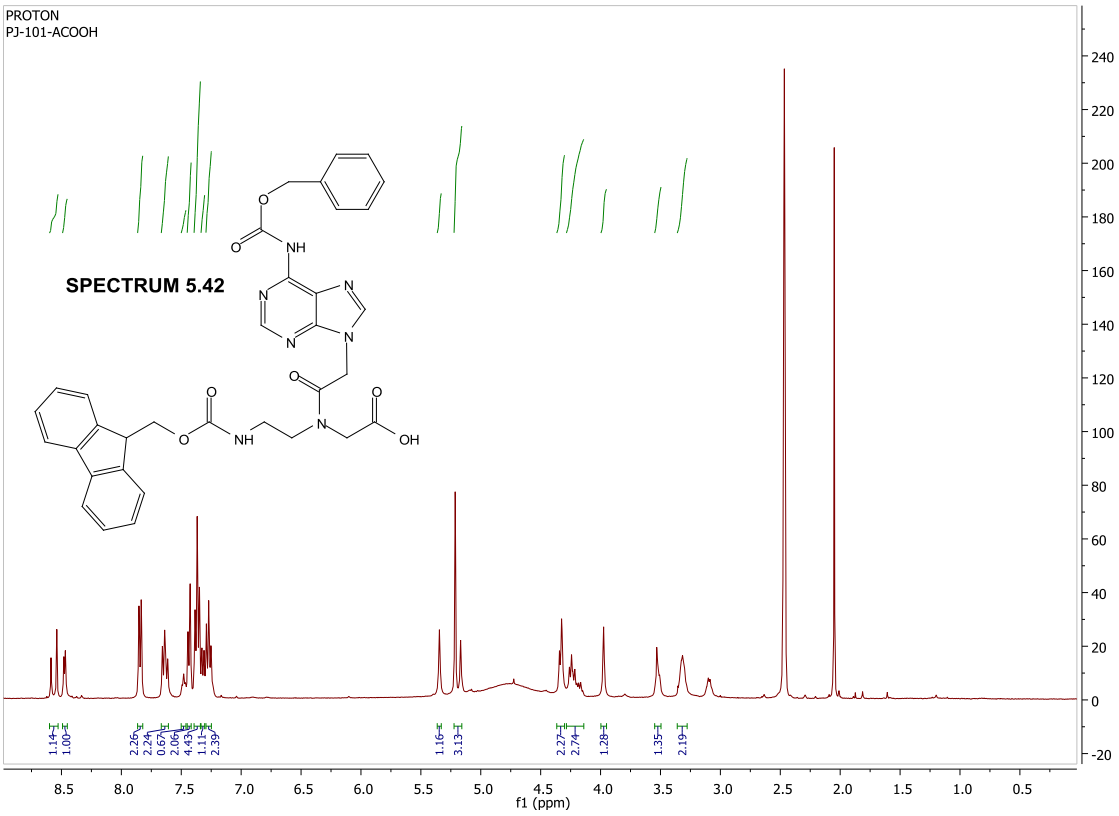
PROTON
PJ-101-ACOOH
SPECTRUM 5.42
f1 (ppm)

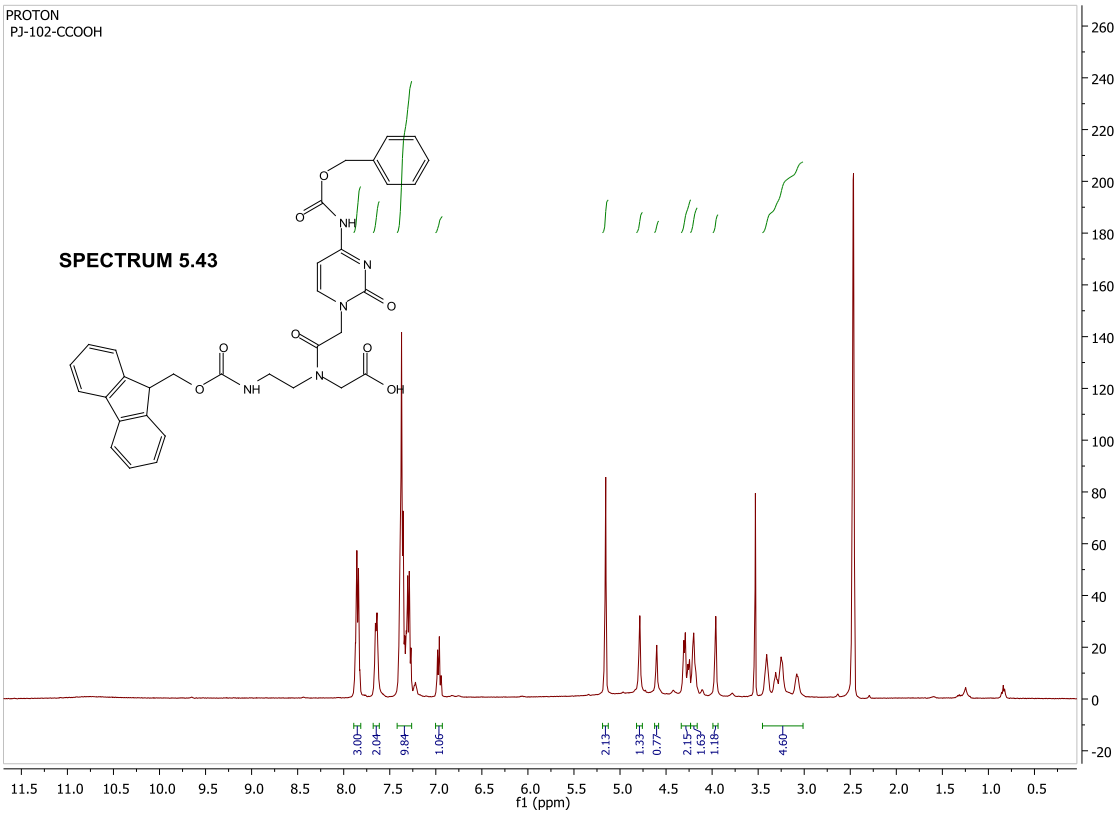
PROTON
PJ-102-CCOOH
SPECTRUM 5.43
f1 (ppm)

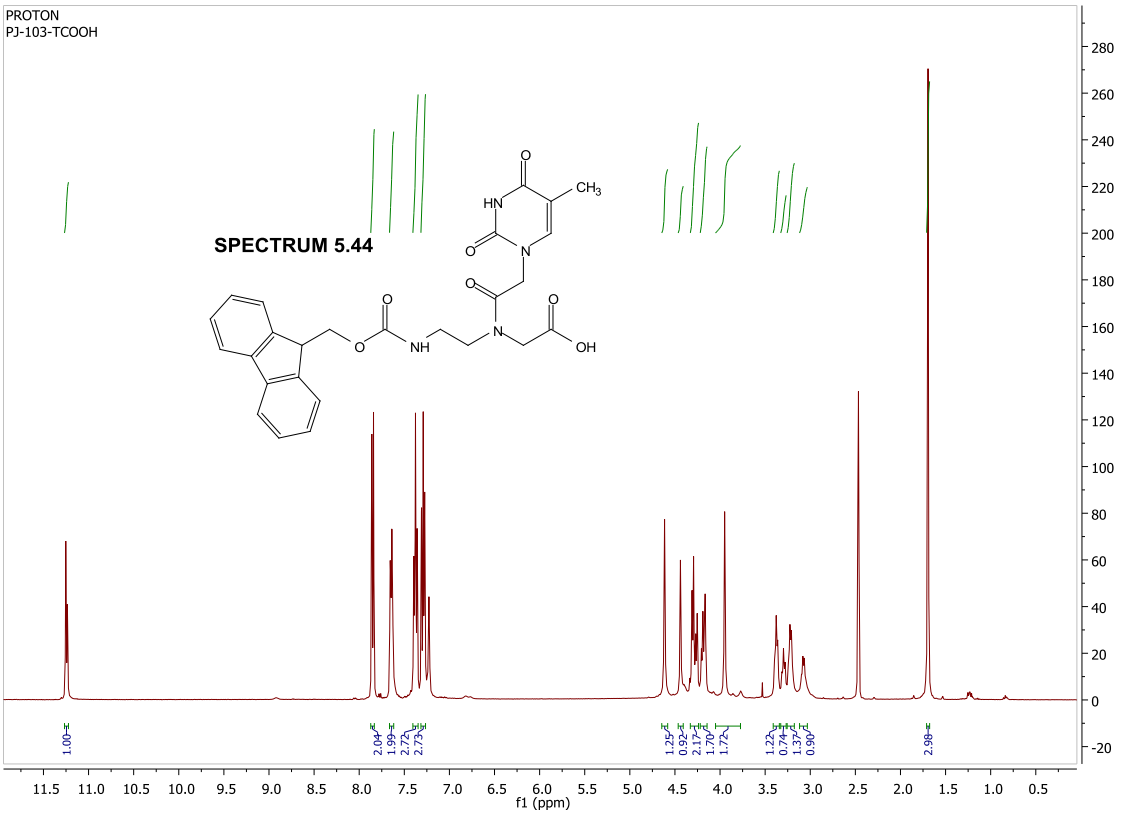
PROTON
PJ-103-TCOOH
SPECTRUM 5.44
f1 (ppm)

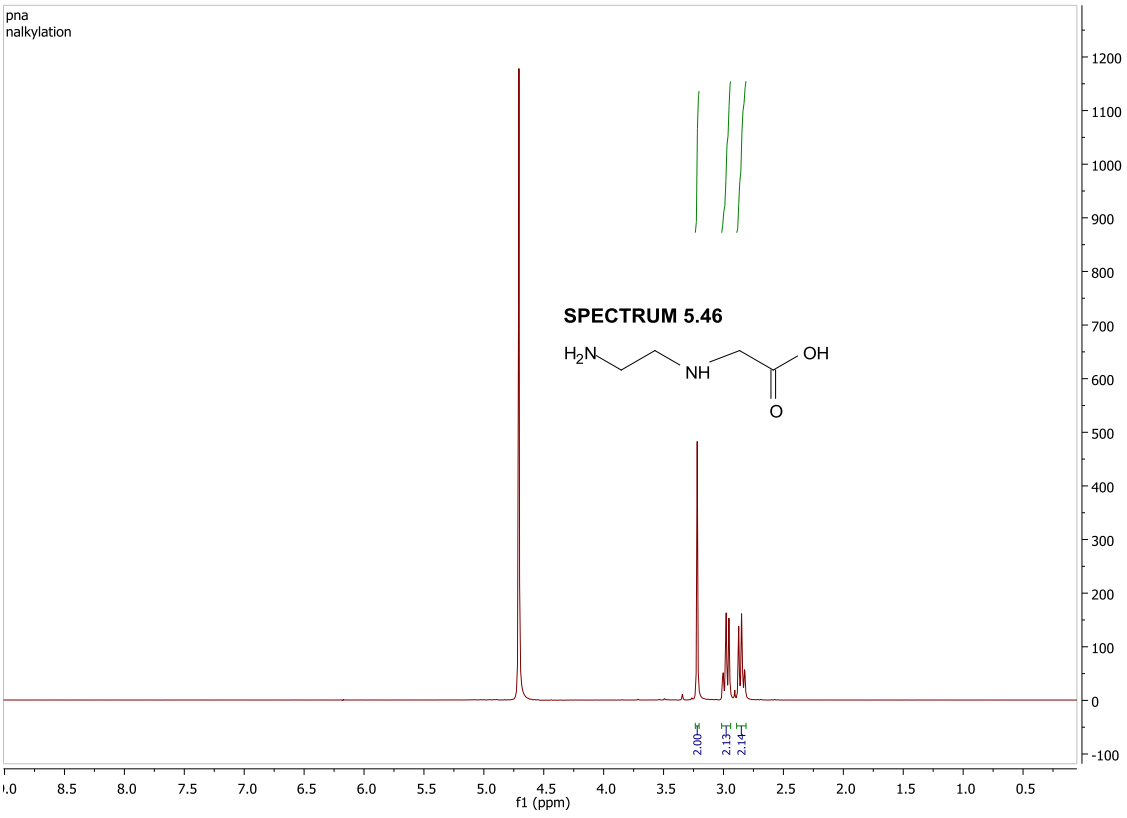
pna
nalkylation
SPECTRUM 5.46
f1 (ppm)

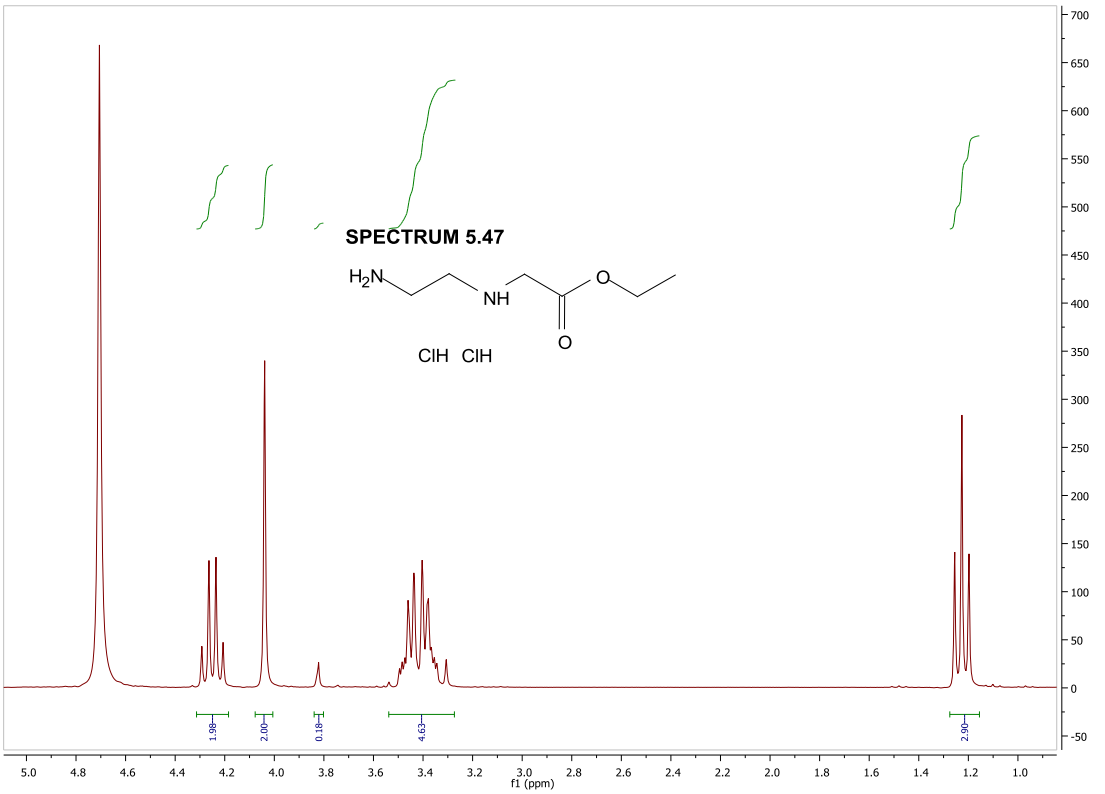
SPECTRUM 5.47
H2N
NH
O
O
ClH ClH
1.98
2.00
0.18
4.63
2.90
f1 (ppm)

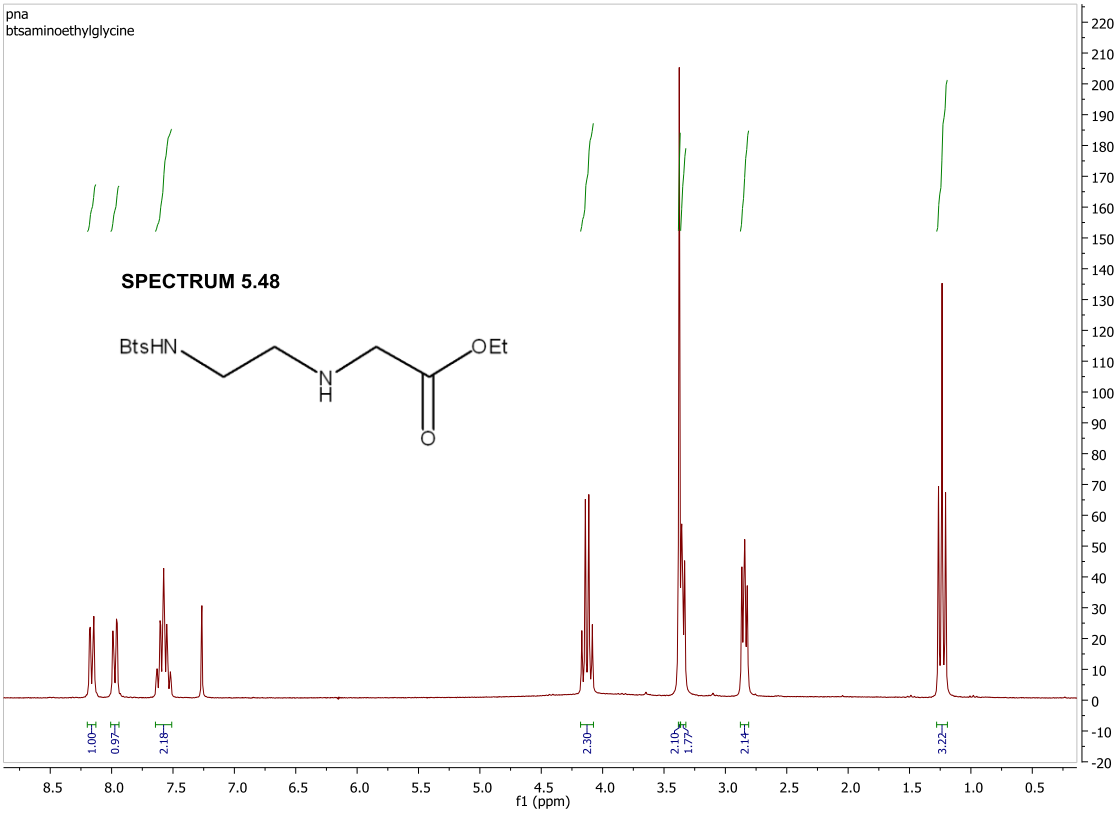
pna
btsaminoethylglycine
SPECTRUM 5.48
BtsHN
N
H
OEt
O
1.00
0.97
2.18
2.30
2.10
1.77
2.14
3.22
f1 (ppm)

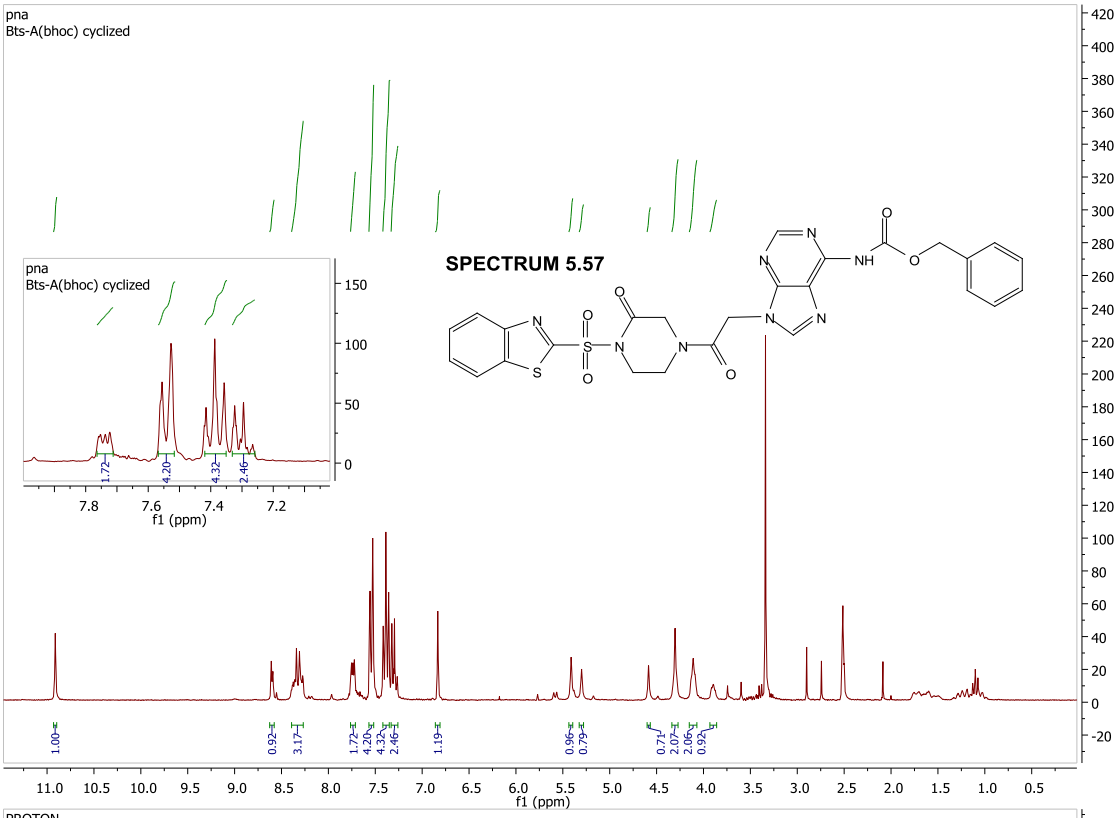
pna
Bts-A(bhoc) cyclized
SPECTRUM 5.57
f1 (ppm)

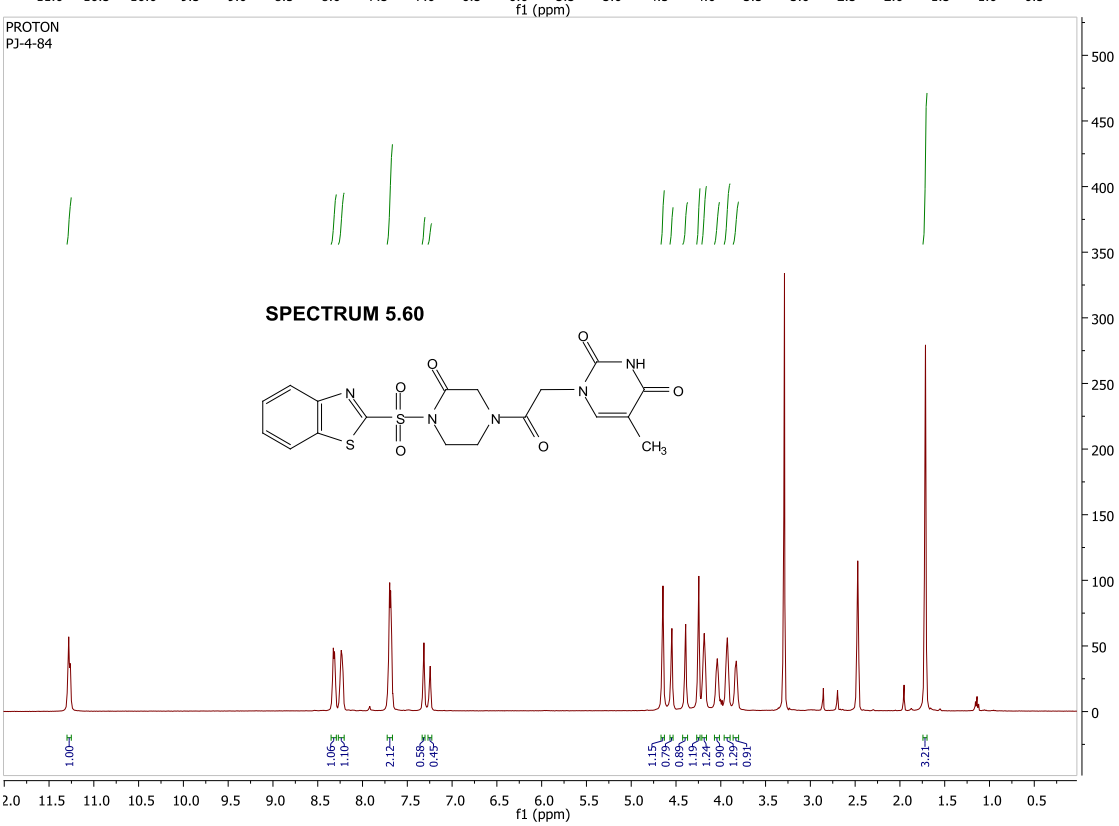
PROTON
PJ-4-84
SPECTRUM 5.60
f1 (ppm)

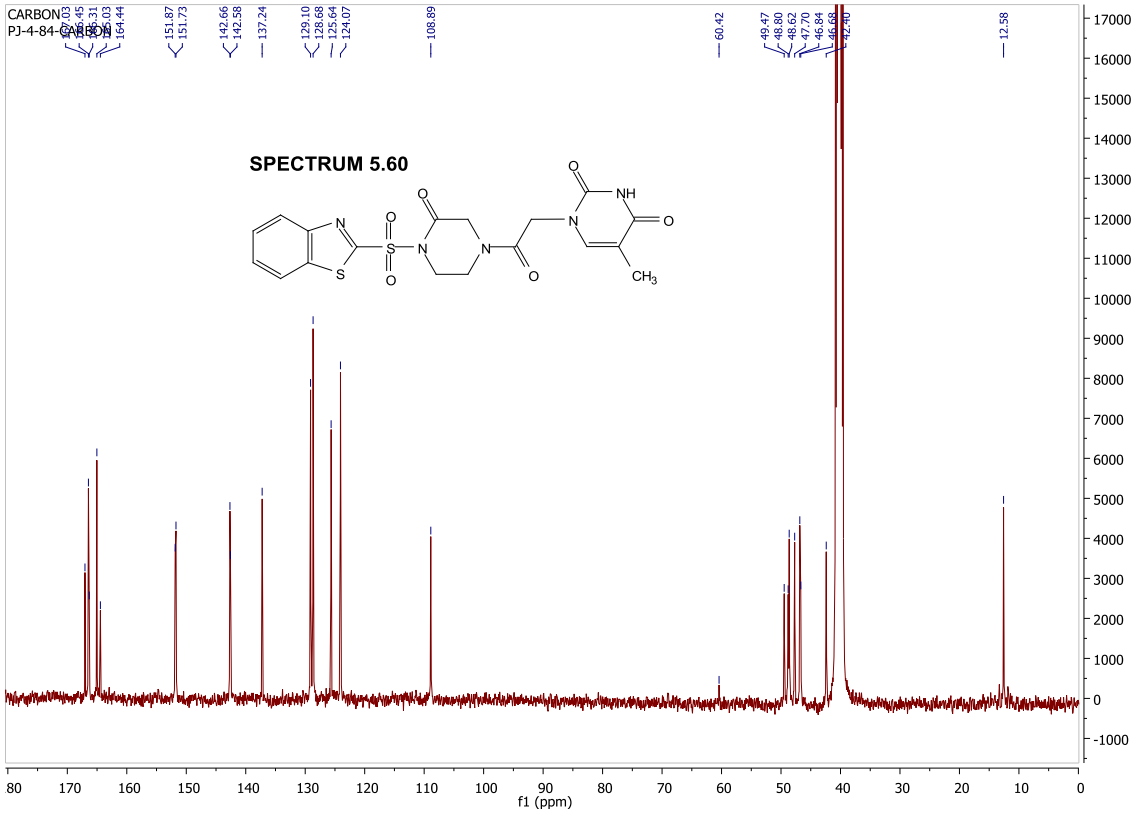
CARBON
PJ-4-84-CARBON
SPECTRUM 5.60
f1 (ppm)

Peptide 2.17

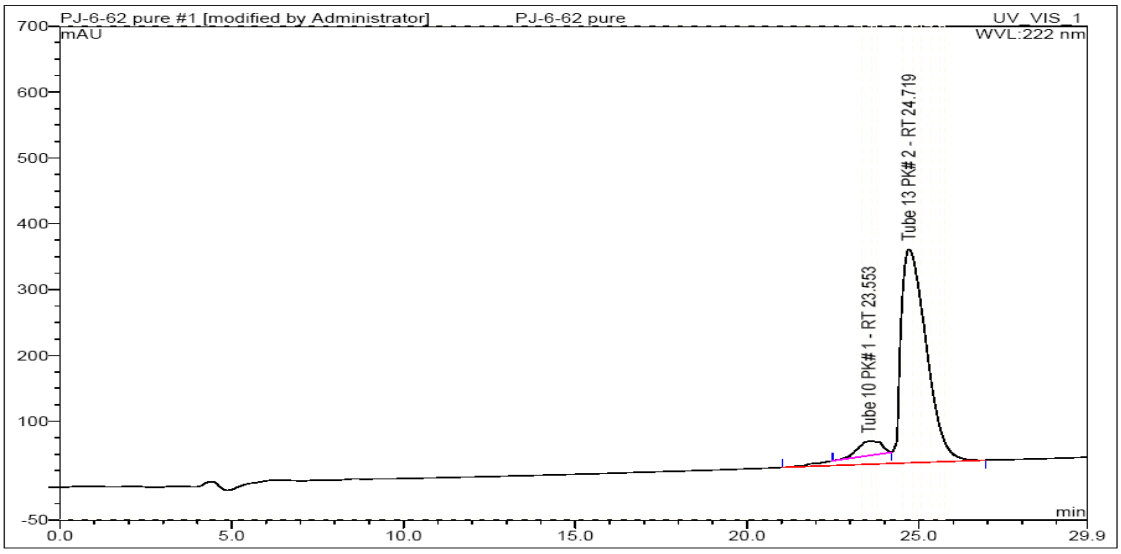

No.	Ret.Time min	Peak Name	Height mAU	Area mAU*min		Rel.Area %	Amount
1	23.55	n.a.	21.705	17.462		5.49	n.a.
2	24.72	n.a.	324.450	300.424		94.51	n.a.
Total:			346.154	317.886	100.00	0.000	

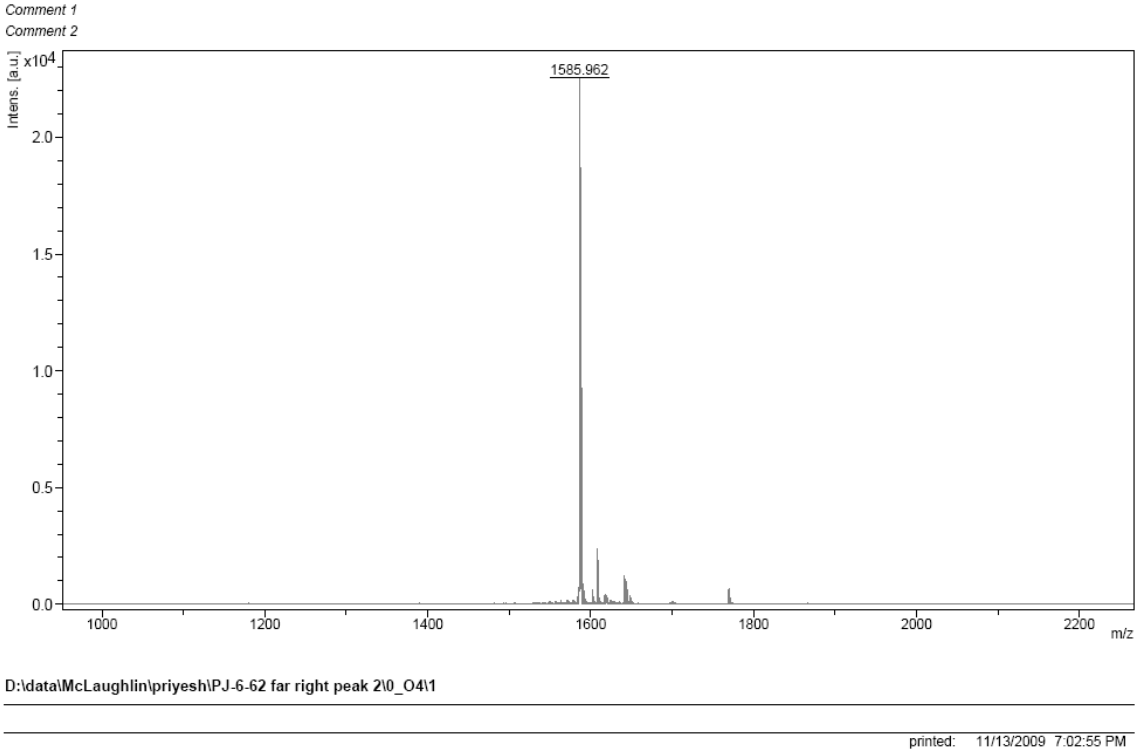

Peptide 2.1

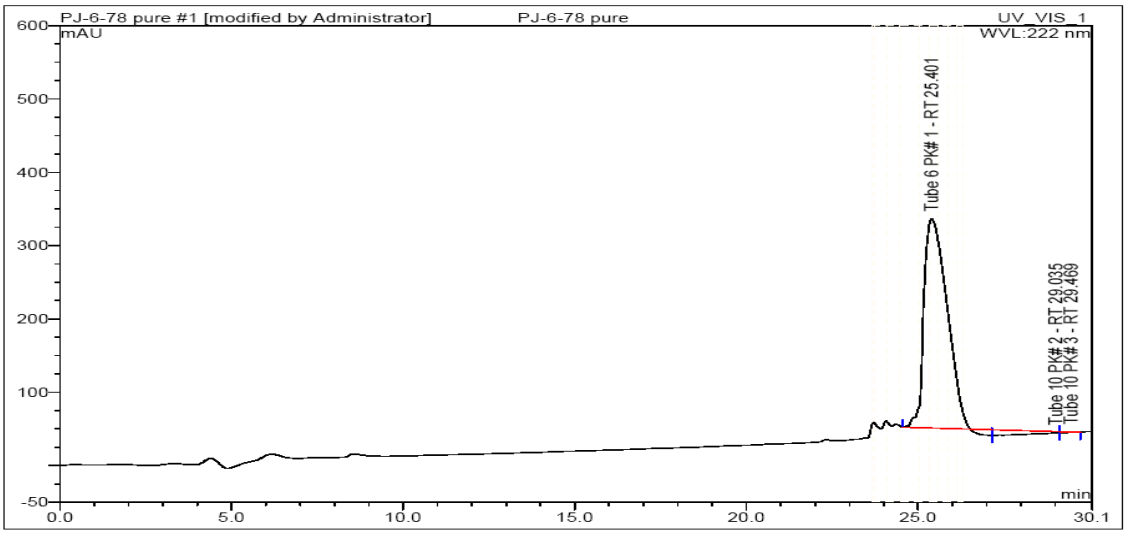

No.	Ret.Time min	Peak Name	Height mAU	Area mAU*min		Rel.Area %	Amount
1	25.40	n.a.	285.280	220.421		95.71	n.a.
2	29.03	n.a.	1.506	9.488		4.12	n.a.
3	29.47	n.a.	0.153	0.382		0.17	n.a.
Total:			286.940	230.291	100.00	0.000	

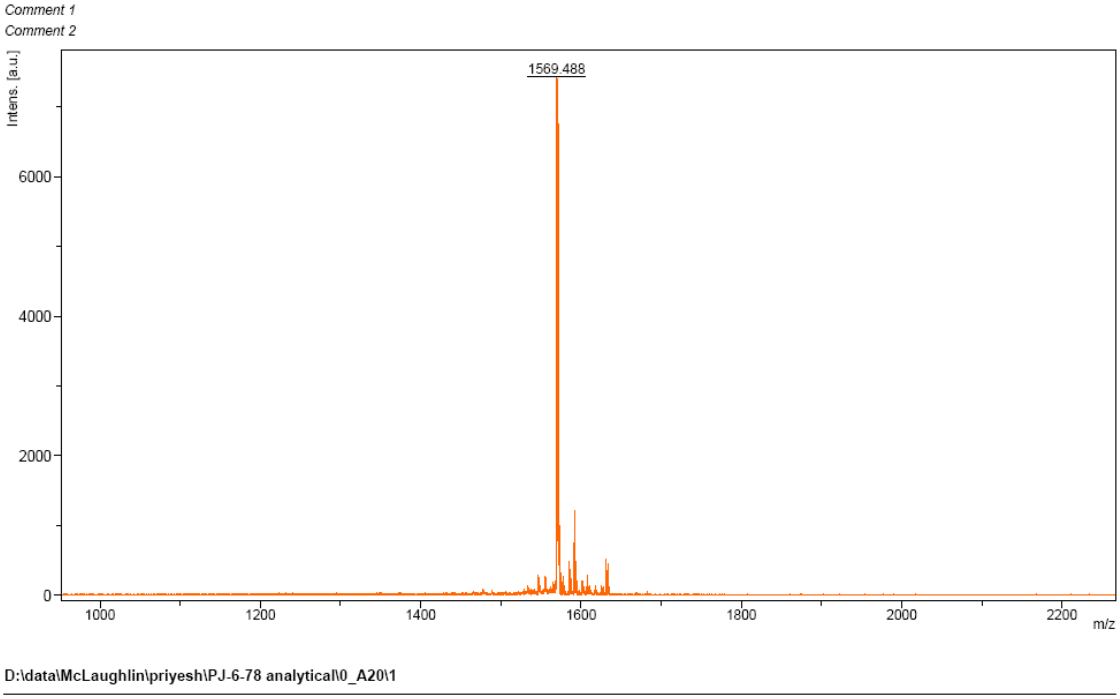

Peptide 2.2

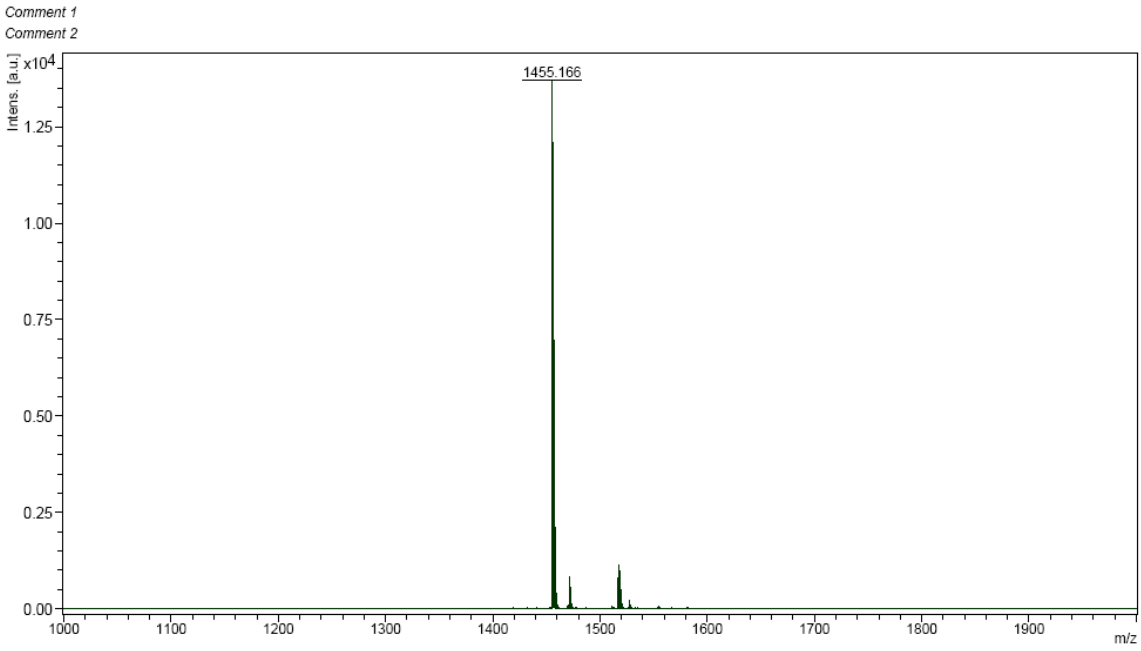
Comment 1
Comment 2
Intens. [a.u.]
x10^4
1.25
1.00
0.75
0.50
0.25
0.00
1455.166
1000
1100
1200
1300
1400
1500
1600
1700
1800
1900
m/z
D:\data\McLaughlin\priyesh\PJ-6-104 analytical\PJ-6-104\0_A6\1
printed: 1/27/2010 2:49:41 PM

Peptide 2.3

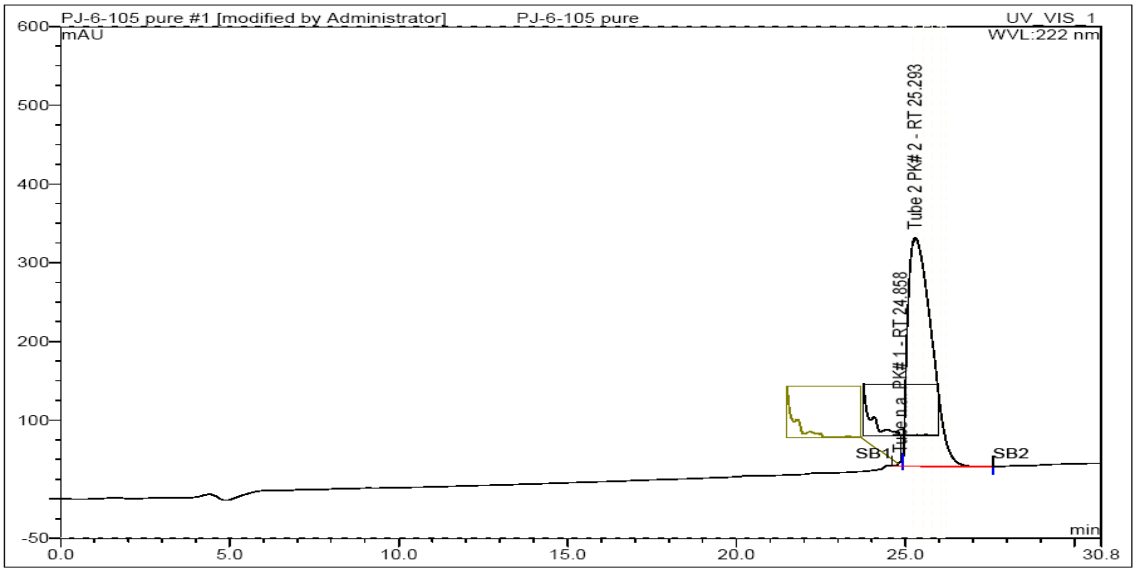

No.	Ret.Time min	Peak Name	Height mAU	Area mAU*min		Rel.Area %	Amount
1	24.86	n.a.	6.081	0.704		0.30	n.a.
2	25.29	n.a.	290.486	234.760		99.70	n.a.
Total:			296.568	235.463	100.00	0.000	

Comment 1
Comment 2

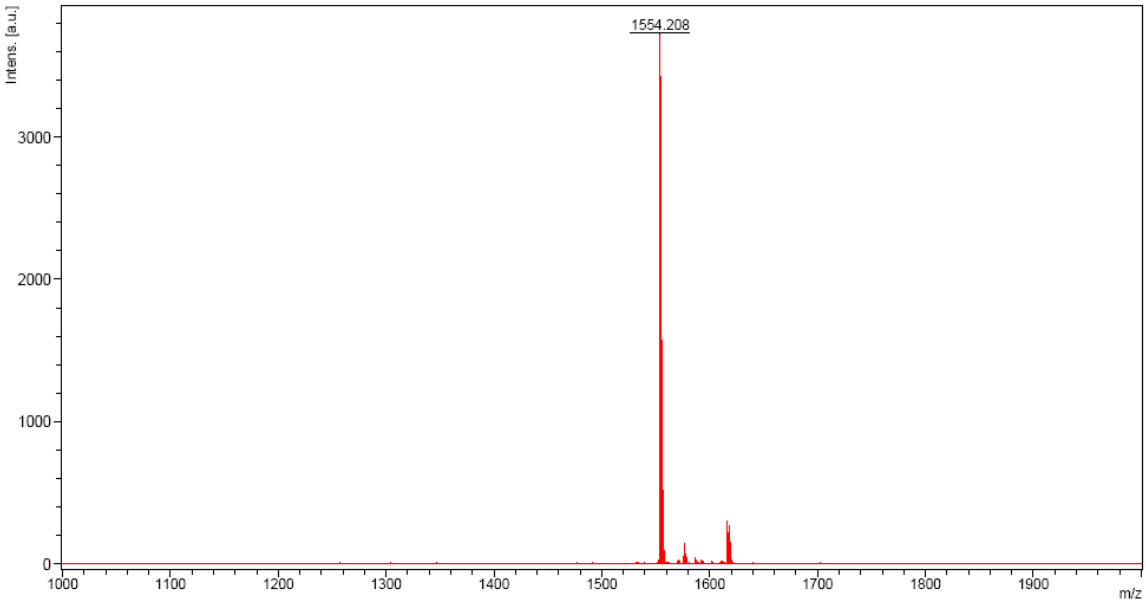

D:\data\McLaughlin\priyesh\PJ-6-105 analytical\PJ-6-105\0_A8\1

printed: 1/27/2010 2:51:44 PM

Peptide 2.4

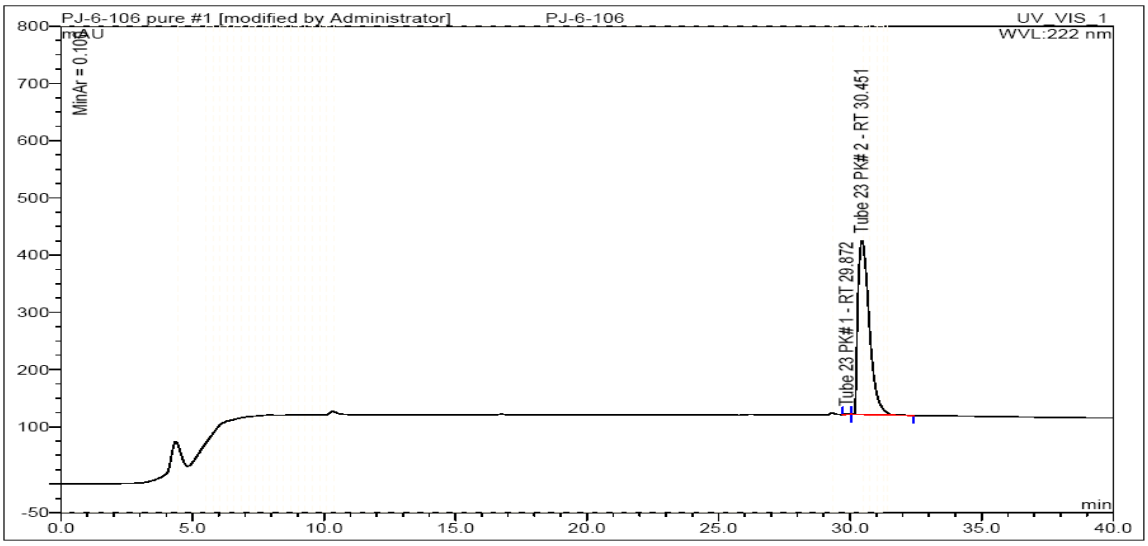

No.	Ret.Time min	Peak Name	Height mAU	Area mAU*min		Rel.Area %	Amount
1	29.87	n.a.	0.942	0.138		0.09	n.a.
2	30.45	n.a.	303.679	152.184		99.91	n.a.
Total:			304.620	152.322	100.00	0.000	

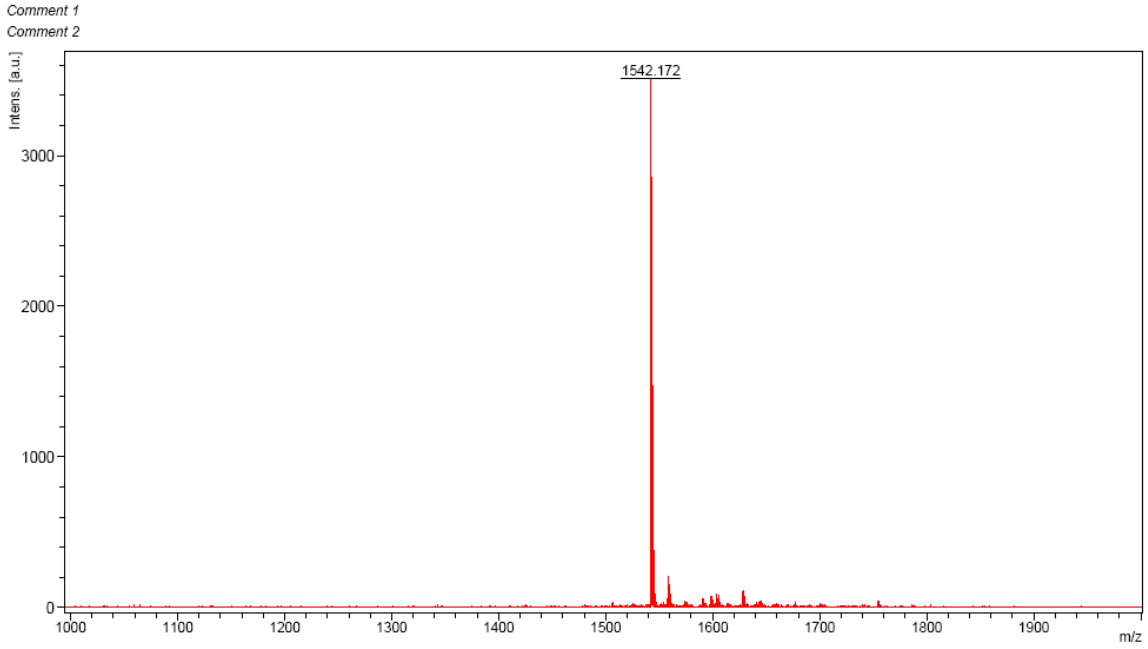

D:\data\McLaughlin\priyesh\PJ-6-106 analytical\PJ-6-106\0_A12\2

printed: 1/27/2010 2:57:15 PM

Peptide 2.5

Comment 1
Comment 2

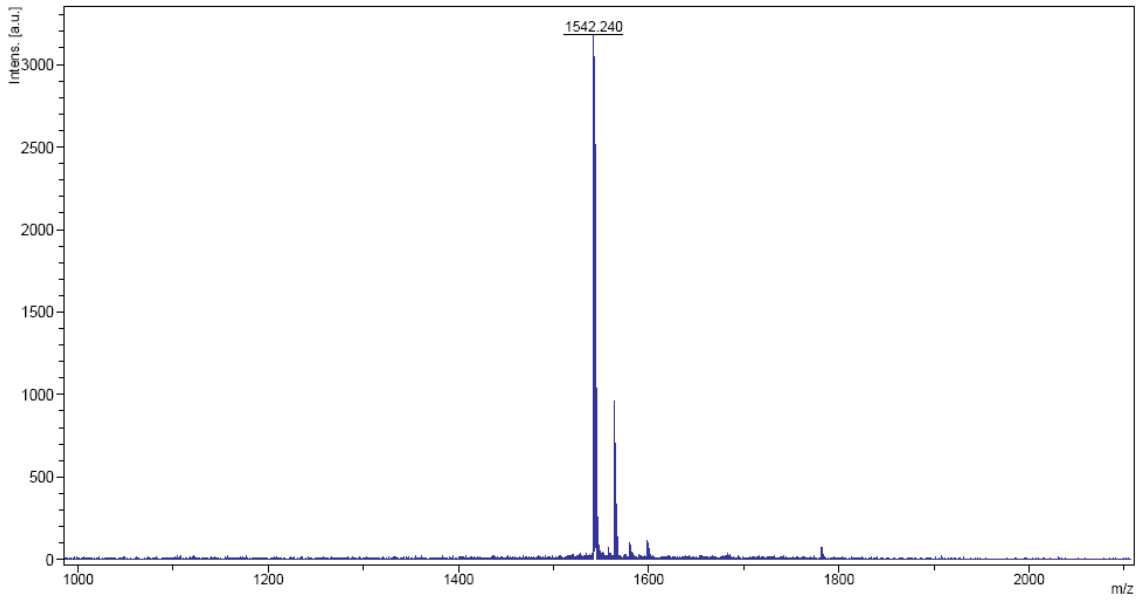

D:\data\McLaughlin\priyesh\PJ-6-107 pure\PJ-6-107 pure\0_I2\2

printed: 1/29/2010 4:50:06 PM

Peptide 2.6

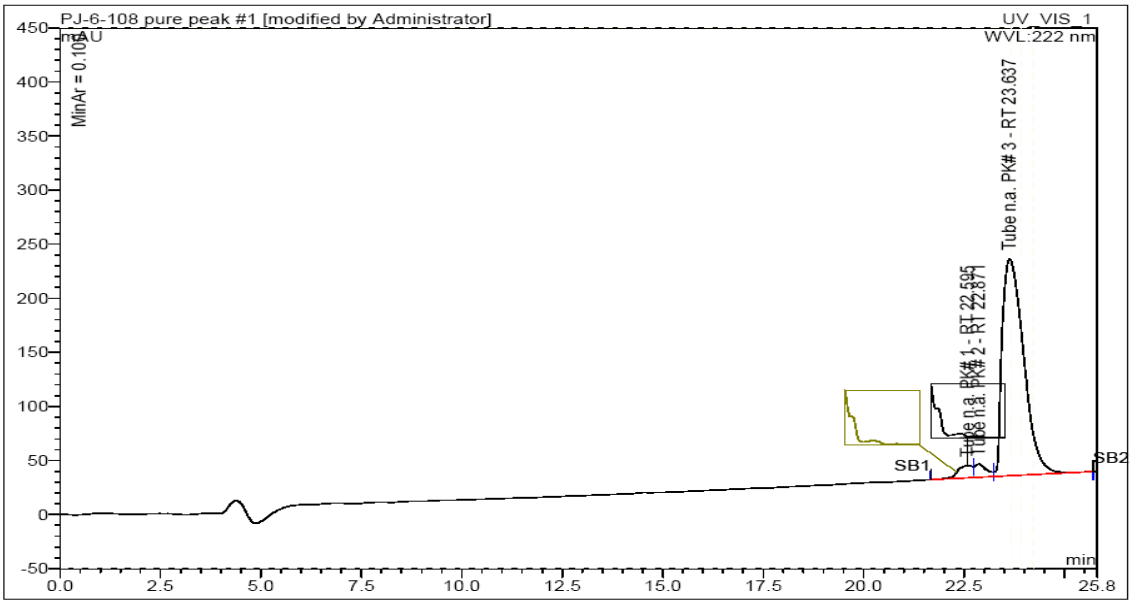

No.	Ret.Time min	Peak Name	Height mAU	Area mAU*min		Rel.Area %	Amount
1	22.60	n.a.	11.581	4.955		3.73	n.a.
2	22.87	n.a.	12.076	4.133		3.11	n.a.
3	23.64	n.a.	200.552	123.895		93.17	n.a.
Total:			224.209	132.982	100.00	0.000	

Comment 1
Comment 2

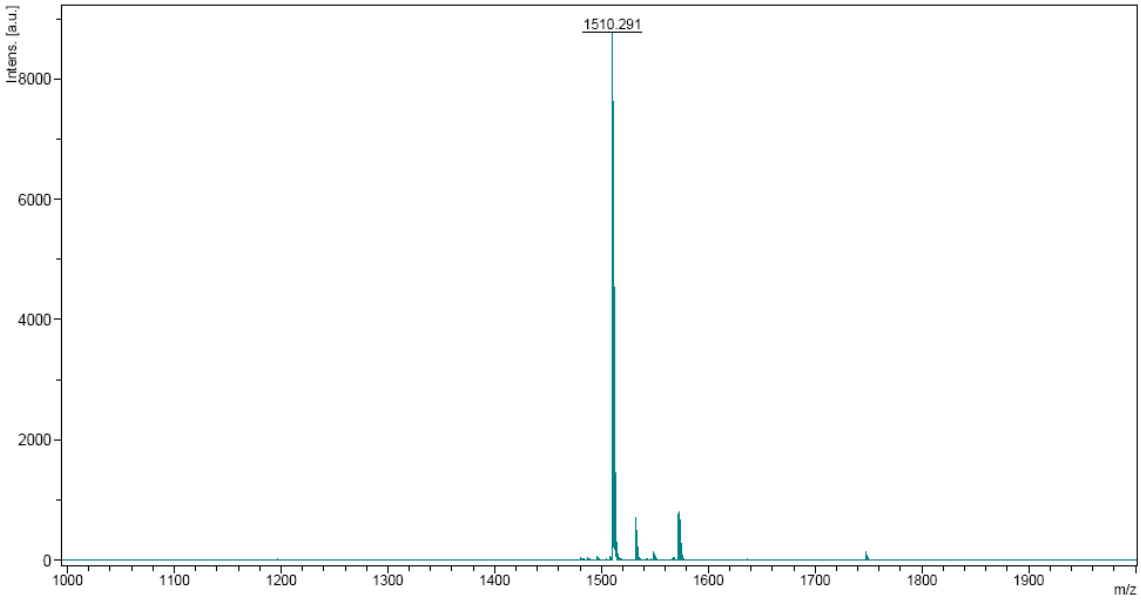

D:\data\McLaughlin\priyesh\PJ-6-108- analytical\PJ-6-108 prep hplc\PJ-6-108\0_D10\1

printed: 1/27/2010 3:04:28 PM

Peptide 2.7

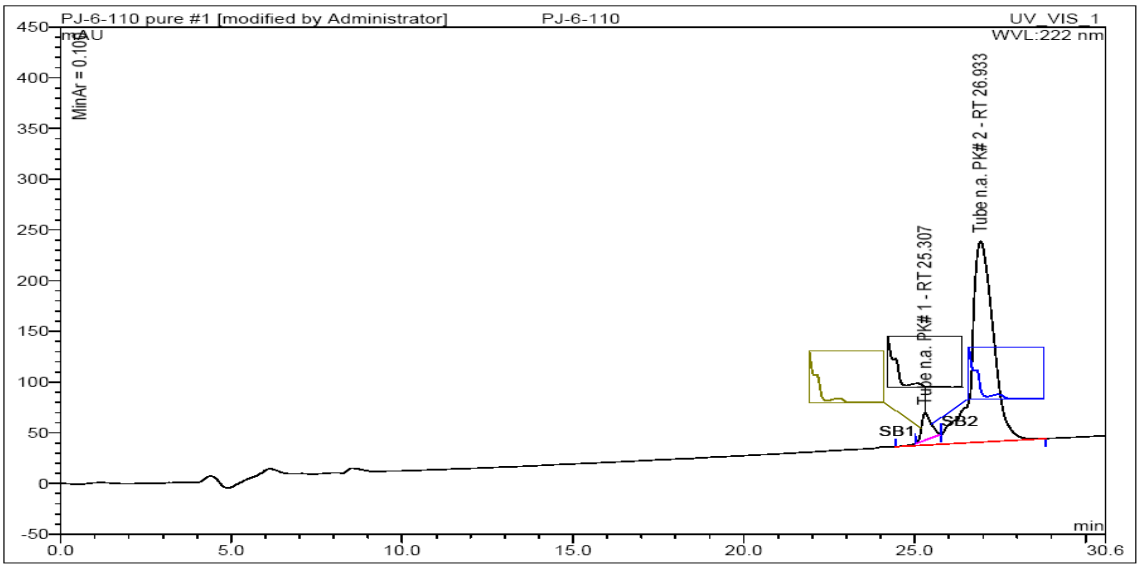

No.	Ret.Time min	Peak Name	Height mAU	Area mAU*min		Rel.Area %	Amount
1	25.31	n.a.	26.854	8.542		5.22	n.a.
2	26.93	n.a.	197.961	155.054		94.78	n.a.
Total:			224.814	163.595	100.00	0.000	

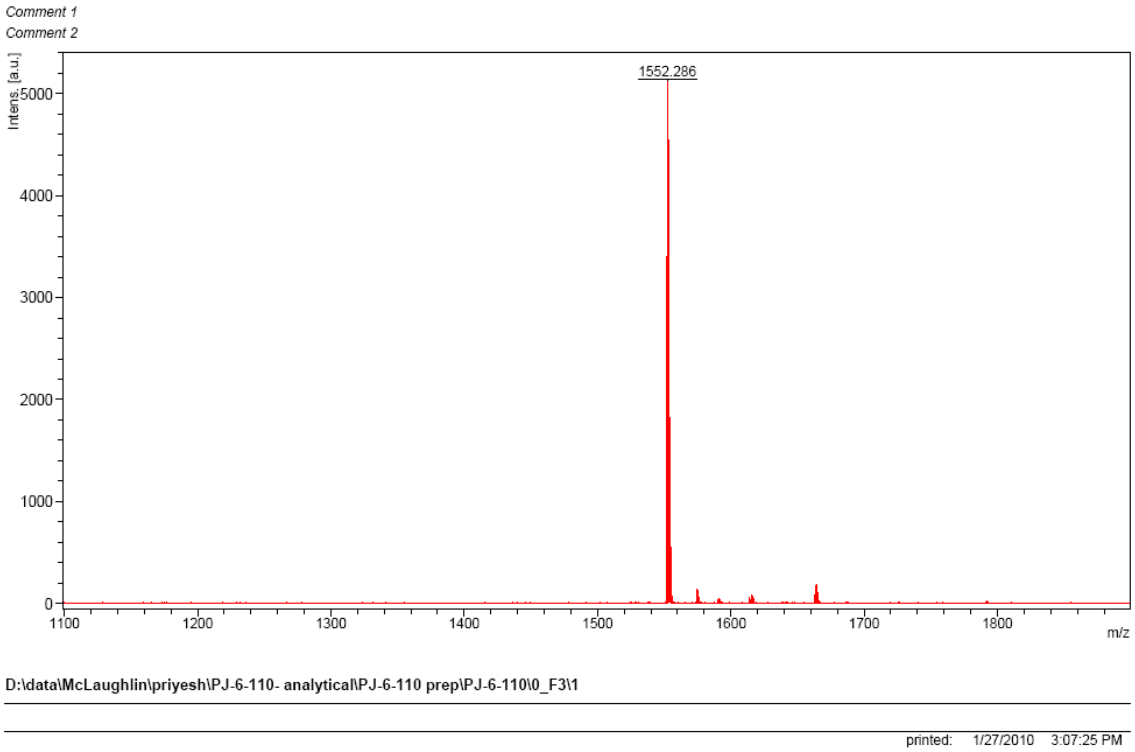

Peptide 2.8

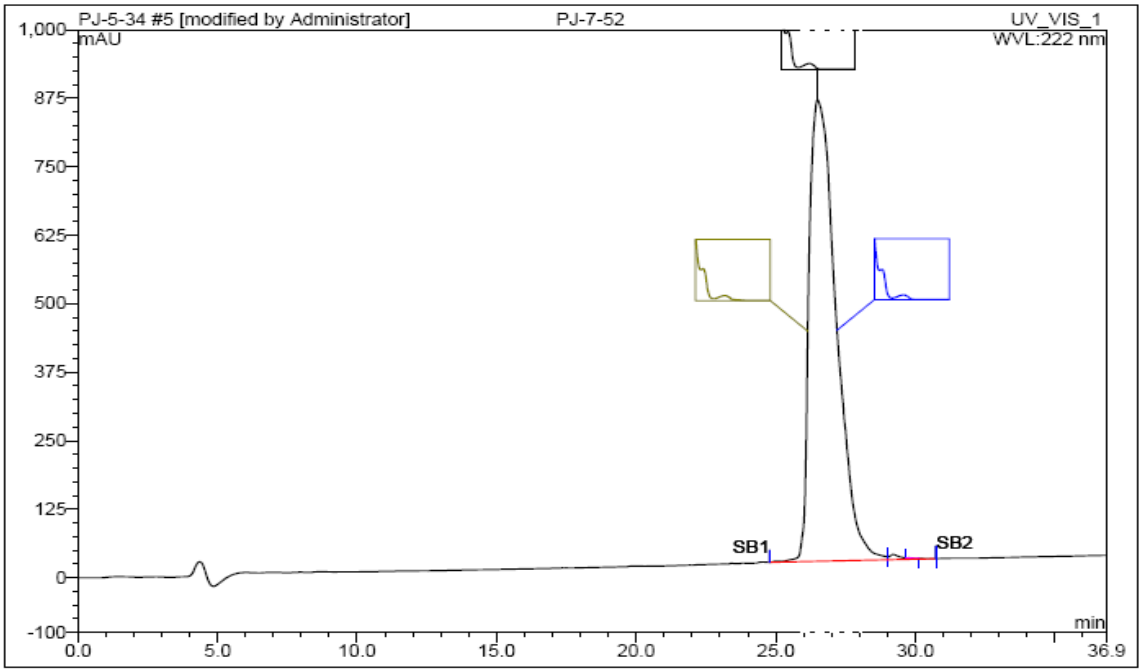

No.	Ret.Time min	Peak Name	Height mAU	Area mAU*min		Rel.Area %	Amount n.a.
1	26.52	n.a.	841.677	948.266		99.48	n.a.
2	29.21	n.a.	9.268	4.802		0.50	n.a.
3	29.78	n.a.	0.664	0.148		0.02	n.a.
Total:			851.608	953.216	100.00	0.000	

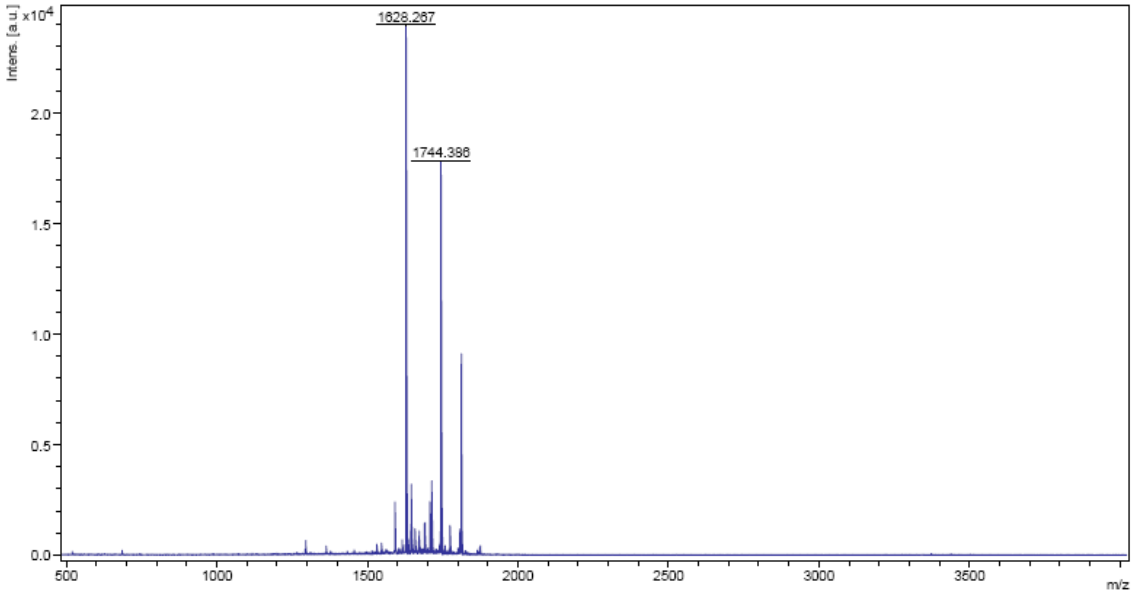

D:\data\McLaughlin\priyesh\PJ-7-52\PJ-7-52\0_O10\1

Peptide 2.9

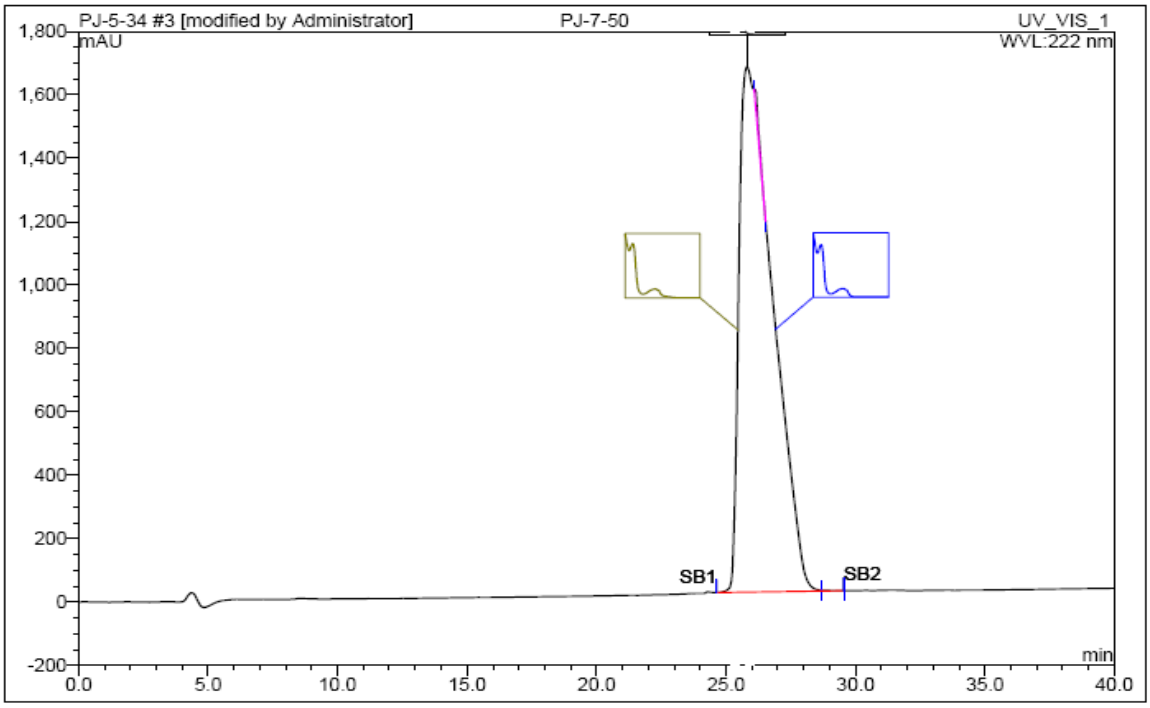

No.	Ret.Time min	Peak Name	Height mAU	Area mAU*min		Rel.Area %	Amount n.a.
1	25.82	n.a.	1657.685	2496.065		99.50	n.a.
2	26.10	n.a.	18.841	11.628		0.46	n.a.
3	28.78	n.a.	2.537	0.931		0.04	n.a.
Total:			1679.063	2508.624	100.00	0.000	

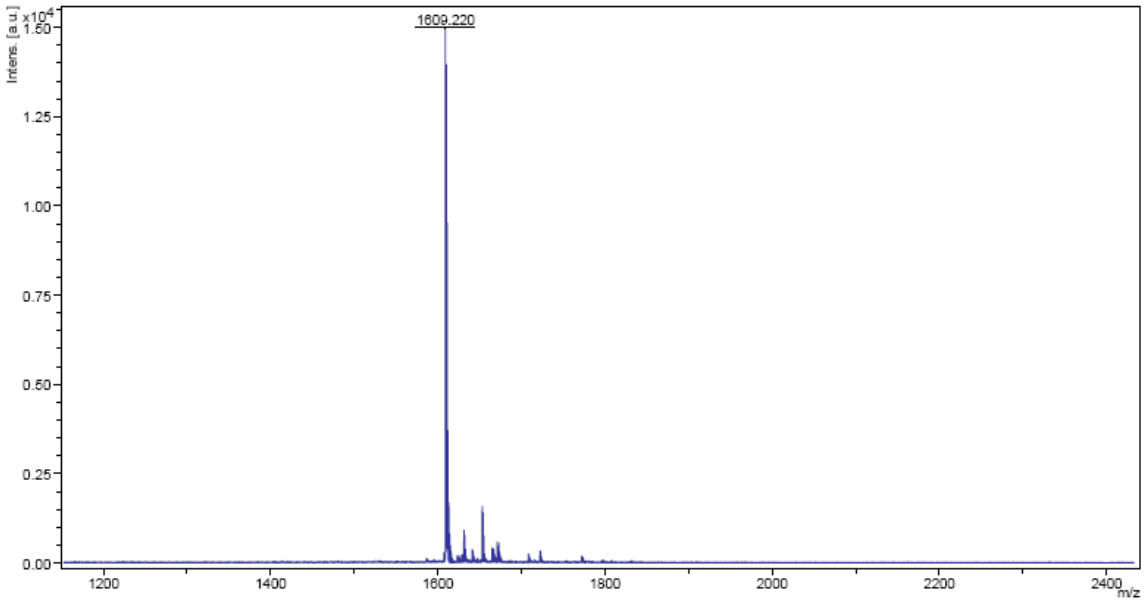

D:\data\McLaughlin\priyesh\PJ-7-50 analytical\PJ-7-50 prep\PJ-7-50 prep\0_N18\1

Peptide 2.10

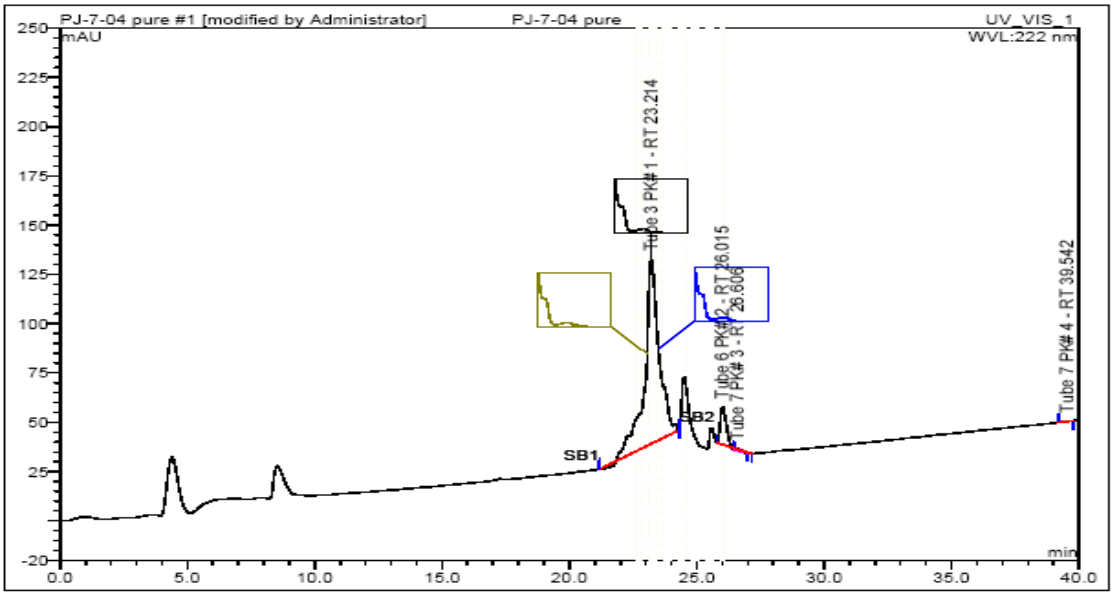

No.	Ret.Time min	Peak Name	Height mAU	Area mAU*min		Rel.Area %	Amount
1	23.21	n.a.	93.227	61.296		92.49	n.a.
2	26.01	n.a.	19.039	4.657		7.03	n.a.
3	26.61	n.a.	1.283	0.289		0.44	n.a.
4	39.54	n.a.	0.118	0.033		0.05	n.a.
Total:			113.667	66.276	100.00	0.000	

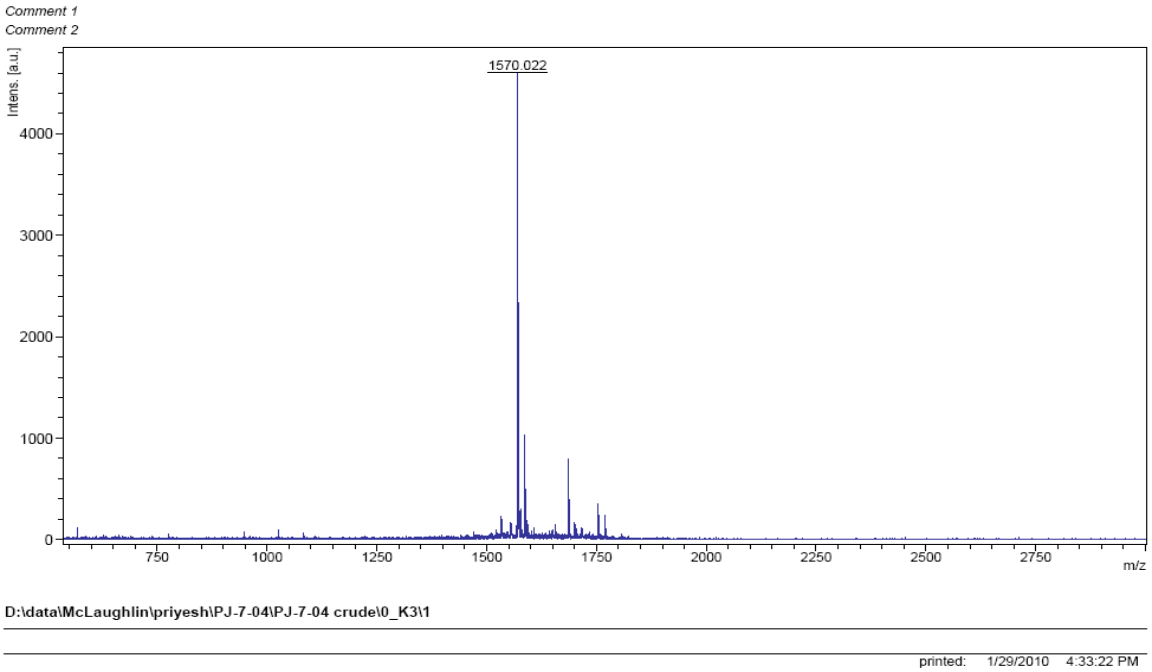

Peptide 2.11

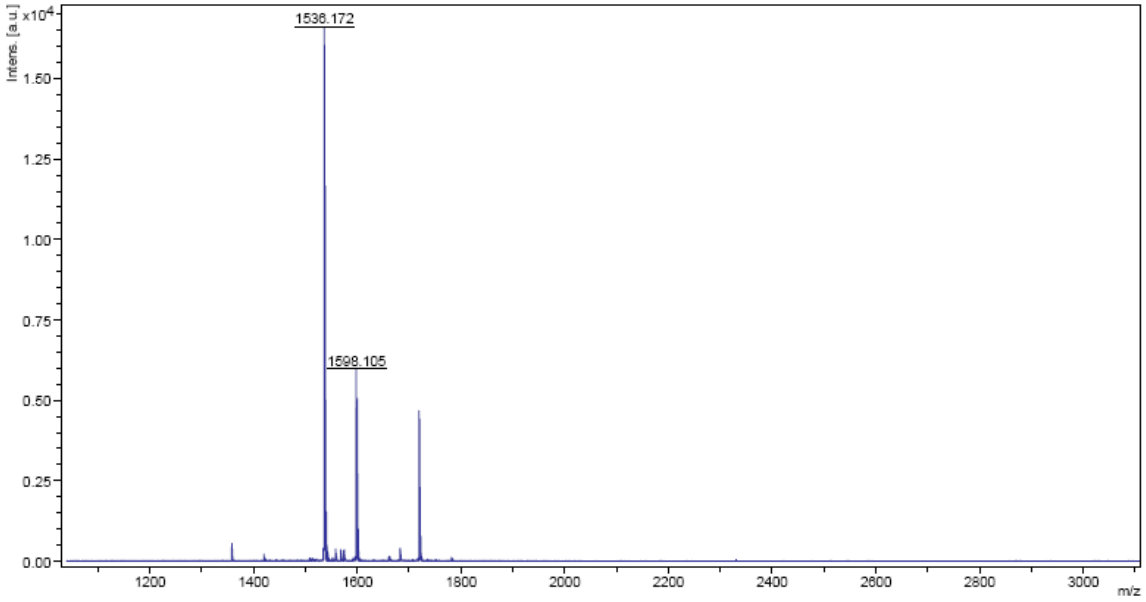

D:\data\McLaughlin\priyesh\PJ-7-95\PJ-7-95-analytyical\PJ-7-95-analytical RT=26.4\0_N18\1

Peptide 2.12

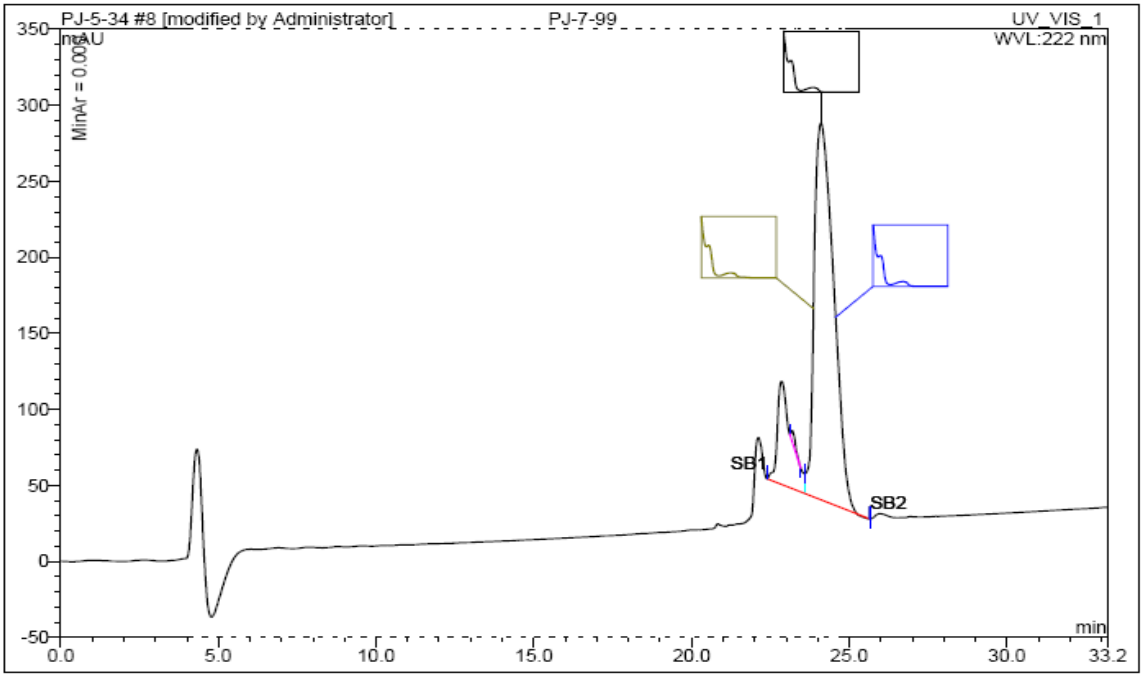

No.	Ret.Time min	Peak Name	Height mAU	Area mAU*min		Rel.Area %	Amount n.a.
1	22.86	n.a.	67.792	34.533		16.14	n.a.
2	23.20	n.a.	7.511	1.252		0.59	n.a.
3	24.11	n.a.	247.725	178.118		83.27	n.a.
Total:			323.028	213.903	100.00	0.000	

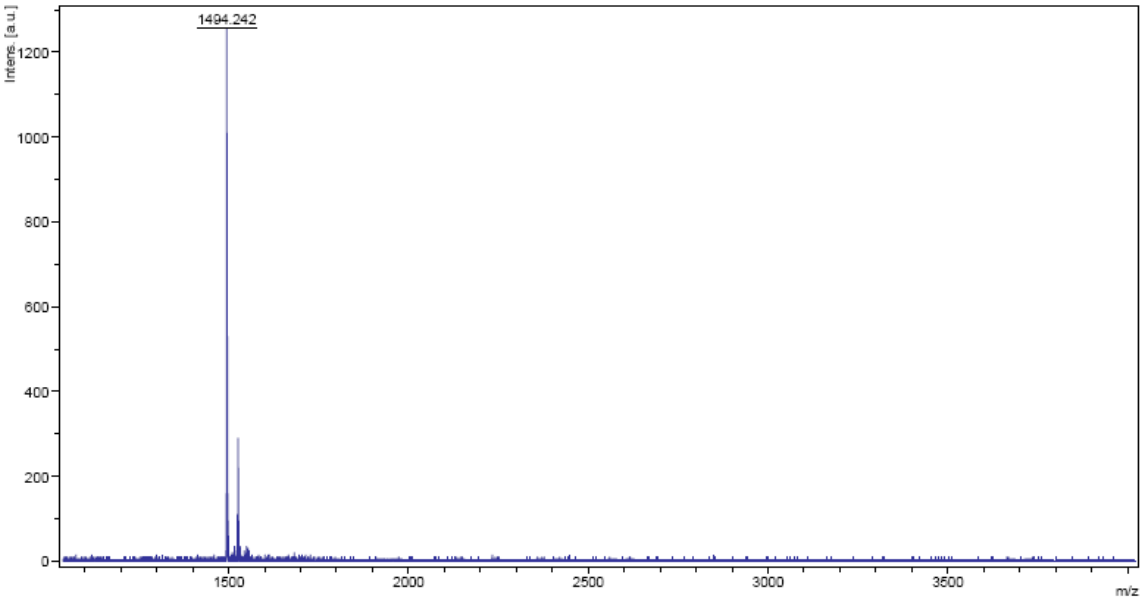

D:\data\McLaughlin\priyesh\PJ-7-99\PJ-7-99-analytical RT=24\0_L6\1

Peptide 2.13

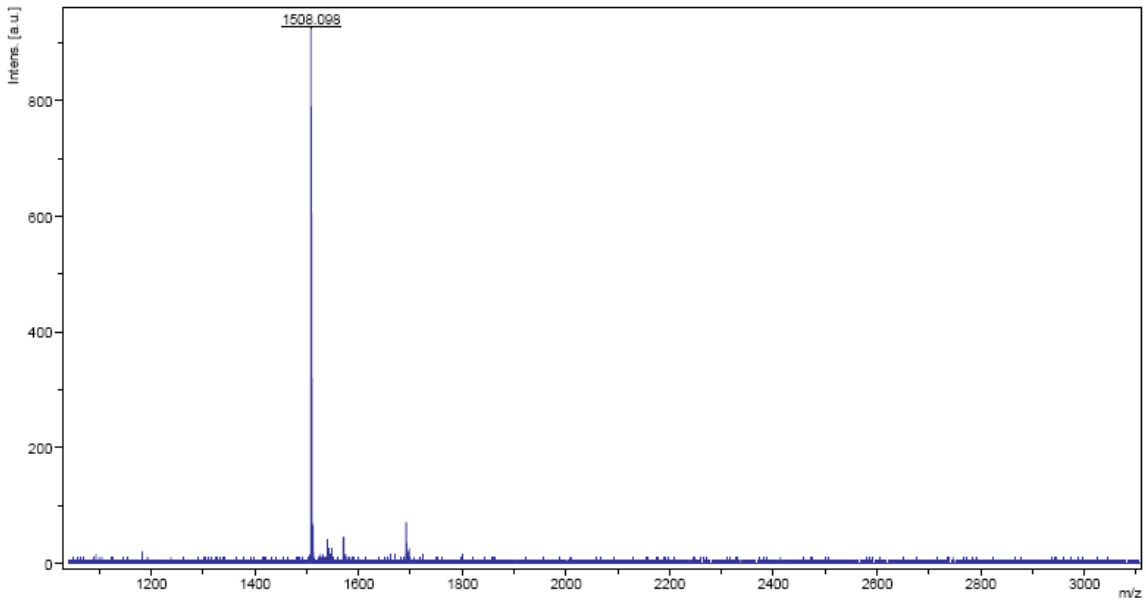

D:\data\McLaughlin\priyesh\PJ-7-96\PJ-7-96-analytical\PJ-7-96-analytical RT=25.67\0_N16\1

Peptide 2.14

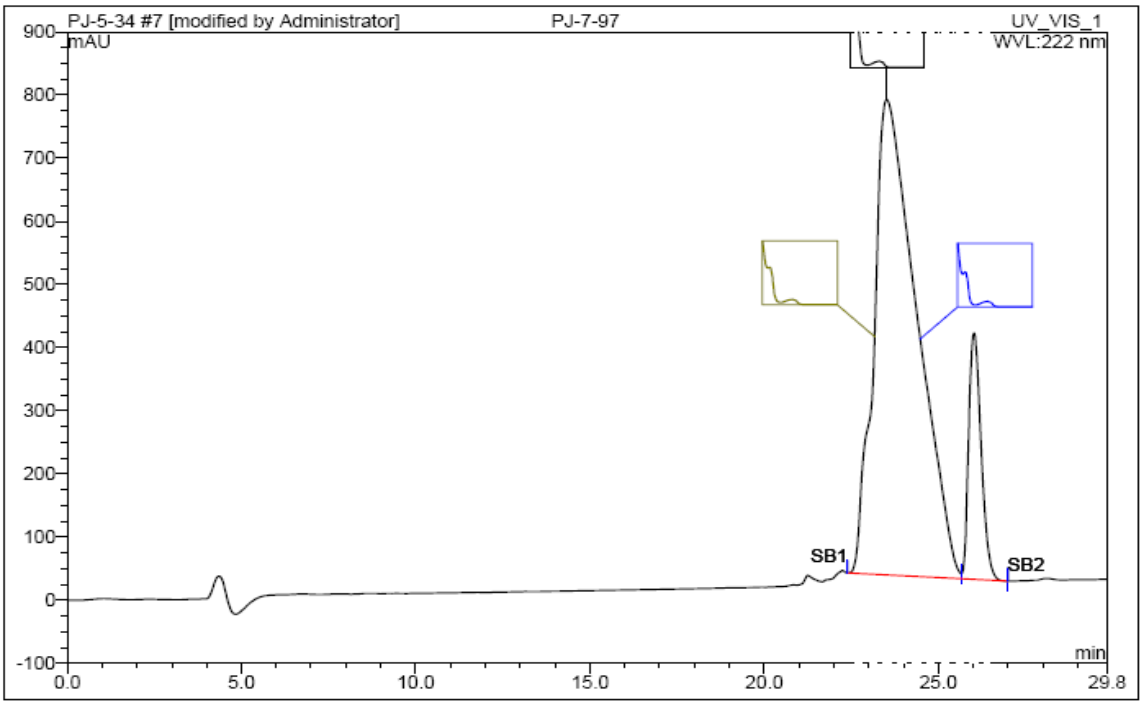

No.	Ret.Time min	Peak Name	Height mAU	Area mAU*min		Rel.Area %	Amount n.a.
1	23.52	n.a.	753.135	1076.488		86.90	n.a.
2	26.02	n.a.	390.426	162.220		13.10	n.a.
Total:			1143.561	1238.707	100.00	0.000	

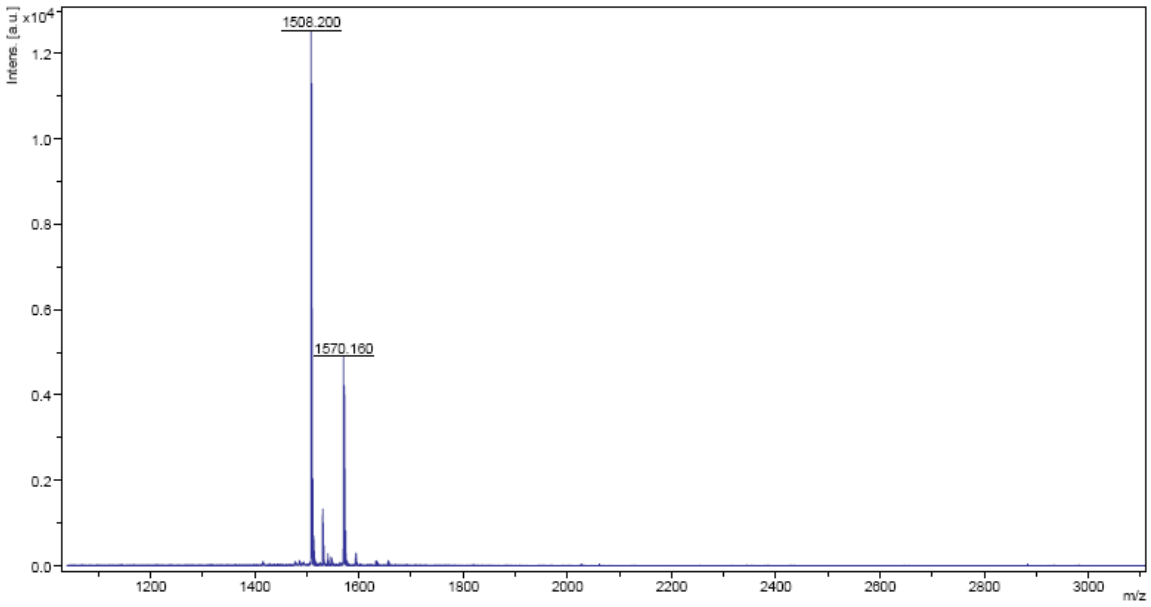

D:\data\McLaughlin\priyesh\PJ-7-97\PJ-7-97-prep\PJ-7-97-prep\0_N5\1

Peptide 2.15

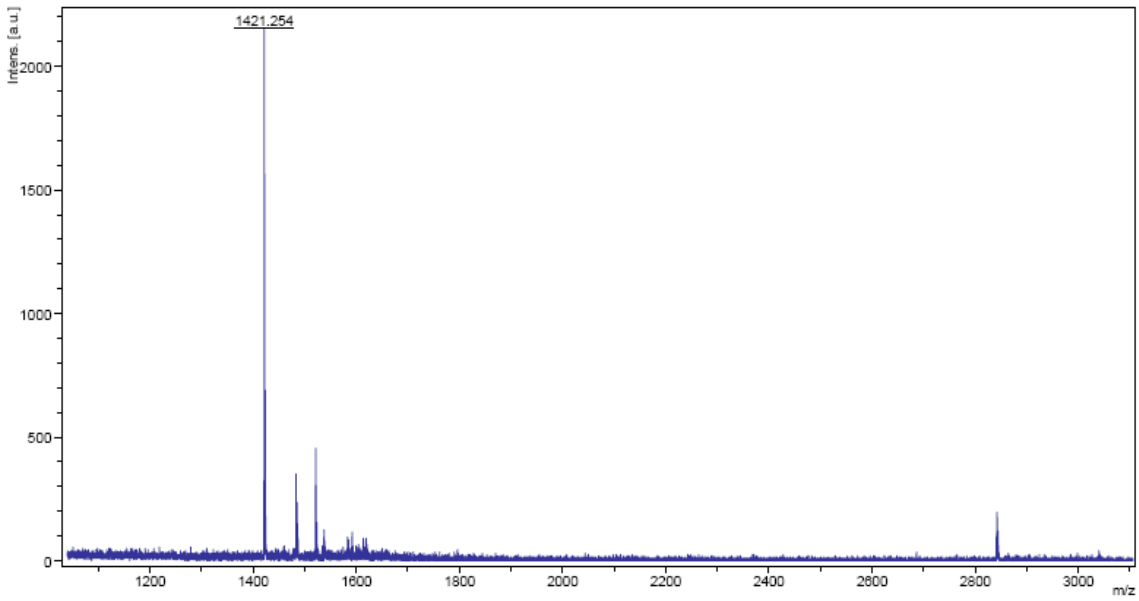

D:\data\McLaughlin\priyesh\PJ-7-98\PJ-7-98-analytical RT=25.8\0_N15\1

Peptide 2.16

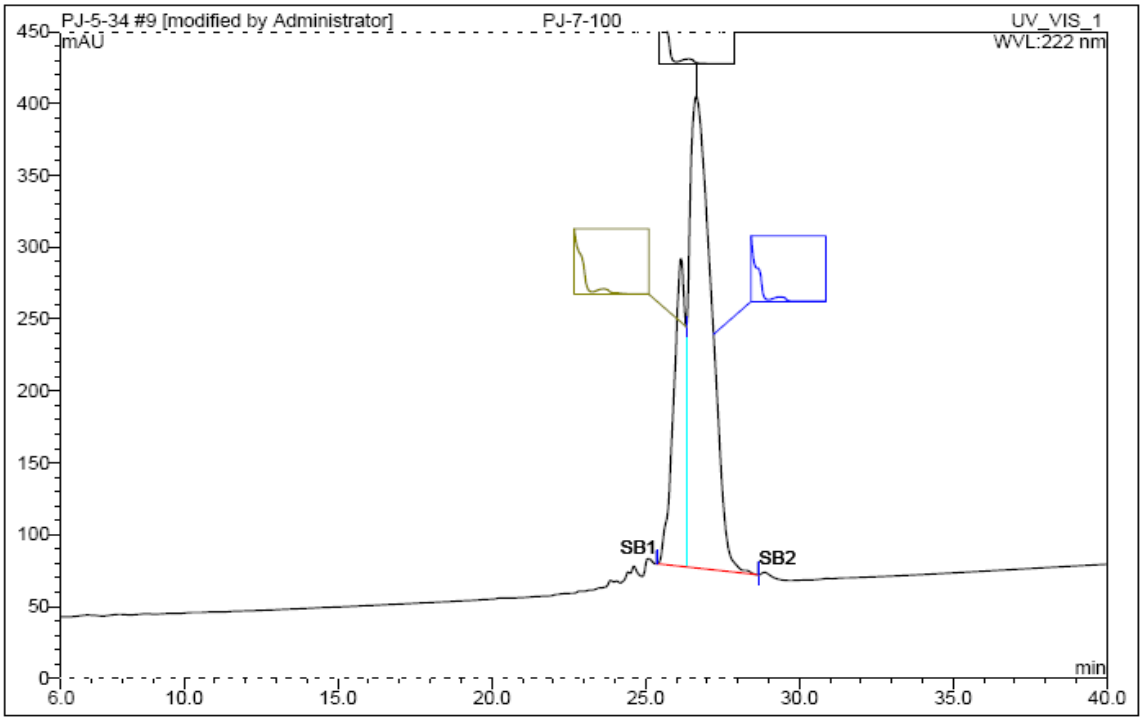

No.	Ret.Time min	Peak Name	Height mAU	Area mAU*min		Rel.Area %	Amount n.a.
1	26.15	n.a.	214.082	92.528		25.25	n.a.
2	26.65	n.a.	328.164	273.858		74.75	n.a.
Total:			542.246	366.386	100.00	0.000	

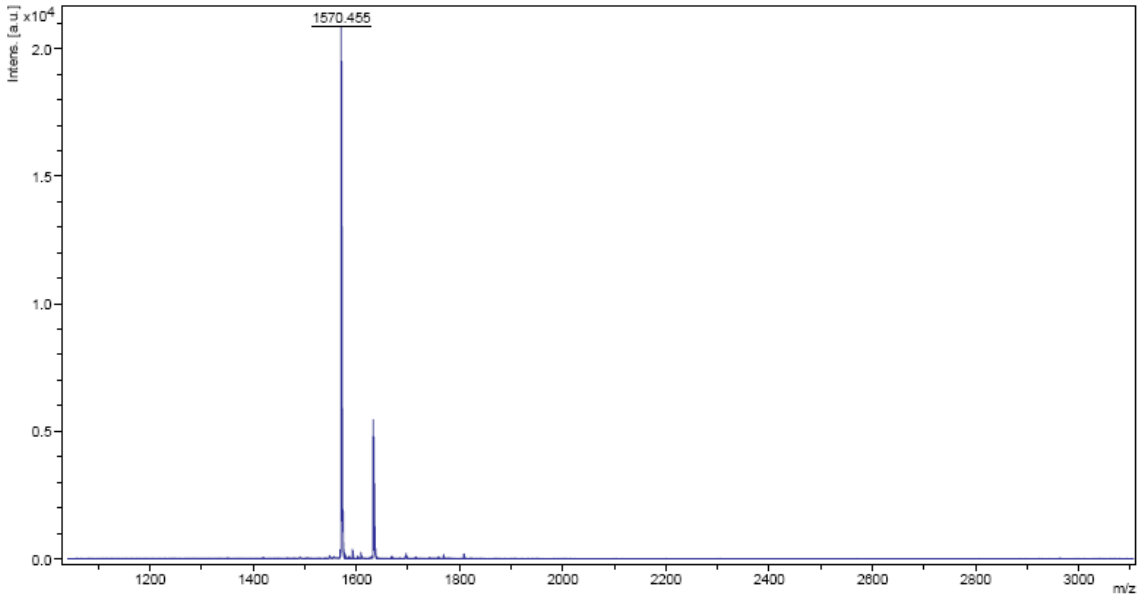

D:\data\McLaughlin\priyesh\PJ-7-100\PJ-7-100-prep\PJ-7-100-prep\0_O7\1

Peptide 2.17

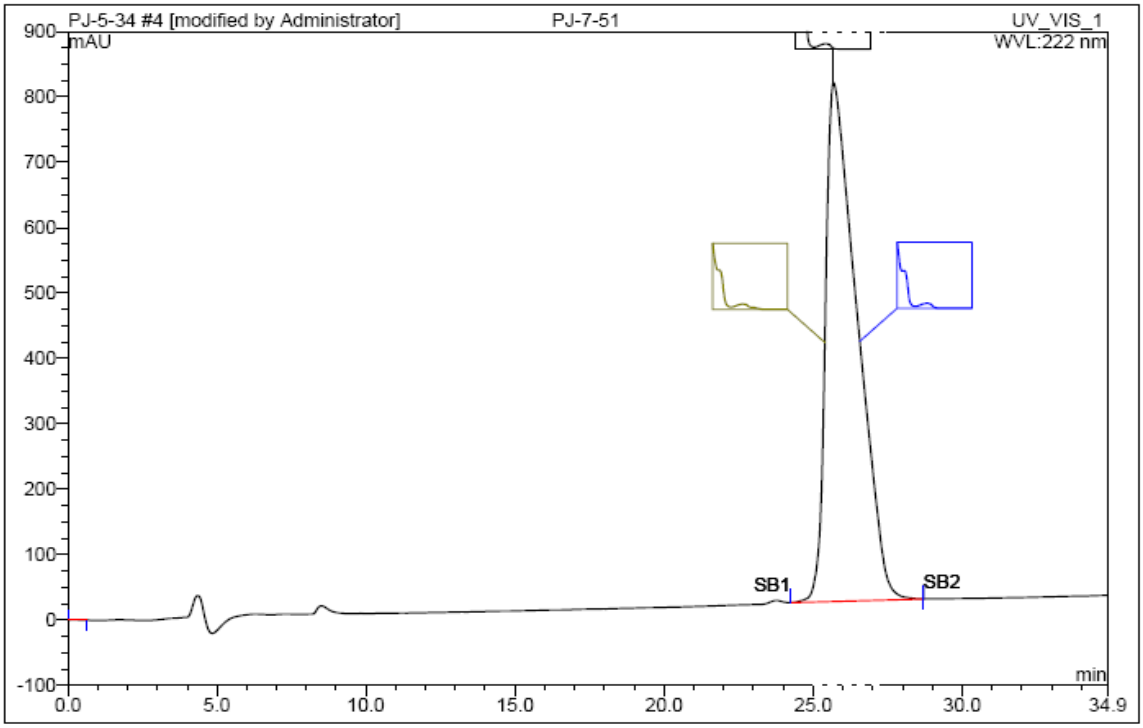

No.	Ret.Time min	Peak Name	Height mAU	Area mAU*min		Rel.Area %	Amount n.a.
1	0.19	n.a.	0.263	0.094		0.01	n.a.
2	25.69	n.a.	793.404	974.640		99.99	n.a.
Total:			793.667	974.734	100.00	0.000	

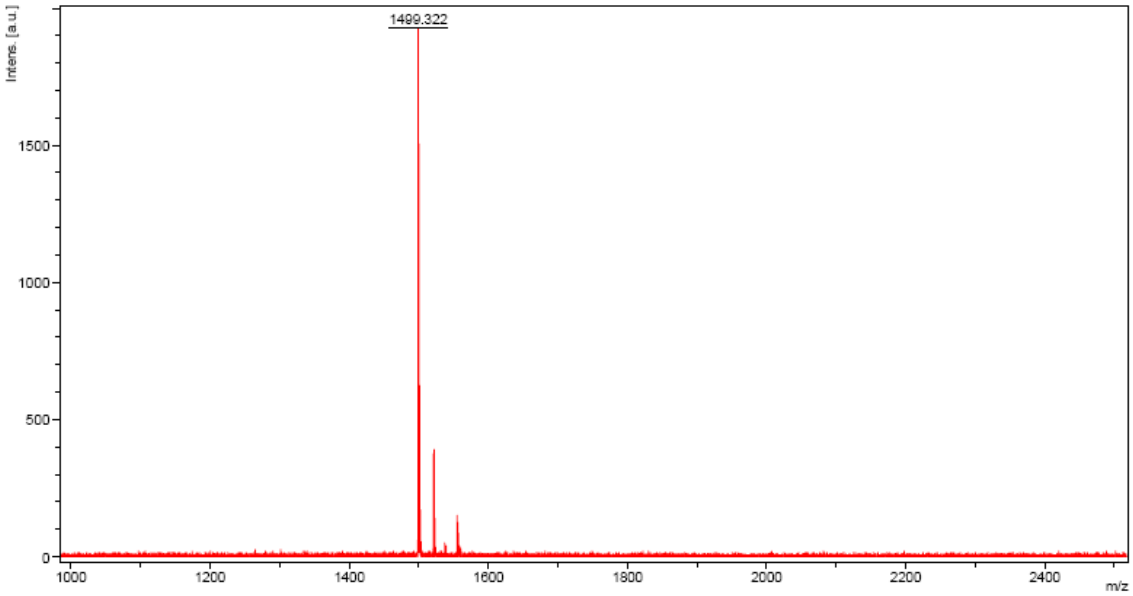

D:\data\McLaughlin\priyesh\PJ-7-51 analytical\PJ-7-51 prep\PJ-7-51 prep\0_K8\1

Peptide 2.18

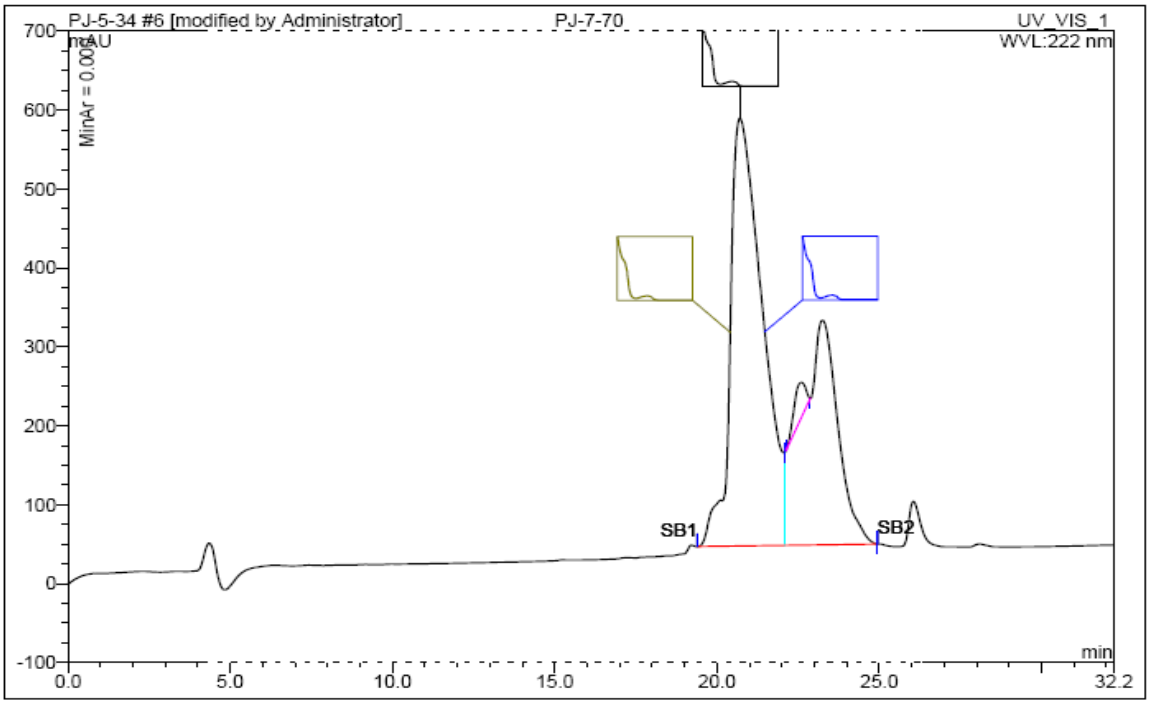

No.	Ret.Time min	Peak Name	Height mAU	Area mAU*min		Rel.Area %	Amount n.a.
1	20.71	n.a.	542.313	621.334		61.25	n.a.
2	22.60	n.a.	44.708	19.376		1.91	n.a.
3	23.25	n.a.	284.733	373.773		36.84	n.a.
Total:			871.755	1014.482	100.00	0.000	

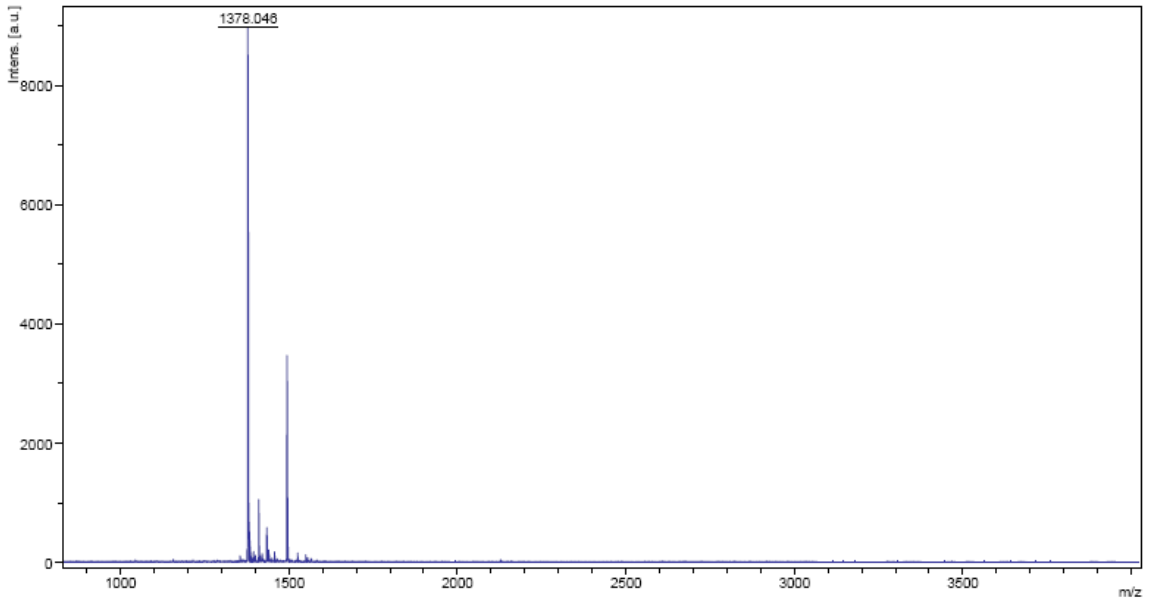

D:\data\McLaughlin\priyesh\PJ-7-70 PREP\PJ-7-70\0_O7\1

Peptide 3.1

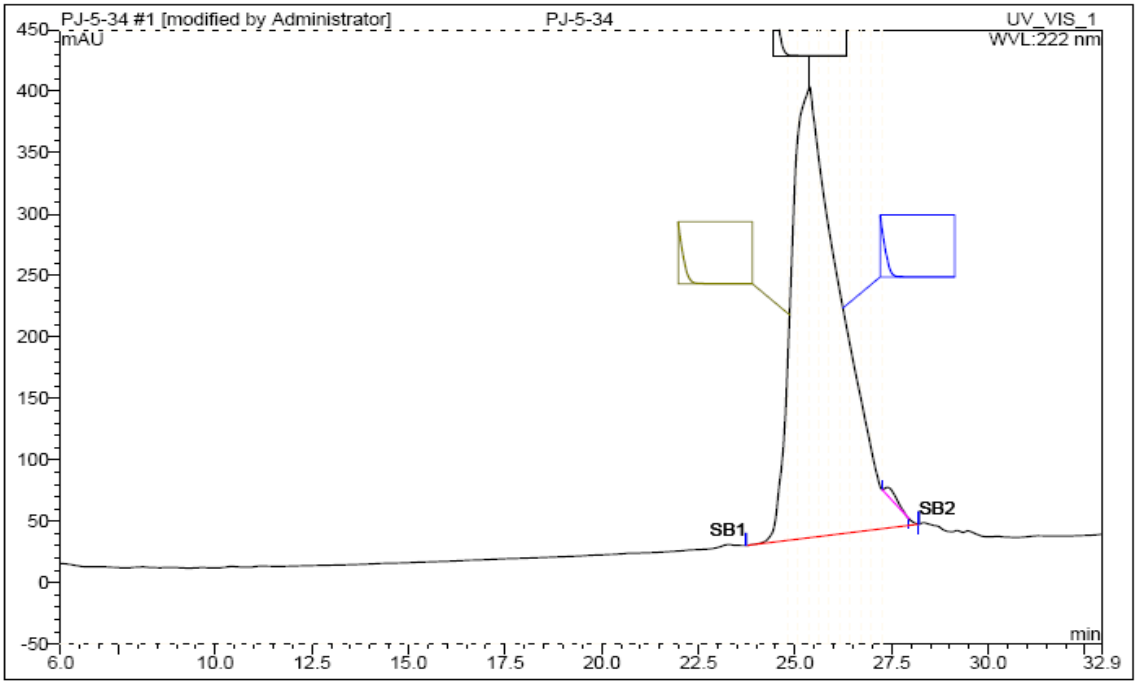

No.	Ret.Time min	Peak Name	Height mAU	Area mAU*min		Rel.Area %	Amount n.a.
1	25.38	n.a.	366.934	543.412		99.49	n.a.
2	27.39	n.a.	6.353	2.768		0.51	n.a.
Total:			373.287	546.180	100.00	0.000	

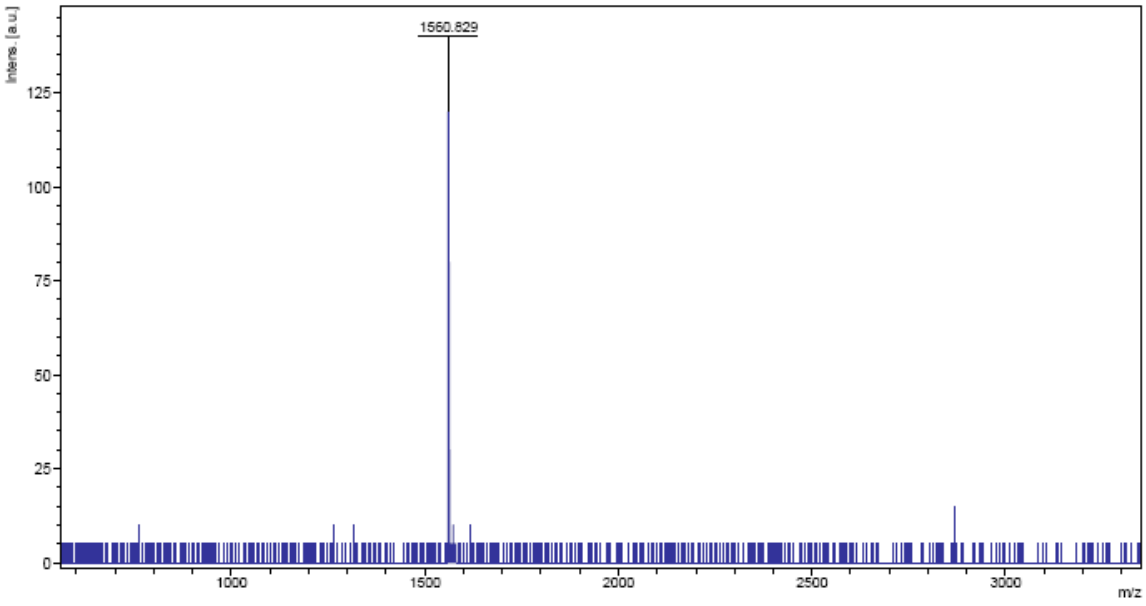

D:\data\McLaughlin\priyesh cAbA\PJ-5-34 pure\0_B22\1

Peptide 3.2

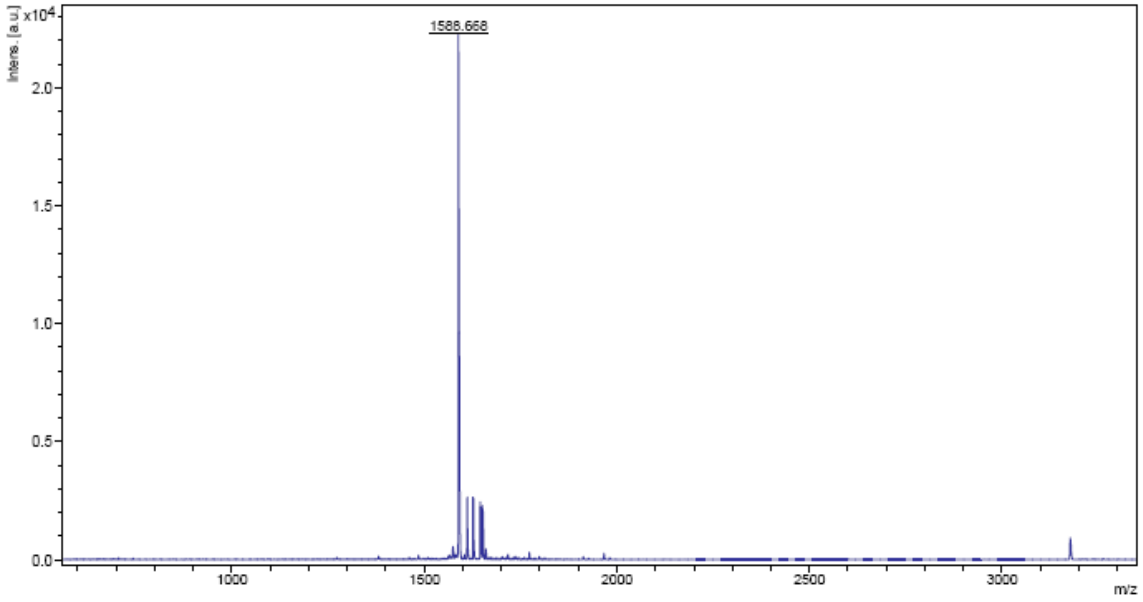

D:\data\McLaughlin\priyesh cAbA\cyclic ABeta 061109\0_P13\1

Peptide 3.3

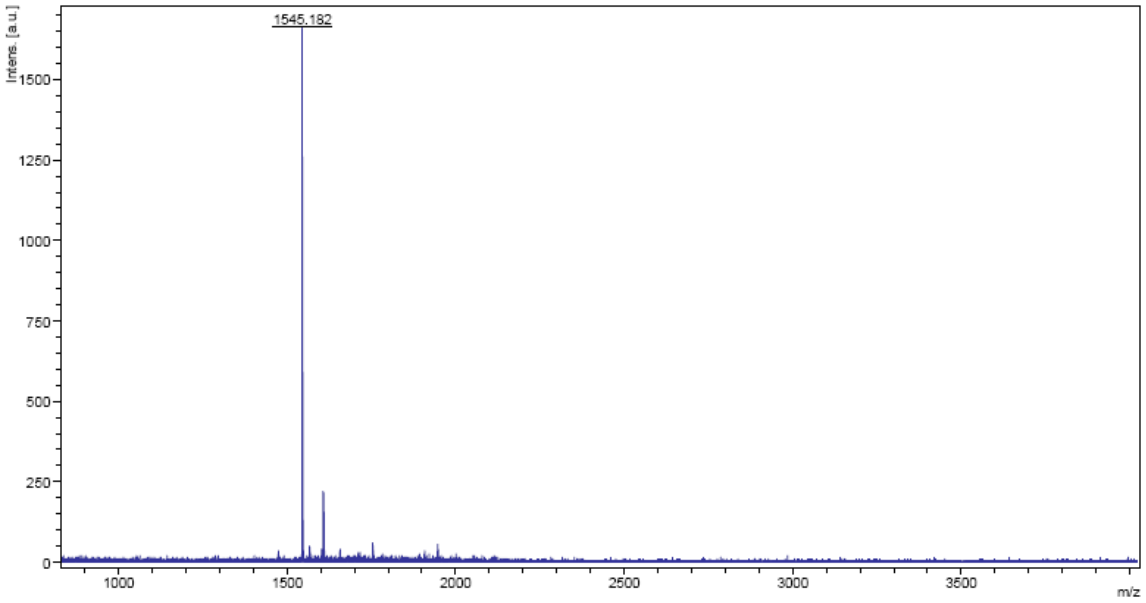

D:\data\McLaughlin\priyesh\PJ-7-106\PJ-7-106-crude\0_F11\1

Peptide 3.4

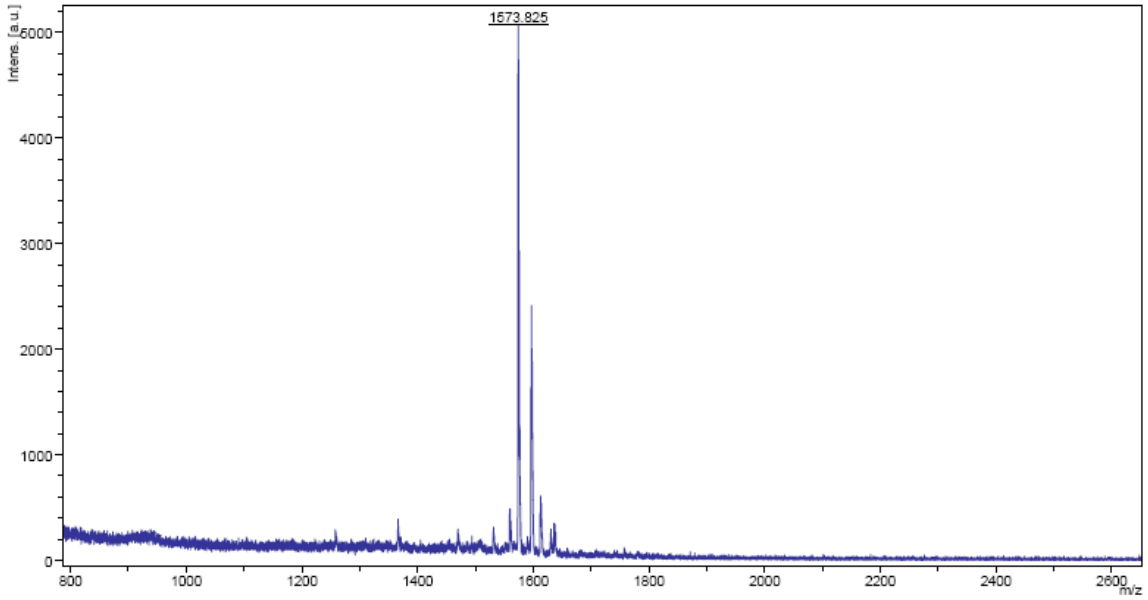

D:\data\McLaughlin\Cyclic Abeta PJ5108\0_A9\1

Peptide 3.5

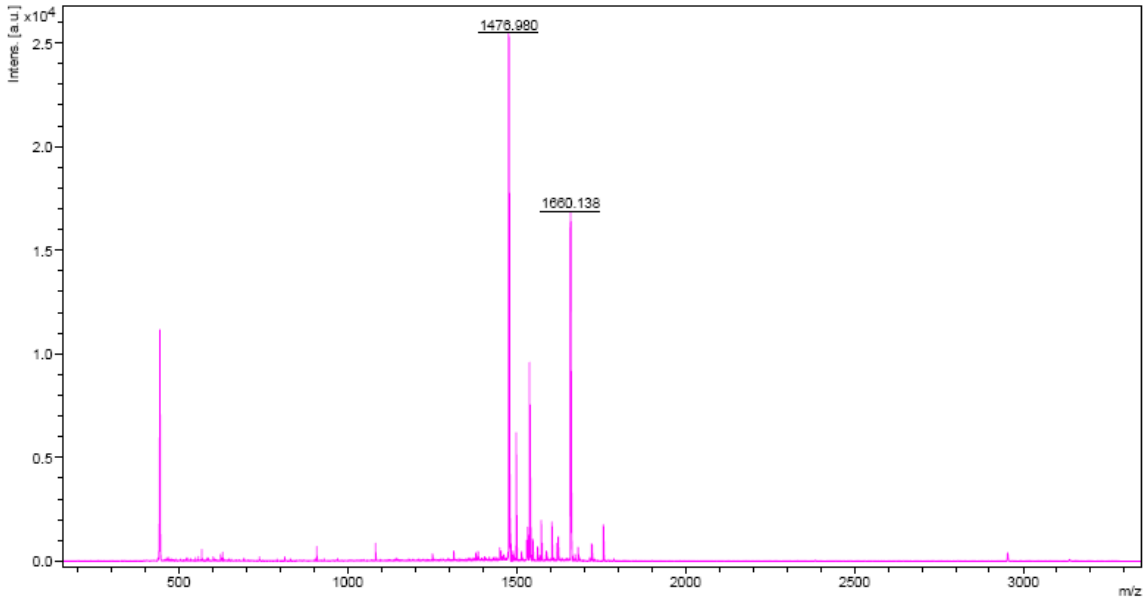

D:\data\McLaughlin\priyesh\PJ-6-60\0_N16\1

Peptide 3.6

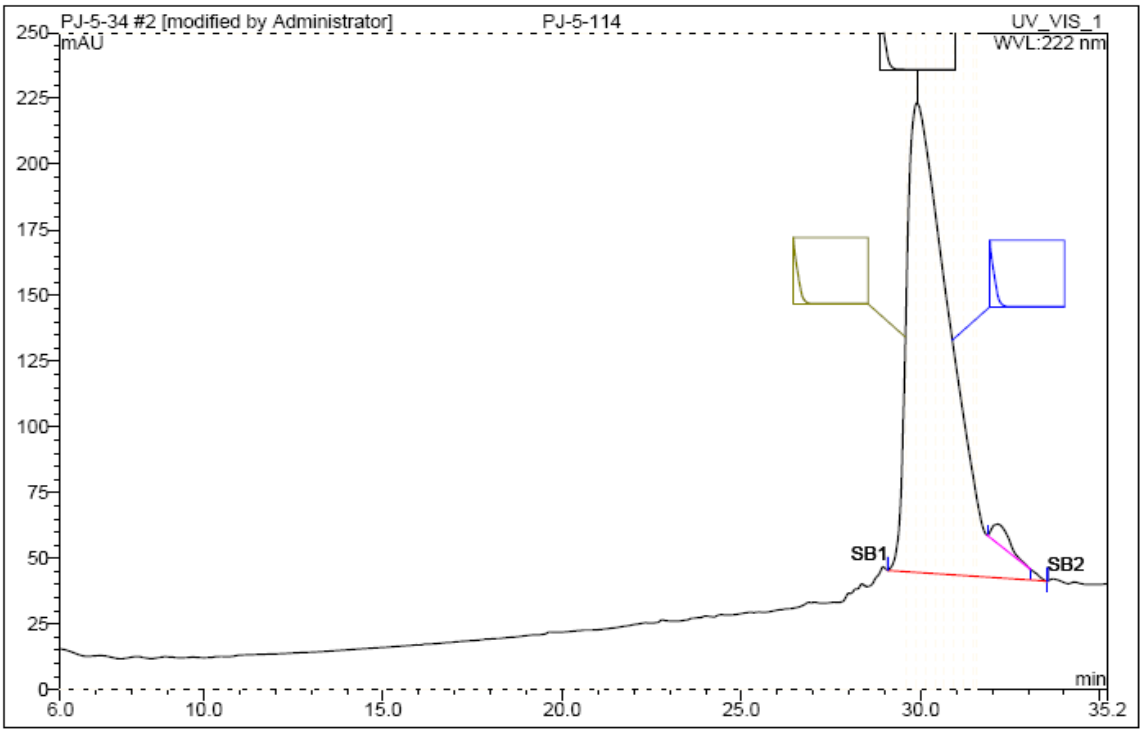

No.	Ret.Time min	Peak Name	Height mAU	Area mAU*min		Rel.Area %	Amount n.a.
1	29.90	n.a.	178.658	254.095		98.38	n.a.
2	32.15	n.a.	7.415	4.173		1.62	n.a.
Total:			186.073	258.269	100.00	0.000	

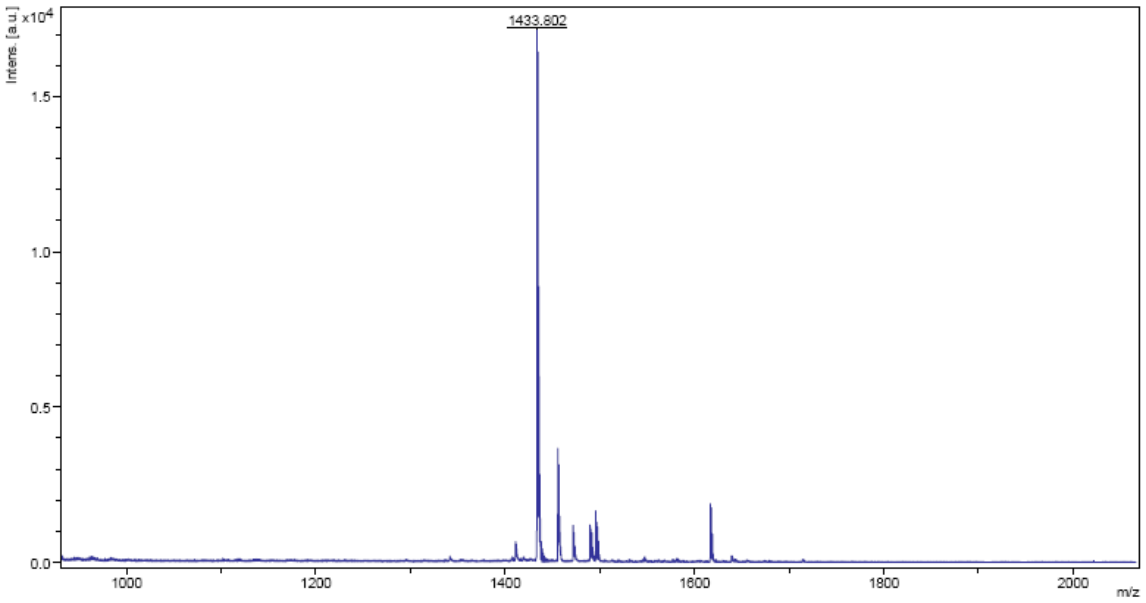

D:\data\McLaughlin\Cyclic Abeta Pg 5114\0_A7\1

Peptide 4.1

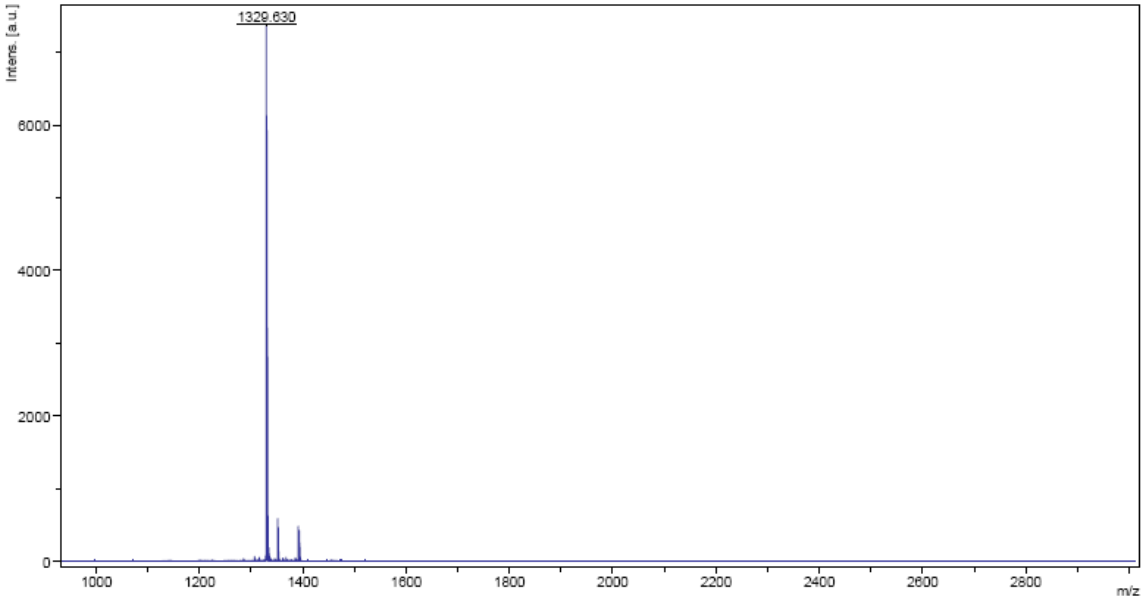

D:\data\McLaughlin\priyesh\PJ_7-17 analytical\PJ-7-17 Prep\PJ-7-17\0_H1\1

Peptide 4.2

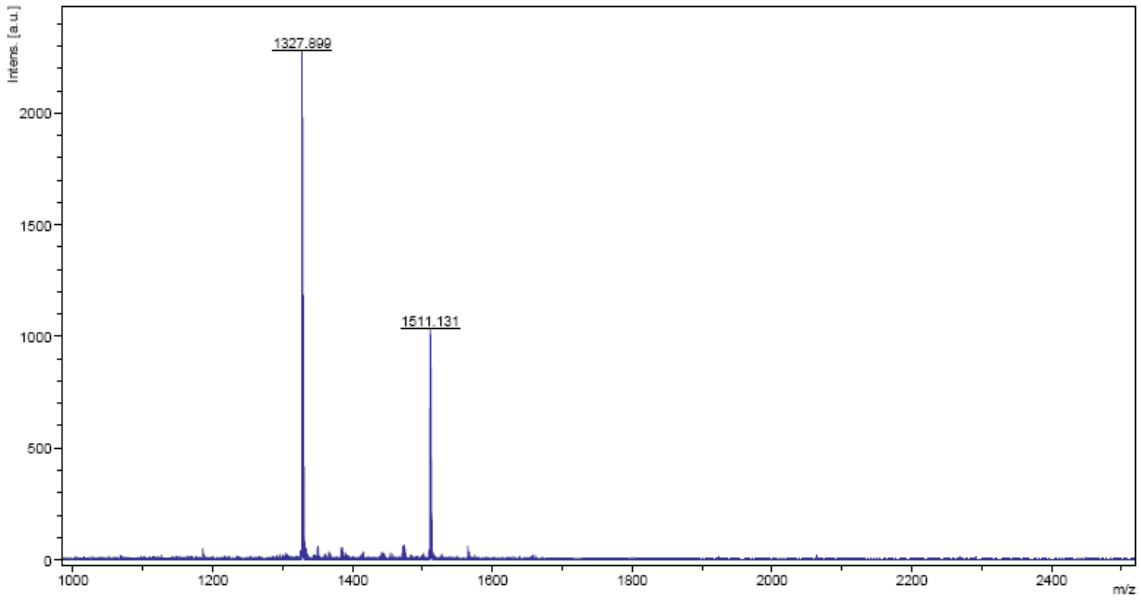

D:\data\McLaughlin\priyesh\PJ-7-72 crude\PJ-7-72 crude\0_M9\1

Peptide 4.3

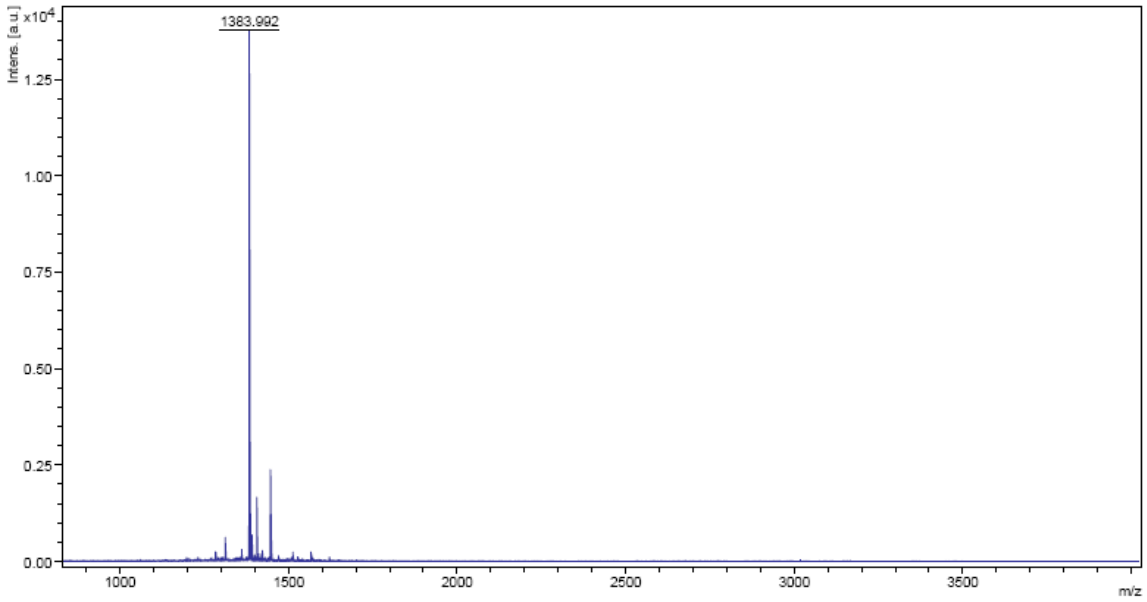

D:\data\McLaughlin\priyesh\PJ-7-102\PJ-7-102-crude\0_F10\1

About the author

Mr. Priyesh Jain received his Bachelor's degree in Paints & Polymer Technology from University Department of Chemical Technology, University of Mumbai, India in 2000. He worked as Technical officer (R&D) in Goodlass Nerolac paints, Mumbai till September 2001. He completed his Master's degree in Paints & Polymer Technology from UDCT in August 2003. Later he worked for Anmol Chemical Industries, New Delhi, India as Assistant Manager (R&D). Mr. Jain started his career at USF in Spring 2005 as a graduate student in Dr. Mark McLaughlin's group. He continued his research in synthetic organic chemistry and medicinal chemistry to receive doctoral degree in Fall 2010.